GRAHAM HAMILTON ROWE

APPLIED GEOLOGY OF WELLINGTON ROCKS FOR

AGGREGATE AND CONCRETE

Submitted for the degree of Doctor of Philosophy

in Geology at Victoria University of Wellington

November 1980

SODD'S FIRST LAW:

*When a person attempts a task, he or she
will be thwarted in that task by the
unconscious intervention of some other
presence (animate or inanimate). Never-
theless, some tasks are completed, since
the intervening presence is itself attempt-
ing a task and is, of course, subject to
interference.*

ABSTRACT

This study was initiated to examine geological aspects of Wellington grey-wacke-suite rocks in relation to their end use as an engineering material - aggregate, particularly for concrete.

An attempt has been made to map (at least in part), identify and categorise rocks for quarrying in the Wellington region, to evaluate and quantify their properties as aggregates and to appraise their qualities in concrete - in short to equate rock geology to aggregate and concrete performance as a tool for resource management.

Study of bedding led to a classification into three lithofacies and some 70 representative samples were examined petrographically. For engineering purposes, Wellington rocks may be divided into two categories, greywacke and argillite, each having separate and distinct mineralogies and chemistries which do not alter significantly between lithofacies. Greywacke is coarser and may be distinguished from argillite texturally at a mean grain size of 5 phi (0.031 mm).

Rock properties, in particular strength, modulus, density, hardness and degradation tendencies, are linked directly or indirectly with mean grain size. Argillites, though more dense, are generally weaker, softer, less elastic and degrade more readily than greywackes, the latter property being readily assessed from a newly devised test based on the destruction of chlorite by hydrochloric acid.

As aggregates, greywackes produce similar particle shapes irrespective of grading. Argillites, which are generally more angular, produce concretes which are more difficult to work. Physical properties of aggregate, inherently those of its parent rock, are reflected in concrete made from it. The possibility of laumontite promoting cement alkali-silicate reaction is obviated by the mode of occurrence of minerals within the rock.

Although argillite aggregates are unsuitable in certain environments and return lower strength in concrete than do greywacke aggregates, they still have a place in low strength concrete applications.

FOREWORD

For too long a lack of detailed knowledge of the properties of rocks for concrete aggregates has precluded the use of anything but the 'best'. Recent consciousness of the need to conserve all natural resources has encouraged a re-think of past attitudes toward what is acceptable. Such re-appraisals are not wholly useful without the sort of information contained in this thesis.

Mr Rowe's long association with the concrete industry and his proposed topic made him the ideal first recipient of the New Zealand Concrete Research Association's Research Fellowship. The industry has followed Mr Rowe's progress with interest and have been kept fully informed of his progress by regular reports, some of his findings are already in use.

Now that the thesis is completed it is to be hoped that it will encourage similar studies elsewhere.

J.E.F. Field,
Director,
New Zealand Concrete Research Assn,

October, 1980.

ACKNOWLEDGEMENTS

Most chapter quotations are from Bloch, A. (1977) "Murphy's law and other reasons why things go 6uoɹʍ", Magnum books, London: 96 pp.

CONTENTS

LIST OF TABLES

LIST OF FIGURES

Page

LIST OF PLATES

CHAPTER ONE

INTRODUCTION

For some 25 years, the aggregate industry of New Zealand has been aware of many problems associated with rock products derived from Lower Mesozoic rocks, which form the country's main mountain ranges.   With increasing use of quarried rock and as alluvial deposits are depleted or become less accessible, the problems assume greater significance.

Greater Wellington is increasingly dependent on quarried Lower Mesozoic rocks for use as aggregates of all types.   The amount of material quarried for use as concrete aggregate is substantial (280,000 tonnes annually on average) even when compared with national production (Figure 1.1).   Increase in population has been paralleled by increase in aggregate consumption and although low (4.5 tonnes/person a year) by national standards (6.3 tonnes/person in 1976) growth is expected to continue (Ward and Grant, 1978).

It seemed appropriate therefore, that an applied geological study be undertaken to provide fundamental data for some of the physico-mechanical properties of Lower Mesozoic rocks in the Wellington area, particularly as engineering difficulties associated with them are rarely found outside New Zealand. Impetus is added from a growing awareness world-wide that all natural resourses are finite to be husbanded if only, initially, for economic reasons.

1.1   The meaning of "greywacke"

The Lower Mesozoic rocks forming the axial ranges of New Zealand are often loosely described as "greywacke".   The nomenclature and classification of greywacke-type rocks has been extensively discussed but no satisfactory agreement on a precise definition has been reached.

The term "greywacke" was first proposed by Lasius (1789), but by 1854 the term had fallen into disrepute and its abandonment was recommended.   In New Zealand the term is in common usage but with indefinite meaning, such that it is likely to be applied to any hard, dark grey, metasedimentary rock.   Indeed in the Wellington region all rocks of this type are often grouped together and referred to as "Wellington greywacke" - the term including the sandstones mostly referred to as "greywacke" and the mudstones referred to as "argillite",

**SAND, ROCK (BUILDING AGGREGATE)
QUARRIED IN WELLINGTON**

$NZ

x 10^6
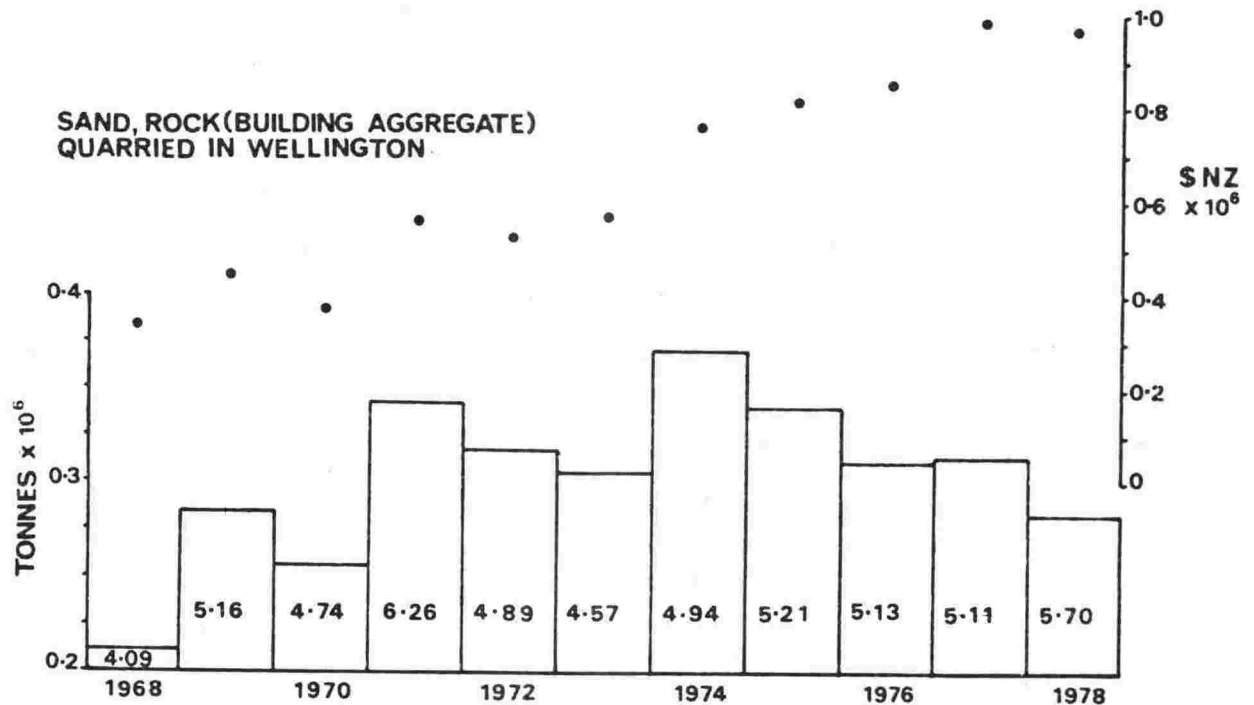
Figure 1.1 : Statistics of building aggregate quarried in the
Wellington region 1968-1978.

Quantity and value of quarried rock for building (concrete) aggre-
gate produced in Wellington by the following quarries: River
Shingle and Sand (1935) Ltd., Wellington City Council (Kiwi Point),
Carsons Quarry - formerly K.T. Wilkinson Ltd., (only since 1969),
Horokiwi Quarry Ltd., (only since 1971), and Owhiro Bay quarries.
Figures within histogram columns represent Wellington production
(percent) in terms of national production of building aggregates,
the average for the period being 5.07 percent.

Source: Annual returns of production from quarries and mineral
production statistics, Mines Division, Ministry of Energy 1968-
1978.

as defined by Flawn (1953) and Gamble (1971). To avoid the confusion associated with the grouping connotation implied by the term "greywackes", the rocks of the Wellington region could more appropriately be referred to as Wellington "greywacke-suite" rocks.

The basis of subdivision of Wellington greywacke-suite rocks into greywacke and argillite components will be discussed later but the terms are retained even though, in the case of greywackes, subtly different rock types may be identified within the limits of its definition. Such differences are even more subtle in the argillites, where there is not as broad a range in rock type.

Retention of the terms "greywacke" and "argillite" is felt justified because no one geological term has superseded greywacke as a term that has found acceptance to engineers, quarrymen, etc., in addition to geologists. If more precise classification or description is needed, then Folk *et al.* (1970) have provided a basis of classification which allows some resolution, of a geological nature, to be made within the greywackes.

For this study it is proposed that rocks of the greywacke-suite include greywacke and argillite.

1.2   Known industry-related problems

Greywacke-suite rocks provide many problems for the concrete and aggregate industries. Those discussed at the 1969 New Zealand Conference on Concrete Aggregates and the 1970 and 1979 New Zealand Roading Symposiums are detailed below.

1.2.1   The greywacke-argillite problem

Although greywacke and argillite occur together in Wellington and elsewhere (Reed, 1957, 1967) differentiating between them in the field and in the laboratory is not always easy. The recognition of these two rock types under varied conditions of weathering and/or tectonic shattering is important to the engineer. For this reason clear definitions and simply applied identifying test procedures need to be developed.

The common consumer misconception (and in some cases an academic preconception) that "argillite is bad, greywacke is good" for engineering purposes, stems from practical experience and the literature on soft rocks. Arbitrary limits have been imposed by some authors on maximum argillite percentage allowed in concrete aggregates (e.g. Grant-Taylor, 1976). No research seems to have been undertaken to justify these limits, however.

1.2.2   The zeolite problem

Investigation of zeolite bearing rocks overseas has led to claims that local aggregates made from zeolite bearing greywacke, could be responsible for destructive alkali-reaction if used with high alkali cement, and cause excessive shrinkage of concrete. Also they could cause unacceptable particle size reduction of graded aggregate whilst stored in stockpiles (Watters, 1969).

1.2.3   The aggregate degradation problem

This is related to the greywacke-argillite problem (section 1.2.1), confusion arising from apparent differences in the interpretation of the word degradation as well as from the recognition of the two rock types. Degradation may have different meanings to the quarryman, roading engineer, concrete technologist and geologist.

Degradation is a term used for different processes, not all being deleterious. Usually the roading engineer uses the term as Minor (1959) describes, and Buckland (1967) has clarified the term as used by New Zealand roading engineers. To the concrete industry, aggregate degradation is the non-mechanically induced breakdown of aggregate particles into smaller pieces by natural chemical and physical processes. Such a process is regarded as deleterious, with significant alteration imparted to grading. The release of deleterious minerals from vesicles, veins and/or joints is not regarded as degradation in itself although the presence of these features may contribute to degradation. The process seems to be a physical alteration of the aggregate and is a forerunner to more advanced states of degradation (weathering) but these are not found in concrete aggregate conforming to existing New Zealand Standards. Degradation by attrition produces fine mineral dusts, generally of more concern in roading than in concrete.

Two additional problems (Craven, pers. comm.; Ward and Grant, 1978) now confront the aggregate industry:

(i)   The production of ultra-fine materials in quarry washing operations - quarry sludges and their disposal.

(ii)   The depletion of good quality and easily won aggregates in areas of high demand.

CHAPTER TWO

FOURTH LAW OF REVISION

*After painstaking and careful analysis
of a sample, you are always told that
it is the wrong sample and doesn't apply
to the problem.*

Geological properties of Wellington greywacke-suite rocks

A quarryman needs two pieces of information from a geological investigation:

(i)   Whether the rock investigated meets the specifications for the job.

(ii)   Where it is located and how much is available.

Obviously the Wellington greywacke-suite rocks are useful; Mines Department returns (Figure 1.1) and discussions by other authors (Reed and Grant-Taylor, 1966; Grant-Taylor, 1976; Ward and Grant, 1978) indicate that they are extremely important.   Quantitative data on resources have been provided by Ward and Grant (1978) but a compilation of localities for what may be deemed the "most useful" greywacke-suite materials for Wellington is lacking.

The geology of the region has been presented by Stevens (1974) in an excellent book and specific aspects by Grant-Taylor (1976) and Ward and Grant (1978). Geological dating has been undertaken by Park (1975), McKean (1976) and Bird (in prep.).   Smaller studies of relevance include those by Barnes (1979) and Cranney (1979).   For a bibliography of Wellington geology, Williams (1975) should be consulted.

2.1   The *in situ* nature of Wellington greywacke-suite rock

Rock masses are never homogenous, isotropic bodies.   Their physico-mechanical properties alter according to interactions of mineral composition and fabric (including texture) and physical/chemical conditions throughout their geologic history, manifest on all scales from the individual grains, though the rock sample, to the rock mass or even the geologic region.   In this section the properties of outcrops are considered.

The greywacke-suite rocks are steeply dipping (generally more than 60°) and isoclinally folded about north-south trending axes (map in flap pocket). The sequence is dominated by alternations of "couplets" of sandstone (greywacke) and mudstone (argillite) that are evident even in the more metamorphosed areas. The alternations are, in some places, the result of deposition from a turbidity current and the essential features of the sequence of Bouma (1962) can be seen in many beds (Figure 2.1). However, some sand beds have different features (Table 2.1) and may have resulted from deposition by traction or contour currents.

The greywacke and corresponding argillite is referred to as a couplet as generally, despite diagenesis and metamorphism, a clear distinction can be made between the sandy lower portion (greywacke) and the upper portion (argillite) of each couplet regardless of the completeness of the Bouma sequence.

Conglomeritic deposits (Grant-Taylor, 1976) and volcanic rocks (Stevens, 1974) are small in volume, widely separated and not of importance to the aggregate industry and are therefore not part of this study.

The rocks of the region can be divided into three mappable lithofacies, sandstone, thick-bedded and thin-bedded, using as parameters average couplet thickness, average greywacke thickness, average argillite thickness and range of couplet thickness (Table 2.2).

Consistent with the nature of turbidite beds, the greywackes exhibit graded bedding, sometimes more than one sequence within a single greywacke bed. The grain orientation within greywacke and argillite is parallel to bedding (Onions and Middleton, 1968), and has been enhanced by metamorphism hence the rocks are anisotropic. Because of size grading, anomolies may arise from taking random samples from turbidite beds therefore a representative sample was taken from the mid-point of each bed to make petrographic comparisons.

As will be discussed, the many discontinuities within greywackes and argillites frustrate efforts to break handspecimens along planes which have not already experienced fracturing or veining. To examine sedimentary structures, fabrics and grain size, all rocks not sampled from stream beds or the coast require cutting in the laboratory.

	Grain Size		Bouma (1962) Divisions	Interpretation
	Mud	E	Interturbidite (generally shale)	Pelagic sedimentation or fine grained, low density turbidity current deposition
		D	Upper parallel laminae	? ? ?
	Sand-Silt	C	Ripples, wavy or convoluted laminae	Lower part of Lower Flow Regime
		B	Plane parallel laminae	Upper Flow Regime Plane Bed
	Sand (to granule at base)	A	Massive, graded	? Upper Flow Regime Rapid deposition and Quick bed (?)

Figure 2.1 :   Ideal sequence of structures in a turbidite bed.

After Bouma (1962) with interpretation after Walker (1965), Walton (1967) and Middleton (1967).   From Blatt *et al.* (1972).

Table 2.1 : The Heezen-Hollister-Bouma criteria for the recognition of turbidites and contourites (from Stow and Lovell, 1979).

	Turbidite	Contourite	Conclusions
Size sorting	moderate to poorly sorted >1.50 (Folk)	well to very well sorted <0.75 (Folk)	contourite is better sorted
Bed thickness and frequency	usually 10 - 100 cm infrequent	usually <5 cm abundant	contourite has thinner bedding, and many more beds per core length
Primary sedimentary structure			
grading and bedding contacts	normal grading ubiquitous, bottom contacts sharp, upper contacts poorly defined	normal and reverse grading, bottom and top contacts sharp	contourite tends to be less regularly graded and has sharp upper contacts
cross laminations	common, accentuated by concentrations of lutite	common, accentuated by concentration of heavy minerals	contourite contrasts sharply with turbidite in that heavy mineral placers are in the form of small-scale stratification
horizontal laminations	common in upper portion only, accentuated by concentration of lutite	common throughout, accentuated by concentrations of heavy minerals or foraminifera shells	
massive bedding	common, particularly in lower portion	absent	contourite is ubiquitously laminated
grain fabric	little or no preferred grain orientation in massive graded portions	preferred grain orientation paralell to the bedding plane is ubiquitous throughout bed	contourite has better grain orientation
Principal constituents of sand and silt beds			
matrix (<2 μm)	10 - 20 percent	0 - 5 percent	contourite has less
microfossils	common and well preserved, sorted by size throughout bed	rare and usually worn or broken, often size sorted in placers	contourite shows more evidence of reworking
plant and skeletal remains	common and well preserved, sorted by size throughout bed	rare and usually worn or broken	contourite shows more evidence of reworking
Classification (Pettijohn)	greywacke and sub-greywacke	sub-greywacke, arkose and ortho-quartz	contourite is more "mature"

2.1.1   The sandstone lithofacies

This is composed of couplets having excess thickness of greywacke with respect
to argillite thickness (Table 2.2).   They are often poorly graded or
ungraded, with no clear grain orientation.   The beds have distinctly regular
joint sets which are oriented obliquely to bedding.   The lithofacies may be
made up of successive greywacke beds about 2 m thick, separated by thin layers
of highly comminuted and polished slabby argillaceous material which has
accommodated relatively large amounts of slip.   This may be the result of
bedding plane slippage rather than argillite sedimentation.   Many greywacke
beds may accumulate (Walker, 1967) up to 30 m thick (Plate 2.1).

Possibly the most frequent assemblages of Bouma divisions are AE or AC (Figure
2.1), but in quarry outcrops the detection of Bouma divisions is difficult.
Veining is common, both as linear infillings to tens of millimetres width
vugs forming in larger examples or as infilled tension gashes.   Principal
vein minerals are prehnite, quartz and calcite.

2.1.2   The thick-bedded lithofacies

In the thick-bedded lithofacies, couplet thickness is generally about the same
as in the sandstone lithofacies but the couplets contain a higher proportion
of argillite.

Thicker greywackes are not as well graded as thinner greywackes.   Bouma
divisions include ABCE, AE, ACE.

The mean grain size variation is greatest in greywacke beds within the thick-
bedded lithofacies.   Clasts from argillaceous beds which have been ripped up
by a turbidity current may have become included, to appear in flaky or slab-
like form (colloquially known as "chipwackes").   Individual clasts may mea-
sure 0.4 m (Plate 2.2).   Little if any grain orientation was noted in grey-
wacke beds although in the coarser beds larger grains and argillite clasts
did show some orientation.

Jointing is commonly at right angles to bedding in well developed sets in the
greywackes and in thicker argillites.

Table 2.2 : Parameters used to differentiate lithofacies within the
Wellington greywacke-suite rocks.

Parameter	Thin-bedded			Thick-bedded	Sandstone
	RSS	BQ	DC	HQ	KTW
Avge. argillite bed thickness	5 cm	12.5 cm	8.9 cm	68 cm	16 cm
Avge. greywacke bed thickness	13.9 cm	14.4 cm	18.8 cm	164 cm	100 cm
Avge. argillite:greywacke ratio	1:2.8	1:2.1	1:2.1	1:2.4	1:6.3
Thickest couplet	30 cm	46 cm	107 cm	2.5 m	4.6 m
Thinnest couplet	8 cm	9 cm	45 cm	2.2 m	0.15 m
Avge. thickness of couplets	19 cm	36 cm	28 cm	2.35 m	1.16 m
Length of section	2.48 m	3.63 m	5.26 m	11.6 m	30 m
Normal range of couplet thickness	10 to 30 cm			50 to 300 cm	
Percentage of argillite	25 to 40				<20

A

B

Plate 2.1 : Two views of the sandstone lithofacies at Owhiro Bay
quarry; (A) shows a more extensively shattered out-
crop than (B), which shows some obvious argillite bedding.
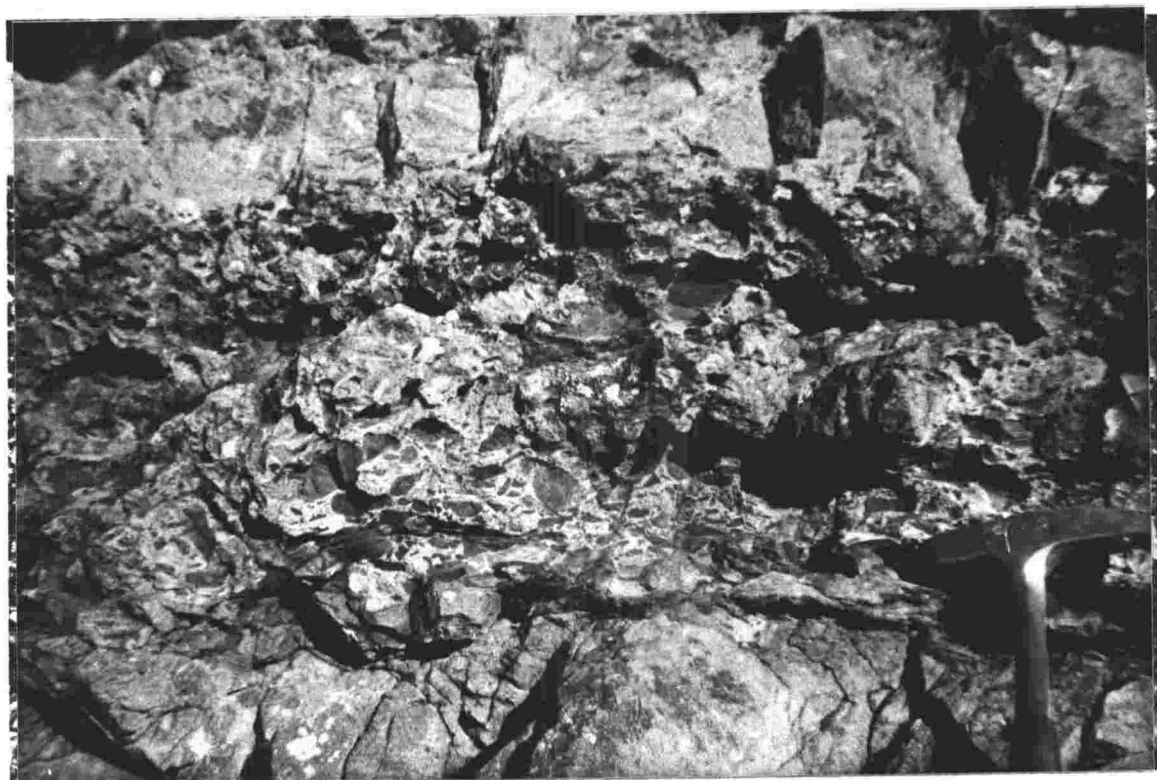
Plate 2.2 : Sedimentary rock fragment clasts (argillite) in
              "chipwacke" from Eve Bay (NZMS 1, N164/384163).
At this locality clasts may reach 0.4 m in length displaying
their original sedimentary structures.   They were incorporated
as turbidity currents dislodged large flakes and slabs of pre-
sedimented argillaceous material which achieved an initial
coherence as a soft plastic sediment.

Veining is frequent in the greywackes but rather less so in the argillites. Principal vein minerals include prehnite, quartz, calcite and laumontite.

The thick-bedded lithofacies (Plate 2.3A) are commonly transitional between the sandstone and the thin-bedded lithofacies.

2.1.3   The thin-bedded lithofacies

These include turbidities, contourites and inter-turbidite materials.   Inter-turbidite materials include the D and E divisions of Bouma sequence;   turbidites are represented by ABCE, ACDE, ACE and AC divisions.   Evidence of contourites comes from large sequences of unknown total thickness, some with at least 10 m of thin, regular couplets,apparently devoid of an A division. Greywacke beds are more even grained than those of the other lithofacies, while laminations and rarer cross laminations are made more obvious by heavy mineral concentrations.   Contacts between beds are sharp and grain orientation in the greywacke is well developed.

The lithofacies include contorted strata due to slumping (Plate 2.3B). Occasionally the lithofacies pinch out laterally to become massive argillite of reduced thickness.

Jointing is generally intense,with greywacke beds broken by large numbers of sets perpendicular to bedding.   Argillites are often intensely shattered. Veining is again better developed in the greywacke beds though it does occur, often in ptygmatic style, in the argillites.   Vein minerals are mainly prehnite, quartz, calcite or laumontite.

2.2   Mapping of lithofacies

Difficulty in mapping the region stems from a lack of outcrops suited to establishing lithofacies and structural relationships,in areas away from the coastline, new road cuts, quarries and the like.   Even stream beds proved disappointing.

A map compiled from lithofacies is presented for part of the Wellington region east of Wellington Fault (map in flap pocket) and shows regional trends.

Strike of beds trends north-south; they are steeply dipping and young west.

A

B
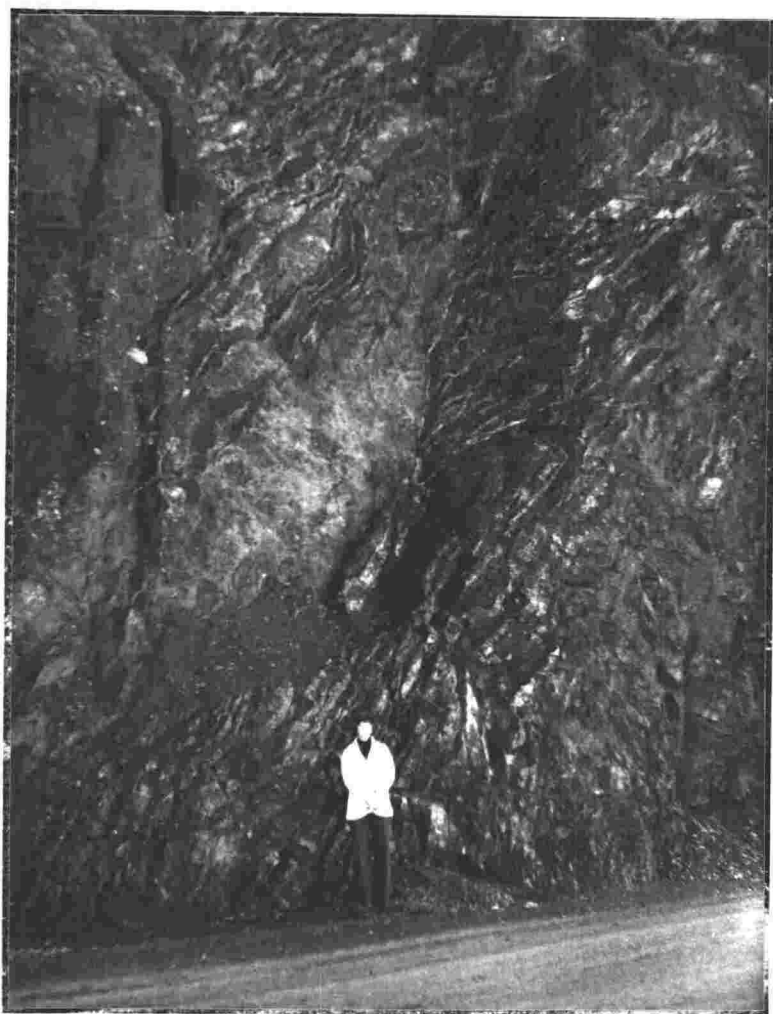
Plate 2.3 :

(A) The thick-bedded
lithofacies and
(B) the thin-bedded
lithofacies at Owhiro
Bay quarry.   Note the
extensive distortion
and disruption of the
thin-bedded material.

The magnitude of folding is difficult to establish accurately but appears to fall into two ranges - less than 5 m and in excess of 60 m - see also mapping by Brodie (1953) and Grant-Taylor *et al.* (1974).

2.3 Causal geology

Lithofacies control much of the topography and structural trends.

Examination of field relationships and structure revealed several interesting observations (map in flap pocket):

(i)   Bays or inlets are associated with the thin-bedded lithofacies.

(ii)   Major and minor headlands are coincident with the sandstone and thick-bedded lithofacies respectively.

(iii)   Most fault movement seems to have been accommodated in the thin-bedded lithofacies.

(iv)   Slumping and contorted bedding (usually on a scale of 1 m to 30 m) was observed only in the thin-bedded lithofacies.

More obscure information comes from observations by Stevens (1976), who plotted greywacke to argillite ratios enabling him to isolate what he termed the Waitangirua sandstone, which contains little argillite and corresponds well with the most resistant topographical features of the area.

Slumping, ptygmatic veining, drag folding, discontinuity spacing and boudinage structures all indicate that the thin-bedded lithofacies is incompetent just as argillite between greywacke beds is incompetent.

For engineering work these observations are significant.   Slippage of fresh rock tunnel portals at Karori and at Northland (NZMS 1 grid refs. N164/317217 and N164/317220 respectively, both situated in crush zones of the Wellington fault), is aggravated by their situation in thin-bedded lithofacies material.

Continuing road pavement damage in Lennel Road and Chaytor Street (N164/338247 and N164/317217 respectively) are pertinent examples of problems which can arise from subterranean drainage associated with the thin-bedded lithofacies.

2.4 Paleontology

Webby (1967) provided an historical summary of paleontology from the Wellington region and recently Speden (1976) published fossil localities of Lower Mesozoic rocks of the North Island.

During this study two new fauna (Rowe, in prep.) and numerous unidentifiable floral debris were found (Plates 2.4, 2.5) in greywacke (KS-2) and argillites (IB-13A)

2.5 Petrographic methods

Samples of both greywacke and argillite beds were obtained from quarries and outcrops for microscopic study to see how features seen in this section might relate to the physical properties of the rocks. Fieldwork was concentrated on existing main quarries (Figure 2.2) and about the southern coast of Wellington.

Appendix 1 lists the sample numbers for each sample location site and Appendix 33 correlates sample numbers with the Petrology collection, Geology Department, Victoria University of Wellington.

For the reasons outlined in section 2.1 samples were taken from the mid-point of each bed.

Thin sections were cut, usually perpendicular to bedding, to avoid biasing textural, modal and fabric determinations due to microlaminations and the natural sorting and anisotropic characteristics of preferred grain orientation. Portions of some greywacke thin sections were stained for K-feldspar or plagioclase feldspar, or both, using modified techniques (Appendix 2). It was found necessary to expose the thin sections to hydrofluoric acid fumes for relatively long periods to adequately etch the felsic grains but this destroyed other important minerals, notably zeolite and calcite, therefore only about 10 percent of any thin section area was stained (Appendix 2).

The preparation of thin sections for detailed petrographic work was of particular importance. For some samples, sections slightly thicker than the usual 0.03 mm were cut, especially in strongly oriented or coarser grained rocks to

5mm

7mm
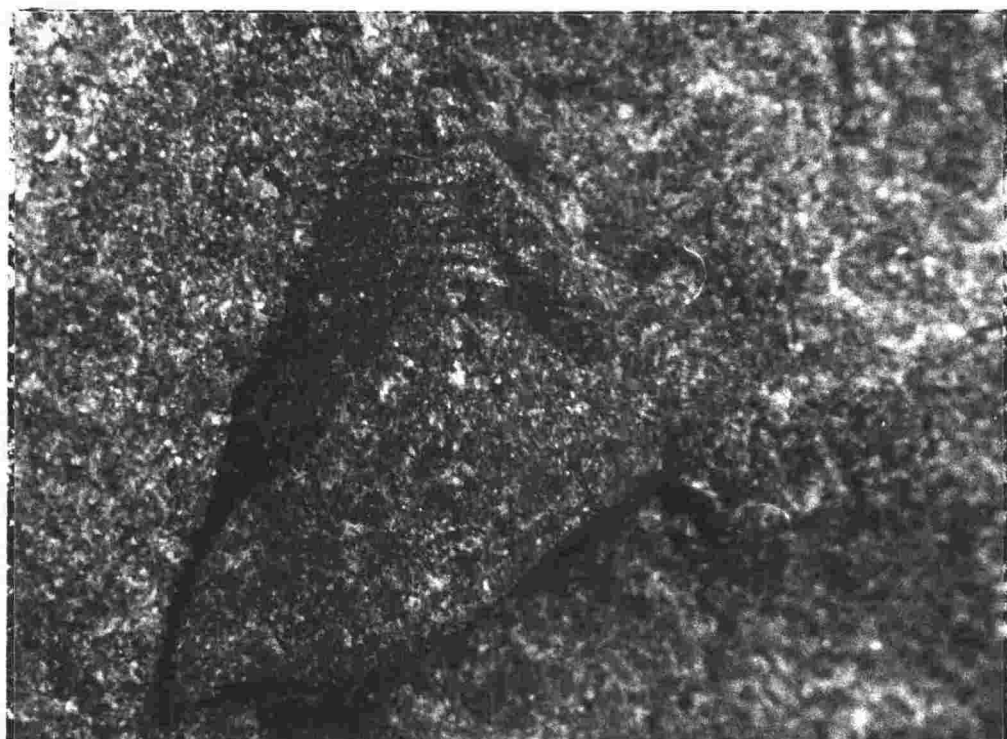
Plate 2.4 : Floral debris in greywacke is rare:

(A) and (B) are corresponding portions of KS-2,
clearly showing botanical detail in a carbonaceous film.

20mm

A
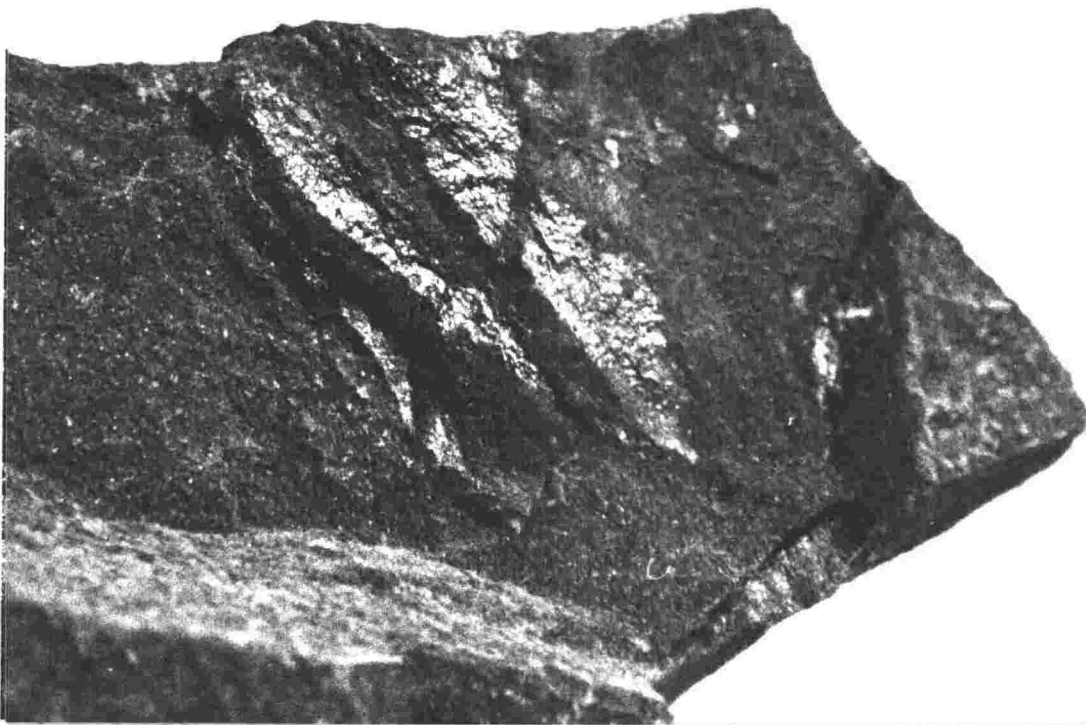
12 mm

B

Plate 2.5 : Floral debris in argillites (sample 1B-13A) show good
continuity of some carbonaceous films.
(A) and (B) are corresponding pieces at different scales.
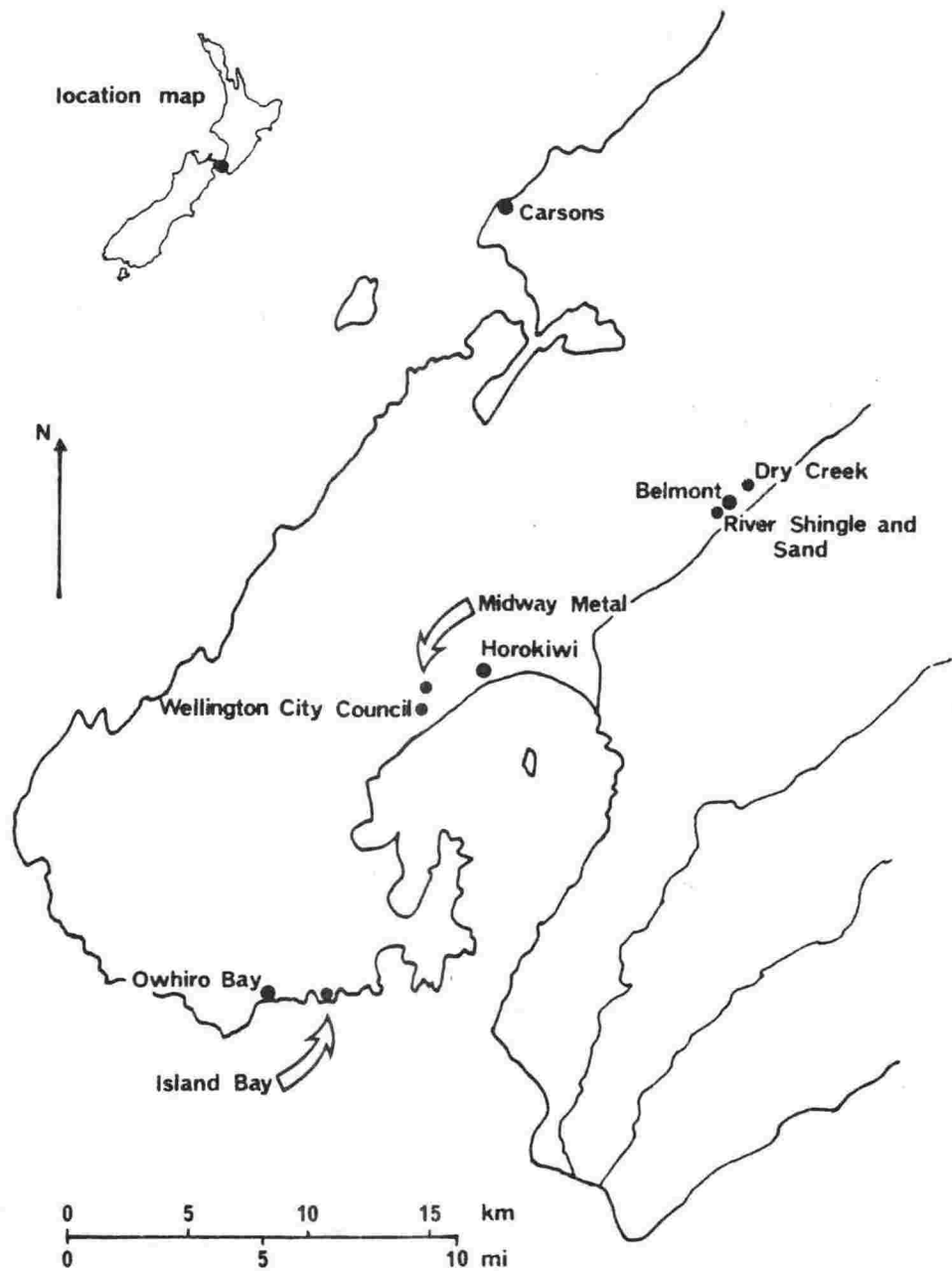
Figure 2.2 : Quarry sites sampled for this study. Quarries from which samples were taken but which are no longer operating are indicated by arrows. Shown by larger symbols are those quarries which will be most important in satisfying Wellington's future demands for aggregate (Ward and Grant, 1978).

enable the habit of larger phyllosilicates to be better determined. Being cut
perpendicular to bedding, thin sections adequately displayed preferred orienta-
tions of minerals, but true lengths of some mineral grains were indeterminate
due to deviations of the mineral in and out of the plane of the thin section.
Thicker sections were useful also in differentiating acid from basic volcanic
rock fragments.

Ultra-thin rock sections were preferred in studying finer and more opaque
rocks. Some were carefully polished to zero thickness at an edge to enable
reliable grain size measurements in rocks with mean sizes finer than 5 phi
(0.03 mm).

In argillite thin sections, overlapping grains were common so for optic modal
analysis and size analysis, the thicker (= deeper) grain under the cross-hairs
took precedence.

Modal and size analyses of rocks were made from thin sections by following
the recommendations of Chayes (1956). As noted previously, thin sections
were cut perpendicular to preferred orientation (= bedding) and thin sections
having strong preferred orientations or laminations were positioned, where
practicable, so that preferred orientation was at an angle to the long axis
of the glass slide.

For point counting, the vertical interval between counted rows was chosen so
that all the slide was covered in the examination. Horizontal intervals were
ideally suited to most greywackes, being approximately the same as the mean
maximum grain size, i.e. approximately 0.4 mm. For finer rocks it was not
practicable to change the gearing of the click stage and trials were carried
out to determine whether more points should be counted by increasing the
number of horizontal traverses or whether the slide should be reversed in its
holder and re-examined in the usual way. It was found that both these alter-
natives were effective in duplicating analyses but results varied little from
a single analysis. Reasons for this are:

(i)   The fine grained rocks are relatively homogenous so that examination
of a proportionally smaller area gives acceptable results, particularly for
modes.

(ii)   Size analysis histograms of fine rocks showing the effects of
mineral recrystallisation are leptokuritic.   Therefore variations due to
horizontal click interval are within an acceptable maximum.

Welsh (1967) has shown that acceptable reliability may be achieved between
different operators examining optical mineral modes of greywackes even though
the major source of error is operator error.   There is a need for strict con-
sistency.   For this study much time and trouble was taken to become familiar
with thin sections before modal or size analyses were attempted.   Mineral
staining helped in this regard and several modal analyses were duplicated
months apart to maintain a record of consistency.   Similar tests were done
for grain size analysis (Appendix 5).   With practice a very close approxima-
tion of mean grain size was achieved by observation alone (within 0.03 phi for
rocks with a mean grain size between 5 and 6 phi, 0.031 and 0.0156 mm).   Point
counting of thin sections is the only practical means of acquiring grain size
data from greywacke-suite rocks, though it is recognised that the present
size distribution is now rather different from the original size distribution.
However, because we are now concerned mainly with a comparison of rocks in
this size no attempt was made to convert the thin section size data to sieve
equivalents (Adams, 1974).   Results from this study are, however, directly
comparable, as they are with other data similarly obtained.

An attempt was made to use rock slabs to determine mean grain size as des-
cribed by Marshall (1974) but, compared with thin section analysis, mean grain
size was over estimated due to the "blanketing" effect of matrix and smaller
mineral grains.   Induced shattering of grains by cutting and grinding pre-
paration is never eliminated and confusion arises even after coating the
surface with a clear lacquer or varnish.   For rocks with mean grain sizes
finer than about 3 to 3.5 phi (0.125 to 0.088 mm) the technique is of no prac-
tical use.

2.6   Petrography

The purpose of this section is to outline the features and distribution of
common minerals in Wellington greywacke-suite rocks, because mineral composi-
tion is likely to be an important factor in determining engineering properties
of aggregate.   Detailed petrographic descriptions are given in Appendix 3.

The composition of sand sized material was determined as if there had been
no alteration after deposition.   For example grains of volcanic rocks now
containing much chlorite were counted as rock fragments and feldspar grains
altered to white mica were counted as feldspar.   Vein minerals were not inclu-
ded in the modal analysis but cements and authigenic minerals were.   The grey-
wackes were examined in terms of the following modal classes:

quartz	biotite
feldspar	chlorite
rock fragments	metamorphic accessories and cements
muscovite	detrital accessories

                    matrix

Argillite mineral components were classified twice:

(i)   Using the following modal classes

quartz	chlorite
feldspar (all varieties)	non-opaque detrital heavy minerals
rock fragments (all varieties)	opaque minerals
white mica	metamorphic accessories and cements

                    matrix

(ii)   Without a matrix class so that every grain was counted in a mineral
mode.   Grains which were so fine as to be unidentifiable were placed in a
class replacing matrix, called "unidentifiably fine material".

In this way operator consistency was checked and an estimate made on mineral
composition of the matrix;   such an estimate, taken for 10 argillites, may be
considered similar to the matrix composition of the greywackes.

Modal analyses of greywackes were based on at least 500 counts and argillites
on at least 300 counts.   Although many modal analyses were undertaken, only
42 greywacke slides were examined in great detail;   20, 10 and 12 from the
sandstone, thick-bedded and thin-bedded lithofacies respectively.

2.6.1.   Quartz

Varieties of quartz include monocrystalline, polycrystalline (excluding chert), wavy (quartz with undulose extinction) and non-wavy quartz (Figure 2.3).

Quartz plotted according to the method of Basu *et al.* (1975) gave inconclusive provenance although the scatter so determined indicated a low or middle rank metamorphic terrain for quartz origin (see section 2.10).

Significant differences between greywackes of different lithofacies were not detected by statistical analysis of quartz modes (P is greater than 0.1).

Recrystallised quartz associated with veining and shearing was not included in modal analyses.

2.6.2   Feldspar

Two classes of feldspar were recognised (Figure 2.4), though in the finer grained rocks they were difficult to differentiate.   The first, K-feldspar (potassium feldspar) occurs as monocrystalline grains of orthoclase, microcline, perthitic or granophyric grains.   In the case of orthoclase and microcline the grains have been altered mainly to white micas (sericitised).   This class was included in a general feldspar mode for greywackes of the thin-bedded lithofacies because of their relative paucity and finer grain size in those rocks.

The second class, plagioclase, occurs as monocrystalline grains both fresh and altered.   Grains of authigenic albite and albitised plagioclase were included where they were distinct grains - authigenic albite was often very difficult to differentiate from detrital plagioclase.   Authigenic plagioclase cements are rare and were included in the cement rather than the feldspar class.

The ratio of plagioclase to K-feldspar (Figure 2.4C) ranged from 3:1 to 23:1 for the sandstone lithofacies.   The mean for the sandstone lithofacies and thick-bedded lithofacies was similar, i.e. 8:1.   The ratio for the thin-bedded lithofacies averaged 10.5:1 and showed K-feldspar to be relatively scarce.
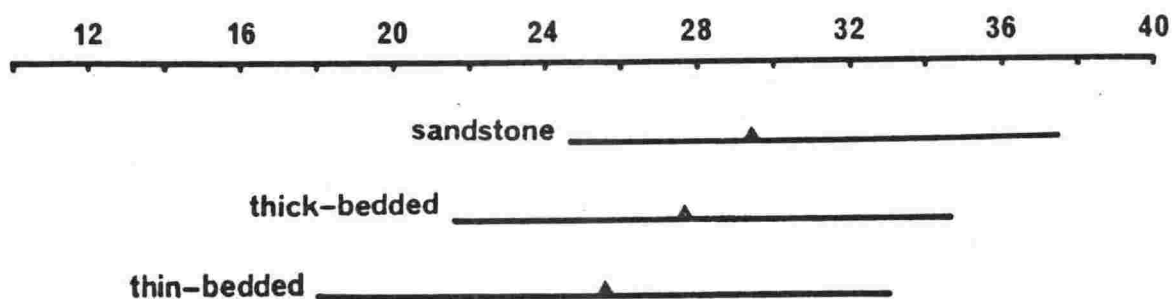
Figure 2.3 : Average and range in percentage of quartz estimated from thin sections (500 counts) for each lithofacies in the Wellington region.
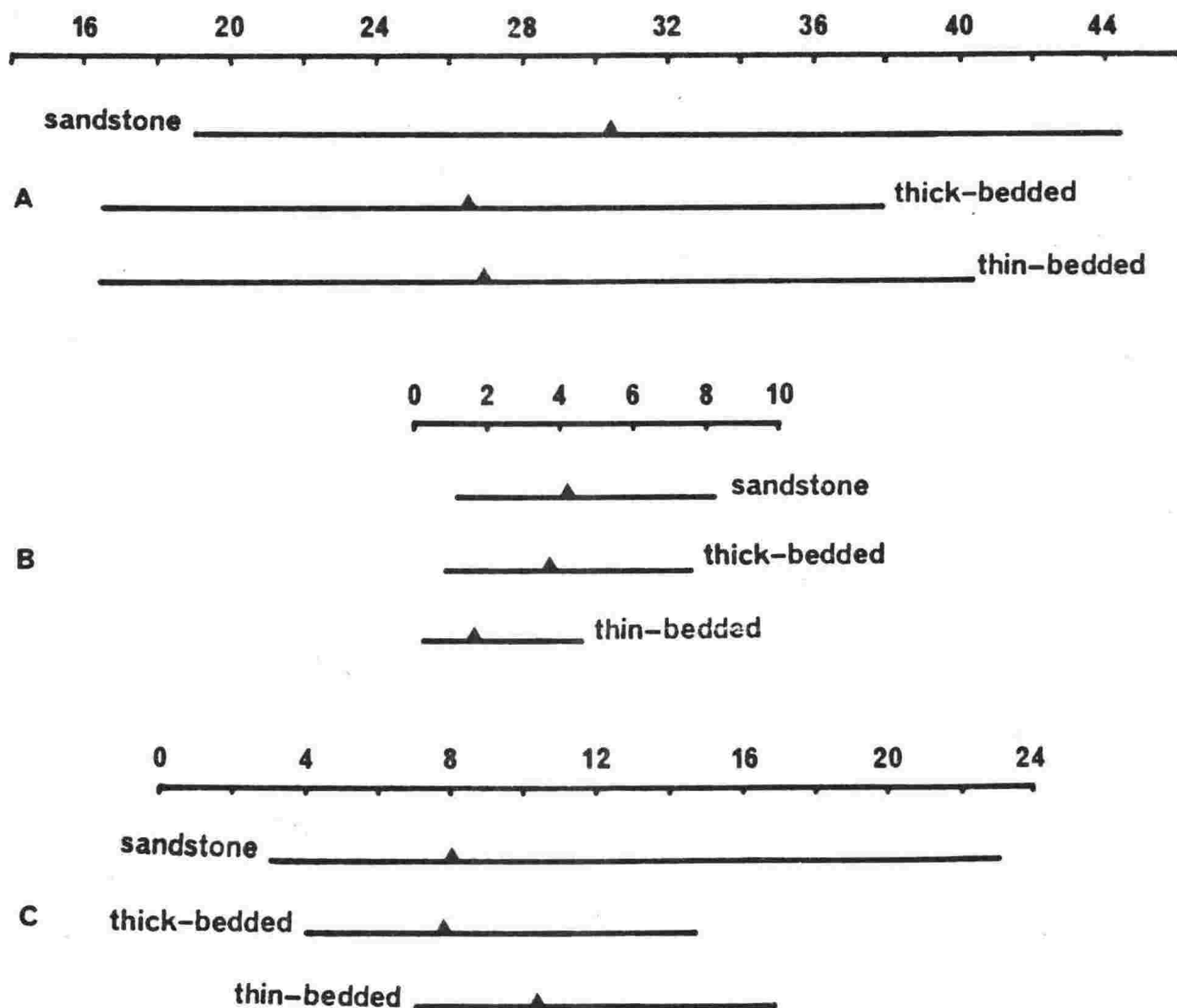
Figure 2.4 : Average and range in percentage of (A) plagioclase (B) potassium feldspar and (C) the ratio of plagioclase to potassium feldspar estimated from thin sections (500 counts) for each lithofacies in the Wellington region.

The mean ratio from all lithofacies was similar to that established by Reed (1957), 10:1.

2.6.3 Rock fragments

Rock fragments (Figure 2.5) were divided into four classes:

(i) Sedimentary rock fragments include both intrabasinal and extrabasinal grains. Most are intrabasinal (derived from within the basin of sediment deposition), detrital chert being the only obvious extrabasinal sedimentary rock. They are mainly siltstones or mudstones but some have grain sizes of the same magnitude as the host rock and these were recognised from subtle differences in grain orientation, packing, roundness, sphericity, matrix content and contrast, sorting, boundary continuity, opacity and constituent mineralogy. Fine grained sedimentary rock fragments, in places, form "pseudomatrix" (Dickinson, 1970), where they have deformed around adjacent rigid grains. Such material was classified as a sedimentary rock fragment as it was obviously deposited as a rock fragment.

(ii) Metamorphic and plutonic rock fragments are mainly irregularly shaped aggregates of quartz, albite, perthite, orthoclase, microcline, muscovite, biotite, chlorite or epidote. The metamorphic fragments are schistose and the plutonic fragments, medium to coarse grained and holocrystalline. Both types lack ground mass. Metamorphic fragments are rounded and elongate or flaky in contrast to plutonic fragments which are generally larger in size. A few large euhedral feldspar grains had small pieces of quartz or other feldspar adhering to ends or edges of the grain (DC - 1); these were included in this class.

(iii) Acid volcanic rock fragments include glassy materials with or without aggregated sodic feldspar laths (where recognisable) whether altered or not. They are best identified under plane light with the substage diaphram stopped down to impart refractive index contrast between component minerals. Altered grains are often very difficult to differentiate from basic volcanic rock fragments, however the former tend to be more distorted.

(iv) Basic volcanic rock fragments are mainly identified by the presence of amphibole and pyroxene grains, plagioclase composition and micro-porphyritic
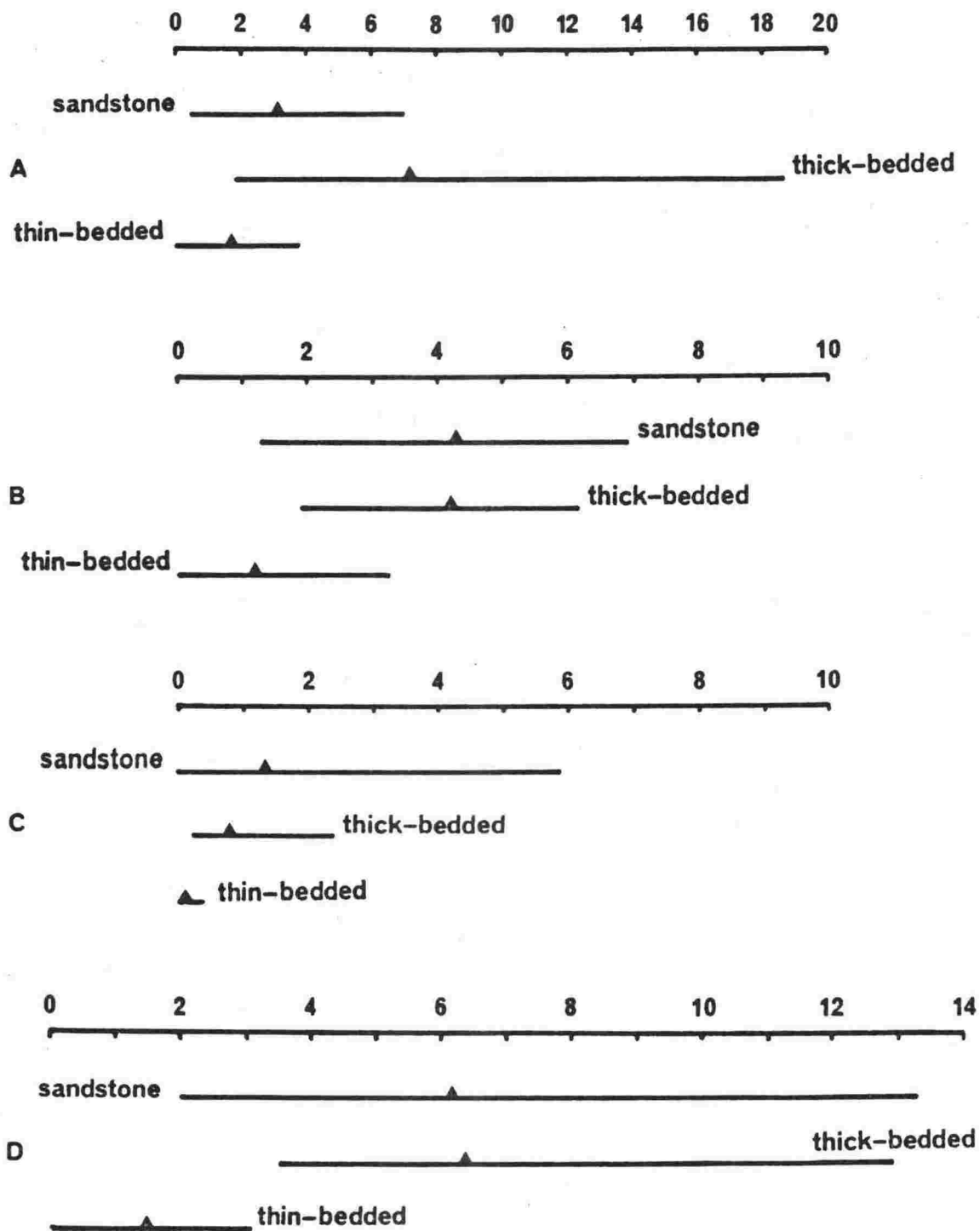
Figure 2.5 : Average and range in percentage of (A) sedimentary
(B) metamorphic and plutonic (C) acid volcanic and
(D) basic volcanic rock fragments estimated from thin sections
(500 counts) for each lithofacies in the Wellington region.

textures ranging from trachytic to pilotaxitic and hyalopilitic with increasing randomness of microlite orientation. Zeolitised, chloritised and basic volcanic rock fragment grains being replaced by iron oxides etc. were counted in this category. Fragments in greywackes of the thin-bedded lithofacies are so altered that grain size measurement is impossible, in which case the size of the largest included constituent grains were averaged to represent the size of the fragment.

2.6.4   Muscovite

This is not prolific in any but the coarsest greywackes (Figure 2.6). It is relatively easy to identify and, combined with other phyllosilicates, indicates preferred orientation and compaction. Fine grained material, less than 5.65 phi (0.02 mm), was arbitrarily termed sericite as were the products of feldspar decay unless grain size exceeded 5.65 phi (0.02 mm). Differences in structure between the two white micas is apparent, however, from X-ray diffractometry and infrared analyses.

Collectively termed "white mica" they are important constituents for considerations of rock end use.

2.6.5   Biotite

Most mineral matter termed biotite by Reed (1957) is in fact chlorite, a fact discovered independently by McKean (1976), Sameshima (1977), Bird (pers. comm.) and this study. The two minerals are difficult to differentiate, especially in greywackes with a mean grain size finer than 2 phi (0.25 mm). Most biotite is altering to chlorite or has zeolite extending along its cleavage planes. Only in a few cases has biotite been counted separately - otherwise it has been counted with chlorite. For engineering assessment of the rocks, the chlorite mode includes biotite where biotite was not counted separately.

2.6.6   Chlorite

This is the most important mineral occurring in the greywacke-suite rocks from the viewpoint of engineering use (Figure 2.7). Several categories were recognised but all were included in one class. Recrystallised chloritic material in areas of matrix was counted as chlorite only if grain size exceeded 5.65 phi (0.02 mm). Detection of chlorite was often hampered by anomolous or low order interference colours.
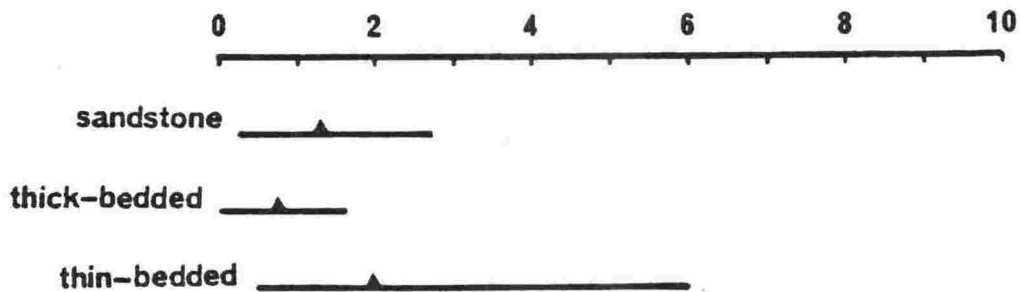
Figure 2.6 : Average and range in percentage of muscovite
estimated from thin sections (500 counts) for each
lithofacies in the Wellington region.
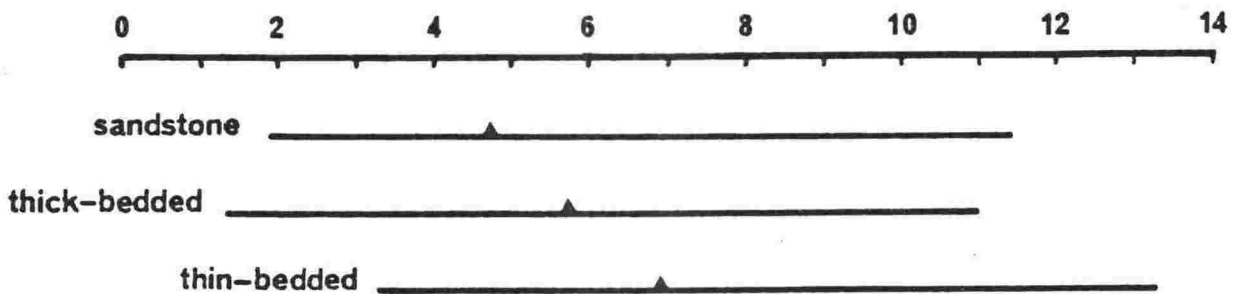
Figure 2.7 : Average and range in percentage of chlorite estimated
from thin sections (500 counts) for each lithofacies
in the Wellington region.

2.6.7   Metamorphic accessories and cements

This mode includes such minerals as calcite, laumontite, prehnite, pumpel-
lyite and axinite (Bird, in prep.) provided their greatest grain dimension
exceeded 5.65 phi (0.02 mm) (Figure 2.8). Veined materials were not included.

2.6.8   Detrital accessories

These include amphiboles, apatite, allanite, opaque iron oxides (mainly
pyrite), carbonaceous material, sphene, garnet, zircon, zoisite, epidote and
augite (Figure 2.9).   Most occur in very small quantities and are of little
importance to engineering properties with the exception of pyrite and carbon-
aceous material.   For this and identification reasons, authigenic pyrite was
also included in this portion of the mode.   Sometimes carbonaceous material
occurred in long ribbons parallel to bedding (DC-LAM) and was counted as a
detrital accessory. Where carbonaceous material was distinctly granular and
dispersed, grains were usually of matrix size or smaller and were counted as such.

2.6.9   Matrix

This included all material, authigenic or detrital, less than 5.65 phi
(0.02 mm) measured along the mean long axis of the mineral grain or aggregate
(Figure 2.10).

2.7   Petrographic comparison of lithofacies

The results of 42 modal analyses of greywackes are shown in Tables 2.3, 2.4
and 2.5.

Differences in petrography between greywackes of different lithofacies are small,
with a wide range in most mineral modes (Figure 2.3 to 2.10).

Most contrast is apparent when the thin-bedded lithofacies is compared with
either the sandstone or the thick-bedded lithofacies.   General increase in
felsics (56 to 61 percent) and rock fragments (5 to 16 percent), are accom-
panied by decrease in matrix (22 to 17 percent), phyllosilicates (9 to 6 per-
cent), detrital accessory minerals (3.5 to 1.5 percent) and in most samples,
metamorphic accessories and cements.
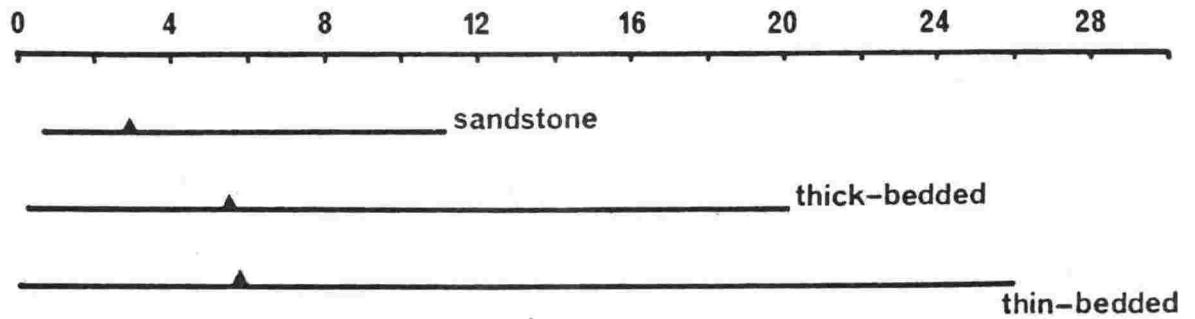
Figure 2.8 : Average and range in percentage of metamorphic accessories and cements estimated from thin sections (500 counts) for each lithofacies in the Wellington region.
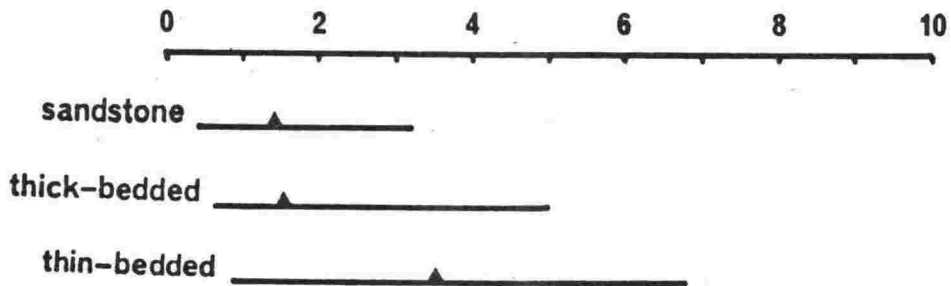
Figure 2.9 : Average and range in percentage of detrital accessory minerals estimated from thin sections (500 counts) for each lithofacies in the Wellington region.
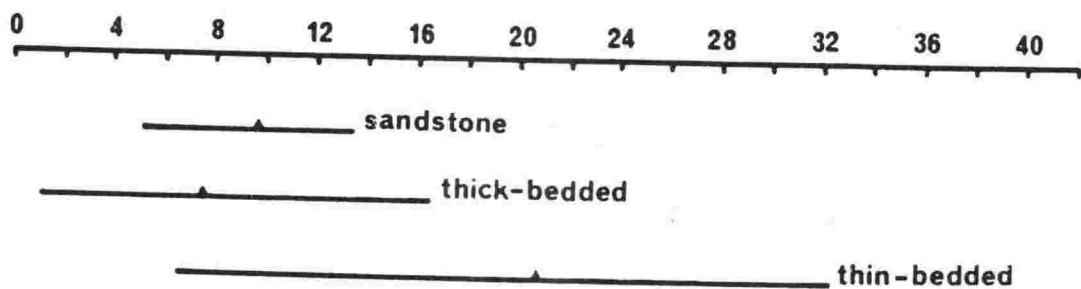
Figure 2.10 : Average and range in percentage of matrix estimated from thin sections (500 counts) for each lithofacies in the Wellington region.

Table 2.3 : Composition (in percent) for greywackes of the sandstone lithofacies (500 counts/thin section) arranged in order of decreasing mean grain size.

Sample	KTW-13	KTW-14	RSS-12	BQ-xviii	DC-1	DC-2	BQ-V
Mean grain size, phi (mm)	2.4(0.19)	2.6(0.17)	2.6(0.17)	2.63(0.16)	2.65(0.16)	2.72(0.15)	2.73(0.15)
Quartz	27.2	28.3	30.7	24.7	27.0	29.2	29.9
K-feldspar	5.5	3.8	3.8	7.9	5.5	3.6	5.2
Plagioclase	36.7	31.0	27.6	27.9	27.1	32.0	18.2
Sedimentary rock fragments	0.7	2.2	4.4	4.4	6.3	4.1	6.3
Metamorphic and plutonic rock fragments	4.3	6.3	4.2	6.2	6.5	5.3	6.9
Acid volcanic rock fragments		0.2	-	0.8	3.2	3.0	2.0
Basic volcanic rock fragments	8.1	3.2	6.3	6.0	9.7	6.7	13.3
Muscovite	0.9	1.8	0.8	0.2	0.2	0.8	0.6
Biotite*	-	-	-	-	2.2	3.2	3.2
Chlorite	6.6	7.9	11.4	4.4	2.6	2.6	3.2
Metamorphic accessories and cements	0.6	3.4	1.9	11.2	2.0	2.8	1.8
Detrital accessories		2.4	1.0	1.2	1.2	0.4	0.4
Matrix	9.6	9.7	8.0	5.2	6.7	6.5	9.1
Total:	100.2	100.2	100.1	100.1	100.2	100.2	100.1

Sample	WCC-13A	KTW-15	KTW-17	SJ-6	KTW-16	BQ-IXA	OB-21
Mean grain size, phi (mm)	2.78(0.15)	2.78(0.15)	2.79(0.15)	2.8(0.14)	2.83(0.14)	2.9(0.13)	2.93(0.13)
Quartz	32.1	27.6	37.5	29.3	31.7	27.9	31.5
K-feldspar	3.4	1.5	3.0	3.0	8.2	5.5	3.2
Plagioclase	35.0	34.4	30.2	37.7	25.1	25.1	30.0
Sedimentary rock fragments	3.4	1.7	0.8	2.4	0.4	2.6	1.3
Metamorphic and plutonic rock fragments	3.2	3.9	4.5	4.0	5.4	4.0	1.2
Acid volcanic rock fragments	-	-	-	0.6	2.2	5.9	2.6
Basic volcanic rock fragments	5.5	3.7	2.5	2.0	5.0	9.6	7.4
Muscovite	1.3	2.4	1.0	1.6	1.9	0.9	0.9
Biotite*	-	-	-	-	4.8	3.6	0.2
Chlorite	2.5	6.8	3.0	4.6	2.4	1.9	3.8
Metamorphic accessories and cements	1.7	4.4	6.6	0.8	1.9	2.8	5.6
Detrital accessories	2.1	3.2	0.5	1.4	0.6	0.8	1.3
Matrix	9.6	10.5	10.3	12.8	10.6	9.4	11.1
Total:	99.8	100.1	99.9	100.2	100.2	100.0	100.1

Sample	DC-3	HQ-27	SJ-2	KS-2	NC-8	KS-10
Mean grain size, phi (mm)	3.08(0.12)	3.13(0.11)	3.2(0.11)	3.27(0.1)	3.37(0.1)	3.38(0.1)
Quartz	27.3	24.9	36.6	29.9	29.6	30.2
K-feldspar	3.3	1.1	2.0	5.1	2.1	3.3
Plagioclase	26.9	44.2	31.7	26.6	27.7	29.8
Sedimentary rock fragments	1.7	3.4	2.4	5.1	7.0	1.4
Metamorphic and plutonic rock fragments	2.5	3.0	2.5	3.5	3.3	5.2
Acid volcanic rock fragments	4.8	-	0.2	-	-	-
Basic volcanic rock fragments	6.1	5.3	2.7	9.3	7.5	6.5
Muscovite	2.7	1.0	1.0	0.8	2.3	1.9
Biotite*	7.5	-	-	-	-	-
Chlorite	3.5	4.2	7.4	4.3	5.0	7.5
Metamorphic accessories and cements	3.8	0.8	2.0	0.6	1.6	0.8
Detrital accessories	1.5	1.5	2.0	1.8	0.8	2.1
Matrix	8.5	10.6	9.6	13.4	13.2	11.4
Total:	100.1	100.0	100.1	100.0	100.1	100.1

* Dashes indicate biotite included in chlorite mode.

Table 2.4 : Composition (in percent) for greywackes of the thick-bedded lithofacies (500 counts/thin section) arranged in order of decreasing mean grain size.

Sample	DC-6	HQ-17	$SJ-3_1$	HQ-21	HQ-23
Mean grain size, phi (mm)	1.25(0.42)	1.317(0.4)	1.32(0.4)	2.7(0.16)	2.7(0.16)
Quartz	21.5	24.2	22.8	34.2	29.6
K-feldspar	2.1	7.6	6.0	3.8	3.4
Plagioclase	30.8	38.2	26.3	24.9	17.2
Sedimentary rock fragments	18.7	4.5	15.3	2.3	3.8
Metamorphic and plutonic rock fragments	1.9	6.1	5.4	4.3	3.2
Acid volcanic rock fragments	0.6	0.6	0.4	0.9	0.2
Basic volcanic rock fragments	5.0	12.9	4.5	6.2	6.5
Muscovite	0.2	0.2	-	1.3	1.0
Biotite*	-	-	-	-	-
Chlorite	3.0	1.3	6.2	7.2	5.1
Metamorphic accessories and cements	12.3	2.5	6.0	2.3	20.1
Detrital accessorites	0.8	0.6	5.0	1.3	1.6
Matrix	3.4	1.1	2.1	11.3	8.5
Total:	100.3	99.8	100.0	100.0	100.2

Sample	HQ-16	HQ-25	HQ-19	KTW-G	BQ-21
Mean grain size, phi (mm)	2.77(0.15)	2.83(0.14)	3.08(0.12)	4.07(0.06)	4.13(0.06)
Quartz	28.0	34.8	27.1	27.1	16.8
K-feldspar	2.6	3.3	1.9	}21.0	2.2
Plagioclase	30.2	24.6	24.8		16.6
Sedimentary rock fragments	3.6	4.5	3.5	0.7	1.8
Metamorphic and plutonic rock fragments	4.8	4.8	4.7	4.6	2.6
Acid volcanic rock fragments	2.4	1.4	0.6	} 1.8	0.6
Basic volcanic rock fragments	6.4	8.3	7.8		3.6
Muscovite	0.8	0.6	1.2	8.3	1.6
Biotite*	0.4	0.6	-	-	-
Chlorite	5.8	4.1	9.7	22.5	11.0
Metamorphic accessories and cements	2.2	1.6	1.4	7.5	0.2
Detrital accessories	1.4	0.6	0.8	0.6	1.6
Matrix	11.7	11.0	16.7	6.1	41.5
Total:	100.3	100.2	100.2	100.2	100.1

* Dashes indicate biotite included in chlorite mode.

Table 2.5 : Composition (in percent) for greywackes of the thin-bedded lithofacies (500 counts/thin section) arranged in order of decreasing mean grain size.

Sample	BQ-iv	DC-10	BQ-iii	RSS-i	RSS-iii	KTW-i
Mean grain size, phi (mm)	3.3(0.1)	3.7(0.08)	3.78(0.07)	3.82(0.07)	4.08(0.06)	4.23(0.05)
Quartz	18.1	26.8	26.3	31.9	20.5	32.9
K-feldspar	2.0	0.2	2.9	1.7	1.0	4.6
Plagioclase	24.0	40.5	25.9	28.6	33.0	34.9
Sedimentary rock fragments	3.8	1.9	3.1	2.9	2.5	0.4
Metamorphic and plutonic rock fragments	1.2	1.5	2.5	3.3	1.7	0.4
Acid volcanic rock fragments	0.2	-	0.4	-	-	-
Basic volcanic rock fragments	2.4	1.9	3.1	1.9	2.6	0.4
Muscovite	0.8	1.0	0.4	1.0	1.3	3.6
Biotite*	-	-	-	-	-	-
Chlorite	5.2	3.4	4.4	4.1	5.5	9.4
Metamorphic accessories and cements	21.8	5.2	13.7	2.9	0.2	0.4
Detrital accessories	1.2	5.4	0.8	1.7	1.3	6.6
Matrix	19.4	12.4	16.6	20.1	30.5	6.6
Total:	100.1	99.8	100.1	100.1	100.1	100.2

Sample	DC-8	SJ-T	DC-LAM	BQ-i	KTW-V	RSS-ii
Mean grain size, phi (mm)	4.5(0.04)	4.72(0.04)	4.8(0.04)	4.87(0.03)	5.0(0.03)	5.18(0.03)
Quartz	27.6	33.4	31.5	18.2	31.3	24.3
K-feldspar	0.3	} 30.1	} 16.1	1.8	} 28.1	1.9
Plagioclase	28.4			16.6		23.3
Sedimentary rock fragments	0.8	1.0	0.2	1.2	-	-
Metamorphic and plutonic rock fragments	0.3	0.8	0.2	-	-	1.0
Acid volcanic rock fragments	-	-	-	0.2	-	-
Basic volcanic rock fragments	1.4	-	0.8	0.2	0.4	-
Muscovite	2.8	2.7	6.0	1.4	4.2	1.0
Biotite*	-	-	-	-	-	-
Chlorite	3.3	8.8	11.2	9.4	13.4	13.3
Metamorphic accessories and cement	0.6	0.2	-	26.0	-	-
Detrital accessories	4.5	2.5	6.8	3.2	2.6	3.9
Matrix	30.1	20.5	27.3	22.0	20.0	32.3
Total:	100.1	100.0	100.1	100.2	100.0	101.0

* Dashes indicate biotite included in chlorite mode.

The sandstone and thick-bedded lithofacies are not easily contrasted by petrography alone, due to the wide textural range displayed by the thick-bedded lithofacies. The petrography of rocks within the same textural range for both lithofacies is similar, differences being limited to higher total feldspar modes in the sandstone lithofacies and large modes of metamorphic accessories and cements in the thick-bedded lithofacies. The magnitude of the difference is the same in both cases, i.e. approximately 4 percent.

There is no statistical evidence of any significant difference between the lithofacies based on the quartz mode (P is greater than 0.1) even though modes for a lithology may deviate by up to 1.5 percent from the mean i.e. 1.5 percent is the standard error for about 15 samples. Confidence interval for the standard error is 3 percent at the 95 percent confidence level.

2.8 Argillite petrography

Table 2.6 presents the data from modal analyses of argillites. Two analyses were undertaken, one counting matrix as material less than 0.02 mm in size, the other with no lower limit to grain size, every identifiable grain being allocated a mode class. Where identification was impossible a mode class "unidentifiably fine" was used. Comparison shows that an average of 85 percent of mineral components can be identified from thin section.

On average, matrix comprises some 60 percent, with chlorite and quartz occurring in subequal quantity and feldspar representing 30 percent of the fabric minerals. White mica contents vary from 1 to 7 percent, averaging 4 percent.

The proportions of quartz, feldspar, white mica and chlorite are similar regardless of how the modal analysis is done. Components not commonly occurring in sizes greater than 0.02 mm are opaque minerals and detrital heavy minerals.

Matrix therefore consists largely of chlorite and quartz, the former slightly dominant, with lesser amounts of white mica and feldspar - plagioclase is often twinned in grains 0.01 mm in size (WCC-8A). Small amounts of opaque minerals (3 percent average) and detrital heavies (2 percent average) constitute the remainder.

Table 2.6 : Composition (in percent) for argillites (300 counts/thin section) arranged in order of decreasing mean grain size.

A Optic modal analyses of argillites

Sample	HQ-26	NC-15	HQ-24	OB-W	HQ-20	WCC-8A	WCC-5A	HQ-18	BQ-vii	HQ-22	OB-13	AVERAGE
Mean grain size, phi	5.4	5.49	5.58	5.6	5.87	5.87	5.9	5.95	6.18	6.28	6.39	NA
Quartz	16.4	30.0	12.2	14.0	5.8	16.4	16.1	10.1	8.0	6.1	3.8	12.6
Feldspar	14.8	10.4	8.0	15.3	7.8	14.1	11.4	5.1	6.0	6.5	3.8	9.4
White mica	2.8	7.7	5.0	5.0	1.3	3.2	6.6	3.3	5.8	1.0	1.8	4.0
Chlorite	13.4	7.7	15.9	13.1	13.3	13.4	9.8	9.6	12.8	4.9	8.5	11.1
Heavies	2.2	2.7	0.5	0.6	2.0	1.6	1.6	0.8	0.3	0.4	0.3	1.2
Opaques	0.8	1.1	2.0	0.9	3.3	0.6	1.9	3.5	3.5	0.6	0.6	1.7
Rock fragments	0.5	0.3	0.2	-	-	-	0.3	-	-	0.2	-	0.1
Metamorphic - accessories	-	-	-	-	0.7	-	-	0.3	-	0.2	-	0.1
Cements	-	-	-	-	-	-	-	-	0.3	-	-	tr
Matrix (0.02 mm)	49.0	40.1	56.2	51.1	65.9	50.7	52.5	67.4	63.3	80.2	81.3	59.8
Total:	99.9	100.0	100.0	100.0	100.1	100.0	100.2	100.1	100.0	100.1	100.1	100.0

B Optic modal analyses of argillites disregarding matrix as a mode class

	HQ-26	NC-15	HQ-24	OB-W	HQ-20	WCC-8A	WCC-5A	HQ-18	BQ-vii	HQ-22	OB-13	AVERAGE
Quartz	36.5	45.9	21.6	26.0	14.9	30.9	23.3	26.1	26.2	19.6	Asses-	27.1
Feldspar	18.9	10.3	12.0	20.8	10.8	18.0	18.6	13.2	6.9	10.1	ment	14.0
White mica	7.0	9.5	10.6	8.3	6.8	8.5	8.5	10.2	10.7	9.4	not	9.0
Chlorite	20.6	15.5	26.9	18.4	39.9	32.2	18.0	27.1	33.1	36.5	practi-	26.8
Heavies	4.3	3.8	0.8	3.4	1.9	1.9	5.3	4.0	0.9	4.6	cable	3.1
Opaques	0.9	0.8	5.0	4.0	7.4	1.6	3.2	7.3	8.3	9.6		4.8
Rock fragments	2.2	0.3	-	-	-	-	0.3	0.7	0.2?	0.2		0.4
Metamorphic - accessories	-	-	0.3	-	-	-	0.5	0.3	0.2?	0.5		0.2
Cements	-	-	-	-	-	-	-	-	0.2	-		tr
Unidentifiably fine	9.6	13.9	22.7	19.3	18.3	6.9	22.3	11.2	13.2	10.3		14.8
Total:	100.0	100.0	99.9	100.2	100.0	100.0	100.0	100.1	99.9	100.8		100.2

C Optic modes of matrix (<0.02 mm) by difference, from analyses A and B above

	HQ-26	NC-15	HQ-24	OB-W	HQ-20	WCC-8A	WCC-5A	HQ-18	BQ-vii	HQ-22	OB-13	AVERAGE
Quartz	20.1	15.9	9.4	12.0	9.1	14.5	7.2	16.0	18.2	13.5	Asses-	13.6
Feldspar	4.1	-	4.0	5.5	3.0	3.9	7.2	8.1	0.9	3.6	ment	4.0
White mica	4.2	1.8	5.6	3.3	5.5	5.3	1.9	6.9	4.9	8.4	not	4.8
Chlorite	7.2	7.8	11.0	5.3	26.6	18.8	8.2	17.5	20.3	31.6	practi-	15.4
Heavies	2.1	1.1	0.3	2.8	tr	0.3	3.7	3.2	0.6	4.2	cable	1.8
Opaques	0.1	1.0	3.0	3.1	4.1	1.0	1.3	3.8	4.3	9.0		3.1
Metamorphic - accessories	-	-	0.3	-	-	-	0.5	-	-	0.3		0.1
Unidentifiably fine	9.6	13.9	22.7	19.3	18.3	6.9	22.3	11.2	13.2	10.3		14.8
Total: cf. matrix of A	47.4	41.5	56.3	51.3	66.6	50.7	52.3	66.7	62.9	80.6		57.6

2.9　Comparison of greywacke and argillite

A direct comparison of argillite modes with greywacke modes is difficult because of different mode class requirements for the rock types but there is a striking difference in grain size.

As a generalisation, argillites have half as much quartz, two-thirds the total feldspar and no rock fragments, but four times the white mica and double the chlorite.

Non-opaque detrital accessories (heavies) are more abundant in argillites than greywackes, excepting some greywackes of the thin-bedded lithofacies.　Metallic opaques are more abundant in argillite than greywacke as is carbonaceous material but they take different forms.　Metallic opaques in argillites are sometimes apparent as large flakes of pyrite along planes of parting, having no relationship with bedding, or as nodules up to 10 mm long in bedding planes. Organic matter in argillites is more finely dispersed than in greywackes.

Metamorphic accessories, other than minerals included in modes, e.g. chlorite and metallic opaques, are absent in argillites.

Argillites possess six times as much matrix as greywackes of the sandstone and thick-bedded lithofacies and two to three times that of the thin-bedded lithofacies.

Generally, detrital grains in argillites are equant, angular to subrounded and most grains are fresh and monocrystalline.

2.10　Provenance

The provenance of sediments may be indicated by various physical and mineral characteristics of the rock concerned.　In this study mineral characteristic methods were chosen using quartz, feldspar, rock fragments and heavy minerals.

The method used for quartz was suggested by Basu *et al*. (1975) based on a simple four category grouping, utilising undulosity and polycrystallinity of medium sand sized quartz to discriminate plutonic grains from those of low and high rank metamorphic affinity.　Results for the Wellington greywacke-suite rocks

are shown in Figure 2.11. Only greywackes from the sandstone and thick-bedded lithofacies have sufficient medium sand sized quartz to provide plots based on 50 grains (Appendix 4).

The data suggest that most medium sand sized quartz is of low rank metamorphic origin. However, the interpretation is complicated by the possibility that the grains were strained after deposition.

Basu acknowledges the possibility of tectonic strain in folded sediments but maintains that careful sampling and examination of rocks containing softer matrix and rock fragments can minimise these effects. Packing proximities are high in Wellington greywackes (Appendix 7) therefore cushioning effects from matrix and rock fragments are minimal.

Blatt and Christie (1963) and Blatt (1967) have shown undulatory quartz to be less stable than non-undulatory quartz and that polycrystalline quartz breaks down relatively quickly to produce monocrystalline quartz. Older sediments, or those reworked should, on the Basu plot, trend towards a more plutonic affinity. Such a trend was not evident in this study.

Other detrital minerals, e.g. microcline and feldspar with perthitic and myrmekitic intergrowths, indicate an acid plutonic source but the provenance of most feldspar (plagioclase) is obscured by alteration of grains to sodic affinities (Appendix 3). Further indications of an acid igneous rock source, are minerals such as apatite, sphene, zircon and tourmaline (Pettijohn, 1957). Biotite, muscovite and tourmaline may be derived from metamorphic rocks or acid igneous rocks and epidote and zoisite indicate a high-rank metamorphic provenance (Table 2.7).

In coarser grained rock types, the mineral association most frequently encountered is that of an acid igneous rock source. Finer sediments (thin-bedded lithofacies), although having similar acid igneous rock affinities, also have assemblages indicative of basic igneous rock sources and characteristics of reworked sediments, not unexpectedly if some of these greywackes are contourites (section 2.1).

Fine grained sediments possess heavy mineral assemblages typical of basic igneous rock sources, e.g. ilmenite, magnetite, chromite, apatite, zircon

POLYCRYSTALLINE QUARTZ
(2-3 CRYSTAL UNITS PER GRAIN; ≥75 PERCENT
OF TOTAL POLYCRYSTALLINE QUARTZ)

NON-
UNDULATORY
QUARTZ

UNDULATORY
QUARTZ

PLUTONIC

MIDDLE & UPPER RANK
METAMORPHIC

LOW RANK
METAMORPHIC

POLYCRYSTALLINE QUARTZ
(>3 CRYSTAL UNITS PER GRAIN; 25 PERCENT
OF TOTAL POLYCRYSTALLINE QUARTZ)
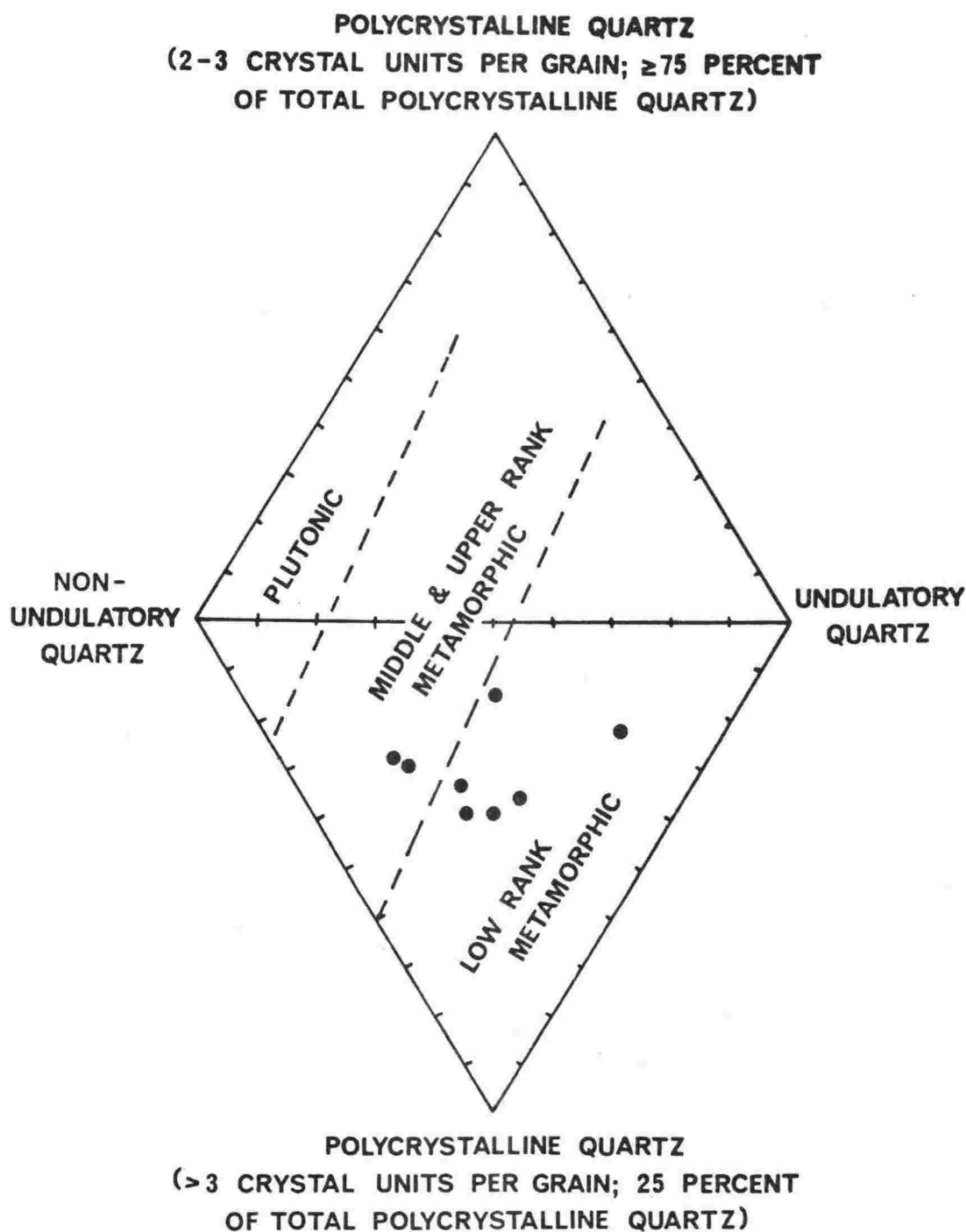
Figure 2.11 : Quartz grains of medium sand size from greywackes of the
sandstone and thick-bedded lithofacies plotted on
the Basu plot. Fifty grains were counted for each plot. Raw
data is given in Appendix 4.

Table 2.7 : Detrital mineral suites characteristic of source rock types*
(after Pettijohn, 1957).

Reworked sediments

Barite   Rutile
Glauconite
Quartz (esp. with worn overgrowths)   *Tourmaline*, rounded
Chert   *Zircon*, rounded
Quartzite fragments (orthoquartzite type)
Leucoxene

Low-rank metamorphic

Slate and *phyllite fragments*   *Quartz* and *quartzite* fragments (meta-
Biotite and muscovite   quartzite type)
Chlorite (if clastic)   *Tourmaline* (small pale brown euhedra
Feldspars generally absent   carbonaceous inclusions)
                                                Leucoxene

High-rank metamorphic

Garnet   *Staurolite*
Hornblende (blue-green variety)   *Quartz* (metamorphic variety)
Kyanite   Muscovite and biotite
Sillimanite   Feldspar (acid plagioclase)
Andalusite   *Epidote*
                                                Zoisite
                                                Magnetite

Acid igneous

Apatite   Sphene
Biotite   *Zircon*, euhedra
Hornblende   *Quartz* (igneous variety)
Monazite   *Microcline*
Muscovite   *Magnetite*
                                                Tourmaline, small pink euhedra

Basic igneous

Anatase   Leucoxene
Augite   Olivine
Brookite   *Rutile*
Hypersthene   Plagioclase, intermediate
Illmenite and magnetite   Serpentine
Chromite

Pegmatite

Fluorite   Monazite
Tourmaline, typically blue (indicolite)   *Muscovite*
Garnet   Topaz
                                                Albite
                                                Microcline

---

* Italicized species are more common.

and rutile, as these minerals are all relatively stable.   In coarser grained
greywackes, basic igneous rock fragments as well as some of their heavy
minerals occur together.

Rock fragment contents, particularly in the coarser grained greywackes, are
of valuable assistance in determining source rock lithology.   Lithologies
identified have been described (Appendix 3).   Sedimentary rock fragments
probably come from penecontemporaneous erosion of the sea floor.   This is
substantiated by a positive relationship between sedimentary rock fragment
size with mean grain size of host sediment and a positive relationship, by
volume, of sedimentary rock fragments with increasing mean size of host
sediment.   They are most obvious in the greywackes of the thick-bedded
lithofacies (chipwackes), where they occur as angular elongate flakes up to
0.4 m long, in which lamination and convolutions are still preserved.   They
deform to form pseudomatrix more readily than igneous rock fragments.   In a
plastic state, they must have been more susceptible to mechanical erosion than
any other variety of rock fragment observed and therefore must have been
added to the sediment immediately prior to its final emplacement.   Reworked
fine grained greywackes (thin-bedded lithofacies) have no significant
sedimentary rock fragments.

Volcanic debris is mechanically weak and chemically unstable.   Grains are
rounded and the ratio of acid to basic volcanic debris is consistently small
for all lithofacies (Figure 2.12).   Only in greywackes of the thin-bedded
lithofacies do the volcanic rock fragments diminish in volume - a response to
reduced mean grain size and reworking.   The volume in greywackes of the
thick-bedded lithofacies is only slightly greater than that in the sandstone
lithofacies indicating that, for the greywacke source sediments, volcanic
debris was maintained at a consistent volume and is possibly intrabasinal (i.e.
derived from a source within the basin of greywacke sedimentation) being
relatively weak compared with metamorphic and plutonic rock fragments.

The latter rock fragments are probably extrabasinal in origin, schists, phyl-
lites, quartzites and gneiss fragments being subordinate to granitic fragments,
even in the size range 0.5 to 2 mm required for accurate identification of
metamorphic rock fragments (Boggs, 1968).   This indicates that, even though
a wider range of metamorphic rock types is represented, granitic rocks are
more likely to have produced the bulk of sediments forming the Wellington
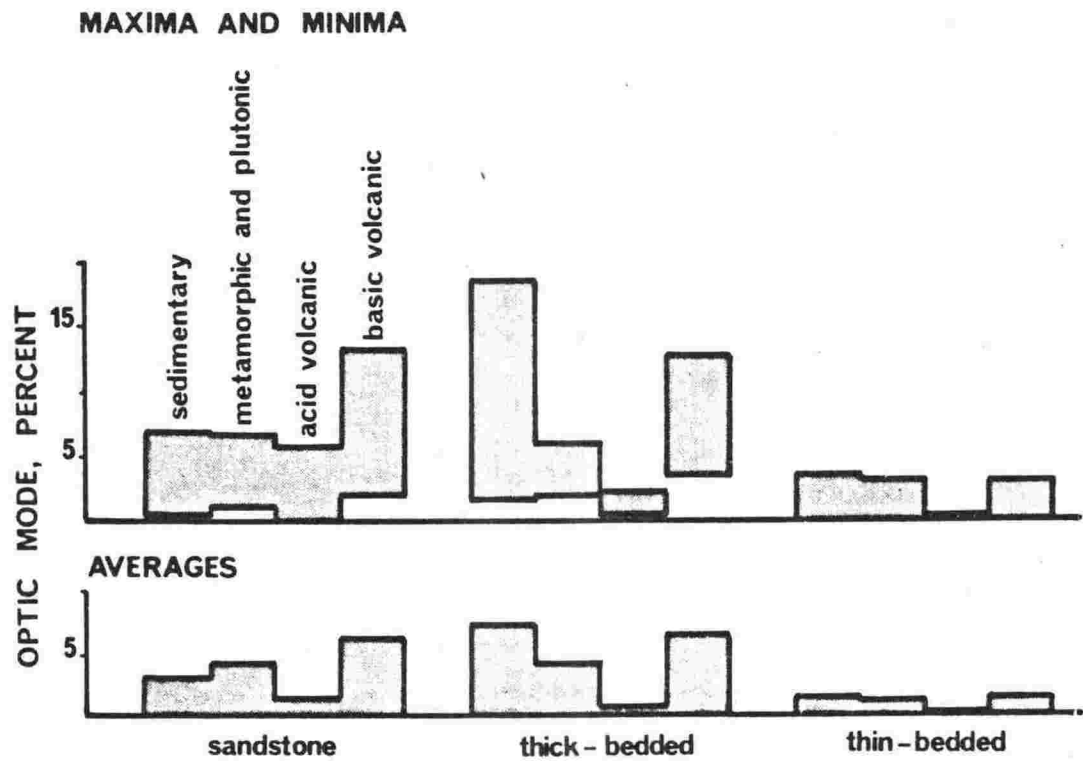
Figure 2.12 : Range and average concentrations of rock fragment
types for greywackes by lithofacies.

greywacke-suite greywackes.   The presence of large myrmekitic and perthitic aggregates, with orthoclase crystals having euhedral grain boundaries with each other and quartz, indicate this.

The range in volumes of metamorphic and plutonic rock fragments in greywackes of each lithofacies is the same, within about 1 percent; gradual decrease both in range and maximum volume being evident from the sandstone lithofacies, through the thick-bedded to the thin-bedded lithofacies.   This indicates that this chemically relatively stable debris forms the basis of greywacke sediments, a slight concession being made to volume with reduced mean grain size.

Approximate relative contributions of source rocks providing debris for the Wellington greywacke sediments is estimated to be:

Source	Percentage contribution
acid and basic plutonic	50
low rank metamorphic	20
basic igneous derived	10
acid igneous derived	5
redeposited sediments	15

2.11   Classification of greywackes by mineral composition

Folk *et al.* (1970) published a classification system for detrital sediments in New Zealand, based on relative abundances of quartz (excluding chert), feldspar and rock fragments (igneous, metamorphic and sedimentary, including chert).   These three parameters recalculated to sum to 100 percent, are determined from optical modal analysis and are end members on a triangular (QFR) diagram.   Figure 2.13 shows the QFR diagram (primary arenite triangle) with greywackes plotted by lithofacies association.

The conclusions drawn from the classification are that all the rocks examined are (lithic) feldsarenites, difference being due to grain size.   All the rocks represent a single population i.e. all the greywackes in the study region had basically the same mineralogical starting point.
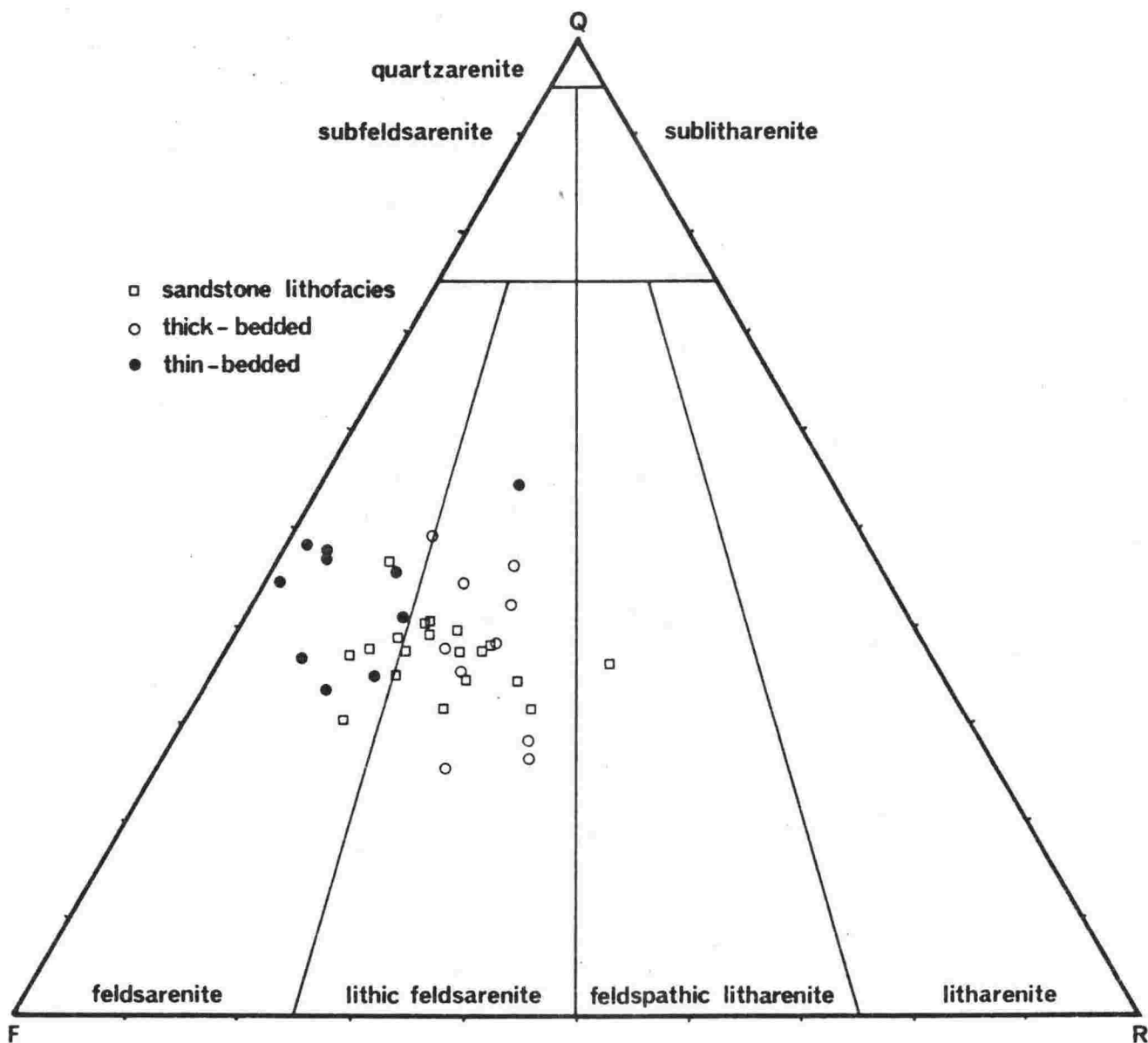
Figure 2.13 : Primary arenite triangle (after Folk *et al.*, 1970)
with plots representing the modal compositions of
greywackes from each lithofacies. Q = monocrystalline and
polycrystalline quartz (excluding chert), F = monocrystalline
feldspar, R = rock fragments (igneous, metamorphic and sedi-
mentary, including chert).

2.12 Grain size

The grain size distribution of greywacke and argillite samples was determined from thin section measurement. The apparent long axes of at least 250 grains were measured using a graduated micrometer eyepiece and magnifications from x35 to x250. The spacing of the counting "grid" was adjusted to cover the whole section. Although Adams (1974) has shown a reliable relationship between thin section and sieve statistics, he recognised problems in converting the distributions. Therefore the data presented and discussed here have not been manipulated in any way, being the size distributions of apparent long axes in thin section.

Grain size distribution histograms (Figures 2.14 to 2.17) were plotted and graphic statistics were calculated (Folk, 1968) according to the formulae:

$$\text{Graphic mean} \quad (M_z) = \frac{\phi16 + \phi50 + \phi84}{3} \text{ phi}$$

Inclusive graphic standard deviation (σ_I)

$$= \frac{\phi84 - \phi16}{4} + \frac{\phi95 - \phi5}{6.6} \text{ phi}$$

Graphic standard deviation (σ_G)

$$= \frac{\phi84 - \phi16}{2} \text{ phi}$$

used where the 5 and 95 percentiles were not obtainable.

Inclusive graphic skewness (SK_I)

$$= \frac{\phi16 + \phi84 - 2\phi50}{2(\phi84 - \phi16)} + \frac{\phi5 + \phi95 - 2\phi50}{2(\phi95 - \phi5)}$$

Graphic kurtosis (K_G)

$$= \frac{\phi95 - \phi5}{2.44(\phi75 - \phi25)}$$
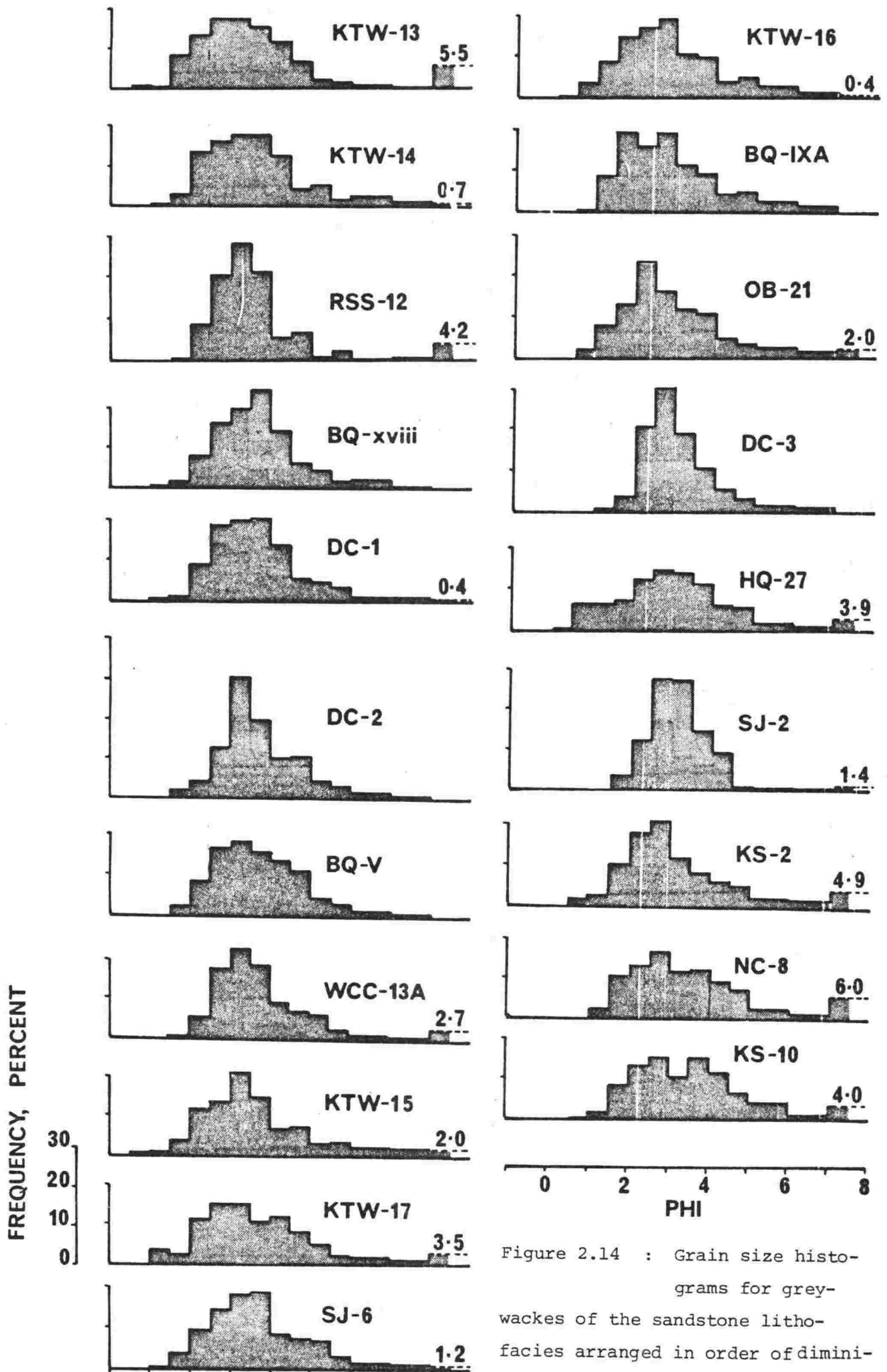
Figure 2.14 : Grain size histograms for greywackes of the sandstone lithofacies arranged in order of diminishing mean grain size, see Table 2.8.
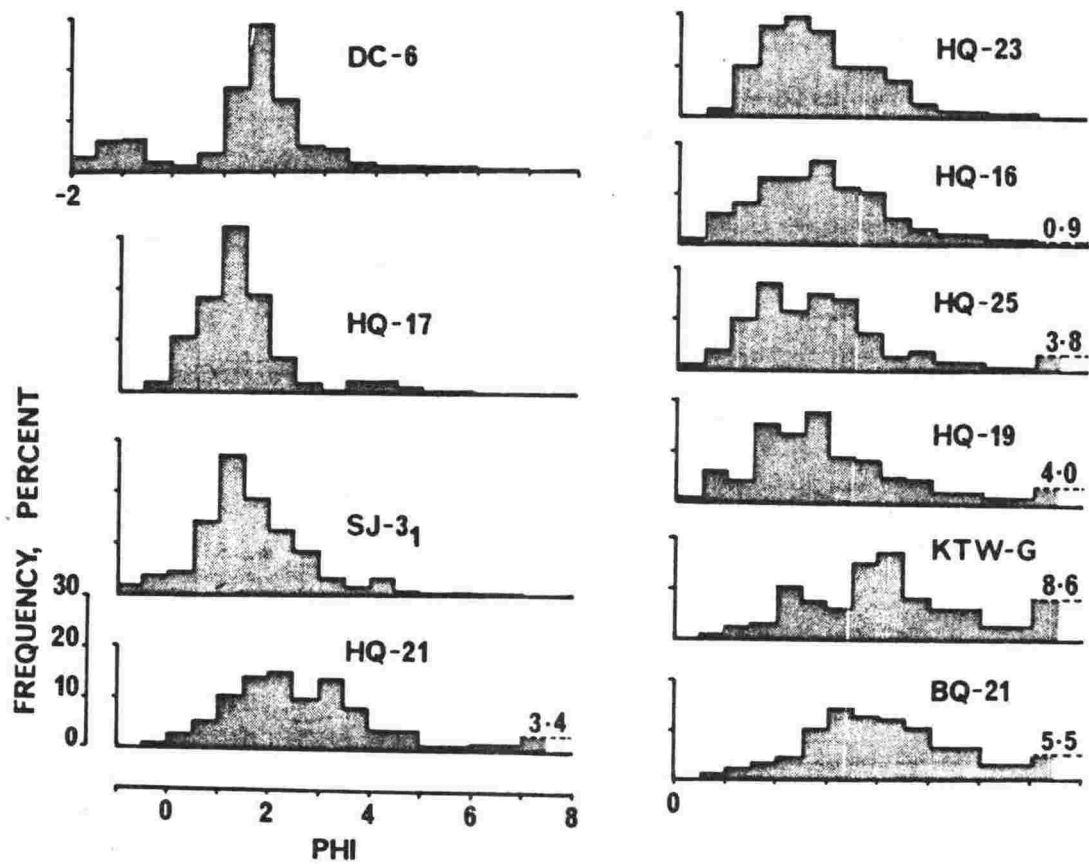
Figure 2.15 : Grain size histograms for greywackes of the thick-
bedded lithofacies arranged in order of diminishing
mean grain size, see Table 2.8.
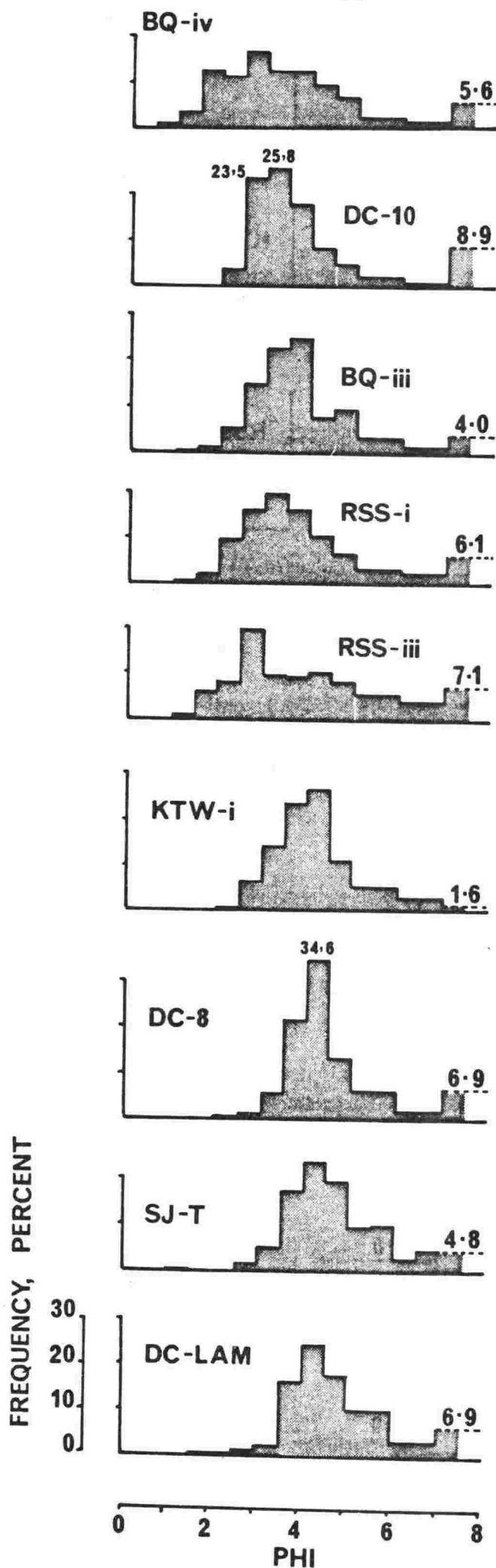
Figure 2.16 : Grain size histograms for greywackes of the thin-bedded lithofacies arranged in order of diminishing mean grain size, see Table 2.8.
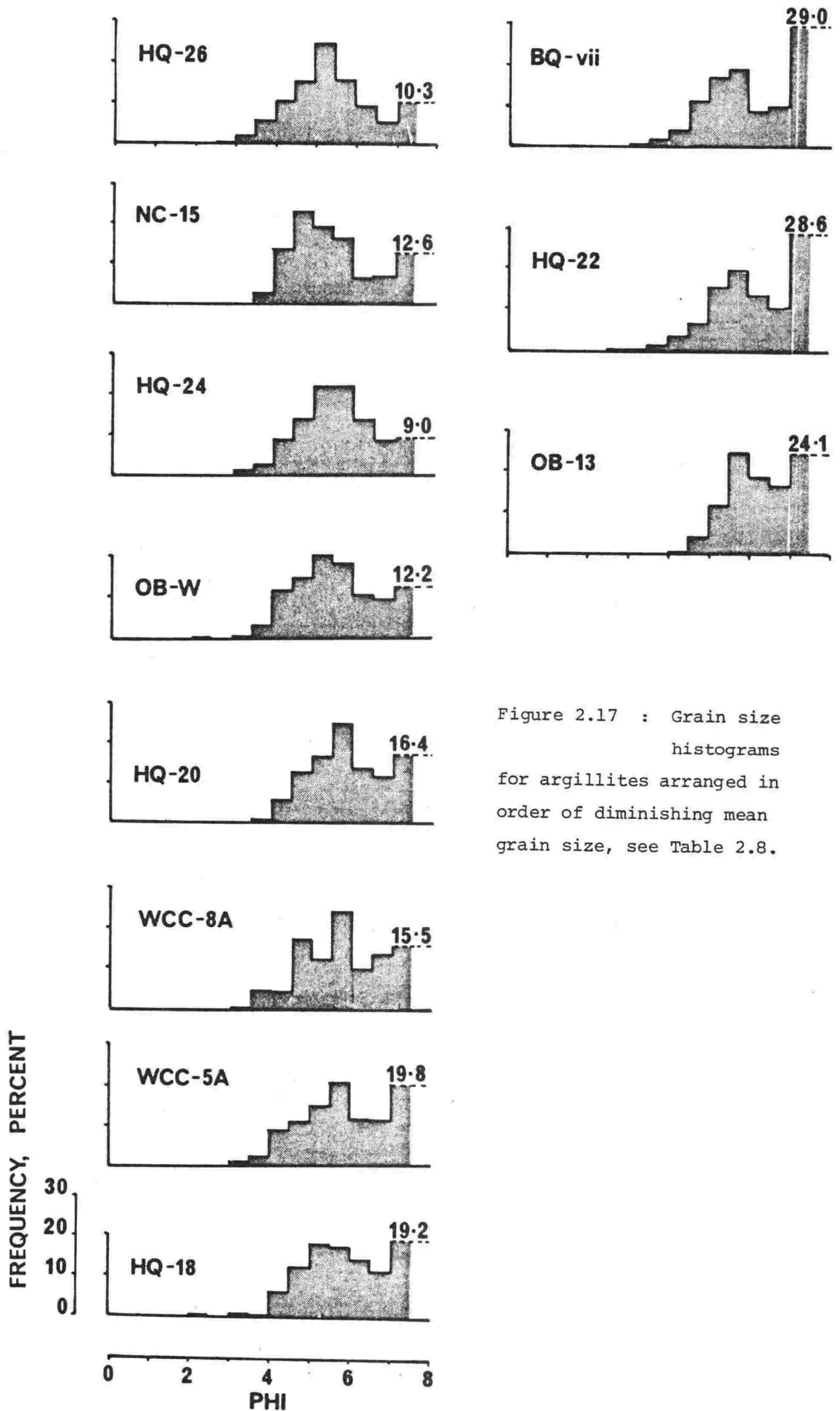
Figure 2.17 : Grain size histograms for argillites arranged in order of diminishing mean grain size, see Table 2.8.

Grain size data provide a reliable basis for differentiating lithofacies in thin section.   Figure 2.18 shows the relationship of rock mean grain size to bed thickness.

Greywackes of the sandstone lithofacies are restricted in mean grain size (2.4 to 3.38 phi) and are poorly sorted (σ = 1.25 average).   Grain size distributions are more positively skewed and are less peaked than for greywackes of any other lithofacies.

Greywackes of the thick-bedded lithofacies have the greatest range in textural parameters.   They overlap other greywackes in mean grain size (1.25 to 4.13 phi) but are generally finer than greywackes of the sandstone lithofacies and coarser than those of the thin-bedded lithofacies.   They are more poorly sorted than those of the sandstone lithofacies.   Grain size histograms may be skewed positive or negative, the negative skew being due to greywackes possessing large sedimentary rock fragments (chipwackes).   Although they display the widest range in skewness values, these greywackes have grain size histograms most closely approximating a normal distribution.

Greywackes of the thick-bedded lithofacies have wider ranging Kurtosis values (Table 2.8) than those of the sandstone lithofacies and histograms are more leptokurtic.   They include the most peaked grain size distributions.

Greywackes of the thin-bedded lithofacies have silt sized mean grain sizes. Sorting is better than in other greywackes and there is a smaller range of relatively high (+0.21 to +0.37) skewness values.   Kurtosis values are also limited (1.18 to 1.39).

Argillites are similar in size regardless of lithofacies affiliation.   Modes vary between 5 and 6 phi (0.03 and 0.015 mm) and mean grain sizes are finer than 5.4 phi (0.023 mm).   Most argillites are poorly sorted.

Post-depositional effects (diagenesis) have reduced grains in size by erosion and alteration.   Smaller grains have been reduced in size faster and more
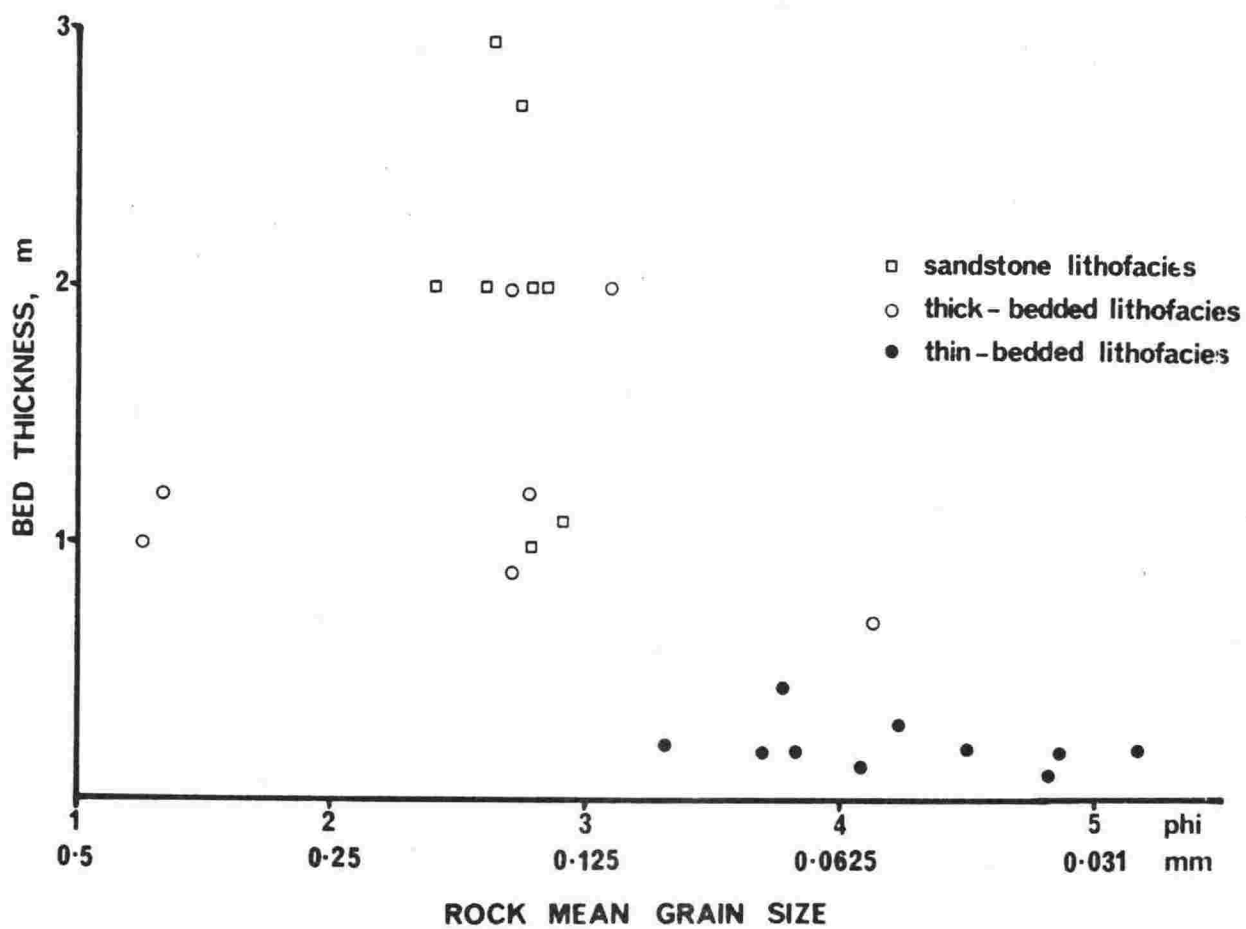
Figure 2.18 : Plot of greywacke bed thickness and rock mean grain

size at mid-bed.

Table 2.8 : Grain size parameters determined for Wellington greywacke-suite rocks. Raw data is tabled in Appendix 5. Phi units used.

Sample	Mean (M_z)	σ_I	σ_G	Sorting term	Skewness SK_I	Skewness description	Kurtosis K_G	Kurtosis description
KTW-13	2.4		1.15	poorly sorted	NA		NA	
KTW-14	2.6	1.27		poorly sorted	+0.25	fine skewed	1.26	leptokurtic
RSS-12	2.6	1.03		poorly sorted	+0.54	strongly fine sk.	1.73	very leptokurtic
BQ-xviii	2.63	0.98		moderately sorted	+0.16	strongly fine sk.	1.10	mesokurtic
DC-1	2.65	1.03		poorly sorted	+0.22	strongly fine sk.	1.08	mesokurtic
DC-2	2.72	0.96		moderately sorted	+0.34	strongly fine sk.	1.13	leptokurtic
BQ-V	2.73	1.13		poorly sorted	+0.19	fine skewed	1.03	mesokurtic
WCC-13A	2.78	1.17		poorly sorted	+0.39	strongly fine sk.	1.23	leptokurtic
KTW-15	2.78	1.54		poorly sorted	+0.36	strongly fine sk.	1.32	leptokurtic
KTW-17	2.79	1.57		poorly sorted	+0.30	fine skewed	1.18	leptokurtic
SJ-6	2.8	1.37		poorly sorted	+0.29	fine skewed	1.15	leptokurtic
KTW-16	2.83	1.36		poorly sorted	+0.25	fine skewed	1.08	mesokurtic
BQ-IXA	2.9	1.30		poorly sorted	+0.30	fine skewed	1.04	mesokurtic
OB-21	2.93	1.38		poorly sorted	+0.35	strongly fine sk.	1.22	leptokurtic
DC-3	3.08	0.91		moderately sorted	+0.41	strongly fine sk.	1.21	leptokurtic
HQ-27	3.13	1.63		poorly sorted	+0.16	fine skewed	1.29	leptokurtic
SJ-2	3.2	0.75		moderately sorted	+0.14	fine skewed	1.12	leptokurtic
KS-2	3.27	1.49		poorly sorted	+0.46	strongly fine sk.	1.23	leptokurtic
NC-8	3.37	1.57		poorly sorted	+0.40	strongly fine sk.	1.27	leptokurtic
KS-10	3.38	1.41		poorly sorted	+0.21	fine skewed	1.09	mesokurtic
AVERAGE	2.88	1.25						
DC-6	1.25	1.56		poorly sorted	-0.3	coarse skewed	2.05	very leptokurtic
HQ-17	1.317	0.94		moderately sorted	+0.23	fine skewed	1.73	very leptokurtic
SJ-3₁	1.32	1.22		poorly sorted	-0.01	near symmetrical	1.10	mesokurtic
HQ-21	2.7	1.58		poorly sorted	+0.30	fine skewed	1.29	leptokurtic
HQ-23	2.7	1.80		poorly sorted	+0.23	fine skewed	0.94	mesokurtic
HQ-16	2.77	1.44		poorly sorted	+0.14	fine skewed	1.07	mesokurtic
HQ-25	2.83	1.54		poorly sorted	+0.26	fine skewed	1.34	leptokurtic
HQ-19	3.08	1.67		poorly sorted	+0.33	fine skewed	1.24	leptokurtic
KTW-G	4.07	1.78		poorly sorted	+0.11	fine skewed	1.08	mesokurtic
BQ-21	4.13	1.58		poorly sorted	+0.13	fine skewed	1.13	leptokurtic
AVERAGE	2.62	1.51						
BQ-iv	3.3		1.43	poorly sorted	NA		NA	
DC-10	3.7		1.05	poorly sorted	NA		NA	
BQ-iii	3.78	1.12		poorly sorted	+0.36	strongly fine sk.	1.38	leptokurtic
RSS-i	3.82		1.35	poorly sorted	NA		NA	
RSS-iii	4.08		1.75	poorly sorted	NA		NA	
KTW-i	4.23	0.99		moderately sorted	+0.21	fine skewed	1.29	leptokurtic
DC-8	4.5		0.8	moderately sorted	NA		NA	
SJ-T	4.72	1.19		poorly sorted	+0.37	strongly fine sk.	1.39	leptokurtic
DC-LAM	4.8		1.0	mod./poorly sorted	NA		NA	
BQ-i	4.87	0.89		moderately sorted	+0.25	fine skewed	1.18	leptokurtic
KTW-v	5.0		1.13	poorly sorted	NA		NA	
RSS-ii	5.18		1.38	poorly sorted	NA		NA	
AVERAGE	4.33	1.17						

Left margin groupings (vertical labels): FIELD SAMPLED BY BED ASSOCIATION AS GREYWACKES — SANDSTONE LITHOFACIES; THICK BEDDED LITHOFACIES; THIN BEDDED LITHOFACIES

NA = not able to be calculated

Table 2.8 : (continued)

	Sample	Mean	Standard deviation		Sorting term	Skewness	Skewness	Kurtosis	Kurtosis
		(M_z)	σ_I	σ_G		SK_I	description	K_G	description
ARGILLITE BY BED ASSOCIATION	HQ-26	5.4		1.03	poorly sorted				
	NC-15	5.49		1.13	poorly sorted				
	HQ-24	5.58		0.95	moderately sorted				
	OB-W	5.6		1.15	poorly sorted				
	HQ-20	5.87		1.05	poorly sorted				
	WCC-8A	5.87		1.05	poorly sorted				
	WCC-5A	5.9		1.25	poorly sorted				
	HQ-18	5.95		1.18	poorly sorted				
	BQ-vii	6.18		1.38	poorly sorted				
	HQ-22	6.28		1.23	poorly sorted				
	OB-13	6.39		0.99	moderately sorted				

NOT ABLE TO BE CALCULATED

significantly than larger grains, due to their larger surface area to volume ratios (section 2.14.3).   In grain size populations less than, say, 0.02 mm recrystallisation due to diagenesis has probably meant that rocks have some mineral types enhanced in grain size (chlorite and white mica) relative to the grain population at deposition.

The effect of this is to increase positive skewness (reduce sorting) in greywackes and to perhaps enhance sorting and even mean grain size in argillites.

It is doubtful whether the most marked grain size changes in the population finer than 0.02 mm will have influenced textural distinctions - greywackes are still comparable one with another and argillites are of little help in discriminating lithofacies association.

2.13   The relationship of mineralogy to texture

In the course of the microscope work it became apparent that the mineralogy of the greywacke-suite rocks was related to texture and, in particular, mean grain size.   This section examines that relationship,by plotting the main mineral modes against mean grain size (Figure 2.19).

The proportion of felsic grains remains more or less constant between 50 and 70 percent over the range 1 to 4 phi (0.5 to 0.063 mm), but declines markedly from 5 to 6 phi (0.03 to 0.015 mm) with a corresponding increase in phyllosilicates;   rock fragments also decline dramatically at about 5 phi (0.03 mm). While limitations of microscopic resolution can not be overlooked,there appears to be a mineralogical trend towards a higher proportion of phyllosilicates, which in these rocks are chlorite and white mica.   These minerals appear,on average,to maintain similar proportion (Figure 2.20).

2.14   X-ray diffractometry

X-ray diffractometry (XRD) was used to establish the bulk mineralogy of the rocks as they occur in the field today and as a means of determining variations in metamorphic grade by assessing the crystallinity of white mica, particularly in the argillites.
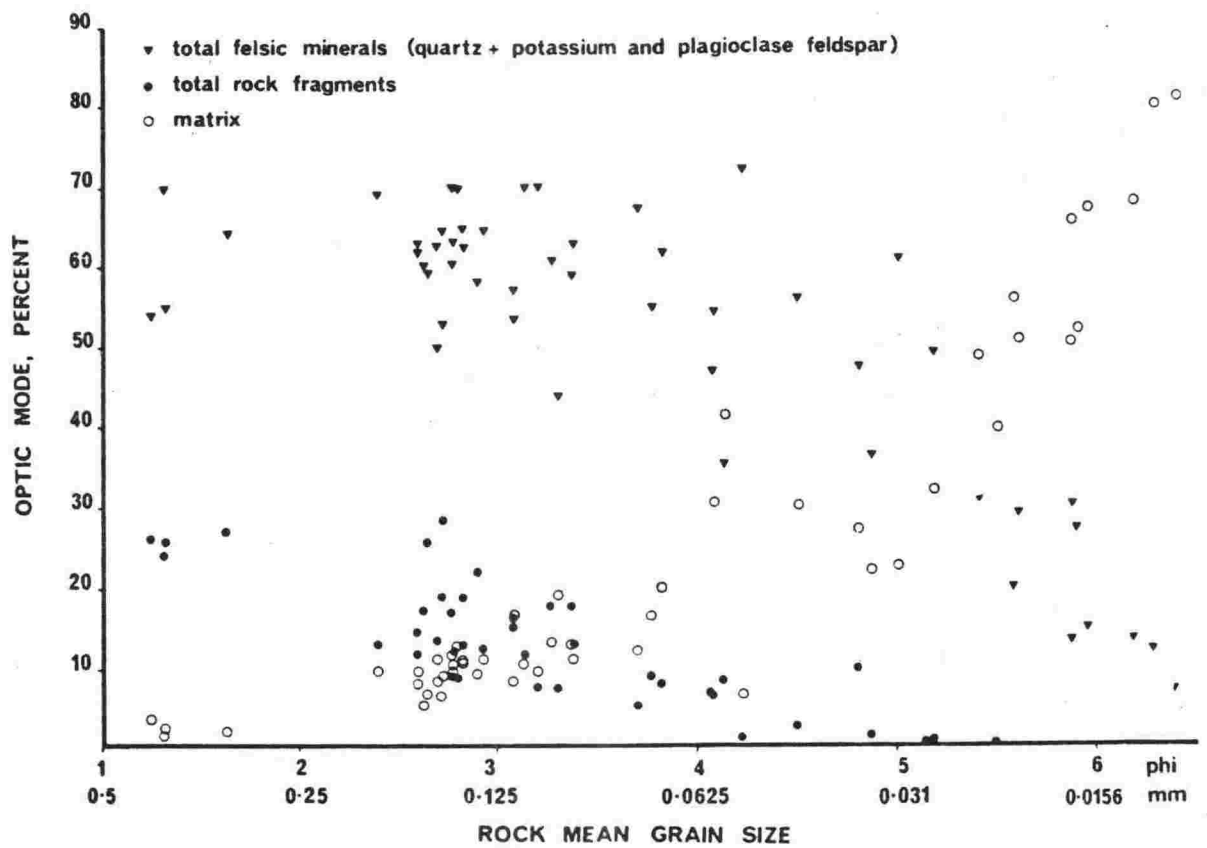
Figure 2.19 : Optically determined mineral modes show dramatic
response to rock mean grain size. Note cross-
over at 5 phi, where matrix and felsic components are subequal and
rock fragments assume negligible importance. cf. Figures 2.20 and
2.21.
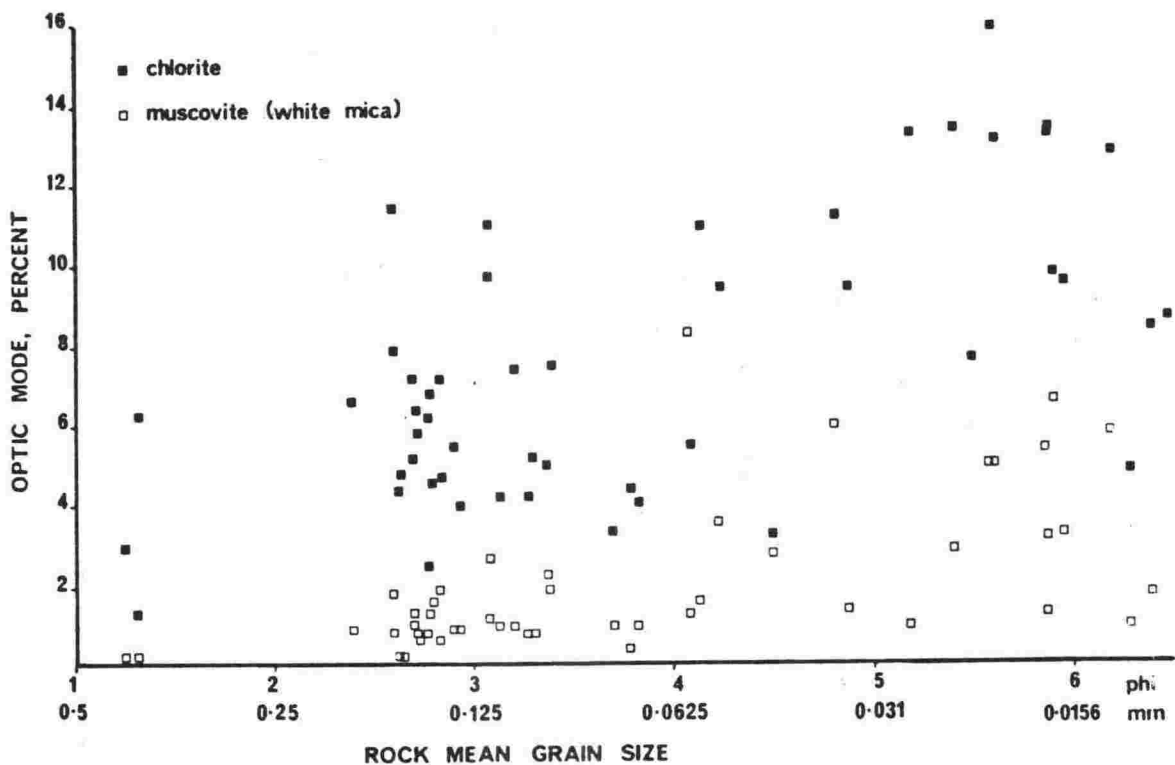
Figure 2.20 : Superior chlorite modes (optically determined), com-
pared with white mica, exist throughout Wellington
greywacke-suite rocks. Chlorite increases in approximately constant
ratio with muscovite with reduced rock mean grain size. cf. Figure
2.21.

This investigation was undertaken on an assumption that the physical proper-
ties of rock would be influenced by degrees of metamorphic change undetectable
by any other means.   Such properties as strength, hardness, and resistance
to weathering, all important in engineering use , improve with higher degrees
of metamorphism.

Whole rock samples were prepared, by crushing, in two ways:

(i)   By using a hand operated agate pestle and mortar to powder the sample.

(ii)   By using a tungsten carbide "Tema" swing mill.

A vibrating stylus was used to obtain material to establish the mineralogy
of veins and surface coatings.   For whole rock analyses, samples were selec-
ted free of veins, shears, slickensides and surface coatings to avoid
enhancing certain mineral modes and to minimise effects of differing mineral
crystallinity, strain, polytypism etc.

2.14.1   Whole rock quantitative analysis

An internal standard method of quantitative diffractometry was used (Klug and
Alexander, 1974), see Appendix 6.   Samples were prepared and run by Mr B.
Yardley.   After grinding sample powder and internal standard (LiF), a dis-
oriented (back filled) powder mount was analysed using a Siemens (X-ray
diffractometer, with nickel filtered CuKα -radiation generated from 35 kV at
20 mA and directed by a 1° beam slit and a 0.2° detection slit.   Samples were
scanned at 1 2θ/minute from 4° to 40° 2θ.   Chart speed and flow counter count
rate settings were adjusted for optimum results.   Time constant (seconds) was
adjusted with scanning speed (degrees/minutes) so that the product of the
settings was 1 or 2 (Schoen, 1962) at which values peak distortion is small
(Parrish, 1960).

Diffractograms of known minerals and the ASTM Powder Data File were used to
interpret results.   Accurate d-spacings were obtained by reference to detri-
tal quartz in the samples.   Results should be accurate to ±3 percent
(Appendix 6).

XRD indicated a higher white mica content than optical petrography had
revealed.   Presumably this resulted from altering feldspar and rock fragments

or possibly the masking of white mica by chlorite during optical examination.

Results (Table 2.9) also show the content range of minerals to be greatest for plagioclase (15 percent) with white mica (11 percent) and chlorite least (5 percent).

Composition determined by XRD indicates that felsics constitute at least 80 percent of any greywacke-suite rock, whereas composition determined optically show a maximum of 70 percent. Quartz content is also indicated to be higher by XRD than by optical means, almost doubled in greywackes and by at least 10 percent in argillites counted without a matrix category. (Table 2.6B). Optical quantification of argillite matrix showed white mica not to exceed 10 percent and its ratio to chlorite to be less than 1 (Table 2.6C), but even this is in doubt as XRD did not confirm the strong dominance of chlorite. However, trends of mineralogy with mean grain size to those established optically in section 2.13 are confirmed (Figure 2.21).

2.14.2   Semi-quantitative analysis of the whole rock fraction finer than 0.015 mm.

Diffractograms, similar whether sample powder was prepared by hand or "Tema" mill, indicated fresh greywacke and argillite to include only four main minerals; quartz, sodic plagioclase, white mica and chlorite. Of these minerals, white mica and chlorite are the most important from an engineering viewpoint since they may induce plasticity in rock fines, are soft, assume preferred orientation, are structurally weak, constitute most of the matrix material, and chlorite is chemically unstable.

Further investigation of these phyllosilicates was necessary because diagnostic peaks of both minerals at low 2θ angles mask peaks of clay minerals such as kaolinite, vermiculite, illite and chlorite mixed-layer minerals with expanding lattices, e.g. chlorite - montmorillonite, which are of importance for engineering purposes.

As phyllosilicates and clay minerals generally, have much finer natural size ranges than other detrital minerals, separation of finer materials from the powdered samples was necessary. A separation of clay minerals including phyllosilicates was required for XRD detection (Table 2.10). All methods of sample preparation were aimed at providing a well oriented, fine grained

Table 2.9 : Quantitative XRD modes for whole rock powders, arranged in order
of diminishing mean grain size.   Results should be accurate
±3 percent (Appendix 6).

Sample	M_z phi	Run	Quartz	Plagioclase	White Mica	Chlorite	Totals
HQ-17	1.317	avge. 3 runs %	48	45	4	4	101
RSS-12	2.6	1	41	52	1	5	99
		2	42	53	0	5	100
		3	44	51	0	5	100
		avge. %	42	52	<1	5	99
NC-8	3.37	1	40	49	0	11	100
		2	41	52	0	7	100
		3	44	49	0	7	100
		avge. %	42	50	0	8	100
KS-10	3.38	1	44	50	0	6	100
		2	35	59	2	4	100
		3	42	50	2	5	99
		avge. %	40	53	2	5	100
BQ-21	4.13	1	47	40	6	7	100
		2	42	45	7	6	100
		3	47	38	9	6	100
		avge. %	45	41	7	6	99
KTW-V	5.0	1	45	42	6	7	100
		2	42	50	4	5	101
		3	38	52	3	7	100
		avge. %	42	48	4	6	100
NC-15	5.49	1	38	52	5	5	100
		2	44	47	5	5	101
		3	42	48	3	6	99
		avge. %	41	49	4	5	99
WCC-8A	5.87	1	38	44	7	11	100
		2	35	48	9	8	100
		3	39	47	8	7	101
		avge. %	37	46	8	9	100
HQ-22	6.28	1	49	37	8	6	100
		2	41	38	11	11	101
		3	38	40	13	8	99
		avge. %	43	38	11	8	100
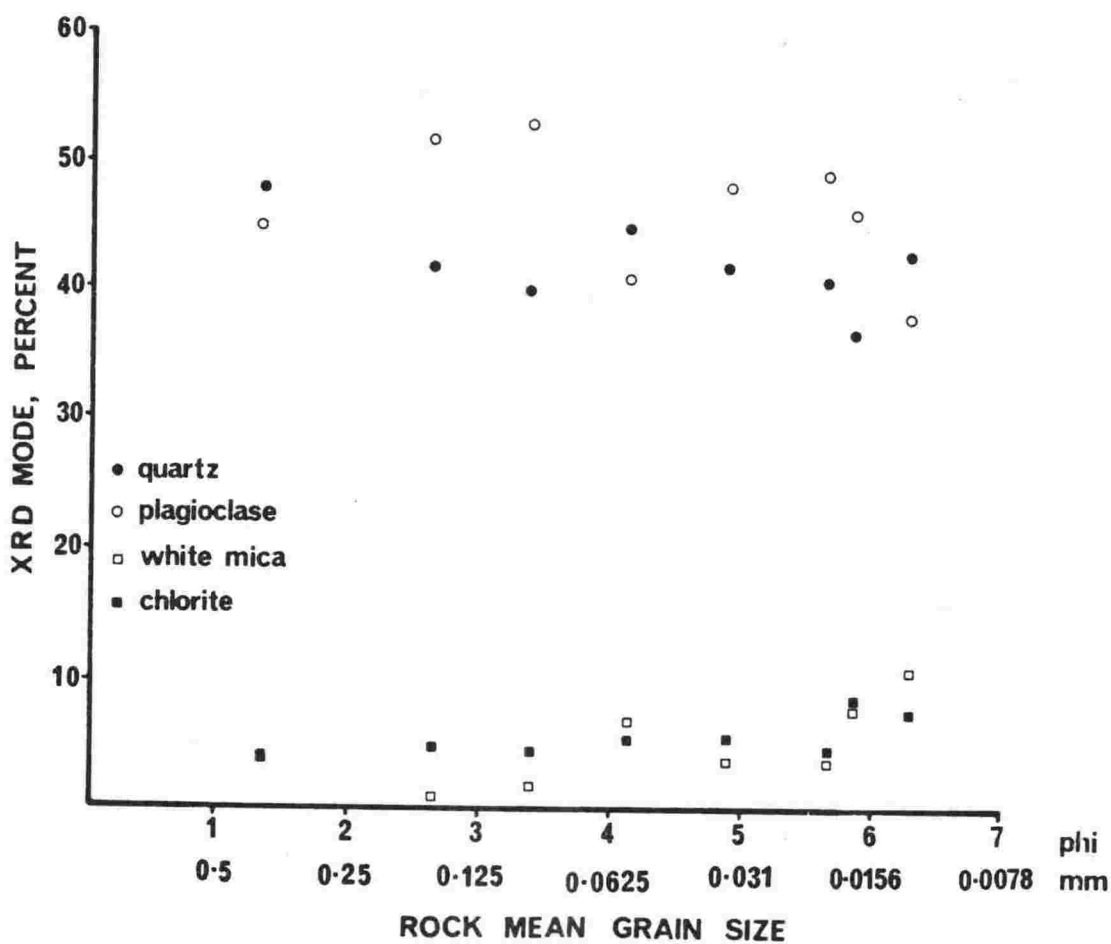
Figure 2.21 : Relationship between mineral proportions from XRD
analysis and rock mean grain size for some
Wellington greywacke-suite rocks. The trends are similar to those
found from optical petrography (Figure 2.19).

Table 2.10 : Quantitative resolution by X-ray diffraction of clay minerals and certain others in the clay fraction (<2 microns) of sedimentary materials (Cu $K\alpha$; 50 kV, 20mA, 1° scatter slit, 006" receiving slit, 10^3 cps., multiplier 1, ratemeter 4; oriented mount on tile). 1° 2θ per minute; chart speed 0.5" per minute. (after Carroll, 1970).

Mineral	Lowest percentage identifiable	Principal d spacing used for identification	$2\theta^\circ$ (approx.)
Kaolinite	5	7.13 - 7.16	12.36 - 12.4
Kaolinite, disordered	1 - 5	7.15	12.38
Halloysite, $4H_2O$	10	10.1	8.75
Halloysite, $2H_2O$	10	7.21	12.26
Mica, $2M_1$	1	9.99 - 10.4	8.85 - 8.80
Illite, mixed layer 1b mica polytype	5	10.16	8.70
Biotite	1	10.1	8.77
Vermiculite	5	14.2	6.22
Smectite group, (montmorillonite)	10	15.4 (variable)	5.7
Chlorite, Mg	1	14.1 - 14.2	6.27 - 6.22
Chlorite, Fe	10	14.1 - 14.2	6.27 - 6.22
Quartz	1	3.34	26.66
Orthoclase feldspar	5	3.25 - 3.28	27.4 - 27.16
Plagioclase feldspar	5	3.17 - 3.18	28.14 - 28.0
Calcite	5	3.08	29.47
Ferric oxide, crystalline or amorphous mineral coatings	<1		

sample over a large area of the glass slide, mounted so that basal d-spacings of minerals at low 2θ angles would give enhanced diffractogram peak heights i.e. maximum intensities. Best results were obtained from "Tema" ground whole rock samples separated by settling through water (Sameshima 1977). From nomographs of particle settling times through water (Tanner and Jackson, 1948) the resultant oriented material was less than 0.015 mm in size, entirely covering the slide (necessary for low angle diffractometry, Soong, pers. comm.), with a uniform layer 0.015 to 0.03 mm thick (Schoen, 1962).

Diffractograms of these fine fractions were used to obtain semi-quantitative data, by utilising peak heights above background to establish relative peak intensities (Moore, 1968) at 28° 2θ, 26.8° 2θ, 12.5° 2θ and 8.8° 2θ, representing quartz, K-feldspar, plagioclase, chlorite and sericite respectively. Adjustments were calculated directly from intensity values, some of the usual uncertainties of clay phyllosilicate semi-quantitative analysis from XRD, being reduced by the nature of chlorite and sericite - they are not as variable in behaviour as other clay minerals (Soong, pers. comm.).

Relative abundancies of all five minerals are shown (Table 2.11) though quartz and feldspar relative abundancies are important only for rocks finer than, say, 5 phi (0.031 mm). The results confirm the optic modal data on chlorite content over the range in rock mean grain size represented. Sericite, too, shows increase with reduced mean grain size, but in a more linear fashion and in direct antipathy with plagioclase. The reduction in K-feldspar parallels the trend for this mineral established by optical means. Quartz shows a scattered trend, averaging about 40 percent for any mean grain size. This may reflect a more perfect crystalline habit of what must be mostly detrital quartz, or more reasonably, indicates quartz to occupy larger size fractions in coarser rocks and to be more easily removed during sample preparation.

The fine mineral separates agree extremely well with the relative order of abundance of argillite matrix contents (determined optically) except the relative dominance of chlorite over quartz, the two most abundant matrix components in argillite. XRD data are probably reflecting absorption characteristics of mostly authigenic chlorite and better crystallinity of detrital quartz.

Table 2.11 : Relative abundancies of main minerals, determined from diffractogram peak height intensities of minus 0.015 mm whole rock oriented, sedimented samples.

Sample	M_z, phi	Relative diffractogram Peak heights					peak height Sum	Recalculated peak heights, percent					Totals	Remarks
		Quartz	Plagioclase	K-feldspar	Chlorite	White mica		Quartz	Plagioclase	K-feldspar	Chlorite	White mica		
DC-6	1.25	10.8	4.1	2.1	4.2	2.9	24.1	44.8	17.0	8.7	17.4	12.0	99.9	
HQ-17	1.317	14.6	12.0	4.2	4.3	3.2	38.3	38.1	31.3	11.0	11.2	8.4	100.0	Laumontite also
SJ-3₁	1.32	6.0	3.2	1.5	8.2	3.3	22.2	27.0	14.4	6.8	36.9	14.9	100.0	
KTW-13	2.4	12.8	8.8	3.4	5.5	2.8	33.3	38.4	26.4	10.2	16.5	8.5	100.0	
HQ-21	2.7	11.1	7.8	4.2	6.4	3.9	33.4	33.2	23.4	12.6	19.2	11.7	100.1	expanding 14Å peak?
BQ-V	2.73	10.1	4.7	2.0	6.2	3.1	26.1	38.7	18.0	7.7	23.8	11.9	100.1	
BQ-IXA	2.9	10.9	4.8	2.5	5.5	3.4	27.1	40.2	17.7	9.2	20.3	12.6	100.0	
OB-21	2.93	9.7	5.9	3.5	5.5	3.4	28.0	34.6	21.1	12.5	19.6	12.1	99.9	
HQ-19	3.08	12.8	6.4	3.3	6.1	3.5	32.1	39.9	19.9	10.3	19.0	10.9	100.0	
KS-2	3.27	8.2	3.3	2.3	3.8	2.1	19.7	41.6	16.8	11.7	19.3	10.7	100.1	expanding 14Å peak?
BQ-iii	3.78	11.8	6.2	2.2	4.4	4.0	28.6	41.3	21.7	7.7	15.4	14.0	100.1	calcite also
KTW-G	4.07	7.4	3.7	2.0	4.5	5.2	22.8	32.5	16.2	8.8	19.7	22.8	100.0	
RSS-iii	4.08	8.6	4.2	2.1	6.1	4.0	25.0	34.4	16.8	8.4	24.4	16.0	100.0	
BQ-21	4.13	9.2	3.0	1.5	4.0	3.0	20.7	44.4	14.5	7.3	19.3	14.5	100.0	very ragged feldspar peak
KTW-i	4.23	10.0	4.4	1.8	3.3	3.1	22.6	44.3	19.5	8.0	14.6	13.7	100.1	ragged feldspar peak
KTW-i(R)	4.23	9.7	4.3	2.1	3.1	2.3	21.5	45.1	20.0	9.8	14.4	10.7	100.0	
DC-8	4.5	13.1	4.4	2.4	5.2	2.8	27.9	47.0	15.8	8.6	18.6	10.0	100.0	
BQ-i	4.87	7.1	2.8	1.3	3.4	4.1	18.7	38.0	15.0	7.0	18.2	21.9	100.1	calcite also
RSS-ii	5.18	5.0	2.7	1.4	6.5	4.7	20.3	24.6	13.3	6.9	32.0	23.2	100.0	
HQ-26	5.4	7.0	3.0	1.8	2.6	2.1	16.5	42.4	18.2	10.9	15.8	12.7	100.0	
HQ-24	5.58	8.8	1.8	1.2	4.5	3.3	19.6	44.9	9.2	6.1	23.0	16.8	100.0	expanding 14Å peak?
OB-W	5.6	11.7	1.9	1.0	5.4	5.3	25.3	46.3	7.5	4.0	21.3	21.0	100.1	ragged feldspar peak
HQ-20	5.87	7.0	2.3	tr.	4.2	3.4	16.9	41.4	13.6	tr.	24.9	20.1	100.0	ragged feldspar peak
HQ-18	5.95	9.0	1.8	1.0	4.0	3.4	19.2	46.9	9.4	5.2	20.8	17.7	100.0	ragged feldspar peak
BQ-vii	6.18	9.5	2.2	1.3	6.5	6.0	25.5	37.3	8.6	5.1	25.5	23.5	100.0	expanding 14Å peak?
HQ-22	6.28	19.4	4.6	3.2	9.5	7.9	44.6	43.5	10.3	7.2	21.3	17.7	100.0	expanding 14Å peak?
OB-13	6.39	6.0	1.4	tr.	3.9	4.5	15.8	38.0	8.9	tr.	24.7	28.5	100.1	

tr = trace

From Figure 2.22 it may be concluded that orthoclase has a relatively smaller grain size population than plagioclase, in greywackes finer than about 4 phi (0.0625 mm) mean grain size. It is unlikely that the relatively low plagioclase to K-feldspar ratios, seen in Figure 2.22 in rocks of finer mean grain size, have been induced by comminution of the larger K-feldspar grains (later discussed in section 2.14.3). The altered condition of finer plagioclase could enhance this trend.

A full discussion of mineral characteristics from XRD data has been provided by McKean (1976).

2.14.3   Degree of phyllosilicate crystallinity

Weaver (1960) showed that crystal ordering in phyllosilicate minerals increases with diagenesis and metamorphism. Burst (1959) studied the trend in chlorite in the Eocene of Texas and Flawn *et al.* (1961) incorporated Weavers work to quantify crystallinity of illite and relate it to metamorphism established by microscope study of slabs from the Ouachita Mountains, Texas, as follows

Degree of metamorphism	Sharpness ratio
Low-grade	12.1
Weak to very weak	6.3
Incipient to weak	4.5
Incipient	2.3
Unmetamorphosed Stanley	2.3
Unmetamorphosed Atoka	1.8

The most abundant references are for illite (Kubler, 1967). The crystallinity of illite or mica polymorphs increases almost universally with temperature and pressure. A "muscovite" with relatively small d-spacing is easier to study in this regard than chlorite as possible variations are less numerous and better known than in the chlorite group and white micas occur more frequently in sedimentary rocks than chlorite. Consequently, most studies of subtle diagenetic/metamorphic change in sediments have utilised the crystallinity of white mica polymorphs, usually illite, since it undergoes greater morphologic changes with temperature/pressure difference than other white mica types.
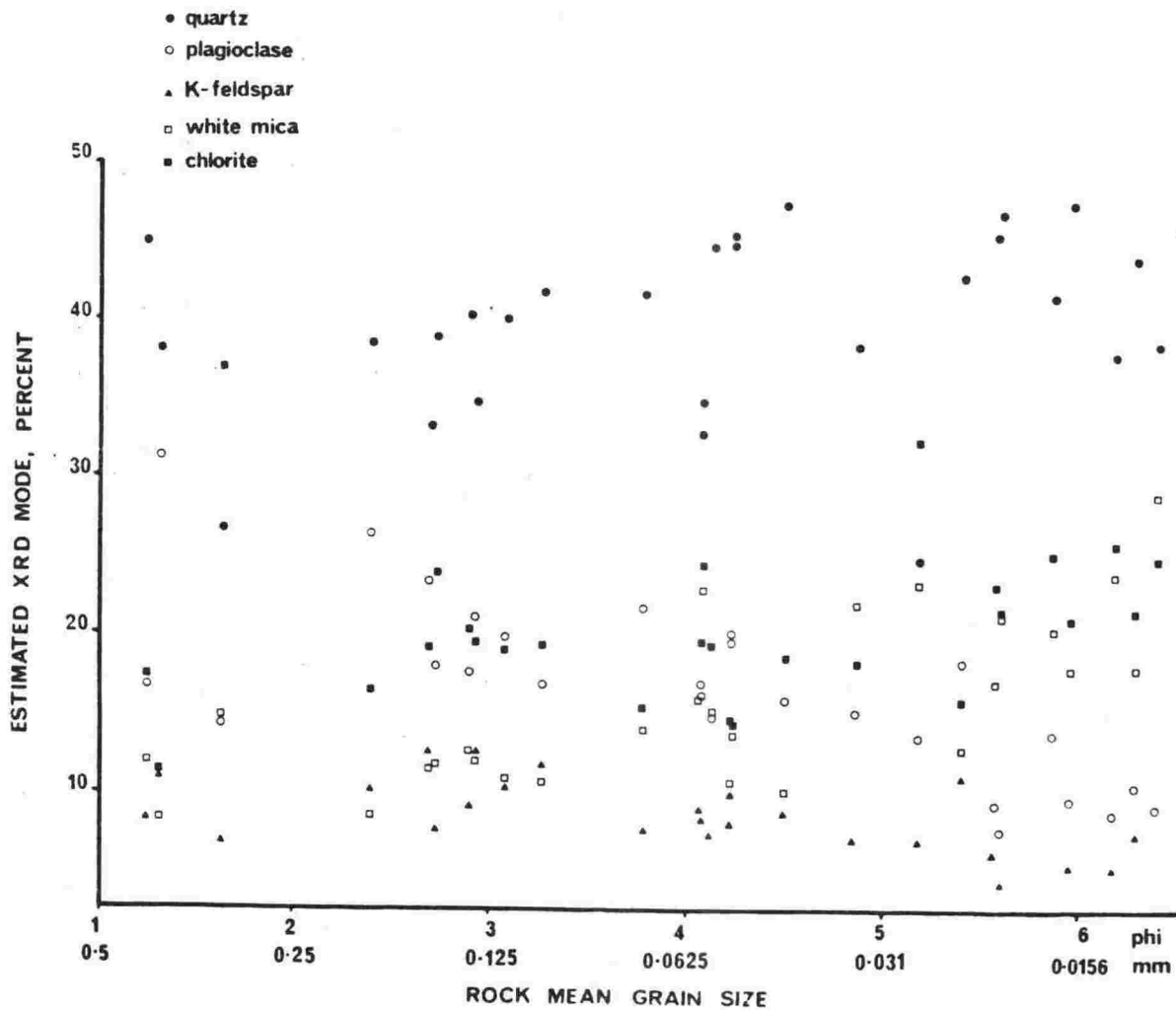
Figure 2.22 : Relationship of mineral abundance, from whole rock
powder fractions finer than 0.015 mm, with rock
mean grain size.   The trend reflects modal analyses obtained by
quantitative XRD and optical determination.   cf.   Figures 2.19
and 2.21.

For this study the sharpness ratio method of Weaver (1960) was employed using the 10Å (8.8° 2θ) diffractogram peak of oriented sericite in the less than 0.015 mm size whole rock fraction. Since peak intensities are related to both grain size (Carroll, 1970), and crystallite size (Rau, 1963) sampling rock mineral separates of very small grain size may cause a loss in resolution.

Generally, well developed (well crystallised) phyllosilicates afford stronger, more intense X-ray reflections than poorly crystalline ones.

To determine the relative sharpness of the 10Å peak measurement was made from the baseline of the peak vertically to its tip and from the baseline of the peak to the point where a 10.5Å vertical line intersected the side of the peak. The ratio of these two measurements give a measure of the relative sharpness of the 10Å peak (Figure 2.23). As the shape of the 10Å peak is comparatively similar, it is not necessary to measure values for both sides of the peak and calculate a Kurtosis value.

Kubler (1967) recommended a change in the method of Weaver (1960) i.e. that a single measurement be made of peak width at a point half way up the 10Å peak. This is the method Rau (1963) adopts for measuring crystallite size. However, Weaver's method was used in this study as Kubler's method ignores peak asymmetry which is a crystallinity indicator (Carroll, 1970).

As a check, Kubler's method was used to measure the 7Å (12.5° 2θ) chlorite peak for the reasons below:

(i)   This was the most intense peak in the low angle 2θ range making it easier to measure.

(ii)   Chlorite crystallinity changes with diagenetic/metamorphic grade in the same manner as white mica.

(iii)   The 7Å peak was more symmetrical than the 10Å peak.

(iv)   For a restricted particle size range (effectively a maximum of about 0.015 mm) width at half-peak height should be a reasonable indicator of crystallinity.

(v)   The 7Å peak is purely a chlorite reflection.
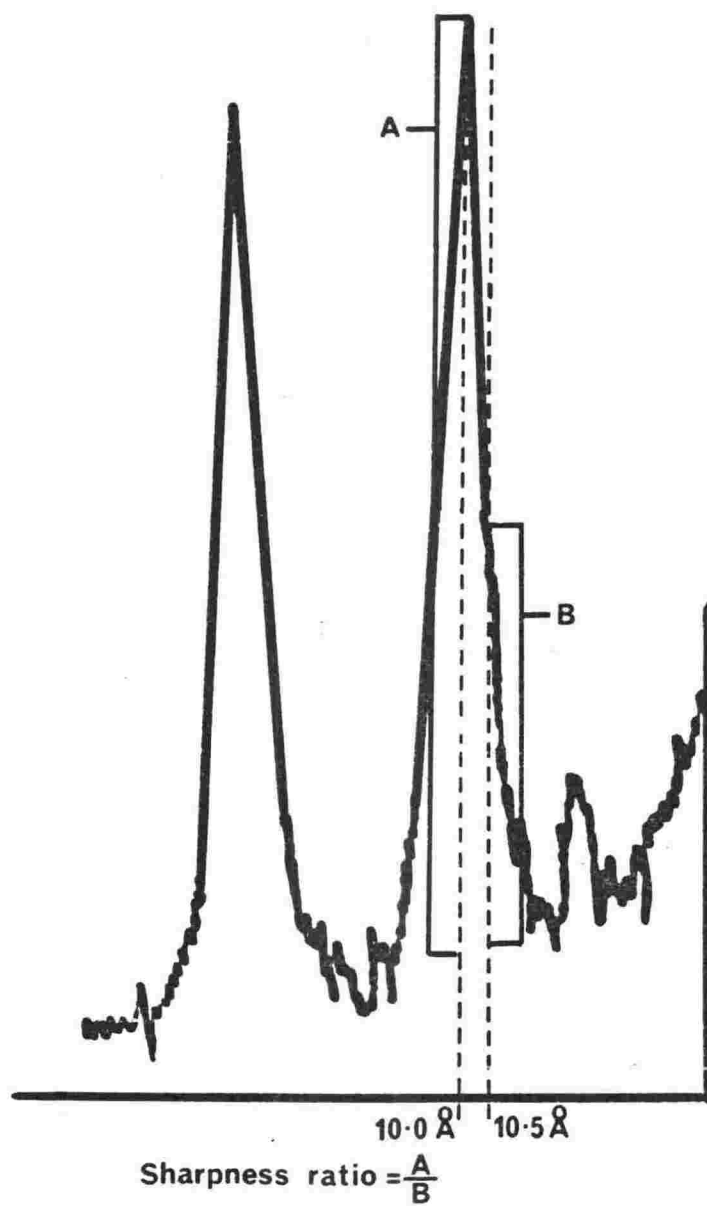
Figure 2.23 : Part of an X-ray diffractogram showing how relative
sharpness of the 10Å illite peak is measured
(after Weaver, 1960).

The results (Tables 2.12, 2.13 Figures 2.24, 2.25) show the same trend for the
two minerals measured by different means,i.e. the crystallinity of phyllo-
silicates in the finer than 0.015 mm (less than 7 phi) fraction is lower in
rocks of smaller mean grain size.

To check both methods, five additional diffractograms were made from material
settled to provide oriented slides of phyllosilicates with grain sizes of
less than 1.5 μm (less than 9.5 phi).   The trend towards decreased crystal-
linity with reduced rock mean grain size is even more evident (Figure 2.24,
2.25).

The trend observed is not as might be expected nor is it apparent from a
casual visual assessment of the diffractograms (Figure 2.26).   It can be
argued that rocks with reduced mean grain size have increased internal surface
areas, of benefit to diagenetic/metamorphic reactions, bringing argillaceous
rock to metamorphic equilibrium relatively quickly and more completely than
coarser grained greywackes.

The trends shown could indicate a degradation of phyllosilicates within argil-
laceous rocks (e.g. from the strenuous action of the "Tema" mill) but several
lines of evidence suggest that differences between rocks are real and not due
to sample preparation.

(i)   MacKenzie and Milne (1953) show considerable grinding (8 hours) is
required to alter mica crystallinity significantly in an agate mill.   Samples
were ground in a "Tema" mill for only one minute.

(ii)   The relative lack of introduced mineral materials in argillites may be
due to reduced permeability (Bucke and Mankin, 1971) during diagenesis and
metamorphism.   This decrease in permeability does not allow percolation of
fluids which aid the solution/deposition of minerals.   These fluids are
responsible for the recrystallisation of other minerals and if their passage
is restricted,recrystallisation is also reduced.   Then,in what were initially
fine argillites, phyllosilicates may be expected to be relatively poorly
developed in spite of large surface areas.

Maintenance of this situation after lithification is due to rock incompetence.

Table 2.12 : Sharpness ratio, or peakedness, of the 10Å white mica peak measured from diffractograms by a method after Weaver (1960). Each measurement was an average of at least three sets of data from diffractograms of one slide. Those values marked (?) were not included in means. Five determinations, listed at the bottom of the table, were included as the method was not expected to operate where small peak intensities were encountered - a peak may occupy less physical space on a diffractogram than is provided between 10Å and 10.5Å points. To increase peak intensities a finer sediment (oriented) was used, i.e. $<1.5\mu m$ - the five samples at base of the table.

Sample	M_z phi	Peak height measurement A	B	A:B ratio	Mean A:B ratio
DC-6	1.25	40	6	6.67	
		28	8.5	3.3	
		27	6.5	4.2	4.42
		42	15	2.8	
		36	7	5.14	
HQ-17	1.317	33	5	6.6?	
		72	16	4.5	4.0
		67	19	3.5	
SJ-3$_1$	1.32	33	5	6.6	
		32	3	10.7	
		39	6.5	6.0	7.38
		31	5	6.2	
KTW-13	2.4	27	4	6.8	
		30	7	4.3?	
		42	5	8.4	7.4
		28	4	7.0	
HQ-21	2.7	39	9.5	4.1	
		33	9	3.7	
		36	9	4.0	4.0
		40	10	4.0	

Table 2.12 : (continued)

Sample	M_z phi	Peak height measurement		A:B ratio	Mean A:B ratio
		A	B		
BQ-V	2.73	30	8.5	3.5	
		27	5.5	4.9	
		28	5.5	5.1	4.4
		29	7	4.1	
BQ-IXA	2.9	33	7	4.7	
		24	6	4	5.13
		20	3	6.7	
OB-21	2.93	33	7	4.7	
		72	14	5.1	4.6
		70	18	3.9	
HQ-19	3.08	35	12	2.92	
		40	12	3.33	
		40	10	4.0	3.36
		35	11	3.18	
KS-2	3.27	20	2	10.0?	
		59	9	6.6	5.65
		56	12	4.7	
BQ-iii	3.78	40	8.5	4.7	
		100	18	5.6	5.6
		110	17	6.5	
KTW-G	4.07	49	5.5	8.9	
		127	37	3.4	7.5
		132	13	10.2	
RSS-iii	4.08	40	4.5	8.9?	
		97	26	3.7	4.3
		106	22	4.8	
BQ-21	4.13	29	6	4.8	
		78	18	4.3	4.6
		65	14	4.6	

Table 2.12 : (continued)

Sample	M_z phi	Peak height measurement A	B	A:B ratio	Mean A:B ratio
KTW-i	4.23	30	3	10.0?	
		73	15	4.9	4.8
		63	13.5	4.7	
KTW-i(R)	4.23	23	4	5.8	
		22	3.5	6.3	
		27	4.5	6.0	5.75
		22	4.5	4.9	
DC-8	4.5	28	8	3.5	
		35	11	3.2	3.6
		42	10	4.2	
BQ-i	4.87	41	12	3.4	
		87	28	3.1	3.2
		93	31	3.0	
RSS-ii	5.18	47	9	5.2	
		127	30	4.2	4.6
		132	30	4.4	
HQ-26	5.4	20	4	5.0	
		41	12	3.4	4.5
		67	13	5.2	
HQ-24	5.58	33	9.5	3.5	
		85	32	2.7	4.3
		86	26	3.3	
OB-W	5.6	52	14	3.7	
		122	43	2.8	3.0
		125	48	2.6	
HQ-20	5.87	33	7	4.7	
		78	22	3.6	3.7
		86	30	2.9	

Table 2.12 : (continued)

Sample	M_z phi	Peak height measurement A	B	A:B ratio	Mean A:B ratio
HQ-18	5.95	34	12	2.8	
		43	15	2.87	
		41	11	3.73	3.1
		36	12	3.0	
BQ-vii	6.18	60	16	3.75	
		67	18	3.72	3.9
		63	15	4.2	
HQ-22	6.28	38	11	3.5	
		82	23	3.6	3.5
		79	24	3.3	
OB-13	6.39	44	9	4.9	
		41	9.5	4.3	
		42	10	4.2	4.3
		32	9	3.6	
HQ-17	1.317	32	5	10.6	10.6
KTW-13	2.4	53	14	3.8	3.8
KS-2	3.27	40	6	6.7	6.7
DC-8	4.5	40	13	3.1	3.1
HQ-22	6.28	105	43	2.4	2.4

Table 2.13 : Relative crystallinity from peak widths at half peak height of the chlorite 7Å peak. The determinations are from the less than the 0.015 mm fraction of whole rock powders. The five results at the end of the table were determinations from the <1.5 μm fraction. (Kubler's method).

| Sample | Run | | | Mean |
	1	2	3	Value
DC-6	3.0*	3	2.25*	2.9
HQ-17	2.5	3	2.5	2.67
SJ-3$_1$	2.5*	2.5	3	2.63
KTW-13	3.5*	4.5	3	3.63
HQ-21	3.0*	3.5	2	2.88
BQ-V	3.5*	2.5	3	3.13
BQ-IXA	3.0*	3.5	3	3.13
OB-21	2.5	3	3	2.8
HQ-19	3.5*	3.5	3.5	3.5
KS-2	3.5	4	3	3.5
BQ-iii	2.5	2.5	3	2.67
KTW-G	3.5	4	4	3.8
RSS-iii	2.5	3	2.5	2.67
BQ-21	3	4	4	3.67
KTW-i	3.5	3	3.5	3.3
KTW-i(R)	2.25*	2.5	2.5	2.38
DC-8	3.0*	3	-	3.0
BQ-i	2.5	2.5	2.5	2.5
RSS-ii	3	3.5	3	3.17
HQ-26	3.5	4	3	3.5
HQ-24	3	4	3.5	3.5
OB-W	3	3.5	4	3.5
HQ-20	4	4.5	3	3.8
HQ-18	2.75*	3.5	4	3.25
BQ-vii	3.0*	-	3.5	3.17
HQ-22	3.5	4	3	3.5
OB-13	3.25*	3	3.5	3.25

* Obtained by duplication of run.

Table 2.13 : (continued)

Sample	Run			Mean value
	1	2	3	
HQ-17	3	—	—	3
KTW-13	4	—	—	4
KS-2	3.5	—	—	3.5
DC-8	4.5	—	—	4.5
HQ-22	4.5	—	—	4.5
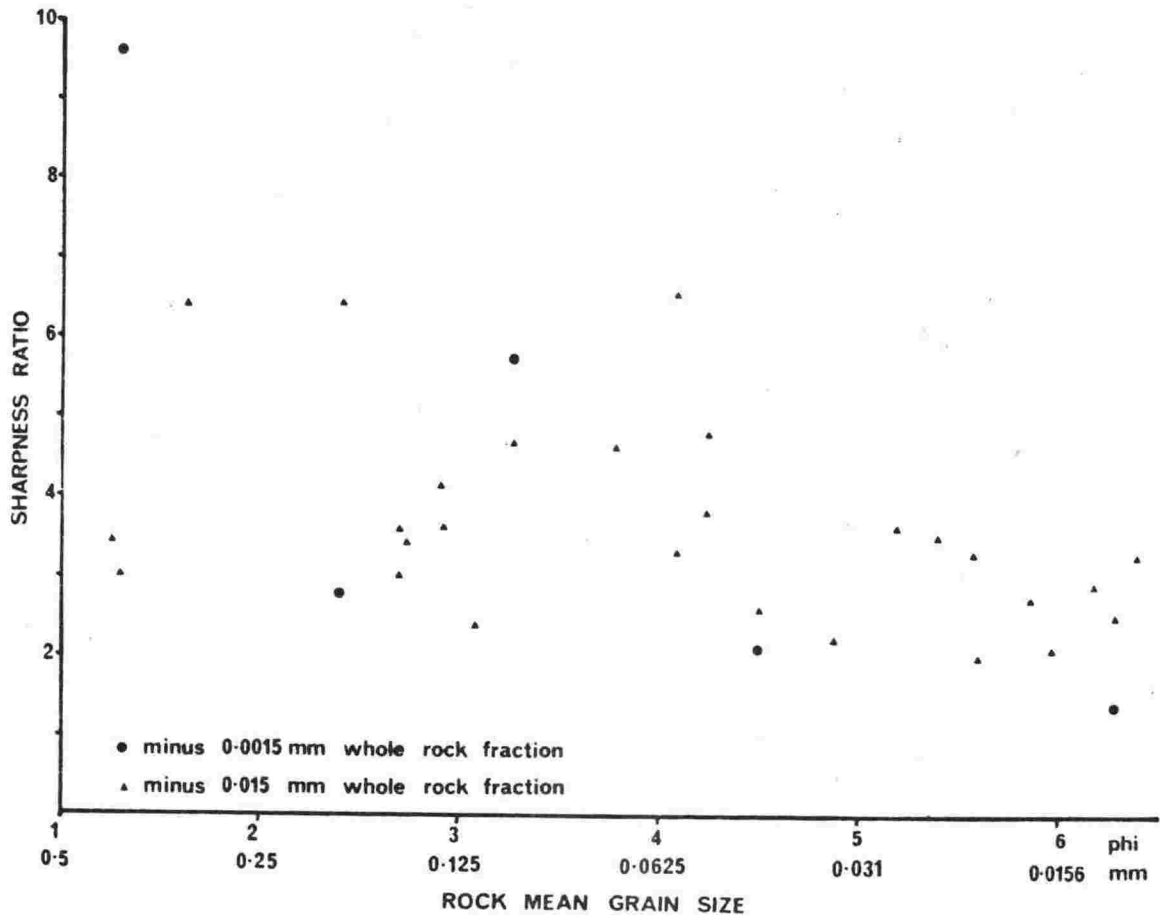
Figure 2.24 : Sharpness ratio of illite (Weaver, 1960) indicates
that metamorphic change has taken place more com-
pletely in coarser grained greywacke-suite rocks. Circular points
are values for whole rock powder fractions finer than 1.5 µm, trian-
gles for whole rock powder fractions finer than 0.015 mm.
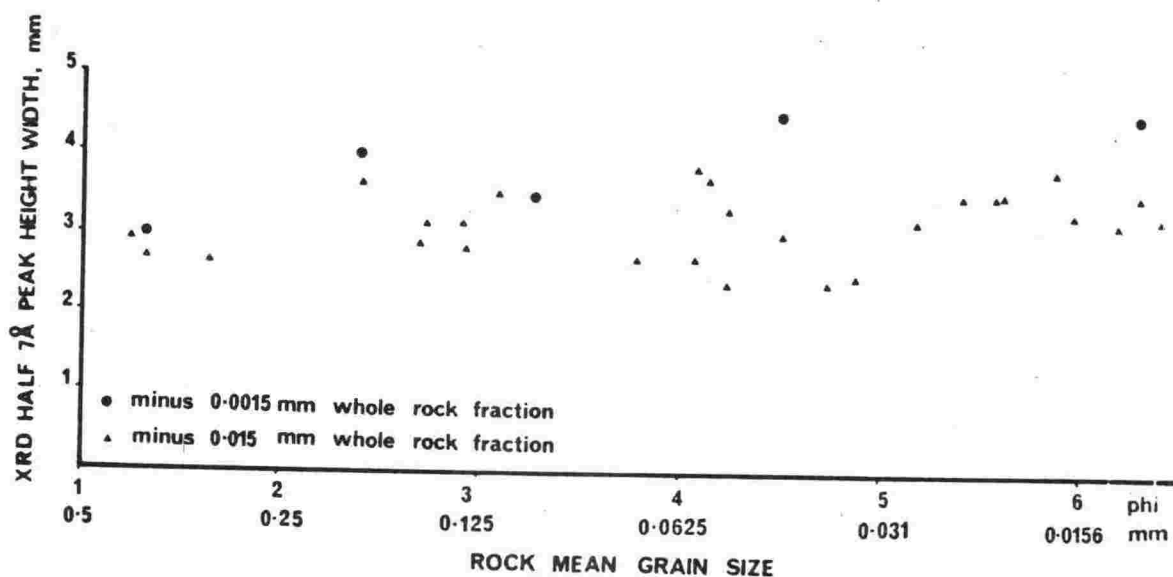
Figure 2.25 : Relative crystallinity (Kubler, 1967) of chlorite
(7Å diffraction peak) assessed by measuring peak
width at half peak heights. Circular points finer than 1.5 μm.,
triangles for whole rock powder fractions finer than 0.015 mm.
Increasing values indicate reduced crystallinity.
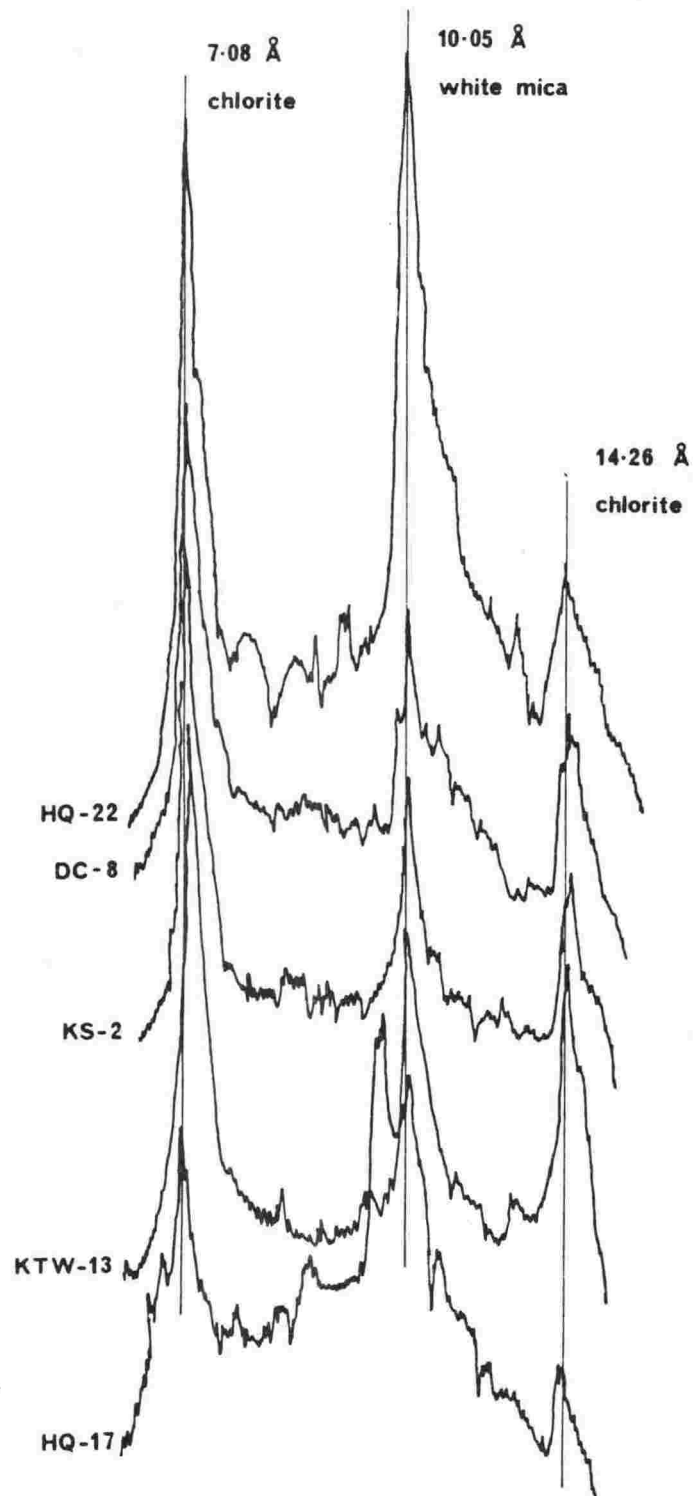
Figure 2.26 : X-ray diffractogram of whole rock materials finer
than 1.5 μm from five lithogies assembled to show
contrast between peak intensity and sharpness ratio or half peak
height widths, i.e. relative mineral abundance and crystallinity.

(iii)   The fineness of material to emerge after "Tema" crushing is the same
whether the crushed rock is a greywacke or argillite.   Indeed, argillites
sometimes emerged noticeably more "gritty" but they tend to smear the mill
more than greywackes and smeared material was not included in the powder
sample.   Smeared material probably acted as a buffer minimising metal-to-
metal contact within the mill.

2.15   Fissility

Some argillites display fissility, the ability to split easily along closely
spaced parallel planes.   This influences the physical and chemical breakdown
of the rock and so features of fissility in the Wellington greywacke-suite
rocks are reviewed below.

Ingram (1953) classified mudrocks by fissility type i.e. massive, flaggy and
flaky.   The Wellington argillites fit the flaky category, described as rocks
that "split along irregular surfaces parallel to bedding into uneven flakes,
thin chips and wedge-like fragments whose length seldom exceeds 3 inches
(76 mm)" and they are "predominantly grey or grey-black in colour".

From the literature, several reasons have been given for fissility in mud rocks:
fabric, organic material, felsic grain content, mineral cement content, sand
and silt size particle content (Ingram, 1953);   overburden pressure applied to
newly deposited clay material and the amount of liquid and rigid water in the
clay at the time of application of pressure (O'Brien, 1963).   The interface
between zones of preferentially oriented grains and organic material, inter-
faces between zones of randomly oriented grains and organic material, and
zones of preferentially oriented grains have been shown by Gipson (1965) to
provide fissile planes.   More recently Blatt *et al*. (1972) have claimed that
type and crystallinity of clay minerals is important, fissility being favoured
by higher proportions of well crystallised clays with bonding sites on surfaces
rather than edges (Kaarsberg, 1959).   Spears (1976) has shown how laminations
within mudrocks can influence fissility and states the importance of preferred
orientation of clay minerals may have been over estimated.   Indeed, many
inconsistencies arise, most "controls of fissility" not being universally
applicable.

The fissile argillites of Wellington do possess two features that distinquish them from the non-fissile argillites; stronger grain orientation and better-formed more coarsely crystalline phyllosilicates.

Fissility appears to be independant of rock mean grain size (Ingram, 1953), though some fissile argillites have larger phyllosilicate minerals. Fissility is enhanced by weathering (Ingram, 1953), splitting more easily and producing a flakier form in resultant particles (section 2.12; Appendix 25).

The presence of carbonaceous (organic) material in a concentrated seemingly structureless layer (Gipson, 1965), was conducive to controlling fissile planes but a continuity of these materials was required (IB-13A, Plate 2.5).

Fissility can occur within a layer at the interface between oriented fine grained phyllosilicate materials and non-oriented or poorly oriented, felsic, coarser grained materials.

All of the above features of fissility are consistent with general descriptions by White (1961).

2.16   Weathering

Convenient classifications of weathering variation observed in greywacke-suite rocks have been based on a simple grading system (Raisbeck, 1973; Marshall, 1974; Riddolls and Perrin, 1975), the nomenclature being shown in Table 2.14.

Although this study was based on fresh samples, some weathered samples were examined. Microscopic study was made of incipient chemical weathering, taken as that stage between categories 1 and 2 and often observable only by microscopic means in category 1 (Table 2.14). This is important for engineering considerations as it indicates the order of destruction of the various minerals, where it is concentrated and at what rate it proceeds.

While it is convenient to differentiate between physical and chemical weathering, it is improbable that either process acts alone (Sparks, 1960). Early experiments by Barton (1916), Blackwelder (1925) and Griggs (1936) showed the importance of chemical weathering in physical processes. Various physical

Table 2.14 : Categories of greywacke-suite rock weathering (after Marshall, 1974), based on handspecimen colour changes and strength loss.

Category 1   Fresh rock: Dark grey or dark blue-grey. Signs of weathering absent, apart from slight surface staining along open joints and fractures.

Category 2   Slightly weathered: Discolouration along joints and fractures. Grey-brown colour penetrates less than 10 mm.

Category 3   Moderately weathered: Rock decomposition will advanced. Weathering aureole around blocks, fresh material at centre of broken fragments. Clay materials form, especially along joint and shear planes. Rock appreciably weakened by weathering - is easily shattered by hammer blow.

Category 4   Heavily weathered: Equivalent to "rotten rock" of contractors and farmers. Colour varies from brown, through red-brown and lighter yellow-brown. No fresh material remains. Rock able to be broken by hand. An abundance of clay minerals. Rock retains original structures and is strong enough to maintain a steep cut face.

Category 5   Completely weathered: Material approaches soil in character (saprolite). Crushes between fingers. Original structure is lost and material will not maintain a steep face.

and chemical processes and their sequential developments have been discussed elsewhere (Rowe, 1979; Appendix 25).

Factors influencing weathering of any rock were listed by Sparks (1960) as follows:

(i)   Mineral composition.   Of the four main component minerals of grey-wacke-suite rocks Marshall (1974) indicated chlorite to be most vulnerable, an observation made also by Goldich (1938).

(ii)   Texture.   Under certain conditions,coarse grained rocks should weather more rapidly than fine grained rocks of the same mineral composition.

(iii)   Effects of minor structures.   Minor structures in greywackes,and especially in argillites, dominate initial (and direct subsequent) weathering patterns once rocks are unconfined.   Such effects as lamination (Spears, 1976), preferred orientation (Hedberg, 1936; Ingram, 1953), recemented shears, microcracking and veining are included in this category; any feature allow-ing ingress of chemical weathering agents or increasing surface area also increases rates of chemical weathering.

(iv)   Climate.   This is assumed to have been consistent for the Wellington greywacke-suite rocks over the period of development of a natural weathering profile (10,000 years).

(v)   Time.

Microscopic examination shows the association of the above factors clearly. Minor structures, notably veining and microcracking, play the most obvious role and are now discussed in some detail.

2.16.1   Veining

Some veins, notably those of prehnite (OB-21), allow access for weathering agents.   Bright yellow and yellow-brown to black weathering products (semi-opaque in polarised light) were observed adjacent to vein boundaries.   The materials were fine grained (about 0.001 mm) and massed at the vein boundary in a zone about 0.03 mm wide but extended up to 0.7 mm where colouration was patchy and consisted of red-brown, isotropic discontinuous blebs and

aggregates, brown-red in reflected light.   Within the veins some shapeless

and ramifying material was observed as an extremely fine layer between grains

(less than 0.006 mm) but obliquity of grain contacts increased the apparent

width observed - a problem solved only with the use of a universal stage

(Glover, 1964).

2.16.2   Microcracking

Microcracks are here considered to be open cracks of such a size that on a

smooth dry rock surface they are invisible to the naked eye (less than

0.004 mm wide).   On wetting, such cracks become visible (in argillaceous

rocks) as a relatively wetter, or darker linear feature, the width of which

may vary visibly by application of hand pressures.   Due to coarser texture,

microcracks in greywackes may be wider than those in argillite and still be

invisible to the naked eye.   In any case they are much fewer and less persis-

tent.   They are more linear in greywackes than argillites, with local aber-

ations due to textural considerations.   Grains of quartz and feldspar are

skirted rather than broken, the path of the crack often including the long

axes of chlorite grains, with less than 0.001 mm displacement across the

crack.   Red-brown to black isotropic limonite may accumulate in cracks with

the onset of weathering.

2.16.3   Lamination, preferred orientation, recemented shears

Quartz veins in greywackes of the thin-bedded lithofacies and argillites may

be relatively sinuous (ptygmatic).   Associated with these are ubiquitous

microcrush or shear zones, evident as linear concentrations of foliated matrix

and highly comminuted fabric minerals to 0.12 mm.   Calcite, prehnite, zeolite

or authigenic albite are not associated with these features.   Shear zones are

up to 0.35 mm wide but are often not obvious other than at low magnification,

so subtle are the changes in matrix orientation and grain size reduction.

Generally colour value is increased in these zones, often black, with grains

about 0.005 mm in size.   White mica is occasionally associated with both

veins and shear zones.

The microcrush zones are here termed recemented shears, implying small size,

physical continuity of the rock across them, and comminution.   They are very

common in argillites and, in these rocks, are almost undetectable with the naked

eye (OB-12).   They formulate conditions which may promote parting and/or

weathering of the rocks (RSS-i).

Laminations, preferred orientation and recemented shears are all minor structures, constituting a linear plane of weakness.   Porous organic matter with associated chlorite and pyrite is concentrated along laminations.   Preferred orientation arranges chlorite so that weathering may extend along cleavage planes which are oriented end-to-end.   Laminations originate from successive differences in grain size of detrital grains in confined thin (0.016 to 2.2 mm) layers, planar concentrations of carbonaceous material, detrital (and authigenic) pyrite and/or detrital heavies;   they may be disrupted by bioturbation (Plate 2.6).   Carbonaceous material may occupy large areas parallel to bedding.

The effects of texture are less than those of minor structures, but are still important.   In coarse grained rocks the weathering of one constituent may have a proportionally larger effect than the weathering of the same constituent in a finer grained rock.   This is true for *in situ* chemical weathering of Wellington greywacke-suite rocks but after quarrying the effects of minor structures are more important.   Physical *in situ* weathering of greywacke-suite rocks shows argillite to be less resistant on the sea coast or where chemical weathering is advanced.   Coarse grained greywackes (chipwackes) displayed the contrast well (see Plate 2.2).   In newly exposed fresh outcrops, however, chemical weathering is suppressed in argillites and enhanced in the greywackes,i.e. the coarser grained rocks.   Vertical or steeply dipping beds and induced secondary porosity (joints, shears and faults) facilitate chemical weathering to deep levels.   For reasons discussed later, this induced perm-
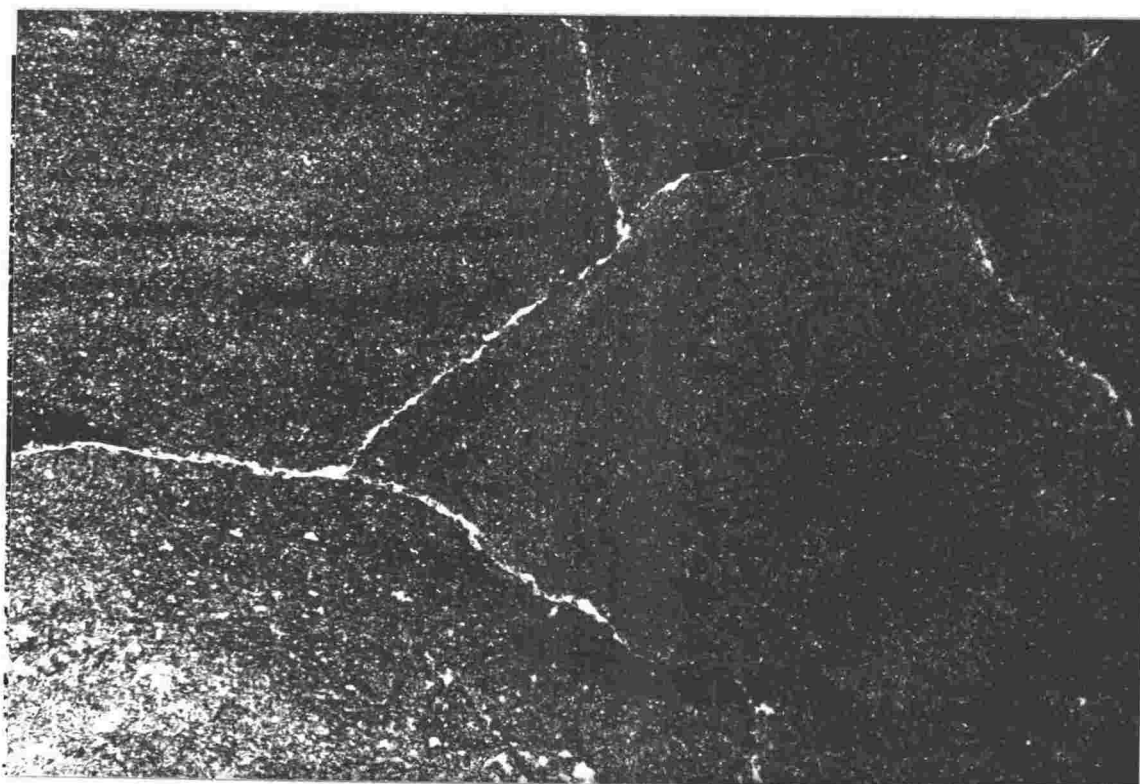
5·5 mm

Plate 2.6 : Bioturbation may disrupt fissility lamination in
                argillaceous rocks by attenuating sedimentary
laminations.   Some benefit may result for engineering purposes.
Shown is a sample (IB-6) of argillite (rock mean grain size
0.016 mm) showing cracking in rock 'circumnavigating' a bioturbation
structure (centre right) which destroys laminations (upper left),
in this case controlling fissility.   The photomicrograph shown (in
plane light) did not have the crack pattern "manufactured" during
thin section production.

that chlorite and white mica would behave similarly proved erroneous. Mica
schist rock fragments adjacent to an alteration zone showed no sign of
staining but chlorite, in any form, including that in sedimentary rock frag-
ments, was affected.

2.17   Geochemistry

Greywackes as a rock type are very homogeneous chemically throughout the
world despite large differences in age (Pettijohn et al. 1972), i.e. they are
rich in Al_2O_3, $FeO + Fe_2O_3$, MgO and Na_2O - as may be seen in Table 2.15.

Most authors regard the alkali ratio $Na_2O:K_2O$ as being highly significant in
the classification and interpretation of sedimentation of greywackes
(Middleton, 1960; Pettijohn, 1963; Crook, 1974).   The alkali content is of
particular importance to this study as Reed (1957) and Sameshima (1977) both
show rocks regarded as greywackes to have $Na_2O:K_2O$ ratios greater than unity
and argillites less than unity.   Reed (1966) used alkali contents to clas-
sify rock-types from aggregates that degraded on a motorway project.   He
showed (Reed, 1966, 1967) that alkali ratios for the failed aggregate were
greater than unity and contended that this was due to secondary "albitisation".
The failed aggregates were partially weathered and were in the mean grain size
range 0.06 to 0.005 mm.   Most photomicrographs (Reed, 1966) indicate many of
the rock types to be argillites on the textural parameters of this study and
tests recently performed (Rowe, 1979).

The aim of this section is to present further chemical data on the Wellington
rocks and to relate this to the petrography (section 2.6).   Thirty samples of
various lithofacies, representing the textural range apparent in the
Wellington greywacke-suite rocks, were analysed for major and trace elements.
The major element analyses are listed in Table 2.16.

2.17.1   Major elements

Rocks were prepared by crushing for one minute in a "Tema" mill.   X-ray
fluorescence (XRF) analyses were performed on glass fusion discs following the
preparation and correction procedures given by Norrish and Hutton (1969).
Analyses were carried out on Siemens SRS-1 Spectrometer at Victoria University
by the late Mr F. Shafer.

Table 2.15 : Representative chemical analyses of greywackes, after Pettijohn *et al.* (1972) compared with analyses of this study.

	A	B	C	D	E	F	G	H	I	J	K	L
SiO_2	60.51	61.39	76.84	69.11	68.85	74.43	73.04	71.10	68.84	65.05	69.06	59.44
TiO_2	0.87	0.62	-	0.60	0.74	0.83	0.15	0.50	0.25	0.46	0.52	0.81
Al_2O_3	15.36	16.97	11.76	11.38	12.05	11.32	10.17	13.90	14.54	13.89	14.74	18.29
Fe_2O_3	0.76	0.39	0.55	1.41	2.72	0.81	0.56	trace	0.62	0.74	0.59	0.75
FeO	7.63	5.32	2.88	4.64	2.03	3.88	4.15	2.70	2.47	2.60	2.87	5.47
MnO	0.16	0.12	trace	0.17	0.05	0.04	0.18	0.05	nil	0.11	0.05	0.07
MgO	3.39	3.84	1.39	2.06	2.96	1.30	1.43	1.30	1.94	1.22	1.52	2.58
CaO	2.14	3.21	0.70	1.15	0.50	1.17	1.49	1.80	2.23	5.62	2.05	1.58
Na_2O	2.50	2.78	2.57	3.20	4.87	1.62	3.56	3.70	3.88	3.13	3.45	1.80
K_2O	1.69	1.25	1.62	1.76	1.81	1.74	1.37	2.30	2.68	1.41	2.89	4.56
H_2O+	3.38	2.44 }	{ 1.87[1]	{ 4.13	2.30	2.15 }	{ 2.36[1]	{ 1.90	1.60	2.30 }	2.03[1]	4.08[1]
H_2O-	0.15	0.06 }		{ 0.05	0.77	0.20 }		{ 0.26	0.35	0.28 }		
P_2O_5	0.27	0.19	-	0.03	0.06	0.18	0.23	0.10	0.15	0.08	0.17	0.19
ZrO_2	-	0.07	-	-	-	-	-	-	0.05	-	-	-
CO_2	1.01	0.88	-	-	0.08	0.48	0.84	0.12	0.14	2.83	-	-
SO_3	-	-	-	-	-	-	-	-	0.15	-	-	-
S	0.42	0.15	-	-	0.08	0.12	0.10	trace	-	0.05	-	-
Cr_2O_3	-	0.01	-	-	-	-	-	-	-	-	-	-
BaO	-	0.06	-	-	trace	-	-	-	0.04	-	-	-
C	-	-	-	-	0.07	0.17	0.17	0.09	-	-	-	-
	100.24	99.75	100.18	99.69	99.94	100.45	99.80	99.80	99.93	99.77	99.94	99.62

(1) Loss on ignition.

A. Greywacke (Archean), Manitou Lake, Ontario, Canada, B. Brunn, analyst (Pettijohn, 1957b. p.306).

B. Greywacke (Archean), Knife Lake, Minnesota, U.S.A., F.F. Grout, analyst (Grout, 1933, p. 997).

C. Greywacke Tyler slate (Precambrian Animikian), Hurley, Wis., H.N. Stokes, analyst (Diller, 1898, p. 87).

D. Rensselaer Greywacke (Ordovician?), near Spencertown, N.Y., H.B. Wiik, analyst (Balk, 1953, p.824).

E. Tanner Greywacke (Upper Devonian - Lower Carboniferous), Scharzfeld, Germany, R. Helmbold, analyst (Helmbold, 1952, p. 256).

F. Greywacke from Stanley Shale (Carboniferous), near Mena, Arkansas, B. Brunn, analyst (Pettijohn, 1957b, p. 306).

G. Kulm (Carboniferous), Steinback, Frankenwalk, Germany (Eigenfeld, 1933, p. 58).

H. Composite sample (Lower Mesozoic), prepared by using equal parts of 20 greywackes exposed along shoreline between Palmer Head and Hue-Te-Taka, Wellington, N.Z., J.A. Richie, analyst (Reed, 1957, p. 16).

I. Franciscan Formation (Jurassic?), Quarry Oakland Paving Co., Piedmont, California, Jas. W. Howson, analyst (Davis, 1918, p.22).

J. Greywacke (Cretaceous?), Olympic Mountains, Washington, near Solduc, B. Brunn, analyst (Pettijohn, 1957b, p. 306).

K. Average of analyses for 19 Wellington greywacke-suite rocks in mean grain size range 1.25 to 4.5 phi.

L. Average of analyses for eight Wellington greywacke-suite rocks in mean grain size range 5.58 to 6.39 phi. Compare K with H.

Table 2.16 : New major element analyses (percent) of the Wellington greywacke-suite rocks. LOI = loss on ignition. * Analysed by B. Roser.

Sample	DC-6	HQ-17	SJ-3₁	KTW-13	KTW-14*	RSS-12*	HQ-21	BQ-V	BQ-IXA	OB-21
M_z (phi)	1.25	1.317	1.32	2.4	2.6	2.62	2.7	2.73	2.9	2.93
SiO_2	66.54	77.63	67.65	69.80	69.55	69.51	68.62	67.90	69.05	69.45
Al_2O_3	15.69	13.31	14.93	14.19	14.11	14.33	15.01	14.99	14.56	15.05
TiO_2	0.59	0.27	0.55	0.49	0.50	0.46	0.51	0.54	0.53	0.42
Fe_2O_3	0.59	0.24	0.44	0.69	0.76	1.20	0.42	0.40	0.48	0.32
FeO	3.20	1.32	3.32	2.51	2.36	2.32	2.80	3.68	3.02	2.36
MnO	0.05	0.04	0.06	0.04	0.04	0.04	0.06	0.08	0.04	0.05
MgO	1.61	0.57	1.71	1.54	1.47	1.66	1.45	1.66	1.74	1.34
CaO	3.05	2.12	3.08	1.71	2.03	1.89	2.08	2.07	2.13	1.15
Na_2O	2.75	3.82	3.09	3.87	3.90	3.64	3.44	3.53	3.53	4.05
K_2O	3.29	2.31	2.74	2.66	2.61	2.91	3.17	2.52	2.51	3.54
P_2O_5	0.17	0.10	0.16	0.15	0.16	0.14	0.13	0.17	0.12	0.16
LOI	2.16	2.20	2.02	1.77	1.89	1.70	1.94	1.99	1.90	1.52
Total:	99.69	99.93	99.75	99.42	99.38	99.80	99.63	99.53	99.61***	99.41**

Sample	HQ-19	KS-2	KS-10*	BQ-iii	KTW-G	RSS-iii	BQ-21	KTW-i	DC-8	BQ-i
M_z(phi)	3.08	3.27	3.38	3.78	4.07	4.08	4.13	4.23	4.5	4.87
SiO_2	68.28	67.77	70.23	68.54	65.77	68.10	66.57	70.70	70.45	61.52
Al_2O_3	15.07	15.12	15.16	13.50	15.64	15.12	15.93	14.18	14.11	14.56
TiO_2	0.53	0.53	0.47	0.49	0.63	0.59	0.63	0.64	0.54	0.50
Fe_2O_3	0.54	0.50	1.49	0.33	0.56	0.59	0.57	0.64	0.46	0.06
FeO	3.16	3.43	2.00	2.45	3.84	3.16	3.72	2.86	2.98	2.74
MnO	0.04	0.06	0.03	0.06	0.06	0.06	0.05	0.04	0.08	0.13
MgO	1.69	1.64	1.50	1.20	1.85	1.53	1.93	1.40	1.45	1.33
CaO	1.64	2.00	2.00	4.00	1.41	1.59	1.97	1.73	1.35	7.06
Na_2O	3.58	3.32	3.59	3.40	3.08	3.15	3.98	3.61	3.26	2.85
K_2O	2.99	3.19	3.14	2.03	3.51	3.30	3.05	2.45	2.95	2.71
P_2O_5	0.13	0.16	0.16	0.20	0.19	0.19	0.21	0.23	0.20	0.19
LOI	1.94	1.82	1.42	3.18	3.00	2.17	2.37	1.60	1.90	6.09
Total:	99.59	99.59	101.19	99.41	99.54	99.55	99.98	100.08***	99.73	99.74

Sample	RSS-ii	HQ-26	HQ-24	OB-W	HQ-20	WCC-5A*	HQ-18	BQ-vii	HQ-22	OB-13
M_z(phi)	5.18	5.4	5.58	5.6	5.87	5.9	5.95	6.18	6.28	6.39
SiO_2	62.75	66.97	60.18	60.10	58.07	57.98	59.83	59.51	59.69	60.18
Al_2O_3	10.69	15.83	17.74	18.57	18.76	18.62	17.97	18.33	18.17	18.17
TiO_2	0.70	0.68	0.81	0.84	0.83	0.83	0.80	0.77	0.82	0.81
Fe_2O_3	0.60	0.38	0.54	0.86	0.67	0.93	0.65	0.80	0.69	0.88
FeO	4.66	3.52	5.64	5.14	6.22	5.52	5.56	5.12	5.58	4.96
MnO	0.08	0.06	0.06	0.05	0.06	0.07	0.05	0.07	0.07	0.09
MgO	2.26	1.69	2.43	2.43	2.95	2.70	2.57	2.82	2.40	2.34
CaO	1.65	1.66	1.56	1.36	1.63	1.44	1.71	1.41	1.60	1.94
Na_2O	2.74	3.02	2.04	1.44	1.88	1.70	1.94	1.81	1.83	1.78
K_2O	3.73	3.83	4.48	4.91	4.44	4.75	4.25	4.50	4.60	4.51
P_2O_5	0.22	0.23	0.17	0.13	0.15	0.19	0.16	0.19	0.24	0.25
LOI	3.26	2.31	4.08	3.93	4.39	4.21	4.07	3.93	4.16	3.88
Total:	99.34	100.18	99.73	99.76	100.05	98.94	99.56	99.26**	99.55**	99.79

**   Average of two analyses

***   Average of three analyses

Initially, multiple analyses from each sample were averaged but the degree of correlation proved this unnecessary as did the comparison with check discs prepared by Mr B. Roser. Morris (1979) also found excellent agreement with major elements in subsequent analyses. Loss on ignition was determined by heating in excess of one gram of sample powder at 1,000°C for one hour. FeO was determined by, at least duplicate, wet chemical analyses (Shapiro and Brannock, 1956) and attempts made to establish CO_2 by a quick chemical method also by these authors, but for small quantities of CO_2 (less than 0.4 percent) the accuracy is unreliable and precision is very poor (Roser pers. comm.). Major element composition of the Wellington greywacke-suite (Table 2.16) shows strong affiliation to mineralogic modes. The greywackes range in SiO_2 content from 66 to 71 percent, have a $Na_2O:K_2O$ ratio greater than unity, Al_2O_3 between 13 and 16 percent and less than 3 percent CaO. Argillites, by contrast, contain appreciably less SiO_2, the $Na_2O:K_2O$ ratio is less than 1 and Al_2O_3 significantly greater (17.7 to 18.8 percent). Loss on ignition for argillites is appreciably higher.

Higher phyllosilicate content in the argillites is indicated by higher potassium and alumina content together with higher losses on ignition, the latter due to combined water, organic matter and pyrite contents. Rocks with lower felsic modes give lower sodium and silica values.

These trends were noted by McKean (1976) and Nathan (1976) and are consistent with other analyses of Wellington greywacke-suite rocks (Reed, 1957). The ACF diagram (Figure 2.27) compares analyses of this study with those of Reed (1957) and Pettijohn (1963). The diagram shows good agreement of data and indicates a clear distinction between greywackes and argillites. The trend toward the C (molar CaO) portion of the diagram is protracted because of three samples, HQ-17, BQ-i and BQ-iii; HQ-17 having significant modal laumontite, the others calcite.

Figure 2.28 shows an inverse relationship between silica and alumina contents in greywackes and argillites, governed by felsic and phyllosilicate modes respectively. From section 2.13, it is the gradual transition of these modes, in response to textural considerations, that determines whether a rock is "greywacke" or "argillite". The abundance of SiO_2 in sandstones and Al_2O_3 in shales is an indication of mineralogic maturity of these rocks (Pettijohn, 1957) and when plotted, the inverse relationship is apparent (Figure 2.28). When compared with Kawachi (1974) and Nathan (1976), it appears that these
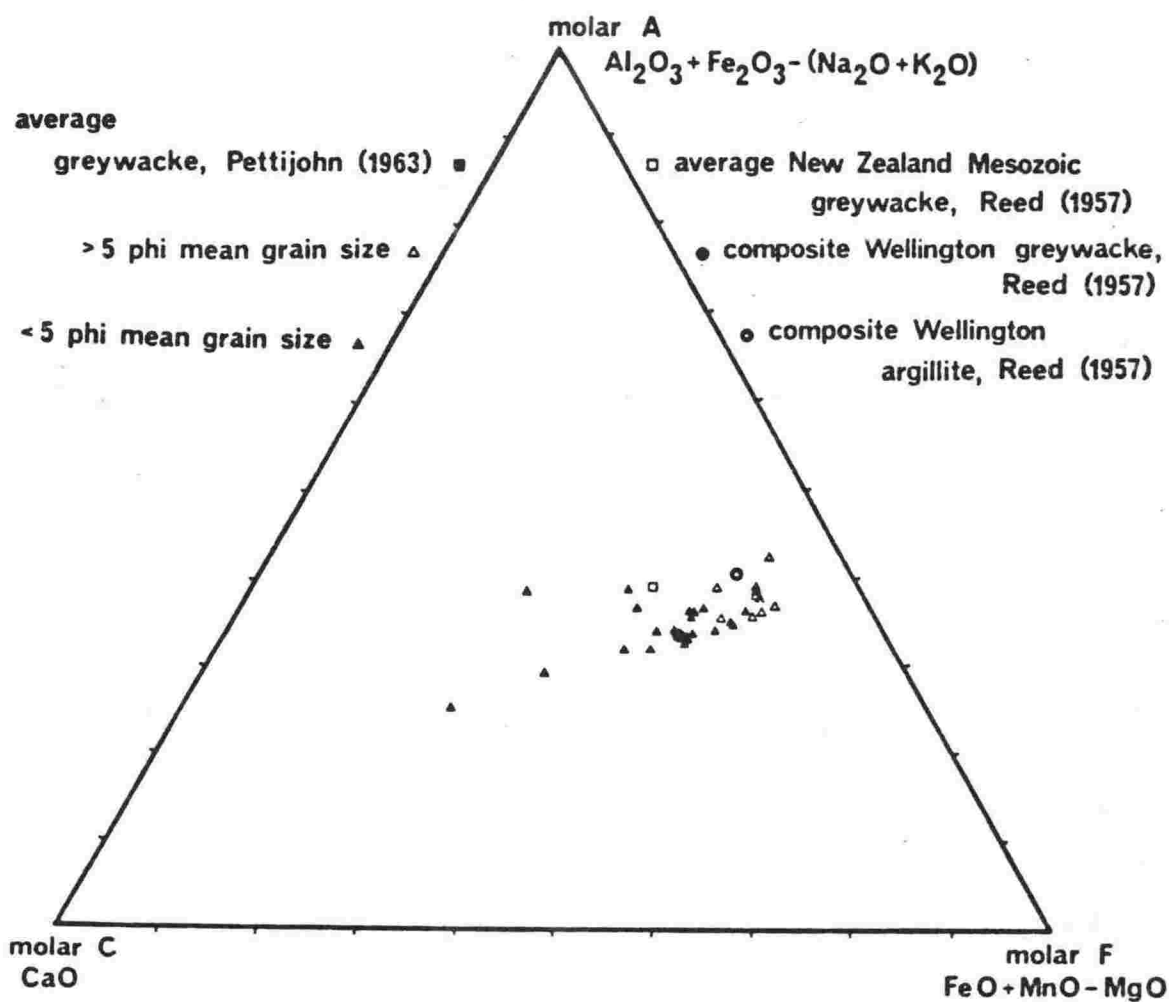
Figure 2.27 : ACF diagram for comparison of Wellington greywacke-
suite rocks of this study with Reed (1957) and
Pettijohn (1963).
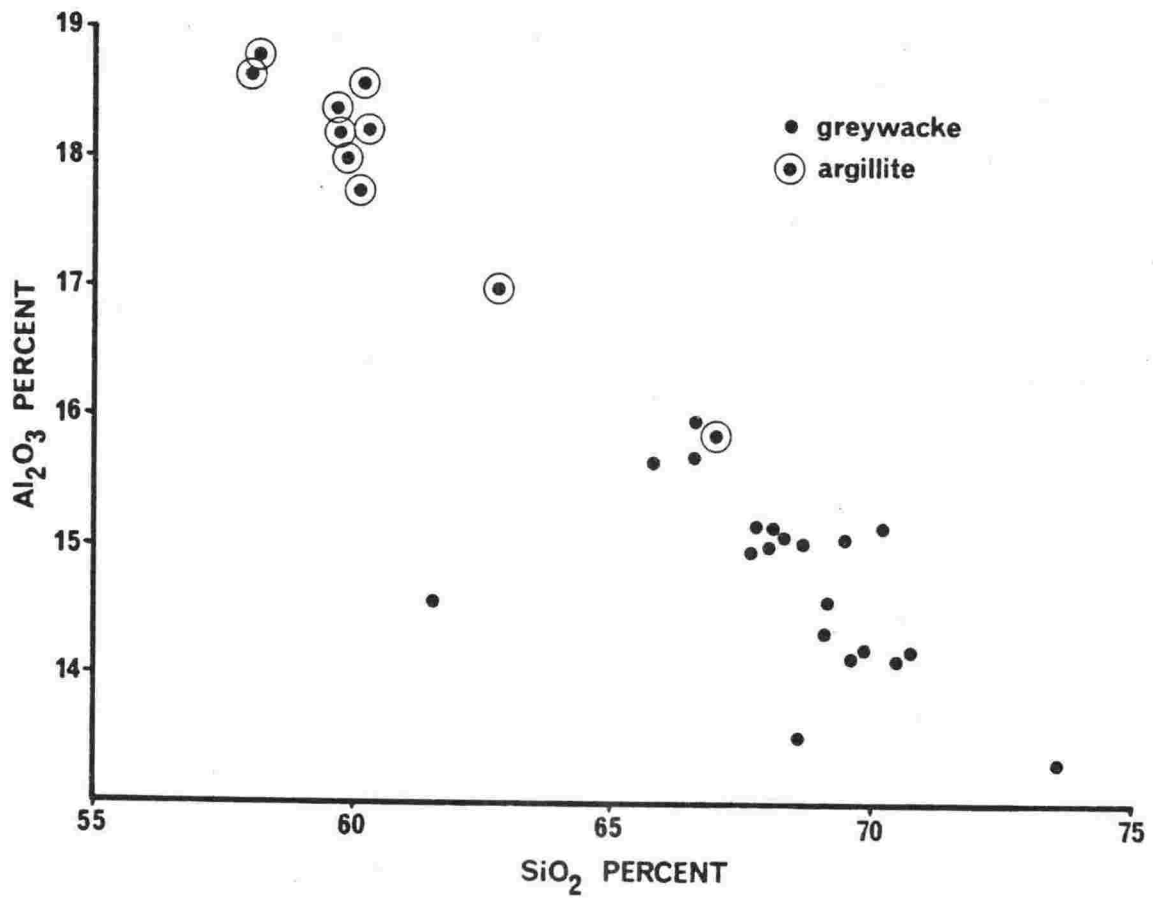
Figure 2.28 : Relationship of silica to alumina contents of grey-
wacke-suite rocks. The inverse relationship shown
is in response to relatively high felsic and phyllosilicate modes
in greywackes and argillites respectively.

trends are best displayed where mineralogical diversity is small.   Further
means of indicating the transition from greywackes to argillites may be seen
by plotting a $Na_2O:K_2O$ diagram (Figure 2.29).   The inverse relationship indi-
cates that a 1:1 ratio may separate the rocks.   This was a means by which
Reed (1957) displayed the defective albitised argillite aggregates.   It is
noteworthy that most greywackes of the Wellington area plot in this field with
"albitised" argillites.

Greywackes show relatively constant values of K_2O (2 to 3.5 percent), the
range of total alkalis ($Na_2O + K_2O$) being due to the trend of Na_2O.   From
Figure 2.30, relating major element chemistry to rock mean grain size, the slight
rise in Na_2O content in greywackes with mean grain sizes between 2.4 and
3.8 phi (0.19 and 0.07 mm), provides a larger scatter in the range of total
alkalis of greywackes - 5.4 to 6.9 percent.   Argillites have total alkali
contents in the range 6.2 to 6.6 percent.   The potassium content of greywackes
reflects the stability of the matrix mode through their range.   Sodium is
enriched due to slightly higher feldspar and volcanic rock fragment modes in
the fine and very fine sand size ranges of the greywackes (2.0 to 4.0 phi).

$FeO:Fe_2O_3$ ratios of the Wellington greywacke-suite rocks confirmed a lack of
weathering in any of the rocks analysed.

2.17.2   Trace Elements

All trace element work was undertaken by Mr B. Roser using pressed rock
powder mounts analysed by XRF.   Among elements analysed were Cu, Ni, Zn, Y,
Cr, U, Th and Nb.   Trace element data are summarised in Figure 2.31.   With
a few exceptions trace elements show positive correlation with phi unit values
and inverse relationship with SiO_2.   This is because SiO_2 decreases with
finer mean grain size of rocks and phyllosilicates (low in SiO_2 and of small
particle size) absorb alkali metals of increasing atomic number preferentially.
Heier and Adams (1964) note that most marine clays are enriched in K, Rb and
Cs with respect to sea water.   Strontium shows an inverse trend with phi
units (positive with silica) due to the metamorphic rock fragments apparent
in coarser grained greywackes.   Zr occurs in greater concentrations in rocks
of the coarse silt size range (4 to 5 phi).   This is due to zircon having a
preferred grain size range in natural sediments.   These heavy minerals,
together with opaque heavy minerals, help provide the laminations commonly seen
in greywackes of this grain size range.
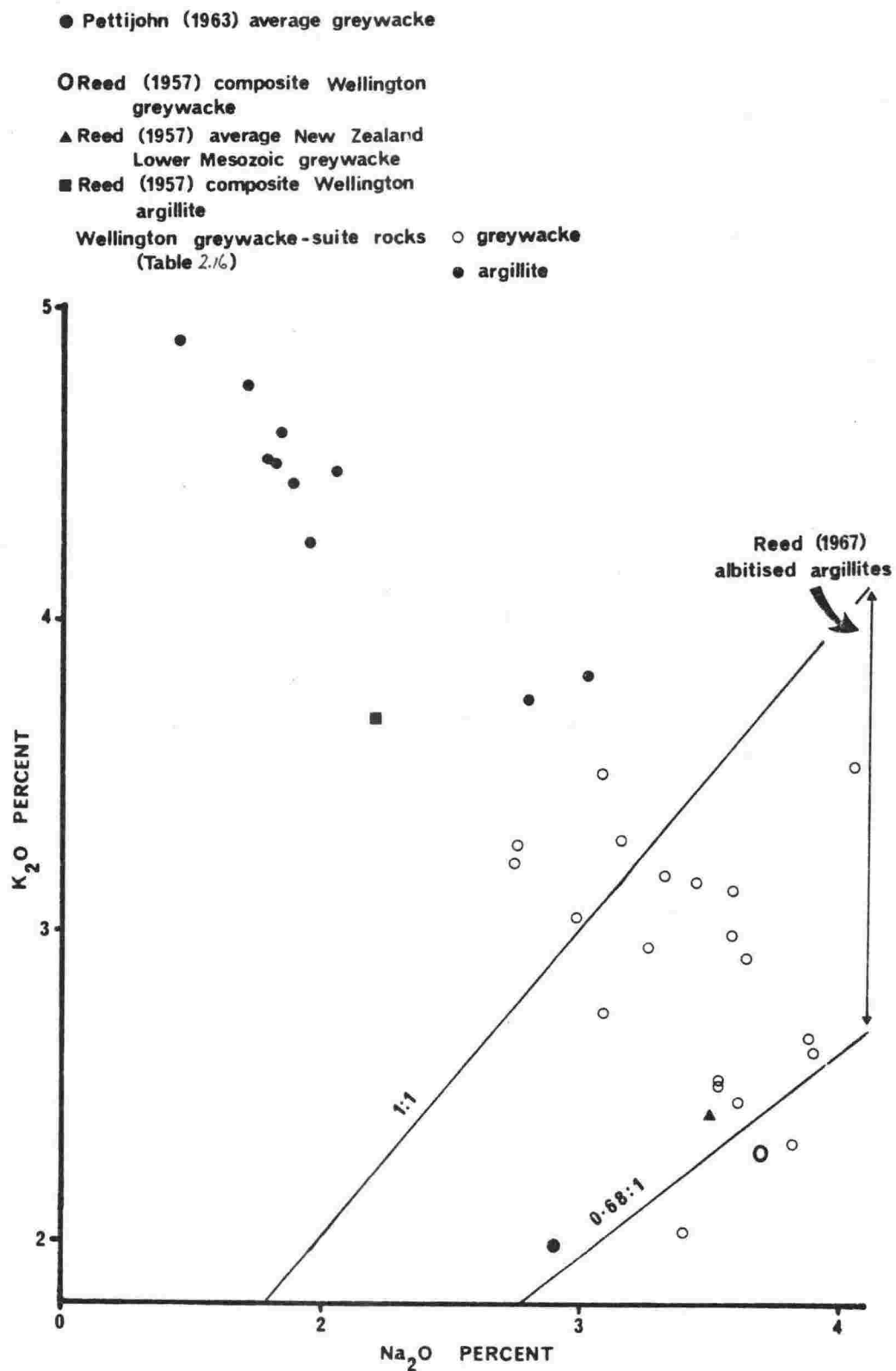
Figure 2.29 : Greywacke - argillite classification according to
alkali content. Argillite is generally assumed
to be rock material which plots above 1:1 line.
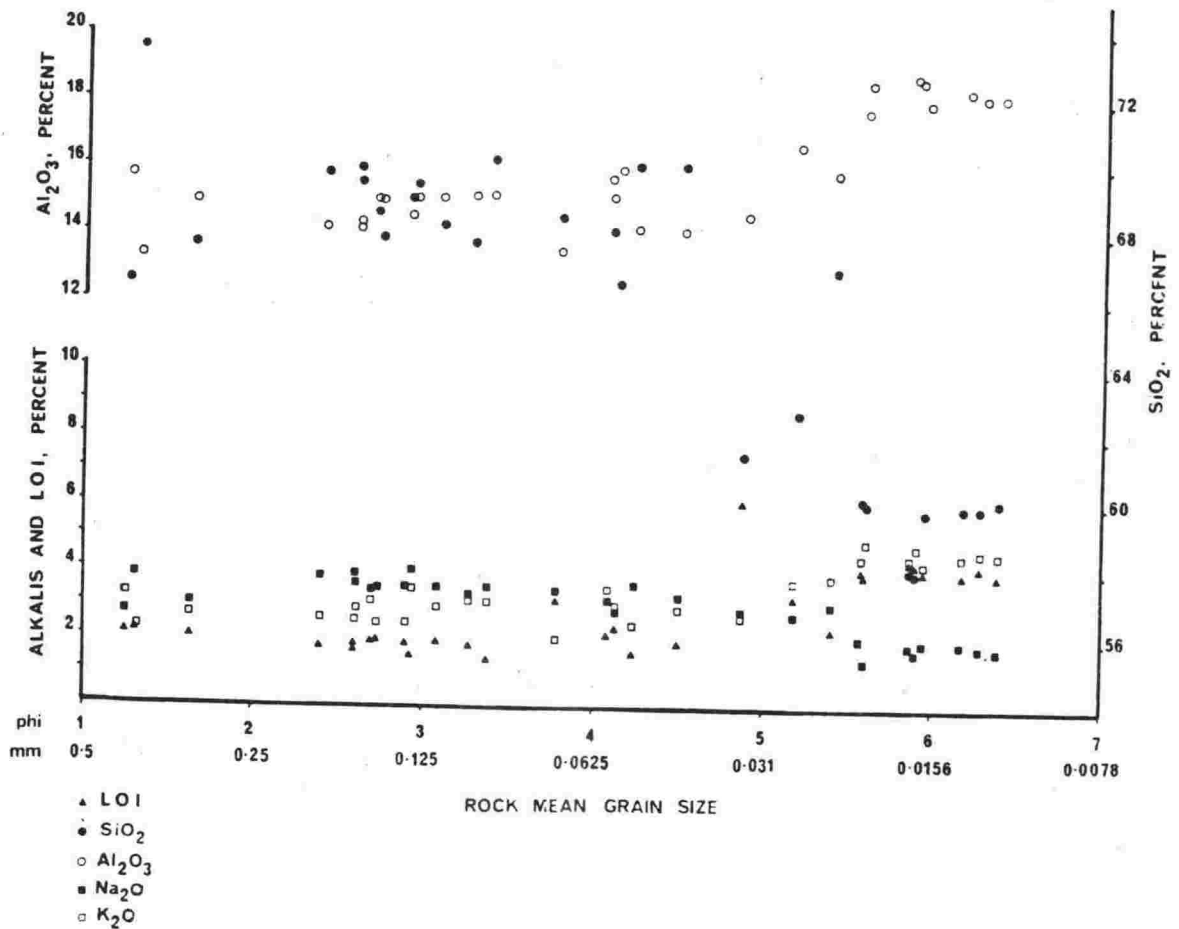
Figure 2.30 : Major element chemistry related to rock mean grain size. The transition of greywackes to argillite at the mean grain size of 5 phi (0.03 mm) is shown well by four major oxides and ignition loss.
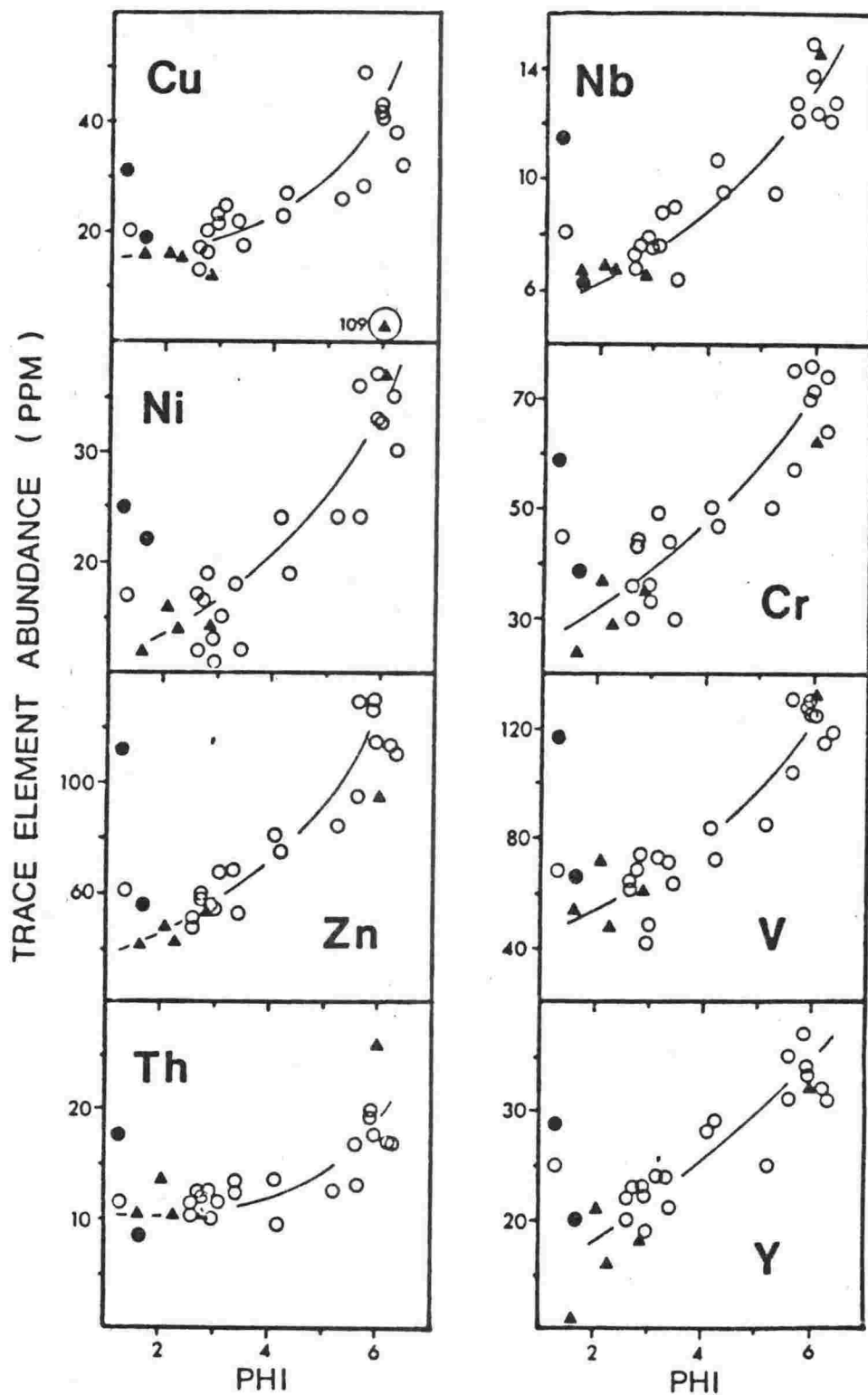
Figure 2.31 : Trace elements in Wellington greywacke-suite rocks; elements with positive correlation with phi unit values.

For more comprehensive discussions on trace element data see Roser (in prep.) or Rowe and Roser (in prep.).

Geochemistry of the greywacke-suite rocks is controlled by mineral modes which, for these rocks, depend on mean grain size. From the chemical data it appears that there are at least four main oxides, and loss on ignition (LOI), that may be useful for distinguishing greywacke from argillite (Figure 2.30). However, the distinction can be made only from fresh rock analyses as hydro-thermal effects and weathering will alter parent rock chemistry.

The trend in silica is somewhat scattered but maintains a mean value (69.1 percent) with mean grain size to about 5 phi (0.031 mm) where, from a value of 70.5 percent, it drops to a mean of 59.4 percent in rocks finer than this size. The alumina trend is less scattered and maintains a very slight increase through the greywackes, again to approximately 5 phi where a jump of about 4 percent occurs. Sodium describes a trend, gently convex upwards, with mean grain size to a maximum in the fine and very fine sand sized greywackes, becoming more and more steeply decending after 5 phi. Potassium and LOI figures follow similar trends, remaining relatively constant to about 5 phi then rising gently some 2 percent.

Loss of ignition is lowest in the fine and very fine sand sizes.

In the very coarse greywackes (chipwackes) a drop in SiO_2 and Na_2O is due to the presence of argillaceous rock fragments but Na_2O still exceeds K_2O due to the relatively large grains of sodic feldspar and relative paucity of micaceous minerals elsewhere in these rocks.

From section 2.13, the conclusion of petrographic data, and the findings of Rowe (1979), argillite is defined as that rock material in the Wellington grey-wacke-suite rocks with a mean grain size finer than 5 phi (0.031 mm). The geochemical data strongly support this: the $Na_2O:K_2O$ ratio reversing at 5 phi, the drastic reduction of SiO_2 and rise of Al_2O_3 at the same point and LOI indicating more combined water apparent in rocks finer than 5 phi.

Although there is good correlation between sedimentology, petrography, geo-chemistry and service records in the Wellington greywacke-suite rocks, this may not hold for other parts of New Zealand as alteration, which could change

chemistry markedly, may have misleading effects. For example, the Auckland greywacke-suite rocks used to produce aggregate which failed in service (Reed, 1966, 1967) were described as albitised argillites and, "plotted" in terms of alkali ratios, might reasonably have been expected to behave as greywackes. In fact the rocks were often incipiently weathered and were of a mean grain size finer than the 5 phi (0.031 mm) criterion which this study suggests is more reliable. Clearly, a single chemical parameter is not sufficient to ascertain rock capabilities for engineering purposes.

Chemical composition of sedimentary rocks is a function not only of grain size, but also provenance, degree of induration/metamorphism and other post-depositional changes besides weathering (Pettijohn, 1963). The Wellington greywacke-suite greywackes show more chemical diversity than the argillites due to a greater range in texture, differing cements, and greater ranges of mineral alteration.

Probably the main reason for argillite homogenity is the lack of rock fragments and fresh feldspar.

Because of the observed chemical changes with texture, chemical differentiation may be expected within one greywacke bed due to vertical textural change. This and lithofacic differences make it extremely difficult to obtain a single reliable chemical analysis - an average - for Wellington greywacke-suite rocks. As vital as any other factor is the manner in which samples are collected.

The data expresses the *range* of chemical variability likely to be encountered within the suite but to use it in an attempt to average all, or even part, of the suite would be no more than speculation, without a weighting factor derived from textural considerations of constituent rocks and relative abundance within the suite.

Methods used in mapping Wellington greywacke-suite rocks (Brodie, 1953; Grant-Taylor *et al.*, 1974; Stevens, 1976) have been too rudimentary to provide such a factor but, should bulk chemical assessment be deemed necessary, current work by D. Williams (New Zealand Geological Survey) and relevant portions of this study may provide a suitable basis.

It does appear, however, that there is relative consistency of major oxide values within each of two groups based on mean grain size: greywackes (1.25 to 4.5 phi, 0.42 to 0.044 mm), and argillites (5.58 to 6.39 phi, 0.021 to 0.012 mm), (see Table 2.15).

CHAPTER THREE

COOPERS LAW:

All machines are amplifiers

Physical properties of Wellington greywacke-suite rocks

Results from the previous chapter indicate that the Wellington greywacke-suite rocks have the following features:

(i)   They comprise two dissimilar rock types; greywacke and argillite, with a rock mean grain size of 5 phi (0.031 mm) clearly differentiating the two.   Argillites are those rocks with a mean grain size finer than 5 phi.

(ii)   Greywackes and argillites have separate and distinctive mineralogies and chemistries which are directly related to the division based on size.

(iii)   There is no significant difference in mineralogy or chemistry in either greywacke or argillite between lithofacies.

The most useful means by which the Wellington greywacke-suite rocks may be characterised is their mean grain size.   In this chapter, therefore, physical properties will be examined with respect to each other and to rock mean grain size.

Probably the most difficult task in assembling data was sampling, particularly where rock cores were required, made very time consuming by considerations of homogeneity, weathering, orientation and representation of *in situ* rock. Variation in handspecimen samples is readily observed from density and compressional wave velocity (ultrasonic velocity) data.

The physical parameters described and quantified in this chapter are those that may link fundamental geological properties with those of concrete made from derived aggregates.

Tests and/or properties, e.g. plasticity, which may be important to other
rock uses were not examined in this study which is confined to aggregate
source rocks.

Unless specifically stated, no *in situ* information has been included and such
tests as permeability, moisture movement and uniaxial compression strengths
have been carried out on as homogeneous a piece of rock material as could be
found (coherent rocks, Friedman, 1966).

3.1   Rock colour

The importance of colour in establishing both rock type and degree of weather-
ing has long been acknowledged (Speden, 1971).   In geological and quarrying
pursuits the colour of fresh Wellington greywacke-suite rocks range from very
light grey (N7) to black (N1), with modes, at medium grey (N5) and greyish
black (N2), very crudely delineating greywacke from argillite.   Colour is
imparted to the rocks by their mineral components, most important of which
are felsic minerals, rock fragments (especially sedimentary rock fragments),
matrix and organic matter.   The importance of phyllosilicates increases with
diminishing mean grain size to overshadow the felsic content.   Colour value
(density) is enhanced by greater internal surface area so that even very
felsic rocks may, if of small mean grain size, appear quite dark.   Because
mineralogy is related to grain size it follows, apart from the anomaly just
outlined, that finer grained rocks are darker in colour.   Veining tends to
lighten the overall colour in the field, or in *in situ* rock as vein minerals
such as zeolites, calcite and quartz are white.

When wetted, all rocks examined assumed higher colour values, but finer rocks
have greater colour retention.

Classification by fresh rock colour is therefore possible but only where
large colour contrasts exist and it is not quantitative.   Rocks with similar
colour values may vary geologically and/or in their physical properties.

A classification of weathering of greywacke-suite rocks has been established
for Wellington (Raisebeck, 1973) and Auckland (Marshall, 1974).   Both rely
on colour differences for distinguishing lightly weathered rocks (Table 2.14).

3.2 Rock hardness

This is a most complex property. In general, hardness implies resistance to deformation. Richards (1961) defines technological hardness as "the resistance of a material to permanent deformation of its surface". When metals are deformed or indented the deformation is predominantly outside the elastic range and often involves considerable plastic or permanent deformation. However, in dynamic hardness measurement, the elastic properties may be as important as the plastic properties. In all types of hardness, the properties of strength and elasticity are involved to some degree. The hardest rocks comprise those having hard minerals embedded in a tough* matrix or cement (Shepherd, 1951). Hardness depends on the type of binding forces between atoms and molecules and increases with the magnitude of these forces; it is closely related to the yield strength of the material.

Hardness was gauged in this study by the relative ability to withstand scratching by a specified stylus when applied to the rock surface under specified load conditions (Appendix 9). The test method adopted was that of ASTM C851-76 (1976, discontinued 1978) used to identify the quantity of soft particles in coarse aggregates, particularly those so poorly bonded that rock grains are easily detached. The test which is easy, quick, repeatable and provides comparative results was used on Wellington greywacke-suite rocks with a mean grain size range between 1.25 and 6.39 phi (0.42 and 0.012 mm) and established those rocks with a mean grain size finer than 5.5 phi (0.022 mm) as being soft. Hence for engineering purposes, aggregate use particularly, argillites should be considered soft rocks.

The hardness of rock is due to a summation of many parameters, but mainly mineralogy, fabric and texture. From Chapter Two, both mineralogy and fabric are related to texture. The minerals mainly responsible for the relative degree of hardness in the greywacke-suite rocks are chlorite (H = 2.0 to 2.5 Mohs scale) and white mica (H = 2.0 to 2.5) and perhaps organic matter but to a lesser extent in greywackes. Chlorite and white mica increase with diminishing mean grain size and organic matter occurs in greater concentration in argillites.

---

* toughness: the resistance of aggregate to failure by impact (Neville, 1975).

3.3   Rock integrity

The physical integrity of an outcrop is important to the study of rocks for use as engineering material, as it effects the major problems of quarrying, slope stability, winning methods, processing methods and economics.

The factors of rock integrity important to any extractive industry or engineering use include the following:

(i)   Surface discontinuities - faults, bedding planes, shears, slickensides, foliation, joints, veins (their orientation, development, state of saturation and contribution to *in situ* permeability).

(ii)   Contrasts in shear and tensile strength between the discontinuities and the rock material within which they occur.

The relationships between regional geological structural trends and folding, faulting and jointing are, as yet, unstudied (a basis for study could possibly come from guidelines set out by Harding, 1974).   Certain effects of lithological control of faulting and jointing can be seen from a study of lithofacies.   The lengths, widths and surface areas of discontinuities are difficult to interpret genetically but their abundance is probably the most important, and most easily quantified parameter.

The abundance of discontinuities, apart from bedding planes, veins and foliation, i.e. fractures generally:

(i)   Increases in the vicinity of major faults and areas of high strain.

(ii)   Increases with decreasing bedding thickness.

(iii)   Is greater in brittle (competent) rocks rather than in ductile or less brittle (incompetent) rocks which tend to shear and squeeze.

(iv)   Increases near the surface of the outcrop and in regions of high relief.

In Wellington rocks, faults, joints and the like far outweigh other discontinuities.   Furthermore, the tensile strength between discontinuity faces is

very low, since the surfaces are systematic, smooth, planar and continuous, without being "keyed" by large irregularities (Plate 3.1). The abundance of rock discontinuities is, therefore, of paramount important to the quarry industry and to engineering (tunnelling, base rock foundations for large structures etc.), as it directly influences slope stability, permeability, the ability of rock to be weathered, strength of the rock mass and the susceptibility of structures to earthquake damage. On a more specific scale it influences the number of discontinuities likely to be encountered in individual aggregate particles, which has been shown to be of significance (Cornwell, 1966; Marshall, 1974).

Relative abundance of rock mass discontinuities may be ascertained in several ways:

(i)   By discontinuity spacing (Deere, 1964; Terzaghi, 1965; Watkins, 1970; a good summary is provided by Roberts, 1977).

(ii)   By expressing a total length of discontinuities (veins) exposed in a measured area of prepared rock surface (Marshall, 1974).

(iii)   By comparing the ultrasonic velocity of the rock mass with the ultrasonic velocity of a piece of intact rock material from the rock mass (Deere *et al.*, 1969).

All three methods were used in this study but method (ii) was discontinued after correlation with method (i) was found to be poor and that it was time consuming for data yield. Problems associated with the method were outlined by the Geological Society Engineering Group Working Party (1977).

3.3.1   Quantitative assessment of discontinuities

A method for quantitative description of rock mass and its classification was developed by Deere (1964). The classification index, called rock quality designation (RQD), was based on analysis of recovered core; it has since been used on exposed rock faces. Pieces of core exceeding 100 mm in length are expressed as a total length and divided by the depth from which the total core was recoved. This fraction expressed as a percentage is the RQD for the rock mass. The selection of 100 mm as the unit for reckoning or discarding the core in the determination
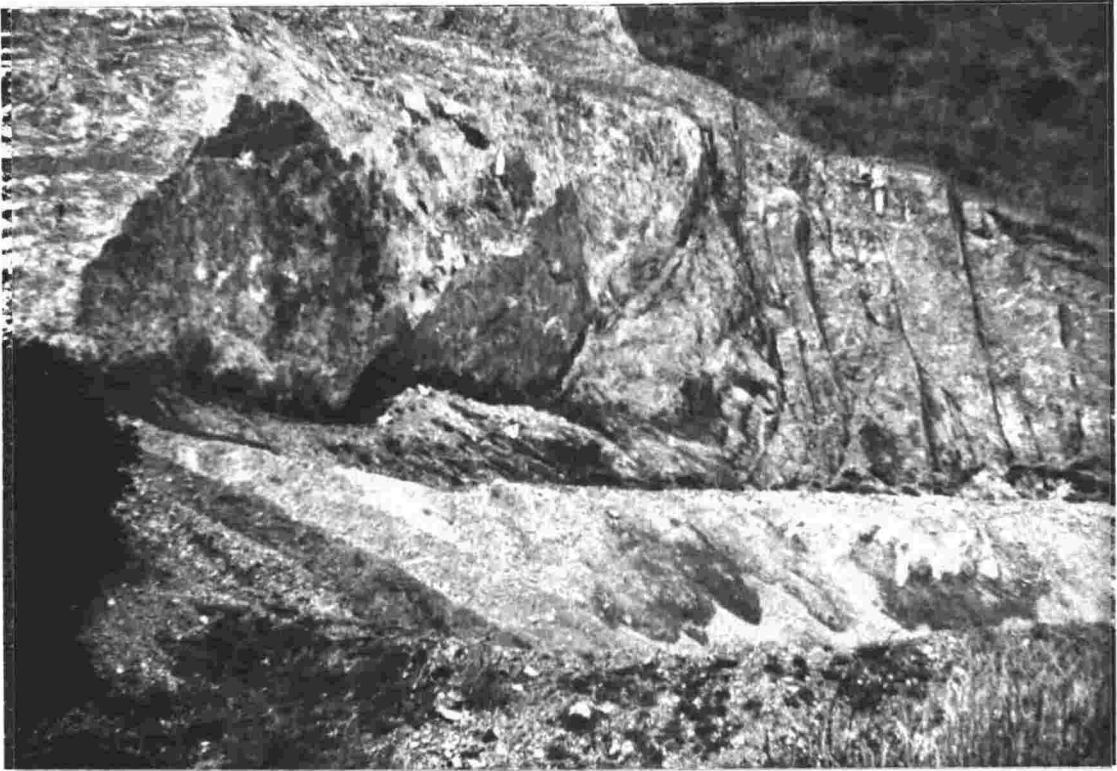
Plate 3.1 : A large bedding plane slickenside exposed in Kiwi
            Point quarry, Ngauranga Gorge.   The quarry face
is established parallel to strike.   The surface shown is
approximately 6 m high.

of RQD has no justification except experience. Some modifications to the method have been made to obtain correlation between RQD and other parameters (Deere, *et al.*, 1969).

Priest and Hudson (1976) found good correlation (within 5 percent) between RQD and joint frequency per metre.

Rock quality designation is a subjective observation because it is based on the number of discontinuities which are visible in *in situ* rock. Discontinuities include faults, shears, joints, veins, foliation, slickensides and bedding planes. These are not always discernable in the field as details are invariably lost due to dirt. The Geological Society Engineering Group Working Party (1977) affirmed RQD as a subjective technique and recommended a minimum of 200 readings per locality over continuous distances of 30 m or more. Where practicable these criteria were met for Figure 3.1. Raw data is presented in Appendix 11.

Spacings of discontinuities were taken along a traverse using a tape measure stretched across the outcrop perpendicular to bedding.

Individual beds within the traverse were assessed and additional data gained by shorter linear traverses within beds, measured parallel to bedding. Expressing discontinuity spacing by RQD provided little resolution, especially in the thick-bedded lithofacies, so frequency histograms were plotted for each bed (Figure 3.2).

Several trends, related to lithofacies, described in section 2.1 are apparent.

Results indicate a trend from the sandstone lithofacies through thick-bedded to the thin-bedded lithofacies of increasing numbers of closer spaced discontinuities, i.e. the sandstone lithofacies is more competent than the thick-bedded lithofacies which is more competent than the thin-bedded lithofacies for any given locality. For a particular lithofacies the greywacke beds are more competent than their complementary argillite beds (Figure 3.2). Between localities, however, the same lithofacies may alter discontinuity characteristics, so that an argillite of the thick-bedded lithofacies at one locality (away from faulted areas) may have fewer discontinuities visible *in situ* than a greywacke of the sandstone lithofacies at another locality near faulting.
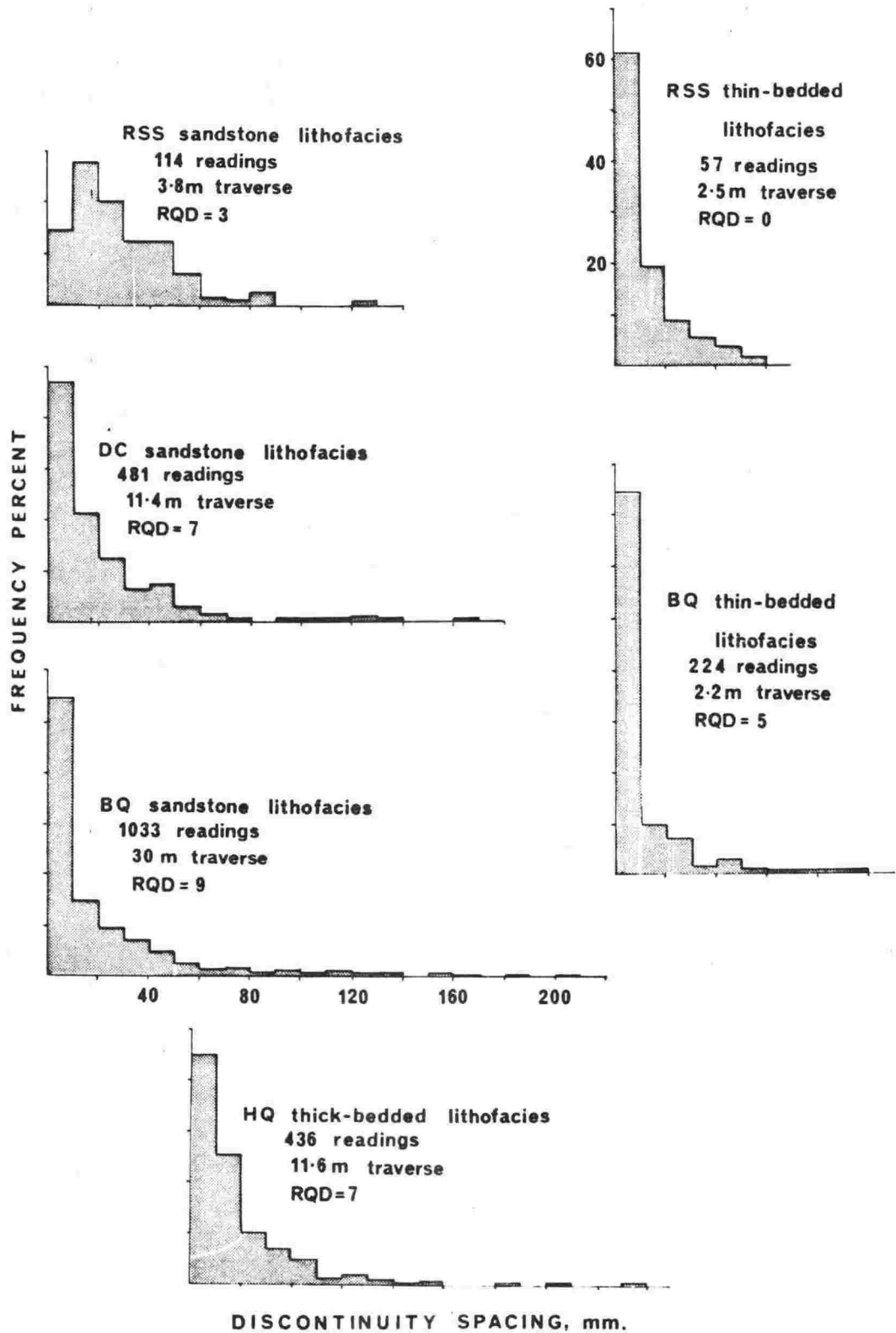
Figure 3.1 : Histograms showing discontinuity differences between the sandstone lithofacies (greywackes), thick-bedded and thin-bedded lithofacies of Wellington.
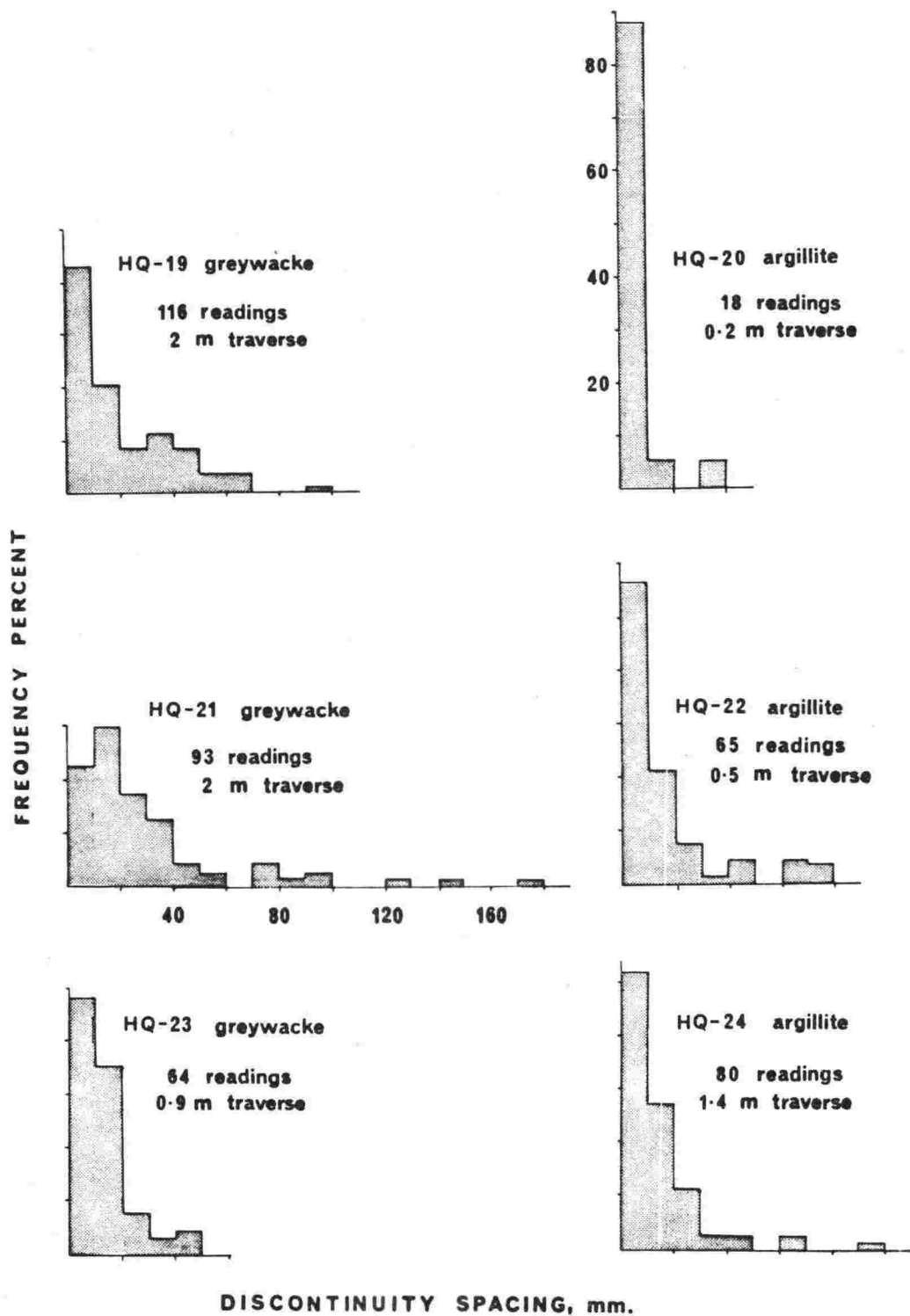
Figure 3.2 : Histograms showing discontinuity differences between
greywacke and argillite beds of the thick-bedded
lithofacies at Horokiwi quarry, Wellington.

3.3.2 Ultrasonic velocity

The propagation of waves in rocks is dependent upon rock type, mineralogy, texture, density, porosity, stress, moisture content and temperature.   It is related to the dynamic elastic modulus of the rock by the expression:

$$v = \sqrt{\frac{E}{\rho} \cdot \frac{(1 - \nu)}{(1 + \nu)(1 - 2\nu)}}$$

where -   v = ultrasonic velocity

E = dynamic elastic modulus - or for compact rocks, a value close to the static elastic modulus, especially at low stress levels.

ν = Poisson's ratio.

ρ = rock density

The measurement is precise, easy to undertake, may be performed on a wide range of sample sizes, and provides an assessment of rock integrity and static properties.

The ultrasonic (compressional wave) velocity of Wellington greywacke-suite rocks was measured in three different ways:

(i)   Field measurements on *in situ* rocks of differing lithofacies to better understand the effects of discontinuities in the rock mass.

(ii)   Handspecimens in the laboratory, to isolate differences in lithology.

(iii)   Rock cores prepared in the laboratory.

(i)   *In situ* testing:

Field ultrasonic velocity measurements were taken with a Geochrone manufac-tured by the Thiokol Chemical Corporation, Bristol, Pennsylvania, U.S.A. The instrument has been described and its performance discussed by Zachariadis (1966).

Three traverses over 21.3 m, 15.2 m and 30.5 m (70, 50 and 100 feet) in the sandstone, thick and thin-bedded lithofacies respectively were examined (see Map 7, Appendix 1).

In situ rock ultrasonic velocities are dependant on many parameters which may cause fluctuation at any given locality, water content and the degree of openness of joints both having very marked effects. To ensure stability of test conditions, measurement was carried out on a shore platform above high water mark, within a 4 hour period after a long dry spell with the following results:

Sandstone lithofacies	Thick-bedded lithofacies	Thin-bedded lithofacies
2438 m.s^{-1}	2514 m.s^{-1}	2629 m.s^{-1}
(8000 ft.s^{-1})	(8250 ft.s^{-1})	(8625 ft.s^{-1})

The least jointed sandstone lithofacies has a marginally lower ultrasonic velocity than the generally closely jointed thin-bedded lithofacies even though greywacke cores have consistently higher velocities than argillities cores (Appendix 10). This is probably due to the open nature of jointing in greywacke which generally allows free draining whereas, discontinuities induced by stress in the thin-bedded lithofacies, although more prolific, are closed, causing water retention.

The results indicate that even when compared to the liberal allowances made for bulldozer performance (Figure 3.3), greywacke-suite rocks generally will require blasting and at best will be difficult to rip.

As already mentioned, joints are probably the most prolific form of discontinuity existing in the Wellington greywacke-suite rocks and a transition to shears and faults is apparent. In most areas joints are planar and systematic in parallel sets. Several systems may be superposed. Their frequency and attitude to bedding, discussed by Stevens (1974), is related to the proximity of faulting.

Open joints minerally infilled, generally with calcite but sometimes zeolite, may be confused with veins, particularly near the joint.
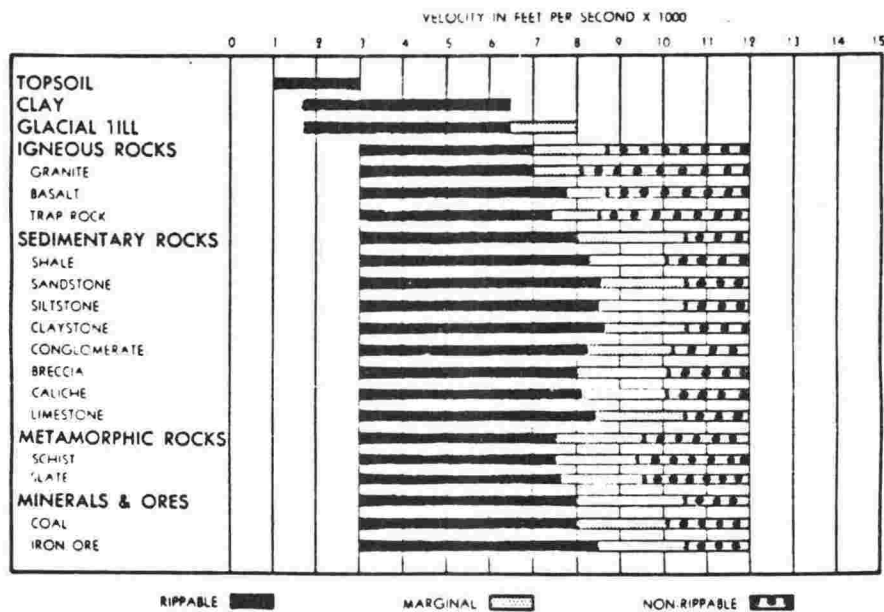
Figure 3.3 : Ripper performance as related to ultrasonic velo-
cities (from Roberts, 1977).

(ii)   Laboratory testing:

Laboratory measurements were made using the PUNDIT (portable ultrasonic non-destructive digital indicating tester).   Laboratory measurements using the PUNDIT showed the same shortcomings experienced by New (1976) and a wide scatter of results from handspecimen samples is apparent (Figure 3.4, Appendix 10).   Samples were prepared with 3 pairs of parallel faces for authogonal velocity studies to assess their degree of anisotropism both saturated and oven dried.

Cores used for uniaxial compression tests (section 3.5) were measured for ultrasonic velocity in two conditions;   soaked in water (at $20\pm1^{\circ}$C) for a minimum period of 30 days and at equilibrium with an environment of 50 percent R.H. at $20\pm1^{\circ}$C.   PUNDIT readings were taken using 15 mm diameter transducers and a frequency of 200 kH$_z$ (least lateral dimension approximately 25 mm). Results are summarised in Table 3.1 and shown in complete form in Appendix 10.

The results (rock core data) indicate that there is a reduction of elasticity in rocks of finer mean grain size when saturated but that ultrasonic velocity is constant for different moisture contents of rocks in the 4 to 5 phi mean grain size range.   From handspecimen data (Appendix 10) anisotropism increases with decreasing grain size which is consistent with findings of preferred orientation (Appendix 7) and ultrasonic velocity is higher parallel to sheet layering in the phyllosilicates (Boguslavskiy, 1976).

Attempts have been made to use ultrasonic velocity as a guide to establishing rock suitability for various engineering purposes, e.g. De Puy (1965).   He provides a general classification of "poor", "fair" and "good" quality rock as being rock with an ultrasonic velocity of less than 4572 m.s^{-1}, 4572 to 5182 m.s^{-1} and greater than 5182 m.s^{-1} respectively.

From Figure 3.4 the inconsistencies arising from handspecimen data are very marked and generally show reduced ultrasonic velocity values compared with rock core data.   A trend of reduced ultrasonic velocity is apparent with reduced rock mean grain size.   In the coarse grained greywackes (chipwackes) zeolitisation has a pronounced effect in reducing ultrasonic velocities, especially where the mineral occurs as a vein transecting the signal path. Homogenous, flawless samples (rock cores) show that the moisture content of the rock is relatively unimportant except in the case of argillites mentioned
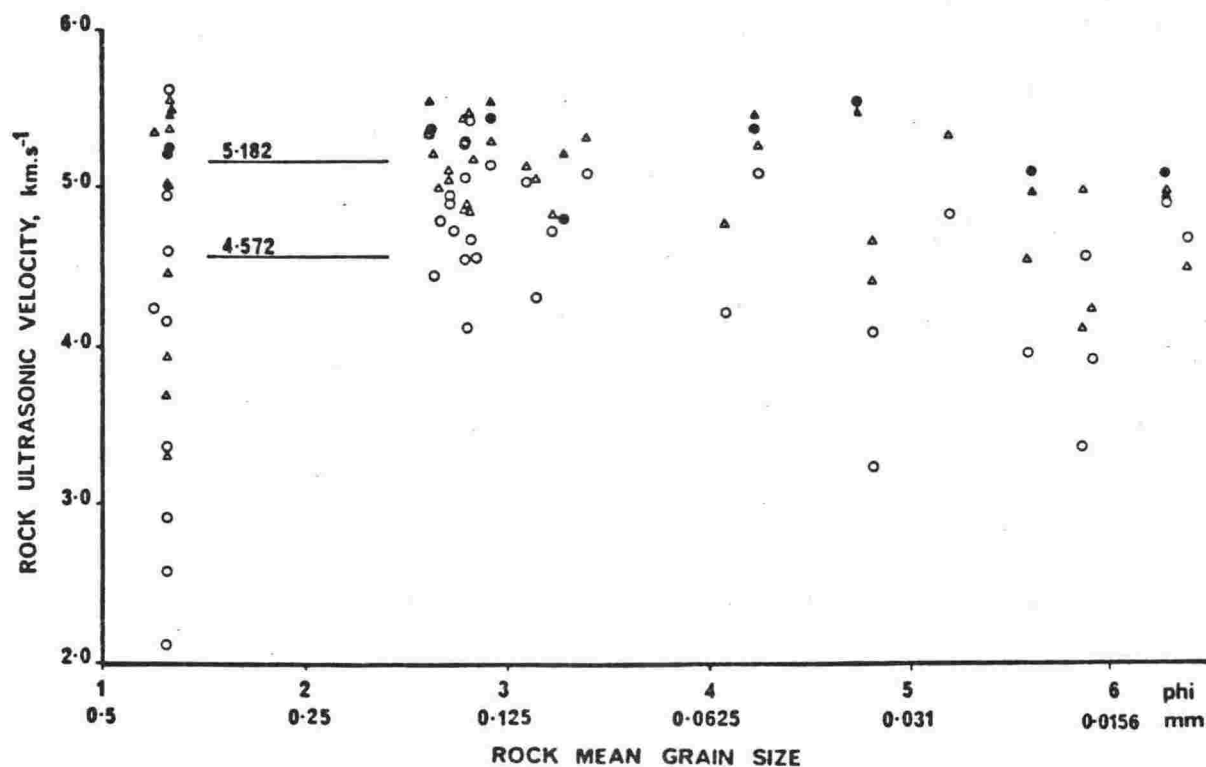
Figure 3.4 : Ultrasonic velocities diminish in value in finer

greywacke-suite rocks.   Handspecimen samples return

scattered data compared to homogenous, flaw-free rock cores (solid

points).   Circular symbols denote rocks tested dry, triangles

indicate saturated samples.   The cored samples at 3.27 phi returned

lower ultrasonic velocities due to relatively high porosities

imparted by organic material.   Ultrasonic velocity boundaries of

De Puy (1965) are shown as horizontal lines.

Table 3.1 : Summarised density, ultrasonic velocity and apparent porosity
data from rock core samples.

Sample	Rock mean grain size	Ultrasonic velocity $m.s^{-1}$		Density $kg.m^{-3}$		Effective porosity
	phi	Dry	Wet	Dry	Wet	percent
DC-6	1.3	-	-	2643	-	-
HQ-17	1.3	5230	5412	2653	2665	0.28
SJ-3$_1$	1.3	5251	5484	2670	2692	0.27
KTW-14	2.6	5368	5528	2673	2679	0.29
BQ-V	2.7	-	-	2659	-	-
BQ-1XA	2.9	5424	5526	2667	2678	0.34
KS-2	3.3	4878	5220	2627	2636	0.48
KTW-i	4.2	5399	5438	2673	2679	0.29
SJ-T	4.7	5524	5464	2696	2707	0.30
OB-W	5.6	5084	4945	2714	2723	0.38
HQ-22	6.3	5107	4969	2685	2702	0.51

above. All values from greywacke rock cores indicate this rock type to be of "good" quality (de Puy, 1965), with one exception, KS-2, which is relatively porous because of the presence of organic material.

3.4 Density and effective porosity

Density and effective porosity values were determined in the laboratory, in conjunction with ultrasonic velocity measurements, on handspecimens and cored rock samples prepared for uniaxial compression testing (section 3.5). This was done as a potential for further classification of greywacke-suite rocks and to gain insight of their mechanical behaviour.

3.4.1 Density

Density determinations were undertaken using the method of Hatherton and Leopard (1964) although in some cases handspecimen sample weights did not conform to the 100 - 150 gm guidelines of that paper.

To remove organic debris and loose material all samples were scrubbed thoroughly before testing. As constant temperature conditions were not available, measurements were confined to a fixed time on consecutive days during a period of stable weather. Temperature variation at the time of measurement was not great. Duplicate determinations were frequently made (Appendix 10). Rock core mean density values are shown in Table 3.1.

Some density/porosity methods require a standard sample expressed by weight, by surface area to volume ratio, or by surface preparation (ASTM C97-47; Hatherton and Leopard, 1964). However, because of the relatively large handspecimens measured and the low values of effective porosity, the density measurements are considered accurate. The cored samples, though smaller, have a constant geometry and were measured under controlled conditions and results are again considered accurate ± 20 kg.m^{-3}.

When plotted as histograms (Appendix 10) the results of handspecimens show a bimodal distribution for particle density. The scatter apparent in the dry and wet density histograms are attributable to micro-cracking, especially in the argillites and in greywackes which are fine grained and/or laminated or extensively veined by zeolite. Incipient weathering of some samples also gives anomolous values but bimodality may be seen in all density types.

From Appendix 10, the particle densities reflect a change in mineralogy between modes, and this relationship is also evident from a plot of particle density against mean grain size (Figure 3.5). With smaller mean grain sizes there is an obvious increase in particle density due to a higher proportion of chlorite (s.g. = 2.6 to 2.9), white micas (s.g. = 2.76 to 3.1) and heavy accessory minerals, e.g. pyrite, sphene, etc. (s.g. = 3.5 to 5.0) with a reduction in the proportion of quartz and feldspar (s.g. 2.57 to 2.65). The densities corresponding to a mean particle size of 5 phi, however, cannot be used with confidence to differentiate greywackes from argillites (Figures 3.6, 3.7) because of the scatter in the data.

3.4.2   Effective porosity

Porosity is expressed as either total or effective porosity. Total porosity is a measure of the total pore volume including pores which may be sealed off, as well as those connected with the surface of the test specimen. It may be expressed:

$$\text{Total porosity} = P_T = 100 \left(1 - \frac{V_G}{V_B}\right)$$

where V_G is grain volume and V_B is total or bulk volume of rock. More usually grain density (D_G) is substituted for grain volume, and bulk density (D_B) for bulk volume:

$$P_T = 100 \left(1 - \frac{D_B}{D_G}\right)$$

Effective porosity (P_E), also known as apparent porosity or nett porosity, excludes sealed off or non-communicating pores. Pore volumes, V_P, which are interconnected and communicate with the surface of the test specimen are measured and expressed as a percentage of V_B:

$$P_E = 100 \frac{V_P}{V_B}$$

Clark (1966) discusses how the method of determining porosity may affect the values obtained.
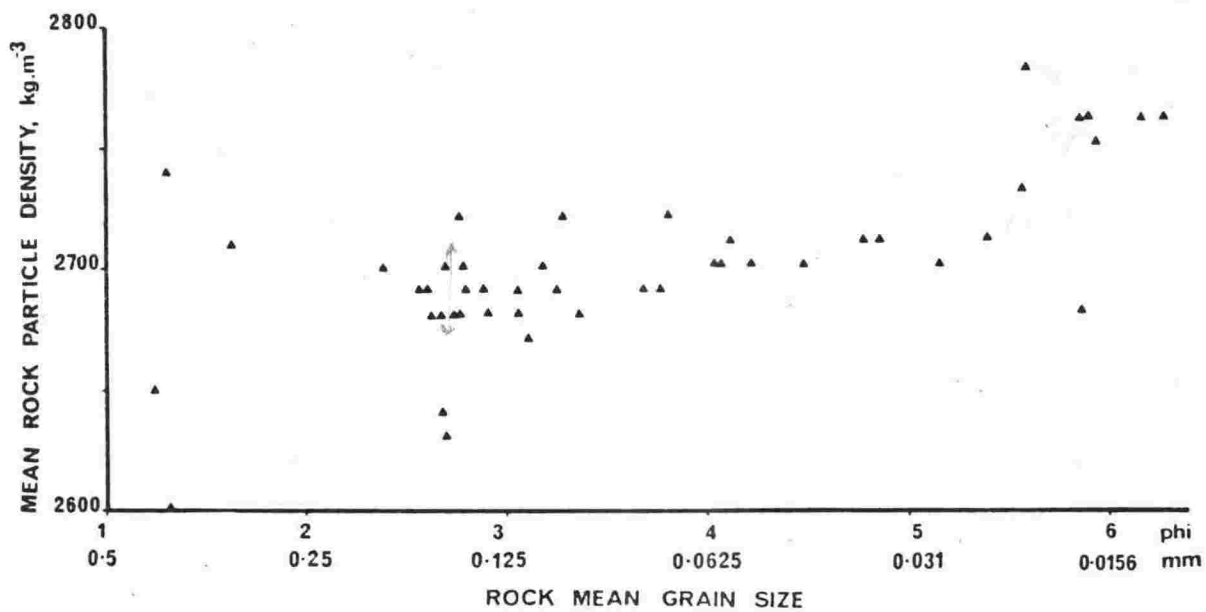
Figure 3.5 : A trend of increasing rock particle density is
apparent in finer greywacke-suite rocks, particu-
larly in those rocks finer than 5 phi.
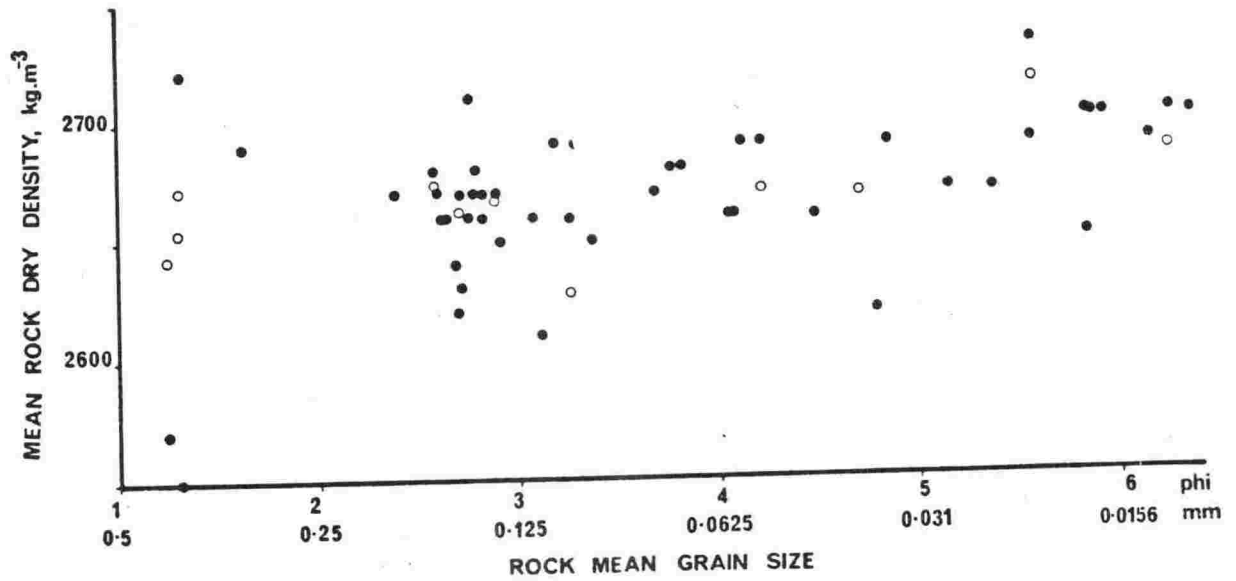
Figure 3.6 : Dry density appears to increase slightly with mean
grain size. Circled points indicate core samples,
which produce, for reasons of geometry and integrity, rather less
scatter than handspecimens.
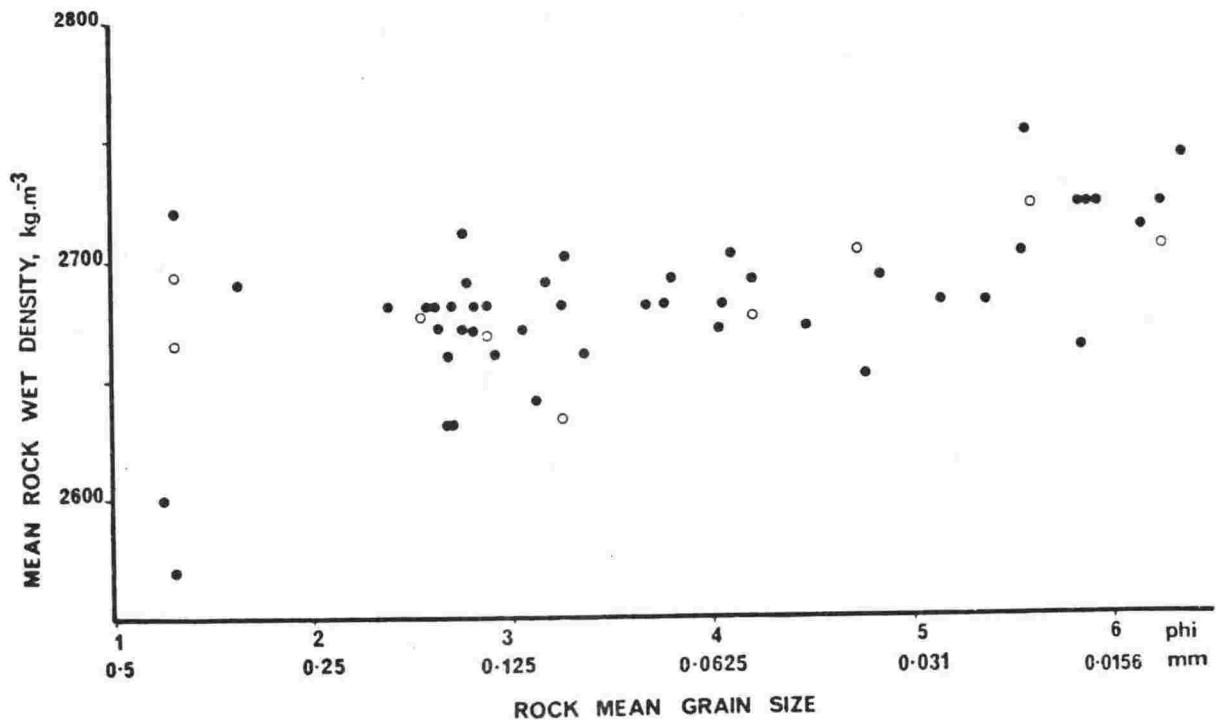
Figure 3.7 : Wet density also increases slightly with mean grain
size, but the increase is much greater in rocks
finer than 5 phi. Circled points are rock cores, the solid are
handspecimens.

In this study, oven dried (constant weight at $105\pm5^{\circ}C$) samples were weighed, immersed in distilled water under vacuum (737 mm = 29 inches of mercury) for a minimum period of 18 hours then reweighed, firstly in water then in air, in a saturated surface dry (SSD) condition (NZS 3111:1974, Neville, 1975) to give both density and effective porosity data.

Vacuum was released 15 minutes before wet weighing so that air pressure could aid water penetration. Such an elaborate procedure was deemed necessary as low effective porosity was expected.

Core sample dry weight was measured at equilibrium after 5 weeks in an environment of 50 percent R.H. at $20\pm1^{\circ}C$ and wet weight at equilibrium after 5 weeks in distilled water at $20\pm1^{\circ}C$. Weighing was carried out in the former environment.

Results of handspecimen measurements may be found in Appendix 10. Results from rock cores are presented in Appendix 10 and are summarised in Table 3.1.

The reduction of all strength properties of rocks with increasing porosity is well established; Lama and Vutukuri (1978) give a good modern summary of reductions in rock compressive and tensile strengths, ultrasonic velocity and density.

Handspecimen porosity data and to a lesser degree core data, are very scattered. Figure 3.8 provides an indication of how porosity increases with reduced mean grain size - consistent with interpretation of ultrasonic velocity investigation.

In greywackes, porosity values are lower in handspecimen samples than in rock cores, in spite of vacuum assistance, probably as a direct result of the lower surface area to volume ratios of the former. For argillites the reverse is true, this being due to handspecimens having many fine fractures which open with wetting (Appendix 25) to hold relatively large volumes of water. Samples which contain organic matter, zeolite, large argillaceous rock fragments and/or are strongly laminated, generally show relatively high porosity values.

Increased porosity with reduced mean grain size does not reflect the usual

Figure 3.8 : Effective porosity values of greywacke-suite rocks
increases in rocks of reduced mean grain size.

Rocks which are zeolitised, strongly laminated, contain organic
matter and/or large argillaceous clasts show general increases in
porosity. Rock core specimens are shown as solid symbols, hand-
specimens are circles. The single circled point is a very pro-
fusely microcracked argillite.

reduction in density as with other rock types (Lama and Vutukuri, 1978) as
density also increases with reduced mean grain size. The reason for this is
that argillites are composed of relatively heavy minerals, mainly phyllosili-
cates, which possess large d-spacings. If mineral modes remained constant
with reduced mean grain size and metamorphic effects remained constant
throughout the range of mean grain size, then an inverse relationship between
porosity and density could be expected.

3.5   Uniaxial compressive strengths and static elastic modulus

Uniaxial compressive strength and static elastic modulus are two of the most
fundamental and informative parameters of rock materials. Both tests offer
a means of engineering classification (Appendix 16).

The elastic modulus of a concrete aggregate particle influences many proper-
ties of the concrete of which it is part, i.e. flexural strength and the
modulus of the concrete. Determination of strength aids in determining the
types and applications of concrete, as inadequate strength of aggregate is a
factor in limiting concrete strength even when the aggregate itself is strong
enough to resist premature fracture.

3.5.1   Uniaxial compressive strength

The uniaxial compressive strength of rock is relatively easy to determine
but requires meticulous preparation of many samples to give meaningful results.
Sample preparation procedures are given in Appendix 12.

Compressive strength of concrete aggregate is an important consideration in
concrete mix design because the strength of a concrete can never exceed that
of the strongest predominant aggregate particles and the required strength of
aggregate is generally considerably higher than the normal range of concrete
strengths. This is because the actual stresses at the points of contact of
individual particles within the concrete may be far in excess of the nominal
compressive stress applied. Aggregate strengths are difficult to measure
directly, and indirect test methods are usually used - point load tests,
impact tests, crushing of bulk aggregate samples, crushing of geometrically
prepared specimens and crushing of cast concrete specimens made with the
aggregate in question. In this section results are presented from the

crushing (uniaxial compression) of geometrically prepared greywacke-suite rock specimens.

The results (Table 3.2) show that mean dry compressive strengths are high (245 MPa, all rocks), even for argillaceous samples.   Mean wet and dry argillite strengths (140 MPa and 196 MPa respectively), are lower than those for greywacke (187 MPa and 258 MPa), although some argillites are as strong as greywackes for loads applied perpendicular to bedding.   The scatter of mean values, for both wet and dry strengths of all rocks are about the same, the mean standard deviation being 58 MPa and 53 MPa respectively.   The average difference between wet and dry mean strength is 45.7 MPa, with, in one case only (SJ-T), a wet strength higher than the corresponding dry strength.   The ratio of the mean wet to dry strength of argillites and greywackes are comparable, 0.71 and 0.72 respectively.

The ratio of wet to dry strength is often stated to be an indication of rock softening (Michalopoulos and Triandafilidis, 1976); the higher the ratio, the lower the softening effect and the better the durability expectancy. But as argillites have been established as soft rocks (section 3.2) dynamic elastic modulus from ultrasonic velocity measurements (section 3.3.2) may provide a means of predicting durability quality.

The effect of water saturation, from a durability stand point, is more clearly seen from ultrasonic velocity measurements.   Although wet and dry strength comparisons are useful, they are not important as a measurement of hardness for greywacke-suite rocks.   Strength loss of a rock from water saturation is due to induced positive pore pressures (Young, 1974) and reduced bond strengths, especially in greywackes, as their behaviour is similar to that described in "undrained" tests (Paterson, 1978).   For the argillites, reduced bond strength is probably the most important factor (Colback and Wiid, 1965).

Differences in mean compressive strength of cores (BQ-IXA and HQ-22) prepared and left at room temperature (18 to 23°C) for approximately 18 months, compared with those prepared and tested after 2 months (1 month being at 20$\pm$1°C, 50 percent R.H.), are interesting (Appendix 13).

In this example the strength gain over 18 months averaged 29 MPa for BQ-IXA and 51 MPa for HQ-22 but core height to diameter ratio (h:d) of HQ-22 was 1.5 rather than 2.   Winkler (1973) suggests that higher strength of "older"

Table 3.2 : Summary of uniaxial compressive strengths of rock cores with h:d
ratios of 2, full data appear in Appendix 13.

Sample	Mean grain size, phi	Moisture condition	Number of samples tested	Mean Strength, MPa	Standard deviation, MPa	Coefficient of variation, percent
HQ-17	1.3	dry	9	221	25.6	11.6
		wet	8	194	32.1	16.6
SJ-3₁	1.3	dry	6	234	22.2	9.5
		wet	6	149	41.7	28.0
KTW-14	2.6	dry	7	260	23.5	9.0
		wet	7	239	40.4	16.9
BQ-V	2.7	dry	3	263	19.7	7.5
		-	-	-	-	-
BQ-1XA	2.9	dry	6	262	21.7	8.3
		wet	7	196	15.7	8.0
BQ-1XA	2.9	dry	6	291	53.3	18.3
		wet	3	257	21.0	8.2
KS-2	3.3	dry	9	243	25.2	10.4
		wet	9	182	33.7	18.5
KTW-i	4.3	dry	3	324	42.3	13.1
		wet	2	278	4.2	1.5
SJ-T	4.7	dry	4	254	36.5	14.4
		wet	2	259	24.0	9.3
OB-W	5.6	dry	9	245	34.3	14.0
		wet	11	195	23.6	12.1
HQ-22	6.3	dry	4	147	30.6	20.8
		wet	2	86	48.1	55.9

[BQ-1XA core samples stored at room temperature 18 months before testing.

cores is due to water of various affinities gradully being lost with time.
Stone masons often refer to this water as "quarry sap" (Hills, 1963); its
loss increases durability but decreases workability (Appendix 25).

Results from uniaxial compressive strength tests suffer from high variability
regardless of care in sample preparation and test execution. This is due to
platen restraint and the presence of weakness planes in the rock which gen-
erally have less effect with decreased specimen size yielding a higher rock
strength. This may be seen in Appendix 13 by comparing results from cores
with h:d ratios of 1.5 and 2. Results of core uniaxial compression tests
are difficult to relate to strength tests applied to the rock when crushed
as an aggregate, mainly because of factors of geometry, but the test is still
a means of comparing different parent lithologies.

A table from Neville (1975) is reproduced in part (Table 3.3A) to show the
relative reproducibilies of different strength assessing tests commonly
performed on aggregates.

The number of core sample tests required to establish means at various confi-
dence levels has been calculated based on this study (Table 3.3B).

Results from uniaxial compressive strength testing show that mean rock strength
of Wellington greywacke-suite rocks is related to mean grain size (Figure 3.9)
with both ends of the textural range having relatively lower strength.
Change of state from dry to wet displaces the strength curve to a lower value.
Brace (1961) explained the lower compressive strength of quartzite, basalt,
dolomite and limestone with increased maximum grain diameter, in terms of
Griffith crack theory. This was confirmed by tests on a number of specimens
of different textures but cut from a common block (SJ-3_1); the strength of
the coarser specimens was lower without exception (Appendix 13). For the
greywackes generally, an increase in dry and (particularly) wet strength with
finer mean grain sizes is apparent to 5 phi (0.031 mm). A comprehensive
discussion on brittle rock failure and Griffith theory is presented by
Paterson (1978).

The lower strength of the argillaceous materials, in contrast to the gener-
ally observed trend that fine grained rocks withstand higher stresses
(Paterson, 1978), may be attributed to the plastic nature of the bulk of
their mineral grains - phyllosilicates. These are softer and weaker than
the felsic minerals that predominate in coarser greywacke-suite rocks.

Table 3.3(A) : Reproducibility of strength test results on aggregate. After
Neville (1975).

Test	Coefficient of variation percent	Number of samples to be tested to ensure 0.9 probability that mean will be -	
		within ±3 percent of true mean	within ±10 percent of true mean
Impact of prepared specimen	17.1	90	8
Impact of bulk aggregate	3.0	-	-
Aggregate crushing strength	14.3	60	6
Aggregate crushing value	1.8	1	-
Los Angeles test	1.6	1	-

Table 3.3(B) : Reproducibility of uniaxial compressive strength test
results on rock cores from this study:

Number of greywacke-suite rock core samples required to estimate a mean
uniaxial compressive strength (MPa) by a confidence level, within a prescribed
confidence region.

±Difference from mean (MPa)	D — R — Y			W — E — T		
	uniaxial c.l.	comp. 95%	strength 99%	uniaxial c.l.	comp. 95%	strength 99%
1		3940	9000		5100	11800
5		158	361		206	470
10		39	90		51	120
20		10	23		13	30
50		2	4		2	5

Statistics by T. Aldridge, Applied Maths. Division, DSIR.
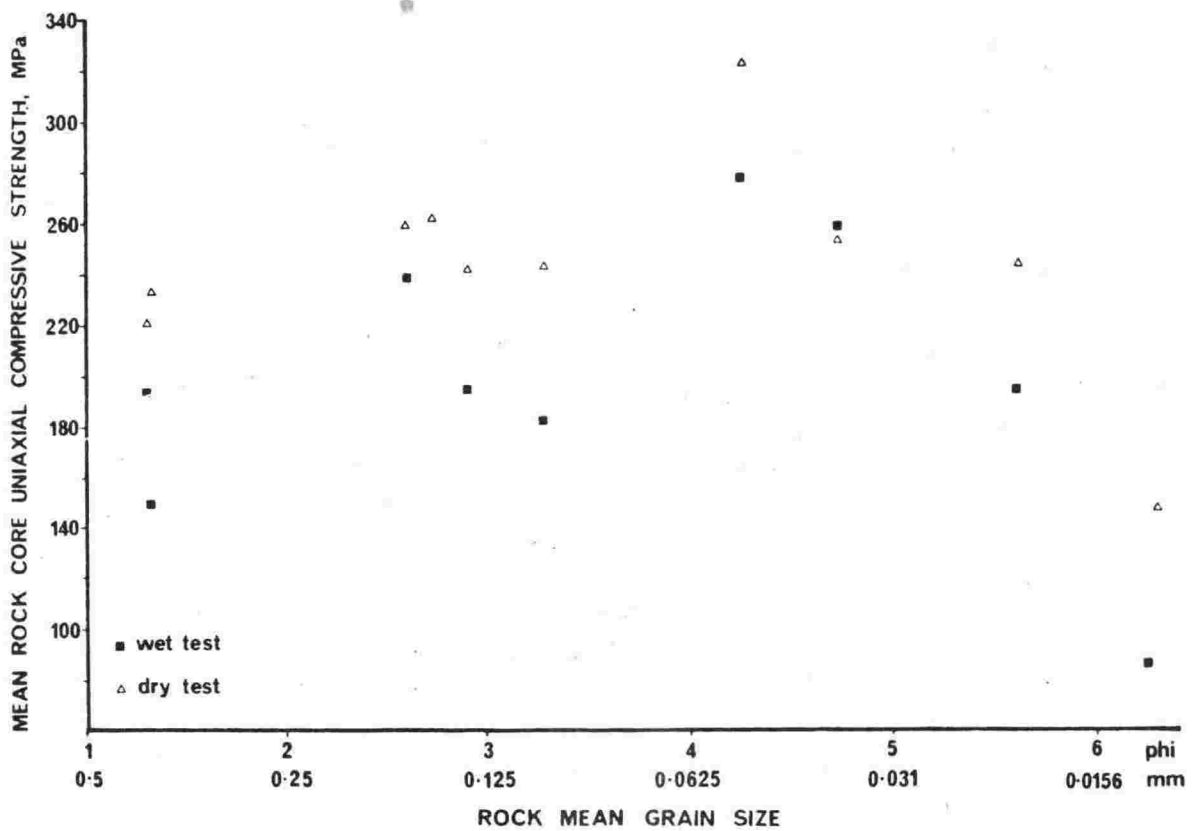
Figure 3.9 : Rock core uniaxial compressive strength related to rock mean grain size. Greywacke-suite rocks with mean grain sizes finer than 5 phi (argillites) display reduced strengths compared to greywackes which have increased strength with reduced mean grain size. Wet strengths are generally lower than dry strengths.

There may even be a trend within the argillites of increasing strength with increasing mean grain size for reasons of crystallinity. This argument is supported by strength tests on two argillites (Table 3.2).

It is important to recognise that although the argillites have similar strengths to the greywackes tested, load was applied in a direction perpendicular to bedding. The strength of argillites where load is applied parallel to bedding would probably be reduced by approximately 10 percent due to fissility (section 2.15).

3.5.2   Static elastic modulus

The static elastic modulus (Young's modulus, compression modulus, modulus of elasticity or modulus of deformation) was established for each lithology tested in uniaxial compression.

This parameter is rarely determined for aggregate material but is important, as it is directly related to the elastic modulus of concrete although other factors are involved. The elastic modulus of aggregate also affects the magnitude of creep and shrinkage that can be realised by the concrete. Aggregate of low elastic modulus can be valuable in preserving the durability of concrete subject to volume changes. Lower stresses arise in concrete made with compressible aggregates when changes in temperature or moisture conditions may otherwise cause cracking of cement paste about rigid aggregate particles.

Stress-strain relationships were established, for each of three cores from each lithology both water saturated ($20 \pm 1^{\circ}C$) and dry $20 \pm 1^{\circ}C$, 50 percent R.H.), by using wire resistance strain gauges (Appendix 14).

One cycle of load to failure, during which the rocks behaved as linear elastic solids, produced stress-strain curves (Figure 3.10) used to obtain the static elastic modulus of three stress levels (Table 3.4). These show interesting relationships with other physical parameters.

The initial tangent modulus (E_i) - defined in Appendix 15 - of a saturated sample is influenced by predeformation stresses from a preliminary expulsion of water, e.g. from between platen and sample. The tangent elastic modulus
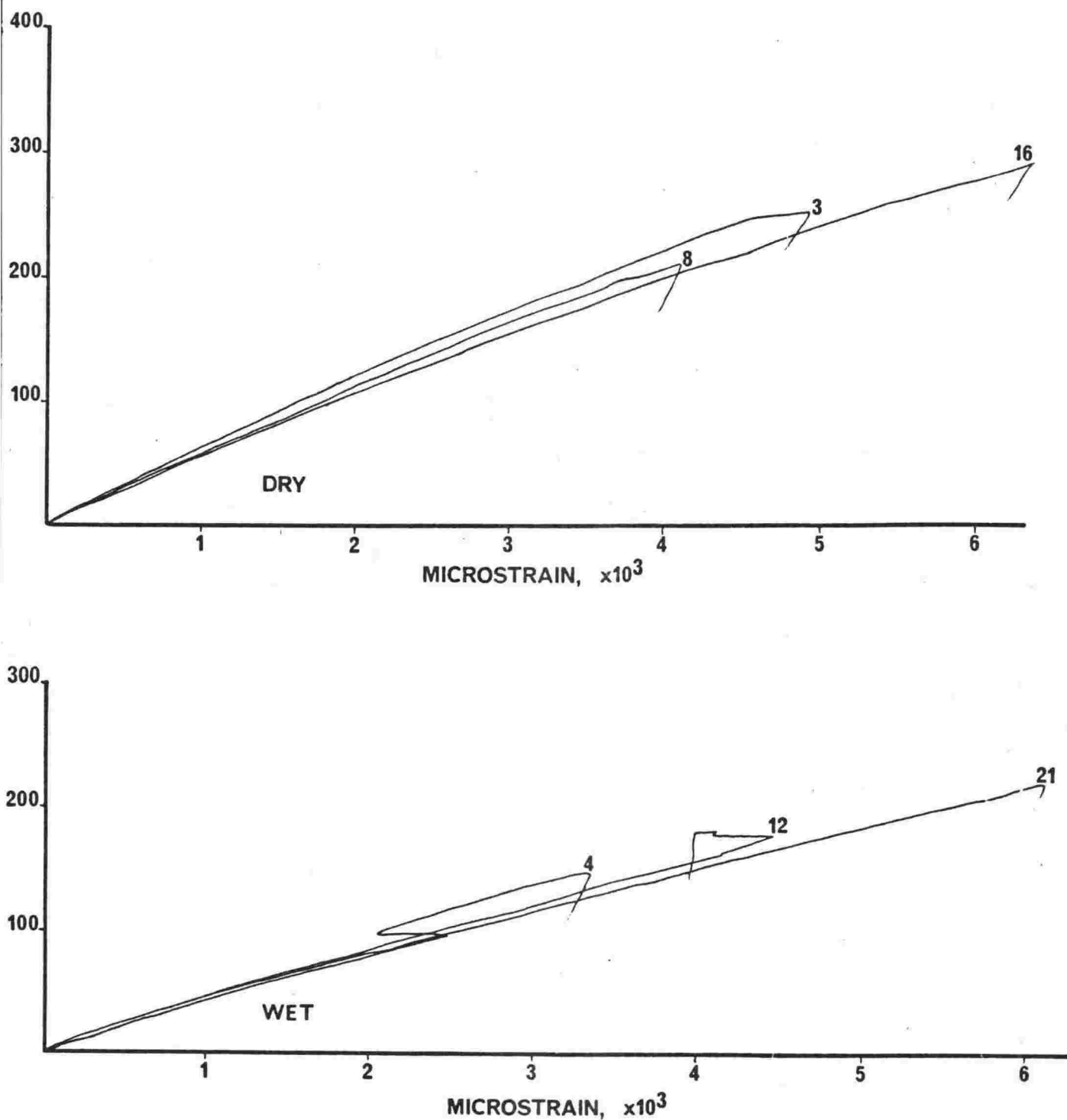
Figure 3.10 : Stress-strain curves of OB-W argillite (5.6 phi,

mean grain size), provide a typical contrast of

wet and dry testing.   Curve numbers indicate core sample numbers

which, with other curves, may be found detailed in Appendix 13.

N.B. Strain axes not identical scales.

Static elastic modulus figures are:

		Dry	Wet
E_i		63.9 GPa	55.5 GPa
E_t		51.6 GPa	37.1 GPa
E_s		48.1 GPa	38.3 GPa

N.B. 1000 microstrain = 1 mm.m^{-1}.

Table 3.4 : Summary of static elastic moduli from rock cores. Full data appear in Appendix 15.

Sample	Rock mean grain size, phi	Mean initial tangent modulus (E_i),GPa		Mean tangent modulus at 50 percent ultimate stress (E_t),GPa		Mean secant modulus to ultimate stress (E_s), GPa	
		dry	wet	dry	wet	dry	wet
HQ-17	1.3	69.5	74.0	66.6	65.1	67.2	60.3
SJ-3	1.3	73.5	85.8	73.7	67.5	73.4	47.7
KTW-14	2.6	77.8	88.8	82.6	65.3	80.6	58.8
BQ-V	2.7	67.1	-	63.0	-	64.3	-
BQ-1XA	2.9	74.7	81.5	68.3	64.4	64.4	66.5
KS-2	3.3	48.4	46.1	56.3	48.3	51.7	51.7
KTW-i	4.2	77.7	62.0	64.3	59.5	63.3	60.2
SJ-T	4.7	94.0	59.1	72.7	65.2	70.2	61.0
OB-W	5.6	63.9	55.5	51.6	37.1	48.1	38.3
HQ-22	6.3	68.3	14.0	68.4	11.2	60.9	10.9

at 50 percent ultimate stress (E_t) is reduced by saturation as is the secant modulus at ultimate stress (E_s),   though reduction is not uniform.

Deere and Miller (1966) compared static and dynamic properties of rocks and concluded that their magnitudes are equal for compact rocks at low stresses, although at high stress levels the dynamic properties are greater than static properties by about 10 to 20 percent.   Similar findings were published by Ide (1936).

The PUNDIT tests on cores were undertaken at low stress levels (normal temperatures and pressures) and the ultrasonic velocity is related to the dynamic elastic modulus, E (comparable with the static elastic modulus, E_i) by the relationship:

$$E = \rho v^2 \cdot \frac{(1 + \nu)(1 - 2\nu)}{(1 - \nu)}$$

where   v =   ultrasonic velocity

E =   dynamic elastic modulus - or for compact rocks, a value close to the static elastic modulus, especially at low stress levels.

ν =   Poisson's ratio.

ρ =   rock density

The greatest influence on ultrasonic velocity will be E, since wet and dry densities of greywackes or argillites differ only slightly (Table 3.1).   A reduction in value of E will lower the ultrasonic velocity as observed in the argillites (Appendix 10).

3.5.3   Rock strength and ultrasonic velocity relationships

It was hoped that ultrasonic velocity may provide means of evaluating rock strength.   However, correlation between rock strengths and ultrasonic velocity is poor, mainly because of the inherent variability of strength test results (Table 3.3B).

It is interesting to note a tendency for dry rocks to be better resolved by ultrasonic velocity and wet rocks by compression testing (Figure 3.11).
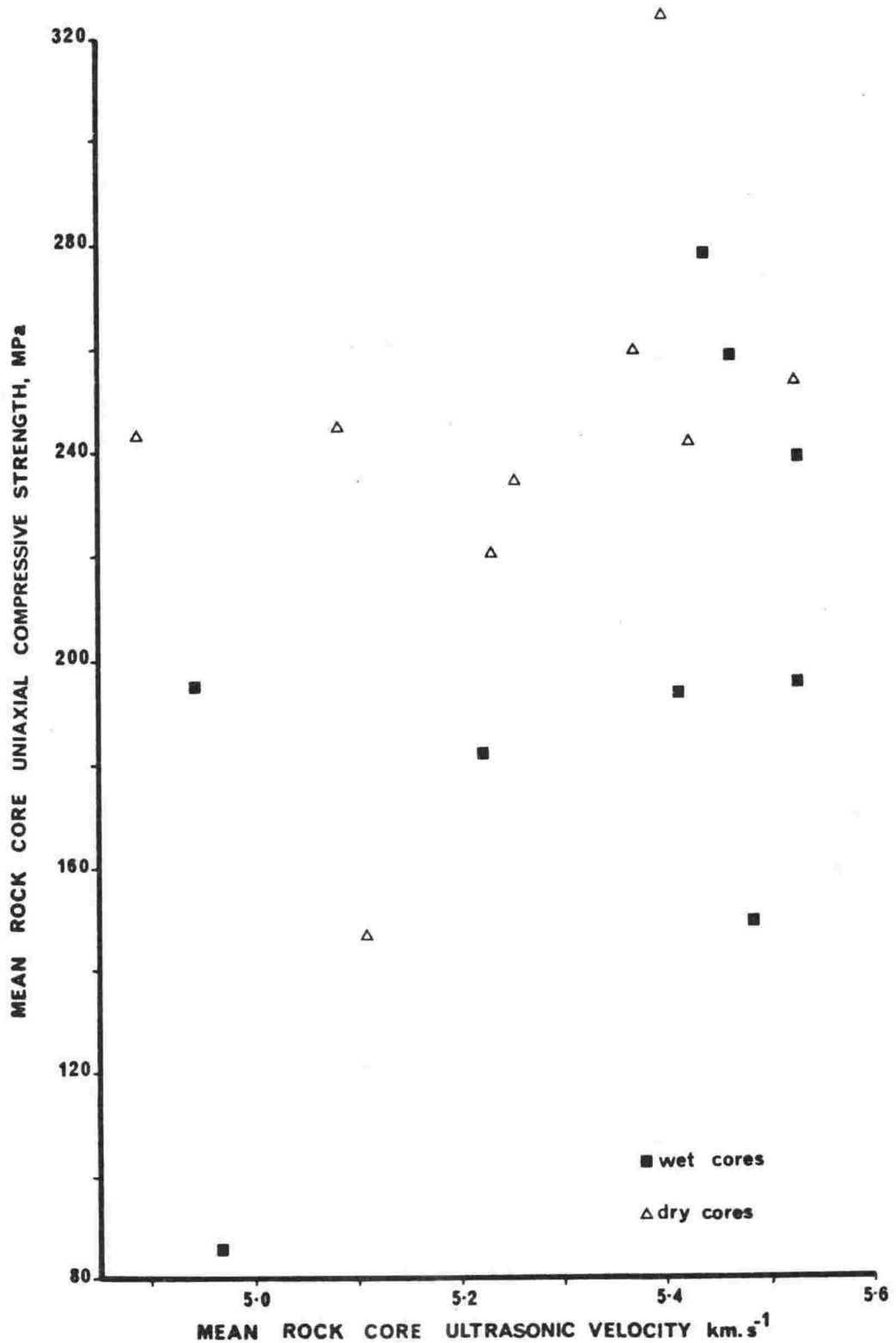
Figure 3.11 :⸱ Rock core uniaxial compression strength related to
rock ultrasonic velocity. A poor correlation
exists between these two parameters.

3.5.4   Static elastic modulus and rock texture relationships

The main contrast between Figures 3.12 and 3.13 is the tendency for dry rock static elastic moduli to remain linearly related to mean grain size whereas in wet rocks the relationship becomes rapidly more inverse with mean grain size finer than 5 phi.   Moduli correlation improves from E_i through E_t to E_s in dry rock but remains poor in wet rock. E_t provides the best correlation in greywackes.   The moduli spread appears greater in coarser rocks.

Correlation disparity is explained by Belikov (1967) "the elastic parameters of rocks are a function of the elastic constants of the constituent minerals, but the former are generally lower than the latter because of the rock porosity which weakens the bonding between the mineral grains".   He also determined elastic constants for some of the main rock forming minerals.

The felsic minerals, quartz and alkali feldspars, are more elastic than phyllosilicates and, if compared with the mineralogy of the rocks (section 2.7), the elastic modulus may be expected to be reduced in finer grained greywacke-suite aggregates.   Some coarse grained greywackes (chipwackes) contain large clasts of argillaceous material (sedimentary rock fragments, section 2.12) and it is these that produce the levelling effect in the curve in Figure 3.13.

3.6   Degradation

An important engineering characteristic of any aggregate material is stability when stockpiled, i.e. physical and chemical properties should not change to an extent where the material no longer meets specification.

These changes (collectively termed degradation when the process is deleterious) and the rate at which they take place, are especially important where an aggregate is to be exposed to weathering in service, e.g. as exposed aggregate in a concrete panel, railway ballast, road surfacing chip, rip-rap or filter blanket.
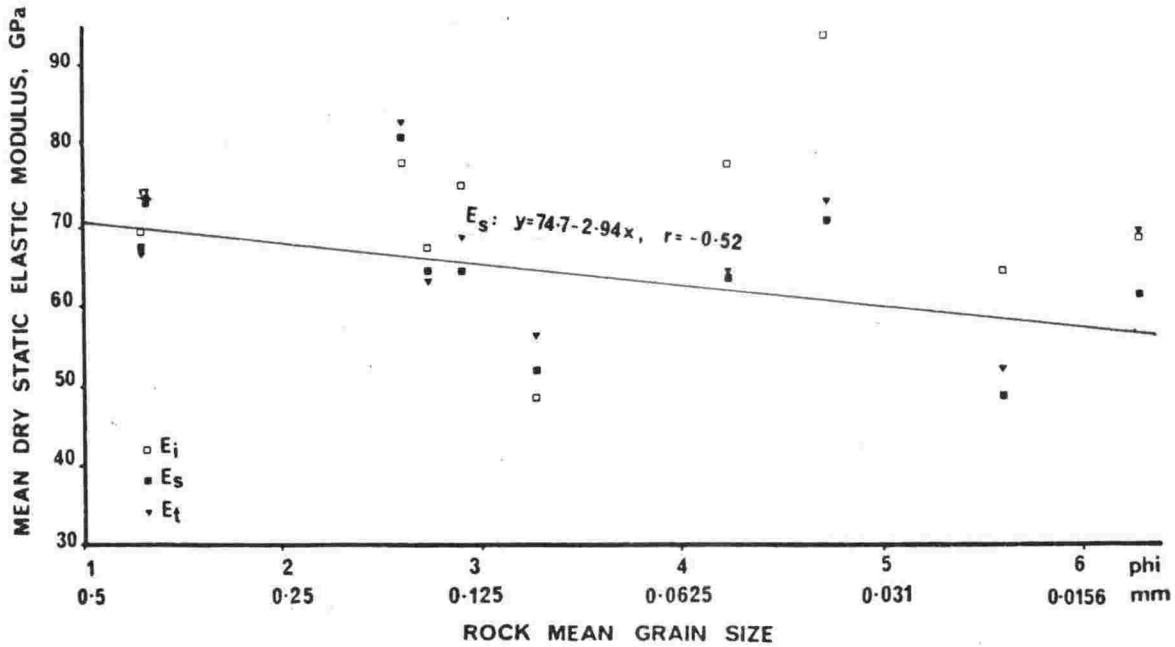
Figure 3.12 : Dry rock static elastic modulus related to rock
mean grain size.
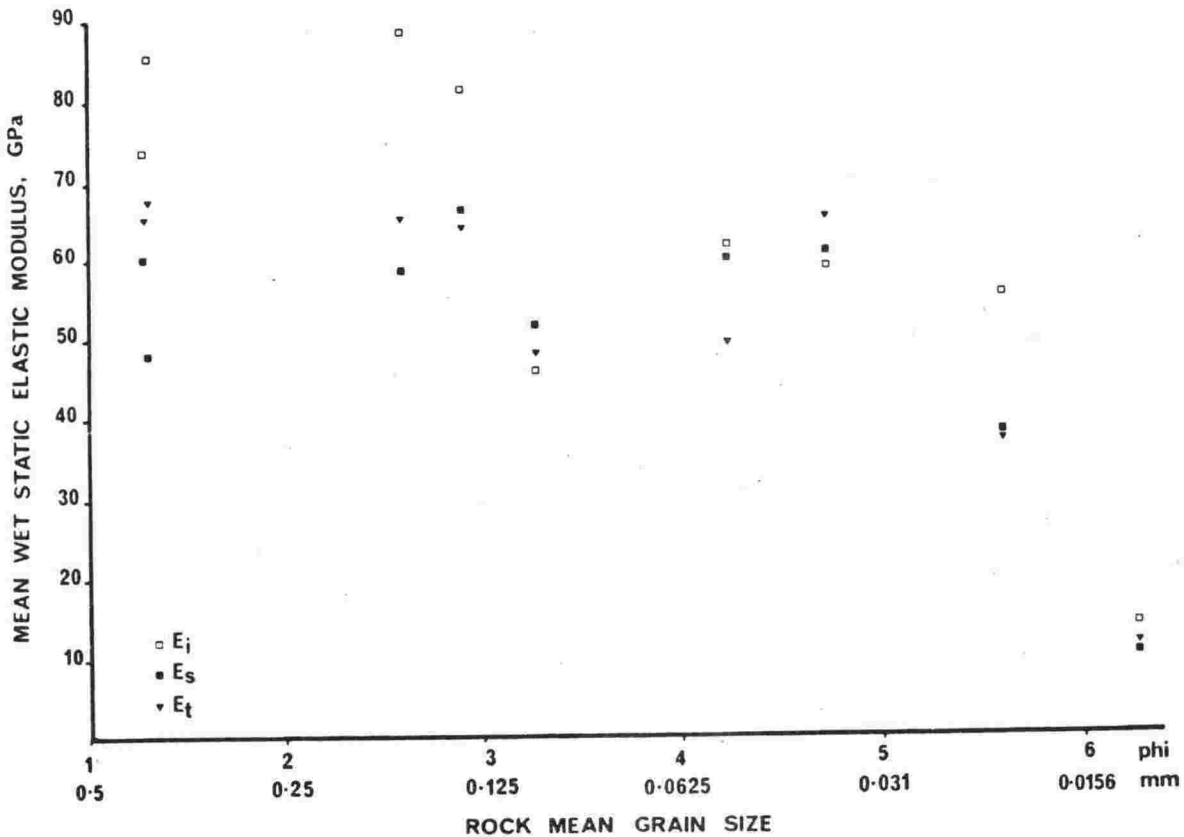
Figure 3.13 : Wet rock static elastic modulus related to rock
mean grain size. Averaged wet rock static elastic
moduli show an increasingly rapid decrease as mean grain size
decreases.

3.6.1   "A method for assessing degradation in New Zealand grey-
         wackes", a paper presented at the New Zealand roading
         symposium, 1979.

Some greywacke-suite rocks do degrade and this paper and information else-
where (Appendix 23, 24, 25) are included since relevant quantitative data is *are*
scarce.

A METHOD FOR ASSESSING DEGRADATION IN
NEW ZEALAND GREYWACKES.

G.H. Rowe, First New Zealand Concrete Research Association Research Fellow

SYNOPSIS

A laboratory method for determining the degradation potential of New Zealand greywacke-suite rocks has been developed to degrade rock aggregate in an accelerated and quantitative manner.

The test gives a Rock Stability value, here defined as the percent weight loss after 10 days treatment in 10 percent HCl at $80^{\circ}C$ under standard conditions. The percent weight loss results from the solution of chlorite, and to lesser extents calcite and zeolite, and is a function not only of the proportions of these minerals but also of the degree of veining, fracturing and intergranular permeability.

The laboratory apparatus for performing the test is simple to construct and operate and requires minimal operator attention; it may be used to test aggregate chips or prepared rock samples.

1. INTRODUCTION

Over the last 15 years there has been much concern expressed over the "degradation" of aggregates (Buckland, 1967; Clelland, 1967; Cornwell, 1966; Dekker and Scott, 1969; Kear, 1965; Kear and Hunt, 1969; Reed, 1965, 1966, 1967; Skinner, 1970; Watters, 1969), particularly "wacke"-type aggregates (Kear, 1965; Reed, 1966), whilst stockpiled or otherwise exposed to weathering. This paper presents a new test developed to provide a means of better forecasting rock behaviour during storage and use as aggregate.

2. THE DEGRADATION PROCESS

Degradation is here regarded as the detrimental physico-chemical alteration (weathering) of rock. The two main factors influencing this alteration are mineral composition and texture (grain size). Throughout New Zealand the main mineral components of the greywacke-suite rocks are quartz, sodic plagioclase, white micas and chlorite, with a texture range from gravel to silt size.

Marshall (1974) has shown that chlorite is the first of the four main minerals to be eliminated during weathering, the dominant processes being oxidation and hydration. Chloritic materials are common in greywacke-suite rocks, ranging from 7 percent to 90 percent (Rowe, in

prep.). It was therefore concluded that the loss of chlorite was a critical factor in the degradation of aggregate. Degradation should also be influenced by the effects of inherent fabric structures, microcracks, preferred orientation etc. and the effects of elastic relief and desication rock experiences during quarrying before being subjected to heating/cooling and wetting/drying cycles of natural weathering.

3. TEST PRINCIPLE AND ASSUMPTIONS

It was assumed that chlorite is the first common mineral to be destroyed by weathering and that therefore an indication of rock performance could be gained by measuring the loss of chloritic components. The method adopted follows that of Carroll (1970), utilising a 10 percent concentration of Hydrochloric acid (by volume) at $80^{\circ}C$, and relates percent weight loss to rock stability.

The weight loss, due largely to the solution of chlorite is a function not only of the proportion of chlorite in the sample but also to the degree of veining, fracturing and intergranular permeability.

Preliminary tests were on small chips of greywacke-suite rocks in open beakers. Dramatic changes occurred after only six days; the finer grained, more chlorite rich rocks were physically disrupted by crystallising iron compounds as the acid solution dried. Flaws, invisible prior to testing, were enhanced and disruption duplicated degradation effects observed in the field. Colour changes, too, were consistent with those seen in naturally degrading rock being leached to a lighter value* accompanied by concentrations of iron oxide giving yellow, yellow-brown and light red-brown surfaces and margins. Pieces able to be pulled apart in the fingers after testing often displayed a mineral coating on the parted planes which possessed a blue-grey metallic sheen. The coating is pyrolusite (MnO_2), chlorite having manganese occurring within its crystal lattice (B. Roser, pers. comm.; G. Bird, pers. comm.; Deer et al., 1971).

Degraded rock material from these tests was generally one to six millimetres in size, equidimensional with sharp, flaky form. A type of exfoliation process was seen in samples possessing strong preferred orientation, a phenomena more apparent with decreasing mean grain size. Samples all assumed a lighter colour after testing, with an increase in porosity and loss in weight. X-ray

Research Fellow
Geology Department, Victoria University
of Wellington.

*   Rock - colour chart; Geol. Soc. America 1970.

diffractometry confirmed chlorite has been removed from samples along with zeolite (laumontite) and calcite apparent in some samples.

4. DEVELOPMENT OF TEST APPARATUS

Following encouraging preliminary tests an apparatus was designed and built (Fig. 1), essentially an insulated wooden box with a heat source to one side (a 60 watt light bulb serving as a pilot and illuminating light). A partition divided the box to give slight heat gradient both horizontally and vertically so that convection tubes (Fig. 1), which contained the sample were held perpendicular to the partition and allowed the acid solution placed within the tube to slowly circulate. After inclusion of the sample and the acid, the top was sealed with acid resisting plastic film, heat resisting plastic film and a rubber bung.

5. DEVELOPMENT OF TEST PROCEDURE

Time taken to reach the test temperature did not exceed one percent of the total testing time so that the temperature rise had little significant effect on samples. Numerous trials of using different sample loadings and heat source wattages were used to establish an optimum test situation in which the apparatus maintained a temperature of $84 \pm 3^{\circ}C$ with ambient temperatures between $16^{\circ}C$ and $22^{\circ}C$.

A small sample of VUW standard chlorite, 196/1/1(b), was tested over 10 days to establish a maximum percent weight loss for chlorite and to ensure that the volume of acid used in the test was sufficient to prevent it being exhausted by the reaction. The percent weight loss of the chlorite standard was 60.7 percent. The sample after testing was a soft skeletal, porous mass with a pearly lustre: the "talc" layers of mainly Si and Al. Chemical analyses (Deer et al., 1971) of chlorites indicate that major oxides other than SiO_2 and Al_2O_3 i.e. MnO, Fe_2O_3, FeO, MgO and H_2O, sum to an average of approximately 60 percent.

Samples were cut to give an approximate weight of 18 grams and dried to constant weight at $105 \pm 3^{\circ}C$, cooled in a dessicator and weighed to four decimal places before being tested.

Relative performance between samples was quantified by establishing a percent weight loss.

Two trials, one using an argillite (mean grain size 6.28 phi = 0.013 mm) and the other a greywacke (mean grain size 2.9 phi = 0.13 mm) established that the precision of the test method at 10 days of testing to be $\pm$ 2.4 percent weight loss and $\pm$ 0.8 percent weight loss respectively (fi.g 2). The trials also showed the trend of percent weight loss with time to be linear after four days of testing. Argillite lost more weight over any given interval of time than greywacke and its rate of weight loss is therefore

higher at any time but especially the first four days of testing.

Plate 1. Showing the Rock Stability apparatus in operation. Note the wire strand, to hold convection tubes in an upright position. Insulation is provided by 12 mm polystyrene plastic covered with aluminium foil.
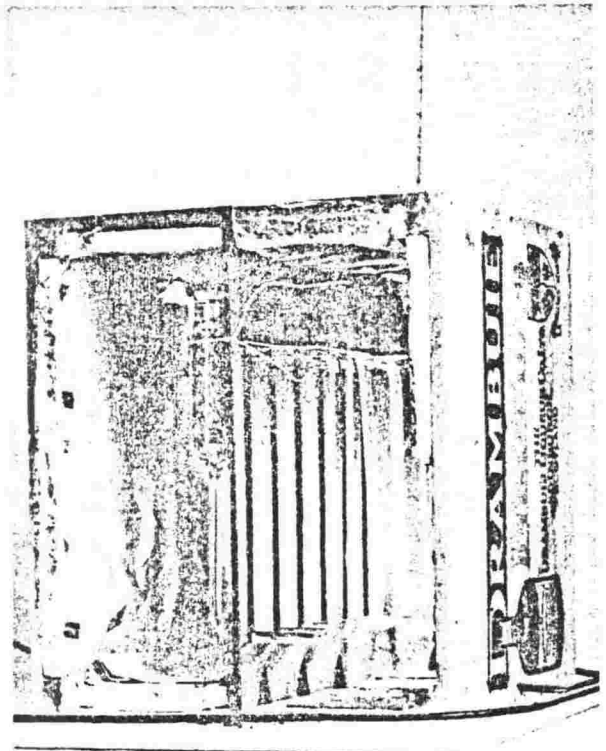
Surface area/volume ratios of samples were assumed to have a significant effect on test results, the larger this ratio the higher the expected percent weight loss. Trials were made with similar specimen shapes of differing dimensions so that weights differed. Weights and test results are shown in Table 1.

Samples cut after testing showed that leaching had occurred to a depth related to the manner in which the sample was prepared as well as rock type. There was a slight leaching to form a halo beneath a slickensided surface; the leaching halo being deeper beneath the surface for a naturally fractured surface than a sawn surface for any given rock type. The depth of leaching did not exceed four millimetres for most samples. Destruction of chlorite, i.e. halo penetration, did not proceed to the centre of the sample unless it was extremely flaky or small. Visible and invisible fractures (microcracks), iron oxides, the occurrences of calcite, laumontite and chlorite, especially along foliation planes, yielded higher percent weight losses.

It was apparent that though there may be changes in the Rock Stability value for different size aggregates due to differences in surface area/volume

Figure 1

Rock Stability apparatus shown in vertical and horizontal section to give basic dimensions and illustrate relative positions of internal fittings. A maximum of six convection tubes were used. c.f. Plate 1. Dimensions in millimetres.
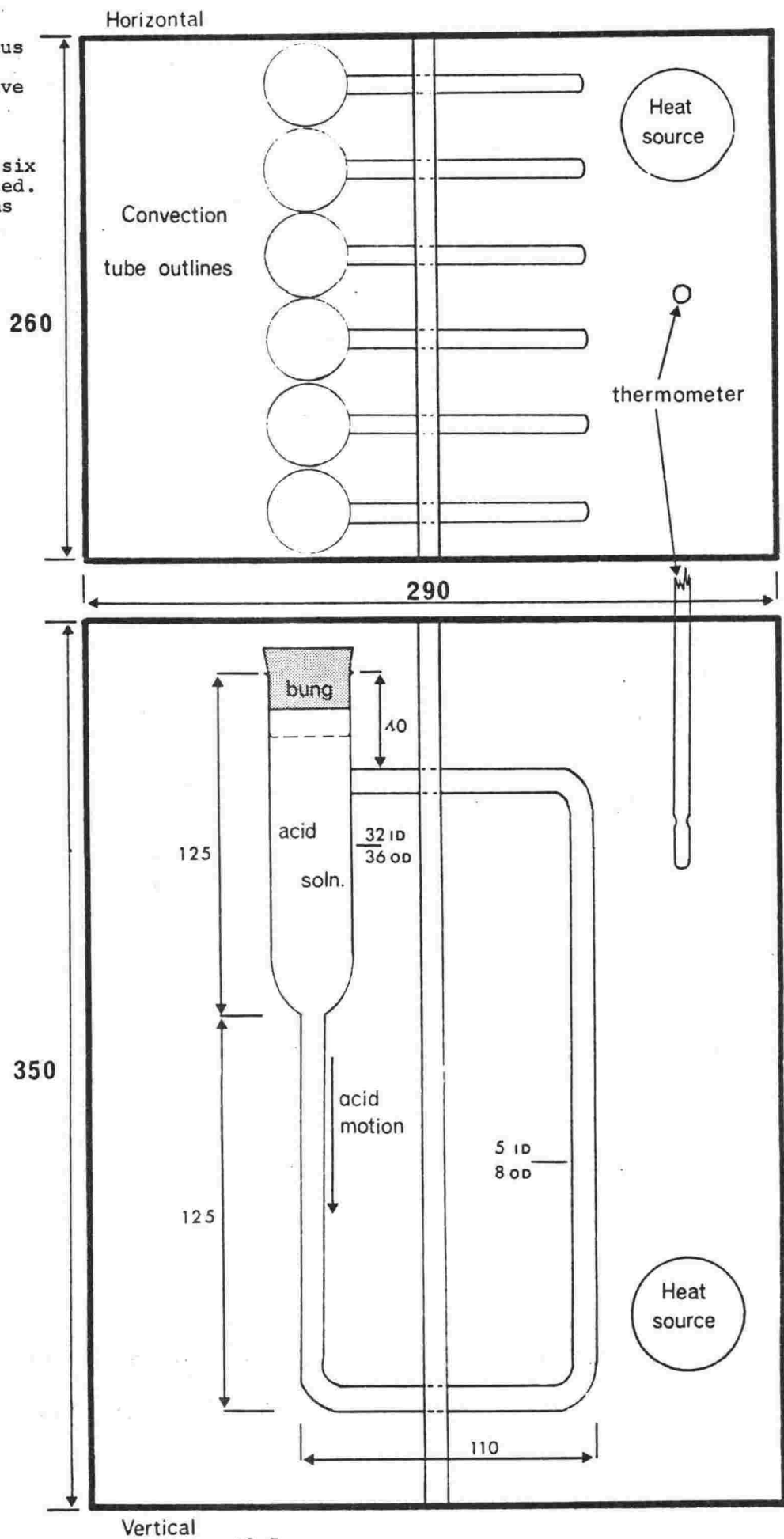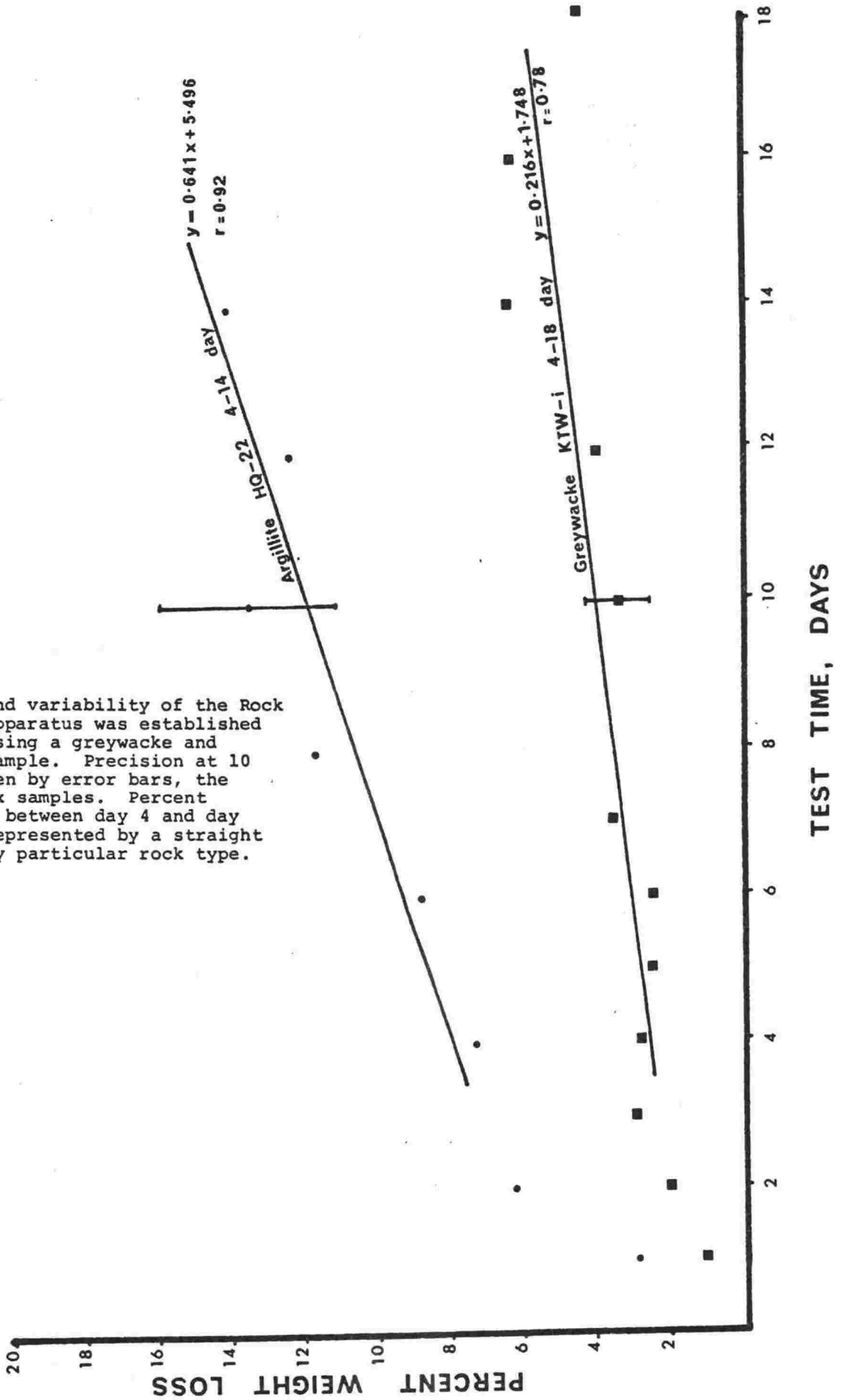
Figure 2

Precision and variability of the Rock Stability apparatus was established by trials using a greywacke and argillite sample. Precision at 10 days is given by error bars, the range of six samples. Percent weight loss between day 4 and day 12 may be represented by a straight line for any particular rock type.

ASSESSING DEGRADATION IN NEW ZEALAND GREYWACKES

Table 1

The effects of surface area to volume
ratio are indicated by using samples of
different weight for a similar geo-
metrical shape. Argillites show a
tendency towards higher percent weight
loss in heavier samples. Greywackes show
highest percent weight loss with the
lightest sample; scatter within the
samples indicates surface area:volume
ratio of samples of given weight
relatively unimportant.

Oven dry sample weight before testing (gm)	Rock Stability Value
GREYWACKE BQ-IXa	
46.0954	4.2
41.9840	4.2
36.4027	5.1
34.6257	4.9
33.1153	5.5
29.6689	4.9
24.3285	5.6
mean	4.9
ARGILLITE HQ-22	
50.8953	11.5
37.4426	11.4
31.4076	16.2
25.9724	15.0
22.9726	14.1
19.0884	13.7
18.9196	12.3
mean	13.5

ratios there was no significant effect
for samples in the weight range 18-50 gm
(Table 1), which corresponds to the size
range 19-25 mm.

Samples are subjected to physico-chemical
degradation in the same way as natural
weathering agencies. The test therefore
indicates the vulnerability of rock
particles to degradation.

In quarried aggregates irregularities
in gross surface texture and shape may
increase percent weight losses.

6. ROUTINE RESEARCH METHOD USED

Approximately 120 greywacke-suite rock
types, mostly from Wellington, have been
tested in the following manner:

Representative samples were cut from
large hand-specimens to measure approx-
imately 25 - 30 mm x 12 mm x 12 mm with
flat, coarse ground sides and weighing

between 10 and 25 gm but averaging 18 -
19 gm. Commercially available aggregates
were tested by selecting six pebbles
typical of a 25 - 20 mm grading and
meeting the overall criteria of dimensions
and weight mentioned above.

Samples were dried in an oven ($105 \pm 3°C$) until they reached constant weight
(six hours minimum), cooled in a vacuum
desiccator and weighed (to four decimal
places), before being sealed in the
convection tubes with 10 percent HCl and
subjected to a temperature of $83 \pm 3°C$ in
the apparatus for four days. They were
then removed from their acid solutions,
rinsed overnight in slowly circulating
tap water to leach all acid and soluble
reaction products, dried, weighed, then
returned to their respective tubes (and
acid) and tested for a further eight days.

The percentage weight losses at four
and 12 days was calculated for each
sample:

$$\frac{w_o - w_x}{w_o} \times 100\%$$

where w_o = pretest oven dry weight, w_x = oven dry weight at four and 12 days respectively

The average percent loss per day for
each sample was calculated over the period
between day four and day 12 i.e. the
gradient of a straight line joining the
four and 12 day percent weight losses on
a percent weight loss versus time graph:

$$\frac{W_{12} - W_4}{8} = \% \text{ weight loss per day.}$$

The physical condition of the specimens
before and after testing were recorded.

7. RESULTS

Figure 3 summarises the results
obtained (based on approximately 120
samples), which are clearly separated
into two groups by a well defined band
(hachured in the figure) in which few
samples plotted.

7.1 Geological factors influencing results

Significantly weathered rock tended to
have high percent weight loss rates, initially,
due to higher porosity, permeability and
concentrations of susceptible iron in
readily mobile forms (samples 1B 17,
1B 22; fig 3). Other samples (DC-LAM,
KTW-iii, WCC-23A) are laminated sand and
silt sized rocks with increased effective
porosities due to fissility developed
parallel to bedding and high preferred
orientation, encouraging permeability
parallel to bedding. Concentrations of
organic material in finer laminations
also increases porosity and permeability.

Fresh samples with high weight percent
losses (HQ-22) are susceptible to
treatment due to microcracking giving
increased surface area. The cracks
(less than 0.004 mm wide) had not been
detected with the naked eye before
testing.

Figure 3   The relative effects of microcracking, lamination, weathering, zeolites and organic matter content of rocks subjected to the Rock Stability test.
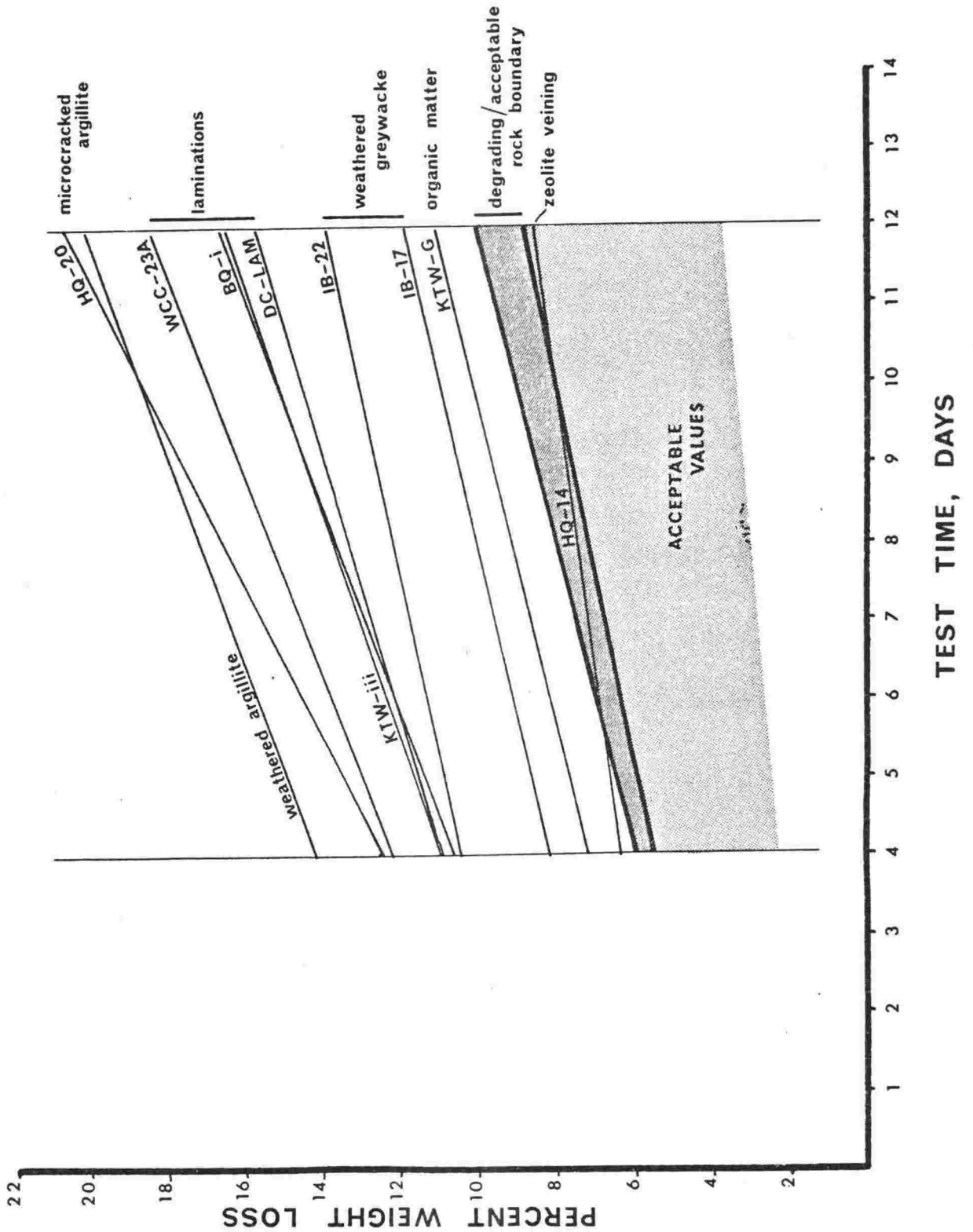
7.2 Rock Stability

From figure 3 the range of percent weight loss values separating rocks with low and high weight losses increases with time. For a laboratory test to be used routinely in assessing aggregates only one determination of weight percent loss, rather than two, undertaken at four and 12 days, is desirable. A 10 day test was considered definitive, resolution of results being consistent with acceptable testing time - the Accelerated Weathering test (Clelland, 1967) takes a similar length of time.

Weight percent loss of a rock sample at 10 days is therefore defined as the Rock Stability value (RSV).

As may be expected there is a positive, scattered correlation between RSV and the percentage sum of chlorite components of rocks (Fig. 4) established by modal analysis of the sample rocks in thin section. Percentage sum of chloritic components (chlorite) was taken as the sum of the percentage of sedimentary rock fragments, basic volcanic rock fragments and detrital and authigenic chlorite with grain sizes larger than 5.65 phi (0.02mm) and matrix - material with a grain size less than 5.65 phi (0.02mm). X-ray diffractometry estimates of chlorite percentage reveals a similar trend with RSV.

There is also a positive non-linear scattered correlation between diminishing mean grain size of samples and RSV, due to an increase in chloritic material, preferred orientation, organic matter, and microcracking which accompanies reduced mean grain size. A similar trend is seen for chlorite and mean grain size (Figs 5 and 6).

Results from tests of four commercially available greywacke aggregates, where RSV is an average from six aggregate particles, are shown in Table 2 with corresponding Los Angeles abrasion, 10 percent fines and Accelerated Weathering test results.

8. DISCUSSION

Results indicate that a sample with a RSV exceeding 8 percent can be expected to degrade. This delineation is supported by field evidence, physical testing and petrography. Exceptions arise in weathered materials which have a high RSV for particular mean grain sizes and reduced percent weight loss rates per day; these materials are usually yellow-brown in colour, have lower densities and give poor performances in normal aggregate tests.

Coarser grained greywacke-suite rocks often have argillite fragments included in their clastic components i.e. sedimentary rock fragments. These fragments may range in size from 2 mm to

400 mm or more but are commonly in the range 5 mm to 60 mm. These rocks have a rather higher RSV than may be expected from their mean grain size but it is the large fragments of included argillite which reverse the trend of fig. 6. If these rocks are crushed to yield aggregate then portions of the rock with clasts exceeding, say, 15 mm may well have excessive argillite particles and therefore a higher chance of degradation.

Crushed aggregates give a higher RSV than aggregates from river sources, generally, because of increased surface area induced by irregular surfaces, crushing, etc. Natural degradation is also somewhat enhanced by such effects of manufacture and the test may be considered as having a "built-in" mechanism to assess incipient mechanical weakness induced by manufacture.

The results of most existing test methods are valid only at the time of test and give little indication of performance expectancy over the working life of the aggregate. Some tests have their results "improved" by parameters such as particle morphology e.g. the Los Angeles test gives "poorer" results if aggregates are angular rather than rounded, finer graded rather than coarser (Orchard, 1964). The 10 percent fines test tends to have an "improved" result if the aggregate particles are equidimensional rather than flakey, rounded rather than irregular. Not surprisingly, these two tests show good correlation (Shipway, 1964). A comparison may be seen in Table 2 of two very different rock types juxtaposed in a Wellington quarry.

From Table 2 the fresh argillite gives the impression of being as "good" as the greywacke, and at the time of testing it may well have been, the Rock Stability value however gives a better idea of what may be expected from the argillite. The other tests would have to be repeated with time on the same sample to yield similar information.

The wetting and drying, heating and cooling of the Accelerated Weathering tests (Clelland, 1967) is given a secondary role in the Rock Stability test. The importance of chemical effects in rock decay was indicated well by Griggs (1936) and unpublished research by the author suggests chemical effects may be more important than physical changes in degradation of aggregates below a certain maximum screen size.

Figure 4 A scattered, positive correlation between Rock Stability value and Σ chlorite percent exists. Samples labelled depart from the trend due to influences of organic matter, lamination, calcite or zeolite in greater than normal concentrations.
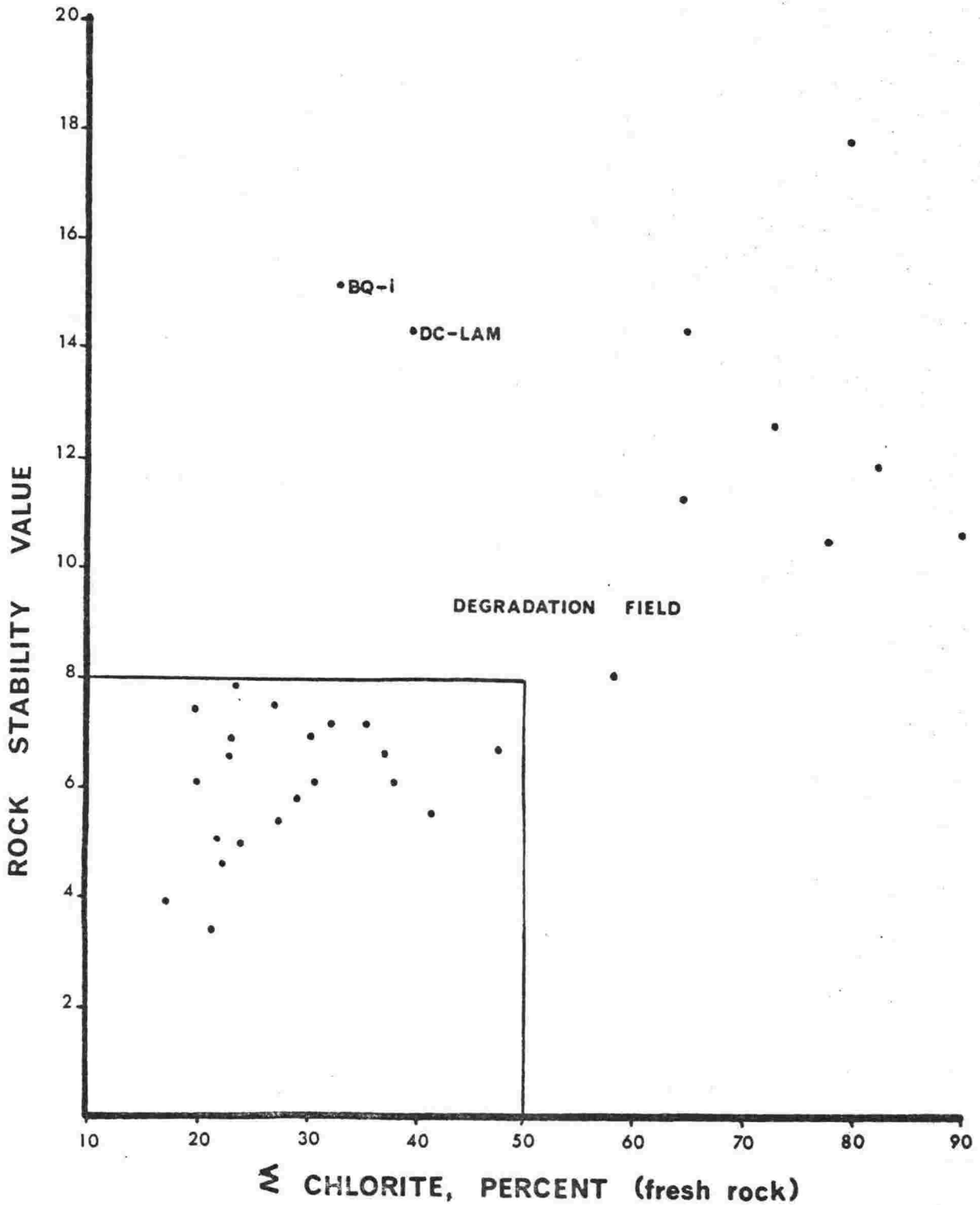
Figure 5 Rock Stability value is enhanced with smaller mean grain sizes in
greywacke-suite rocks due to the increase in chlorite components
in these rocks. The coarsest greywacke-suite rocks also show
increasing Rock Stability values due to a relative increase in size
and number of chlorite bearing rock fragments.
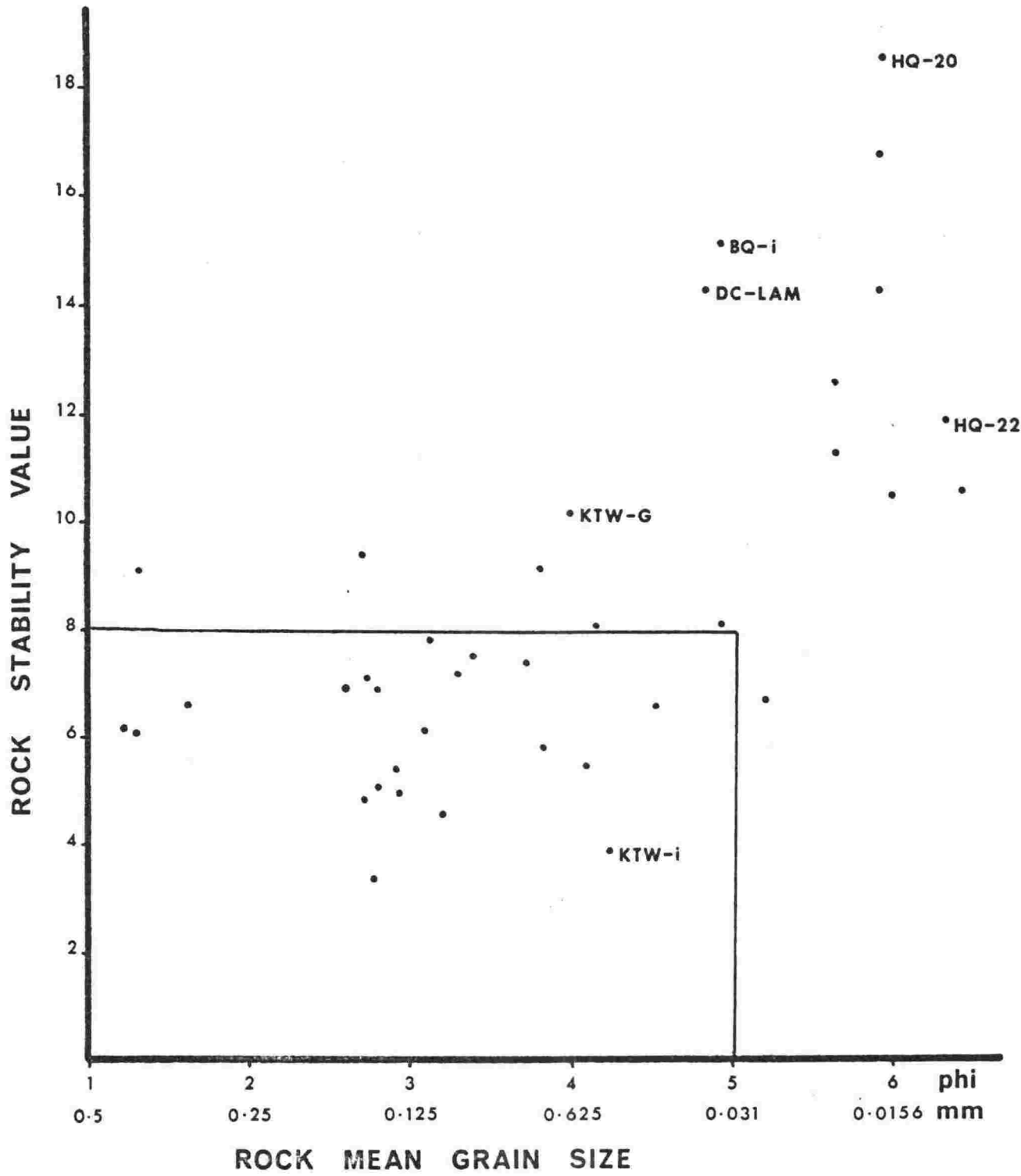
Figure 6   Greywacke-suite rocks rapidly increase in chlorite content with reduced
            mean grain size. The fine grained rocks (Argillites) are susceptible
            to degradation.
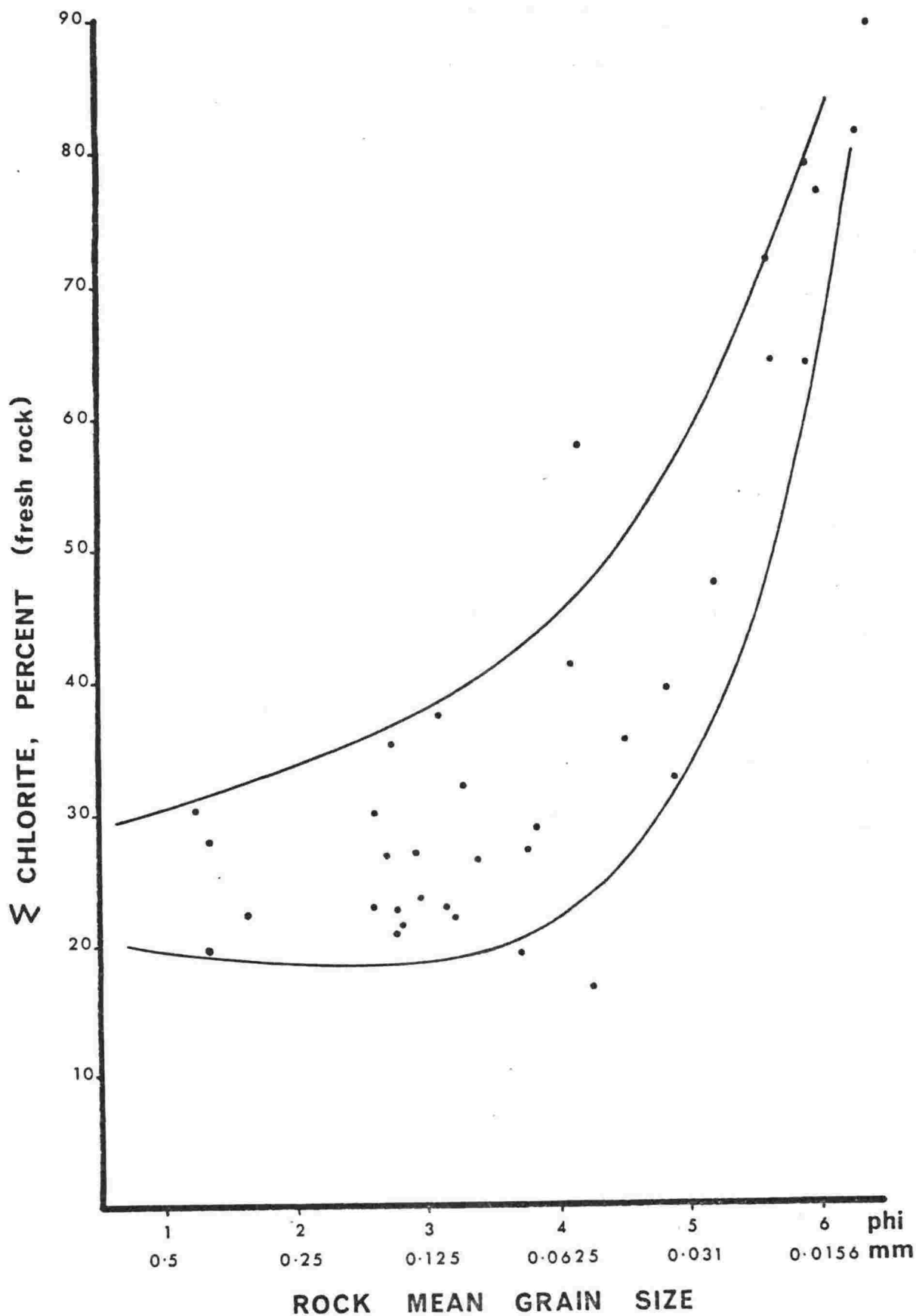
Table 2. A comparison between different aggregate performances for various established tests and the Rock Stability test. (Based on data supplied by the N.Z. Concrete Research Association Laboratories).

Aggregate type	Los Angeles test	10 percent fines test	Accelerated Weathering test	Rock Stability value
Fresh argillite (degrades within three months of initial exposure) Wellington	13%	29 tons	AB	11.9%
Fresh greywacke (adjacent to argillite tested above) Wellington	19%	29 tons	BB	6.1%
Commercially available rounded greywacke, Christchurch	12%	43 tons	AA	5.4%
Commercially available crushed rounded greywacke, Christchurch	12%	36 tons	AA	5.6%
Commercially available crushed greywacke, Whangarei; contains plastic clays.	14%	23 tons	AB	9.8%
Commercially available rounded greywacke, Christchurch	-	61 tons	-	7.2%

9. COST OF THE TEST

The main items of equipment necessary for performing the Rock Stability test are normally found in well equipped laboratories i.e. drying oven, dessicator, and balance (weight to two decimal places would be adequate for routine work). Construction of the Rock Stability apparatus is well within the capability of technician staff at a cost of the order of $NZ200.

Time involved for a routine work is 10 days of testing with perhaps an extra working day required for drying, leaching, weighing, etc. Two litres of acid solution is adequate for 20 samples. Technical personnel need only attend the apparatus for a half hour at the commencement and conclusion of a test. Operator error is at a minimum.

10. CONCLUSIONS

A rock stability test that involves treatment of the sample with 10 percent HCl at 80°C is presented. The test indicates the degradation susceptability of greywacke-suite rocks and should fill a need for means of predicting the performance of greywacke-suite aggregates.

REFERENCES

BUCKLAND, A.H. (1967) The Degradation of Roading Aggregate. Proc. Roading Symp., Road Res. Unit, N.Z. Nat. Roads Board, V.2: 692-715.

CARROLL, D. (1970) Clay Minerals: A Guide to their X-ray Identification. Geol. Soc. Am. Spec. Paper 126: 80 p.

CLELLAND, J. (1967) An Artificial Weathering Test for Roading Aggregates. Proc. Roading Symp., Road Res. Unit, N.Z. Nat. Roads Board, V.2: 743-758.

CORNWELL, W.L. (1966) Assessment of Basecourse Aggregate Quality, Auckland-Hamilton Motorway. M.O.W. Internal Report: 9 p.

DEER, W.A., HOWIE, R.A. and ZUSSMAN, J. (1971) An Introduction to the Rock-forming Minerals. Longman, London: 528 p.

DEKKER, B. and SCOTT, K.O. (1969) Some Aspects of Aggregate Supply for North Island Power Stations. Proc. Nat. Conf. Concrete Aggregates, Hamilton, New Zealand: 26-34.

GRIGGS, D.T. (1936) The Factor of Fatigue in Rock Exfoliation. Jl. Geol. V. 44 (7): 783-796.

KEAR, D. (1965) South Auckland Road - Metal Quarries "Wacke"-type Rocks. N.Z. Geol. Survey Report 2: 24 p.

KEAR, D. and HUNT, J.L. (1969) Aggregate Resources of New Zealand. Proc. Nat. Conf. Concrete Aggregates, Hamilton, New Zealand: 17-25.

MARSHALL, T.W. (1974) A Petrographic Investigation of Greywacke-type Aggregate from the Auckland Region. Unpub. M.Sc. (Hons) Thesis: 125 p.

ORCHARD, D.F. (1964) Factors Influencing the Wear of Coarse Aggregate in the Los Angeles Test. Proc. Second Conf. Australian Road Res. Board, V.2. part 2: 963-980.

REED, J.J. (1965) Mineralogy and Petrology in the New Zealand Geological Survey 1865-1965. N.Z. Jl. Geol. Geophys. V.8 (6): 999-1087.

REED, J.J. (1966) Geological and Petrological Investigations of Wacke Aggregates used in Auckland - Hamilton Motorway, Redoubt and Takanini Sections. N.Z. Geol. Survey Report 20: 47 p.

REED, J.J. (1967) Application of Recent Petrological Advances to Selection of Road Aggregates. Proc. Roading Symp., Road Res. Unit, N.Z. Nat. Roads Board, V.2: 716-742.

SHIPWAY, C.H. (1964) A Study of the Aggregate Crushing Test. Proc. Second Conf. Australian Road Res. Board, V.2 part 2: 981-996.

SKINNER, D.N.B. (1970) Mineralogical changes in some New Zealand Sedimentary and Igneous rocks and their effect on Aggregate Quality. First International Congress of the International Association of Engineering Geology, Paris, France, 8-11 September. Section 1: Natural and Industrial Materials of Construction: 534-547.

WATTERS, W.A. (1969) Petrological Examination of Concrete Aggregates. Proc. Nat. Conf. Concrete Aggregates, Hamilton, New Zealand: 48-54.

APPENDIX 1

Method of test to determine the Rock Stability value of aggregates from greywacke-suite rocks.

Scope

An accelerated laboratory test designed to assess whether greywacke-suite aggregates will degrade by physico-chemical alteration.

Procedure

A. Apparatus

1. An insulated box and fittings of approximate dimensions given in fig. 1, fitted with a heat source such that the box when closed will equilibrate at a temperature of $83 \pm 3°C$ within three hours. A 60 watt electric lamp will suffice.
2. Six convecting tubes with dimensions as in fig. 1.
3. Six rubber bungs to fit 2. above each with an acid resistant (polythene) and a heat resistant ("glad" oven bag) plastic film barrier (a 60 mm square of each material per bung is adequate).
4. One mercury in glass thermometer, capable of being read to $1°C$ in the range $70°C$ to $90°C$.
5. A balance capable of weighing up to 50 gm to ± 0.01 gm.
6. A ventilated oven controllable between $100°C$ and $110°C$.
7. A dessicator (150 mm) with active silica gel, or other suitable dessicant, in its base.

B. Reagents

1. Concentrated Hydrochloric acid (laboratory reagent grade or better) diluted with distilled water to give a 10 percent solution by volume. May be made up and kept, sealed, indefinitely. Approximately 100 ml of the 10 percent solution is required for each test.

WARNING

Hydrochloric acid and its fumes are highly corrosive, protective clothing, gloves and face visor should be worn when mixing this chemical with water. Mixing should be carried out in a fume

cupboard. Always mix by pouring acid into water, NEVER water into acid; mixing should be done slowly as the reaction is exothermic (heat generating). ALWAYS use good quality pyrex or polypropylene mixing vessels. Storage of 10 percent HCl may be in glass or plastic vessels with a screw type plastic cap.

C. Sample Preparation

1. Samples must be selected as being those most representative of a representative sample, with regard to rock type, size, shape and surface texture of the aggregate concerned.
2. A minimum of six samples must be tested for each aggregate type.
3. Samples must be selected from the 25 mm - 20 mm size range and weigh between 15 gm and 25 gm. Should aggregate in question be too large then pieces may be sawn or broken to assume approximate shape of a square right prism and fulfilling the weight requirements above consistent with size to fit the convection tubes.
4. Samples must be scrubbed to remove loose adhering matter, dried to constant weight (about 6-8 hours) in an oven at $105 \pm 3^\circ$C. Allow to cool in the dessicator for 1 hour.
5. Identify and weigh each sample (to two decimal places).

D. Testing Procedure

1. Place samples into convection tubes (one sample per tube) and fill the tube to within 20 mm of the top. Remove air bubbles by tilting the tube.
2. Firmly insert a rubber bung into each tube. The base of the bung should be covered with a piece of heat resisting then acid resisting plastic film before being fitted.
3. Position all tubes in the apparatus in the manner shown in plate 1.
4. Shut the box and monitor the temperature on the light bulb side of the partition; it should remain at $83 \pm 3^\circ$C.
5. Continue for 10 days $\pm$ 4 hours.
6. Remove tubes from the apparatus, remove samples from the tubes by pouring the hot acid from the tubes in a fume cupboard.
7. Place samples in a shallow (40 mm deep) plastic or glass vessel large enough so samples are well separated.
8. Apply a slow flow of tap water over the samples by way of a tube so as not to disturb the samples. Continue for 18 hours.
9. Dry the samples to constant weight, cool in a dessicator for 1 hour and weigh to two decimal places.

Results

The percent weight loss for each sample is calculated from

$$\frac{w_o - w_{10}}{w_o} \ 100\%$$

where w_o = initial oven dry weight of the sample

w_{10} = oven dry weight of sample after 10 days testing

The mean percent weight loss for the aggregate rock-type is reported as the Rock Stability value reported to the nearest 0.1 percent.

The majority of individual results should not depart from the mean by more than 2 percent, in most cases wide variations can usually be explained, and this alone is an indication of Rock Stability.

If the Rock Stability value exceeds 8 percent the aggregate rock-type may be regarded as having a high degradation potential.

APPENDIX 2

Assessment of Rock Stability value with Rocks of Known Performance

To establish the test's ability to identify degrading greywacke-suite rock types, aggregates used in the Auckland-Hamilton motorway, Redoubt and Takanini Sections and described by Reed (1966) were tested in the Rock Stability apparatus. The results are listed below with partial reproduction of Table 2; 'Stages of Albitisation of Silt and Clay Wackes (Argillites) of the Auckland District' from Reed (1966).

From the thin sections studied, the reconstitution of argillites, termed "albitisation" by Reed (1966), is also the geologic process that concentrates and enhances chloritic components, at the same time causing a mean reduction in grain size. All rocks tested have an unsatisfactory Rock Stability value. Significant and intense "albitisation" may have a hardening effect (though P30647 was soft according to ASTM test C235 68 "Scratch Hardness of Coarse Aggregate Particles") but does not significantly increase the ability of argillacous rocks to withstand degradation when used as aggregate. Albite and prehnite are minerals possessing relatively good mechanical properties. It is unlikely therefore that they are reliable indicators of rocks susceptable to degradation. The minerals of paramount importance are those that form the matrix, which commonly encloses, cements and prevents continuity of the more durable mineral components in greywacke-suite rocks. In greywacke-suite rocks these are chloritic in composition.

Stage of Alteration (Reed, 1966)	Sample No. (N.Z. Geol. Survey)	Alkali Content (Reed, 1966) Na$_2$O	K$_2$O	Remarks (Reed, 1966)	Rock Stability Value	Remarks
Insignificant albitisation	P 30663	2.7	3.2	Disintegrating clay-wacke in Kawakawa Bay road cutting	Not tested due to extreme friability. Analogous Wellington rocks gave results of 18%	Weathered, leached, soft and weak; able to be broken in the fingers.
	P 30669	2.5	4.1	Claywacke, Mangatangi water tunnel	9.1%	Fresh argillite with prehnite vein
		(mean of 3)	(mean of 3)			
Significant albitisation	P 30664	3.9	3.0	Stevensons quarry	8.6%	Extensive chlorite matrix
	P 30646	4.0	4.2	Matakana quarry	9.2%)	Contained some calcite, much re-constitution to give broad bands of oriented chlorite. Mean grain size approx. 53 microns (4.25 phi)
	P 30647	3.5	3.5	Matakana quarry	9.5%)	
Intense albitisation	P 30649	6.1	1.6	Petrie's quarry	8.3%	
	P 30653	5.9	2.5	Beachland's quarry	6.6%	Much chloritic and albitic banding and veining
	P 30655	5.0	2.1	Litten Bros. quarry	12.6%	Mean grain size approx. 33 microns (4.9 phi)

CHAPTER FOUR

BOOKERS LAW:

An ounce of application is
worth a ton of abstraction.

Physical properties of Wellington greywacke-suite aggregates

This chapter relates geological and physical properties of the Wellington greywacke-suite rocks to those of their derived aggregates and to the properties of concrete made with these aggregates.

To obtain aggregates for testing and concrete making, samples were selected on the following criteria:

(i)   Samples had to be representative of rock from localities with the greatest future potential for quarrying purposes.

(ii)   Samples had to reflect a representative range of textural features apparent in Wellington greywacke-suite rocks.

(iii)   Samples had to be as free as possible from contamination by close veining, weathering and close jointing.

4.1   Sampling methods and sample preparation

Samples were quarried from a 3 m length of a single bed, in each of four quarries as follows:

Sample	Quarry	Rock mean grain size phi	Rock types	Lithofacies
HQ-17	Horokiwi	1.3	greywacke	thick-bedded
KTW-14	Carsons	2.6	greywacke	sandstone
BQ-IXA	Belmont	2.9	greywacke	sandstone
SJ-T	Owhiro Bay	4.7	greywacke	thin-bedded
OB-W	Owhiro Bay	5.6	argillite	thin-bedded
HQ-22	Horokiwi	6.3	argillite	thick-bedded

These quarries were chosen because they have the largest inferred "reserves" (Ward and Grant, 1978). For economic and logistic reasons, too, these quarries will be the most important to the Wellington region for the next 20 years at least.

Each sample was quarried by hand, using bars and hammers, to obtain approximately 700 kg of cobble and boulder size rock. The material was crushed in a jaw primary crusher and swing hammer mill, then screened to pass 19 mm before being placed in reconditioned, rust free 200 litre (44 gallon) drums as 19 mm "all-in", unscrubbed, unwashed aggregate. All hoppers, crushers, conveyor belts and handling equipment were cleaned before crushing successive samples. All handling, crushing and screening was undertaken by Ryans Quarries, Ngauranga.

To aid the detection of contamination between successive crushing runs the order of crushing was as follows:

KTW-14, HQ-22, HQ-17, OB-W, BQ-IXA, SJ-T

The marked difference in colour and texture between lithogies in this sequence enabled small amounts of contaminating material to be removed by hand later, when the aggregates were coned, quartered and split to obtain representative samples. These were finally screened to 19 - 9.5 mm, 9.5 - 4.8 mm and minus 4.8 mm size fractions. Material coarser than 4.8 mm was thoroughly hand washed.

4.2   Aggregate characteristics

A number of aggregate characteristics were measured to aid concrete mix design and help establish the connection between the rock and concrete produced from it. They included grading, aggregate density, water absorption, bulk density, voids content, and crushing resistance (NZS 3111:1974). In addition, abrasion resistance was assessed by the Los Angeles test and particle angularity was measured by the method of Lees (1964).

Tests for whole rock alkali reactivity were not undertaken as much work of this type had already been carried out by the Inorganic Materials Section, Chemistry Division, DSIR, with the indication that, for Wellington greywacke-

suite rocks, alkali reactivity is not a problem (St John, pers. comm.; see also section 4.4), apart from a few isolated cases observed in the laboratory. The Accelerated Weathering test (Clelland, 1967, NZS 3111:1974 part 202.4) was omitted for reasons outlined elsewhere (Rowe, 1979).

Tests for cleanness, and lightweight particles (NZS 3111:1974 parts 202.2; 201.5) were not necessary because the aggregate had been washed and because of the nature of the rock.

4.2.1   Gradings

All samples were crushed under identical conditions.   They were then screened to passing 19 mm retained 9.5 mm;   passing 9.5 mm retained 4.8 mm;   and passing 4.8 mm fractions.   (Figure 4.1).

Coarse aggregate grading was carried out mainly to see if there was a relationship between grading and rock type, though it was also necessary to separate, physically, the size fractions for later recombination according to concrete mix designs.

No clear relationship emerged between grading and rock mean grain size (Figure 4.1), although there are substantial differences in the gradings (Table 4.1).   No explanation can be offered and this is an area that deserves further study.

4.2.2   Particle shape

Particle shape is important in assessing concrete aggregates as it is a key factor in determining the workability of fresh concrete.

Problems associated with quantifying particle shape have been discussed by many authors (see Barrett, 1980, for a review).   Opinions are split between quantifying particle shape by individual grain measurement and averaging particle shape on a single parameter, e.g. permeability or specific surface area.

The first approach is usually pursued by geologists, the second by those associated with engineering or industry.

136
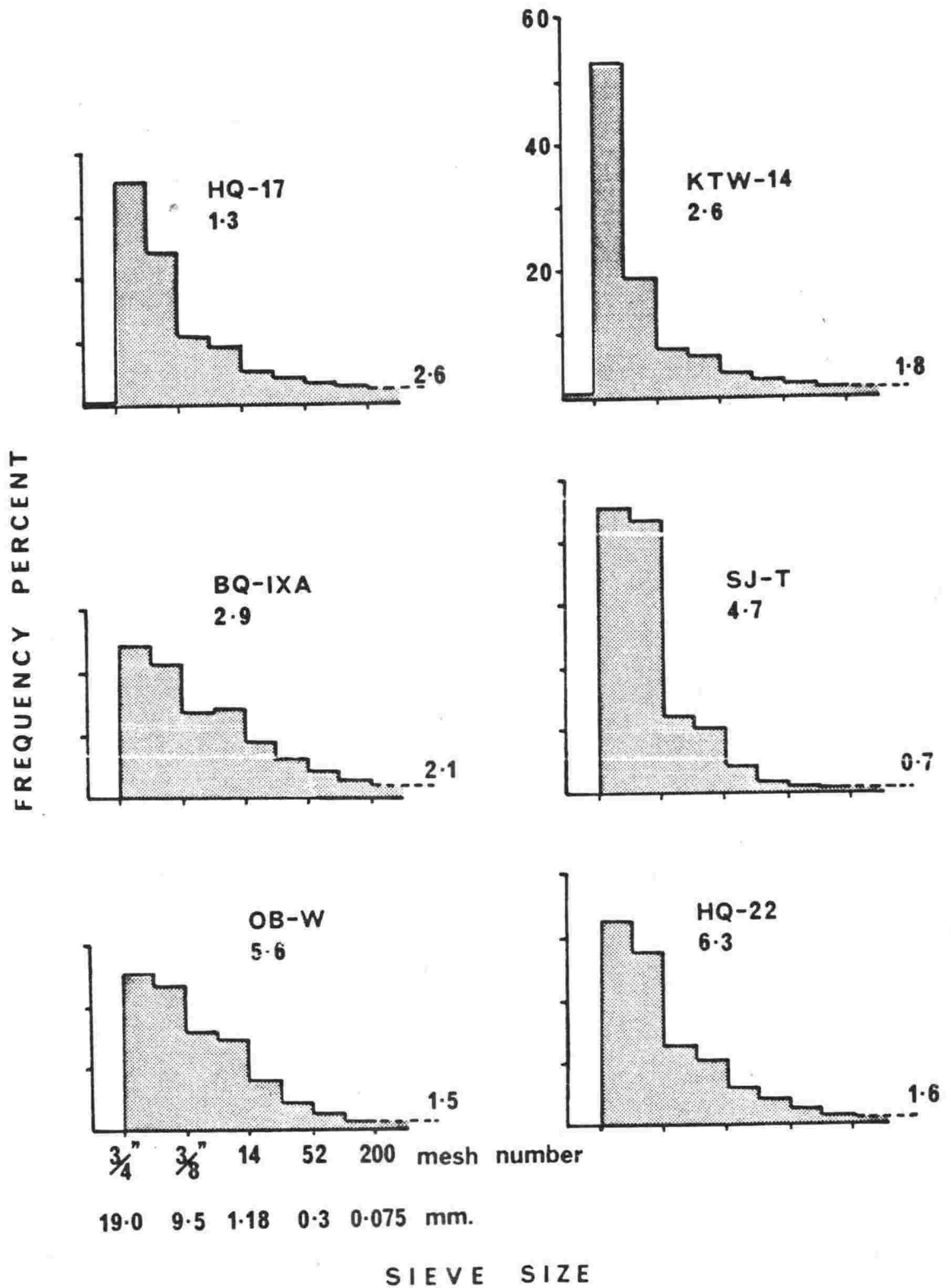
Figure 4.1 : Grading histograms of aggregate samples produced by crushing from quarried blocks, i.e. 19 mm "all in" aggregate. Percentage of material finer than 0.075 mm is shown numerically to the right of each histogram. Rock mean grain size in phi units is shown for each sample beneath sample numbers.

Table 4.1 : Sieve analyses of 19 mm "all-in" aggregates crushed from quarried blocks. (minus 4.8 mm sand sieve analyses by F. Williams).

Sieve sizes	HQ-17 % on	4571 gm. Cumulative % retained	KTW-14 % on	3504 gm. Cumulative % retained	BQ-IXA % on	3465 gm. Cululative % retained
19 mm (3/4")	0.24	0.24	0.9	0.9	-	-
12.7 mm (1/2")	18.24	18.5	34.9	35.8	9.2	9.2
9.5 mm (3/8")	17.7	36.2	18.2	54.0	15.5	24.7
4.75 mm (3/16")	24.3	60.5	18.9	72.9	21.8	46.5
2.36 mm (No. 7)	11.0	71.5	7.8	80.7	14.0	60.5
1.18 mm (No. 14)	9.5	81.0	6.5	87.2	14.5	75.0
600 μ(No. 25)	5.4	86.4	3.9	91.1	9.3	84.3
300 μ(No. 52)	4.4	90.8	2.9	94.0	6.6	90.9
150 μ(No. 100)	3.6	94.4	2.3	96.3	4.5	95.4
75 μ(No. 200)	3.0	97.4	1.9	98.2	3.0	98.4
PAN	2.6	100.0	1.8	100.0	2.1	100.5
	100.0		100.0		100.5	

Sieve sizes	SJ-T	3970 gm.	OB-W	5554 gm.	HQ-22	4316 gm.
19 mm (3/4")	-	-	-	-	-	-
12.7 mm (1/2")	21.7	21.7	8.7	8.7	11.1	11.1
9.5 mm (3/8")	24.1	45.8	16.8	25.5	21.6	32.7
4.76 mm (3/16")	23.5	69.3	23.9	49.4	27.8	60.5
2.36 mm (No. 7)	12.2	81.5	16.0	65.4	12.9	73.4
1.18 mm (No. 14)	10.2	91.7	14.9	80.3	10.6	84.0
600 μ(No. 25)	4.3	96.0	8.3	88.6	6.0	90.0
300 μ(No. 52	2.1	98.0	4.9	93.5	4.2	94.2
150 μ(No. 100)	1.0	99.0	2.9	96.4	2.8	97.0
75 μ(No. 200)	0.7	99.7	1.7	98.1	1.8	98.8
PAN	0.7	100.4	1.5	99.6	1.6	100.4
	100.4		99.6		100.4	

A major problem in this study was one of resolution, i.e. all the aggregates were of similar provenance, metamorphic rank and geologic character. All were crushed using the same plant and subject to the same screening. Quantification of particle shape required a method that would be sensitive to subtle differences in the shapes of crushed rock. Lees (1964) devised a method specifically for this purpose, although his interest was in road aggregate. The method takes cognizance of the number of corners, their sharpness and their degree of projection from the main body of the particle measured. Lees' procedure involves taking measurements from photographs taken in the three planes a/b, b/c, a/c, where a, b and c are the long, intermediate and short axes of particles. Results from the planes were averaged. Such is the tedium of measuring particles in this way that Lees produced a chart for visually determining the degree of angularity of particles. Although not used in this study, the validity of angularity assessment by measurement from a single particle projection plane, was accepted. Measurement was therefore undertaken using two dimensions of the particle, quantified as a dimensionless number (degree of angularity, A_{2D}, Figure 4.2) which increases with angularity.

Measurements were made from a photocopy (Appendix 17) of a section of concrete cast in 200 x 100 mm cylinder moulds (conforming to NZS 3112:1974, 201 method B1), cut longitudinally through a diameter (Plate 4.1; Appendix 17). Particles to be measured, from each photocopied face, were selected by using a 12 x 25 mm grid - generally this meant more particles were counted from mix 1 cylinder photocopies than mix 2. Measurement of angles was done with a protractor and the radii of inscribed circles determined by circular templates of known diameter. Projection of corners was measured with a millimetre scale.

The results (Table 4.2) show that, although standard deviation is large, Lees' angularity is a consistent measure - there is close agreement between means of different mixes of the same aggregate. Also, angularity increases with decreasing rock grain size (Plate 4.1; Figure 4.3; Appendix 17).

It is known that particle shape and hence angularity is strongly influenced in two ways:

(i) The nature of the crushing process, (McIntosh, 1957), the same for each sample in this study (section 4.2.2).
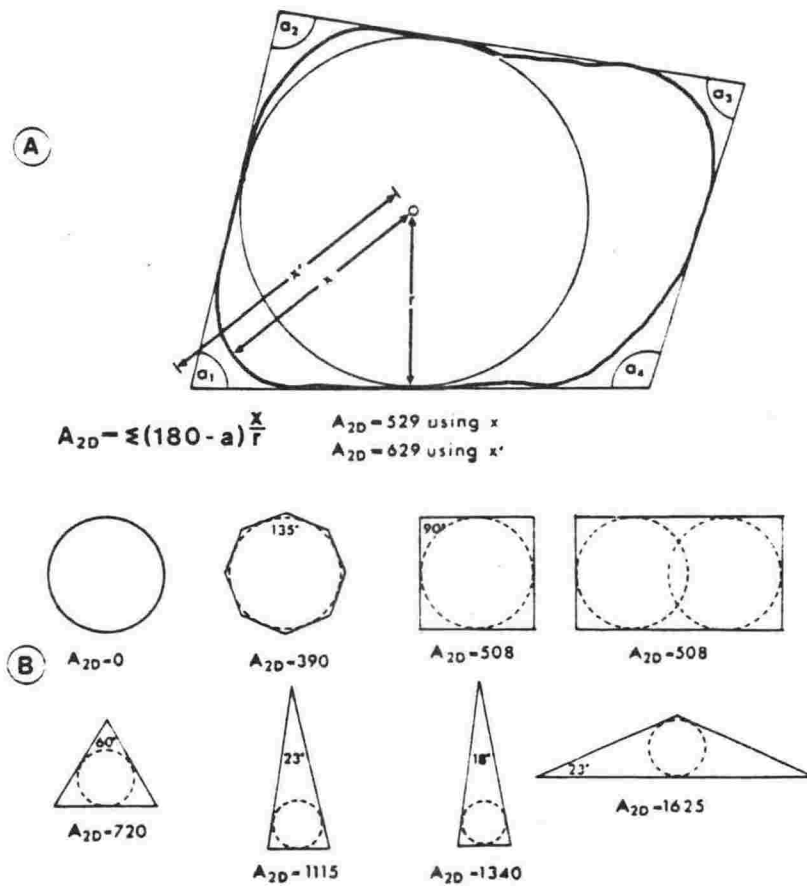
Figure 4.2 : (A) Construction and formula for determining
angularity (A_{2D}) of a particle by the method of Lees
(1964). (B) Values for degree of angularity (A_{2D}) for various
regular figures (mainly from Lees, 1964 , with a corrected value for
the octagon from Barrett, 1980).
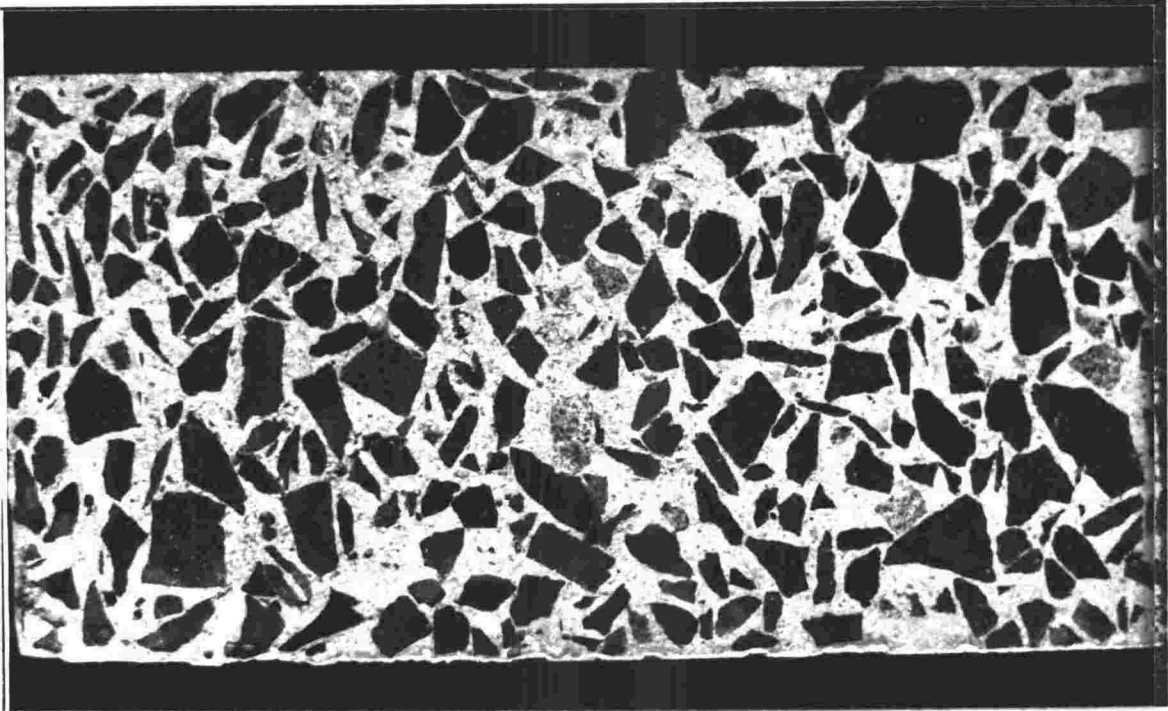
HQ-17
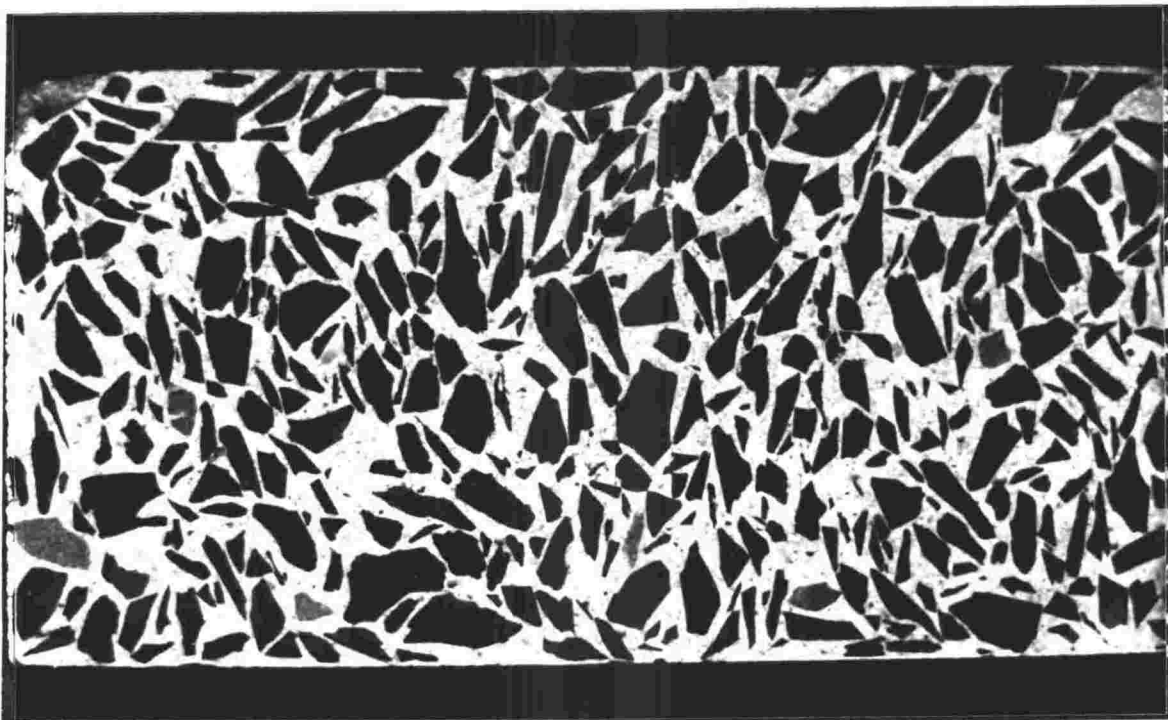
OB-W

Plate 4.1 : Sections of mix 1 design concrete are shown for two
aggregate types to display aggregate particle orien-
tations, angularities (A_{2D}) and packing. The photographs have
been taken from 200 x 100 mm concrete cylinders after they have
been cut in half longitudinally. Both sections are shown with
the uppermost surface (as cast) to the left. Angularities (A_{2D})
were measured from photocopies of these surfaces directly for
both mix designs. Particles for angularity measurements were sel-
ected by grid overlay (Appendix 17).

Table 4.2 : Aggregate particle shape statistics derived using the method of Lees (1964).

Sample	Rock Mean grain size, phi	Mix design	Total angularity (A_{2D}) for mix design	Mean particle angularity	S.D.	Coefficient of variation, percent	Minimum particle angularity	Maximum particle angularity	n.
HQ-17	1.3	1	30640	747	314	42.1	350	1800	41
		2	32347	$\overline{x}\ \frac{789}{768}$	330	41.9	305	1765	41
KTW-14	2.6	1	32338	874	406	46.4	460	2320	37
		2	31394	$\overline{x}\ \frac{826}{850}$	398	48.0	415	2740	38
BQ-IXA	2.9	1	28432	768	238	31.0	400	1315	37
		2	32010	$\overline{x}\ \frac{889}{829}$	325	36.6	385	1965	36
SJ-T	4.7	1	31453	850	359	42.3	380	1895	37
		2	23990	$\overline{x}\ \frac{727}{789}$	247	33.9	340	1350	33
OB-W	5.6	1	46883	1019	474	46.6	350	2325	46
		2	43882	$\overline{x}\ \frac{1070}{1045}$	469	43.8	295	2495	41
HQ-22	6.3	1	33624	934	359	38.4	290	1880	36
		2	36325	$\overline{x}\ \frac{931}{933}$	299	32.1	535	1880	39
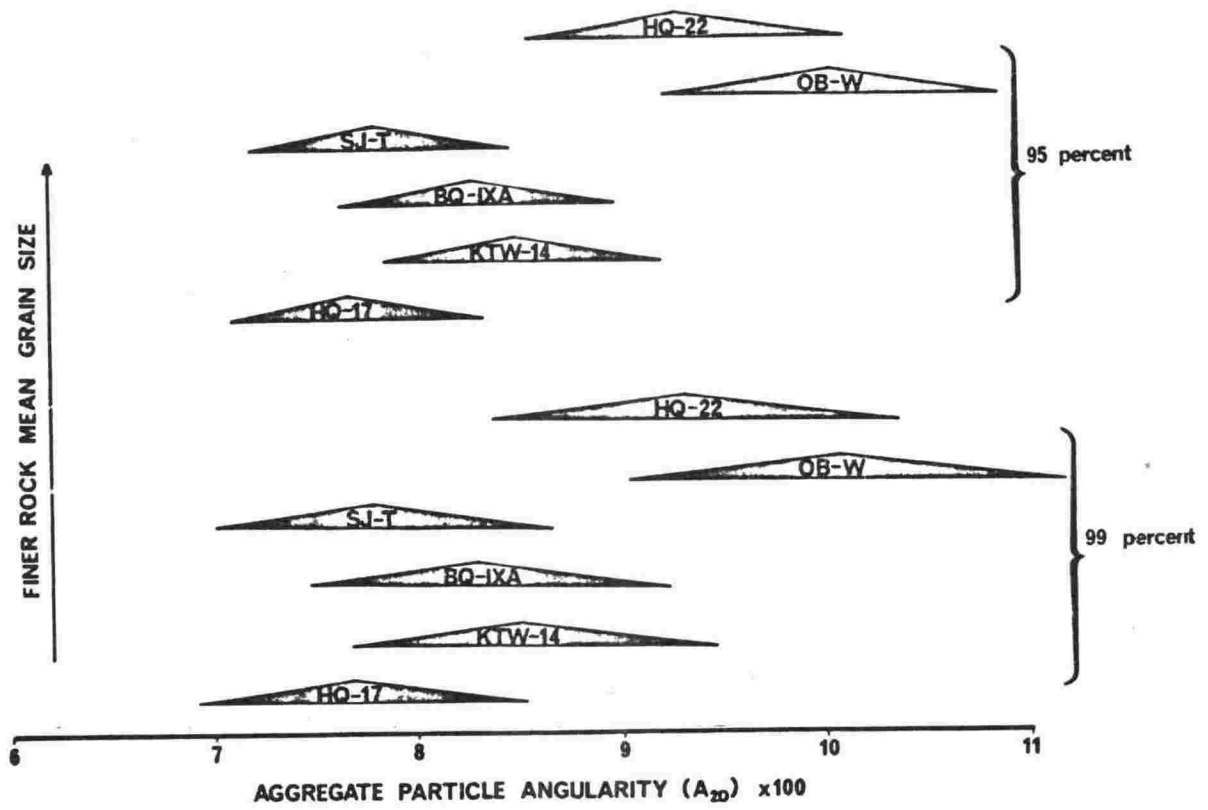
Figure 4.3 : Aggregate particle angularity errors, at two levels of confidence, in order of grain size. The apex of triangles denote mean angularity (A_{2D}); bases span error at confidence levels indicated.

(ii)   The crushing ratio, i.e. the ratio of the size of material introduced to the crusher, to that which the crusher produces.   Large ratios tend to produce flakier particles, which give high values of angularity.

Crushing ratio was large in most cases, certainly for aggregates KTW-14, BQ-IXA (boulder size), less so for HQ-17, OB-W and HQ-22 (boulder and cobble sized material) and very much less, by orders of magnitude, for SJ-T (cobble and pebble size).   However, there is no clear relationship between angularity and crushing ratio, whereas that between angularity and rock mean size is quite well established (y = 38.28x + 719.6;   r = 0.71).

4.2.3   Density and absorption

Tests for density and absorption (NZS 3111:1974, parts 202.1 and 202.3) were undertaken, the results being listed in Table 4.3.   In addition, a 30 minute water absorption was determined for use in concrete mix design (Appendix 27).

Density increases slightly with decreasing rock mean grain size (Table 4.3). Water absorption data reflect surface area to volume ratio differences between different aggregate gradings, i.e. the ratio between the 30 minute water absorption of 19 and 9.5 mm aggregate average 0.55.   Higher values are apparent for greywacke HQ-17, due to the presence of zeolite (Appendix 3) and for argillaceous samples SJ-T, OB-W and HQ-22.

For absorptions obtained to NZS 3111:1974 method 202.1, the ratio between absorption of 19 and 9.5 mm aggregates is higher, average 0.82, because 19 mm aggregate takes a longer time to equilibrate.   Samples OB-W and HQ-22 had the highest values and HQ-17 the lowest.

To better understand the influences of rock crushing on the densities of aggregate produced, aggregate densities were correlated with corresponding rock core densities for both dry and SSD conditions (Figure 4.4).   Correlation was good for both conditions but was not linear in either case, crushing apparently tending to reduce the density of aggregate for all but the most argillaceous samples.   Although dry densities were less than SSD densities in all cases, the density values of 19 mm aggregates correlate well with those of cores. A single trend was apparent in the more argillaceous rock types, i.e. those

Table 4.3 : Density and absorption results for greywacke-suite aggregates
used for concrete making, arranged in order of rock mean grain
size.

Sample	Rock mean grain size, phi	Coarse aggregate grading, mm.	SSD density, $kg.m^{-3}$	Oven dry density, $kg.m^{-3}$	Water-absorption, percent	30 minute water absorption, percent
HQ-17	1.3	19.0	2662	2647	0.56	0.22
		9.5	2653	2632	0.77	0.33
KTW-14	2.6	19.0	2673	2660	0.47	0.15
		9.5	2660	2644	0.61	0.32
BQ-IXA	2.9	19.0	2670	2658	0.48	0.17
		9.5	2666	2651	0.59	0.37
SJ-T	4.7	19.0	2706	2691	0.56	0.21
		9.5	2696	2676	0.76	0.36
OB-W	5.6	19.0	2740	2713	0.96	0.26
		9.5	2730	2699	1.14	0.57
HQ-22	6.3	19.0	2694	2671	0.87	0.33
		9.5	2700	2676	0.88	0.52
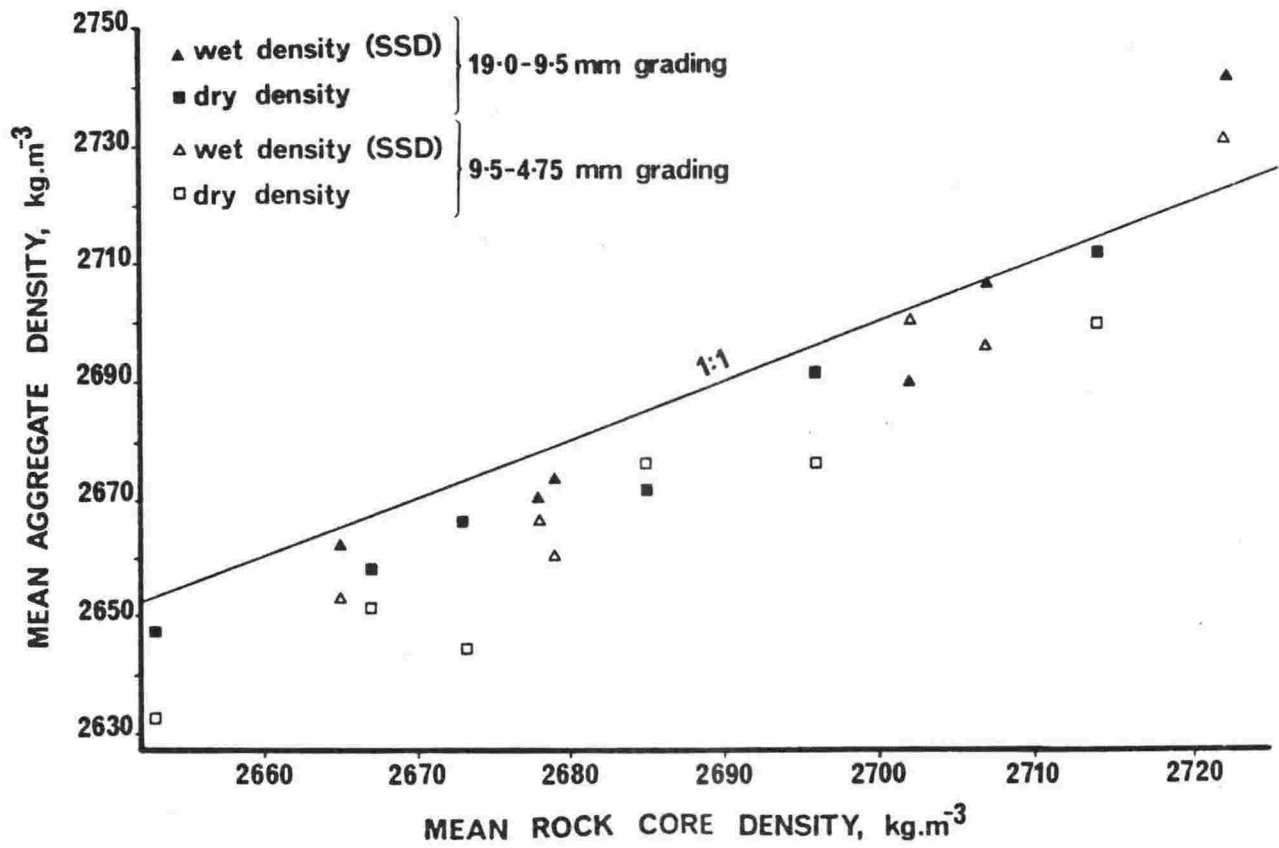
Figure 4.4 : A comparison of densities of identical rock types in two forms, aggregate and cores.

with dry densities in excess of 2690 kg.m^{-3}. Below this value the difference
between SSD and dry densities was less for core material than for aggregate
material (Figure 4.4).   These effects are brought about by the crushing
process; a larger surface area to volume ratio tends to increase a lower dry
density and raise the SSD density of aggregates.   Both density values are
lower than those of equivalent cores.   In the greywackes this is due to sur-
face texture features, microcracking and a resultant increase in capillary
space.

The effect was greatest in the rocks of larger mean grain size.   Disruption
of rock adjacent to a new formed outer surface seems to be greatest in fine
to medium grained greywackes compared with argillites (Appendix 15).   On
close examination surface flaking of small regions of aggregate particles can
be seen.   The flakes may be still attached but translucent due to their
separation from the aggregate particle over their entire area.   Such flakes
are larger than the mean grain size of the rock but are very strongly attached
(Appendix 15).   Further, argillites do not have the well developed surface
texture or small scale surface flaking of greywackes.   The surface may be
very hackly but does not appear to retain the same proportion of trapped water,
except in larger size gradings where irregularites may be well indented - a
possible reason for the trend going above the 1:1 density ratio in Figure
4.4.

The relationship shown by Figure 4.4 for 9.5 mm aggregate is more scattered
but has the same features as the 19 mm aggregate discussed above.

The behaviour of 9.5 mm HQ-22 aggregate seems anomalous in that both its SSD
and dry densities are greater than those of 19 mm HQ-22.   However, differ-
ences between the aggregate densities for both gradings are almost identical
(5 and 6 kg.m^{-3}) and are not significant, as absorption figures for this
particular rock type in both aggregates are almost identical (19 mm, 0.87 per-
cent; 9.5 mm, 0.88 percent).

Comparison of effective porosity of cores with absorption characteristics of
aggregates show no relationship, except that 9.5 mm aggregates have greater
absorptions than 19 mm aggregates for any particular rock type - reflecting
increasing surface area to volume ratios in finer aggregate sizes.   This is
superposed on a tendency for the more argillaceous rocks to absorb more water.
Over 24 hours, 19 mm aggregates absorb between 1.7 and 2.5 times as much as

their cored counterparts and 9.5 mm aggregates between 1.7 and 2.8 times; again, greater scatter is apparent in the finer grading (Figure 4.5).

There is better correlation between effective porosity of cores and 30 minute water absorptions (Figure 4.6) determined for concrete mix designs. In addition, it seems that there is an aggregate surface area to volume ratio which enables a rapid water absorption, equalling the natural effective porosity of the parent rock. The surface area to volume ratio which allows this to take place in, say, 4 to 8 hours and the corresponding particle size may provide valuable information regarding aggregate degradation (Appendix 25).

4.2.4   Bulk density and voids content

The bulk density and voids content of aggregates were measured using NZS 3111:1974 method 201.6 (Table 4.4). The measurement is of direct use in concrete mix design (NZS 3111:1974 method 201.4 "Method for determining aggregate performance in concrete").

Results represent the efficiency with which aggregate can be packed into a container. For aggregate of a particular specific gravity, bulk density depends on size grading and particle shape; the more well sorted the aggregate, i.e. the more uniform particles are in size, the greater the space left unfilled. Aggregates with greater variation in particle size may be packed more closely giving higher bulk densities. More equant and less angular particles also pack closer. In fact some tests for measuring the angularity of coarse aggregate particles have been based on theoretical and loose poured bulk densities (Shergold, 1953; Hughes, 1966). It is interesting to note that argillites, in spite of higher rock densities, have lower bulk densities and higher voids contents in both 19 and 9.5 mm gradings. This is directly attributable to their flaky particle shapes.

4.2.5   Crushing resistance

The strength of aggregate as a particulate mass is a difficult property to measure. Approaches to strength assessment for aggregates include uniaxial compression strengths of prepared samples (section 3.5), strengths of concrete made with the aggregate, the 10 percent fines test (forerunner to the crushing resistance test), aggregate impact value (BS 812: part 3:1978), point load tests on prepared rock specimens or aggregate particles (Bieniawski,
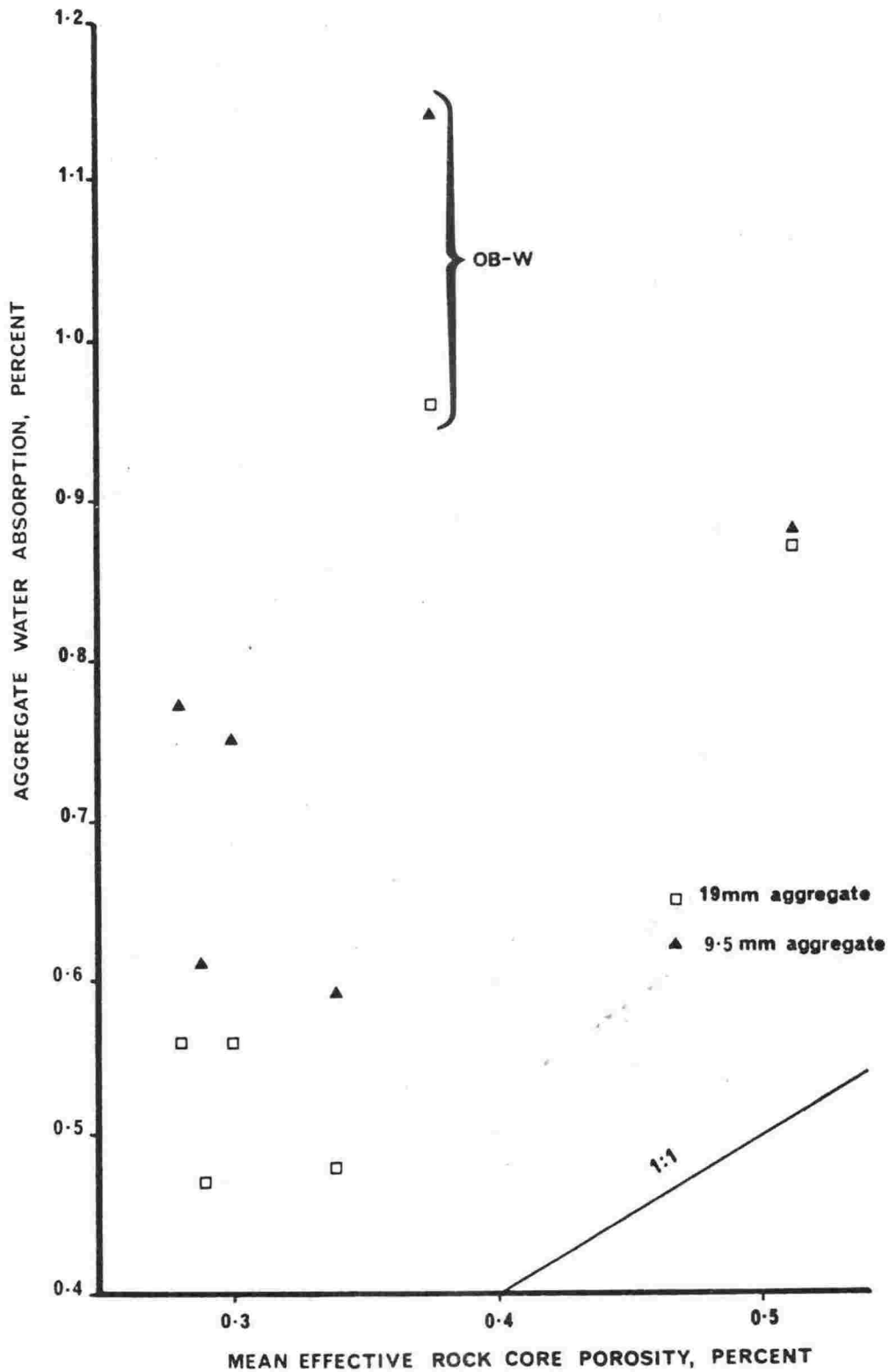
Figure 4.5 : Little correlation exists between 24 hour aggregate
           absorption and rock core effective porosity.   Note
that scatter is greater for finer aggregate fractions.   A large
surface area to volume ratio for OB-W is apparent from its absorption.
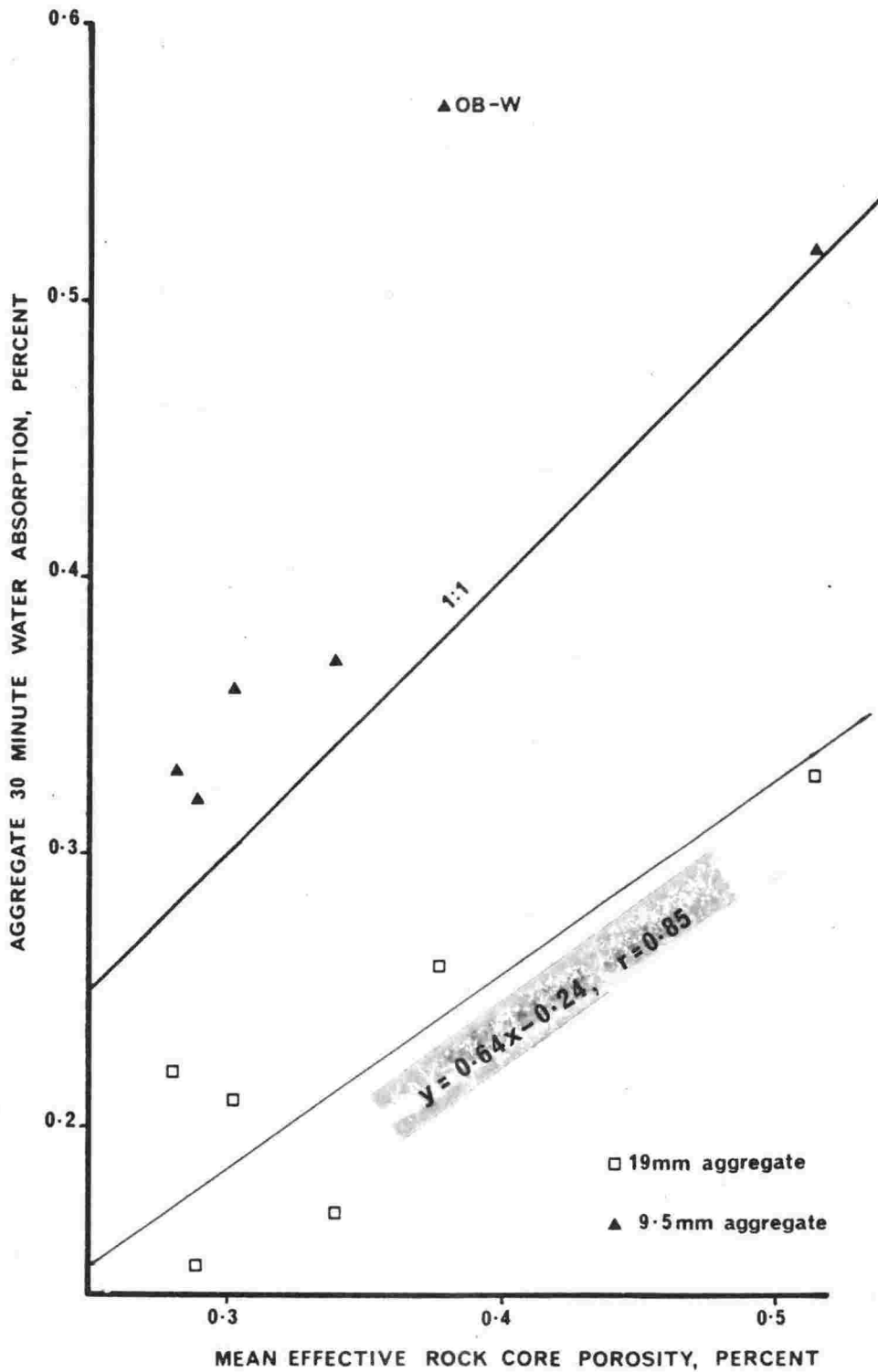
Figure 4.6 : Rock core effective porosities show good correla-
tion with aggregate 30 minute water absorptions.
Again the relatively high surface area to volume ratio of 9.5 mm
OB-W aggregate is readily satisfied even within 30 minutes of
soaking.

Table 4.4 : Aggregate test results for all rock types.

Aggregate test	A G G R E G A T E S A M P L E					
	HQ-17	KTW-14	BQ-IXA	SJ-T	OB-W	HQ-22
Rock mean grain size, phi	1.3	2.6	2.9	4.7	5.6	6.3
Los Angeles, percent wear	12.2	11.7	11.4	11.3	18.8	14.9
Crushing resistance, kN, see also Table 4.5	350	340	370	360	190	290
Mean particle angularity (A_{2D})	768	850	829	789	1045	933
19 - 9.5 mm						
SSD (wet) density kg.m^{-3}	2662	2673	2670	2706	2740	2694
Dry density kg.m^{-3}	2647	2660	2658	2691	2713	2671
Absorption, percent	0.56	0.47	0.48	0.56	0.96	0.87
30 minute absorption, percent	0.22	0.15	0.17	0.21	0.26	0.33
Compacted bulk density, kg.m^{-3}	1499	1513	1496	1518	1435	1473
Void content, percent	43.4	43.1	43.7	43.6	47.1	44.9
9.5 - 4.8 mm						
SSD (wet) density kg.m^{-3}	2653	2660	2666	2696	2730	2700
Dry density kg.m^{-3}	2632	2644	2651	2676	2699	2676
Absorption, percent	0.77	0.61	0.59	0.75	1.14	0.88
30 minute absorption, percent	0.33	0.32	0.37	0.36	0.57	0.52
Compacted bulk density, kg.m^{-3}	1450	1466	1441	1469	1410	1415
Void content, percent	44.9	44.5	45.6	45.1	47.8	47.1

1975), testing large (cobbles) and small (pebbles) irregular rock specimens
(Hobbs, 1963; Ramsay *et al.*, 1974; Vutukuri *et al.*,1974), and the crushing
resistance test (NZS 3111:1974, method 202.3). The latter method was used
in this study.

All tests mentioned above have different applications. When bulk aggregate
particles are tested for crushing resistance, results are influenced by the
effects of packing, particle shape (Figure 4.7), point loading, and abrasion
resistance, which provide better resolution of performance in strong aggregates.

The crushing resistance of the samples tested appears to be more related to
angularity of the particles (Figure 4.7), than mean grain size (Table 4.4) or
strength of the rock (Table 3.2), though effects of packing will have had
some influence. Particle shape is already known to affect aggregate impact
values (Ramsay *et al.*, 1974), which measures a similar aggregate property.
Crushing resistance results from aggregate tested wet and dry also allow some
assessment of rock durability (Table 4.5).

Table 3.3A, in part reproduced from Neville (1975), gives an indication of the
relative precision of several commonly used methods of assessing aggregate strength.

4.2.6 Los Angeles abrasion test

This test measures the combined effects of attrition and abrasion and consists
of grinding the aggregate with steel balls in a rotating drum for a set time.
The Los Angeles value is the percentage of ground material passing a 1.7mm
sieve; details of the test are given by ASTM C131-76. It has been found to
correlate well with the compressive strength and wearing characteristics of
concrete (Neville, 1975). As with the crushing resistance test, the results
depend very much on toughness, hardness, elasticity, strength and especially
particle shape (Figure 4.8) - most of these properties being better assessed
by other means. Use of the Los Angeles test is declining in New Zealand as
in most cases results are difficult to apply, by direct means, to aggregate
use. Results presented (Table 4.4) are included for completeness.

The Los Angeles values for the aggregates tested also show a close relationship
to crushing resistance (Figure 4.9), indicating that both tests yield the same
sort of information.
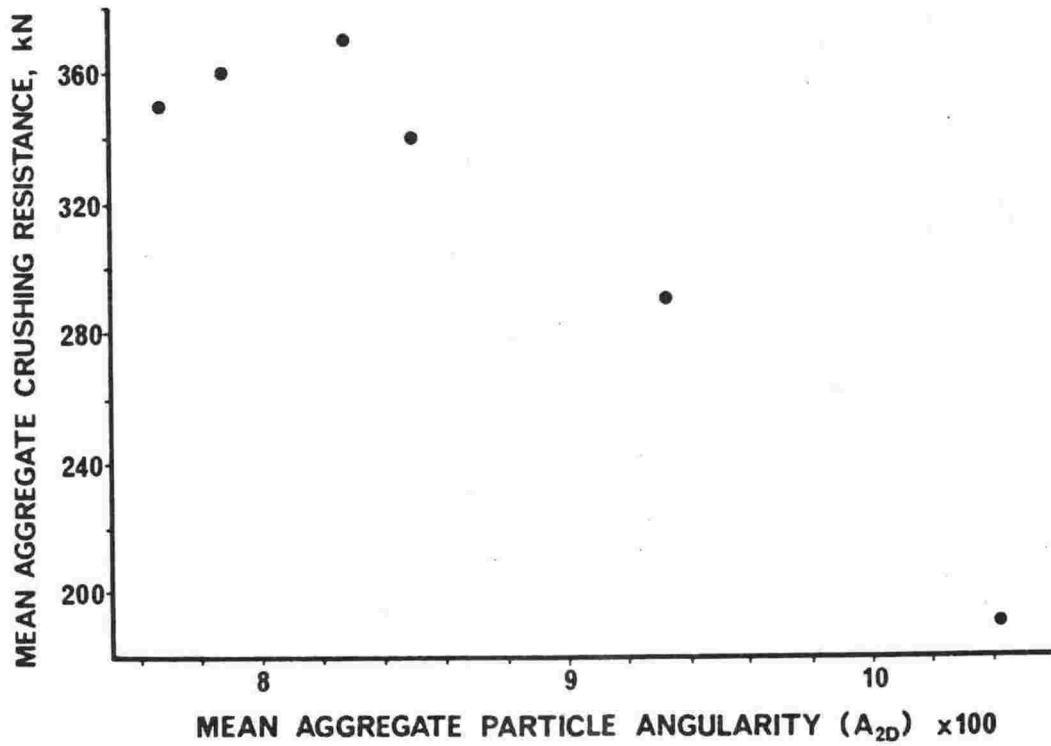
Figure 4.7 : Aggregate particle shapes affect aggregate crushing
            resistance results.   More angular materials
return a lower crushing resistance.

Table 4.5 : Comparison of aggregate relative durability, as measured by wet and
dry crushing resistance. Samples tested wet were soaked seven
days beneath a 100 mm head of water before being otherwise tested
according to test method T215, Department of Main Roads, N.S.W.,
Australia: durability of coarse aggregate by the ten percent fines
(wet/dry variation) procedure; April 1979.

Sample	Rock mean grain size, phi	Crushing resistance, kN		Wet crushing resistance as percentage of dry*
		dry	wet	
HQ-17	1.3	350	320	91
KTW-14	2.6	340	330	97
BQ-IXA	2.9	370	360	97
SJ-T	4.7	360	320	89
OB-W	5.6	190	140	74
HQ-22	6.3	290	220	76

* A minimum value of 65 percent is required by the DMR for their aggregates.
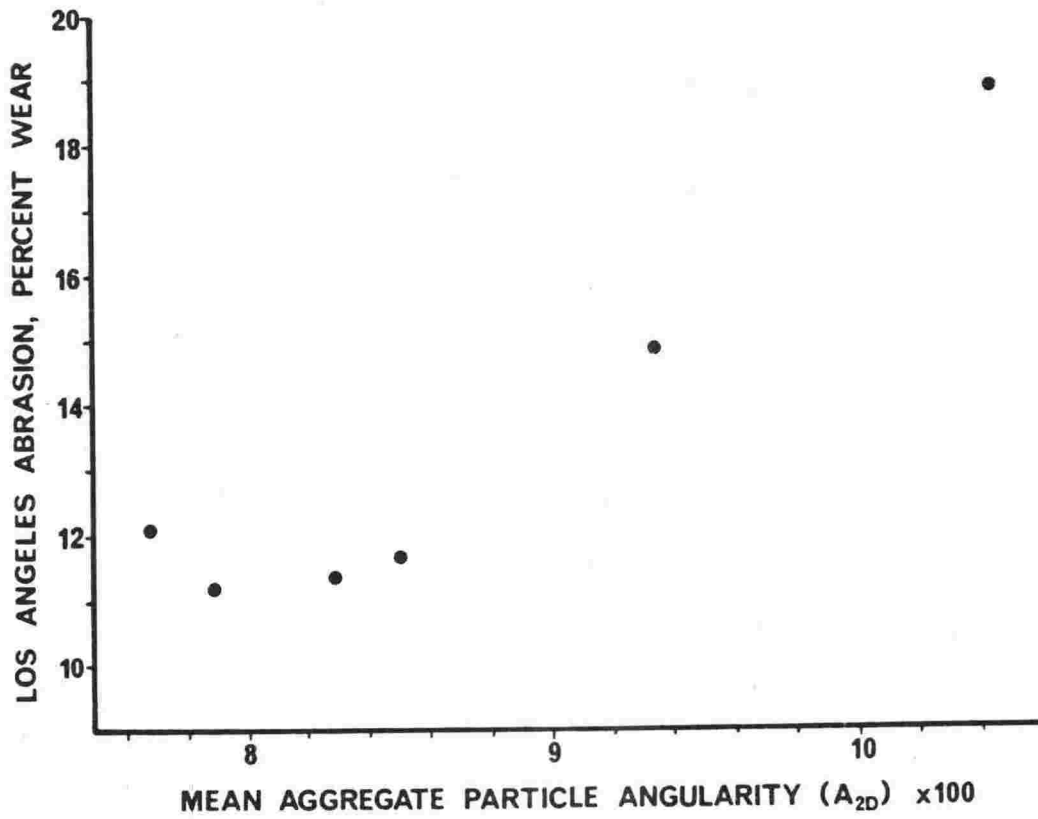
Figure 4.8 : Aggregate particle shape affect the abrasion resis-
tance of aggregate.   More angular materials return
a greater loss due to abrasion.

4.2.6a Results of bulk testing

The uniformity in the results of bulk testing shown by greywackes is in marked contrast to the difference between the two argillites tested (Table 4.4). Some parameters, Los Angeles abrasion test and crushing resistance, show direct relationships with particle angularity and therefore are only indirectly related to rock mean grain size. Generally, the argillites show an increase in Los Angeles abrasion percentage wear over greywackes (3 to 7 percent), lower crushing resistance (approximately 100kN less), increased wet density (20 $kg.m^{-3}$), higher absorption (0.4 percent), compacted bulk density reduced by 40-50 $kg.m^{-3}$ and higher (1-4 percent) voids content.

4.2.7 Fines from crushing and abrading

Fines produced during crushing can influence significantly the quality of the aggregate, which acquires a fine dust coating that is only partly removed by washing. This coating is probably formed initially by electrostatic charge generated by friction during crushing but the fineness of the dust is responsible for adhesion which makes separation by washing difficult.

Different crushing methods produce different proportions of fines, but whatever the method used, argillite yields more and finer material than greywacke (Figure 4.10).

4.3 Alluvial versus quarried aggregate

Traditionally the use of greywacke-suite aggregates from alluvial and quarried sources has been dependent upon place value and ease of production. Prior to law amendments from the early 1950's, alluvial and beach gravels and sands were the most important source of aggregate in Wellington. These sources were accessible, easily extracted, were clean and without soft or weathered particles, due to sorting by moving water. Even today Owhiro Bay Quarries use the sea as a "scrubber" and crude sieve by deliberately placing freshly won material on a small beach, adjacent to the quarry, for a period of time (Rowe, in prep.).

Pressures from increased population have had the effect of increasing demand for aggregates whilst also requiring maintenance of alluvial aquifers, beaches and river channels. For these reasons most aggregate in the Wellington region (Grant-Taylor, 1976; Ward and Grant, 1978) is now quarried. One major advantage inherent to alluvial aggregates, is that the particles are rounded in contrast to the sharp corners of crushed aggregate. The rounded particles improve the workability of concrete (section 5.1.1), which is especially important for pumped concretes, where strict size gradings must be adhered to, to allow minimum cement, sand and water contents for economy and strength. Other advantages of alluvial material are cleanness and a general freedom from deleterious matter.
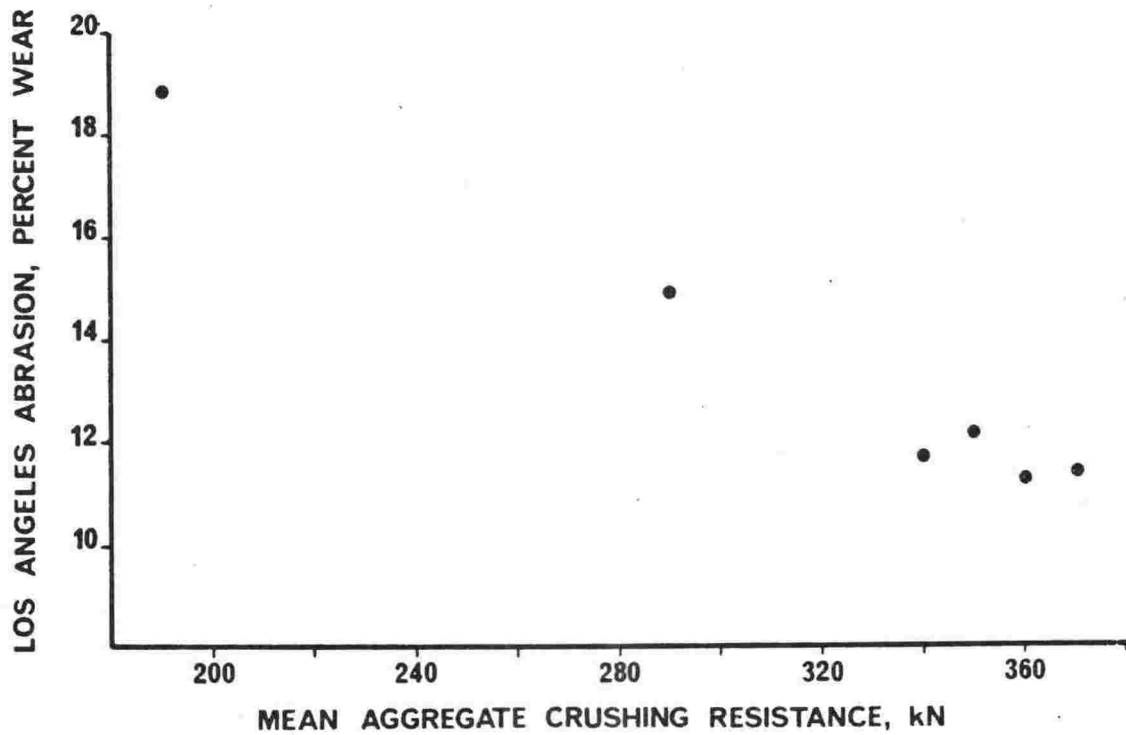
Figure 4.9 : Los Angeles results relate well with the crushing

strength of bulk aggregate. A similar trend is

apparent for uniaxial compression strength of rock cores (Appendix

18).
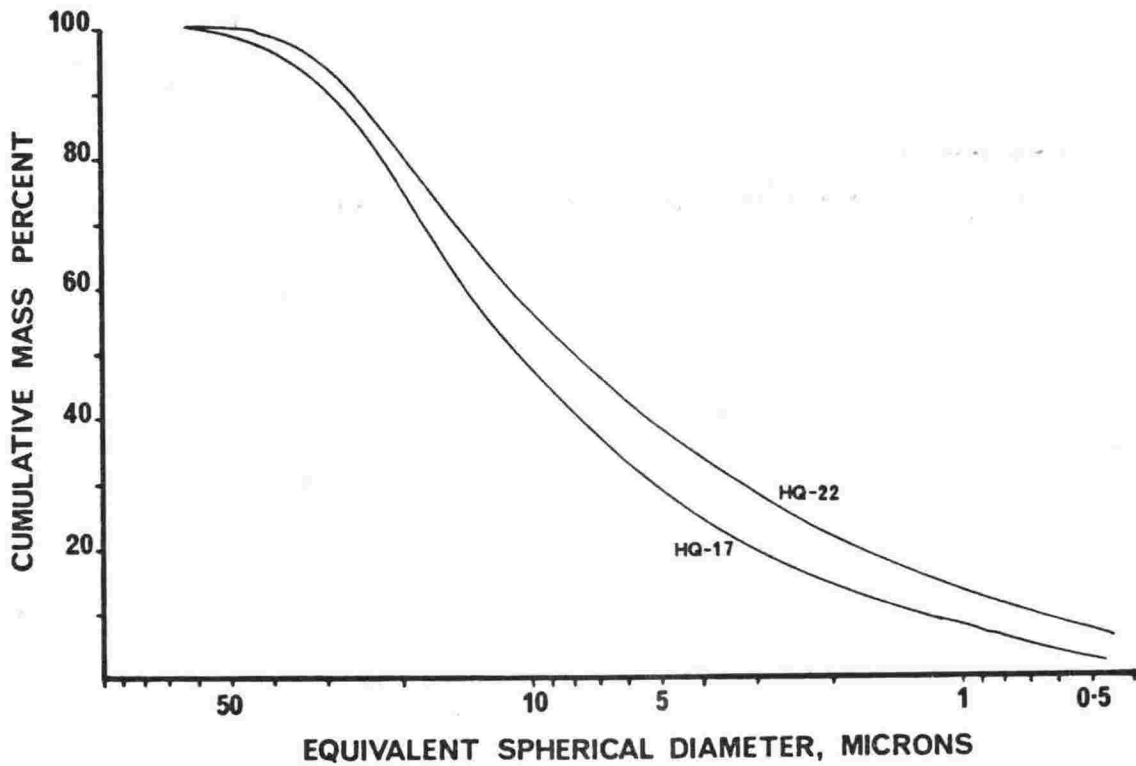
Figure 4.10 : A comparison between the coarsest greywacke and
            finest argillite aggregate fines (minus 0.065 mm)
produced by the Los Angeles test indicates that finer material is
produced from argillites.   The other four aggregates tested in
the study have curves that plot between those shown and are
arranged from the HQ-17 curve to the HQ-22 curve in order of
decreasing rock mean grain size.

Grant-Taylor (1976), comparing several different quarried road basecourse aggregates with river-won aggregates, concluded that for river gravel "Los Angeles abrasion test results appear to be consistantly 3 to 5 percent lower (better) than for similar rock from a quarry. This difference will be due to the presence of rounded faces". However, it is also worth noting that quarried basecourse aggregate, although angular, invariably contains more weathered and therefore softer rock, (see Grant-Taylor, 1976, Table 1), which also yields high Los Angeles values.

Grant-Taylor (1976) also points out that rock jointed "to include the product grade range, would be expected to give a better Los Angeles test than rock which is all artifically crushed" and has greater angularity. Rocks crushed for aggregate used in this study were selected for their lack of geological discontinuity - veining etc., and included large boulders. Their Los Angeles values are even lower than those of the best (large river) gravel deposits (minimum Los Angeles test values), and rocks from "best" quarries (minimum Los Angeles test values) of Grant-Taylor (1976):

Average Los Angeles test minimums for eight best quarries in Wellington region, (Grant-Taylor, 1976, Table 5)	Averaged Los Angeles test minimums for gravel from nine large river sites, (Grant-Taylor, 1976, Table 6).	Average of four greywackes, this study.
13.3 percent highest minimum	13.7 percent highest minimum	11.7 percent maximum
14.7 percent lowest minimum	16.5 percent lowest minimum	12.2 percent minimum
11.6 percent	12.2 percent	11.3 percent
n = 376	n = 241	n = 4

Differences are not significant between Grant-Taylors' minimum values for either aggregate source and this work.*   This may imply that veining and other discontinuities do not affect Los Angeles values as much as, say, the type of crushing machinery, which influences particle shape, and hence Los Angeles results (Orchard, 1964).

A comparison of some commercially available quarried and alluvial greywacke-suite concrete aggregate is presented in Table 4.6.   Generally this shows agreement with Grant-Taylors' (1976) data indicating that alluvial greywackes are more consistent in the Los Angeles test than quarried greywackes.   This is probably because the quarried aggregate normally includes some argillite which is more easily comminuted, more absorbent and contains more incipient flaws than greywacke.   The aggregate may also include some weathered material.

4.4   Alkali reactivity

Zeolites have been placed, as a mineral group, into the category of reactive components when aggregate particles, containing it, are used in con-junction with high alkali cements to make concrete (Rhoades and Mielenz, 1946;   Swenson and Chaly, 1956;   Hansen, 1966;   Neville, 1975).

Gillott (1975) has described three subdivisions of alkali-aggregate reactions and has given a good summary of the problem.   The type of reaction discussed here is an alkali-silicate reaction.

---

*   "For nominal 19.0 mm maximum size coarse aggregate with percentages of wear in the range of 10 to 45 percent, the multilaboratory coefficient of variation has been found to be 4.5 percent.   Therefore, results of two prop-erly conducted tests from two different laboratories on samples of the same coarse aggregates should not differ from each other by more than 12.7 per-cent of their average.   The single-operator coefficient of variation has been found to be 2.0 percent.   Therefore, results of two properly conduc-ted tests by the same operator on the same coarse aggregate should not differ from each other by more than 5.7 percent of their average."
Extracted from ASTM C131-76, 'Resistance to abrasion of small size coarse aggregate by use of the Los Angeles Machine'.

Table 4.6 : A comparison of test results of New Zealand greywacke-suite aggregates from quarried and alluvial sources .

QUARRIED GREYWACKES

AGGREGATE TEST	Same Aggregate*			Same aggregate*					This study			
	1/002	1/003	1/044	1/011	SP7-75	SP2-69B	1/019B	1/061	HQ-17	KTW-14	BQ-1XA	SJ-T
Crushing resistance, kN	260	220	450	230	230	290	320	320	350	340	370	360
Cleanness value	81	86	91	73	79	84	81	85	-	-	-	-
Bulk density, kg.m^{-3}	1446	1455	1540	1528	1528	1546	1562	1600	1499	1513	1496	1518
Voids contact, percent	42.2	41.1	42.0	42.5	42.5	41.0	40.5	40.0	43.4	43.1	43.7	43.6
S.S.D.(wet) density, kg.m^{-3}	2630	2650	2680	2670	2650	2640	2660	2690	2662	2673	2670	·2706
Dry density, kg.m^{-3}	2590	2640	2670	2660	2610	2600	2640	2660	2647	2660	2658	2691
Absorption, S.S.D.(wet) basis, percent	1.20	0.44	0.5	0.78	1.44	0.95	0.95	0.89	-	-	-	-
Absorption, oven dry basis, percent	1.22	0.44	0.5	0.79	1.46	0.96	0.96	0.90	0.56	0.47	0.48	0.56
Accelerated weathering test	AA	BA	-	AB	-	BB	AA	-	-	-	-	-
Los Angeles abrasion test percent wear	17.2	15.5	-	14.2	-	18.8	13.4	-	12.2	11.7	11.4	11.3
Sodium sulphate soundness test, percent loss	1.6	2.5	-	13.8	-	5.4	7.4	-	-	-	-	-

AGGREGATE TEST	QUARRIED ARGILLIES				ALLUVIAL GREYWACKES		
	Same aggregate*		This study				
	1/019A	SP2/69A	HQ-22	OB-W	1/012A	1/012B	1/017
Crushing resistance, kN	250	290	290	190	360	430	300
Cleanness value	45	69	-	-	86	94	89
Bulk density kg.m^{-3}	1573	1532	1473	1435	1608	1693	1682
Voids contact, percent	39.8	42.5	44.9	47.1	38.6	35.9	37.1
S.S.D.(wet) density, kg.m^{-3}	2650	2650	2694	2740	2630	2660	2710
Dry density, kg.m^{-3}	2610	2620	2671	2731	2620	2640	2680
Absorption, S.S.D(wet) basis, percent	1.39	1.48	-	-	0.73	0.63	1.18
Absorption, oven dry basis, percent	1.41	1.50	0.87	0.96	0.74	0.64	1.19
Accelerated weathering test	BB	AB	-	-	AA	AA	-
Los Angeles abrasion test percent wear	17.0	13.1	14.1	18.8	12.0	11.6	16.1
Sodium sulphate soundness test, percent loss	12.8	12.5	-	-	2.09	5.62	11.2

* Same aggregate tested twice in last 10 years.

Data applies only to 20 mm aggregate.

All data other than of this study supplied by New Zealand Concrete Research Association. Sample numbers from aggregate testing programme.

A cement is considered to have a high alkali content where Na_2O percent + (0.658 x K_2O percent)= 0.6 percent minimum (Lerch, 1962). All New Zealand cements produced at present have low alkali contents, i.e. less than 0.6 percent as calculated above. Exceptional cases of low alkali cements reacting with aggregates have been recorded (Neville, 1975).

Hutton (1945) tested various New Zealand aggregates for alkali reactivity including 18 greywackes; he concluded greywackes were non-reactive with cement and could perhaps be used with high alkali cements. One greywacke tested, however, had "a large number of intermediate to basic volcanic fragments, some with a residuum of dusty isotropic material, probably glass, although due to general neomineralization, one could not be too definite about this. In one case this glassy material gave n = 1.525 by the immersion method". This greywacke reacted slightly, suggesting to Hutton that it should be used with low alkali cements. It may be that the material observed was laumontite, which though not isotropic, has a changing refractive index depending on hydration state:

laumontite (hydrated form) n_x = 1.509, n_z = 1.525

leonhardite (dehydrated form) n_x = 1.502, n_z = 1.518

                                                   Coombs (1952).

The petrographic associations of laumontite are discussed in Appendix 3. Laumontite is often a replacement product of calcic plagioclase, volcanic glass, or nepheline in basic volcanic rocks due to late-stage hydrothermal alterations or as an authigenic cement or replacement product in sediments due to incipient metamorphism.

To test mineral aggregates for their potential alkali reactivity there are at least three orthodox approaches:

(i)   The mortar-bar test, NZS 3111:1974, part 201.7 and ASTM C227-71.

(ii)   The quick chemical test, ASTM C289-71.

(iii)   The rock cylinder test, ASTM C586-69: for carbonate rocks.

Although not normally used for pure mineral samples, as the results are
difficult to interpret, the quick chemical test was used by Dr N. Milestone,
Chemistry Division, DSIR, - because of its simplicity and speed - to assess
potential reactivity of leonhardite.   Five grams of sample taken from 1 mm
wide veins in Horokiwi quarry produced the following measurements:

Quantity S_c - dissolved silica (millimoles per litre)   = 28

Quantity R_c - reduction in alkalinity (millimoles per litre) = 45.5

Rationalising these figures for a pure mineral test gave a plot shown in
Figure 4.11.   Within Wellington greywacke-suite rocks, laumontite is most
commonly found in veins and because of its weakness, generally coats exterior
surfaces of aggregate particles when crushed.   Surface material surviving
the production processes is then in a locality best suited to reaction with
cement paste.   Aggregate stockpiling allows desiccation of the mineral and it
becomes a fluffy, friable, anhydrous powder of crystalline mineral coating
(leonhardite) which is weaker and more easily removed than laumontite.
Relatively small amounts of zeolite, as surface coatings, may therefore remain
on aggregate particles.

From permeability studies (Appendix 22) access by solutions containing calcium
ions (e.g. the liquid phase of concrete) to replace sodium and potassium ions
in the lattices of zeolite, within the rock, would take place only if hydrostatic
head exceeded about 20 metres.

The mechanism of alkali reactivity by base exchange suggested by Swenson and
Chaly (1956) is: "zeolite minerals ..... are subject to base exchange in
which the calcium ions from the cement paste solutions are absorbed, replacing
Na or K ions originally present in these materials.   The change in composi-
tion of the paste solution may affect the setting and hardening of the
concrete.   The resulting increase in the alkali content in the paste solu-
tion appears to be one of excessive efflorescence, and may also promote
reaction with alkali-reactive aggregates".   From this argument, the
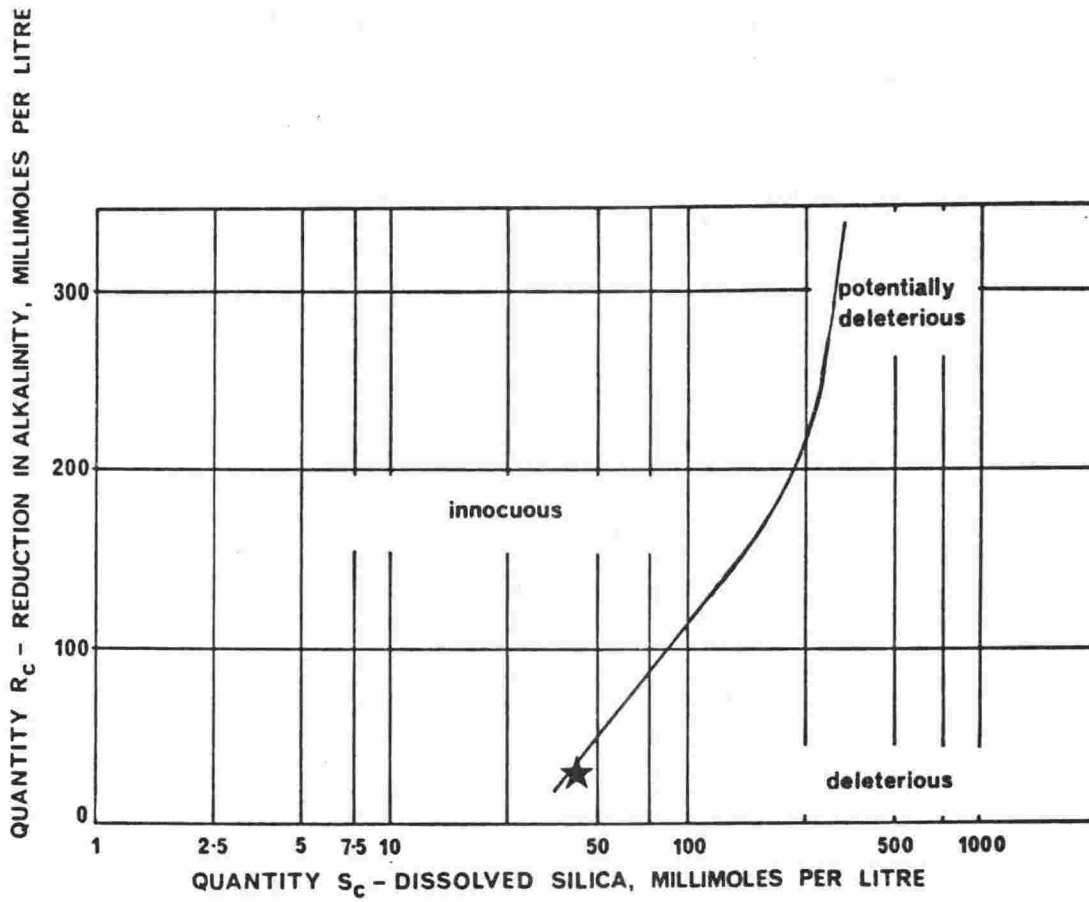
Figure 4.11 : Illustration of the division between innocuous and
deleterious aggregates on the basis of reduction
in alkalinity test (from ASTM C289-71).

orthorhombic zeolites such as natrolite*, ferrierite* and mordenite*, rather than laumontite* would be better able to provide enrichment of the cement paste in Na and K. Also, alkali reactivity is then brought about only if an alkali reactive aggregate is present, the zeolite acting merely as a catalyst for enhanced alkali content of cement paste.

A further concern with aggregate containing laumontite in particular, is that the mineral may be responsible for the disruption of concrete by volume change with varying degrees of hydration. Disruption of laumontite bearing rock has been established as being deleterious to aggregate production else-where (Appendix 25).

Hansen (1963) states "the zeolite laumontite on exposure to air or to gentle heat loses about 0.125 of its water to form leonhardite. This occurs with a change in the volume of the unit cell of about 1.5 percent. Sometimes this occurs with the crystal changing to a powder. The reaction is rever-sible and fairly rapid. According to Coombs (1952) the rehydration may be as brief as one or two hours. It appears from this that this rehydration process might be sufficiently slow to produce a volume change in concrete that would result in harmful expansion if leonhardite were a component of an aggregate".

Physical disruption of concrete due to volume change of leonhardite bearing aggregate is unlikely, however, because:

(i) The presence of hydration expansion is not likely to be great enough to exert pressures exceeding the tensile strength of the fresh greywacke-suite rocks. Coombs (1952) gives measurements of expansion of leonhardite, "after soaking in water to convert to laumontite form, the (100) lattice spacing of the (same) crystal increased from 13.68 to 13.86$\overset{o}{A}$ and the (010) from 13.10 to 13.17$\overset{o}{A}$, all ±0.01 to 0.02$\overset{o}{A}$". Lattice spacings of this order

---

*	Natrolite	Na_2 $(Al_2Si_3O_{10})$ $.2H_2O$
	Ferrierite	(Na,K) $4Mg_2$ $(Al_6Si_{30}O_{72})$ $(OH)_2$ $.18H_2O$
	Mordenite	(Na_2, K_2, Ca) $(Al_2Si_{10}O_{24})$ $.7H_2O$
	Laumontite	Ca $(Al_2Si_4O_2)$ $.4H_2O$

and an open alumino-silicate framework of channels and cavities which give laumontite a specific gravity of 2.2 to 2.3 combined with its hardness of between 3.5 to 5.5 (Mohs scale) suggests that distortion of the mineral lattice would accompany any increase in stress due to hydration expansion.

(ii)   Zeolite minerals are all permeable (Hurlbut, 1971) and excess water beyond that required for hydration of leonhardite is not "stored" or "contained" to produce excess pressures if confined.

(iii)   "The amount of laumontite (three samples of nine examined) is so small that it can probably be neglected, particularly in unveined rocks" (Watters in Grant-Taylor, 1976).   See Appendix 3.

Recent work by Duncan et al. (1973) and Gillott (1975) showed that alkali treatment - 2M NaOH at 38°C (100°F) for one month - of greywackes, phyllites and argillites from Nova Scotia, containing a vermiculite-type mica (after biotite and chlorite) resulted in expansive reactions as the vermiculite mineral "exfoliated".   An expansive reaction reported by Oberholster and Brandt (1974) in illite rich shales and summarised by the formula:

$$\text{K-illite (10Å)} + 0.5\ Ca^{++} \longrightarrow \text{Ca - vermiculite (14Å)} + K^{+}$$

may be disruptive in its own right or may promote alkali-reaction in concrete bearing alkali reactive aggregates, by the release of K to the cement paste, even where low alkali cements have been used.

A note by Watters (in Grant-Taylor, 1976), briefly describing mineralogy of some greywackes from Wellington, mentioned the findings of Gillott (1975) and predicted a potential for expansion cracking in concrete made with greywackes, should they be shown to contain vermiculite or montmorillonite.   Neither of these minerals have been found in the present study (section 2.14.2).

With weathering, however, both vermiculite (Barnes, 1979) and montmorillonite (Appendix 24) may form.

Recent experiments have shown the expansion of a greywacke from a sheared greywacke-argillite interface, when subjected to alkali treatment (St John, pers. comm.).   It may be that an illite-vermiculite type reaction

(Oberholster and Brandt, 1974) could occur in such materials due to the presence of illite in fault zones (Barnes, 1979).

Alkali aggregate reactions are becoming increasingly significant to New Zealand, with approximately 25,000 square kilometres of rock-types considered potentially reactive with high alkali cements. Although Neville (1975) claims alkali-aggregate reactions in concrete are widespread in New Zealand, no real problem presently exists (all New Zealand made cements are currently low alkali) although potentially, difficulties could be acute. If high alkali cement were used with these aggregates without proper mix design consideration exposure reactions would create massive damage, often over a long (20 or 30 year) time interval.

High alkali cement production is attractive for a very impelling reason - production cost reduction.

Rising energy charges, an appreciable contribution of production cost, can be offset by increasing the alkali content of the raw mix or recycling kiln stack dust in raw mix of relatively low alkali content to induce clinkering at lower temperature. The end product in both cases is cement of higher alkali content (Gillott, 1975; Gratten-Bellew *et al.*, 1978).

Aggregate related durability problems may then compound since:

(i)   High alkali cements are often used with relatively inferior aggregates.

(ii)   Premium material is increasingly remote from urban areas.

(iii)   New technologies and legislation aimed at environmental protection may also increase costs of aggregate production.

New Zealand will probably manufacture high alkali cements in the near future (Kennerly, pers. comm.; Field, pers. comm.) for reasons outlined above. Increasingly, therefore, there is a need for aggregates to be carefully examined and zoned geologically for their potential use in concrete as aggregates and/or use as engineering materials.

CHAPTER FIVE

"So, Nat'ralists observe, a Flea
Hath smaller Fleas that on him prey.
And these have smaller Fleas to bite 'em,
And so proceed ad infinitum."

Dean Swift (1733) On Poetry: a rhapsody: 20pp.

Utilisation of greywacke-suite aggregate in concrete

This chapter investigates the properties of concrete made of aggregate from
Wellington greywacke-suite rocks, and attempts to relate these properties to
those of the aggregate and rock.

In chapter 4, links were established between quarried aggregate and the parent
rock, in particular with angularity, density, bulk density, crushing resistance
and Los Angeles test values. Of these properties, all of which are related to
rock mean grain size, angularity, density and crushing resistance were selected
as being those most likely to influence concrete properties.

Because the results of chapter 3 and 4 indicate greywacke-suite rocks (and
especially the greywackes) to be very strong, elastic materials with close
ranging physical properties, it was decided to design the concrete mix so that
the sometimes subtle differences in the physical properties of the aggregate
were more readily discernable and comparable. To gauge the importance of
aggregate strength, a very high strength concrete was necessary. Although the
strength of the cement paste would invariably be much lower than that of the
rock materials used as aggregate, a reasonable matching of static elastic
properties was considered desirable and attainable

High strength concrete calls for low water to cement ratios, as concrete strength
is inversely related to the water to cement ratio in fully compacted concrete
(Neville, 1975). Initial testing of mixes with water to cement ratios of 0.4
and 0.5 did not provide concretes of sufficient strength and showed that such a
difference in ratios masked subtle workability effects imparted by the aggregates
thus precluding confident comparison of aggregate performance.

The two mixes finally chosen (Appendix 27) used water to cement ratios of 0.375 (mix 1) and 0.4 (mix 2). They were designed to achieve very high strengths with high aggregate to cement ratios without the use of additives or admixtures. This provided a good basis for comparing performance of different aggregates from Wellington greywacke-suite rocks. A special interest was shown in concrete from argillite, because this rock type has been traditionally unacceptable to the building industry.

Although concrete strengths from the chosen designs are well in excess of those normally required of concrete in commercial use, the mix designs would not be commercially viable as workability and cohesion are too low due to the low sand content.

The sand chosen for the study was monomineralic, well graded, and consisted of rounded grains. The latter properties are well suited to impart plasticity to concrete ar moderate water requirements (Appendices 26, 28).

Each concrete mix design was used with each aggregate in $0.03m^3$ batches which provided twelve 100mm diameter x 200mm long cylinders to NZS 3112:1974 clause 201. Mix designs and calculations may be found in Appendix 27 while ingredients, moulding, curing and testing is detailed in Appendix 28.

At age 3, 7, 28 and 90 days, three cylinders, randomly selected from each batch, were removed singly from the curing chamber and immediately weighed in air, then in water, their long axis ultrasonic velocity determined with the PUNDIT, and measured longitudinally and across two diameters, 22.5^o each side of the cylinder mould seam at mid-height. They were then tested in uniaxial compression (Appendix 28). All tests were carried out in accordance with NZS 3112:1974 "Methods of test for concrete".

At 28 days, the static elastic modulus was determined using temperature compensated half-bridge strain instrumentation, a single PL-60 strain gauge (60mm gauge length) being attached parallel to the longitudinal axis of the cylinder centred on mid-height (Appendix 14).

5.1   Fresh concrete tests

Results are presented in Table 5.1.

5.1.1   "Workability" of fresh concrete

"Workability" of fresh concrete is measured in different ways and tests have
been specifically designed to simulate certain types of "workability", e.g.
its ability to be pumped - pumpability, its deformation under the influence
of gravity - slump, the rate at which it can be transformed from one shape to
another - remoulding effort (Tattersall, 1976).

Two workability tests were used in this study (both mix designs gave concrete
of essentially zero slump):

(i)   Compacting factor: Not often used in New Zealand, this test to
BS 1881:1970; part 2, measures the degree of compaction after a set amount
of work has been imparted to the concrete, and was used for comparative
purposes.

Concrete is allowed to drop through two inverted truncated cones (frustrums)
to fill a standard sized cylinder and its mass is expressed as a ratio to the
mass at optimum compaction required to fill the cylinder.   Compacting factor
is therefore a density ratio , with a range from 0 to 1, which is sensitive to
concrete of low workability provided the mix does not stick or hesitate in the
apparatus during test.   The test mixes performed well in this regard.

(ii)   Vebe consistometer: The Vebe (V-B) apparatus measures the time
(seconds) taken to remould a cone of fresh concrete to a cylinder, under
vibration at a predetermined frequency.   The energy required to compact the
concrete is deemed a measure of workability, simulating compaction into moulds
or formwork.

The V-B test provided better resolution of mix workability than the compac-
ting factor test (Figure 5.1) especially for mix 1.

Test results (Table 5.1, Figures 5.2 and 5.3) showed that workability decreases
with degree of angularity (A_{2D}).   The effect is more marked as workability
increases and in design 2 mixes generally.

Table 5.1 : Fresh concrete test results. Within each mix design the order of concrete made was randomised. Results are listed here in order of diminishing rock mean grain size.

Aggregate Sample	Order in which concrete was made	Rock mean grain size, phi	V-B Consisto-meter seconds	Compac-ting factor	Fresh concrete density, kg.m^{-3}	Concrete yield	Calcu-lated cement content kg.m^{-3}
HQ-17	3	1.3	23.9	0.77	2502 }	}	
KTW-14	5	2.6	26.6	0.71	2494 }	}	
BQ-1XA	1	2.9	29.7	0.69	2509 }	}	
SJ-T	2	4.7	22.1	0.75	2501 }	0.97 }	360.8
OB-W	4	5.6	50.9	0.66	2543 }	}	
HQ-22	6	6.3	34.1	0.69	2504 }	}	
HQ-17	8	1.3	12.0	0.77	2471 }	}	
KTW-14	9	2.6	12.8	0.78	2473 }	}	
BQ-1XA	7	2.9	12.9	0.76	2476 }	}	
SJ-T	12	4.7	10.1	0.76	2505 }	0.97 }	360.8
OB-W	10	5.6	15.8	0.72	2520 }	}	
HQ-22	11	6.3	17.4	0.74	2503 }	}	

MIX 1 (top group), MIX 2 (bottom group)
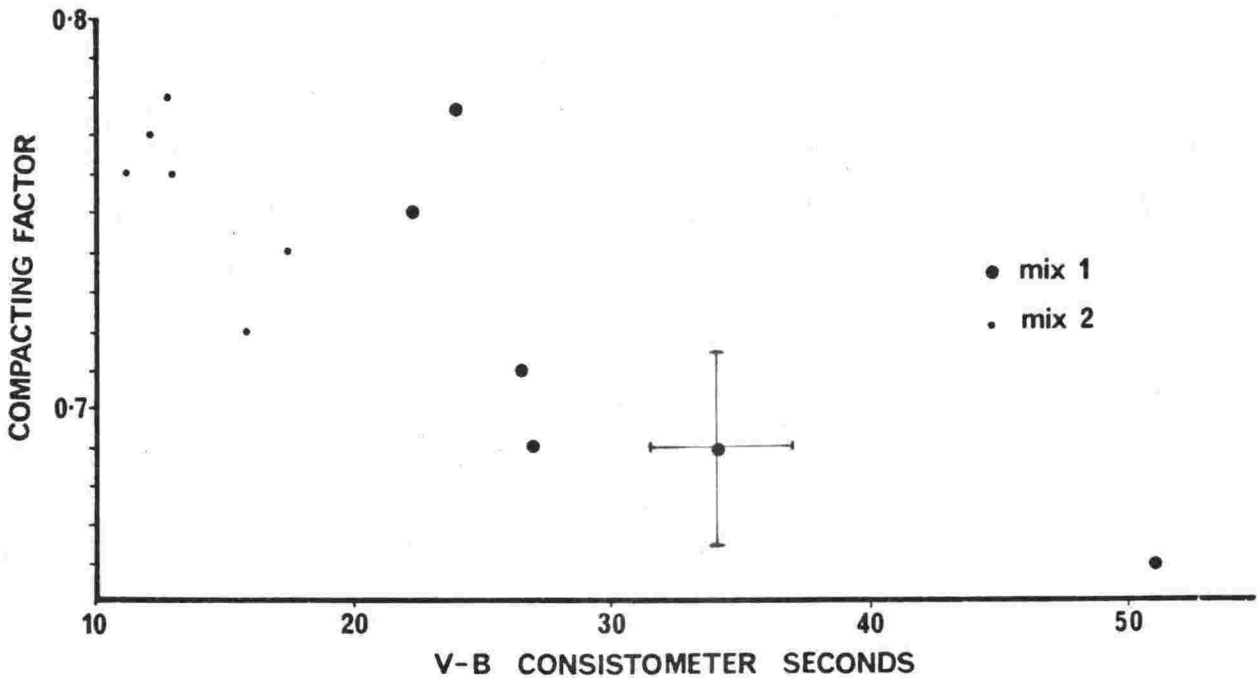
Figure 5.1 : A comparison of workability by compacting factor
and V-B consistometer. Although related and able
to be used with concrete of low workability, the V-B consistometer
provides better resolution. Error bars based on the standard
deviation from 5 runs. Standard deviation for V-B, 2.7 seconds;
for compacting factor 0.024. These data are consistent with the
findings of Clelland (pers.comm.) who indicated respective
repeatibilities of 3 seconds and 0.03 for mixes in the workability
range of this study.
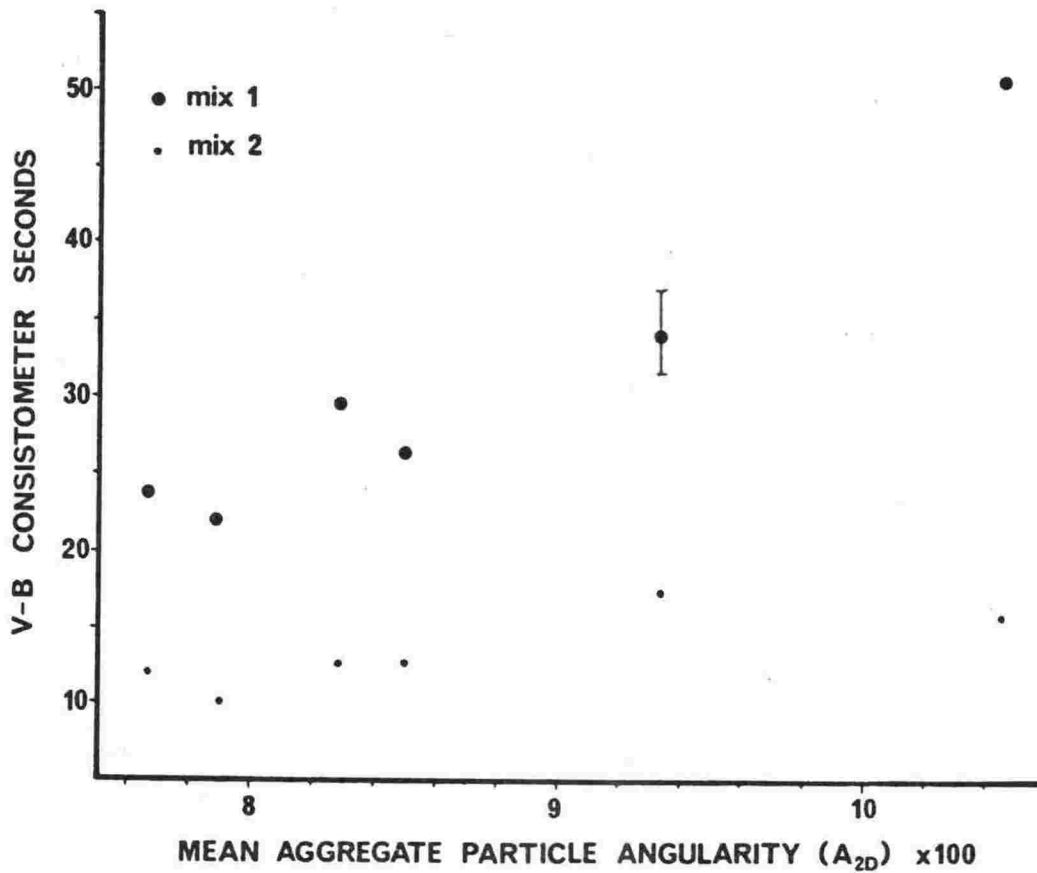
Figure 5.2 : Aggregate particle shape has a profound effect on
V-B seconds workability especially in mixes of
increased aggregate to cement ratio.   Compare with Figure 5.3.
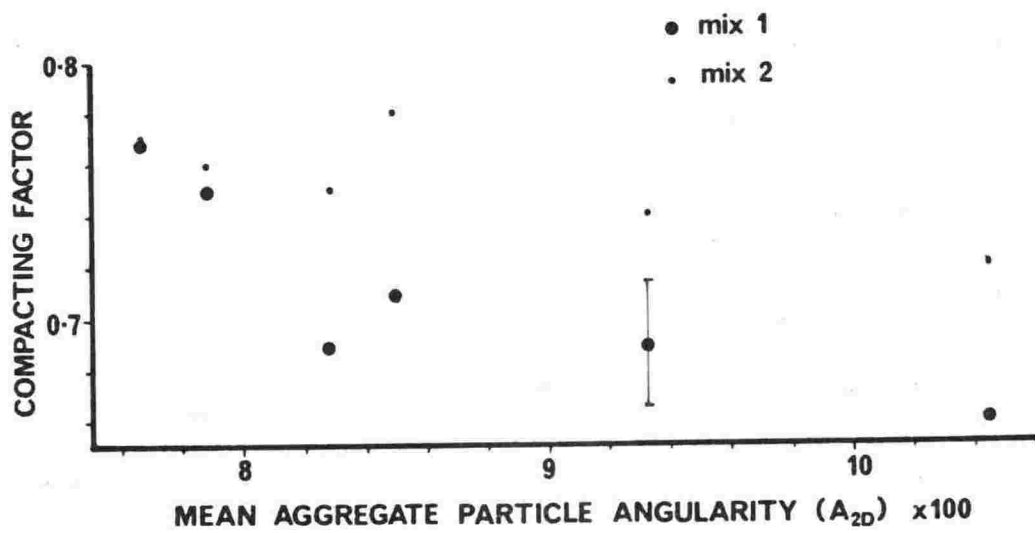
Figure 5.3 : Aggregate particle angularity influence
            over workability as measured by compacting factor,
but does not identify differences in mix design as well as V-B
seconds (Figure 5.2).

Convergence of the two trends shown in Figures 5.2 and 5.3 with decreasing particle angularity values suggests that workability is determined entirely by angularity below 600 A_{2D} for mixes with high aggregate to cement ratios (>5). This trend is best shown by the V-B test, though generally for mixes with a lower aggregate to cement ratio, and slumps greater than 15mm, the test is less sensitive.

5.1.2 Density (unit mass) of fresh concrete

Densities of mix 1 concrete were higher than those of mix 2, for the same aggregate, due to a lower water to cement ratio and corresponding increase in aggregate to cement ratio in the mix design.

Mix 1 results show no clear relationship between fresh concrete density and that of rock core and aggregate (Figures 5.4 and 5.5), though one sample, OB-W, had a significantly greater core, aggregate and fresh concrete density.

Mix 2 concretes show clear linear relationships (very high correlation coefficients for rock and aggregate densities, Figures 5.4 and 5.5), presumably because the concrete density scatter was much greater than in mix 1. Rock density influences are probably better assessed from mix 2 concrete because the higher water to cement ratio produces a sand/cement paste mortar of lower density.

5.2 Hardened concrete tests

Though many tests may be performed on hardened concrete to assess its properties, only those most likely to illustrate the role of aggregate were carried out. Therefore tensile strength and more time consuming investigations of concrete shrinkage, thermal conductivity and coefficient of linear thermal expansion were not determined. Instead uniaxial compressive strength, ultrasonic velocity, static elastic modulus and density were measured. Complete results are presented in Appendix 29 except those for static elastic modulus which are in section 5.2.2.

The quality of bond in concretes of this study followed the normal pattern (Table 5.1A). However, bond strength was not measured because:

(a) the greatest interest for this study was aggregate performance which is well recorded from measurements of ultrasonic velocity, compression strength and elastic modulus.

(b) no widely accepted method of measuring bond strength exists.

A recent review of the cement-aggregate bond (Struble *et al.*, 1980*) concluded that the nature of the bond is far better understood than is the influence of the bond on concrete performance, although most workers apparently agree that the bond is an important factor in the strength of concrete, especially the flexural strength (Neville, 1975). "Generally, when bond is good, a crushed concrete specimen should contain some aggregate particles broken right through, in addition to the more numerous ones pulled out from their sockets. An excess of fractured particles, however, might suggest that the aggregate is too weak. Because it depends on the paste strength as well as on the properties of aggregate surface, bond strength increases with the age of concrete; it seems that the ratio of bond strength to the strength of the paste increases with age. Thus, providing it is adequate, the bond strength *per se* may not be a controlling factor in the strength of concrete. However, in high strength concrete there is probably a tendency for the bond strength to be lower than the tensile strength of the cement paste so that preferential failure in bond takes place". (Neville, 1975).

The effect of the bond on concrete performance is a subject of controversy but a positive relationship between concrete strength and bond strength seems to exist. (Struble *et al.*, 1980).

Further study in this field would have required very considerable research effort - beyond that which would seem reasonable within the context and scope of this study.

5.2.1   Uniaxial compressive strength

The compressive strength of concrete is one of its most useful and important properties. It is one of the most easily determined and the most directly

---

*Struble, L., Skalny, J. and Mindess, S. (1980).   A review of the cement-aggregate bond. *Cement and Concrete Res., Vol.10* : 277-286.
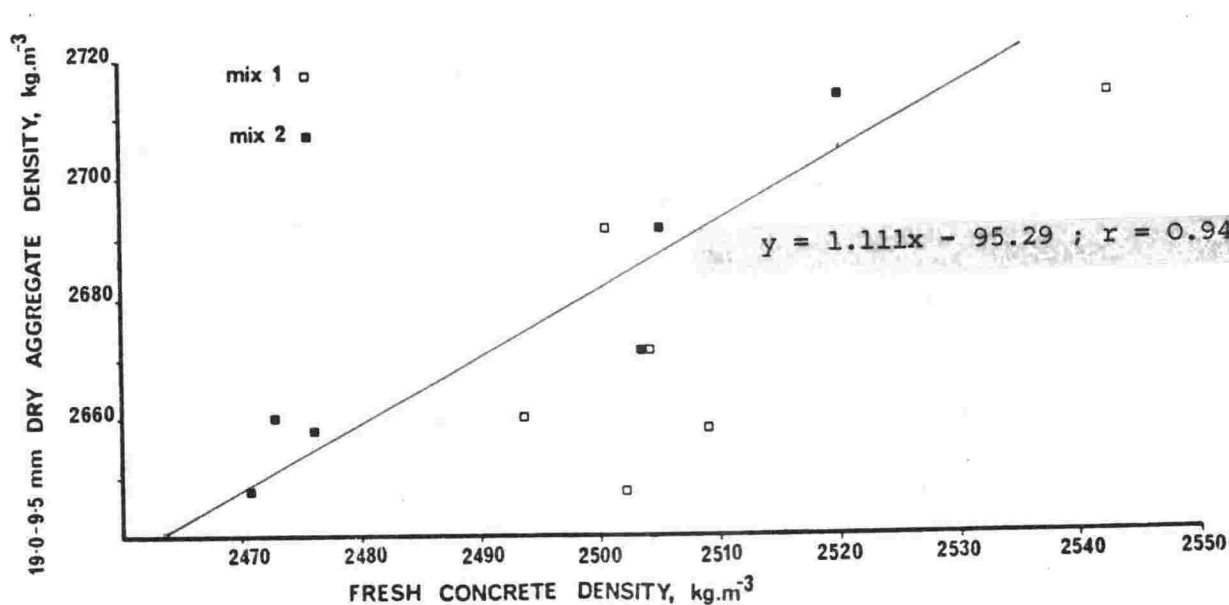
Figure 5.4 : Dry 19mm aggregate density related to fresh concrete density. A clearer relationship is apparent in concretes of mix 2 design.
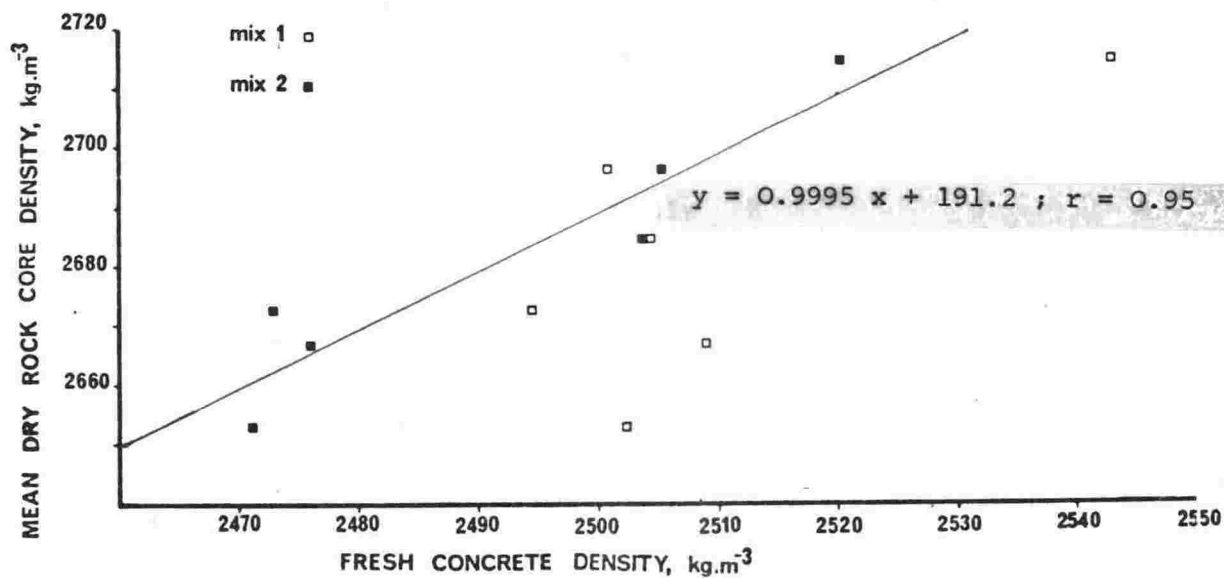
Figure 5.5 : Dry rock core density related to fresh concrete density. As in Figure 5.4, better correlation is apparent in concretes of mix 2 design.

Table 5.1a: Bond qualities from all mixes of this study. A
subjective assessment from failure surfaces.
B = aggregate not broken   A = aggregate broken

Aggregate sample	Concrete age	Mix 1 Concrete failure surfaces		Mix 2 Concrete failure surfaces	
HQ-17	3		B		B
	7		B		B
	28		A		A
	90		A		A
KTW-14	3		B		B
	7	mainly	B		B
	28		A		A
	90		A		A
BQ-1XA	3		B		B
	7	mainly	B	mainly	B
	28		A		A
	90		A		A
SJ - T	3		B		B
	7	mainly	B		B
	28		A		A
	90		A		A
OB-W	3		B	mainly	B
	7	mainly	A	mainly	A
	28	mainly	A	mainly	A
	90		A		A
HQ-22	3	mainly	B	mainly	B
	7	mainly	A	mainly	A
	28		A		A
	90		A		A

applicable, so compressive strength is the parameter generally used to assess quality.

Test results relating compressive strength to age, aggregate type and mix design are shown in Tables 5.2, 5.3 and Figures 5.6, 5.7.

Concrete of both mix designs behaved in a manner consistent with concrete of more orthodox designs.   Several observations may be made from Figures 5.6, 5.7:

(i)   The rate of strength development, initially rapid, decreased exponentially.

(ii)   There is little significant strength difference in concrete younger than seven days, but from 28 days, differences in aggregate become apparent e.g. OB-W, a low strength aggregate, yields a lower strength concrete.

(iii)   From 28 days, the strength of OB-W concrete is significantly weaker than the rest in each of the mix designs.

(iv)   At days 3 and 90 respectively, the strength of mix 2 concrete was 80 and 90 percent that of mix 1 except for OB-W, (75 and 95 percent).

5.2.2   Static elastic modulus

The range in rock strengths and the greater degrees of angularity of aggregates from the (generally) weakest rocks (sections 3.5.1, 4.2.2) prompted the investigation of concrete static elastic modulus.   Weak rocks are generally considered to have low elastic moduli.   High values of aggregate angularity give lower concrete workabilities and lead to preferred orientation of aggregate particles.

The difference between static and dynamic elastic moduli data is greatly influenced by the presence of fractures, cracks or cavities, static data generally providing lower values (see Boult, 1979).

The static elastic modulus was measured in preference to the dynamic elastic modulus because the latter can be readily determined only at low stress levels

Table 5.2 : Summary of hardened concrete test results for concrete of Mix 1
             design.   Full data appear in Appendix 29.

Aggregate,	Concrete age, days	Mean density, kg.m^{-3}	Mean strength, MPa	Mean ultrasonic velocity, m.s^{-1}
HQ-17	3	2475	30.1	4570
	7	2478	49.3	4727
	28	2482	74.4	4896
	90	2481	88.0	4956
KTW-14	3	2482	30.3	4685
	7	2480	49.8	4786
	28	2484	73.9	4979
	90	2483	85.5	4963
BQ-IXA	3	2482	29.8	4604
	7	2480	48.0	4734
	28	2491	74.0	4946
	90	2485	87.2	5011
SJ-T	3	2500	28.4	4553
	7	2496	49.9	4708
	28	2502	73.8	4883
	90	2505	83.4	4955
OB-W	3	2515	31.4	4360
	7	2520	48.6	4499
	28	2518	62.7	4641
	90	2523	67.9	4702
HQ-22	3	2489	29.9	4446
	7	2494	48.5	4591
	28	2498	71.3	4771
	90	3497	82.4	4789

Table 5.3 : Summary of hardened concrete test results for concrete of Mix 2
design.   Full data appear in Appendix 29.

Aggregate,	Concrete age, days	Mean density, kg.m^{-3}	Mean strength, MPa	Mean ultrasonic velocity, m.s^{-1}
HQ-17	3	2463	22.1	4504
	7	2464	41.4	4715
	28	2467	66.9	4872
	90	2471	79.6	4937
KTW-14	3	2473	25.4	4528
	7	2475	42.1	4741
	28	2479	68.8	4912
	90	2479	80.0	4967
BQ-IXA	3	2469	21.7	4503
	7	2468	38.2	4671
	28	2471	65.9	4841
	90	2477	75.6	4909
SJ-T	3	2489	22.8	4511
	7	2493	38.2	4648
	28	2489	64.0	4807
	90	2497	72.5	4864
OB-W	3	2505	23.6	4242
	7	2512	42.4	4464
	28	2513	60.5	4629
	90	2513	65.4	4684
HQ-22	3	2483	23.6	4339
	7	2480	41.1	4507
	28	2486	68.0	4704
	90	2486	72.8	4746
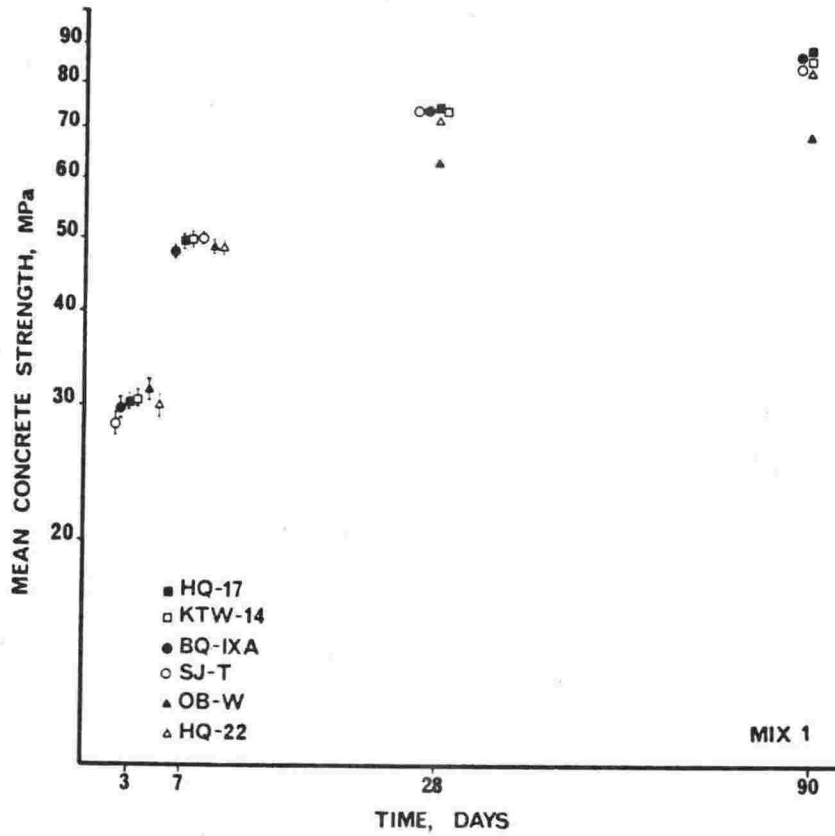
Figure 5.6 : Concrete strength related to time: mix 1.
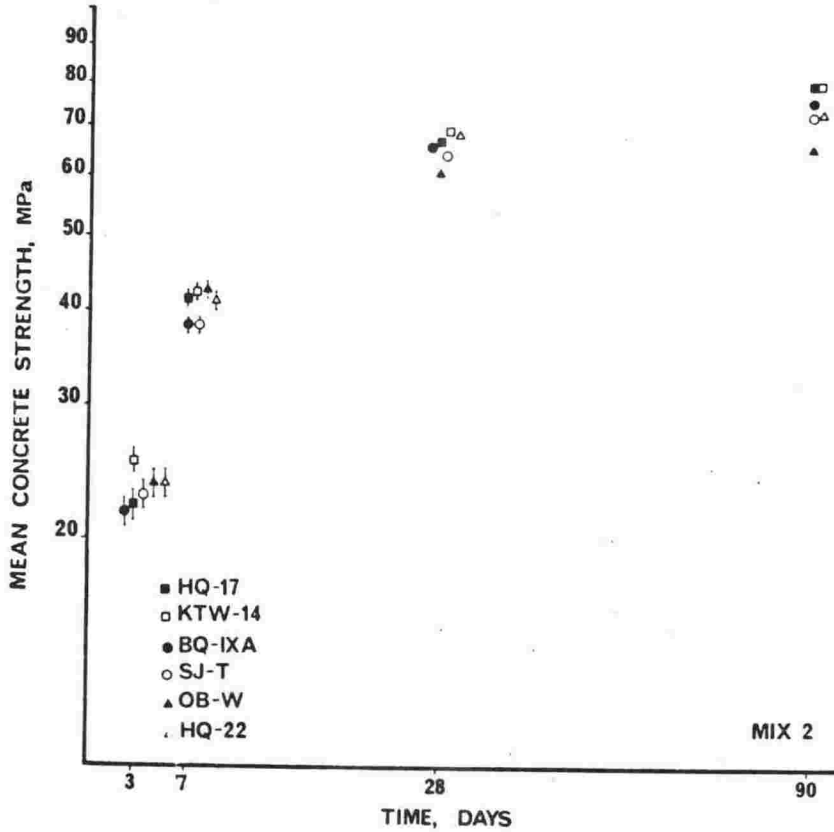
Figure 5.7 : Concrete strength related to time: mix 2

Comprehensive strength of concrete of two mix designs with different greywacke-suite aggregates at ages of 3, 7, 28 and 90 days.   Both axes are logarithmic scales.   Standard error about the mean is ±1.02 MPa, shown as bars at 3 and 7 days.   Symbol size precludes error bars at 28 and 90 days.   Symbols are slightly offset from test ages for clarity.

and there it is comparible with the initial tangent static elastic modulus
(E_i).

Elastic moduli are of interest in the design of concrete structures and
although not normally used routinely*, may be required in:

(i)   Reinforced concrete design theory.   Concrete has negligible strength
in tension thus reinforcing steel is used to accommodate tensile strain imposed
by loads.   Deflection calculations for beams and pillars and the positioning
of lever arms, two-way spanning slabs and the like also require its use.

(ii)   Calculation of the slenderness effects of columns in high-rise
structures.

The method of determining the static modulus of concrete specimens at 28 days
is discussed in Appendix 14:   results are shown in Table 5.4.

Stress-strain curves are shown in Figures 5.8, 5.9.   The elastic modulus is
valid only from the more linear part of the curve as the strain increase at
the top of the curve is considered to be due to creep (Neville, 1975).

As no universally accepted method of determining the elastic modulus of con-
crete appears to exist, the secant elastic modulus (E_c) at 50 percent ultimate
stress was chosen as the most appropriate for the comparison of data and
representation of concrete (Neville, 1975).

---

*   For practical purposes the elastic modulus of any normal weight concrete
      may be found from:

$$E_c = 4700 \sqrt{f'c}$$

where E_c = concrete elastic modulus, MPa

        $f'c$ = concrete compressive strength, MPa

see the "New Zealand reinforced concrete design handbook".   Preferred
concrete strengths $(f'c)$ are listed in DZ 3109 "Concrete construction"
as 17.5, 20, 25, 30, 35, 40 and 45 MPa.

Table 5.4 : Static elastic moduli for concrete of all aggregate samples
of Mix 1 and 2 design,obtained as the secant elastic modulus
at 50 percent ultimate stress.

Aggregate sample and concrete cylinder number		Mix 1		Mix 2	
		Static elastic modulus (E_c) at 50 percent ultimate stress, GPa	Mean E_c GPa	Static elastic modulus (E_c) at 50 percent ultimate stress GPa	Mean E_c GPa
HQ-17	1	50.9		44.4	
	2	56.1	55.2	37.3	39.3
	3	58.5		36.1	
KTW-14	1	67.8		34.4	
	2	81.6	76.6	58.2	44.8
	3	80.4		41.7	
BQ-IXA	1	57.8		51.7	
	2	35.1	54.5	37.6	42.4
	3	70.7		37.8	
SJ-T	1	59.0		-	
	2	41.2	48.6	47.9	42.8
	3	45.6		37.6	
OB-W	1	41.4		39.4	
	2	35.2	37.7	35.0	35.6
	3	36.6		32.5	
HQ-22	1	69.7		37.4	
	2	68.7	69.2	43.6	43.8
	3	69.2		50.4	
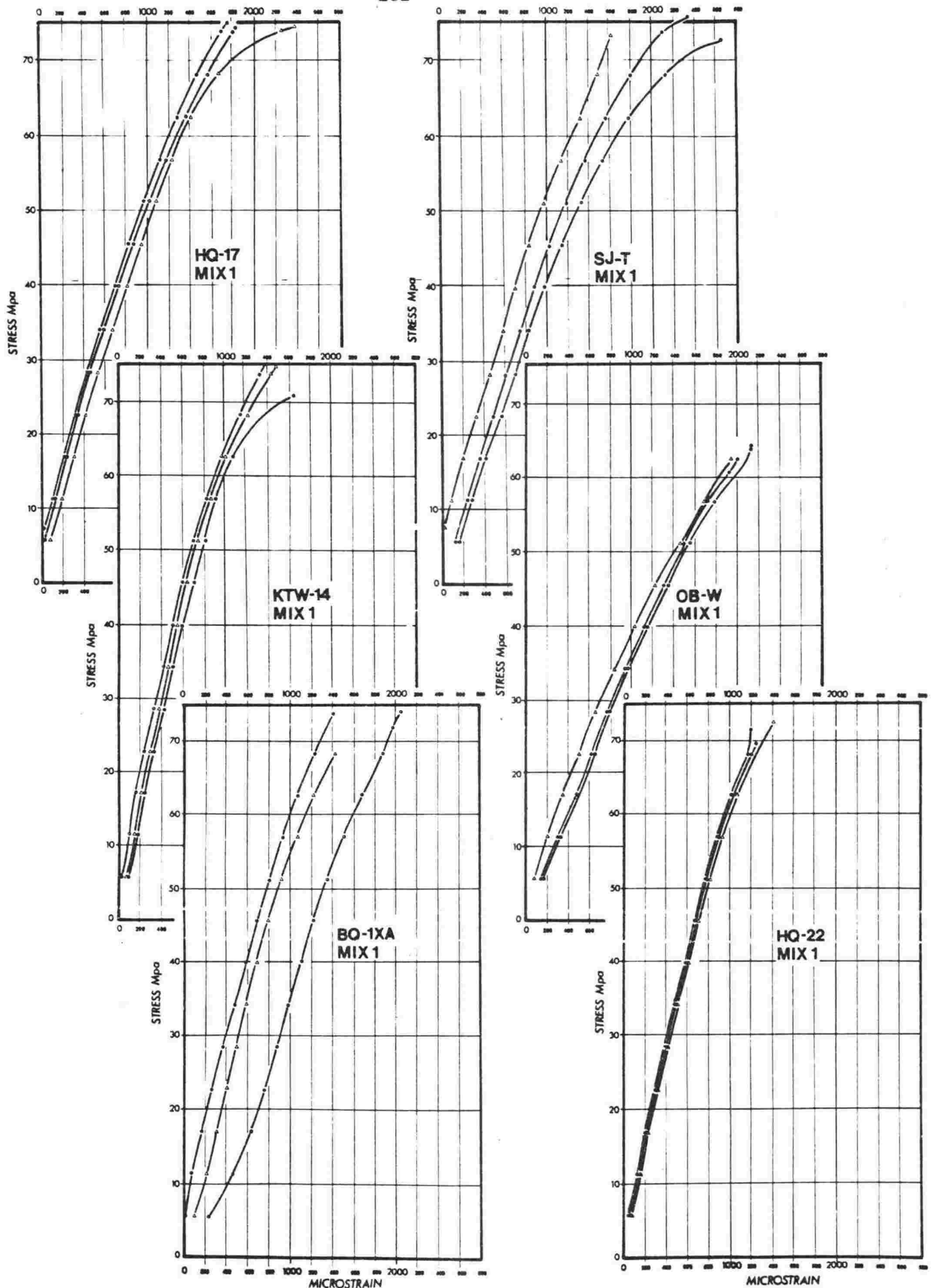
Figure 5.8 : Mix 1 concrete 28 days stress-strain curves.

N.B. Mpa should read MPa.
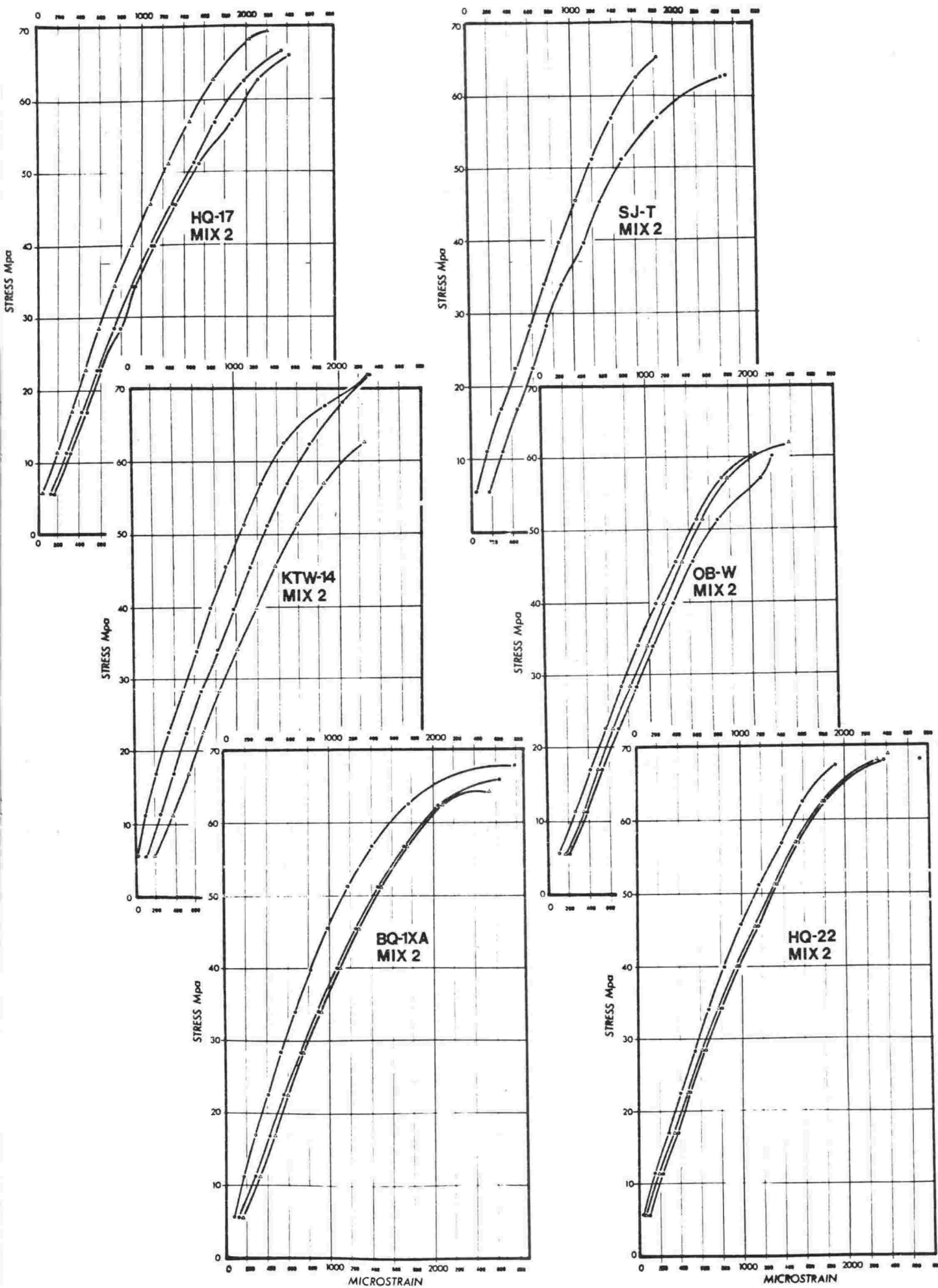
Figure 5.9 : Mix 2 concrete 28 day stress-strain curves.

N.B. Mpa should read MPa.

Table 5.4 shows that mix 1 concretes have higher E_c values than mix 2 concretes, within each aggregate type, i.e. the elastic modulus is higher in stronger concretes for any aggregate type.   This is due to the higher strength cement paste and the higher proportions of aggregate in the mix 1 design.

It is also interesting to note that results from the stronger concrete from mix 1 are more scattered than those from mix 2 concrete.

Neville (1975) has shown the relationship between static elastic modulus and ultrasonic pulse velocity, and his graph is extended by this study (Figure 5.10) although in practice generalisations can not be made regarding the relationship.

Generally, it is contended that the static elastic modulus of concrete is related to the static elastic modulus of the rock from which the included aggregate is made.   Woolf (1966) declares such a relationship to be no more than "fair" having regard for the difficulties in determining moduli, the non-uniformity of rock specimens and of derived aggregates, in bulk and as they occur in concrete, together with the problems inherent in instrumentation. However, results from this study (Figure 5.11) indicate that a linear relationship does exist.

The two main components of concrete, aggregate and sand/cement paste, each have
(Neville, 1975, Fig. 6.4)
more or less linear stress-strain curves but combined as concrete the resultant curve shows strain rate acceleration as ultimate stress is approached due to the development of microcracking at the interfaces between the components. It is not surprising, then, that relationships exist between aggregate particle shape, static modulus and the shape of stress-strain curves (Woolf, 1966;   Neville, 1975).

La Rue (1946) working with four limestone aggregates found the relationship between aggregate and concrete modulus to be exponential;   given by the expression:

$$E_c = 5.875 \ (1 - 0.08^{e - 0.3 \cdot E_s})$$

where E_c = concrete modulus

and E_s = coarse aggregate modulus
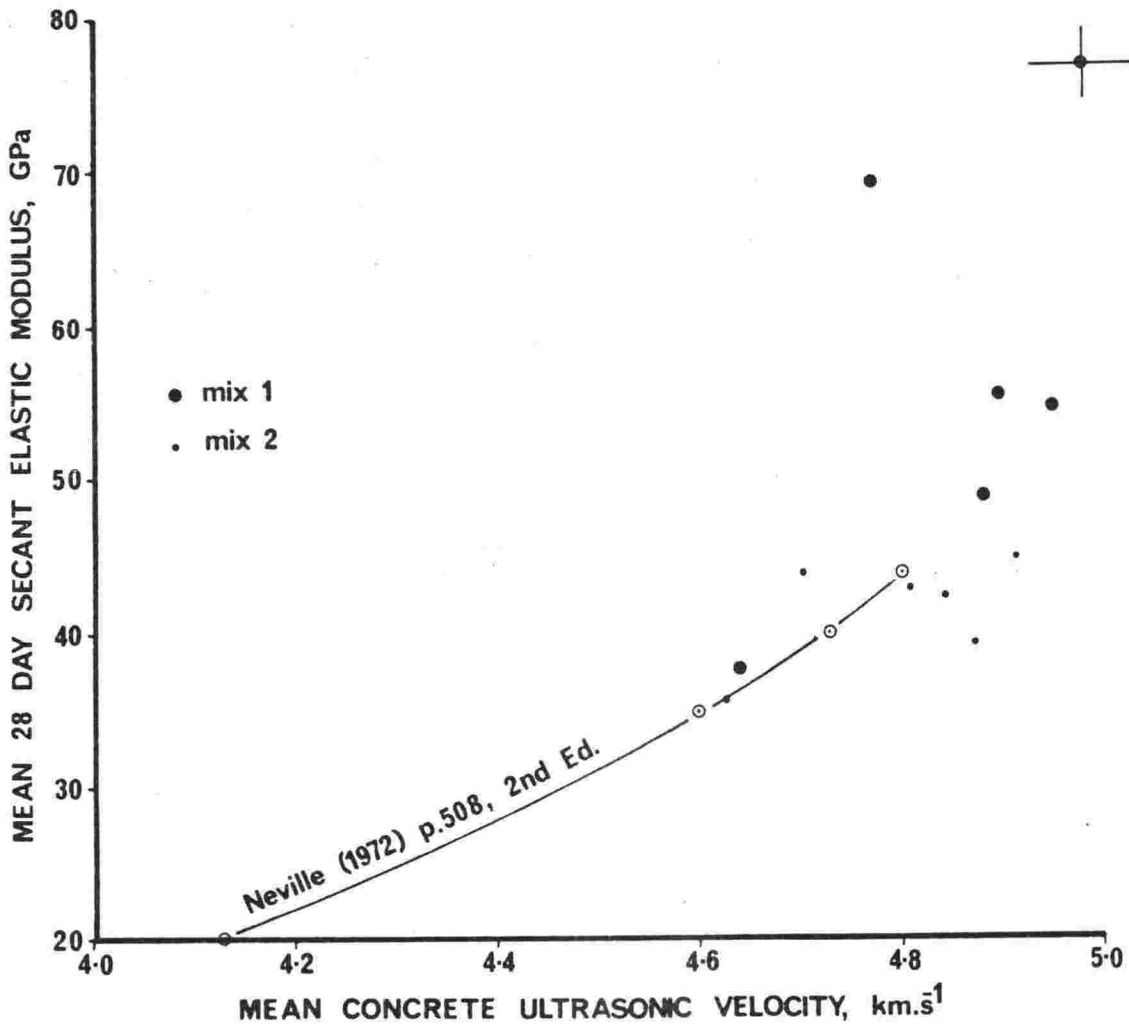
Figure 5.10 : The static elastic modulus of concrete may be
used as an indicator of dynamic properties when
related to ultrasonic velocity. Error bars are shown on one
sample.
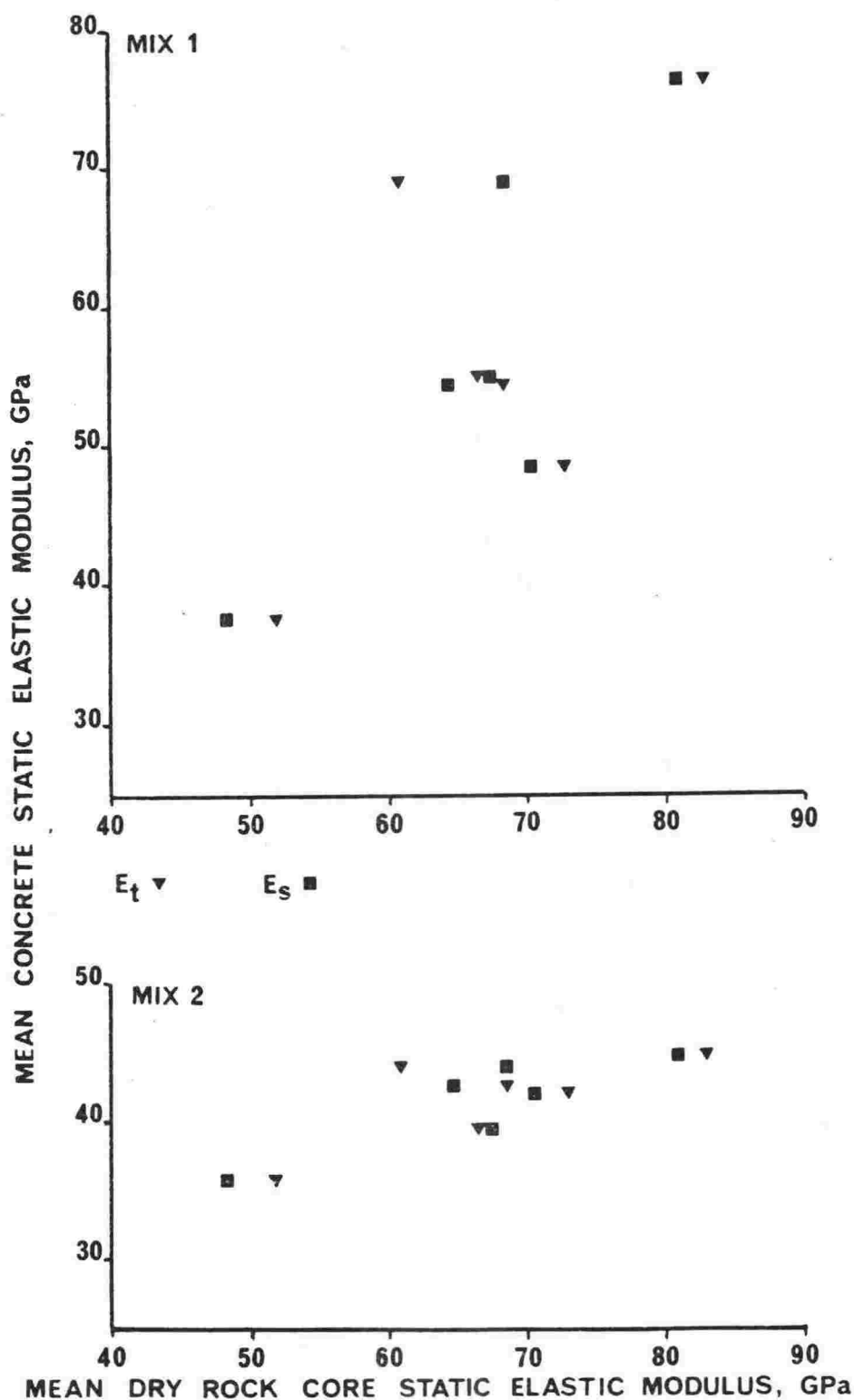
Figure 5.11 : Static elastic modulus relationship of concrete
and dry rock core.   A linear relation appears
to exist.   For mix 1, rock core E_t correlation coefficient = 0.81
and for E_s = 0.71
For mix 2, rock core E_t correlation coefficient = 0.91
and for E_s = 0.78.

5.2.3   Ultrasonic velocity

The PUNDIT apparatus mentioned earlier (section 3.3.2) was originally pro-
duced in response to a demand for non-destructive assessment of relative
strengths of *in situ* concrete,as laboratory strength testing does not accur-
ately represent the strength of the same concrete in a structure.   Ultra-
sonic velocity has been found to be directly related to strength under certain
conditions,although there is no universally applicable relationship between
them (Jones and Gatfield, 1955).

The axial ultrasonic velocity of each cylinder was determined using 50 mm
transducers with a frequency of 50 kH$_z$.   Templates were used to locate the
transducers centrally on the cylinder ends with glycerine and talcum powder
paste to ensure acoustic contact.

There is a direct relationship between ultrasonic velocity and strength for
each concrete made,with a numerical displacement between corresponding samples
from each mix design (Figures 5.12, 5.13).   Ultrasonic resolution is good
until aggregate strength exceeds concrete strength, generally at about 28 days
and except for 3 day samples in mix 2, incorporating greywacke aggregates.

Comparison of Figures 5.12 and 5.13 shows differences in young concrete strengths
are not influenced by aggregate parameters where sand/cement paste is strong
(mix 1).   Indeed, they are only marginally capable of resolution in concretes
of mix 2 design and this is probably due to increased workabilities allowing
angularity dependent particle packing to be better established.

Although, generally, there is no universally applicable correlation between strength and
ultrasonic velocity in concrete (Neville, 1975), there is a strong relation-
ship between the ultrasonic velocity of parent rock and concrete made with
derived aggregate,which becomes apparent when wet rock core velocities are
compared with those of corresponding hardened concrete (Figures 5.14, 5.15).
The relationship is similar at all ages and both mixes.

As parent rock density is reflected through its derived aggregate to become a
determinant in the density of concrete in which it is included,and as density
is related directly to elastic modulus and inversely to ultrasonic velocity,
any assessment of concrete by ultrasonic velocity must have due regard for
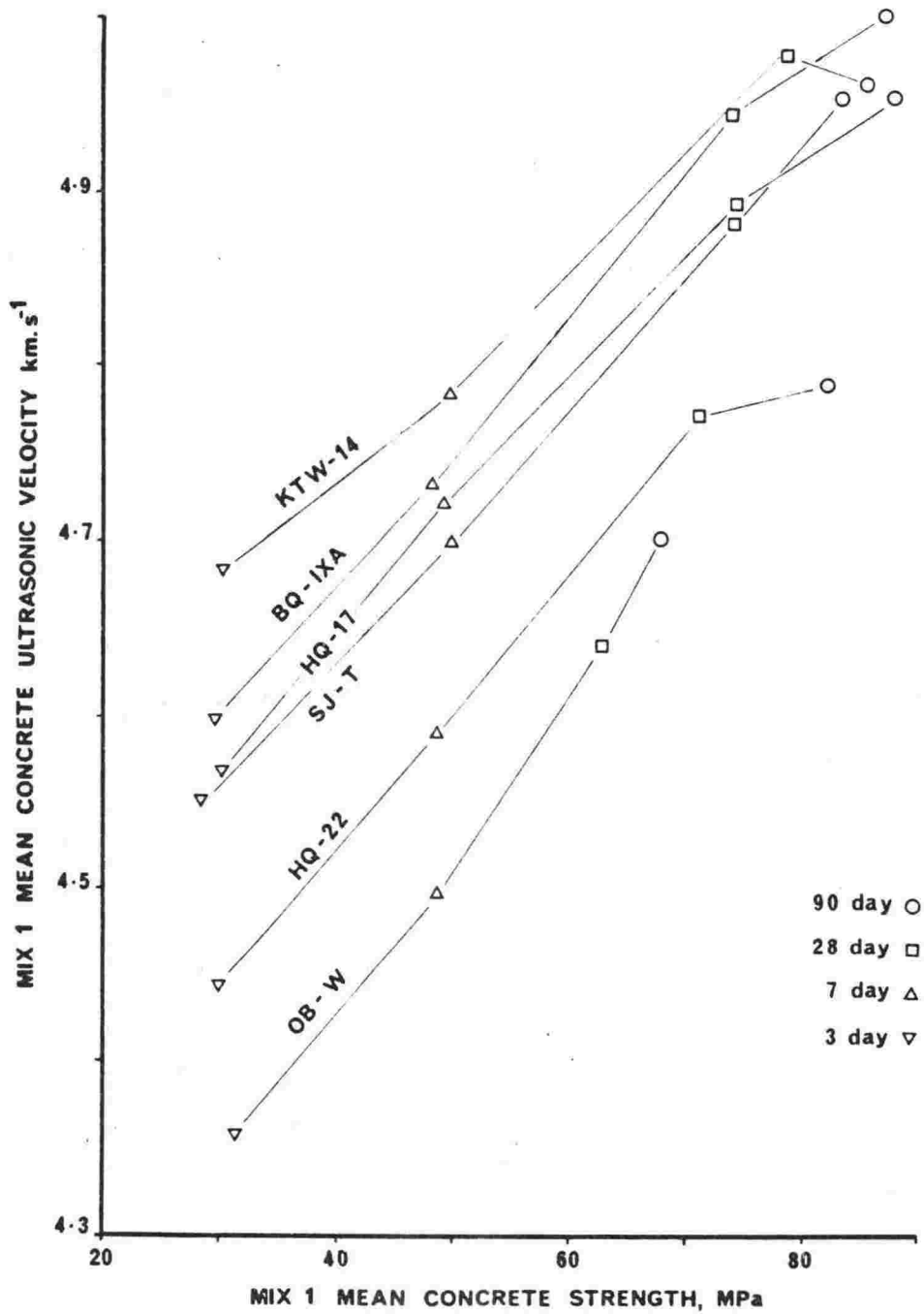
Figure 5.12 : Mix 1 concrete strength related to ultrasonic velocity showing influence of aggregate strength with hardening sand/cement paste.
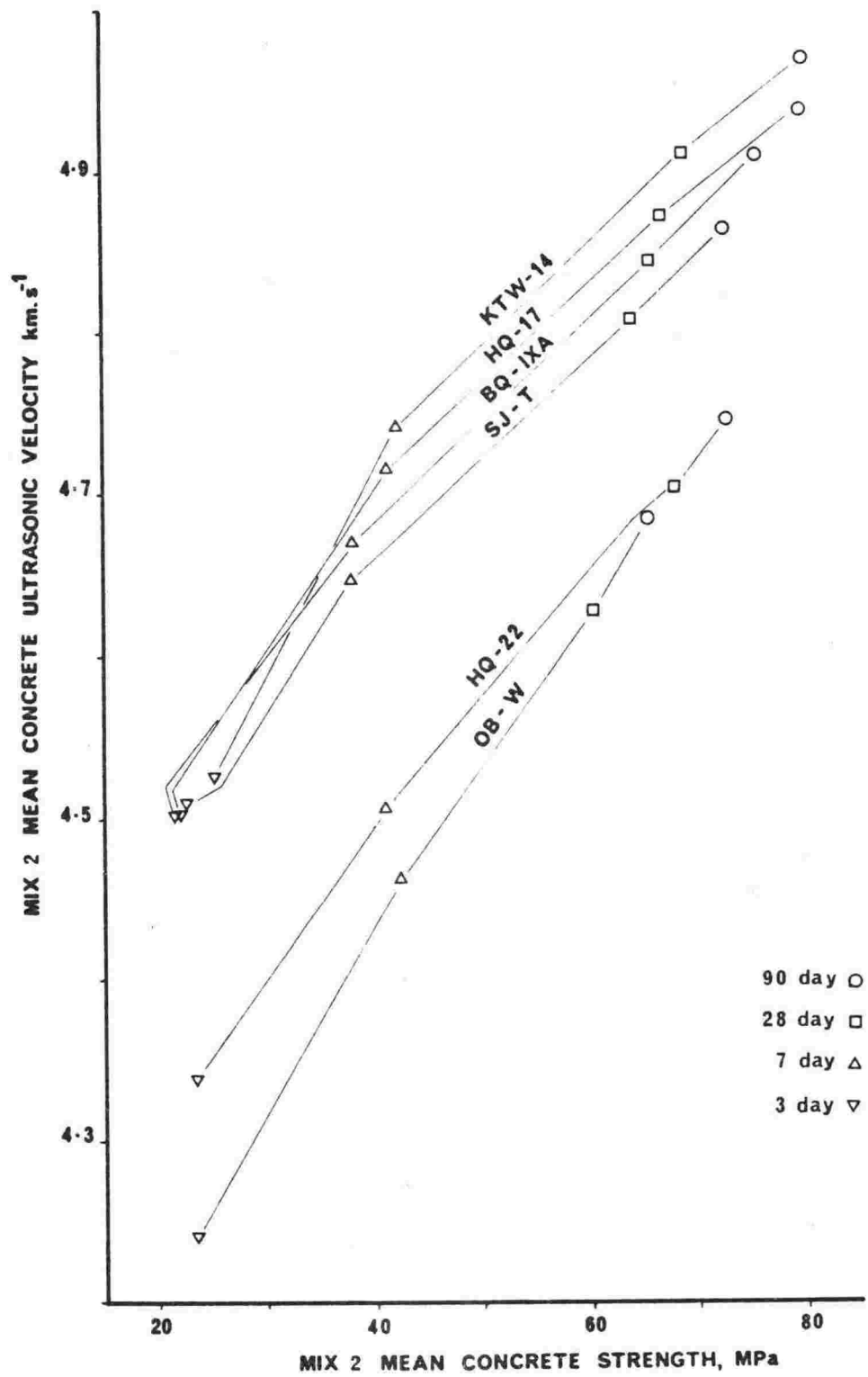
Figure 5.13 : Mix 2 concrete strength related to ultrasonic velo-
city showing influence of aggregate strength with
hardening sand/cement paste.
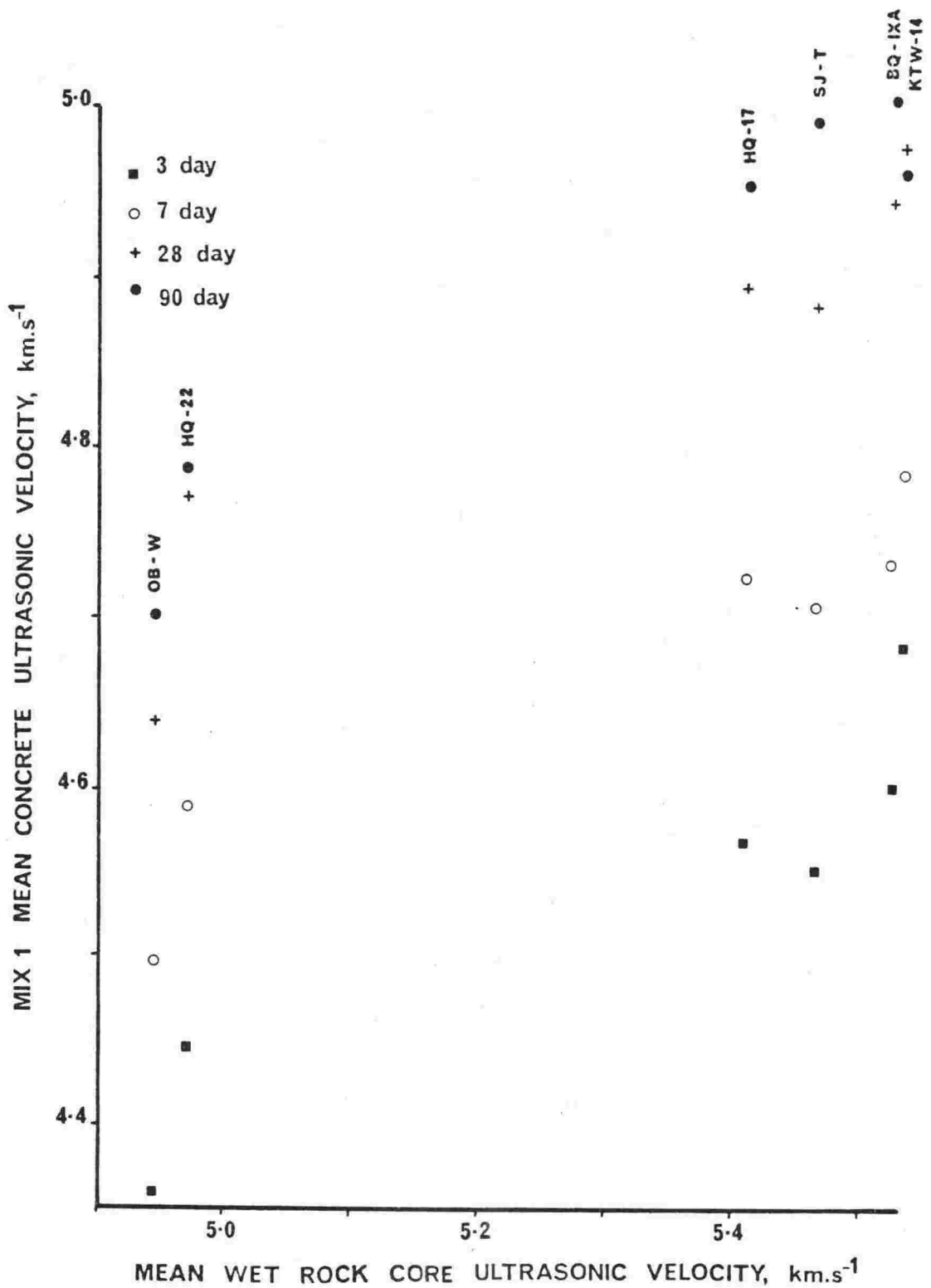
Figure 5.14 : Ultrasonic velocities of wet rock cores are reflected
in concrete ultrasonic velocities up to 90 day con-
crete ages, when sand/cement paste alters the trend as it gains
strength.
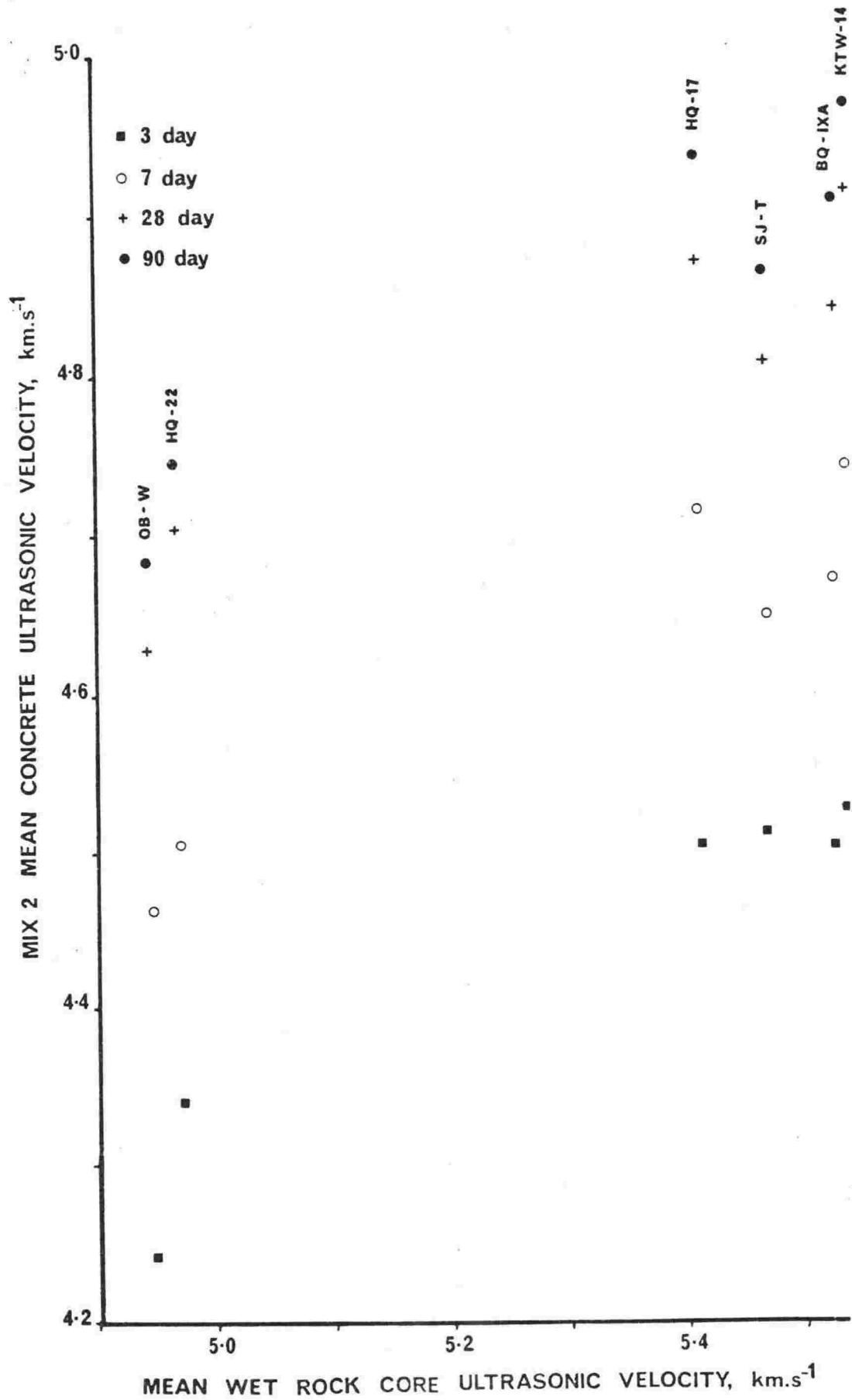
Figure 5.15 : Ultrasonic velocities of wet rock cores are
reflected in concrete ultrasonic velocities,
but with less resolution than in concretes of mix 1 design con-
cretes (Figure 5.14).   Mix 1 contains more aggregate per unit
volume.

elastic modulus (Figure 5.10). This is well demonstrated in this study, where concretes made to the same design from aggregates derived from a range of rocks of varying density, showed an inverse relationship between concrete density and ultrasonic velocity at a given concrete age (Figure 5.16, 5.17).

5.3 Strength - density relationships in concrete

For any concrete, the ratio of compacted density achieved to density attainable is related to the resulting strength of that concrete (Neville, 1975).

Neville's statement is no less applicable to this study where each concrete had, as far as practicable, achieved maximum compaction and therefore maximum concrete density. However most of the concrete density differences, within each mix series were related to aggregate density differences (with differences of mix design and time of secondary and tertiary importance respectively), and aggregates of greater density (argillites), with lower crushing resistances, lower elastic moduli and more angular particle shapes, produced relatively dense concrete of reduced relative strength (Figures 5.18, 5.19).

Compressive strengths and ultrasonic velocities of concrete were lower for aggregate types from rocks of finer mean grain size (Figure 5.20, 5.21) although the effect is more marked in mix 1, which had slightly higher aggregate to cement ratios.

5.4 Aggregate strength as a factor of concrete strength

Ingredients of concrete are nearly always assessed in terms of concrete strengths they produce in predetermined conditions. If aggregate imparts a strength to concrete lower than proven aggregates in the same mix design, then its strength is generally lower than the nominal compressive strength of the concrete. Clearly, such aggregate is better used in concrete of lower strength.

McIntosh (1957) stated that every aggregate has a compressive strength ceiling which should become evident as concrete strength is increased. Therefore aggregate crushing resistance, a measure of the ceiling, was plotted against concrete compressive strength (Figure 5.22). Aggregate crushing resistance is also influenced by particle shape (section 4.2.5). Trends of mix 1
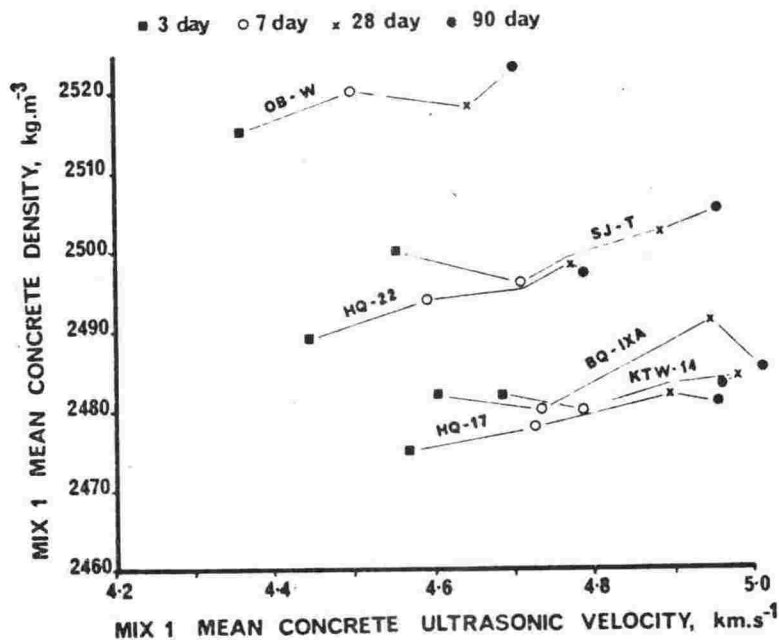
Figure 5.16 : See caption below.
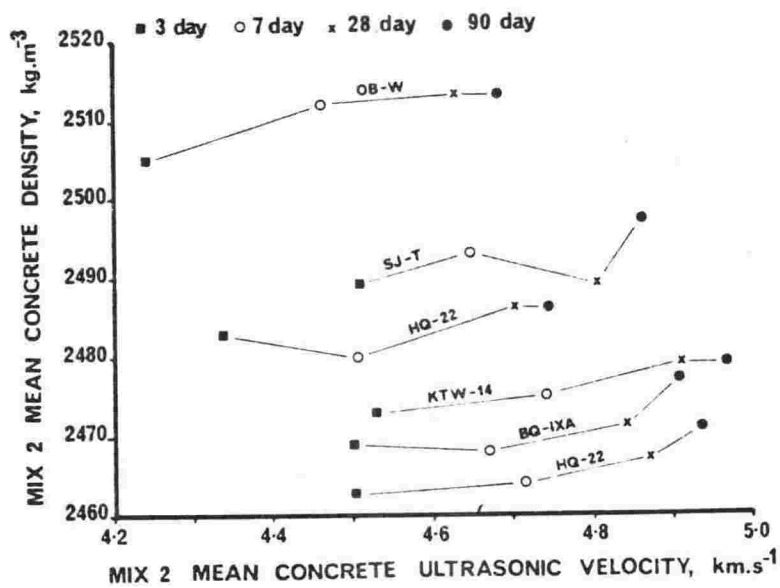
Figure 5.17 : Concrete density shows a positive relationship with ultrasonic velocity of concrete for any particular aggregate. Denser concretes produce lower ultrasonic velocities at any given concrete age, however.
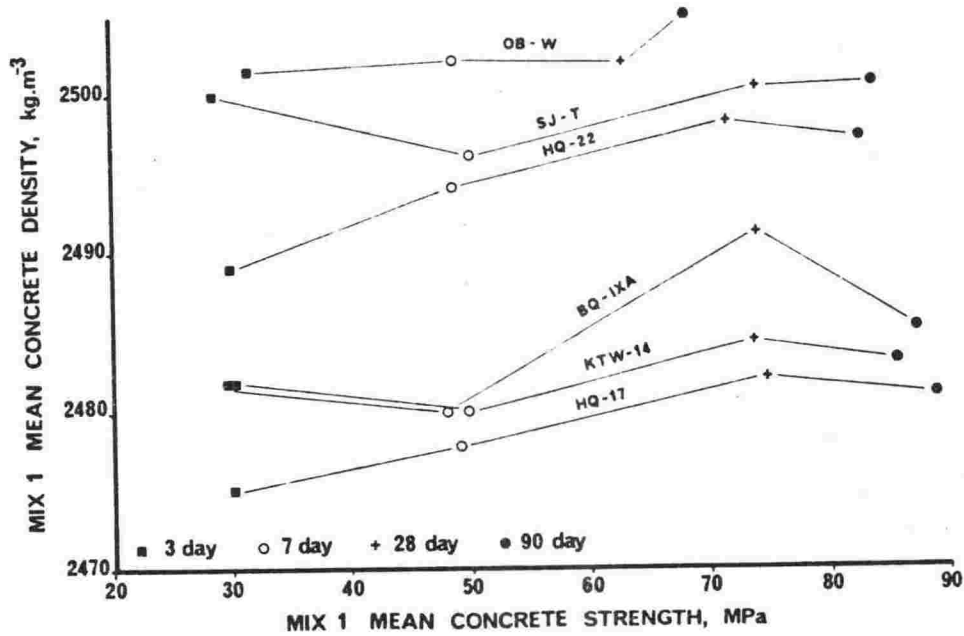
Figure 5.18 : See caption below.
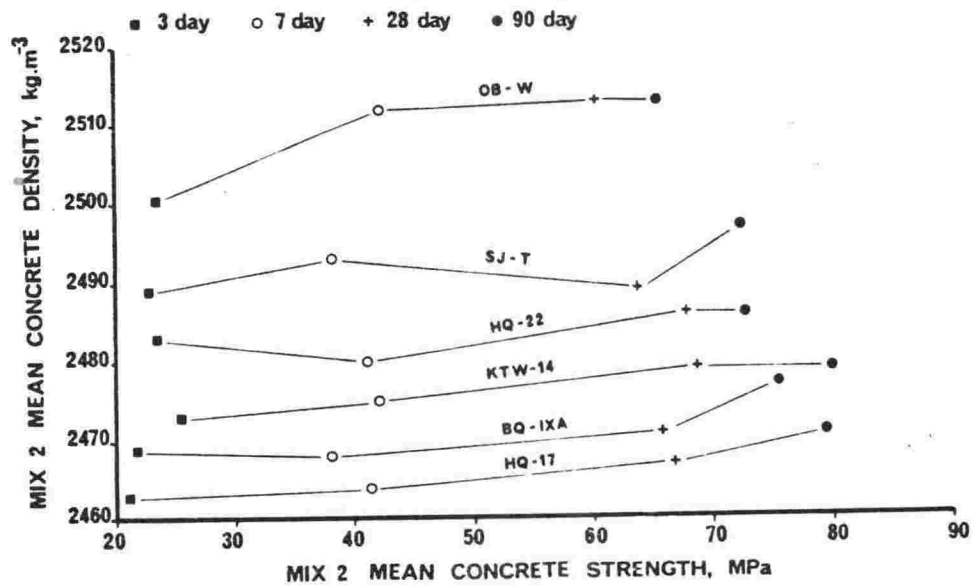
Figure 5.19 : For each aggregate type, density and strength of
concrete increases with age.   At each test age,
however, denser concretes tend to produce lower strengths due to
aggregate type.
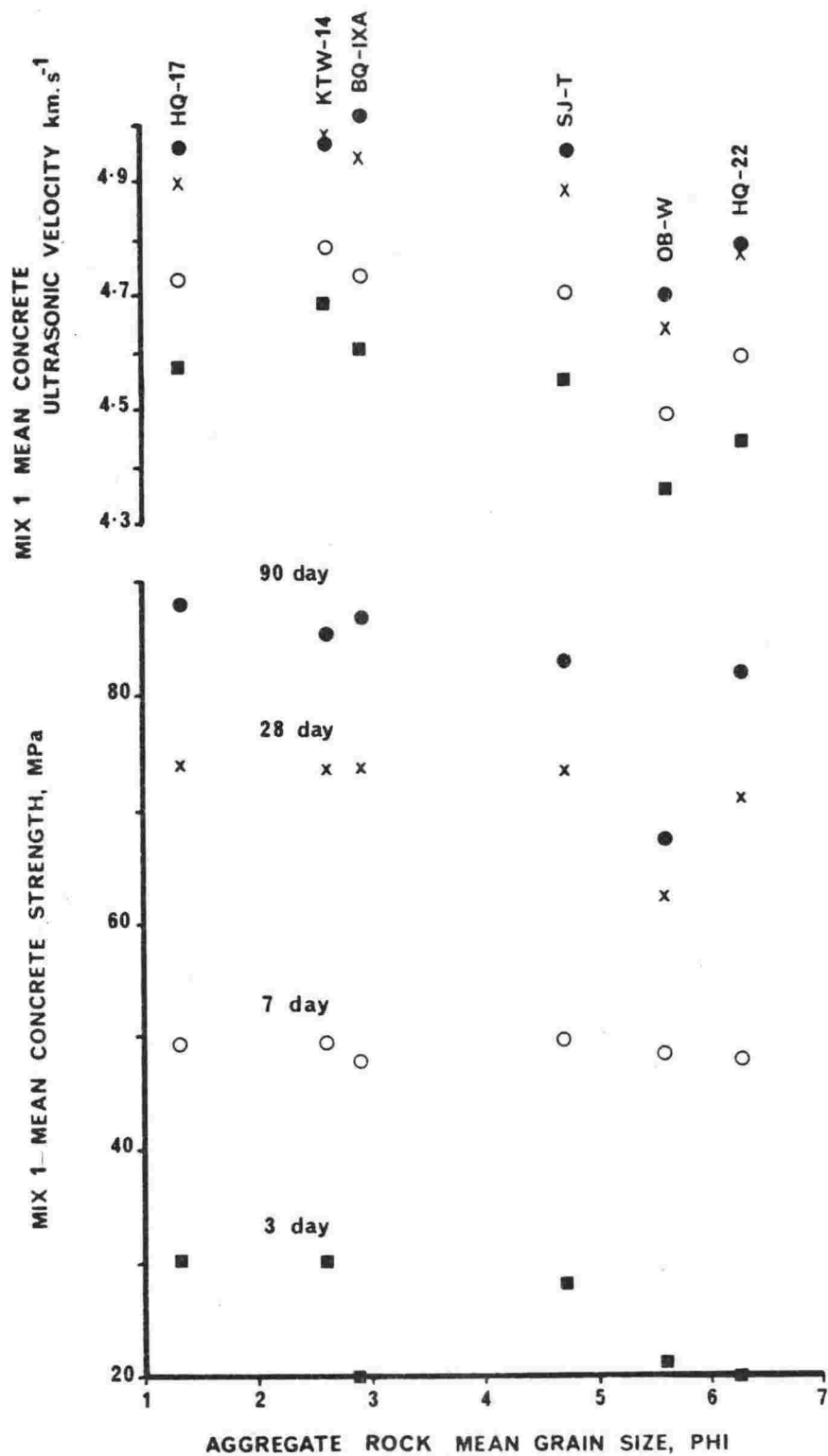
Figure 5.20 : Concrete strength and ultrasonic velocity are
reduced at all ages, in concrete of mix 1 design,
when aggregates of finer mean grain size are used.
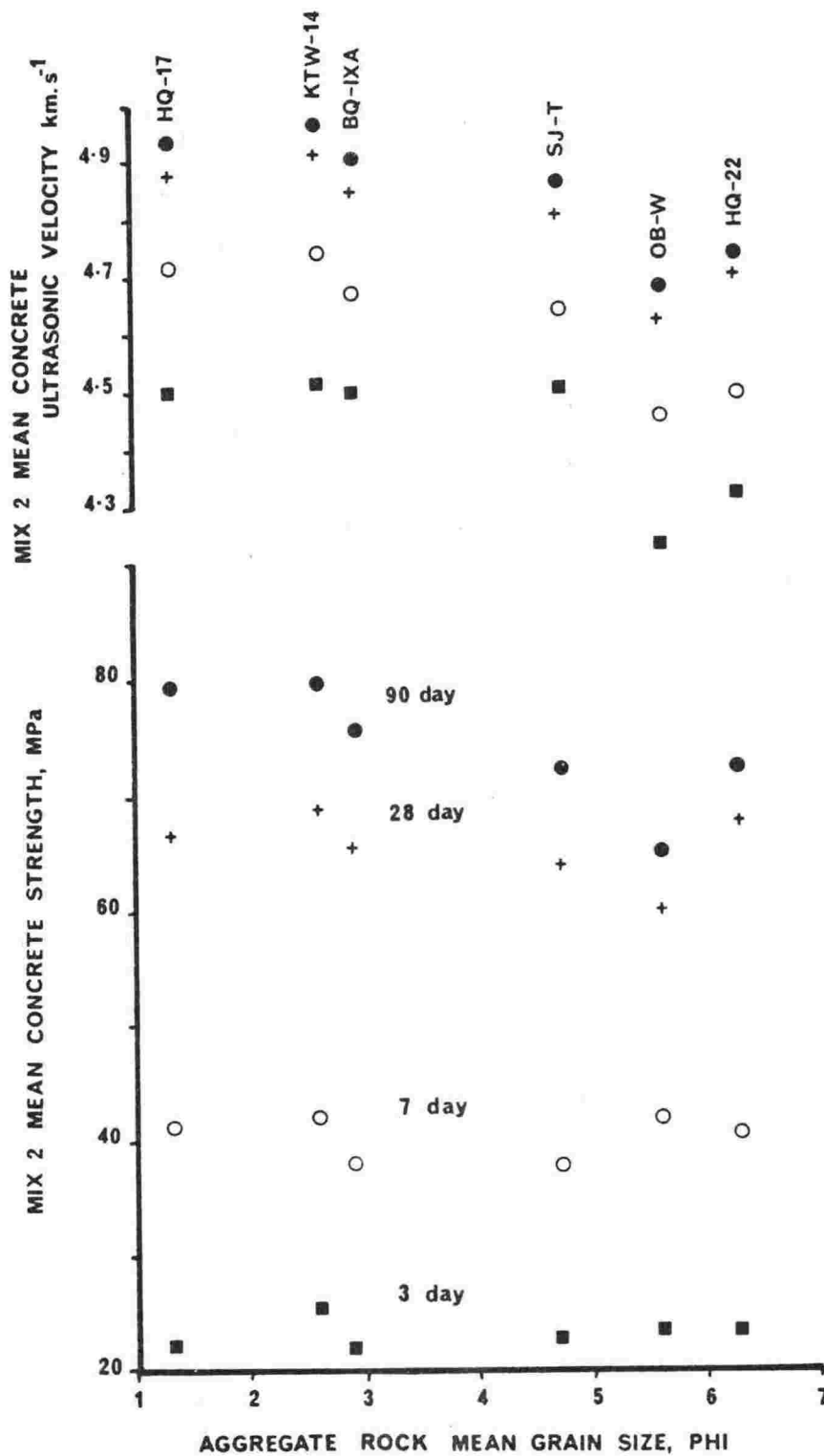
Figure 5.21 : Concrete strength and ultrasonic velocity are
reduced especially at older concrete ages, in
concrete of mix 2 design, when aggregates of finer mean grain
size are used. Compare with Figure 20.
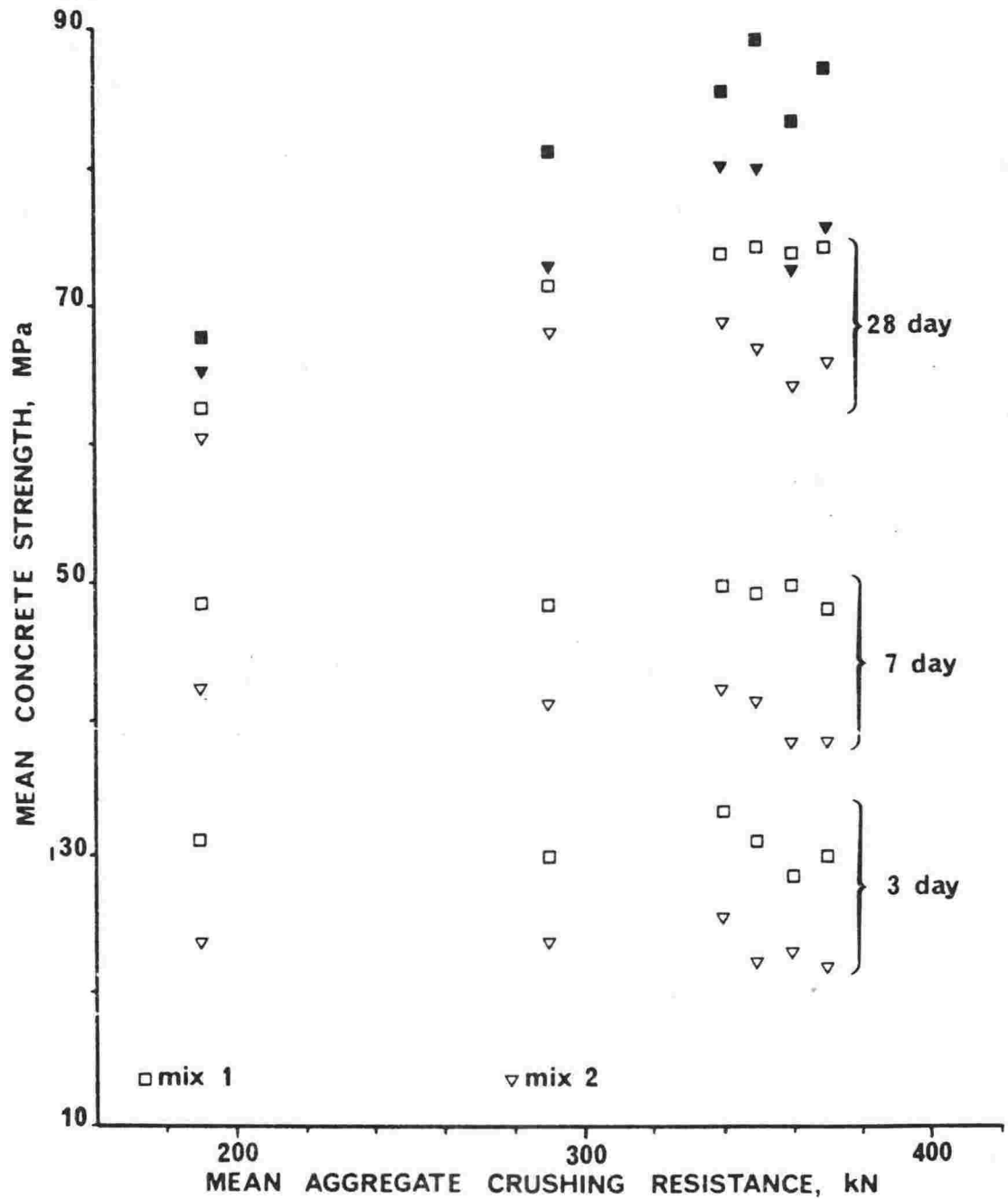
Figure 5.22 : Strength relationship between concrete and aggregate. Increase in concrete strength with increased aggregate crushing resistance is more apparent in high strength concrete (mix 1). Black symbols denote 90 day old concrete.

noticeably increased in gradient at 28 days. In mix 2 the same trend emerged but is not as pronounced.

At 90 days, trends indicate that aggregates of low crushing resistance, could possibly make even higher strength concrete. Mix 1 concretes certainly indicate that potentially higher concrete strengths are available from aggregates of high crushing resistance.

A similar conclusion is reached by relating rock core strengths to the compressive strengths of concrete made with corresponding aggregates (Figure 5.23), although the influence of particle shape is also evident.

Results suggest that there are real advantages, at least in material usage efficiency, in matching the physical characteristics of aggregates to those of the hardened sand/cement paste in the mix, which in turn is designed to meet the in-service conditions. Certainly strong concrete cannot be made with weak aggregate, nor hard (abrasion resistant) with soft aggregate, but a strong aggregate in a weak sand/cement paste may induce lower compression strength in concrete than one more closely matched to the mortar characteristics.

Practical considerations (handling, transport) dictate a minimum strength for precast concrete products but where this is not a requirement, lower preferred strengths, e.g. DZ 3109 "Concrete construction", could well be met with so called marginal aggregates provided they conform to the grading and organic impurity requirements of NZS 3111:1974. For concrete not exposed to the weather, weathering resistance of the aggregate is not important nor is cleanness if the nature of the "dirt" is known and can be accommodated by mix design.

5.4.1 Effects of aggregate angularity

Bache and Nepper Christensen (1965) noted that concrete tested in compression often displays bond failures along the underside of aggregate particles (with respect to how they have been cast), at early ages. This feature was noted during 3 day testing, particularly in concretes with highly angular aggregates. The effect has been attributed to a relative increase in the water to cement ratio localised beneath elongated or flaky particles as a result of laitance and/or entrapment of air (Plates 5.1, 5.2).

198
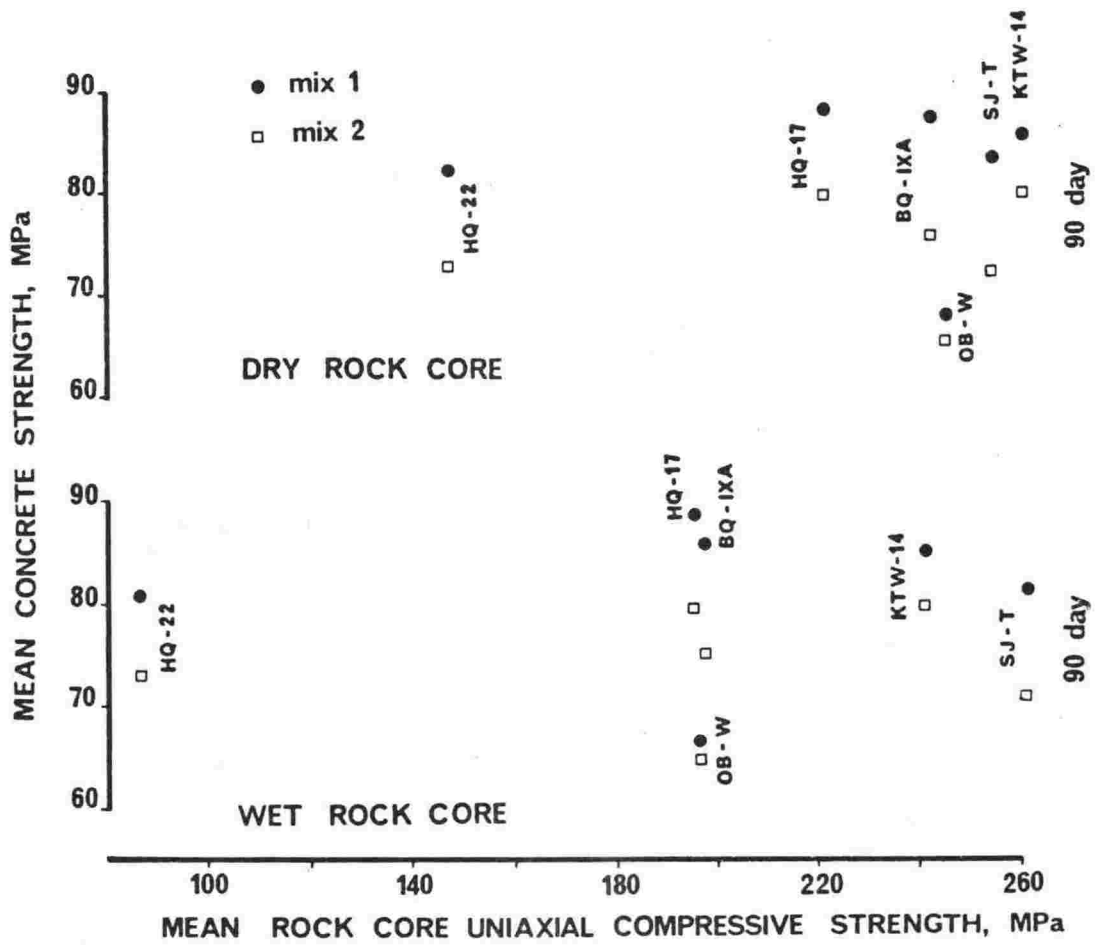
Figure 5.23 : A correlation, especially at later concrete ages,
between dry rock core compressive strength and
concrete strength is probably influenced by aggregate particle
shape.
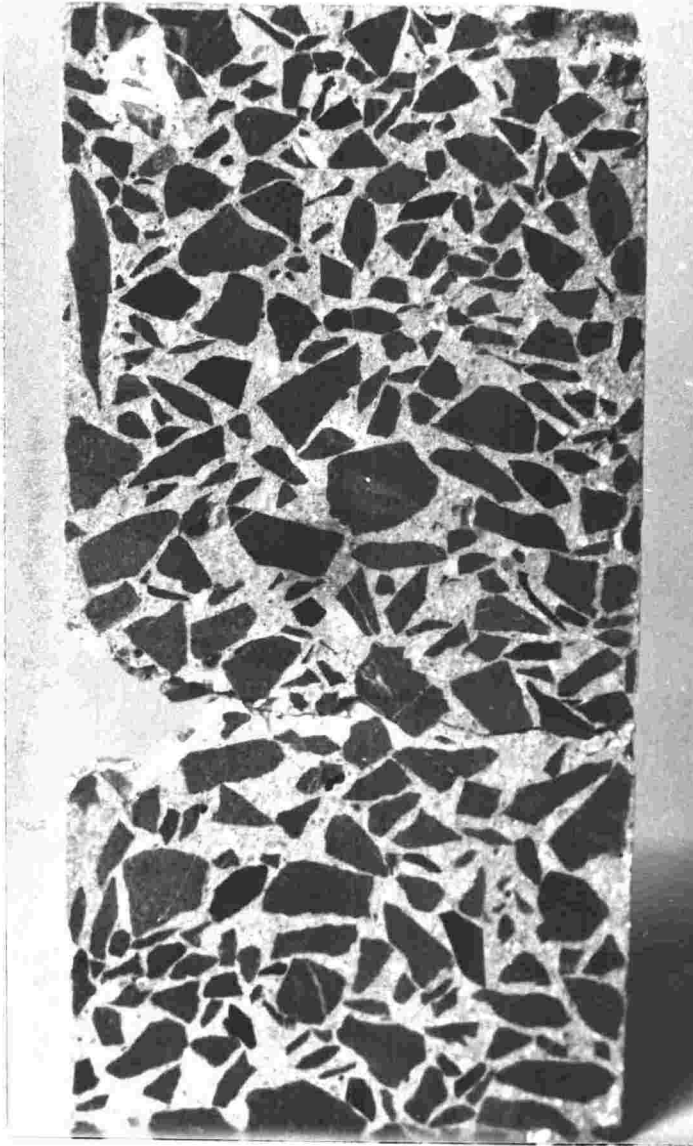
Plate 5.1 : The failure mode of BQ-1XA (mix 1) at 3 days is a
            horizontal plane, which has traversed the cylinder
about 67 mm above its base, as cast.   The plane shows integrated
bond failures at the bottom surfaces of aggregate particles.
The cylinder measures 200 x 100 mm.

Plate 5.2 : The upper and lower portions of concrete shown in Plate

5.1 are photographed here as complimentary surfaces.
Almost all the coarse aggregate particles adhere in the upper
portion of the cylinder (top section in photograph), the portion
that was uppermost during compaction of the fresh concrete.

The lower portion of the cylinder (bottom section shown) has its
fracture plane displaying numerous air voids, indicating that
segregation and local increase in water to cement ratio has
resulted in a preferred bond failure. See also Bache and
Nepper-Christensen (1965). The cylinder is 100 mm in diameter.

Figure 5.24 shows concrete strengths plotted with angularity. The very
slight increase in 3 day strength with angularity value (mix 1) suggests that
aggregate flakiness may actually increase early strength, possibly due to a
mechanically stable packing of particles, normal to the applied load, during
compaction (Plate 4.1, Appendix 17).

In high strength concrete (mix 1) at increased age, more equant grains (which
are also the mechanically stronger rock types) appear to enhance strengths.
The trend is more scattered for mix 2. More equant particles may be expected
to promote higher strengths as, for a given particle size, greatest strengths
will be provided by those with the greatest volumes displaying the mean
angularity for the aggregate as a whole.

5.5 Aggregate performance in old concrete

A search of literature has provided only one reference supporting a suggestion
"that aggregates could continue to degrade even after (the) concrete has
hardened" Corlett and De Gast (1963*) in West and Aughenbaugh (1964), and
there appear to be no reports opposing this view with the possible exception
of Kear and Hunt (1969).

Corlett and De Gast (1963) base their contention on "stress relaxation within
rock pieces" and this type of phenomenon is relevant to greywacke-suite rocks
(Appendix 25) in that desiccation and subsequent wet and dry cycling is seen
as a probable cause of microcracking in argillite. Clasts (flakes and chips)
of argillite included in greywacke (chipwackes) exposed in outcrops, display
microcracking parallel to preferred orientation within the clasts. This is
analogous to argillite particles in concrete.

A long term assessment of aggregate degradation within concrete was not pos-
sible in this study but to ascertain whether argillaceous particles known to
degrade on exposure and in roading situations did degrade in concrete, samples
of known age and from various localities, were assessed in thin sections
and slabs

---

* The original work of these authors was unobtainable.
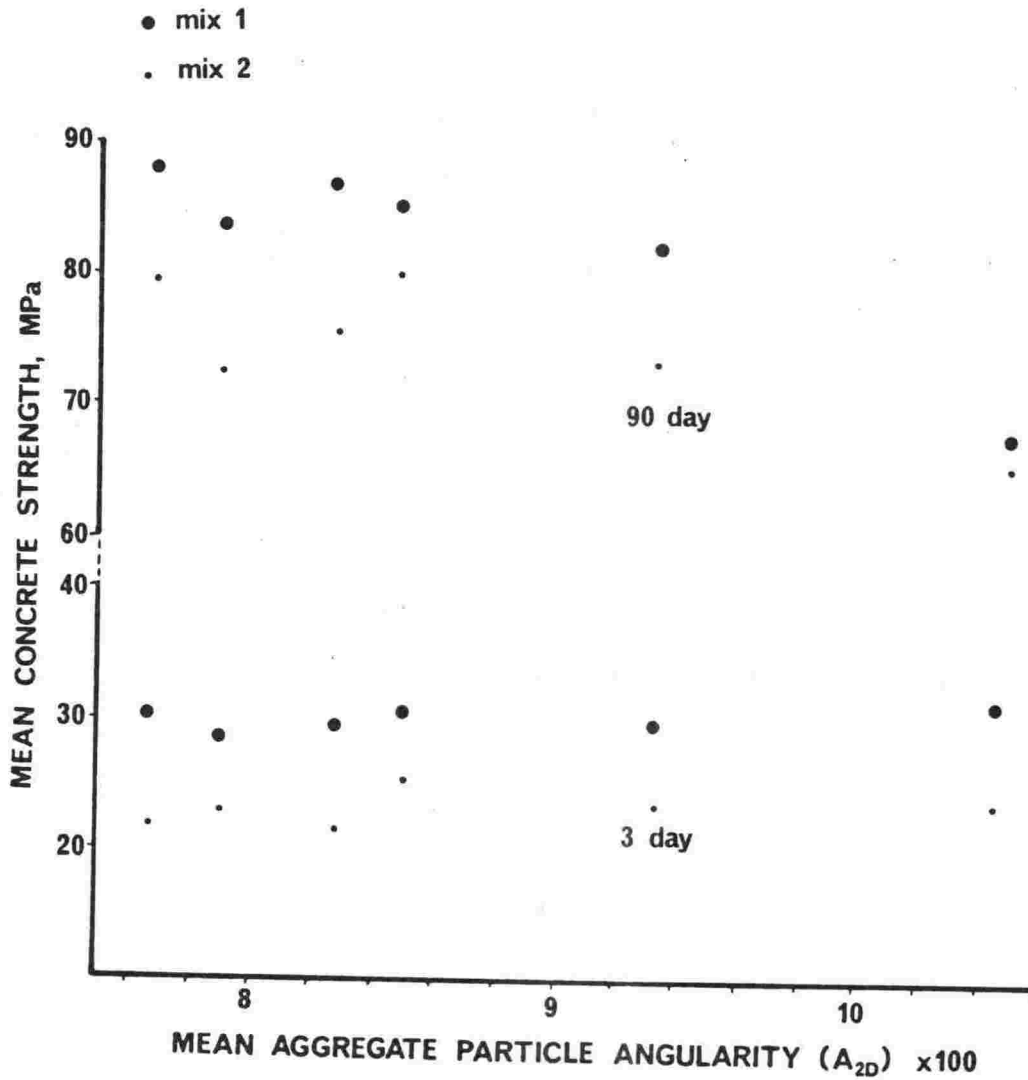
Figure 5.24 : Angularity of aggregate particles is reflected in concrete strength. The more angular particles have produced concrete of lower strength (other factors equal) for two reasons:

(i) Rock which produces angular particles tends to be argillaceous and is strongly anisotropic.

(ii) Flaky particles have high surface area to volume ratios and are therefore weaker for any given size.

The effect is not apparent at early concrete ages as failure then is almost entirely within sand/cement mortar.

Prior to 1950 most aggregate for Wellington was alluvial or beach derived, mostly free from argillite but not from weathered greywacke particles and it often contained significant amounts of shell material. Weathered particles had well rounded surfaces facilitating examination for particle/cement bond.

From the late 1950's quarried material, including argillite, was used so that argillite-bearing concrete is still relatively young in the area.

Results of the survey are shown in Table 5.5. One sample taken from a demolition site showed some argillite microcracking which may have been caused by degradation in the concrete but possibly by desiccation and weathering after exposure resulting from demolition or even induced by the demolition process. The latter cause would seem unlikely when compared with cracking induced by uniaxial compression testing. Here the cracks in argillite particles could generally be traced through the cement paste as well, and were generally wider than microcracks induced by desiccation.

Shrinking aggregates in concrete have been shown (Roper *et al.*, 1964) to have a crack pattern mainly concentric about, and at the particle/cement paste interface, i.e. a bond failure, but degradation is unlikely if the particle is wholly within the concrete because:

(i) Potential argillite volume change is significant (0.2 percent, Appendix 20) but if desiccation occurred it would be very slow because of low permeability.

(ii) Argillite clasts in chipwackes are as fresh as the surrounding greywacke until they are exposed at the surface, at which time microcracks within argillite do not extend into the greywacke fabric.

This survey is inconclusive but desiccation of argillite in concrete, if it occurs at all, must be slow, otherwise bond strength would exceed the lowest tensile strength of the argillite particle since argillite is grossly anisotropic (Appendix 7) and any strain consequent to volume reduction is relieved by microcracking within that particle.

Microcracking could be minimised by confining argillite particles to a maximum nominal particle size of less than, say, 10 mm or accepting a relatively large surface area to volume ratio, say, 6:1 for argillite particles in concrete aggregate (Appendix 25). The latter choice would cause low workabilities in in fresh concretes.

Table 5.5 : Summary of survey on aggregate performance in old concrete.

Concrete source	Age of concrete	Brief description of concrete	Remarks
Tinakori Gun Emplacements, Tinakori Hill, 255 m (837 ft.)	37 years	Most coarse and fine aggregate weathered. Aggregate rounded. Argillite in finer aggregate population. Concrete appeared of good quality.	Some dark rims about weathered greywacke material. This material appears less porous at particle/cement paste interface than elsewhere in particle. No detectable degradation of any material.
Karori Cemetery, Karori Road.	60 years	Very lean, highly porous and permeable concrete. Rounded aggregate. Most particles fresh, very little argillite. Concrete surface weathered at least 1 mm.	No visible signs of aggregate degradation.
Inland Revenue Building, Cnr. Manners St. and Taranaki St.	No date, confirmed at least 44 years	Approximately 40 percent of coarse aggregate weathered. Coarse aggregate is rounded to angular. Limited argillite.	Building extensively cracked in earthquake of November, 1968. No degradation of argillite. Darkened rim about some weathered particles.
Old house foundation, 18A St Michael's Cres., Kelburn.	No construction date available, at least 30 years	Rounded aggregate, approximately 10 percent of coarse aggregate weathered. Negligible argillite.	Weathered particles possess dark rim only if relatively coarse or medium grained. Fine grained greywackes and argillites not affected.
Old Pearse House, Cnr. Sturdee St. and Dixon St.	35 years	Angular, flakey, coarse aggregate. Concrete appeared rich. Argillite and weathered particles both approximately 20 percent by volume of total aggregate.	Dark rim occurring in some weathered material. Some larger fresh argillite particles (larger than 9 mm) microcracked.
Cnr. Farish St. and Manners St. Building had no particular name.	73 years	Angular and rounded coarse and fine aggregate. Coarse aggregate mostly incipiently weathered. Very few argillite particles. Relatively lean, unworkable concrete - voids adjacent to aggregate boundaries.	Weathered particles show dark rims if relatively coarse grained.
Concrete retaining wall, 21 Wilton Rd., Wilton.	25 years	Rounded aggregate, porous and honeycombed concrete, sampled with diamond drill. Little argillite but 30 percent aggregate weathered. Builder acknowledges a dry mix was used.	Weathered particles show dark rims if relatively coarse grained.

The occurrence of dark rim material in some weathered greywacke particles (Table 5.5) is unusual and difficult to interpret (Mather, 1973). Thin sections of concrete from the Inland Revenue Building, 18A St Michael's Crescent, and 21 Wilton Road all showed little resolution of the dark rim surrounding weathered aggregate particles. Because the rim appears to be merely a colour contrast and is seen in rocks with relatively large mean grain sizes, it is probably due to an absorption of cement paste material (perhaps the lime diffusion front of Stocker, 1972), changing the colour of intergranular materials of aggregate particles to a depth of up to 0.6 mm from their interface with cement paste and extending along recemented shears locally to 1.2 mm. Penetration may depend on relative water contents of cement paste and aggregate particles.

Several thin sections showed microcracks about the interface of weathered aggregate and cement paste, some, the result of thin section preparation but others, clearly a feature of the concrete. The cracking around particles is consistent with shrinking aggregates and probably resulted from the high moisture content of weathered greywacke-suite particles.

Reaction products observed in the concretes examined, all appeared innocuous and it is probable that if argillite does microcrack in concrete the process may be reduced or eliminated by careful aggregate production to a finer maximum nominal size grading, which, due to the nature of the material, should be a relatively easy and low cost undertaking.

CHAPTER SIX

Summary, conclusions and future work

A wide range of properties of Wellington greywacke-suite rocks, unprocessed, as aggregate, and in concrete (2 mix designs), were measured to find out how closely concrete properties could be related to rock properties. A summary of properties of typical samples, along with those of aggregates and concrete from them, is presented in Table 6.1. In addition, other specific problems, e.g. aggregate degradation and alkali-silicate reactivity, were investigated.

6.1   Principle conclusions from this study.

(i)   The Wellington greywacke-suite rocks comprise two rock types, greywacke and argillite, which have separate and distinctive mineralogies and chemistries. The fundamental basis for distinction is grain size, argillites having a mean grain size finer than 5 phi (0.031 mm). There is no significant difference in mineralogy or chemistry in greywacke in each of the three lithofacies. Argillite also shows no difference.

(ii)   The crushing strength of aggregate from Wellington greywacke-suite rocks is related to the uniaxial compression strength of its parent rock, and determines to some degree the resulting strength of concrete in which it is used.

(iii)   Greywacke-suite aggregates produce concrete which are, for the most part, unaffected by alkali-silicate reactions. Laumontite is present locally but does not react because of its habit.

(iv)   Discontinuity spacing indicates that the thin-bedded lithofacies may be easier to win and process than other lithofacies but would create more waste.

(v)   A test for degradation potential of greywacke-suite rocks, based on destruction of chlorite by hydrochloric acid, has been successfully devised.

TABLE 6.1 : A summary of results for typical greywacke-suite rocks from the Wellington region. Values listed are averages for samples tested dry.
* denotes parameters measured from cores.

Sample	HQ-17	SJ-3$_1$	KTW-14	BQ-V	BQ-IXA	KS-2	KTW-i	SJ-T	OB-W	HQ-22
Rock type	gwke.	gwke.	gwke.	gwke.	gwke.	gwke.	gwke.	gwke.	argill.	argill.
Lithofacies	thick	thick	sstn.	sstn.	sstn.	sstn.	thin	thin	thick	thick
Rock mean grain size, phi	1.317	1.32	2.6	2.7	2.9	3.3	4.2	4.7	5.6	6.3
Phyllosilicate content, percent										
Hardness	hard	hard	hard	hard	hard	hard	hard	hard	soft	soft
Ultrasonic velocity km.s^{-1}*	5.230	5.251	5.368	–	5.424	4.878	5.399	5.524	5.084	5.107
Uniaxial compressive strength, MPa*	221	234	260	263	262	243	324	254	245	147
Static elactic modulus, E_t, GPa*	66.6	73.7	82.6	63.0	68.3	56.3	64.3	72.7	51.6	68.4
Dry density, kg.m^{-3}*	2650	2670	2670	2660	2670	2630	2670	2700	2710	2690
Effective porosity, percent*	0.28	0.27	0.29	–	0.34	0.48	0.29	0.30	0.38	0.51
Rock stability value, percent	6.1	6.6	6.5	7.1	5.4	7.2	3.9	8.8	11.3	11.9
Angularity, A_{2D}	768	–	850	–	829	–	–	789	1045	933
Crushing resistance, kN	350	–	340	–	370	–	–	360	190	290
Los Angeles abrasion, percent wear	12	–	11	–	11	–	–	11	19	15
Density, kg.m^{-3}	2647	–	2660	–	2658	–	–	2691	2713	2671
Absorption, percent	0.56	–	0.47	–	0.48	–	–	0.56	0.96	0.87
Compacted bulk density, kg.m^{-3}	1499	–	1513	–	1496	–	–	1518	1435	1473
Voids content, percent	43.4	–	43.1	–	43.7	–	–	43.6	47.1	44.9
V-B, seconds	23.9	–	26.6	–	29.7	–	–	22.1	50.9	34.1
Compaction factor	0.77	–	0.71	–	0.69	–	–	0.75	0.66	0.69
Fresh concrete density, kg.m^{-3}	2502	–	2494	–	2509	–	–	2501	2543	2504
28 day mean density, kg.m^{-3}	2482	–	2484	–	2491	–	–	2502	2518	2498
28 day mean strength, MPa	74.4	–	73.9	–	74.0	–	–	73.8	62.7	71.3
28 day mean ultrasonic velocity, km.s^{-1}	4.896	–	4.979	–	4.946	–	–	4.883	4.641	4.771
28 day mean static elastic modulus (E_s), GPa	55.2	–	76.6	–	54.5	–	–	48.6	37.7	69.2

Row group labels (left margin): ROCK PROPERTIES; AGGREGATE PROPERTIES 19mm-9.5mm; CONCRETE PROPERTIES MIX 1

(vi)   Greywacke aggregates will, with confidence, produce concrete to meet not only the strength requirements of common commercially viable mixes, but also the special requirements of very high strength concrete.

Argillite aggregates, which on average are more angular, produce concretes that are harder to work and, when compacted, particles tend to align.   Use of argillites also results in lower maximum strength concrete and it should not be used where low strength concretes will be subjected to great ranges in moisture content, temperature, or where abrasion resistance is necessary.   In particular, argillite aggregates should not be used as exposed aggregate unless protected against wetting and drying.   Nevertheless, there are still many concretes in which argillite can be safely used.

6.2   Future work

The following are pure and applied geological research topics which require further work to allow proper understanding of the processes involved.

(i)   A study of greywacke weathering rates and changes.   The study would involve researching techniques for better studies of internal surface areas of fresh and weathering rocks.   An application of this work to the aggregate industry could show whether rocks, now considered waste materials or over-burden, could be safely utilised in concrete, or in bound granular form.

(ii)   Argillite tends to degrade after being won because of its geological and physical properties.   Optimum gradings for argillaceous rock types should be measured and uses for the argillaceous fines, even considering quarry sludges, whould be found to minimise wastage in the aggregate industry.

R E F E R E N C E S

PARKINSONS SIXTH LAW:

The progress of science varies inversely
with the number of journals published.

ADAMS, J.E. (1974) Empirical determination of sieve size statistics from grain measure-
        ment. Unpub. M.Sc. thesis, Geology Dept., Victoria University of Wellington:
        155 pp.

ALEXANDER, K.M. (1963) A study of concrete strength and mode of fracture in terms of
        matrix, bond and aggregate strengths. *Tewksbury Symp. on Fracture, University of*
        Melbourne: 25 pp.

ARCHIE, G.E. (1950) Introduction to petrophysics of reservoir rocks. *Bull. Am. Assoc.*
        Petrol. Geologists, V. 34: 943-61.

ATTEWELL, P.B. and FARMER, I.W. (1976) "Principles of engineering geology". Chapman and
        Hall, London: 1045 pp.

BACHE, H.H. and NEPPER-CHRISTENSEN, P. (1965) Observations on strength and fracture in
        lightweight and ordinary concrete. *In* "The Structure of Concrete and its
        behaviour under load". *Conf. Proc., Session B;* (Eds.) Brooks, A.E. and Newman, K;
        C. and C.A.: 93-108.

BADGER, C.W., CUMMINGS, A.D. and WHITMORE, R.L. (1956) The disintegration of shales in
        water. *Jl. Instit. Fuel. V. 29:* 417-23.

BAILEY, E.H. and STEVENS, R.E. (1960) Selective staining of K-feldspar and plagioclase
        on rock slabs and thin sections. *Am. Min., V. 45:* 1020-5.

BARNES, C.J. (1979) Structure and petrography of Rimutaka greywackes and associated
        rocks. Unpub. B.Sc. (Hons.) thesis, Geology Dept., Victoria University of
        Wellington: 59 pp.

BAROID DRILLING MUD DATA BOOK (1954) Estimation of cation exchange capacity of clays.
        Section 900: 44-5.

BARRETT, P.J. (1980) The shape of rock particles, a critical review. *Sed., V. 27:*
        291-303.

BARTON, D.C. (1916) Notes on the disintegration of granite in Egypt. *Jl. Geol., V. 24:*
        382-93.

BASU, A., YOUNG, S.W., SUTTNER, L.J., JAMES, W.C. and MACK, G.H. (1975) Re-evaluation
        of the use of undulatory extinction and polycrystallinity in detrital quartz for
        provenance interpretation. *Jl. Sed. Pet., V. 45(4):* 873-82.

BELIKOV, B.P. (1967) Plastic constants of rock forming minerals and their effect on the
        elasticity of rocks. *In* Zalesskii, B.V. (Ed.) "Physical and Mechanical Proper-
        ties of Rocks". *The Israel Prog. for Scientific Trans:* 124-40.

BENCE, A.E. and ALBEE, A.L. (1968) Empirical correction factors for the electron microanalysis of silicates and oxides. *Jl. Geol. V. 76:* 382-403.

BIENIAWSKI, Z.T. (1975b) The point-load test in geotechnical practice. *Eng. Geol. V. 9:* 1-11.

BLACKWELDER, E. (1925) Exfoliation as a phase of rock weathering. *J. Geol. V. 33:* 793-806.

BLATT, H. (1967) Original characters of clastic quartz. *Jl. Sed. Pet. V. 37:* 401-24.

_____ and CHRISTIE, J.M. (1963) Undulatory extinction in quartz of igneous and meta-morphic rocks and its significance in provenance studies of sedimentary rocks. *Jl. Sed. Pet. V. 33:* 559-79.

_____, MIDDLETON, G. and MURRY, R. (1972) "Origin of sedimentary rocks". Prentice-Hall. 634 pp.

BOGUSLAVSKIY, M. Ye. (1976) Effects of crystal structure characteristics of mineral formations on anistropy of the speed of ultrasonic waves. *Internat. Geol. Rev. V. 18(6):* 729-33.

BOGGS, S. (1968) Experimental study of rock fragments. *Jl. Sed. Pet. V. 38(4):* 1326-39.

BOULT, B.F. (1979) Thermal properties of concrete. New Zealand Concrete Research Association, GLR 15: 27 pp.

BOUMA, A.H. (1962) "Sedimentology of some flysch deposits". Elsevier Publishing Co., Amsterdam: 168 pp.

BRACE, W.F. (1961) Dependence of fracture strength of rocks on grain size. *In 4th Symp. on Rock Mechanics; Pennsylvania State University:* 99-103.

_____. (1965) Some new measurements of linear compressibility of rocks. *Jl. Geophys. Res., V. 70(2):* 391-8.

BREWER, R. (1964) "Fabric and mineral analysis of soils". John Wiley and Sons, New York: 470 pp.

BRODIE, J.W. (1953) Stratigraphy and structure of the greywackes and argillites on the South Coast of Wellington Peninsula. *N.Z. Jl. of Sci. and Tech., B. 34(4):* 205-26.

BRYANT, J.M. (1977) Some properties of Kaimanawa greywacke. M.W.D. N.Z. C. Lab. Report No. 2-77/1: 20 pp.

BUCKE, D.P. and MANKIN, C.J. (1971) Clay-mineral diagenesis within interlaminated shales and sandstones. *J. Sed. Pet., V. 41 (4):* 971-81.

BUCKLAND, A.H. (1967) The degradation of roading aggregate. *Proc. Roading Symp., Road Res. Unit, N.Z. Nat. Roads Board, V. 2:* 692-715.

BURST, J.F. (1959) Postdiagenetic clay mineral environmental relationships in the Gulf Coast Eocene. *In* "Clays and Clay Minerals" *Proc. 6th. Nat. Conf. on Clays and Minerals:* 327-41; A. Swineford (Ed.): 411 pp.

CARROLL, D. (1970) Clay minerals: A guide to their X-ray identification. *Geol Soc. Am. Special Paper 126:* 80 pp.

CHAYES, F. (1956) "Petrographic modal analysis". Wiley, New York: 113 pp.

CLARK, B.R. (1970) Mechanical formation of preferred orientation in clays. *Am. Jl. Sci.,* V. 269: 250-66.

CLARK, S.P. (Ed.) (1966) Handbook of physical constants. *Geol. Soc. Am. Memoir 97:* 587 pp.

CLELLAND, J. (1967) An artificial weathering test for roading aggregates. *Proc. Roading Symp. 1967. Road Res. Unit, N.Z. Nat. Roads Board,* V. 2: 743-58.

_____. (1971) Russell Road quarry material. Gyratory compactor tests. M.W.D., Central Laboratories, Gracefield, Report No. 400: 20 pp.

COLBACK, P.S.B. and WIID, B.L. (1965) The influence of moisture content on the compressive strength of rocks. *Proc. 3rd Can. Rock. Mech. Symp., Toronto:* 65-83.

COOMBS, D.S. (1952) Cell size, optical properties and chemical composition of Laumontite and Leonhardite. With a note on regional occurrences in New Zealand. *Am. Min.,* V. 37: 812-30.

CORLETT A.V. and DeGAST, A.A. (1963) A study of properties of Kingston limestone deleterious in concrete. Paper presented at the 1963 Annual General Meeting of the Engineering Institute of Canada.

CORNWELL, W.L. (1966) Assessment of basecourse aggregate quality, Auckland-Hamilton motorway. M.W.D. Internal Report: 9 pp.

CRANNEY, P. (1979) Structure and sedimentology of Lower Mesozoic rocks at Titahi Bay. Unpub. B.Sc. (Hons.) thesis, Geology Dept., Victoria University of Wellington: 41 pp.

CROOK, K.A.W. (1974) Lithogenesis and geotectonics: the significance of compositional variation in flych arenites (greywackes). *Soc. Econ. Pal. Min. Special Pub. No. 19:* 304-10.

CURTIS, B.F. (1971) Measurement of porosity and permeability. *In* Carver, R.E. (Ed.) "Procedures in sedimentary petrology". Wiley and Sons, New York: 335-65.

DEER, W.A., HOWIE, R.A. and ZUSSMAN, J. (1971) "An introduction to the rock-forming minerals". Longmans, London: 528 pp.

DEERE, D.U. (1964) Technical description of rock cores for engineering purposes. *Rock Mech. and Engng. Geol.,* V. 1: 17-22.

_____ and MILLER, R.P. (1966) Engineering classification and index properties for intact rock. Air Force Weapons Laboratory Research and Technology Div; Tech. Report No. AWFL-TR-65-116, Kirtland Air Force Base, New Mexico: 300 pp.

_____, MERRITT, A.H. and COON, R.F. (1969) Engineering classification of in-situ rock. Air Force Weapons Laboratory Research and Technology Division; Tech. Report No. AFWL-TR-67-144, Kirtland Air Force Base, New Mexico: 272 pp.

DEKKER, B. and SCOTT, K.O. (1969) Some aspects of aggregate supply for North Island Power Stations. *Proc. Nat. Conf. Concrete Aggregates, Hamilton, N.Z.:* 26-34.

De PUY, G.W. (1965) Petrographic investigations of rock durability and comparisons of various test procedures. *Bull. Ass. Engng. Geologists, V. 2(2):* 31-46.

DICKINSON, W.R. (1970) Interpreting detrital modes of greywacke and arkose. *Jl. Sed. Pet., V. 39:* 1243-55.

DUNCAN, M.A.G., SWENSON, E.G., GILLOTT, J.E. and FORAN, M.R. (1973) Alkali-aggregate reation in Nova Scotia. *Cement and Concret Res. V. 3(1,2,3,5) Parts 1,2,3 and 4:* 55-69, 119-28, 233-45, 521-35.

DUNCAN, N. (1969) "Engineering geology and rock mechanics". Vol. 1. Leonard Hill, London: 252 pp.

EKSE, M. and MORRIS, M.C. (1959) A test for production of plastic fines in the process of degradation of mineral aggregates. *ASTM Spec. Tech. Pub. No. 277:* 122-6.

FAIRBURN, P.E. and ROBERTSON, R.H.S. (1957) Liquid limit and dye absorption. *Clay Minerals Bull., V. 3(17):* 129-36.

FLAWN, P.T. (1953) Petrographic classification of argillaceous sedimentary and low-grade metamorphic rocks in subsurface. *Bull. Ass. Am. Petrol. Geol., V. 37:* 560-5.

_____, GOLDSTEIN, A., KING, P.B. and WEAVER, C.E. (1961) The Ouichita system. *Pub. Texas Bur. Econ. Geol., University of Texas Pub. 6120:* 401 pp.

FOLK, R.L. (1968) "Petrology of sedimentary Rocks". Hemphill's, Texas: 170 pp.

_____, ANDREWS, P.B. and LEWIS, D.W. (1970) Detrital sedimentary rock calssification and nomenclature for use in New Zealand. *N.Z. Jl. Geol. Geophys. V. 13(4):* 937-68.

FRIEDMAN, M. (1966) Description of rocks and rock masses with a view to their physical and mechanical behaviour. *Theme 2; Proc. Int. Cong. Rock Mech., 1st., V. 3, Lisbon.*

GAMBLE, J.C. (1971) Durability-plasticity classification of shales and other argillaceous rocks. Unpub. PhD. thesis, University of Illinois at Urbana-Champaign: 161 pp.

GEOLOGICAL SOC. ENGINEERING GROUP WORKING PARTY (1977) The description of rock masses for engineering purposes. *Quat. Jl. Engng. Geol., V. 10:* 355-88.

GILLOTT, J.E. (1975) Alkali-aggregate reactions in concrete. *Eng. Geol. V. 9:* 303-26.

GIPSON, M. (1965) Application of the electron microscope to the study of particle orientation and fissility in shale. *Jl. Sed. Pet., V. 35(2):* 408-14.

GLOVER, J.E. (1964) The universal stage in studies of diagenetic textures. *Jl. Sed. Pet., V. 34(4):* 851-4.

GOLDICH, S.S. (1938) A study in rock-weathering. *Jl. Geol., V. 46:* 17-58.

GOONEWARDANE, K. (1977) Behaviour of aggregate in the Washington degradation test. *Jl. Testing and Evaluation, V. 5(1):* 16-25.

GRAMBERG, J. (1962) Rock mechanics. The axial cleavage fracture in brittle materials at compressive loading. Technological University Delft, The Netherlands; Report No. 1.07: 36 pp.

_____ (1965) Axial cleavage fracturing, a significant process in mining and geology. *Eng. Geol., V. 1(1):* 31-72.

GRANT-TAYLOR, T.L. (1976) Aggregates from quarries in the Wellington region. N.Z. Geological Survey unpublished report, M 52: 75 pp.

_____, ADAMS, R.D., HATHERTON, T., MILNE, J.D.G., NORTHEY, R.D. and STEPHENSON, W.R. (1974) Microzoning for earthquake effects in Wellington, New Zealand. *N.Z. DSIR, Bull. 213:* 62 pp.

GRATTAN-BELLEW, P.E., SEREDA, P.J. and DOLAR-MANTUANI, L.M.M. (1978) The aggregate shortage and high alkalai cement in a changing energy situation. *Can. Jl. Eng., V. 5(2):* 250-61.

GRIGGS, D.T. and HANDIN, J. (1960) Observations on fracture and hypothesis of earthquakes. *In* Rock Deformation , *Geol. Soc. Am. Mem. 79:* 347-64.

GRIGGS, P.T. (1936) The factor of fatigue in rock exfoliation. *Jl. Geol., V. 44(7):* 783-96.

HANDIN, J. (1966) Strength and ductility. *In* Clark, S.P. (Ed.). Handbook of physical constants; *Geol. Soc. Am. Mem. 97:* 224-89.

HANSEN, W.C. (1963) Anhydrous and organic materials as sources of distress in concrete. Properties of concrete, Highway Research Record No. 43, Highway Research Board: 1-7.

_____ (1966) Chemical Reactions of concrete aggregates. Concrete and concrete-making materials, ASTM. STP 169A: 487-96.

HARDING, T.P. (1974) Petroleum traps associated with wrench faults. *Am. Ass. Pet. Geol. Bull., V. 58(7):* 1290-304.

HATHERTON, T. and LEOPARD, A.E. (1964). The densities of New Zealand rocks. *N.Z. Jl. Geol. Geophys., V. 7(3):* 605-25.

HAWKES, I. and MELLOR, M. (1970) Uniaxial testing in rock mechanics laboratories. *Eng. Geol., V. 4(3):* 177-285.

HAYES, J.R. and KLUGMAN, M.A. (1959) Feldspar staining methods. *Jl. Sed. Pet., V. 29:* 227-32.

HEDBERG, H.D. (1936) Gravitational compaction of clays and shales. *Am. Jl. Sci., V. 31:* 241-87.

HEIDECKER, E. (1968) Rock Pressures induced by weathering and physiocochemical processes. *Proc. Aust. Instit. Mining and Metallurgy, V. 226(1):* 43-5.

HEIER, K.S. and ADAMS, J.A.S. (1964) The geochemistry of the alkali metals: 253-382. *In* Ahrens, L.H., Press, F. and Runcorn, S.K. (Eds.): "Physics and Chemistry of the Earth" V. 5. McMillan, New York.

HEY, M.H. (1954) A new review of the chlorites. *Min. Mag., V. 30:* 277-92.

HILLS, E.S. (1963) "Elements of structural geology". Methuen, London: 483 pp.

HOBBS, D.W. (1963) A simple method for assessing the uniaxial compressive strength of
    rock. *Int. Jl. Rock Mech. Min. Sci.*, V. 1: 5-15.

HOGAN, J.A. (1979) Stratigraphy and sedimentology of the Kapuni formation Taranaki, New
    Zealand. Unpub. MSc. thesis, Geology Dept., Victoria University of Wellington:
    189 pp.

HOWIE, J.A. (1910) "The geology of building stones". Edward Arnold, London: 455 pp.

HUGHES, B.P. (1966) A laboratory test for determining the angularity of aggregate.
    Magazine of Concrete Res., V. 18(56): 147-52.

HURLBUT, C.S. (1971) "Dana's manual of mineralogy". 18th Ed., J. Wiley and Sons, New
    York : 579 pp.

HUTTON, C.A. (1945) The problem of reaction between aggregate materials and high
    alkali cements. *N.Z. Jl. Sci. Tech.*, V. 266(4): 191-200.

IDE, J.M. (1936) Comparison of statically and dynamically determined Young's modulus of
    rocks. *Proc. Nat. Acad. Sci.*, V. 22(2): 81-92.

INGRAM, R.L. (1953) Fissility of mudrocks. *Bull. Geol. Soc. Am.*, V. 64: 869-78.

INOMATA, M. and TATEYAMA, H. (1974) Titano-penninite from the phlogopite-bearing
    ultramafic rocks in the Ufu-san ultramafic body, the Mikabu zone, Central Japan.
    Jl. Japan Assoc. Min. Pet. Econ. Geol., V. 69(9): 332-7.

JAEGER, C. (1972) "Rock Mechanics and Engineering".Cambridge University Press: 417 pp.

JAEGER, J.C. and COOK, N.G.W. (1976) "Fundamentals of Rock Mechanics", 2nd Ed. Chapman
    and Hall, London: 585 pp.

JETTER, L.K. and BORIE, B.S. (1953) A method for the quantitative determination of
    preferred orientation. *Jl. Applied Physics*, V. 24(5): 532-5.

JONES, F.O. (1964) New fast, accurate test measurement of bentonite in drilling mud.
    Oil and Gas Jl., V. 1: 76-8.

JONES, R. and GATFIELD, E.N. (1955) Testing concrete by an ultrasonic pulse technique.
    DSIR, Road Research Tech. Paper No. 34., H.M.S.O., London: 48 pp.

KAARSBERG, E.A. (1959) Introductory studies of natural and artificial argillaceous
    aggregates by sound propagation and X-ray diffraction methods. *Jl. Geol.*, V. 67:
    447-72.

KAHN, J.S. (1956) Analysis and distribution of packing properties in sand-sized
    sediments. 2. The distribution of the packing measurements and an example of
    packing analysis. *Jl. Geol.*, V. 64: 578-606.

KAWACHI, Y. (1974) Geology and petrochemistry of weakly metermorphosed rocks in the
    upper Wakatipu District, southern New Zealand. *N.Z. Jl. Geol. Geophys.*, V. 17(1):
    169-208.

KAZI, A. (1975) Quantitative fabric analysis of Drammen clay using X-ray diffraction technique. *Jl. Sed. Pet., V. 45(4):* 883-90.

_____ and AL-MANSOUR, Z.R. (1980) Empirical relationship between Los Angeles abrasion and Schmidt hammer strength tests with application to aggregates around Jeddah. *Quat. Jl. Engng. Geol., London, V. 13(1):* 45-52.

KEAR, D. and HUNT, J.L. (1969) Aggregate resources of New Zealand. *Proc. Nat. Conf. on Concrete Aggregates, Hamilton, New Zealand; N.Z. Portland Cement Assoc.:* 17-25.

KLUG, H.P. and ALEXANDER, L.E. (1974) "X-ray diffraction procedures for polycrystalline and amorphous materials". 2nd Ed. J. Wiley and Sons, New York: 966 pp.

KRYNINE, P.D. and JUDD, W.R. (1957) "Principles of Engineering Geology and Geotechnics". McGraw-Hill Book Co., New York: 730 pp.

KUBLER, B. (1967) La Cristallinite de L'illité et les zones tout à fait supérieures du metamorphisme. *Etages Tectoniques, Coll. Neuchâtel:* 105-22.

KUSHIRO, I. and NAKAMURA, Y. (1970) Petrology of some lunar crystalline rocks. *Proc. Apollo 11 Lunar Sci. Conf. 1:* 607-26.

LAMA, R.D. and VUTUKURI V.S. (1978)"Handbook on Mechanical properties of rocks". Vol 2, Trans Tech. Publications, Germany: 481 p.

LANIZ, R.V., STEVENS, R.E. and NORMAN, M.B. (1964) Staining of plagioclase feldspar and other minerals with F.D. and C. red No. 2. *U.S. Geol. Survey. Prof. Paper 501-13:* B152-3.

LA RUE, H.A. (1946) Modulus of elasticity of aggregates and its effects on concrete. *Proc., ASTM, V. 46:* 1298-310.

LASIUS, G.S.O. (1789) Beobachtungen über das Harzgebirge mit Karte. Hanover.

LEES, G. (1964) A new method for determining the angularity of particles. *Sedimentology V. 3(1):* 2-21.

_____ and KENNEDY, C.K. (1975) Quality, shape and degradation of aggregates. *Quat. Jl. Engng. Geology, V. 8(3):* 193-209.

LERCH, W. (1962) Chemical reactions of aggregates in concrete. *Modern Concrete, V. 25(11):* 41-44.

LOUGHNAN, F.C. (1969) "Chemical weathering of the silicate minerals". Elsevier, Amsterdam: 154 pp.

MacKENZIE, R.C. and MILNE, A.A. (1953) The effect of grinding on micas. I. Muscovite. *Min. Mag., V. 30:* 178-85.

MARSHALL, T.R. (1967) Washington test - A status report. Washington State Highway Commission, Dept. of Highways Materials, Spokane, Report 103: 15 pp.

MARSHALL, T.W. (1974) A petrographic investigation of greywacke type aggregates from the Auckland region. Unpub. M.Sc. (Hons.) thesis. Geology Dept., University of Auckland: 125 pp.

MARTINEZ, J.D.   (1958)   Photometer method for studying quartz grain orientation. *Am. Ass. Petrol. Geol. Bull., V. 42(3):* 588-608.

MATHER, K.   (1973)   Examination of cores from four highway bridges in Georgia.   U.S. Army Eng. Waterways Exp. Stn., Corps. Engng.,Vicksburg, Mississippi. Misc. Paper., C 73-11:   20 pp.

MAYER, A.   (1963)   Recent work in rock mechanics.   *3rd. Rankine Lecture, Geotechnique, V. 13:* 97-120.

McINTOSH, J.D.   (1957)   The selection of natural aggregates for various types of concrete work. *Reinf. Concrete Rev., V. 4(5):* 281-305.

_____   (1966)   "Concrete mix design" Cement and Concrete Assoc., London: 123 pp.

McKEAN, T.A.M.   (1976)   The petrology and K/Ar geochronology of the Wellington argillites - North Island, New Zealand. Unpub. B.Sc. (Hons.) project, Victoria University of Wellington: 60 pp.

MELVILLE, P.L.   (1948)   Weathering study of some aggregates. *Proc. Highway Res. Board, V. 28:* 238-48.

MICHALOPOULOS, A.P. and TRIANDAFILIDIS, G.E.   (1976)   Influence of water on hardness, strength and compressibility of rock. *Bull. Ass. Engng. Geologists, V. 13(1):* 1-22.

MIDDLETON, G.V.   (1960)   Chemical composition of sandstones. *Geol. Soc. Am. Bull., V. 71:* 1011-26.

MINOR, C.E.   (1959)   Degradation of mineral aggregates. ASTM Special Tech. Pub. No. 277: 109-21.

MOORE, C.A.   (1968)   Quantitative analysis of naturally occurring multi-component mineral systems by X-ray diffraction. *Clays and Clay Min., V. 16:* 325-36.

MORGENSTERN, N.R. and TCHALENKO, J.S.   (1967)   The optical determination of preferred orientation in clays and its application to the study of microstructure in consolidated Kaolin (parts 1 and 11). *Proc. Roy. Soc. London, Series A, V. 300:* 218-34 and 235-50.

MORRIS, P.   (1979)   Major and trace element chemistry of volcanic rocks from the Chatham Islands.   Analytical Facility Contribution No. 1; Dept. of Geology Publ. No. 11, Victoria University of Wellington. 32 pp.

MÜLLER, G.   (1967) "Methods in sedimentary petrology". Translated by Hans-Ilrich Schmincke. Stuttgart Hafner Pub. Co., New York: 283 pp.

MURRAY, H.H. and LYONS, S.C.   (1960)   Further correlations of Kaolinite crystallinity with chemical and physical properties. *In Proc. 8th Nat. Conf. on Clays and Clay Min.:* 11-7.

NATHAN, S.   (1976)   Geochemistry of the Greenland Group (Early Ordovician), New Zealand. *N.Z. Jl. Geol. Geophys., V. 19(5):* 683-706.

NEUBERT, H.K.P.   (1967)   "Strain gauges; kinds and uses". McMillan: 164 pp.

NELVILLE, A.M. (1975) "Properties of concrete". 2nd Ed., Pitman Pub., England: 686 pp.

NEW, B.M. (1976) Ultrasonic wave propogation in discontinuous rock. Transport and Road Research Laboratory Report 720: 9 pp.

NORRISH, K. and HUTTON, J.T. (1969) An accurate X-ray spectrographic method for the analysis of a wide range of geologic samples. *Geochim. et Cosmochim. Acta, V. 33:* 431-54.

OBERHOLSTER, R.E. and BRANDT, M.P. (1974) An example of cement-aggregate reaction in South Africa. *Proc. Electron Microscopy Soc. South Africa, V. 4:* 59-60.

O'BRIEN, N.R. (1963) A study of fissility in argillaceous rocks. Unpub. Ph.D. thesis, University of Illinois, Urbana, Illinois, U.S.A.

OLLIER, C. (1969) "Weathering" Oliver and Boyd, Edinburgh: 304 pp.

ONIONS, D. and MIDDLETON, G.V. (1968) Dimensional grain orientation of Ordovician turbidite greywackes. *Jl. Sed. Pet., V. 38(1):* 164-74.

ORCHARD, D.F. (1964) Factors influencing the wear of coarse aggregate in the Los Angeles test. *Proc. of 2nd Conf., Australian Road Res. Board, V.2 part 2:* 963-80.

_____ (1976) "Concrete technology. Vol. 3: properties and testing of aggregates". 3rd. Ed. Applied Science Publishers Ltd., London: 281 pp.

PARK, J.E. (1975) Paleomagnetism of the volcanic rocks at Red Rock Point, Wellington. Unpub. B.Sc. (Hons.) thesis, Geology Dept., Victoria University of Wellington: 31 pp.

PARKS, W.A. (1911) Report on the building and ornamental stones of Canada. Dept. of Mines, Canada, V. 1: 376 pp.

PARRISH, W. (1960) Advances in X-ray diffractometry of clay minerals. Clay and Clay Minerals; *Proc. 7th Nat. Conf., Pergamon Press:* 230-59.

PATERSON, M.S. (1978) "Experimental rock deformation - The brittle field". Springer-Verlag, New York: 254 pp.

PERRY, C.C. and LISSNER, H.R. (1962) "The strain gage primer". 2nd Ed., McGraw-Hill, New York: 332 pp.

PETTIJOHN, F.J. (1957) "Sedimentary rocks". 2nd Ed., Harper, New York: 718 pp.

_____ (1963) Chemical composition of sandstones - excluding carbonate and volcanic sands. *In* Data of Geochemistry (6th Ed.). *U.S. Geol. Survey Prof. Paper 440 S:* 19 pp.

_____, POTTER, P.E. and SIEVER, R. (1972) "Sand and sandstone". Springer-Verlag, Berlin: 618 pp.

PIERSON, A.L. (1959) A photomultiplier photometer for studying quartz grain orientation. *Jl. Sed. Pet. V. 29(1):* 98-103.

PRIEST, S.D. and HUDSON, J.A. (1976) Discontinuity spacings in rock. *Int. Jl. Rock Mech. Min. Sci. and Geomech. Abstr., V. 13:* 135-48.

RAISBECK, D.   (1973)   Strength parameters for weathered sandstone.   *N.Z. Engng.* *V. 28(9):*   254-260.

RAMSAY, D.M., DHIR, R.K. and SPENCE, I.M.   (1974)   The role of rock and clast fabric in the physical performance of crushed-rock aggregate.   *Engng. Geol., V. 8:*   267-85.

RAU, R.C.   (1963)   Measurement of crystallite size by means of X-ray diffraction line-broadening.   *Norelco Reporter, V. 10:*   114-8.

REED, J.J.   (1957)   Petrology of the Lower Mesozoic rocks of the Wellington district.   *N.Z. Geol. Survey Bull. n.s. 57:*   60 pp.

_____   (1966)   Geological and petrological investigations of wacke aggregates used in Auckland-Hamilton Motorway, Redoubt and Takanini sections.   *N.Z. Geol. Survey, Report No.20:*   47 pp.

_____   (1967)   Application of recent petrological advances to selection of road aggregates.   *Proc. Roading Symp. 1967. Road Res. Unit, N.Z. Nat. Roads Board, V. 2:*   716-42.

_____   and GRANT-TAYLOR, T.L.   (1966)   Geological investigations of quarries and potential quarries for road metal production, Wellington area.   *N.Z. Geol. Survey, Report No. 5:*   18 pp.

RHOADES, R. and MIELENZ, R.C.   (1946)   Petrography of concrete aggregate.   *Jl. Amer. Concrete Instit., V.42:*   581-600.

RICHARDS, C.W.   (1961)   "Engineering materials science".   Wadsworth Pub. Co., Belmont, California.

RIDDOLLS, B.W. and PERRIN, N.D.   (1975)   Engineering geological investigations: Wellington urban motorway - The Terrace tunnel.   *N.Z. Engng., V. 15:*   221-4.

ROBERTS, A.F.   (1977)   "Geotechnology - An introductory text for students and engineers".   Pergamon Press, Oxford: 347 pp.

ROPER, H.   (1959)   Study of shrinking aggregates in concrete.   *Nat. Bldg. Res. Instit., South African Council for Scientific and Industrial Res., Special Tech. Report No. 502:*   136 pp.

_____, COX, J.E. and ERLIN, B.   (1964)   Petrographic studies on concrete containing shrinking aggregate.   *Jl. PCA Res. and Develpment Lab., V. 6(3):*   2-18.

ROWE, G.H.   (1979)   A method for assessing degradation in New Zealand greywackes.   *Proc. N.Z. Roading Symp. Road Res. Unit, Nat. Roads Board. Session A:* A2-1 - A2-14.

SALTZMAN, U.   (1975)   Rock   quality determination for large-size stone used in protective blankets.   Unpub. Ph.D. thesis, Purdue University: 246 pp.

SAMESHIMA, T.   (1977)   Hydrothermal degradation of basecourse aggregate.   Pavement Res. Project B.C. 21., Dept. of Geology, University of Auckland: 90 pp.

_____   and BLACK, P.M.   (1979) Clay index - a simple method of assessing the quality and performance of roading aggregates.   *Proc. N.Z. Roading Symp. Road Res. Unit, Nat. Roads Board, Session A:* A3-1 - A3-10.

SCHAFFER, R.J.   (1932)   The weathering of natural building stones.   *Dept. Sci. Indust. Res., Bldg. Res. Spec. Report No. 18, HMSO, London:*   149 pp.

SCHOEN, R. (1962) Semi-quantitative analysis of chlorites by X-ray diffraction. *Am. Min.*, *V. 47:* 1384-92.

SCHULZ, L.G. (1949a) A direct method of determining preferred orientation of a flat reflection sample using a Geiger Counter X-ray spectrometer. *Jl. Applied Phys.*, *V. 20:* 1030-3.

SHACKLOCK, B.W. (1974) "Concrete constituents and mix proportions". Cement and Concrete Ass., London: 102 pp.

SHAPIRO, L. and BRANNOCK, W.W. (1956) Rapid determination of carbon dioxide in silicate rocks. *Analytical Chemistry*, *V. 27(11):* 1796-7.

SHEPHERD, R. (1951) Physical properties and drillability of mine rock. *Colliery Engng, Jan.* p. 28; *Feb.* p. 61; *Mar.* p. 121.

SHERGOLD, F.A. (1953) The percentage voids in compacted gravel as a measure of its angularity. *Magazine of Concrete Res.*, *V. 5(13):* 3-10.

SIEVER, R. (1962) Silica solubility 0°- $200^{\circ}C$ and the diagenesis of siliceous sediments. *Jl. Geol.*, *V. 70:* 127-50.

SIPPEL, R.F. (1971) Quartz grain orientations - 1 (The photometric method). *Jl. Sed. Pet.*, *V. 41(1):* 38-59.

SMITH, J.V. (1974) "Feldspar minerals. Vol. 1. Crystal structure and physical properties". Springer-Verlag, New York: 627 pp.

SPARKS, B.W. (1960) "Geomorphology". Longmans: 371 pp.

SPEARS, D.A. (1976) The fissility of some carboniferous shales. *Sed.*, *V. 23(5):* 721-5.

SPEDEN, I.G. (1971) Geology of Papatowai Subdivision, south-east Otago. *N.Z. Geol. Survey Bull. n.s. 81:* 166 pp.

_____ (1976) Fossil localities in Torlesse rocks of the North Island, New Zealand. *Jl. Roy. Soc. N.Z.*, *V. 6(1):* 73-91.

SPRY, A. (1968) "Metamorphic textures". Pergamon Press, New York: 350 pp.

STEVENS, G.R. (1974) "Rugged landscape". A.H. and A.W. Reed, Wellington: 286 pp.

_____ (1976) Geology of the proposed Belmont regional hill park. Appendix 2 *In* Bagnall (Ed.) Survey of the proposed Belmont Regional Hill Park, part 1, Recommendations on development and management, *VUW Extension Pub. No. 14:* 32-5.

STOCKER, P.T. (1972) Diffusion and diffuse cementation in lime and cement stabilised clayey soils. *Aust. Road Res. Board, Special Report No. 8:* 146 pp.

STOW, D.A.V. and LOVELL, J.P.B. (1979) Contourites: their recognition in modern and ancient sediments. *Earth Sci. Rev.*, *V. 14:* 251-91.

SWENSON, E.G. and CHALY, V. (1956) Basis for classifying deleterious characteristics of concrete aggregate materials. *Jl. Am. Concrete Instit. V. 27(9):* 937-1002. *Proc. V. 52, Title No. 52-8.*

TANNER, C.B. and JACKSON, M.L. (1948) Nomographs of sedimentation times for soil particles under gravity or centrifugal acceleration. *Soil Sci. Soc. Amer. Proc. (1947),* V. *12:* 60-5.

TATTERSALL, G.H. (1976) "The workability of concrete". Cement and Concrete Assn., Slough: 138 pp.

TAYLOR, J.M. (1950) Pore-space reduction in sandstones. *Bull. Am. Ass. Pet. Geol.,* V. *34(4):* 701-16.

TCHALENKO, J.S., BURNETT, A.D. and HUNG, J.J. (1971) The correspondence between optical and X-ray measurements of particle orientation in clays. *Clay Min.,* V. *9(1):* 47-70.

TERZAGHI, R.D. (1965) Sources of error in joint surveys. *Geotechnique,* V. *15:* 287-304.

TEYCHENNE, D.C., FRANKLIN, R.E. and ERNTROY, H.C. (1976) Design of normal concrete mixes. *Transport and Road Res. Lab. Dept. of Environment, London:* 30 pp.

THOMSON, A. (1959) Pressure solution and porosity. *In* Ireland, H.A. (Ed.) Silica in sediments. *Soc. Econ. Paleontologists and Mineralogists Special Pub. 7:* 92-110.

TOBIN, D.G. and DONATH, F.A. (1971) Microscopic criteria for defining deformational modes in rock. *Geol. Soc. Am. Bull.,* V. *82:* 1463-76.

TURNER, F.J. and WEISS, L.E. (1963) "Structural analysis of metamorphic tectonites". McGraw-Hill, San Francisco: 545 pp.

VAN DER PLAS, L. (1966) "The identification of detrital feldspars". Development in sedimentology 6; Elsevier Pub. Co., Amsterdam: 305 pp.

VUTUKURI, V.S., LAMA, R.D. and SALUJA, S.S. (1974) "Handbook on mechanical properties of rocks". Vol. 1. *Trans. Tech. Pub.:* 280 pp.

WALKER, R.G. (1967) Turbidite sedimentary structures and their relationship to proximal and distal depositional environments. *Jl. Sed. Pet.,* V. *37(1):* 25-43.

WARD, M. and GRANT, I.J. (1978) Planning for mineral resources in the Wellington region. Report 78.38. Undertaken for the Wellington Regional Planning Authority and Wellington Regional Water Board: 107 pp.

WATKINS, M.D. (1970) Terminology for describing the spacing of discontinuities of rock masses. *Quat. Jl. Engng. Geol.,* V. *3(3):* 193-5.

WATSON, J. (1911) "British and foreign building stones". Cambridge University Press: 483 pp.

WATTERS, W.A. (1969) Petrological examination of concrete aggregates. *Proc. Nat. Conf. Concrete Aggregates, Hamilton, New Zealand:* 48-54.

WEAST, R.C. (1975) "Handbook of chemistry and physics . A ready-reference book of chemical and physical data". 55th Ed., Chemical Rubber Co. Press, Ohio, U.S.A.

WEAVER, C.E. (1960) Possible uses of clay minerals in search for oil. *Bull. Am. Ass. Pet. Geol.* V. *44(9):* 1505-18.

WEBBY, B.D. (1967) Tube fossils from the Triassic of south-west Wellington, New Zealand. *Trans. Roy. Soc. N.Z., Geol., V. 5(7):* 181-91.

WELSH, W. (1967) The value of point-count model analysis of greywackes. *Scot. Jl. Geol., V. 3(2):* 318-28.

WEST, T.R. and AUGHENBAUGH, N.B. (1964) The role of degradation in highway construction. *15th Annual Highway Geol. Symp., Rolla, Missouri:* 117-32.

WEYL, P.K. (1959) Pressure solution and the force of crystallisation - a phenomenological theory. *Jl. Geophys. Res., V. 64:* 2001-25.

WHITE, W.A. (1961) Colloidal phenomena in sedimentation of argillaceous rocks. *Jl. Sed. Pet., V. 31:* 560-70.

WILLIAMS, D.N. (1975) A bibliography of Wellington Geology, 1855-1970. *N.Z. Geol. Survey, Report No. 71:* 54 pp.

WINKLER, E.M. (1973) "Stone: Properties, durability in man's environment". Springer-Verlag: 230 pp.

WOLF, K.H. (1971) Textural and compositional transitional stages between various lithic grain types (with a comment on "interpreting detrital modes on greywacke and arkose"). *Jl. Sed. Pet., V. 41:* 328-32.

WOOLF, D.O. (1966) Toughness, hardness, abrasion, strength and elastic properties. *In* Significance of tests and properties of concrete and concrete-making materials. *ASTM STP 169-A:* 462-75.

YOUNG, J.F. (1974) An assessment of the influence of microstructure on time dependant deformations of hardened cement paste. *1st Australian Conf. on Engng. Materials, Sydney:* 3-28.

ZACHARIADIS, R.G.P. (1966) Near surface seismic velocities in the Wellington greywackes. Unpub. B.Sc. (Hons.) project, Geology Dept. Library, Victoria University of Wellington: 14 pp.

APPENDICES

What one fool can do, another can.

(Ancient Simian Proverb)

All Tables, Figures and Plates are numbered within each Appendix and bear the prefix 'A' to distinguish them from those in the thesis text.

APPENDIX 1

Sample location sites

Index map for sample location maps of this Appendix.   Numbers within the locality areas shown, correspond with those on the sample location maps. Map 7 is taken from Lands and Survey 1:15,840 Mosaic map series, all others are from the Lands and Survey 1:10,000 Wellington District map series.   Working quarries are shown with a star symbol.   Samples were taken along the traverse arrow shown, in chronological or other order shown.

KTW-i ▸ KTW- viii
KTW-1 ▸ KTW-17
KTW-A ▸ KTW-G

Porirua
△
855 m

N

Map 1, Te Rewarewa Point

Carsons

0   500
metres

Moana Rd.

Map 2, Western Hutt

Map 3, Horokiwi

N

Newlands Rd.

NC-1▶NC-15

WCC-1▶WCC-24

City Council

State highway 1

Drapers

Ryans

0   500
        metres

Map 4, Ngauranga

Hutt motorway

N

Wellington–Johnsonville railway

Kenya St.

Ngaio Gorge Rd.

Kaiwharawhara Stm.

KS-10

Churchill Dr.

Hanover St.

KS-1

Wadestown Rd.

0   500

metres

Map 5, Kaiwharawhara Stm.

N

Happy Valley Rd.

OB-17◄OB-9

Ohiro Bay Pde.

The Esplanade

IB-22◄IB-15

OB-8◄OB-1

OB-21◄OB-18

IB-1►IB-14

Owhiro Bay

0   500

metres

Map 6, Island Bay and Owhiro Bay

Map 7, Sinclair Head
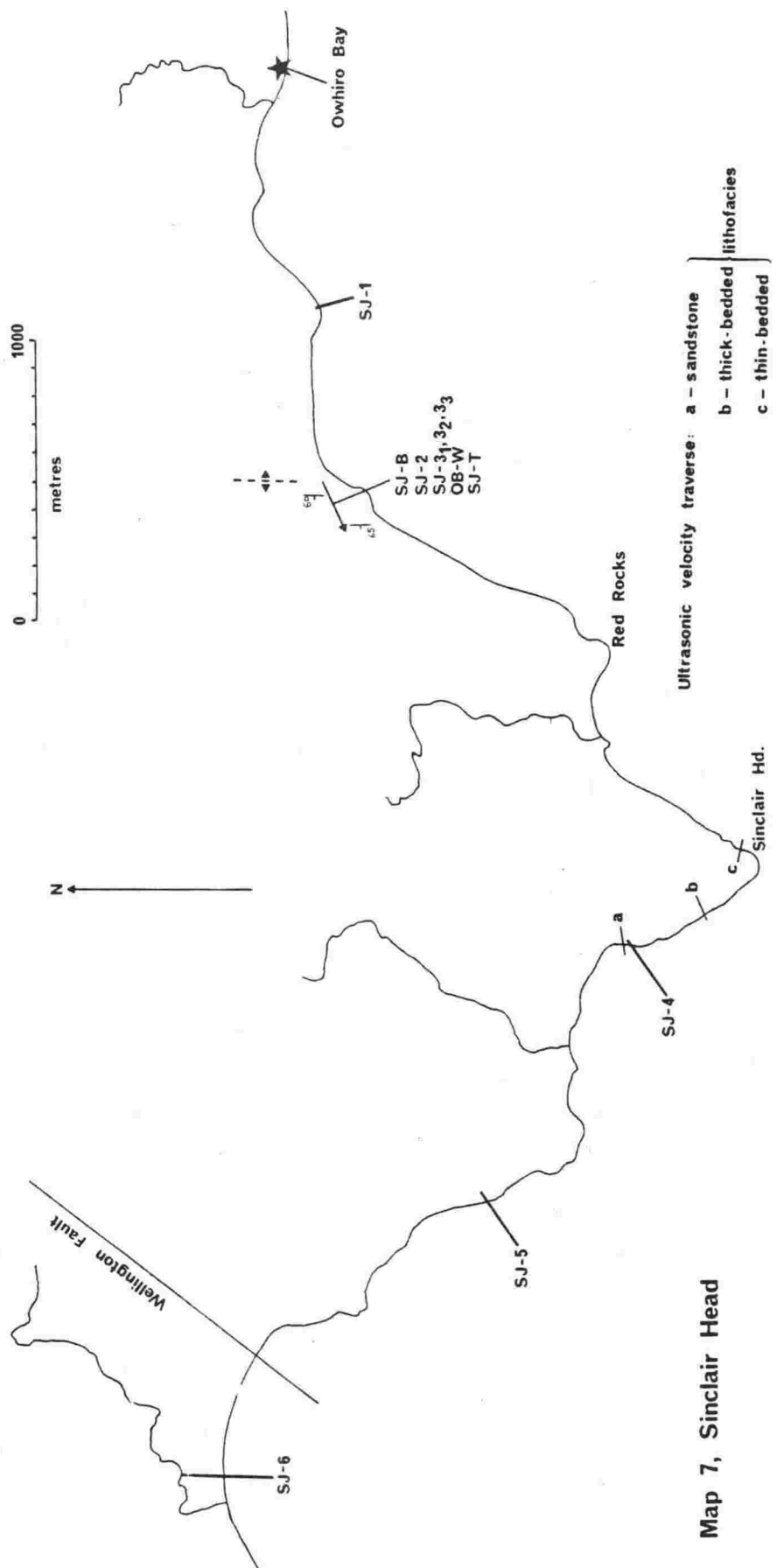
APPENDIX 2

Staining of thin sections for identification of felsic minerals

Etching of thin sections to accomplish staining was carried out using hydrofluric acid
fumes after the final grinding of the thin section. The most suitable etch was obtained
by exposing thin sections to fumes for 90 seconds.

The method described by Bailey and Stevens (1960) was tried but as acid rhodizonate, a
sodium salt, does not stain very sodic plagioclase, potassium chlorite was used. When
immersed in sodium cobaltinitrate, the plagioclase is stained yellow. All etched K-feld-
spar is also stained yellow in sodium cobaltinitrate. Thus all feldspar and potassium
bearing minerals in the matrix were stained yellow, providing differentiation between feld-
spar and quartz but none between K-feldspar and plagioclase.

A technique by Laniz *et al.* (1964) was also tried but the use of calcium chloride to stain
highly sodic plagioclase proved unreliable so staining of K-feldspar only was resorted to
in most thin sections and then only when the rock was relatively "clean" as potassium
bearing minerals had a masking effect.

Müller (1967) suggested a 5 percent barium chloride dip then sodium thiocyanate solution as
a way of staining etched plagioclase with anorthite contents as low as 3 percent. This
also proved unsatisfactory due primarily to authigenic albites.

If all feldspar is etched and stained, relatively accurate quartz to total feldspar ratios
can be determined. From artificially prepared samples, Hayes and Klugman (1959) estab-
lished relative errors of 3.2 percent for quartz, 5.3 percent for K-feldspar and 5.4 per-
cent for plagioclase so by inference a total feldspar count should have a relative error
of about 6 percent.

Although staining of plagioclase proved unsuccessful, etching gave it a whitish appearance
providing a means by which unstained felsics could be differentiated. Etching is obvious
under a microscope in plane polarised light and enhanced by the use of the substage iris.
Hayes and Klugman (1959) had noted this effect and were using medium to fine sand sized
grains (1 to 3 phi, 0.5 mm to 0.125 mm) with counts of 300 to 500. Somewhat greater error
may be expected in this study from reduced stained areas restricting grain counts to 200, the
use of a manual vernier stage instead of a mechanical click stage and the influence of
potassium bearing matrix minerals. However, for rocks of mean grain size coarser than
3 phi (0.125 mm) maximum error will probably not exceed 8 percent.

APPENDIX 3

1.   Quartz

The mean quartz content varies only slightly with lithofacies (Figure 2.3), the average for the greywackes studied being 29.7, 27.7 and 25.8 percent for the sandstone, thick-bedded and thin-bedded lithofacies respectively.   No significant difference between these mean values is apparent (P is greater than 0.1).

The range of quartz content with lithofacies suggests a petrographic continuum.   Quartz varies in its characteristics.   Almost all quartz is monocrystalline, clear and strained. Some display boehm structure (Turner and Weiss, 1963), e.g. SJ-6 and OB-21, or induced twinning (pseudotwins, DC-1) or an impression of laminations within the grains sometimes appearing wavy, an indication that these features have been induced *in situ* (DC-2).   Strain may produce a 2V of about $30°$ to $50°$ (HQ-17, HQ-25).   Only competent rocks are able to withstand such strain and it is noteworthy that although strained quartz exists in the thin-bedded lithofacies, pseudo-twinning is restricted to the more massive greywackes of the other lithofacies, usually near large faults, evidence which corroborates field interpretation well (section 3.3.1).   Occasional grains of high sphericity (equant) occur in all grain sizes though small grains generally are more angular as they result predominantly from fracture of larger grains.   The quartz population in greywackes of the sandstone lithofacies is angular to well rounded (KTW-17) with a few subrounded grains in the natural continuum.   In larger grain sizes, i.e. those more often rounded, subequant grains attributed to breakage of equant rounded grains have a ragged outline.   Extremes in grain shape (KTW-13) are more often associated with smaller grains.   The thick-bedded lithofacies usually has a more poorly sorted population of angular to rounded quartz grains, the subrounded and rounded grains often showing "fresh" breakage - sometimes with long, broken, slivers adjacent to the host grain (HQ-17)

The average size of quartz varies with lithofacies from 0.2 mm in the sandstone lithofacies to 0.36 mm in the thick-bedded lithofacies and 0.073 mm in the thin-bedded lithofacies which also has a smaller maximum size (0.36 mm).   A maximum size of 1.0 mm was obtained in the sandstone and thick-bedded lithofacies.

Quartz recrystallisation is apparent in greywackes of all lithofacies in two forms:

(i)   Cement: intimately packed adjacent quartz grains sometimes indicate overgrowths to be present (DC-1, DC-3).   Some evidence in the form of sericite "entering" quartz may be misleading unless the quartz concerned is authigenic (HQ-25, HQ-16).   Orientation of grain/grain boundary to the plane of the thin section is also important since where this is of low angle, a boundary contact is greatly exaggerated.   With subtle undulose extinction in adjacent grains, optical continuity is sometimes difficult to confirm.   Overgrowth evidence is seen most frequently in the thin-bedded lithofacies and is associated with veining where a quartz vein may include a detrital grain in its fabric.

(ii)   Healed fractures: fractures in quartz are often oriented, e.g. parallel to extinction direction (HQ-17).   Occasionally fractured grains retain their integrity by healing the fracture with quartz in optical continuity to produce a structure resembling an overgrowth (KTW-14).

The differences between overgrowths and healed fractures may be observed by stopping down light and studying optical continuity over the overgrowth boundary;   fractures show as a discontinuity over a distance of about 0.016 mm and the "dust" coating, common to overgrowths, may not be continuous.

Although not common, included mineral grains (maximum size about 0.06 mm), are found in quartz from greywackes of all lithofacies. The larger grains had included sericite, vacuoles, rutile (KTW-15), tourmaline (penetration twins, HQ-25), opaques e.g. magnetite, apatite, epidote group minerals and zircon. Epidote, tourmaline and rutile inclusions persist with decreased quartz grain size.

Most quartz grains show signs of erosion and/or suturing. Suturing occur especially in the more strongly oriented, laminated and finer greywackes (BQ-iv) and in close proximity to detrital grains (especially felsic grains). Erosion is seen in quartz grains which are highly strained or partly shattered and almost always adjacent to zones of sericite, muscovite (KTW-16), calcite, zeolite, pumpellyite or prehnite, which often form blebs or embayments in the grain,e.g. prehnite "enters" quartz (KTW-14) on occasion. A normal surface texture of erosion, or etch, gives up to 0.007 mm penetration in larger quartz grains, smaller grains (thin-bedded lithofacies) eroding to some 0.01 mm or 0.015 mm.

2.   K-feldspar

Identification of potassium feldspar depended strongly on staining for accuracy, and the inability to stain the finest greywackes successfully may have contributed to the trend of lowered K-feldspar percentages through lithofacies; this is true also of quartz (Figure 2.4B).

The average potassium feldspar contents of greywackes is 4.1, 3.7 and 1.8 percent for the sandstone, thick and thin-bedded lithofacies respectively. The K-feldspar mode did not exceed 9 percent for any greywacke studied and does not seem related to plagioclase contents.

K-feldspar is most prolific in the thick-bedded lithofacies, grains average 0.45 mm in this lithofacies compared to 0.25 mm in the sandstone lithofacies and about 0.086 mm in the thin-bedded lithofacies. The rock fragment population follows a similar trend.

The K-feldspar consists of microperthitic string and interpenetrant perthites and mesoper-thites (composition nomenclature of Van der Plas, 1966; textural nomenclature after Spry, 1968), which may be strained (HQ-17) or strained microantiperthite (sodium phase may be compound, rod or banded). Chessboard texture (Smith, 1974) in one mesoperthite grain had patches averaging 0.045 mm (HQ-25). Perthite is more common than microcline.

K-feldspars; microcline, orthoclase, perthite (BQ-IXA), antiperthite and myrmekitic inter-growths with quartz often displayed good cleavage, carlsbad twinning (OB-21, KTW-13) and combined carlsbad - pericline twinning.

The varieties of K-feldspar are reduced in finer grained greywackes, but are generally equant or elongate and angular or subrounded. Compared with plagioclase feldspars,they are more equant and tend to be of larger size, there being a transition between K-feldspar grains and metamorphic and plutonic rock fragments. Individual grains of K-feldspar may be 0.7 mm in size.

Inclusions are common, being tourmaline (0.028 mm long), apatite (residing in fractures, approximately 0.34 mm long), and opaques - sometimes in bands (HQ-25). The minerals are pseudocubic, rectangular or hexagonal and predominantly pyrite.

K-feldspar grains, generally are less rounded than quartz, due to retrogressive rounding induced by calcite erosion (BQ-xviii), prehnite (DC-1), sericite or epidote group minerals.

These minerals also occur within grains in blebs of 0.1 to 0.15 mm. In greywackes of the sandstone lithofacies, approximately 60 percent of the K-feldspar population show some alteration (e.g. KTW-13).

K-feldspar grains are the second largest grains occurring in greywackes, subordinate to rock fragments and phyllosilicates in the coarsest and finest grained greywackes respectively.

3.   Plagioclase feldspar

Greywackes of all lithofacies contain approximately subequal amounts of plagioclase, the least variation being apparent in the thick-bedded lithofacies (Figure 2.4A). When compared with the feldspar ratio figures (Figure 2.4C) this indicates either a more rapid breakdown of K-feldspar from the source sediment, a more prolific plagioclase provenance raw material, together with greater variation in grain size, or an effect of diagenesis to equilibrate plagioclase content by introducing authigenic plagioclase. There is an apparent trend for plagioclase to decrease in concentration from the sandstone to the thin-bedded lithofacies.

Authigenic plagioclase, generally clear, unzoned and untwinned, was also counted in this mode. It was often exceedingly difficult to differentiate between this and detrital plagioclase, and some cements (zeolite and albite) possess undulose extinction making mineral and grain size identification difficult. The presence of authigenic plagioclase is important when engineering properties are considered.

Most detrital plagioclase, and especially that greater than 0.05 mm in size, was albite twinned (composition was obtained by the Michel-Lévy method) and ranged from An_{3-18}. Grain sizes averaged 0.23 and 0.27 mm for the sandstone and thick-bedded lithofacies and 0.074 mm in the thin-bedded lithofacies. Grains are generally equant, elongate but rarely prismatic, angular to subrounded (rounded plagioclase is seen in HQ-23). Although having a less shattered appearance than quartz, deformation twins often kinked, bent (through 20°) and offset, and also combined carlsbad-albite, albite and pericline (KTW-16) twin lamellae are common especially in regions where grains are crushed. Plagioclase tends to fracture along a plane without the brecciation effects seen in quartz. Some grains show signs of healing. Undulose extinction, providing extinction over a 10° angle of stage rotation, altered 2V by up to about 40° and indentation of grains by adjacent grains of quartz and feldspar, indicate this population to be less able to withstand tectonic stress. In spite of this, the mean size of the plagioclase population is exceeded by the quartz population only in greywackes of the thick-bedded lithofacies.

Generally, larger grains are less altered and more angular in the thin-bedded lithofacies. In the sandstone and thick-bedded lithofacies, however, the freshest looking grains are less than 20 percent of the population and are generally smaller than the mean size.

Alteration, erosion and replacement are well established, most alteration probably occurring whilst sediment was in the provenance region. The majority of grains in all lithofacies show some sericitisation, most grains showing at least 10 percent alteration, sometimes with complete destruction of the grain, by prehnite, sericite, calcite, zeolite and to lesser degree, by epidote minerals. Alteration takes place preferentially at the ends of elongate grains, along cleavage planes, along twin planes and about the grain periphery (the interior remaining unaffected). The material observed within and invading plagioclase achieves large grain sizes: calcite blebs 0.01 to 0.032 mm; sericite may average 0.04 mm; epidote group minerals 0.064 mm, sometimes forming clumps 0.2 mm across.

However, the average size of these alteration minerals is 0.006 mm. This is signifi-
cant when the minimum recognizable grain size of plagioclase is about 0.008 mm.

Many grains are partly zeolited, up to 25 percent of the smaller grain being
affected by anhedral crystallite clusters of sutured zeolite 0.005 to 0.019 mm
in size. Zeolite invades plagioclase from the matrix and veins, often completely sur-
rounding grains of highly undulose plagioclase in an undulose cement containing fine
(0.007 mm) sericite which is oriented within the cement in two directions (HQ-17). Erosion
of plagioclase may take place in some regions of a single slide with extensive authigenic
deposition of plagioclase elsewhere.

Heavy sericitisation creates identification problems since some rock fragments, e.g. seri-
cite schist, may resemble fully altered plagioclase, especially where sericite flakes are
oriented. In these circumstances plagioclase may still be identified by observing twin
lamellae (in grains larger than 0.05 mm) under high power using the sensitive tint plate
(λ plate). In untwinned varieties the problem remains unless graphic intergrowths with
quartz are in evidence or refractive index can be checked. For zoned grains (SJ-6) the
sensitive tint plate was again useful. Indistinct grain margins due to erosion were
rationalised by medium to high magnification and stopped down light.

Non-authigenic inclusions in plagioclase are few but, when apparent, constituted zones
0.016 mm wide and parallel with prismatic grain outlines. The inclusions are about
0.003 mm long (HQ-19) and include quartz, zircon, chlorite, sericite and muscovite. The
plagioclase concerned is generally untwinned. Zircon, in particular, was observed in well
formed 0.02 mm rhombs (HQ-17).

Authigenic albite is difficult to identify, ultra-thin sections giving better indication
of important suturing and random growth habits.

4.   Rock fragments

4.1   Sedimentary rock fragments

The thick-bedded lithofacies, in which the intraformational conglomerates (Grant-Taylor,
1976) or "chipwackes" are usually found, possesses the highest concentrations of sedimen-
tary rock fragments (Figure 2.5A). The trend otherwise is for the concentrations of
sedimentary rock fragments to diminish from the sandstone to the thin-bedded lithofacies.

Sedimentary rock fragments may be classified by lithology, based on textural parameters:

(i)   Very fine sandstones: These have a mean grain size of 0.09 mm and are moderately
sorted, often subrounded and rounded felsic detrital fragments "floating" in, and being
replaced by, a fine sericite matrix. Quartz is strained and often polycrystalline.
Fragments are moulded into interstices in the host rock fabric by up to 0.1 mm (pseudo-
matrix; Dickinson, 1970), the rock fragment matrix also eroding the host rock felsic
grains. Small interstitial light brown-green chlorite flakes (0.035 mm) are also present.
This rock fragment type is limited to coarser greywackes of the thick-bedded lithofacies.

(ii)   Siltstones: Rock fragments with a mean grain size of between 16 and 40 mm and
generally more mud rich than the very fine sandstones, they contain smaller equant, angular
to rounded detrital quartz, and more rounded and slightly altering feldspar, floating in
matrix. They constitute the most common sedimentary rock fragments and are ubiquitous in
all greywackes except those of the thin-bedded lithofacies - only the finest textured varie-
ties are found in that lithofacies. Some varieties have a carbonaceous matrix (DC-1) in
fine, sinuous, ramifying bands up to 0.09 mm, providing distinct anisotropy. Most are at

least 30 to 70 percent matrix, composed of chlorite with lesser quantities of sericite, grey ?epidote (and other heavy minerals) and finely disseminated opaques (carbonaceous material). The latter, which in plane light imparts a grey-brown or brown-grey colour, assists readily in the formation of pseudomatrix (KTW-15). Phyllosilicates, subequal in size with felsic grains, are optically less clear than host rock phyllosilicates, oriented, and about 0.02 to 0.06 mm in size.

(iii) Mudstones: This variety of rock fragment is rarely found in other than the thin-bedded lithofacies greywackes. The fragments always form pseudomatrix and are invariably altered except where found in the thick-bedded and sandstone lithofacies (HQ-25). Fragments averaged about 0.19 mm and were the largest detrital grains in some thin-bedded lithofacies greywackes (RSS-i). They were almost totally of matrix sized material (exceeding 80 percent) and occurred only rarely in elongated, subrounded or rounded forms. Their mean grain size varied between 0.004 and 0.019 mm providing a well oriented structure mainly of brown chlorite material, supplimented by sericite, few felsics and heavy minerals. Bands of darker chloritic material indicated distortion of the fragments about more resistant host rock grains.

(iv) Chert: Found in all greywackes, this represents a small fraction of the total sedimentary rock fragment mode. Chert fragments are elongate, angular to rounded, averaging 0.32 mm in size but occurring in grains to 2 mm. Larger grains tend to be subrounded to rounded. The fragments are of anhedral, sutured, equant quartz crystallites averaging 0.045 mm.

4.2 Metamorphic and plutonic rock fragments

Rock fragments under this heading are physically strong felsic rocks. Pseudomatrix formation from, and replacement of, any lithologies in this mode was rarely observed. Variation in greywackes containing this mode is marked only by the thin-bedded lithofacies (Figure 2.58) which averages only 25 percent of the content of other lithofacies. With a slightly increased average, the sandstone lithofacies experiences a much wider range of modal values.

Rock types occurring in this mode include:

(i) Sericite schist: Found in greywacke of all lithofacies, it consists predominantly of quartz, muscovite and sericite. Small (averaging 0.016 to 0.09 mm) strongly oriented, elongate, strained crystallites of quartz were intersutured with easily defined flakes of sericite/muscovite in strands averaging 0.013 to 0.08 mm, but locally 0.5 mm long. The strongly oriented strands often possessed yellow, red or brown second order interference colours and formed foliated zones within the fragment locally, with brown or green chlorite which reached 0.09 mm, and opaques (0.015 mm). The fragments averaged 0.28 mm in size, were subrounded and rounded, elongate - their long axes tending to be parallel to bedding (length to width ratios about 5.8). They occasionally formed pseudomatrix, penetrating the host rock fabric to 0.2 mm.

Some fragments contained carbonaceous matter (?graphite, KTW-16), epidote group minerals and feldspar. Coarser varieties contained chlorite in flakes to 0.64 mm, somewhat less quartz (about 5 percent) in grains averaging 0.16 mm, and pyrite in rounded 0.005 mm grains. Sericite appears to be derived in part from degrading feldspar.

Sericite schist fragments are the most important variety of rock fragments in this mode for greywackes of the thin-bedded variety lithofacies, the only others being quartz schist and some granitic fragments.

Differentiation between sericite "patches" from degrading plagioclase and sericite schist fragments proved difficult but the degree of distortion of the grain was helpful. Plagio-clase, degraded sufficiently to be confusing, would probably not have endured the fluvial processes necessary for sediment accumulation if deposition had taken place after degra-dation. Therefore distorted "patches" of sericite were included as sericite schist fragments if they fulfilled the form and other characteristics indicative of that lithology.

(ii) Quartz schist: These elongate, subrounded and rounded fragments averaged 0.58 mm comprising quartz, feldspar, muscovite and chlorite grains averaging between 0.035 mm and 0.08 mm in intimate, sutured, strongly oriented association. Grains tended to pseudo-matrix in the thin-bedded lithofacies where fragments were smaller, 0.26 mm. Prehnite was sometimes a replacement mineral.

(iii) Granitic fragments: Generally coarse grained, these are seen to advantage only in the thick-bedded lithofacies. They are large (0.85 mm), subrounded, sutured, subhedral intergrowths of string antiperthite with a mineralogy of twinned and untwinned microcline and orthoclase, perthitic and myrmekitic intergrowths of sodic plagioclase (An_{10-14}) and quartz. Zoned feldspars, orthoclase, apatite, quartz, perthite, well crystallised musco-vite and lesser amounts of green biotite with chlorite intergrowths were also present.

These are sometimes the largest rock fragments seen in thin section with elongate fragments rarely smaller than 0.25 mm (0.1 mm in thin-bedded lithofacies, DC-10) with individual component mineral grains equalling the fragment size. Most grains were not altered by more than 5 percent.

(iv) Quartzite: Angular to rounded fragments, averaging 0.5 mm, these are mainly highly intersutured quartz, numerous non-opaque heavy interstitial minerals of 0.008 mm, minor plagioclase and rare mica. Fragments sometimes possess a pronounced fabric orien-tation of crystallites. Crystallites average 0.065 mm.

(v) Gneissic fragments: Subrounded or rounded, elongate, foliated, lepidoblastic, sometimes slightly deformed, these fragments comprise sutured quartz, highly pleochroic biotite and muscovite, averaging 0.09, 0.25 and 0.15 to 0.4 mm respectively. The included phyllosilicates were not as strained as the phyllosilicates of the host greywacke. The fragments were large (mean size 0.78 mm), rare and sometimes eroded (KTW-13).

(vi) Hornfels: This occurred in one thin section (KTW-13) was subangular, fragment measuring 0.7 mm, consisting mainly of biotite, muscovite and sutured quartz with minor plagioclase.

4.3   Acid volcanic rock fragments

Whilst difficulties exist in differentiating rock fragments bearing small grains of quartz (Boggs, 1968; Wolf, 1971), 10 greywackes of the thick-bedded lithofacies were observed to have a mode of acidic volcanic rock fragments consistently. These fragments are chemically unstable, mechanically weak and consequently are found consistently only in the coarsest greywackes with quantity diminishing rapidly from sandstone to thin-bedded lithofacies (Figure 2.5C).

Fragments are mainly devitrifying, glassy, vesicular shards appearing as a brown-grey or dark grey-brown, drusy amorphous mass displaying flow texture in the glass and included microlites/phenocrysts. However a relatively fresh glassy example was observed from BQ-xviii.

Mechanical weakness enables the fragments to assume a pseudomatrix (DC-2) role, especially at their margins, where host rock grains have penetrated fragments to 0.048 mm (HQ-25). Some, lacking microlites, are exclusively pseudomatrix; others, fresh fragments, may be entirely glass with remnant flow banding, the chipped outlines clearly showing conchoidal fracture (HQ-17). In these grains the glass may display slight anisotropy (very slight optically length fast orientation) due mainly to strain and/or very fine (minus 0.002 mm) inclusions. The latter, with opaques (minus 0.002 mm), impart optical drusiness.

Average fragment size is 0.45 mm, varying with lithofacies from 0.032 mm (BQ-i) in the thin-bedded lithofacies and between 0.7 mm to 1.0 mm in the sandstone and thick-bedded litho-facies. Lithofacies association also tends to influence distortion, freshness and grain shape, e.g. fragments occurring in a greywacke with a zeolite or calcite cement dominance are fresher and less distorted than fragments in mainly prehnite cemented greywackes. Grain shapes are typically equant or elongate and subangular to rounded.

Mineralogy of the fragments exclusive of glass are well sorted microlite/phenocryst popu-lations of rounded, granular, euhedral quartz with more common twinned or untwinned, euhedral laths of sodic plagioclase (An_{12}) which may be altering to sericite. Micro-lites average 0.1 mm, with a length to width ratio about 3. Accessories include iron oxides (0.001 to 0.012 mm), the larger grains being euhedral. These opaques influence fragment colour and clarity, imparting a drusy or dusty appearance and increasing colour value as do the rounded, 0.004 mm, heavy minerals.

Microlites or phenocrysts in the otherwise glassy groundmass "stand out" as relatively clear, colourless, elongate patches which assume an apparent pilotaxitic to trachytic texture. These textures aided identification of acid volcanic rock fragments by their patchy light grey or brown-grey appearance and darkness under crossed nicols. Although not as altered as some basic volcanic rock fragments, acid volcanic rock fragments of smaller sizes showed some alteration to chlorite, zeolite (HQ-17), or sericite and promoted vague fragment outlines making size identification impossible.

4.4   Basic volcanic rock fragments

This mode bears close relationship to metamorphic and plutonic rock fragments in that modal averages are relatively distributed between lithofacies, even though average modes and mode ranges from the sandstone and thick-bedded lithofacies are higher than those of volcanic rock fragments. There is no significant difference in mean or range for the thin-bedded lithofacies, between the two mode classes (Figure 2.5D).

Fragments in this mode are chemically unstable but mechanically stronger than acid volcanic rock fragments, so alteration supercedes induration for optical identification.

Textures are mainly hyalopilitic but pilotaxitic and trachytic textures occur which, assum-ing a mobile basic lava, indicates the largest phenocrysts are not represented, fragments merely being groundmass residuals. Texture is well displayed by euhedral and subhedral microlites of plagioclase (An_{22}) measuring to a maximum of 0.23 mm (average 0.06 mm) and appearing as almost acicular laths, sometimes ragged and eroded at the ends. Accessory groundmass minerals(5 percent) include mainly euhedral magnetite and ilmenite 0.016 to 0.02 mm in size (DC-10). Ilmenite, however, (light grey-brown colour in reflected light) may constitute 30 percent of the opaque accessories in skeletal crystals (HQ-25).

Glass in the groundmass is devitrified and most fragments have been altered somewhat to chlorite, yellow drusy elongate prehnite (DC-1), zeolite, calcite, metallic opaque minerals, albite (KTW-15), silica (giving a cherty appearance, HQ-27), sericite (in 0.006 mm flakes to 10 percent replacement), and epidote group minerals (0.006 mm).

Less than 20 percent of the fragments are completely altered.

The quantity of pseudomatrix formed from basic volcanic rock fragments is probably greater than that estimated since alteration (especially to zeolite) tends to round and "fill" the form of the fragments, replacing as necessary, adjacent host rock grains to do so. Deformation is apparent (HQ-25), however, where adjacent host rock grains have been "pushed" into the fabric by 0.06 mm. Generally, the glassy grains are the most readily distored.

Fragment shape is elongate, subrounded and rounded, averaging 0.42 mm in size (1.3 mm maximum), with smaller sizes grouped in the thin-bedded lithofacies (0.14 mm average).

The main alteration processes

(i)   Chloritisation: Alteration begins in the groundmass of the fragment, generally as colourless, brown or yellow-green tinged euhedral grains and blebs which impart, by refractive index difference, a fibrous, felty appearance to the fragment. Chlorite grain size appears to be governed by the size of fragment being replaced, i.e. 0.026 mm in a fragment measuring 0.19 mm. Anomolous interference colours (Berlin blue) may accompany chlorite replacement. Phenocrysts generally remain unchanged.

(ii)   Zeolitisation: Zeolite (laumontite) replaces as fibrous clumps, growing inwards from a locus - usually the rock fragment margin. Individual optically length slow fibrous crystals extend to 0.17 mm in clumps 0.22 mm wide. The "clumped" habit distinguishes completely zeolitised volcanic rock fragments (generally those less than 0.19 mm) from authigenic zeolite cement, especially as most fragments show some zeolitisation e.g. up to 30 percent of the fragments in HQ-25 are totally zeolitised, and RSS-i has almost all the population zeolitised . In rock fragments the "clumps" formation is more complete and is observed as several small spherulites, in optical continuity to 0.026 mm, displaying an "iron cross" extinction. This is quite distinctive and, together with contrasts in refractive index in the rock fragment, aids identification. Authigenic colourless chlorite is often associated with zeolitisation.

(iii)   Authigenic concentration of metallic opaque minerals: Round, symmetrical blebs of euhedral opaque matter which often accompany early stages of zeolite alteration, may occupy the "interior" of basic volcanic rock fragments replacing between 5 and 50 percent of the fragment and leaving the plagioclase laths as residuals. Average size of the blebs is 0.007 to 0.001 mm (BQ-IXA). Under reflected light they have a bright yellow, speckled appearance with no bireflectance, so the material is considered to be pyrite. Calcite is not present.

5.   Muscovite

From Figure 2.6, the relative importance of muscovite as a detrital phyllosilicate to greywackes of the thin-bedded lithofacies is apparent, but the coarsest greywackes bear no more than 2 percent.

Muscovite is always strained and kinked with wavy or incomplete extinction. In places, it may be physically ragged and threaded along the long sides of adjacent grains, in well developed (with included opaques) flakes of high birefringence, sometimes pinched or swollen or slightly anastomosing. Gaps in anastomosing flakes are filled with zeolite (HQ-25).

Grains average about 0.14 mm in length often with large length to width ratios, e.g. 4 to 9.7, the higher value for the thin-bedded lithofacies greywackes. Maximum grain size exceeds 1.5 mm. Muscovite is not as physically disrupted as some detrital phyllosilicates (biotite and chlorite) but may form an epimatrix locally.

Muscovite appears bimodal and grains smaller than about 0.072 mm may belong to a secondary population ranging to matrix size material, predominantly found adjacent to metamorphic and plutonic rock fragments, altering plagioclase or micaseous sedimentary rock fragments. A bimodal population was apparent also in the thin-bedded lithofacies where muscovite grains of reduced size, average 0.085 mm , were in association with rock fragments and plagioclase.

Muscovite, including authigenic white mica , which exceeded matrix size (0.02 mm) was counted with the detrital population.

6.   Biotite

Greywackes of the sandstone lithofacies and, to a lesser degree, the thick-bedded litho-facies contained biotite but it is scarce in the thin-bedded lithofacies greywackes. All biotite has pronounced pleochroism, very light yellow-brown, brown and dark red-brown with second order red, green and blue interference colours. Wavy extinction and kink bands are frequently observed.

Biotite is more disrupted than muscovite and may be squashed into unusual shapes to form epimatrix (KTW-16). Most biotite, especially smaller grains, shows some alteration to chlorite but its cleavage planes are more distinct. Biotite occurs in flakes to 0.9 mm, averaging about 0.2 mm. Biotite chemistry is given in Appendix 8.

7.   Chlorite

Chlorite content increases uniformly from the sandstone to the thin-bedded lithofacies (Figure 2.7) but its range is constant, except for a slight reduction in maxima and minima in the thick-bedded greywackes.

Both authigenic and detrital chlorite were included in this mode for practical reasons. Chlorite quantity does not effect the geological classification of the rock but it may well influence its engineering properties, and optical analyses may be correlated with other methods of assessing quantitative mineralogy, only if genesis is ignored.

Crystallite size of interstitial chlorite was determined by measurement of optical contin-uity limits, which accentuates smaller sizes in strained and wavy populations.

Chlorite was the most deformed of all phyllosilicate minerals and three types were present. (Chlorite chemistry is given and discussed in Appendix 8).

(i)   Chlorite after biotite: Colour - light green, light brown, occasionally colourless. Some, mainly green, shows Berlin blue anomolous interference colour (KS-10). Pleochroic scheme - green variety: colourless or light yellow green, light yellow-brown, light brown. Brown variety: light brown-yellow, brown, red-brown. Optical properties - undulose extinction, 2V about $20° - 60°$ positive (sometimes negative) with length slow orientation.

This is the most abundant ubiquitous variety of chlorite, easily confused with biotite but the latter has more distinct cleavage and stronger colouration.

Chlorite is flaky, often distorted and kinked (sometimes through 100°). Heavy minerals (epidote, euhedral magnetite and pyrite to 0.016 mm) are associated with it, as are authigenic pyrite growths in cleavage traces in bigger grains (1.0 mm) and inclusions of zircon with pleochroic halos (DC-1).

Altered biotite was often in close association with sedimentary and sericite schist rock fragments (DC-2). Biotite alters to chlorite at its periphery and along cleavage planes as seen in BQ-21 which has chlorite as its largest mineral grains. Average grain size was 0.275 mm with a length to width ratio between 3 and 8.

In the thin-bedded lithofacies, grain size was noticeably smaller, averaging 0.136 mm (maximum 0.56 mm) with a length to width ratio of 7 and there were inclusions of up to 0.008 mm, mainly pyrite and magnetite. Green biotite was rare in the lithofacies.

(ii) Detrital chlorite: Colour - as in (i) but brown variety interference colour, light yellow-brown, sometimes blotchy. Pleochroic scheme - green variety; colourless or light yellow-green, light green, green: brown variety; as (i) but lighter. Optical properties - as in (i) but harder to obtain from brown variety which also has a lower refractive index.

This is the least abundant variety of chlorite and is differentiated from authigenic chlorite by grain size and form. It is larger and more colourful than either chlorite after biotite or authigenic chlorite but was not usually as well formed being more crushed, strained and kinked. Cleavage planes were not well defined.

Grain sizes (maximum 0.5 mm, average 0.2 mm green 0.24 mm brown) were smaller than in chlorite pseudomorphs after biotite and measurement is difficult because of indistinct outline and length to width ratios of 1 or 2.

Detrital chlorite may appear in local concentration (BQ-IXA), often in association with smaller muscovite grains, and may contain elongate or equant pyrite in fine (0.005 to 0.021 mm) layers along cleavage planes and between grains (DC-1).

Authigenic chlorite may grow from detrital chlorite grains.

Similar in character in all lithofacies, detrital chlorite mean grain size (0.08 mm) is smaller in the thin-bedded greywackes.

(iii) Authigenic chlorite: In all lithofacies, this chlorite variety is established in matrix size crystallites to grains in optical continuity over 0.048 mm. The mergence of sizes is imperceptable, matrix material often being impossible to resolve into individual crystallites. The largest grains of authigenic chlorite may be associated with detrital chlorite grains and adding to them as a colourless to light green-yellow, equant growth with undulose extinction. Interference colours for such grains are light yellow, light green-brown or blue.

Optic properties include undulose or straight extinction and low 2V. Larger grain sizes are more easily defined and generally replace rock fragments. With decreasing size, authigenic chlorite merges with sedimentary rock fragment pseudomatrix as dark brown, poorly developed crystallites approximately 0.002 mm in size. In some rocks (HQ-17) authigenic chlorite may form interstitial fillings, 0.09 mm in size, (0.18 mm maximum,

DC-3) of type (b) matrix of Dickinson (1970), where it exists often as oriented fibrous clusters of crystallites 0.02 mm long.   In the same form it may be an intergrowth between flakes of non-metallic opaque material.

8.   Metamorphic accessories and cements

From Figure 2.8, the occurrence of authigenic minerals show marked increase from the sand-stone to the thin-bedded lithofacies.

Some authigenic minerals (quartz, albite, chlorite, pyrite), for reasons already discussed (section 2.6), were not included in this mode class since they were better counted in other mode classes for reasons of practicality, rock classification or engineering end use. Also, mainly adjacent to or part of veins (which were not included in optical modal analyses), they are relatively minor components compared with those detailed below, all of which may also be vein minerals.

8.1   Zeolite:

Laumontite and its anhydrous form leonhardite, are found commonly in greywackes of each lithofacies.   Its concentration depends on rock mean grain size and field location.   The radiating fibrous crystallites forming interstitial and replacement clumps, and their orientation, have already been mentioned (this Appendix 4.4(ii)).   These clumps may extend interstitially 0.2 to 0.4 mm in crystallites, typically 0.03 to 0.06 mm long but ranging up to 0.3 mm long and 0.1 mm in diameter.   Calcite is often associated at the base and sides of the clumps, generally in larger euhedral crystals which form after zeolite.   The replacement of basic volcanic rock fragments in radial or quadrant crystal groups has been discussed (this Appendix 4.4(ii)).

Optical properties of laumontite (best observed in HQ-17) show it to be optically negative and length slow, with a 2V of about 20° and undulose extinction.   It is colourless, homogenous and untwinned with interference colours of low first order, and low refractive index.

Adjacent to veins (OB-21) zeolite achieves larger grain sizes (0.48 mm).   Other associa-tions are characteristic, e.g. with sericitising plagioclase, again in spherulite form, and as an extensive cement (HQ-17) it isolates grains, forming sutured boundaries with them, replacing plagioclase and quartz (HQ-25).

Zeolite veins do not have sharply defined edges.   They are well crystallised, with 1° or 2° extinction angles (interstitial material displays undulose extinction) indicating that the crystallites are hydrated (laumontite) as opposed to material exposed in quarry faces on joint planes which is leonhardite.   Blebs of calcite as a late phase also occur in the veins.

The thin-bedded lithofacies has little zeolite cement which occurs mainly as a replacement mineral in basic volcanic rock fragments.

Zeolite may modify rock colour induced by biotite, chlorite, altered feldspars and matrix (e.g. HQ-17), the white colour of the mineral lowering the rock colour value.

8.2   Prehnite

Prehnite exists in a variety of forms:

(i)   A yellow-grey fine drusy material, interstitially (DC-1) eroding plagioclase and basic volcanic rock fragments, which is ubiquitous in some greywackes (KTW-15) as a cement. In this form, prehnite may form a fine rim or discontinuous margin, 0.004 mm wide, about detrital untwinned felspar and quartz (DC-3) and rock fragments (DC-2).   This cement, which may be intensified in areas adjacent to veining, is best seen in ultra-thin sections.

(ii)   A well formed, non-uniformly distributed cement.   In this form, prehnite occupies irregular patches, often as a fibrous, colourless mineral assemblage, with individual crystals varying from 0.016 to 0.7 mm (OB-21) and averaging 0.24 mm.   Interference colours are distinct; yellow-grey, yellow and yellow-red. Prehnite replaces surrounding grains of quartz plagioclase and rock fragments.   Preferentially, it is associated with plagioclase with sericitising twin planes (DC-6) and with basic volcanic rock fragments replaced by calcite (BQ-21).   Often replacement is observed as euhedral, well crystallised, twinned aggregates of prehnite in, and adjacent to, the grain being replaced.

(iii) Occurrance as a mineral in veins, which sometimes exceed 1.7 mm in width, displaying well formed crystals in optical continuity over 0.64 mm.   Often, these veins (KTW-15) host subangular detrital grains which "float" as individual grains of chlorite, quartz or opaques averaging 0.22 mm in size and often very etched.   Generally, vein margins are not well developed and vein prehnite may coalesce locally with interstitial prehnite cement - this is particularly true of smaller veins.   Larger veins usually digress little from a main path, but there is some erosion of adjacent sericitised feldspars and isolated quartz grains, indicative of local crushing which may lead to bifurcation of the vein. In such regions, crushing may rotate some minerals and sericite mixes with prehnite; limonite staining bordering the vein shows how such crushing facilitates water ingress. Epidote group minerals are often associated with prehnite veins (KTW-14).   In greywackes of the thin-bedded lithofacies, prehnite occurs mainly in elongate patches (0.128 mm), rarely interstitially and then poorly crystallised.

8.3   Calcite

In some rocks, calcite is the most obvious and most abundant cement/replacement mineral (BQ-xviii), completely enveloping some acid and basic volcanic rock fragments and feldspar (especially along twin and cleavage planes), replacing zeolite (HQ-16) and actively eroding quartz.   It is responsible in some cases for qualifying rock colouration (BQ-xviii).   Calcite occurs in two forms:

(i)   A discrete mineral, often in association with zeolite, prehnite, sericite and quartz. Veins are generally small and discontinuous, i.e. extending continuously only 0.6 mm in preformed fractures, which may also contain sericite and quartz.   The veins may be up to 0.16 mm wide (HQ-23) with included minerals, other than calcite, of matrix size (BQ-IXA). Calcite often occurs in veins, as a late phase in the centre portion of veins of quartz, prehnite and/or zeolite.

(ii)   Interstitial cement in patches or blebs from 0.01 to 0.3 mm (HQ-17, 1.5 mm), averaging 0.08 mm.   In this form, calcite is often twinned, associated with zeolite, and replaces rock fragments.   Extinction is generally undulose, and rhombohedral crystal outlines are clearly seen where cleavage is developed (HQ-25).   The irregular edges of interstitial calcite patches are a more pronounced brown colour and blebs may be restricted to

particular areas of the slide.   Although less important than zeolite for replacement
considerations,calcite replaces grains measuring 0.29 mm.   Calcite occurs more fre-
quently than zeolite in intersitial habit,though individual zeolite patches are larger.

Calcite also replaces chlorite, sometimes forming a late phase infilling within authi-
genic chlorite.   Calcite cement eliminates much matrix material in association with
severe erosion of detrital grains.   This is especially noticeable in the thin-bedded
lithofacies; in BQ-i all but the largest grains of chlorite in the matrix were replaced.
Detrital grains "float" in calcite cement.

Etching of the surface of grains being eroded or replaced by calcite extends to 0.015 mm.
This is most obvious in the thin-bedded lithofacies,where the restriction of calcite to
specific localities,is an indication of its ability to replace finer grained material
within the rock.   Areas with abundant calcite cement appear "well sorted" (BQ-iv).

8.4   Quartz

This mineral occurs,generally,in small (0.2 mm) interstitial patches and veins (DC-1, DC-2).
Interstitial cementing by quartz (in patches to 0.2 mm) is mostly in areas adjacent to
veining (OB-21) and occurs as a clear assemblage of sutured, strained, subhedral, 0.04 mm
grains, almost always attending a detrital quartz grain and sutured to it.   Sutures have
an amplitude of 0.16 mm.

The recrystallisation of quartz, especially (and plagioclase), is enhanced by recementation
after comminution (RSS-i).   Recrystallised grains are then difficult to distinguish from
detrital grains.   Authigenic quartz is more abundant in regions free of lutum, is associa-
ted with veins of various mineralogies, and has a larger size range than calcite.

Authigenic quartz is more obvious in greywackes of the thin-bedded lithofacies, the largest
grains often associated with quartz veins where recrystallisation has taken place (DC-8).

8.5   Epidote group minerals

These minerals are well formed and are associated with altering grains or may occur in
clumps of 0.3 mm,made up of elongate or subequant, 0.015 to 0.026 mm grains associated
with calcite and white mica and often with an orientation , possibly resulting from plagioclase
or volcanic rock fragment alteration.   They often occur adjacent to or within quartz or
quartz-calcite veins, appearing as fractured grains.

Grains of this group may have been more common than was apparent,as matrix size material
of prehnite, sericite and epidote have similar interference colours.   They are most
easily seen in ultra-thin sections with medium magnification and plane polarised light.

8.6   Pumpellyite

The mineral appears as equant, anhedral, blue-green or green coloured grains (averaging
0.005 to 0.008 mm), occurring interstitally or adjacent to veins.   Optic properties
include undulose or incomplete extinction, length slow orientation and a biaxial positive
(2V about 50°) figure.   The pleochroic scheme is: light green-yellow, light green, green.
The mineral is rare and sometimes formed a "salt and pepper" aggregate (HQ-25) of very
small (0.005 mm) crystals in parallel orientation.   In one such clump measuring 0.11 mm,
crystals were 0.005 mm long, fibrous, distorted and showed undulose extinction.

Pumpellyite is more intense, though generally lighter in colour, than green chlorite, is less pleochroic and under high power is seen to be authigenic.   It was distinguishable, with difficulty, under plane polarised light with low magnification.   Adjacent to veins of prehnite, pumpellyite may occur in larger grain sizes with long, indistinct boundaries and extinction angles of 24°, occasionally containing euhedral, square and hexagonal pyrite crystals 0.006 mm in diameter (DC-3).

8.7   Metallic opaques

These are principally pyrite, which may occur as thin (0.01 mm) flakes on joint faces and bedding planes in finer greywackes and argillites, and may grow to several millimeters. In thin section, the outline is irregular, drusy and eroded.   Single grains may be euhedral, square or hexagonal shaped to 0.012 mm.   In reflected light, pyrite provides a speckled bright yellow colour and is isotropic.   Pyrite (and opaque material generally) increases with increasing fineness of greywackes.   It has affinities to carbonaceous material, basic volcanic rock fragments and chlorite.

8.8   Axinite

A single occurrance of ?axinate has been reported from Wellington greywackes by Bird (in prep.).   ?Axinite may also occur in veins in RSS-ii(2).

From vein intersections, it appears that diagenetic/metamorphic paragenesis continued in the order of quartz - zeolite - prehnite - calcite.   Veins are often polyminerallic, mineral associations being as follows: prehnite - calcite, zeolite - calcite, quartz - zeolite, quartz - zeolite (some prehnite), quartz - calcite (some zeolite), quartz - prehnite - calcite, prehnite - quartz - calcite, albite - quartz - prehnite - zeolite - calcite, quartz - epidote, quartz - calcite - epidote, quartz - sericite.

9.   Detrital accessories

The abundance of detrital accessories was directly related to lithofacies (Figure 2.9), the thin-bedded lithofacies greywackes having most - a mean of 3.5 percent.   Ten accessories were identified.

(i)   Epidote: Probably the most common accessory mineral, it occurred interstitially as elongate, subangular to subrounded grains of moderate relief, high 2V, optically negative and length fast.   It usually displays incomplete, undulose or straight extinction, uneven fracture, and one well developed cleavage with a pleochroic scheme: colourless, yellow, yellow-green.   It is ubiquitous in grains averaging 0.19 mm in the thick-bedded, 0.14 and 0.71 mm in the sandstone and the thin-bedded lithofacies.   With mean size reduction, there was a change of dominance from epidote to zircon with increasing angularity of epidote grains.   A similar trend was noted for other detrital accessories (Table A3.1).

(ii)   Zircon: This occurs as colourless, or brownish, slightly birefringent, equant or elongate, cracked grains of high relief and wavy extinction which may be angular to rounded in form.   Generally, the larger (0.46 mm) grains are more angular, euhedral and twinned and show two cleavages.   Optically, the grains are uniaxial positive, length slow and have parallel extinction.   An euhedral square grain of zircon in biotite (HQ-25) displayed a pleochroic halo.   Zircon is the most common detrital accessory in fine greywackes.

(iii)   Sphene: This appears in grains of high sphericity, high interference colour, and high degrees of rounding (subangular to well rounded) which may be shattered, parallel twinned (BQ-V) and possess imcomplete extinction.   It is optically positive with high 2V (about 40°).   Larger grains may be euhedral or   subhedral, generally broken or chipped. In finer greywackes its mean size is reduced and the degree of rounding increases (DC-10).

(iv)   Apatite: This is present in clear, colourless, angular to rounded, subequant grains up to 0.25 mm in size (KTW-16) with high relief.   Larger grains are angular, smaller grains rounded.   It was observed as   euhedral angular crystals (0.001 to 0.005 mm) in metamorphic and plutonic rock fragments, also as inclusions (0.032 mm) in plagioclase/ quartz myrmekitic intergrowths.   Apatite has first order white interference colours and is near isotropic.   Grains often show plucking due to thin section preparation.

(v)   Tourmaline: Rare but distinctive, it occurs as euhedral broken and worn elongate grains with vivid second order interference colours.   Optically the mineral is length slow, has strain induced extinction angles up to about 7° and is colourless or grey.   It may occur in grains down to 0.009 mm.   Optical properties showed that grains were sodic and the mineral variety elbaite was present.   Tourmaline is often included in quartz and feldspar grains, elsewhere it is interstitial.

(vi)   Hornblende: This has sporadic occurrence but is present in typical form in DC-3 and KS-2, green with good cleavage in broken, ragged, elongate prisms.   Smaller grains can be confused with chlorite.   Chemical data are given in Appendix 8.

(vii)   Allanite: This has an even brown colouration, slightly pleochroic (light brown, green-brown, brown).   It occurs in subrounded grains displaying large 2V and is optically negative.

(viii) Augite: Augite is very rare; it is green, subrounded, subequant with one cleavage displayed.   It is biaxial positive with a pleochroic scheme; green-yellow, brown-green, green.

(ix)   Metallic opaques: Of this category, pyrite is by far the most important.   Pyrite occurred as a detrital grain (though most pyrite present is authigenic) up to 0.24 mm in size and ranging to matrix size.   Skeletal crystals were present in HQ-17, 0.049 mm in size.

Magnetite is also found interstitially, in conglomerates (KTW-16) of grains showing cubic forms   or as rounded and elongate fragments averaging 0.06 mm in size.

Chromite also occurs as discrete subhedral crystal grains, often translucent and brown at the edge of grains (HQ-17).

Detrital metallic opaques in greywacke of the thin-bedded lithofacies are all of matrix size.

(x)   Carbonaceous matter: Already mentioned (section 2.4), these are the leaf impres- sions manifest as carbon films impressed in greywacke and argillite.   The material is ubiquitous but occurs in haphazard fashion in greywackes, being intensely concentrated in some (KTW-G, IB-13A), (Grant-Taylor, 1976).

Carbonaceous matter occurs usually as discontinuous "strings" and patches, about 0.024 mm wide, often in association with authigenic pyrite and chlorite. Although strings of organic matter are irregularly oriented parallel to bedding, sublinear organic blebs, 0.01 to 0.02 mm, amalgamate to extend 1.5 mm, anastomosing through the rock parallel to bedding. Strings have "dusty", or finely (about 0.001 mm) crenulate outlines, (probably induced by scatter of carbon during thin section preparation), and a flaky or platy form. Generally, the more elongate they are, the more wholly carbonaceous. In reflected light the material is black with light grey streaks (HQ-25). Pressure shadow effects are apparent where chlorite has grown between carbonaceous flakes separated perpendicular to bedding (RSS-i). Carbonaceous strings attain a reduced maximum length of 0.48 mm in the thin-bedded lithofacies.

Table A3.1 : Mean grain size of detrital accessory mineral grains by lithofacies.

Detrital accessory mineral	Sandstone	Thick-bedded	Thin-bedded
Epidote	0.14 mm	0.19 mm	0.071 mm
Zircon	0.15 mm	0.24 mm	0.049 mm (max., 0.136 mm)
Sphene	0.16 mm	0.18 mm	0.03 mm
Apatite	0.11 mm	0.156 mm	0.055 mm
Tourmaline	-	0.09 mm	0.036 mm
Hornblende	0.15 mm	-	-
Allanite	0.24 mm	0.06 mm	0.088 mm
Augite	0.1 mm	-	-
Metallic opaques	0.06 mm	0.096 mm	0.024 mm
Carbonaceous matter	0.015 mm	0.029 mm	0.008 mm

10. Matrix

Matrix includes all interstitial detritus, whether recrystallised or not, smaller than the arbitary size of 0.02 mm and has been classified in part after Dickinson (1970). The range of matrix contents increases by lithofacies, from the sandstone to the thin-bedded lithofacies (Figure 2.10).

Dickinson recognises six varieties of interstitial constituents, viz:

(i)   Cement, which may be of calcite, prehnite, zeolite, chalcedony or other easily recognisable minerals uncommon in the rock framework.

(ii)   Homogenous, monominerallic phyllosilicate cement displaying textures indicative of pore filling.

(iii)   Protomatrix, a term for unrecrystallised detrital lutum.

(iv)   Orthomatrix, recrystallised detrital lutum which displays a relict clastic texture.

(v)   Epimatrix, a murky, polymineralic, diagenetic, pore filling material lacking the homogenity and textural evidence required for classification as phyllosilicate cement.

(vi)   Pseudomatrix; this discontinuous interstitial paste is formed by the deformation of weak detrital grains.   Argillaceous and altered volcanic rock fragments especially, fit this description, their boundaries conforming to the outlines of stronger grains and assuming irregular, attenuated shapes occupying volumes interstitial to the rigid grains.

For the greywackes studied, cements were counted in the mode of metamorphic accessories and cements.   The homogenous phyllosilicate cements generally were of larger grain size than 0.02 mm and were counted in the appropriate mineral mode, usually chlorite. Pseudomatrix was almost entirely various distorted rock fragments, but white micas, biotite, some detrital chlorite and carbonaceous matter also assumed pseudomatrix roles. All these grains were counted in their different mineral modes if their grain size exceeded 0.02 mm.

Most of the matrix discussed, therefore, and all counted in the matrix mode (less than 0.02 mm in size), is either protomatrix, orthomatrix or epimatrix.   To better establish interstitial conditions for each lithofacies, however, all six interstitial categories are used to indicate order of importance in interstitial condition.

The three main varieties of matrix occurring in all rocks are epimatrix, pseudomatrix and cements, in their general order of importance, sometimes with local occurrances of homo-geneous, monomineralic phyllosilicate cement and orthomatrix.

All detrital minerals occur in matrix size with the possible exception of biotite and some detrital accessories, e.g. hornblende.   The predominant matrix mineral appears to be chlorite, often with strong orientation, and present as a dark grey-brown or brown but sometimes yellow or yellow-green mass.   The latter colours are often masked by finely divided opaque minerals or cements, indeed, chlorite colouration may mask the true importance of sericite.

Average size for matrix material is about 0.009 mm, for grains resembling fine filaments between larger fragments, commonly separating them be less than 0.001 to 0.01 mm.   However, thin section study often misleads by apparently increasing the distances between adjacent grains.   Sericite, with yellow-white interference colours in flaky or tabular grains, may dominate matrix composition locally, adjacent to veins, rock fragments of schist, sedimen-tary rock fragments or altering plagioclase.   Sericite flakes average 0.01 mm.   Both chlorite and sericite impart a fabric orientation to most greywackes.   Locally, heavy detrital minerals, averaging 0.003 mm, in close proximity may be important (OB-21) matrix components, with or without sericite, and impart a drusy dark appearance;   chlorite is ubiquitous, however, and is of more restricted size range in matrix than sericite.

In the thin-bedded greywackes, slight differences are apparent in matrix constitution, e.g. notably more protomatrix is observed in the form of quartz and feldspar flakes (DC-LAM) augmenting the epimatrix, pseudomatrix and cements. Whereas sericite and chlorite may occur in subequal amounts in other greywackes, those of the thin-bedded facies have signifi-cantly less sericite.   Effects of mineral colouration enhance this reduction, chlorite masking minerals without such colouration (sericite) but distinguishing features include greater widths of chlorite flake with respect to sericite flakes.

Increased matrix modes do not appear to repress authigenic albite formation.

Metallic opaque minerals of matrix size, are more abundant in the thin-bedded lithofacies, although, their parameters are consistent for all lithofacies.   Most grains tend to be concentrated, with or without carbonaceous matter.   Most of the opaque grains are pyrite (60 to 80 percent); other minerals include magnetite, chromite, ?ilmenite, some leucoxene

(? from sphene) and carbonaceous matter.   Most of the pyrite is diagenetic as grains 0.008 mm.   Agglomerates of metallic opaques may extend for 0.16 mm;   carbonaceous matter for 0.2 mm.

Non opaque heavy minerals, e.g. epidote, sphene, tourmaline, are concentrated into fine layers in the rocks of the thin-bedded lithofacies.

Variations of matrix mineral habit are apparent:

(i)   Chlorite to 0.04 mm (in albite flakes), oriented with twin planes (HQ-25).

(ii)   Euhedral calcite crystallising in a "void" in chlorite matrix (type b, Dickinson, 1970, type (ii) this section), between grains (HQ-17).

(iii)   Sericite flakes, 0.009 to 0.04 mm in size, "entering" altering feldspar, and sometimes quartz, to depths of 0.048 mm, and closely surrounding these minerals as a distinct border or layer (KTW-14, KTW-15) 0.006 mm thick - the rock being otherwise cemented by prehnite in the same region.

(iv)   Chlorite, and especially sericite, of matrix size erodes grain boundaries of feldspar, quartz and rock fragments.

Tables 2.3, 2.4, 2.5 present optic modes of greywackes by lithofacies association.

APPENDIX 4

Basu plot: raw data.

These data were used to draft Figure 2.11.

Sample	Rock mean grain size, phi	Polycrystalline quartz, 2-3 units, percent	Polycrystalline quartz, >3 units, percent	Total polycrystalline quartz, percent	Undulatory quartz, extinction angle >5°, percent	Non undulatory quartz extinction angle ≤5°, percent	Metamorphic rank plotted
HQ-17	1.3	13.6	22.0	35.6	35.6	28.8	low rank
BQ-xviii	2.6	3.9	9.8	13.7	15.7	70.6	middle and upper rank
DC-1	2.7	10.4	5.2	15.6	43.0	41.4	low rank
DC-2	2.7	9.4	3.8	13.2	67.9	18.9	low rank
BQ-V	2.7	11.6	17.4	29.0	20.3	50.7	middle and upper rank
HQ-16	2.8	17.4	21.7	39.1	30.4	30.4	low rank
KTW-16	2.8	11.1	22.2	33.3	27.8	38.9	low rank
BQ-IXA	2.9	24.1	14.8	38.9	25.9	35.2	low rank

A minimum of 50 medium sand sized quartz grains were counted for each sample.

APPENDIX 5

Greywacke and argillite grain size data.

Grain size raw data for greywackes and argillites of the Wellington greywacke-suite rocks; tabulated in order of mean grain size by lithofacies association. Size classes are expressed in phi units.

Sample	-2.0 to -1.5	-1.5 to -1.0	-1.0 to -0.5	-0.5 to 0	0 to 0.5	0.5 to 1.0	1.0 to 1.5	1.5 to 2.0	2.0 to 2.5	2.5 to 3.0	3.0 to 3.5	3.5 to 4.0	4.0 to 4.5	4.5 to 5.0	5.0 to 5.5	5.5 to 6.0	6.0 to 6.5	6.5 to 7.0	>7	Totals
SANDSTONE LITHOFACIES																				
KTW-13				0.8	0.4	8.2	12.9	16.9	16.9	14.9	11.4	6.7	2.0	1.6	1.6		0.4		5.5	100.2
KTW-14					0.4	3.0	13.4	16.0	17.5	17.5	12.3	4.5	5.2	1.9	5.6		2.2		0.7	100.2
RSS-12						0.4	8.4	20.2	27.9	21.0	5.7	6.5	0.8	2.3	0.8		1.9		4.2	100.1
BQ-xviii					0.4	1.9	7.9	15.8	19.2	24.1	13.9	6.0	4.5	1.9	4.1		0.4		-	100.1
DC-1				0.8		1.2	8.8	18.3	19.5	19.9	13.2	5.6	4.8	3.6	2.0		2.0		1.0	100.1
DC-2						4.7	13.0	32.7	16.9	9.5	9.1	4.3	3.2	3.5			3.2		-	100.1
BQ-V						2.4	8.8	16.6	18.0	15.9	13.6	11.2	4.8	3.1	3.7		2.0		-	100.1
WCC-13A						0.4	5.8	18.2	23.6	19.3	9.7	7.3	6.6	2.7	2.3		1.5		2.7	100.1
KTW-15			0.4		0.8	3.9	11.8	13.7	20.8	14.9	7.1	7.8	3.5	3.9	5.1		4.3		2.0	100.0
KTW-17					3.9	2.4	11.4	15.3	15.3	11.0	12.2	8.6	5.5	2.8	5.1		3.1		3.5	100.1
SJ-6					0.4	3.9	9.5	14.6	18.1	18.9	8.7	7.5	7.1	3.2	3.9		3.2		1.2	100.2
KTW-16					0.4	3.8	8.6	14.5	16.9	19.0	10.7	9.7	3.8	4.8	5.5		2.1		1.0	100.1
BQ-IXA						0.4	8.2	18.9	15.6	18.9	11.1	9.1	4.5	4.9	4.9		3.3		-	99.8
OB-21						2.0	7.6	12.8	22.4	15.2	11.2	10.4	4.8	3.2	4.8		3.6		2.0	100.0
DC-3							0.8	3.4	20.5	30.0	19.0	10.7	5.7	3.4	3.8		2.7		-	100.0
HQ-27					0.7	6.7	6.7	7.5	12.4	14.9	14.2	11.7	6.7	6.4	4.6		3.6		3.9	100.0
SJ-2								3.4	12.2	27.5	27.1	14.9	9.5	1.0	1.7		1.4		1.4	100.1
KS-2						1.9	2.3	10.1	18.0	21.0	12.0	8.6	6.4	5.2	5.2		4.5		4.9	100.1
NC-8							2.3	11.7	13.5	16.9	12.0	12.4	9.4	7.5	5.3		3.0		6.0	100.0
KS-10						0.3	1.7	8.8	13.5	15.8	10.8	15.2	11.8	6.7	8.4		3.0		4.0	100.0
THICK-BEDDED LITHOFACIES																				
DC-6	3.3	6.3	6.6	2.2	1.5	4.0	16.5	28.7	14.3	5.2	4.8	1.8	1.1	1.1	1.8		0.7		-	99.9
HQ-17				2.0	11.0	18.5	32.5	19.0	7.0	2.0	0.5	2.5	2.5	1.5	1.0		-		-	100.0
SJ-3$_1$			1.7	3.5	4.1	14.1	26.9	18.6	12.8	8.3	3.1	1.7	3.1	0.7	1.0		0.4		-	100.0
HQ-21				0.7	2.8	5.5	10.7	14.4	15.5	10.3	14.1	8.6	4.1	4.1	2.8		3.1		3.4	100.1
HQ-23					0.4	1.8	9.9	17.5	19.3	16.8	9.9	9.9	7.3	2.9	2.9		1.5		-	100.1
HQ-16					1.8	6.7	8.5	13.4	13.4	16.5	11.3	10.7	5.5	3.7	4.9		2.7		0.9	100.0
HQ-25					1.5	4.2	10.4	17.2	11.9	15.3	14.2	7.7	3.1	4.2	4.2		2.3		3.8	100.0
HQ-19					1.2	6.3	4.7	15.4	13.4	17.4	9.1	8.7	5.5	5.1	5.5		3.6		4.0	99.9
KTW-G					0.7	1.0	2.7	3.1	10.3	7.9	6.2	15.1	17.1	8.6	12.7		6.2		8.6	100.2
BQ-21					0.4	1.6	2.4	3.6	4.7	10.3	14.6	13.0	12.3	10.7	13.8		7.1		5.5	100.0
THIN-BEDDED LITHOFACIES																				
BQ-iv				0.4		1.1	3.9	12.6	11.2	16.5	12.3	12.3	9.5	6.7	4.6		3.5		5.6	100.2
DC-10								3.9	23.5	25.8	17.7	8.5	5.0		4.6		2.3		8.9	100.2
BQ-iii							0.4	1.5	5.5	14.7	22.4	24.6	7.7	9.6	6.6		2.9		4.0	99.9
RSS-i							0.7	2.4	9.9	16.0	19.7	16.0	10.5	6.8	6.8		5.1		6.1	100.0
RSS-iii							1.2	6.3	8.2	19.6	9.8	9.4	10.2	8.2	11.4		8.6		7.1	100.0
KTW-i									0.4	6.4	14.3	23.4	26.2	11.1	10.7		6.0		1.6	100.1
DC-8									0.4	1.2	5.8	21.5	34.6	13.5	12.3		3.9		6.9	100.1
SJ-T							0.4	-	-	1.5	5.1	17.6	23.8	19.8	9.5	9.9	2.9	4.8	4.8	100.1
DC-LAM							0.8	0.8	1.5	2.7	16.5	24.9	18.0		20.3		7.7		6.9	100.1
BQ-i									0.8		3.8	8.6	24.0	23.2	29.6		5.6		4.5	100.1
KTW-V											3.5	6.1	25.2	23.5	19.1	5.2	1.7	4.4	11.3	100.0
RSS-ii							0.4	-		2.0	4.0	10.8	14.8	23.2	22.8		7.6		14.4	100.0
ARGILLITES																				
HQ-26									0.4	2.0	5.9	10.7	15.4	24.5	15.8	9.5	5.5		10.3	100.0
NC-15											2.7	13.7	22.8	19.0	16.0	6.5	6.8		12.6	100.1
HQ-24										1.1	2.5	8.7	13.7	21.7	21.7	13.4	8.3		9.0	100.1
OB-W									0.4	-	0.8	3.1	11.5	14.5	19.9	17.9	10.3		9.5	100.1
HQ-20											0.8	5.7	12.2	16.0	24.3	13.3	11.4		16.4	100.1
WCC-8A									0.4		4.7	4.3	16.7	12.0	23.6	9.7	13.2		15.5	100.1
WCC-5A										1.1	2.2	8.6	10.8	14.6	20.2	11.6	11.2		19.8	100.1
HQ-18									0.4	-	0.8	0.4	6.1	12.3	18.0	17.2	14.2		11.5	19.2	100.1
BQ-vii											0.4	1.5	4.0	11.0	16.9	18.8	8.5		9.9	29.0	100.0
HQ-22									0.4	0.4	1.6	3.5	6.7	15.7	19.6	13.3	10.2		28.6	100.0
OB-13													0.4	4.1	11.7	24.5	18.6	16.6	24.1	100.0
TYPICAL REPEATS																				
DC-2						2.0	4.1	12.9	30.1	19.7	10.1	10.2	4.3	3.0	3.5		1.6		-	101.5
KS-10							2.3	17.9	14.5	15.3	10.7	13.4	7.6	3.4	6.9		3.8		4.2	100.0

APPENDIX 6

Quantitative analysis by X-ray diffraction.

Measurements of bulk mineralogy by X-ray diffraction.   Samples and appendix prepared by W. Yardley.

1.   Theory:

Klug and Alexander (1974) showed that:

$$I_j = \frac{C_j X_j}{\rho_j \bar{\mu}}$$

where I_j = net diffracted intensity of jth component in an n-component system.

C_j = constant of diffractometer geometry, and of component $_j$.

ρ_j = density of component $_j$.

$\bar{\mu}$ = linear absorption coefficient of the sample.

Similarly for an internal standard, s, in the sample:

$$I_s = \frac{C_s X_s}{\rho_s \bar{\mu}}$$

where $\dfrac{I_j}{I_s} = \dfrac{X_j C_j \bar{\mu} \rho_s}{X_s C_s \bar{\mu} \rho_j}$

C and ρ are constants, so $\dfrac{X_j}{X_s} = k \dfrac{I_j}{I_s}$

Therefore, if the internal standard is added in a constant proportion, so that X_s is constant for each sample analysed, then:

$$X_j = k \frac{I_j}{I_s}$$

regardless of absorption differences between samples.

2.   Preparation of standard samples:

The following minerals, with respective d-spacings, were used to set up standard calibration curves.

Quartz	Albite	Muscovite	Chlorite
4.27Å	3.19Å	10.0Å	7.14Å

Microcline		Calcite	Dolomite
3.25Å		3.04Å	2.89Å

Lithium fluoride (LiF) was chosen as an internal standard, as its peak at 2.33A does not overlap any peaks of the above minerals.

LiF was added in the proportion 0.250 gm per 1.000 gm of sample, and the materials thoroughly mixed by grinding in an agate mortar for several minutes.   The materials must be ground very fine to minimise scaling errors, which increase with particle size.

Typical scaling errors (Klug and Alexander)

<0.005 mm, 1 percent; 0.005 to 0.015 mm, 2 percent; 0.015 to 0.050 mm, 18 percent

I_j/I_s was measured from the diffractometer trace. Intensities were taken as peak height times peak width at half height (above background level). This takes into account broadening of peaks with size reduction of crystallites.

Calibration charts were drawn up for I_j/I_s (%) versus x_j for different concentrations of the pure minerals. Each point was the average of 3 determinations. The line of best fit, and the value of the constant k for each mineral was determined.

XRD quantitative standards, percent by weight of mineral

Sample	Quartz	Albite	Muscovite	Chlorite	Microcline	Calcite	Dolomite
Q1	80	10	10				
Q2	60	20	20				
Q3	40			40		20	
Q4		80		10		10	
Q5	20		60				20
Q6		40		60			
Q7			40		60		
Q8	10				10		80
Q9				80	20		
Q10		60			40		
Q11				20	80		
Q12						60	40
Q13						40	60
Q14		10				80	10

3.   Results of calibration runs I_j/I_s percent

X_j = k I_j/I____ . k = slope on graph

4.   Proportions from unknown samples:

LiF is mixed with the ground sample in an agate mortar in the proportion 0.250 gm per 1000 gm of sample.

Part of the mixed sample is mounted on a glass plate with acetone and left to dry.   The sample is then run and the peak areas measured.   The ratio I_j/I_s is calculated for each mineral and the corresponding concentration, x_j (%), read off from the calibration charts, or calculated using the correct constant, k.

At least 3 runs should be made for each sample to minimise errors.

5.   Errors:

Automatic scanning produces errors of >10 percent (relative) for mineral concentrations of over 10 percent.   (Klug and Alexander).

By summing all components, and correcting to 100 percent total components, errors can be reduced to probably ±5 percent relative for concentrations over 10 percent.   It would be misleading to present results other than rounded off to the nearest percent.

Obviously, where amorphous material, or uncalibrated minerals are present, this correction cannot be applied.

A further error of unknown magnitude arises where the mineral in the sample has a different composition or has been strained, compared with the mineral standard used for calibration. This is probably most significant with the feldspars.

6   Results:

EN 24/64[+]   XRD Analysis

Mineral	Normative modes from chemical analysis	Run 1 initial	Run 1 final	Run 2 initial	Run 2 final	Run 3 initial	Run 3 final	Average corrected
Quartz	20	19	19	25	21	24	20	20
Calcite	10	9	9	12	10	13	10	10
Dolomite	70	71	72	80	68	85	70	70
	100%	99%	100%	117%	99%	122%	100%	100%

HQ-17	Modal[*] analysis	Run 1 initial	Run 1 final	Run 2 initial	Run 2 final	Run 3 initial	Run 3 final	Average corrected
Quartz	43	55	51	50	47	50	44	48
Total feldspar	48	44	41	48	45	56	49	45
Chlorite	3.8	5	4	4	4	4	4	4
Mica	4.6	4	4	5	5	4	4	4
	99.4%	108%	100%	107%	101%	114%	101%	101%

"initial" — "final" is recalculation procedure to 100 percent.

+   Sample from petrology collection, Geology Department, Victoria University of Wellington.

*   Modal analysis of rock HQ-17 disregarding matrix or rock fragments as mode classes, alteration products within other minerals were counted in the mode of the alteration mineral.   Cements and accessory minerals were disregarded.

APPENDIX 7

Fabric measurement of Wellington greywacke-suite rocks

The term rock fabric refers to the relationship of grains, to each other and to adjacent strata - a fundamental determinant in some engineering properties. The directional aspect of fabric (rock anisotropy) is of particular importance as this affects weathering, strength, elastic modulus and crushed particle shapes.

Two approaches were used in assessing fabric relationships, the natures of grain contacts and grain orientations.

1. Grain contacts (qualitative):

Four grain to grain contact types were considered, using the nomenclature of Taylor (1950).

(i) Sutured contact: stylolitic interpenetration of two or more grains, indicative of pressure solution.

(ii) convex-concave: a contact interface appearing as a curved line in the plane of the thin section.

(iii) Long: a contact appearing as a straight line in the plane of the thin section.

(iv) Tangential: a contact appearing as a point in the plane of the thin section.

The above classification is arranged in order of decreasing diagenesis/metamorphism. Rock fabrics are extremely variable, even within a single thin section, and various grain contact types may occur depending on textural considerations, sorting and mineral composition.

To provide a basis for qualitative assessment each grain contact type was allocated a number.

Sutured	1
Convex-concave	2
Long	3
Tangential	4

The order of abundance of each type was established by assessment at several locations, along a linear traverse of the thin section, using a mechanical stage, normal to any preferred orientation. The sum of the products of abundance order and quality order, gave a qualitative rating, from 20 for the lowest relative diagenetic effect to 30 for the highest, which can be expressed conveniently by histogram. Only greywackes from the sandstone and thick-bedded lithofacies were examined, grain size considerations prevented accurate resolution in the thin-bedded lithofacies (where sutured contacts "appeared" dominant). Argillites were not examined.

The results (Figure A7.1) indicate samples from the sandstone lithofacies to have been compacted and metamorphosed to a greater extent, than samples from the thick-bedded lithofacies.

Sample	Decreasing importance of occurrence				Factor of relative diagnetic effect
	1	2	3	4	
KTW-14	S	C	L	T	30
KTW-15	S	C	L	T	30
OB-21	C	S	L	T	29
DC-3	C	S	L	T	29
BQ-IXA	C	S	L	T	29
KTW-16	S	L	C	T	29
BQ-xviii	L	S	C	T	27
KTW-13	L	S	C	T	27
DC-2	C	L	T	S	24
BQ-V	L	C	T	S	23

S = sutured
C = convex-concave
L = long
T = tangent

Sandstone lithofacies

Thick-bedded lithofacies

HQ-25	C	L	T	S	24
HQ-17	C	L	T	S	24
HQ-19	L	C	T	S	23
HQ-21	T	L	C	S	20
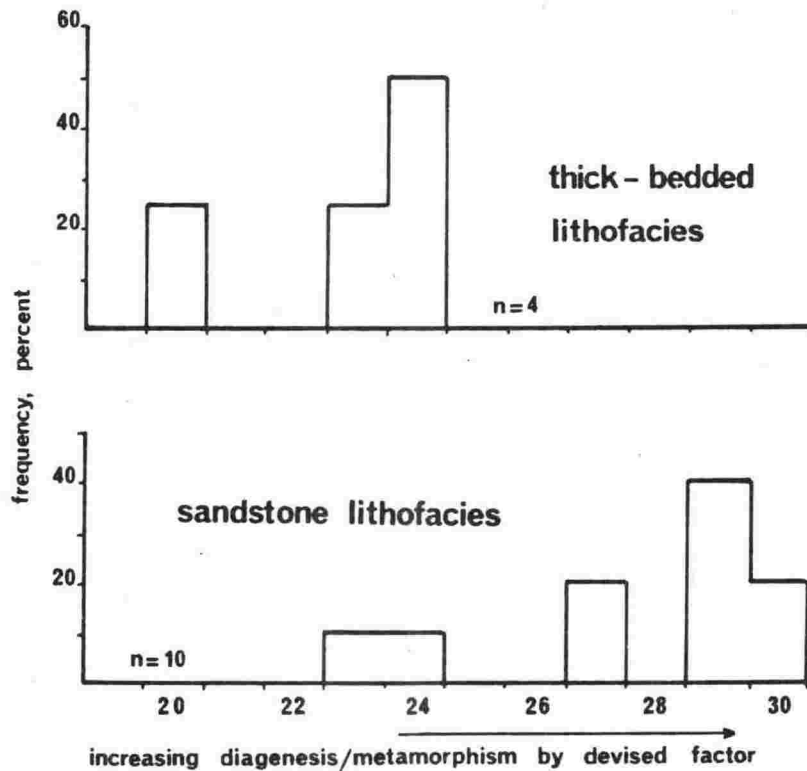
Figure A7.1 : Grain contact types in relative order of importance by lithofacies. By establishing a dimensionless factor (see text) the sandstone lithofacies displays grains in more intimate contact.

Pressure solution of quartz grains (manifest as sutured grain contacts with or without overgrowths) and quartz veining, increases the competence of rocks (Thomson, 1959). This, with other diagenetic/metamorphic processes, reduced porosity to a minimum, limiting later movements of fluids to regions of induced porosity (joints, shears, fissures), often observed as a deposition of saw-tooth quartz or vein infillings. Where fluids are alkaline, pressure solution (with or without clay coatings), erosion and rounding or quartz may proceed as suggested by Thomson (1959) and Siever (1962) and indicated by the presence of calcite, prehnite and laumonite.

In the finer grained greywackes (i.e. the thin-bedded lithofacies) this process must have been particularly significant. Smaller quartz grains dissolved more readily than larger ones (Weyl, 1959) to produce some rounded grains, sutured grain contacts and provide competence in thinly bedded rocks, to enable fracturing and access of metamorphic minerals, and to provide an explanation of the equant felsic grains, high strength and high elastic modulus of thin-bedded greywackes (section 3.5.2).

2.   Quantitative fabric assessment by Packing Proximity (Kahn, 1956).

Packing proximity was measured in conjunction with measurement of grain contact types; it is a measure of grain "closeness". The maximum value is 100 percent, when all grains are in contact with one another. Packing proximity is expressed by:

$$\frac{\text{total number of grain/grain contacts encountered}}{\text{total number of grains encountered}} \times 100 \text{ percent}$$

Several results were averaged for one rock and traverses were made at 90° to any preferred orientation, so that maximum values were recorded. Packing proximities may vary in any direction, and with composition and sorting. Coefficients of sorting should be taken into account when comparing packing proximities (Thomson, 1959), but was omitted in this study as all sediments measured are "poorly sorted" (Folk, 1968; see section 2.12).

Only the sandstone and the thick-bedded lithofacies were examined. Results are listed in Figure A7.2.

The use of packing proximity to assess greywackes is problematic, and results show the sandstone lithofacies to be packed similarly to the thick-bedded lithofacies. Minimum values are the same for both lithofacies but maximum values for the thick-bedded lithofacies are lower.

3.   Measurement of preferred orientation

Settling of particles results in an orientation that tends to parallel the sedimentation surface. The more flaky, prismatic, tabular, elongate or rod-like the mineral shapes, the more pronounced the orientation. Subsequent load, increases the strength of orientation (decreases scatter) by increasing the area of contact between grains, deforming them as necessary and reducing pore space and moisture content. The process continues until lithification is achieved.

Rock deformation has further increased the strength of grain orientation (Clark, 1970), brought about by settling (Onions and Middleton, 1968) and lithostatic loading (diagenesis) so that, ultimately, recrystallisation has further developed preferred orientation

Sandstone lithofacies

BQ-xviii	32
DC-1	67
DC-2	73
BQ-V	69
KTW-14	64
BQ-IXA	54
OB-21	75
DC-3	81
KTW-16	62
KTW-13	48

mean   63 percent

range   32-81 percent

Thick-bedded lithofacies

HQ-25	62
HQ-21	50
HQ-19	66
HQ-23	30
HQ-17	73
DC-6	61
SJ-3_1	75

mean   60 percent

range   30-75 percent
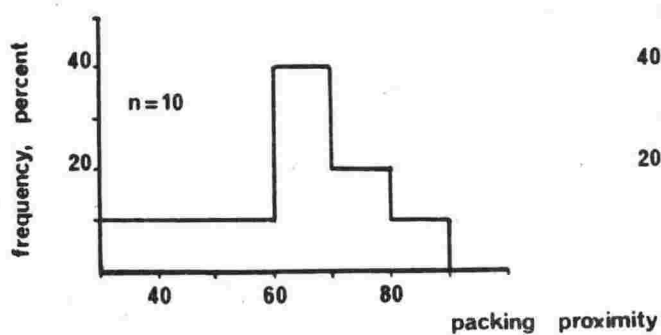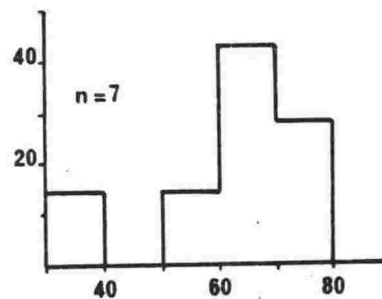
Figure A7.2 : Packing proximities for greywackes of the sandstone and thick-bedded lithofacies measured in directions perpendicular to bedding.

Strong grain orientation results in clustering of optic axial directions.   Quartz, for example, tends to recrystallise with its C-axis parallel to bedding, regardless of initial grain shape.   Recrystallisation of quartz and phyllosilicates, results in mineral growth in the direction of minimum stress, the finer grained greywackes, because of their greater particle surface area, responding faster than coarser greywackes.

Argillites formed from sedimentation of fine muds in various states of flocculation and have achieved degrees of preferred orientation.   Some display orientation textures indicative of shearing, due to large loading increments at low water contents e.g. HQ-18 (Morgenstern and Tchalenko, 1967).   Low water content tends to maintain random grain orientation (O'Brien, 1963) but most argillites display preferred orientation, therefore if original sediments were flocculated, sedimentation must have been rapid to entrap relatively large volumes of water (O'Brien, 1963; Blatt *et al.*, 1972).   Argillites show stronger preferred orientation than greywackes, their fabrics being unistrial similar to those shown by Brewer (1964; figures 115, 116, 117).

Quantification of preferred orientation is generally a time consuming, grain-by-grain measurement of long axes in thin section (Tobin and Donath, 1971).   Due to the large amount of time involved in this type of investigation, a less precise method involving simple techniques, was sought so that patterns of preferred orientation would emerge.

Various methods, using X-rays (Schulz, 1949a; Tchalenko *et al.*, 1971; Kazi, 1975) and/ or elaborate specimen preparation (Jetter and Borrie, 1953; Barrett, pers. comm.) were examined but abandoned in favour of methods used by Martinez (1958), Pierson (1959) and Sippel (1971), based on the orientation of quartz grains, one of several minerals showing definite preferred orientations in greywacke-suite rocks.

Using crossed nicols and a λ plate (older literature refers to a gypsum plate) with a phase difference of 550 nm, producing interference colours of first order red, addition or subtraction of small phase differences, changes the interference colours towards blue or yellow respectively.   The vibration directions of the λ plate, with different mineral orientations and resultant colours, is shown in Figure A7.3.

As thin sections had been cut perpendicular to bedding, maximum preferred orientations (therefore optically slow orientations) and maximum interference colour changes could be observed.   Different degrees of preferred orientation provide different distributions and intensities of yellow and blue colouration, when aligned with the λ plate in the manner shown in Figure A7.3.

Colour intensity, therefore, becomes a measure of preferred grain orientation which can be evaluated readily, on a semi-quantitative basis, by photography.

Thin sections were photographed, using Ilford Pan F black and white film, exposed through a standard blue Leitz microscope filter and a Kodak gelatin photomechanical filter No. 23A which effectively "blocks" blue light.   This allows only yellow and orange colours to be exposed to the film thus, when thin sections were arranged in format A of Figure A7.3, all grains displaying a preferred orientation would appear dark with other grains varying shades of grey.

Negatives were developed and printed on fine grained, hard, black and white paper to produce photographs of good contrast.   Subjective measurement of relative black and white areas of each photograph, to assess degrees of orientation, was not possible as fine grain sizes and low magnifications used were not conducive to this.   Low magnifications were necessary so that differences in preferred orientation were seen over large areas – important in coarser rocks – and also to enable standardisation of exposure settings. Several pictures of each thin section were taken.

slow vibration direction

A

long (slow) axes of minerals – preferred orientation

Blue interference colours;
optical addition

B

sensitive tint plate

long (slow) axes of minerals – preferred orientation

yellow interference colours;
optical subtraction
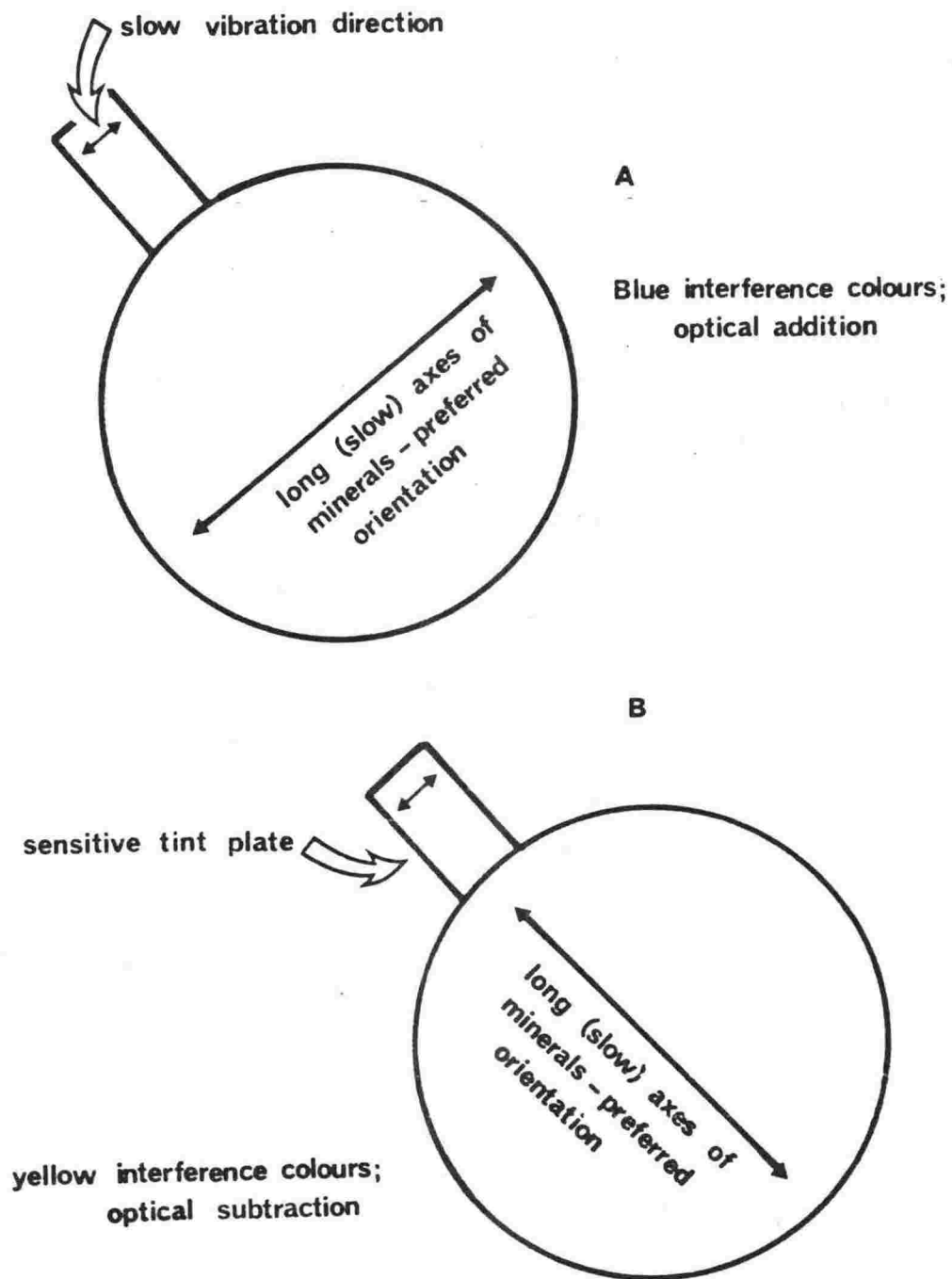
Figure A7.3 : Optical systems used with photomechanical filters to suppress or aid interference colours of optically length slow minerals.

Assessment was undertaken in two ways:

(i)   By inspection of shade, i.e. comparing relative areas of light and dark, and

(ii)   By inspection of observable preferred orientation trends in larger phyllo-silicate minerals.

To ensure impartiality during test, photomicrographs were not labelled and were shuffled face down between tests, while to check consistency, several photomicrographs from different regions of the same rock were included.   Results (Table A7.1) show the relative ranking of rock to be similar by both methods.

Mean grain size was ranked in addition to the fabric properties to check on the procedure ranking.   The close comparison of ranked and measured mean grain size indicates the reliability of the procedure.

Results show relative preferred orientation to correlate well with relative mean grain size, that is, strength of grain orientation increases with decreasing mean grain size (Figure A7.4).

Whilst the techniques is relatively quick, repeatable and convenient, results are not absolute and therefore not directly comparable with other works or engineering parameters. This severely restricts its usefulness.

Table A7.1 : Grain preferred orientation assessed from photomicrographs.

Order by rock mean grain size	Sample	Rock mean grain size, phi	Assessed from photomicrography using photo-mechanical filters		
			Order of diminishing mean grain size	Order of increasing opacity	Order of increasing mineral orientation
1	DC-6	1.25	HQ-17	HQ-17	HQ-17
2	HQ-17	1.317	SJ-3$_1$	DC-6	SJ-3$_1$
3	SJ-3$_1$	1.32	DC-6	SJ-3$_1$	OB-21
4	KTW-13	2.4	KTW-13	OB-21	BQ-IXA
5	HQ-21	2.7	OB-21	BQ-IXA	DC-6
6	BQ-V	2.73	HQ-21	HQ-21	HQ-21
7	BQ-IXA	2.9	BQ-IXA	BQ-V	RSS-ii
8	OB-21	2.93	BQ-V	KS-2	OB-13
9	HQ-19	3.08	HQ-19	KTW-13	BQ-V
10	KS-2	3.27	RSS-iii	HQ-19	KS-2
11	BQ-iii	3.78	KS-2	BQ-21	HQ-20
12	RSS-iii	4.08	BQ-21	RSS-iii	DC-8
13	BQ-21	4.13	BQ-21(R)	BQ-iii	HQ-19
13A	BQ-21(R)	4.13	BQ-iii	BQ-21(R)	BQ-i
14	DC-8	4.5	RSS-ii	RSS-ii	RSS-iii
15	BQ-i	4.87	DC-8	OB-13	KTW-13
16	RSS-ii	5.18	HQ-20	HQ-20	BQ-iii
17	EQ-26	5.4	BQ-i	DC-8	BQ-21
18	OB-W	5.6	BQ-vii	BQ-i	BQ-21(R)
19	HQ-20	5.87	OB-13	BQ-vii	HQ-18
20	HQ-18	5.95	HQ-26	HQ-26	BQ-vii
21	BQ-vii	6.18	HQ-18	HQ-18	HQ-26
22	HQ-22	6.28	HQ-22	OB-W	OB-W
23	OB-13	6.39	OB-W	HQ-22	HQ-22
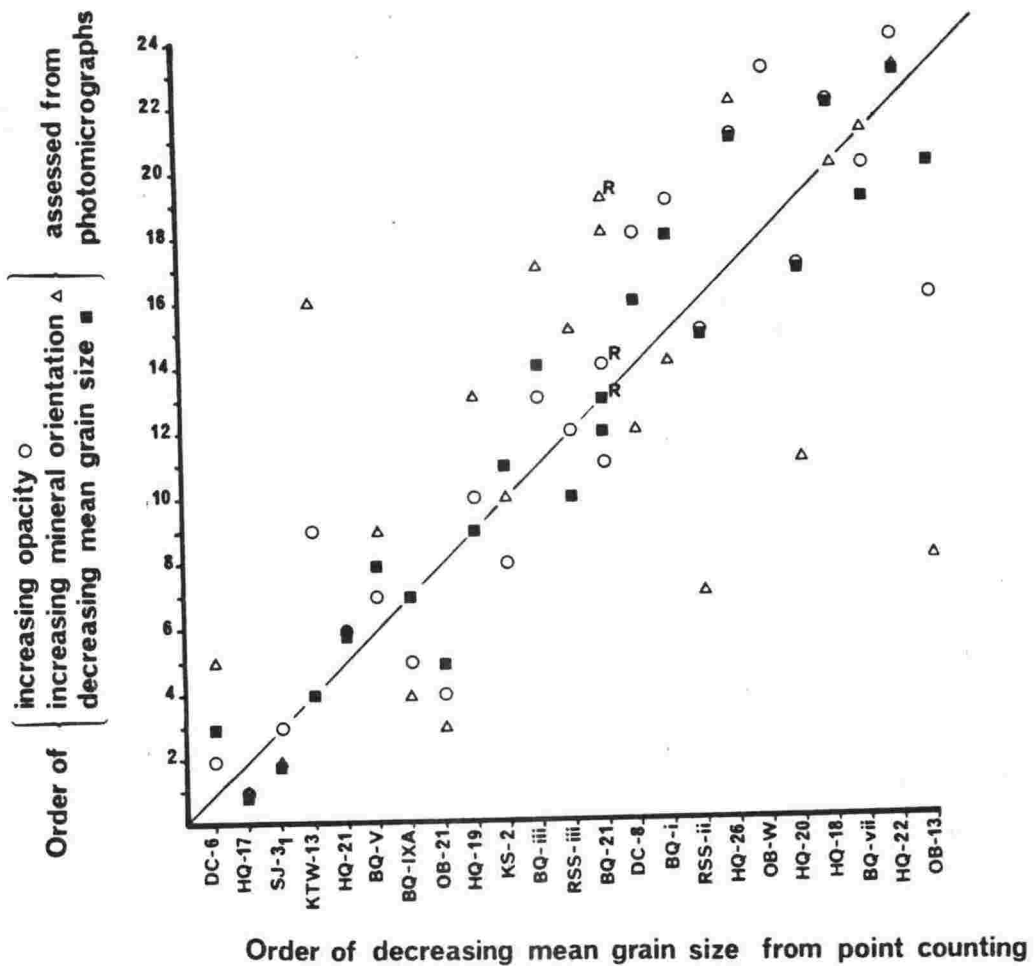
Figure A7.4 : Study of preferred orientation by petrography
indicates that relative mean grain size, degrees of
opacity and preferred orientation are related and show a consistent
trend with mean grain size measurements of Wellington greywacke-suite
rocks.

APPENDIX 8

Chlorite analysis by electron microprobe

Mr I. Pringle (Geology Department, Otago University) used an Electron Optics Laboratory electron microprobe, model JXA-5A, situated at that University, to ascertain the chemical affinities of green and brown detrital and authigenic phyllosilicate minerals, grouped as chlorite in modal analyses (section 2.6.6, Appendix 3). Some brown, broken accessory minerals were also probed for identification.

Test cores, 25 mm diameter, were taken from five greywacke lithologies known to contain adequate subject mineral and representing a wide textural range. Discs, 2.5 mm thick, were cut from the cores, arranged in textural order, stacked with epoxy adhesive to form a composite core, then cut longitudinally through a diameter. One of the half cylinders produced was epoxied to a glass slide and a polished thin section (probe mount), made by fine grinding and polishing to a thickness of 30 microns. A probing map of the grains to be examined was assembled.

1. Analytical method

Instrument settings were: 15 kV accelerating potential, 0.03 μA specimen current and 2-3 micron electron beam diameter. Each complete analysis was prepared by averaging 5 countings of 10 seconds integration time. Correction procedures for absorption, fluorescence and atomic number were those of Bence and Albee (1968) with correction factors given by Kushiro and Nakamura (1970).

Analyses were semi-automated using a PDP 8F computer, controlling peak search at pre-set peak positions, X-ray intensity measurements for peaks and backgrounds, dead time, Bence and Albee corrections and cation calculations. Drift correction was made by measuring probe current (using the synthetic periclase standard) just before the X-ray intensity measurements of each standard and unknown.

Standard materials used were: natural albite from Amelia (Na), adularia from Gotthard (K), hematite from Sennin mine (Fe), maganosite from Nodatamagawa mine (Mn), chromite from Acoje mine (Cr), synthetic corundum (Al), rutile (Ti), quartz (Si), wollastonite (Ca), synthetic periclase (Mg).

Technical problems, associated with probing phyllosilicates, arise from relatively high water contents and varied iron oxidation states. All iron was calculated as FeO. Percentage totals and cation totals are variable and give no indication of analysis accuracy, however beam current stability, and analysis of standards as unknowns, are means by which probe error can be minimised.

2. Results

Analyses shown in Table A8.1 include analyses of grains undergoing a biotite - chlorite transition (Table A8.2). Tables A8.3 and A8.4 present data from hornblende and biotite.

Table A8.1 : Electron microprobe analyses of chlorites and titano-chlorites (the latter five analyses) from Wellington greywacke-suite rocks. Total iron measured as FeO and H_2O determined as difference of analysis total and 100 percent. Numbers in brackets denote different analyses from one lithology.

	KTW-14(1)	KTW-14(2)	HQ-17(1)	DC-6(1)
SiO_2	27.6860	27.7479	27.6466	28.2941
Al_2O_3	16.5720	18.8719	21.1213	16.8992
TiO_2	0.6919	0.1356	0.0216	1.9436
FeO	27.1851	24.4961	22.6487	28.4723
MnO	0.2173	0.2821	0.8091	0.3609
MgO	15.2250	17.3959	17.9222	13.9729
CaO	0.1447	0.0798	0.0441	0.2720
Na_2O	0.0299	0.0256	0.0135	0.0000
K_2O	0.0378	0.0113	0.0270	0.3439
Total	87.7895	89.0462	90.2540	90.5588
H_2O	12.2105	10.9538	9.7460	9.4412

Numbers of ions on the basis of 28 oxygen equivalents ignoring H_2O.

	KTW-14(1)	KTW-14(2)	HQ-17(1)	DC-6(1)
Si	5.8937 } 8	5.7199 } 8	5.5656 } 8	5.8752 } 8
Al	2.1063	2.2801	2.4344	2.1248
Al	2.0514 }	2.3052 }	2.5769 }	2.0108 }
Ti	0.1109 }	0.0211 }	0.0033 }	0.3035 }
Fe^{+2}	4.8395 }	4.2224 }	3.8131 }	4.9442 }
Mn	0.0392 } 11.9284	0.0495 } 11.9725	0.1380 } 11.9317	0.0636 } 10.959
Mg	4.8317 }	5.3446 }	5.3787 }	3.4854 }
Ca	0.0330 }	0.0173 }	0.0095 }	0.0605 }
Na	0.0123 }	0.0100 }	0.0053 }	– }
K	0.0104 }	0.0024 }	0.0069 }	0.0910 }
Mineral colour	green	green	green	brown

	DC-6(4)	KTW-14(1a)	KTW-14(3)	BQ-IXA(1)
SiO_2	28.5256	29.7806	29.0941	29.4984
Al_2O_3	17.0053	16.9933	16.8990	17.8545
TiO_2	2.7756	1.2751	3.0373	1.6157
FeO	26.8845	28.8337	26.0171	24.5462
MnO	0.3229	0.3004	0.4545	0.3678
MgO	13.1658	12.8572	12.4588	15.1307
CaO	0.4049	0.2188	0.6966	0.1154
Na_2O	0.0504	0.0562	0.0393	0.0433
K_2O	0.5404	0.4429	0.5683	0.7240
Total	89.6753	90.7580	89.2650	89.8959
H_2O	10.3247	9.2420	10.7350	10.1041

Numbers of ions on the basis of 28 oxygen equivalents ignoring H_2O

	DC-6(4)	KTW-14(1a)	KTW-14(3)	BQ-IXA(1)
Si	5.9385 } 8	6.1482 } 8	6.0570 } 8	6.0294 } 8
Al	2.0615	1.8518	1.9430	1.9706
Al	2.1108 }	2.2830 }	2.2035 }	2.3306 }
Ti	0.4346 }	0.1980 }	0.4750 }	0.2481 }
Fe^{+2}	4.6805 }	4.9781 }	4.5298 }	4.1956 }
Mn	0.0568 } 11.6231	0.0526 } 11.6563	0.0801 } 11.4774	0.0636 } 11.6719
Mg	4.0860 }	3.9570 }	3.8668 }	4.6083 }
Ca	0.0904 }	0.0484 }	0.1554 }	0.0245 }
Na	0.0204 }	0.0224 }	0.0160 }	0.0146 }
K	0.1436 }	0.1168 }	0.1509 }	0.1866 }
Mineral colour	brown	green	brown	brown

Table A8.2 : Electron microprobe analyses of altering biotite-chlorite minerals.
Total iron measured as FeO and H_2O determined as difference of analysis
total and 100 percent.   Numbers in brackets denote different analyses
from one lithology.

	DC-6(1a)	DC-6(4a)	HQ-17(1a)	KTW-14(2a)
SiO_2	32.4090	32.6519	32.7546	32.2828
Al_2O_3	17.2386	16.7103	15.8706	21.2784
TiO_2	1.5724	3.7986	3.0384	2.6269
FeO	23.9776	22.1925	21.5722	21.2544
MnO	0.3044	0.3976	0.5168	0.3283
MgO	13.8341	13.6615	13.8703	10.9791
CaO	0.3876	0.2445	0.1488	0.1055
Na_2O	0.0430	0.0392	0.0363	0.1689
K_2O	2.0625	4.0039	3.2288	4.5422
Total:	91.8289	93.6998	91.0366	93.5662
H_2O	8.1711	6.3002	8.9634	6.4338
Mineral colour	brown	brown	brown/green	brown

Table A8.3 : Electron microprobe analyses of hornblende from Wellington greywacke-suite
rocks.   Total iron measured as FeO and H_2O determined as difference of
analysis total and 100 percent.   Numbers in brackets denote different
analyses from one lithology.

	KS-2(1a)	KS-2(1b)
SiO_2	46.6092	46.4711
Al_2O_3	7.6579	7.0745
TiO_2	1.4209	1.3268
FeO	14.5285	14.6968
MnO	0.5290	0.4304
MgO	12.7487	13.5782
CaO	11.8306	11.7274
Na_2O	1.3174	1.3307
K_2O	0.7217	0.7378
Total:	97.3638	97.3736
H_2O	2.6362	2.6264

Number of ions on the basis of 23 oxygen equivalents, ignoring H_2O.

	KS-2(1a)		KS-2(1b)	
Si	6.9143	} 8	6.9047	} 8
Al	1.0857		1.0953	
Al	0.2533 }		0.1437 }	
Ti	0.1586 }		0.1482 }	
Fe^{+2}	1.8024 }	5.1002	1.8261 }	5.1801
Mn	0.0666 }		0.0544 }	
Mg	2.8193 }		3.0077 }	
Ca	1.8805		1.8667	
Na	0.3788 }	2.396	0.3834 }	2.3899
K	0.1367		0.1398	
Mineral colour	green		green	

Table A8.4 : Electron microprobe analyses of biotites from Wellington greywacke-suite rocks. Total iron measured as FeO and H_2O determined as difference of analysis total and 100 percent. Numbers in brackets denote different analyses from one lithology.

	HQ-17(2)	HQ-17(3)	HQ-17(4)	HQ-17(4a)	BQ-IXA(2)
SiO_2	35.1198	34.6475	32.2040	34.4313	36.6752
Al_2O_3	19.7249	18.0907	17.1396	17.2256	22.2174
TiO_2	2.9991	6.3035	3.2928	2.8135	1.8269
FeO	19.4696	18.0759	17.5434	18.6475	16.5015
MnO	0.2476	0.4365	0.5366	0.5237	0.2174
MgO	9.3728	11.1126	13.3219	14.2282	9.7464
CaO	0.0470	0.2270	0.1472	0.0496	0.0762
Na_2O	0.1200	0.0753	0.1111	0.0474	0.1275
K_2O	8.9975	5.2318	9.1615	5.1553	5.6785
Total:	96.0981	94.2005	93.4580	93.1220	93.0668
H_2O	3.9019	5.7995	6.5420	6.8780	6.9332

Numbers of ions on the basis of 22 oxygen equivalents, ignoring H_2O

	HQ-17(2)		HQ-17(3)		HQ-17(4)		HQ-17(4a)		BQ-IXA(2)	
Si	5.2923	} 8	5.2043	} 8	5.0335	} 8	5.2536	} 8	5.4622	} 8
Al	2.7077		2.7957		2.9665		2.7464		2.5378	
Al	0.7956 }		0.4068 }		0.1908 }		0.3514 }		1.3619 }	
Ti	0.3399 }		0.7121 }		0.3870 }		0.3227 }		0.2046 }	
Fe^{+2}	2.4537 }	5.7265	2.2706 }	5.9333	2.2931 }	6.0460	2.3795 }	6.3578	2.0552 }	5.8131
Mn	0.0317 }		0.0554 }		0.0710 }		0.0678 }		0.0275 }	
Mg	2.1056 }		2.4884 }		3.1041 }		3.2364 }		2.1639 }	
Ca	0.0077		0.0365		0.0247		0.0081		0.0121	
Na	0.0350 }	1.7727	0.0220 }	1.0609	0.0337 }	1.8852	0.0141 }	1.0258	0.0367 }	1.1277
K	1.7300		1.0024		1.8268		1.0036		1.0789	

Mineral colour	brown	brown	brown	brown	brown

	BQ-IXA(3)	KS-2(1)	KS-2(2)	KS-2(3)	KS-2(4)
SiO_2	33.2146	35.2481	36.0030	35.7041	35.0274
Al_2O_3	20.3431	20.1806	16.1670	18.1081	14.8645
TiO_2	2.8557	3.3771	3.0105	2.0805	3.6369
FeO	18.2542	19.8506	16.3583	19.4379	17.5051
MnO	0.3945	0.2223	0.4440	0.1958	0.2272
MgO	11.2819	8.7518	11.8618	10.9959	13.6015
CaO	0.0397	0.0018	0.0765	0.1405	0.4853
Na_2O	0.1032	0.1242	0.1124	0.0939	0.0967
K_2O	5.7176	8.8649	8.5768	6.1793	5.3351
Total:	92.2043	96.6208	92.6102	92.9359	90.7795
H_2O	7.7957	3.3792	7.3898	7.0641	9.2205

Numbers of ions on the basis of 22 oxygen equivalents, ignoring H_2O

	BQ-IXA(3)		KS-2(1)		KS-2(2)		KS-2(3)		KS-2(4)	
Si	5.1137	} 8	5.2800	} 8	5.5579	} 8	5.4721	} 8	5.4681	} 8
Al	2.8863		2.7200		2.4421		2.5279		2.5319	
Al	0.8051 }		0.8429 }		0.4993 }		0.7428 }		0.2029 }	
Ti	0.3307 }		0.3806 }		0.3496 }		0.2398 }		0.4270 }	
Fe^{+2}	2.3503 }	6.1270	2.4867 }	5.6927	2.1118 }	5.7488	2.4913 }	6.0118	2.2854 }	6.1108
Mn	0.0515 }		0.0282 }		0.0581 }		0.0255 }		0.0301 }	
Mg	2.5894 }		1.9543 }		2.7300 }		2.5124 }		3.1654 }	
Ca	0.0066		0.0004		0.0128		0.0231		0.0369	
Na	0.0308 }	1.1605	0.0363 }	1.7307	0.0337 }	1.7357	0.0279 }	1.2592	0.0293 }	1.1288
K	1.1231		1.6940		1.6892		1.2082		1.0626	

Mineral colour	brown	brown	brown	brown	brown

3.   Mode of occurrence

Chlorite minerals are discussed in section 2.6.6 and Appendix 3 but salient points are restated for convenience.   Most of the chlorite in the Wellington greywacke - suite rocks, not resident in the matrix, is of detrital origin and may be considered as two populations:

(i)   Chlorite from alteration of titanium rich biotite

(ii)   Detrital chlorite.

Titanium rich chlorite constitutes the first population, as microscopic examination shows detrital biotite altering to chlorite along cleavage planes - this was confirmed by microprobe analysis (Table A8.2).

Both populations are considered to have common provenance, indicated as being of mainly metamorphic affinity by biotite chemistry (Deer, et al., 1971) also amphibole chemistry (Table A8.3).

Authigenic chlorites display berlin blue anomalous interference colours more often, perhaps indicating these to be less oxidised.   These chlorites are finer grained than their detrital counterparts, display "pinch and swell" forms (Sameshima, 1977) and grade in grain size to form orthomatrix, pseudomatrix, and epimatrix components (Dickinson, 1970).

The majority of grains analysed are (or altering to) chlorites.   Confusion in identification of biotite and chlorite is due to similarity in colour, habit and optical properties of some grains.   These problems were also noted by McKean (1976) and Sameshima (1977).

The latter studied Auckland greywacke-suite rocks and showed the chlorite to be oxidised (Table A8.5).   Optical properties of chlorite were presented in Appendix 3.   Although microprobe analysis was undertaken to confirm differences in phyllosilicate grains with otherwise similar appearance, an interesting occurrence of titanium-rich chlorite was noted (Table A8.1).   This is a probable product of chemical transition from titanium rich biotites and would explain their red-brown colour.   Such occurrences were noted by Sameshima (1977) and by Inomata and Tareyama (1974), who describe titano-penninite from altering phlogopites in ultramafic rocks of south-west Japan.

If the analysed chlorites are oxidised (Fe_2O_3 >4 percent) then the chlorites may be classified as chamosite (Figure A8.1).   The chlorite in Wellington greywacke-suite rocks is not oxidised, however.   Oxidisation of chlorites may be determined by two means.   In some, a high Fe_2O_3 content is associated with a low value for H_2O (Table A8.5), and when a structural formula is calculated on the basis of 28 oxygen equivalents, the total of the octahedral ions falls somewhat short of the ideal twelve (compare Table A8.1 with Table A8.5).   These are often reported as chlorites which have been oxidised (Deer, et al., 1971).

The oxidising reaction, where $Fe^{+2} \rightarrow Fe^{+3}$ with a loss of hydrogen, indicates that the water content should be low for an internally oxidised chlorite, and thus the elemental oxide total relatively high, say greater than 90 percent.   For these reasons the Wellington greywacke-suite rocks examined are believed to contain ortho-chlorite, specially pynochlorite (Figure A8.1).   Although not apparent from microprobe analyses, optical investigation indicated penninite to be present.   The chlorites plot in a relatively narrow field, variation in iron content being characteristic and high (20 to 30 percent total iron oxide).

Five of the analyses showed that the TiO_2 content, normally not more than 0.8 percent, was unusually high, all in excess of 1.0 percent with a 2.13 percent average.

Table A8.5 : Electron microprobe analyses of oxychlorites, extracted from Sameshima (1977). Structural formulae have been added. Where Fe_2O_3 is absent, total iron is measured as FeO. H_2O determined as difference of analysis total and 100 percent.

	1	2	3	4	5
SiO_2	32.49	29.37	29.81	31.77	30.34
Al_2O_3	15.54	17.93	17.58	17.22	14.20
TiO_2	1.53	1.43	5.61	1.17	2.35
Fe_2O_3	-	-	-	-	-
FeO	28.52	29.94	30.80	29.77	29.24
MnO	0.63	0.50	0.46	0.45	0.34
MgO	13.11	10.45	9.39	12.96	11.35
CaO	1.03	0.19	0.49	0.81	0.49
Na_2O	0.08	0.07	0.05	0.05	0.12
K_2O	0.72	0.56	0.55	0.30	0.43
Total:	93.65	90.49	94.74	94.50	88.86
H_2O	6.35	9.51	5.26	5.50	11.14

Numbers of ions on the basis of 28 oxygen equivalents, ignoring H_2O.

	1	2	3	4	5
Si	6.483 } 8	6.122 } 8	5.953 } 8	6.289 } 8	6.441 } 8
Al	1.517	1.878	2.047	1.711	1.559
Al	2.139 }	2.528 }	2.092 }	2.308 }	1.995 }
Ti	0.230 }	0.232 }	0.843 }	0.174 }	0.375 }
Fe^{+3}	0.000 }	0.000 }	0.000 }	0.000 }	0.000 }
Fe^{+2}	4.759 }	5.219 }	5.144 }	4.928 }	5.191 }
Mn	0.106 }11.567	0.088 }11.532	0.078 }11.216	0.075 }11.575	0.061 }11.489
Mg	3.899 }	3.246 }	2.795 }	3.823 }	3.591 }
Ca	0.220 }	0.042 }	0.105 }	0.172 }	0.111 }
Na	0.031 }	0.028 }	0.019 }	0.019 }	0.049 }
K	0.183 }	0.149 }	0.140 }	0.076 }	0.116 }

	6	7	8	9
SiO_2	28.93	29.75	26.78	27.11
Al_2O_3	15.51	15.22	15.66	17.42
TiO_2	3.17	1.93	1.66	0.35
Fe_2O_3	-	-	-	30.98
FeO	28.98	30.05	30.22	2.91
MnO	0.35	0.35	0.29	0.00
MgO	9.83	11.37	11.49	9.75
CaO	0.65	0.75	0.85	0.21
Na_2O	0.08	0.00	0.05	0.00
K_2O	0.32	0.13	0.00	0.00
Total:	87.82	89.55	87.00	88.73
H_2O	12.18	10.45	13.00	H_2O^- 0.51 H_2O^+ 11.07

Numbers of ions on the basis of 28 oxygen equivalents, ignoring H_2O

	6	7	8	9
Si	6.221 } 8	6.283 } 8	5.888 } 8	5.512 } 8
Al	1.779	1.717	2.112	2.488
Al	2.153 }	2.073 }	1.947 }	1.688 }
Ti	0.513 }	0.307 }	0.274 }	0.054 }
Fe^{+3}	0.000 }	0.000 }	0.000 }	4.740 }
Fe^{+2}	5.212 }	5.308 }	5.557 }	0.495 }
Mn	0.064 }11.363	0.063 }11.535	0.054 }11.818	0.000 } 9.977
Mg	3.150 }	3.579 }	3.765 }	2.954 }
Ca	0.150 }	0.170 }	0.200 }	0.046 }
Na	0.033 }	0.000 }	0.021 }	0.000 }
K	0.088 }	0.035 }	0.000 }	0.000 }

1. Stevenson and Sons Quarry, Drury, bottom cut typical argillite, D-5.
2. Winstones Russel Road Quarry, Whangarei, greywacke.
3. Winstones Russel Road Quarry, Qhangarei, greywacke.
4. Brynderwyn Quarry, Brynderwyn, argillite.
5. Moutohora Quarry, greywacke.
6. Moutohora Quarry, greywacke.
7. Moutohora Quarry, greywacke.
8. Titahi Bay, North Wellington, greywacke.
9. Chlorite, intersertal in spilite, Great Island, Three Kings Group, New Zealand, Battey (1956).
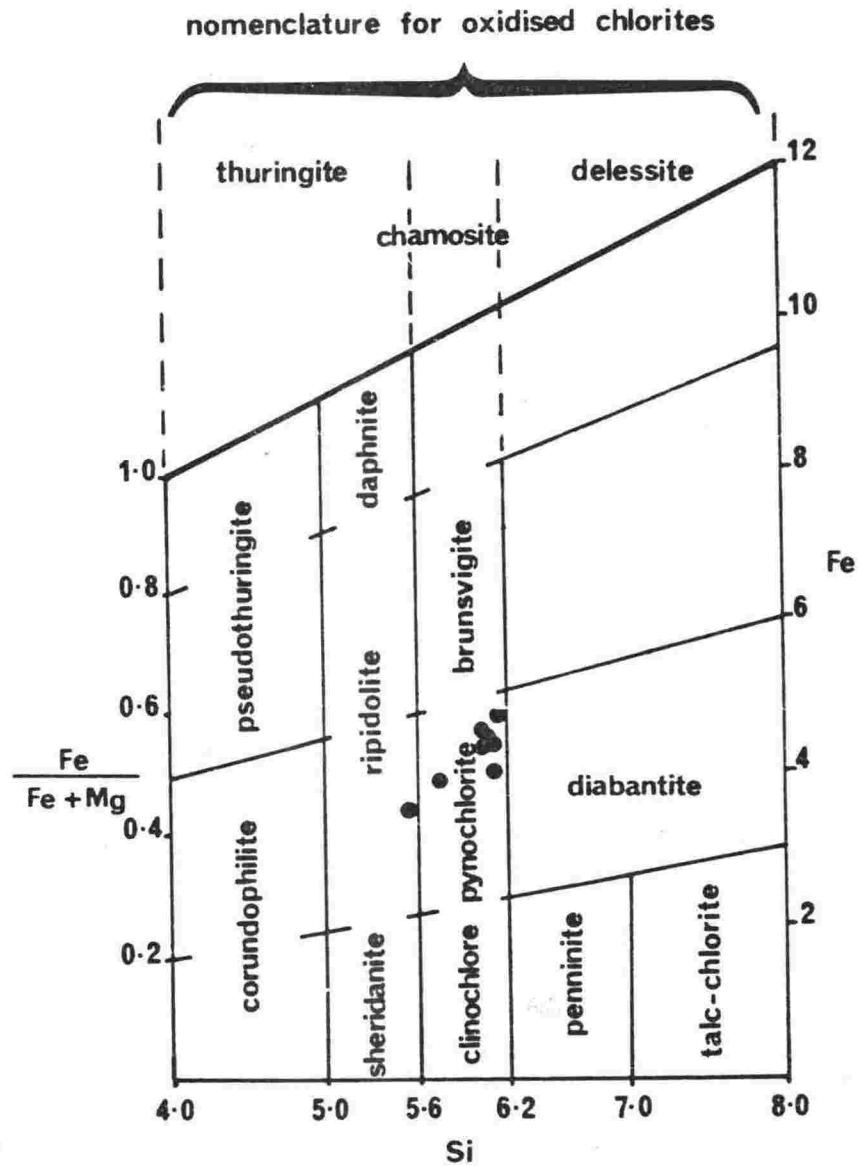
Figure A8.1 : Nomenclature of ortho-chlorites and oxidised chlorites (after Hey, 1954). Specimens for which analyses are given in Table A8.1 are plotted.

APPENDIX 9

Scratch hardness test to ASTM C235-68

This test was used to divide the Wellington greywacke-suite rocks into hard and soft lithologies.

A standard Vicat apparatus (reference ASTM test C191-77 'Standard method of test for time of setting of hydraulic cement by Vicat needle') was adapted to give a brass point, to ASTM C235-68, the required loading of 8.9 ±0.4N (2 ±0.1 lb) by adding weights to the stem (Plate A9.1). Rocks to be tested were positioned under the point and then drawn sideways. Tests were carried out on both natural and prepared planar surfaces.

The equipment is validated by the 1978 Annual Book of ASTM standards which features a specifically designed instrument of similar type, now commercially available (part 14, pages 512-4).
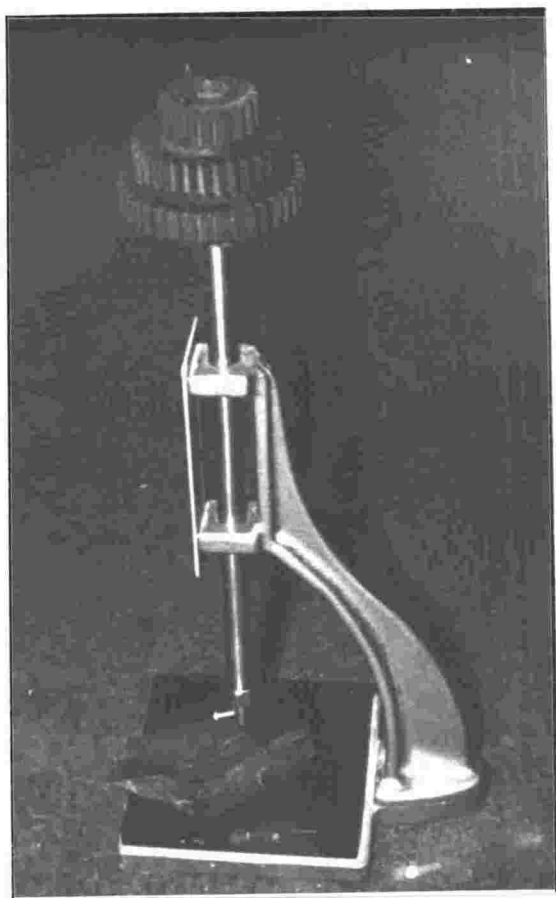
Plate A9.1 : Vicat apparatus (ASTM C191-77, 'Time of setting of hydraulic cement by Vicat needle'), adapted to perform the ASTM C235-68 'Scratch hardness of coarse aggregate particles'. Shown, are the weights added to the top of the spindle to meet weight specifications for the brass rod stylus, seen here easily scratching argillite (OB-W).

APPENDIX 10

Density, effective porosity and ultrasonic velocity of rock cores and handspecimens

The ultrasonic velocity apparatus requires that sample least lateral dimension - the dimension measured perpendicular to the path travelled by the pulse - be not less than the pulse wave length. Handspecimen samples were cut with up to three pairs of parallel faces for authogonal velocity studies to assess the degree of anisotropism. Handspecimen samples were tested saturated and oven dry and results are given in Table A10.1. Figure A10.1 is a graphic summary of handspecimen density data.

Table A10.2 lists density, effective porosity and ultrasonic velocity of rock cores, which were tested saturated and air dried (50 percent R.H.). Both moisture conditions were maintained at $20 \pm 1^{\circ}C$.

Table A10.1 : Densities, effective porosities and ultrasonic velocities of greywacke and argillite handspecimens.

Sample	Ultrasonic velocity $m.s^{-1}$		Rock densities $t.m^{-3}$			Effective porosity,	Ultrasonic velocity orientation w.r.t.
	dry	wet	dry	wet	particle	percent	bedding, and remarks
SJ-2	4724	4787	2.69	2.69	2.70	0.2	
SJ-2(R)	-	-	2.69	2.69	2.70	0.17	90°
SJ-2A	2196	4514	2.73	2.74	2.76	0.41	
SJ-3$_1$	5582	5553	2.72	2.72	2.74	0.3	parallel
SJ-3$_1$(R)	4579	5000	2.69	2.69	2.71	0.32	
SJ-3$_1$(R)	4964	5346	—	—	—	—	
SJ-3$_2$	5464	5431	2.68	2.68	2.69	0.22	
SJ-3$_2$(R)	-	-	2.66	2.67	2.69	0.38	
SJ-3$_3$	5106	5277	2.69	2.70	2.70	0.21	
SJ-3$_3$(R)	-	-	2.68	2.69	2.71	0.3	
SJ-4	5378	5517	2.73	2.74	2.75	0.23	
SJ-5	5472	5472	2.71	2.72	2.73	0.23	parallel
SJ-6	4607	4792	2.69	2.69	2.70	0.14	
SJ-6(R)	5408	5452	-	-	-	-	
SJ-6(R)	-	-	2.68	2.69	2.70	0.25	
KS-1	4525	5162	2.64	2.65	2.67	0.47	} 1 sample
KS-1(R)	4870	5262	-	-	-	-	
KS-1(R)	4423	5000	2.63	2.65	2.67	0.48	
KS-2	-	-	2.66	2.68	2.69	0.41	
KS-4	3269	4825	2.65	2.66	2.68	0.46	
KS-6	4252	4821	2.66	2.67	2.70	0.54	
KS-6(R)	-	-	2.66	2.67	2.68	0.28	
KS-7	-	-	2.56	2.60	2.66	1.38	
KS-7(R)	4261	4523	2.61	2.64	2.69	1.14	parallel
KS-8	4536	4941	2.64	2.65	2.66	0.28	
KS-8(R)	-	-	2.64	2.65	2.68	0.66	
KS-10	5112	5297	2.65	2.66	2.68	0.4	

Table A10.1 : continued

Sample	Ultrasonic velocity m.s^{-1}		Rock densities t.m^{-3}			Effective porosity, percent	Ultrasonic velocity orientation w.r.t. bedding, and remarks
	dry	wet	dry	wet	particle		
RSS-4	5217	5402	2.66	2.67	2.67	0.18	
RSS-5	5114	5226	2.65	2.66	2.68	0.47	
RSS-5(R)	-	-	2.66	2.67	2.68	0.29	
RSS-6	4367	5101	2.65	2.67	2.69	0.65	parallel
RSS-8	5388	5388	2.73	2.74	2.75	0.29	
RSS-8(R)	-	-	2.73	2.74	2.75	0.26	
RSS-12	-	-	2.67	2.68	2.69	0.28	
RSS-i	-	-	2.68	2.69	2.72	0.54	
RSS-ii	4788	5295	2.67	2.68	2.70	0.42	90°
RSS-iii	-	-	2.66	2.68	2.70	0.5	
WCC-2	4606	5191	2.67	2.68	2.69	0.23	
WCC-5A	3879	4206	2.70	2.72	2.76	0.72	90°
WCC-7	4821	5063	2.66	2.67	2.68	0.29	
WCC-7(R)	-	-	2.64	2.65	2.66	0.15	
WCC-8A	4530	4978	2.65	2.66	2.68	0.46	parallel
WCC-13A	5007	5273	2.67	2.67	2.68	0.14	90°
WCC-17	4608	5109	2.64	2.65	2.67	0.47	
WCC-18	4195	4938	2.63	2.65	2.68	0.67	
WCC-22	4459	4650	2.56	2.60	2.66	1.48	
WCC-22(R)	3841	4501	-	-	-	-	
WCC-22(R)	-	-	2.63	2.65	2.67	0.67	
WCC-23A	3820	4277	2.60	2.66	2.75	1.98	parallel
DC-1	4768	4991	2.66	2.67	2.68	0.22	
DC-2	4735	4862	2.63	2.63	2.63	0.13	
DC-3	-	-	2.66	2.67	2.69	0.5	
DC-6	4241	5364	2.57	2.60	2.65	1.07	90°
DC-8	-	-	2.66	2.67	2.70	0.48	
DC-10	-	-	2.67	2.68	2.69	0.24	
DC-LAM	3221	4397	2.62	2.65	2.71	1.36	90°
DC-LAM	4092	4640	-	-	-	-	parallel
NC-8	-	-	2.64	2.66	2.69	0.7	
IB-2	4890	5028	2.65	2.67	2.69	0.48	
IB-7B	4396	4796	2.65	2.66	2.67	0.27	90°
IB-8	3793	4467	2.56	2.59	2.63	1.0	90°
IB-11	3984	4016	2.70	2.72	2.75	0.65	90° cracked
IB-19	2765	3659	2.52	2.58	2.69	0.25	weathered
IB-22	1157	2955	2.41	2.52	2.71	0.46	90° weathered
KTW-1	4866	5046	2.68	2.68	2.69	0.2	
KTW-2	5264	5410	2.69	2.70	2.72	0.37	parallel
KTW-4	4864	5061	2.68	2.68	2.69	0.2	
KTW-4(R)	-	-	2.68	2.68	2.68	0.22	
KTW-13	-	-	2.67	2.68	2.70	0.42	
KTW-14	5321	5321	2.68	2.68	2.69	0.21	
KTW-14(R)	-	-	2.68	2.68	2.69	0.15	
KTW-15	5272	5409	2.70	2.70	2.71	0.14	
KTW-15(R)	-	-	2.72	2.72	2.73	0.08	

Table A10.1 : continued

Sample	Ultrasonic velocity m.s^{-1}		Rock densities t.m^{-3}			Effective porosity, percent	Ultrasonic velocity orientation w.r.t. bedding, and remarks
	dry	wet	dry	wet	particle		
KTW-16	-	-	2.67	2.68	2.69	0.26	
KTW-17	4155	4873	2.68	2.68	2.69	0.28	
KTW-17(R)	-	-	2.67	2.68	2.69	0.25	
KTW-i	5110	5251	2.69	2.69	2.70	0.14	
KTW-i(R)	-	-	2.69	2.69	2.70	0.22	
KTW-ii	5172	5138	2.68	2.69	2.70	0.36	parallel
KTW-ii(R)	-	-	2.69	2.70	2.72	0.44	
KTW-iii	4915	5188	2.70	2.72	2.76	0.87	parallel
KTW-v	-	-	2.70	2.71	2.73	0.34	
KTW-G	4203	4750	2.66	2.67	2.70	0.66	parallel
OB-1	5103	5342	2.65	2.66	2.68	0.47	
OB-1(R)	-	-	2.65	2.67	2.69	0.6	
OB-1(R)	-	-	2.64	2.65	2.68	0.65	
OB-11	2283	4375	2.71	2.73	2.76	0.6	90°
OB-12	4991	6172	2.68	2.69	2.69	0.2	90°
OB-13	4667	4471	2.72	2.74	2.77	0.64	parallel
OB-13(R)	-	-	2.70	2.74	2.81	1.4	
OB-14	4407	4491	2.68	2.69	2.69	0.07	90°
OB-21	-	-	2.65	2.66	2.68	0.44	
OB-W	-	-	2.73	2.75	2.78	0.72	
HQ-13	1636	3798	2.56	2.60	2.67	1.65	zeolitised
HQ-14	3609	4400	2.61	2.63	2.67	0.81	zeolitised
HQ-14(R)	3407	4299	2.61	2.63	2.67	0.92	zeolitised
HQ-15	-	-	2.68	2.69	2.72	0.57	
HQ-16	4527	4867	2.66	2.67	2.68	0.28	
HQ-17	3364	4440	2.57	2.59	2.62	0.85	parallel, zeolite bearing
HQ-17(R)	2895	3929	2.55	2.58	2.63	1.28	
HQ-17(R)	2422	3426	2.53	2.55	2.58	0.68	}
HQ-17(R)	2996	3439	-	-	-	-	} 1 sample
HQ-17(R)	2355	3686	-	-	-	-	}
HQ-17(R)	2336	3344	2.54	2.55	2.58	0.65	}
HQ-17(R)	2278	3576	-	-	-	-	} 1 sample
HQ-17(R)	1725	3113	-	-	-	-	}
HQ-17(R)	4175	5000	2.57	2.60	2.65	1.46	90°
HQ-18	3842	4450	2.49	2.49	2.50	0.29	
HQ-18(R)	4732	-	2.70	2.72	2.75	0.59	
HQ-19	5030	5147	2.67	2.67	2.68	0.25	
HQ-20	3361	4075	2.70	2.72	2.76	0.8	
HQ-21	4882	5108	2.64	2.66	2.68	0.52	
HQ-22	5278	4978	2.70	2.72	2.75	0.67	parallel }
HQ-22(R)	4677	4915	-	-	-	0.75	90° } 1 sample
HQ-22(R)	4711	4872	-	-	-	-	90° }
HQ-22(R)	-	4909	2.70	2.72	2.76	0.75	
HQ-23	4910	5031	2.62	2.63	2.64	0.26	
HQ-24	3915	4529	2.69	2.70	2.73	0.56	90°
HQ-25	4549	5198	2.66	2.67	2.69	0.46	90°
HQ-26	-	-	2.67	2.68	2.71	0.62	
HQ-27	4279	5045	2.61	2.64	2.67	0.88	90°

Table A10.1 : continued

Sample	Ultrasonic velocity m.s.$^{-1}$		Rock densities t.m.$^{-3}$			Effective porosity, percent	Ultrasonic velocity orientation w.r.t. bedding, and remarks
	dry	wet	dry	wet	particle		
BQ-6	4093	4844	2.66	2.67	2.68	0.37	
BQ-6(R)	-	-	2.65	2.66	2.67	0.28	
BQ-8	4446	4817	2.68	2.68	2.70	0.24	
BQ-8(R)	-	-	2.68	2.69	2.69	0.12	
BQ-10	4528	4364	2.67	2.67	2.68	0.18	
BQ-10(R)	-	-	2.66	2.66	2.66	0.07	
BQ-11	3216	4250	2.70	2.72	2.75	0.64	
BQ-15	4157	3926	2.72	2.72	2.72	0.04	90°
BQ-17A	4293	4942	2.67	2.68	2.68	0.06	90°
BQ-17B	5091	5227	2.70	2.71	2.73	0.4	90°
BQ-17B(R)	4776	5261	-	-	-	-	
BQ-18	4768	5294	2.68	2.69	2.70	0.19	90°
BQ-20	4118	4536	2.69	2.70	2.71	0.26	
BQ-21	-	-	2.69	2.70	2.71	0.27	
BQ-22	4902	5111	2.69	2.70	2.71	0.22	
BQ-22(R)	-	-	2.69	2.69	2.70	0.19	
BQ-27	4316	4754	2.71	2.72	2.74	0.33	90°
BQ-27(R)	5081	-	-	-	-	-	parallel
BQ-i	-	-	2.69	2.69	2.71	0.31	
BQ-ii	4817	4857	2.71	2.72	2.73	0.37	90°
BQ-iii	-	-	2.68	2.68	2.69	0.19	
BQ-iv	-	-	2.69	2.70	2.72	0.32	
BQ-v	5351	1473	2.67	2.68	2.70	0.37	
BQ-vii	-	-	2.69	2.71	2.76	0.88	
BQ-xviii	4437	5237	2.66	2.68	2.69	0.38	90°
BQ-IXA	5186	5264	-	-	-	-	
BX-IXA(R)	-	-	2.67	2.68	2.69	0.34	
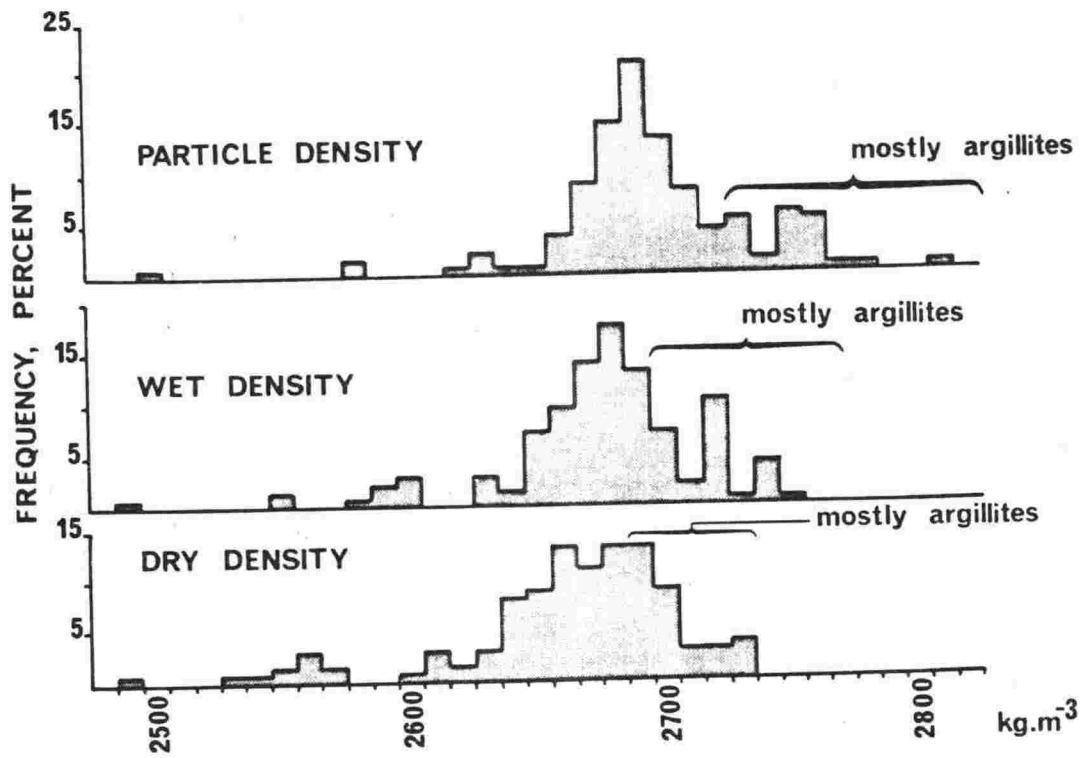
Figure A10.1 : Densities of handspecimen samples, all lithologies;
n = 136.

Table A10.2 : Densities, effective porosities and ultrasonic velocities of greywacke and argillite rock cores.

Rock mean grain size, phi	Sample No.	Core No.	Weight, gm. dry	wet	PUNDIT time secs x10⁻³ dry	wet	Core length h inches	Core volume cm³ $\frac{\pi d^2}{4}$ x h	Density kg.m⁻³ dry	wet	Ultrasonic velocity m.s⁻¹ dry	wet	Apparent porosity, percent
1.25	DC-6	1	56.42				1.708	21.300	2649				
		2	54.22				1.650	20.573	2636				
									2643 mean				
2.73	BQ-V	1	66.17				1.995	24.873	2660				
		2	66.17				1.998	24.912	2656				
		3	66.34				2.000	24.936	2660				
									2659 mean				
		1	49.20				1.497	18.665	2636				
		2	49.04				1.494	18.628	2633				
4.23	KTW-i	1	66.50	66.71	9.4	9.3	1.998	24.912	2669	2678	5399	5457	0.316
		2	66.54				1.997	24.897	2673				
		3	66.72	66.92	9.4	9.4	2.002	24.961	2673	2681	5410	5410	0.300
		4	66.44				1.993	24.848	2674				
		5	66.72				2.002	24.961	2673				
		6	66.47				1.994	24.863	2674				
		7	66.42	66.59	9.4	9.3	1.994	24.863	2672	2678	5388	5446	0.256
									2673	2679	5399	5438	0.291 mean
									2	—	11.0	24.6	0.031 s.d.
1.317	HQ-17	1	66.54				2.002	24.961	2666				
		2	66.40	66.58	9.7	9.4	2.002	24.961	2660	2667	5242	5410	0.271
		3	66.58				2.002	24.961	2667				
		4	66.47	66.66	9.7	9.6	1.999	24.927	2667	2674	5235	5290	0.286
		5	66.53				2.002	24.961	2665				
		6	66.49	66.66	9.7	9.3	2.000	24.936	2666	2673	5237	5462	0.256
		7	66.04				1.997	24.897	2653				
		8	65.21	65.41	9.7	9.4	2.000	24.936	2615	2623	5237	5404	0.307
		9	66.14				2.001	24.951	2651				
		10	66.29	66.50	9.7	9.3	1.996	24.887	2664	2672	5227	5452	0.317
		11	66.40				1.997	24.897	2667				
		12	66.45	66.62	9.8	9.5	2.000	24.936	2665	2672	5184	5347	0.256
		13	66.58				2.002	24.961	2667				
		14	66.60	—	9.7	9.3	2.003	24.976	2667	—	5245	5471	—
		15	66.53				2.001	24.951	2666				
		16	62.27				1.972	24.587	2533				
		17	66.43	66.61	9.7	9.3	1.999	24.927	2665	2672	5235	5460	0.271
									2653	2665	5230	5412	0.281 mean
									33	185	19.4	64.4	0.024 s.d.
4.72	SJ-T	1	67.17				1.994	24.863	2702				
		2	67.27				2.001	24.951	2696				
		3	67.07	67.26	9.2	9.3	1.995	24.873	2697	2704	5508	5448	0.283
		4	67.55	67.76	9.2	9.3	2.005	24.999	2702	2711	5536	5476	0.311
		5	67.06				2.000	24.936	2689				
		6	66.92				1.996	24.887	2689				
		7	67.30	67.51	9.2	9.3	2.002	24.961	2696	2705	5527	5468	0.312
		8	67.12				1.994	24.863	2700				
									2696	2707	5524	5464	0.302 mean
									5	—	14.3	14.4	0.017 s.d.
1.32	SJ-3₁	1	66.09				1.996	24.887	2656				
		2	66.04	—	9.6	9.3	2.000	24.936	2648	—	5292	5462	—
		3	65.80				1.999	24.927	2640				
		4	66.11	—	9.5	9.0	1.999	24.927	2652	—	5345	5642	—
		5	65.97				1.995	24.873	2652				
		6	66.23	66.38	9.6	9.1	2.000	24.936	2656	2662	5292	5582	0.227
		7	66.12				1.998	24.912	2654				
		8	67.00				1.995	24.873	2694				
		9	67.36	67.56	9.5	9.2	1.995	24.873	2708	2716	5334	5508	0.297
		10	66.96				1.996	24.887	2691				
		11	67.41	—	10.5	9.8	2.003	24.976	2699	—	4846	5192	—
		12	67.05	67.24	9.4	9.2	1.998	24.912	2692	2699	5399	5516	0.283
									2670	2692	5251	5484	0.269 mean
									24	—	202.5	156.2	0.037 s.d.

Table A10.2 : continued.

Rock mean grain size, phi	Sample	Core No.	Weight gm.		PUNDIT time secs x10⁻³		Core length h inches	Core volume cm³ $\frac{\pi d^2}{4}$ x h	Density kg.m⁻³		Ultrasonic velocity m.s⁻¹		Apparent porosity, percent
			dry	wet	dry	wet			dry	wet	dry	wet	
2.6	KTW-14	1	66.83	67.04	9.5	9.2	2.004	24.986	2675	2683	5358	5533	0.314
		2	66.71				2.001	24.951	2674				
		3	66.90	67.10	9.5	9.2	2.005	25.000	2676	2684	5361	5536	0.299
		4	66.66				2.003	24.976	2669				
		5	66.87	67.07	9.4	9.1	2.004	24.986	2676	2684	5415	5593	0.299
		6	66.95				2.007	25.024	2675				
		7	66.52				1.999	24.927	2669				
		8	66.54				1.996	24.887	2674				
		9	66.19	66.39	9.3	9.1	2.005	25.000	2648	2656	5476	5597	0.302
		10	66.75	66.93	9.4	9.2	2.002	24.961	2674	2681	5410	5527	0.270
		11	66.70				1.998	24.912	2677				
		12	66.62	66.80	9.5	9.2	1.999	24.927	2673	2680	5345	5520	0.270
		13	66.65				1.997	24.897	2677				
		14	66.73	66.92	9.5	9.2	2.002	24.961	2673	2681	5353	5527	0.285
		15	66.55	66.73	9.7	9.4	1.995	24.873	2676	2683	5224	5390	0.271
		16	66.65				1.997	24.897	2677				
									2673	2679	5368	5528	0.289 mean
									7	9	73.0	63.5	0.017 s.d.
2.9	BQ-IXA	1	66.05				1.995	24.873	2656				
		2	66.82	67.06	9.4	9.2	2.004	24.986	2674	2684	5415	5533	0.359
		3	66.45				2.003	24.976	2661				
		4	66.60	–	9.3	9.2	2.003	24.976	2667	–	5471	5530	–
		5	66.23				1.996	24.887	2661				
		6	66.30	66.56	9.4	9.2	1.998	24.912	2661	2672	5399	5516	0.392
		7	66.55				1.998	24.912	2671				
		8	66.55	66.77	9.3	9.1	1.999	24.927	2670	2679	5460	5580	0.331
		9	66.59				2.000	24.936	2670				
		10	66.47	66.67	9.5	9.3	2.003	24.976	2661	2669	5356	5471	0.301
		11	67.01				2.011	25.074	2673				
		12	66.49	–	9.3	9.2	2.005	25.000	2680	–	5476	5536	–
		13	66.46	66.67	9.4	9.2	1.995	24.873	2672	2680	5390	5508	0.316
		14	66.18				1.997	24.897	2658				
		15	66.33				1.997	24.897	2664				
		16	66.06	–	9.3	9.1	1.996	24.887	2654	–	5452	5571	–
		17	66.53				2.001	24.951	2666				
		18	66.48	66.70	9.3	9.2	1.995	24.873	2673	2682	5448	5508	0.331
		19	66.58	66.81	9.4	9.2	1.999	24.927	2671	2680	5402	5520	0.346
		20	66.12				1.984	24.737	2673				
		21	66.58				1.999	24.927	2671				
		22	66.34	–	9.4	9.2	1.998	24.912	2663	–	5399	5516	–
		23	66.43				2.000	24.936	2664				
									2667	2678	5424	5526	0.339 mean
									7	5	38.9	30.0	0.03 s.d.
3.27	KS-2	1	64.23				1.994	24.863	2583				
		2	66.05	66.40	11.1	10.0	2.001	24.951	2647	2661	4579	5083	0.530
		3	65.87				1.996	24.887	2647				
		4	65.06	65.37	10.6	9.9	2.000	24.936	2609	2622	4793	5131	0.477
		5	64.24	64.53	10.0	9.6	1.997	24.897	2580	2592	5072	5283	0.451
		6	65.60				1.995	24.873	2637				
		7	64.49				2.000	24.936	2586				
		8	64.89	65.15	10.0	9.6	2.005	25.000	2596	2606	5093	5305	0.401
		9	66.28				2.000	24.936	2658				
		10	66.24				2.002	24.961	2654				
		11	64.71	–	10.1	9.6	1.996	24.887	2600	–	5020	5281	–
		12	66.04				1.997	24.897	2653				
		13	65.44	65.70	10.0	9.5	2.001	24.951	2623	2633	5083	5351	0.397
		14	6575				2.000	24.936	2637				
		15	65.82	66.11	10.1	9.6	2.002	24.961	2637	2649	5035	5297	0.441
		16	65.96	66.35	11.1	10.0	1.999	24.927	2646	2662	4575	5078	0.591
		17	65.46				1.996	24.887	2630				
		18	65.60				1.996	24.887	2636				
		19	65.87	66.23	10.9	9.8	1.995	24.873	2648	2663	4649	5170	0.547
									2627	2636	4878	5220	0.479 mean
									26	27	226.8	104.5	0.071 s.d.

Table A10.2 : continued.

Rock mean grain size, phi	Sample	Core No.	Weight gm.		PUNDIT time secs x10^{-3}		Core length h inches	Core volume cm^3 $\frac{\pi d^2}{4}$ x h	Density kg.m^{-3}		Ultrasonic velocity m.s^{-1}		Apparent porosity, percent
			dry	wet	dry	wet			dry	wet	dry	wet	
5.6	OB-W	1	67.39	67.64	10.0	10.5	1.997	24.897	2707	2717	5072	4831	0.371
		2	67.39				2.000	24.936	2703				
		3	67.31				1.998	24.912	2702				
		4	67.42	67.66	10.0	10.3	2.000	24.936	2704	2713	5080	4932	0.356
		5	67.42				1.999	24.927	2705				
		6	67.31				1.995	24.873	2706				
		7	67.19				1.995	24.873	2701				
		8	67.59				1.993	24.848	2720				
		9	67.23	67.48	10.1	10.4	2.000	24.936	2696	2703	5030	4885	0.372
		10	67.54	67.78	9.9	10.2	1.991	24.824	2721	2730	5108	4958	0.355
		11	67.14	67.37	9.9	10.0	1.997	24.897	2697	2706	5123	5072	0.343
		12	67.78	68.05	9.9	10.2	1.994	24.863	2726	2737	5116	4966	0.398
		13	67.97				1.997	24.897	2730				
		14	67.90	68.17	10.0	10.2	1.997	24.897	2727	2738	5072	4973	0.398
		15	67.25	67.51	10.0	10.3	1.992	24.838	2708	2718	5060	4913	0.387
		16	68.06				1.998	24.912	2732				
		17	67.95	68.22	10.0	10.3	1.999	24.927	2726	2737	5078	4930	0.397
		18	67.90				1.999	24.927	2724				
		19	67.19	67.44	9.9	10.1	1.994	24.863	2702	2713	5116	5015	0.372
		20	67.91				2.000	24.936	2723				
		21	67.96	68.23	10.0	10.3	1.997	24.897	2730	2741	5072	4924	0.397
									2714	2723	5084	4945	0.377 mean
									124	139	28.5	63.9	0.019 s.d.
6.28	HQ-22	1	66.57				1.995	24.873	2676				
		2	66.81				1.994	24.863	2687				
		3	66.59				1.995	24.873	2677				
		4	66.77	67.12	10.1	10.3	1.994	24.863	2686	2700	5015	4918	0.524
		5	66.89	67.24	9.9	10.2	1.995	24.873	2689	2703	5118	4968	0.523
		6	66.77				1.995	24.873	2684				
		7	66.97	67.30	9.8	10.1	1.996	24.887	2691	2704	5174	5020	0.493
		8	66.65				1.994	24.863	2681				
		9	66.67	−	9.9	10.2	1.996	24.887	2679	− .	5121	4971	−
									2685	2702	5107	4969	0.513 mean
									5	−	66.5	41.7	0.018 s.d.
		1	50.12				1.495	18.640	2689				
		2	50.04				1.492	18.603	2690				
		3	49.80				1.486	18.528	2688				
		4	49.71				1.490	18.578	2676				
		5	49.78				1.486	18.528	2687				
		6	49.78				1.486	18.528	2687				
		7	49.87				1.491	18.590	2683				
		8	49.76				1.484	18.503	2689				

APPENDIX 11

Discontinuity spacing : table of raw data.

This table is the basis of Figures 3.1 and 3.2.

Sample number/ litho- facies	Discontinuity spacing, mm																				Total number of discon- tinuities percent totals
	10	20	30	40	50	60	70	80	90	100	110	120	130	140	150	160	170	180	190	200	
HQ-19	50	24	10	13	10	4	4			1											116
	43.1	20.7	8.6	11.2	8.6	3.4	3.4			0.9											99.9 percent
HQ-20	16	1		1																	18
	88.9	5.6		5.6																	100.1
HQ-21	21	28	16	12	4	2		4	1	2			1		1			1			93
	22.6	30.0	17.2	12.9	4.3	2.2		4.3	1.1	2.2			1.1		1.1			1.1			99.0
HQ-22	37	14	5	1	3		3	2													65
	56.9	21.5	7.7	1.5	4.6		4.6	3.1													99.9
HQ-23	31	23	5	2	3																64
	48.4	35.9	7.8	3.1	4.7																99.9
HQ-24	42	22	9	2	2		2			1											80
	52.5	27.5	11.3	2.5	2.5		2.5			1.3											100.1
Totals of above con- stitute sample for thick-bed- ded litho- facies, Horokiwi Quarry	197	112	45	31	22	6	9	6	1	4		1		1				1			436
	45.2	25.7	10.3	7.1	5.1	1.4	2.1	1.4	0.3	0.9		0.3		0.3				0.3			100.4
Sandstone lithofacies, Dry Creek Quarry	226	103	58	30	36	12	6	3		1	1	1	2	1			1				481
	47.0	21.4	12.1	6.2	7.5	2.5	1.3	0.6		0.2	0.2	0.2	0.4	0.2			0.2				100.0
Sandstone lithofacies, River Shingle and Sand Quarry	17	32	23	14	14	7	2	1	3				1								114
	14.9	28.1	20.2	12.3	6.1	1.8	0.9	2.6					0.9								100.1
Sandstone lithofacies, Belmont Quarry	576	154	98	72	55	26	13	14	5	8	2	2	1	1		2	1		1		1033
	55.0	15.0	9.5	7.0	5.0	2.5	1.3	1.4	0.5	0.8	0.2	0.2	0.1	0.1		0.2	0.1		0.1		99.2

Also 210 mm : 1 discontinuity = 0.1 percent
300 mm : 1 discontinuity = 0.1 percent

Sample number/ litho- facies	10	20	30	40	50	60	70	80	90	100	Total
Thin-bed- ded litho- facies, River Shingle and Sand	35	11	5	3	2	1					57
	61.4	19.3	8.8	5.3	3.5	1.8					100.1
Thin-bed- ded litho- facies, Belmont Quarry	169	23	16	3	7	2	1	1	1	1	224
	75.0	10.0	7.1	1.3	3.1	0.9	0.4	0.4	0.4	0.4	99.0

APPENDIX 12

Rock core preparation for uniaxial compression testing

Blocks from individual beds, representative of geologic parameters, were hand quarried to enable flaw-free core samples to be cut from them. Blocks from a few kilogrammes to over 50 kg were identified and worked according to bedding plane attitude.

A 24 inch slabbing saw was used to cut blocks into 3 inch slabs parallel to bedding. More than 30 linear feet of rock was cut to provide the number of cores tested. Cores 25 mm in diameter were then taken, perpendicular to bedding, with a continuous rim core bit in a precision drill press with the slabs firmly clamped to prevent "wander". A specially made holding arm was fitted to a Hilquist thin section machine to facilitate cutting and surface grinding of end faces perpendicular to core axis. Other than water coolants, lubricants or solvents were not used at any stage. These precautions were necessary for specimen uniformity and the following criteria were achieved:

(i)   Diameter ±0.0015" (micrometer checked).

(ii)   Sides smooth, free from irregularities and straight to within 0.3 mm over length, checked with straight edge and feeler gauge.

(iii)   Ends flat to within 0.02 mm (microscope inspection).

(iv)   Core sides parallel with end plane vertical to axis. This proved difficult to check with precision but tolerance of the former was of the order of 0.025 mm and the latter four to five minutes.

(v)   Minimum surface contamination.

Hawkes and Mellor (1970) and Vutukuri *et al.* (1974) provided guidance for core geometry, and a length to diameter ratio of 1.5 was chosen to establish a "feel" for the rock types being tested.

Finished cores were thoroughly washed and from that stage not touched by bare hand.

After air drying, they were packed in cotton wool in a constant environment (20 ±1°C, 50 percent R.H.) for one month, when a representative set of cores was removed and immersed in distilled water at 20 ±1°C for one month.

Individual cores or rock types were not tested in any particular order but, generally, stress-strain measurements were done last in both wet and dry core testing programmes and dry testing was carried out before wet testing.

The air dried and saturated cores were tested in the third month after preparation. At the same time cores for two rock types (BQ-IXA and HQ-22) taken 18 months previously were tested air dried for comparison (Appendix 13).

Compression testing was carried out in constant temperature conditions (20° ±5°C) on an Avery universal testing machine with a three range capability of 400,000 lbs graded A to NZS 1021:1965 on all three ranges. The low range up to 80,000 lbs in 50 lb divisions was used. The machine had one spherical platen seat (the upper platen), lightly oiled and held

horizontal by four adjustable coil springs. Cores were accurately placed between test platens with the aid of templates. False platens were used above and below core specimens (Plate A12.1) with no lubricant between platen and sample.

The spherical platen seating conforms to criteria for uniformity assessed by the New Zealand Concrete Research Associations', Foote proving device (Boult, pers. comm.).

A loading rate of 127 lbf.in^{-2} .s^{-1} (0.87 MPa.s^{-1}) was used throughout, i.e. 6,000 lb load per minute on the cores tested.
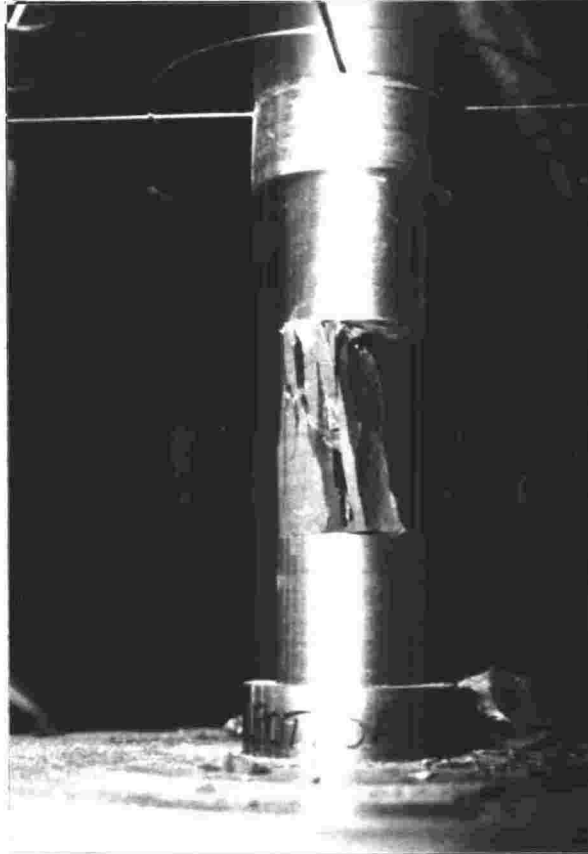
Plate A12.1 : After recommendations of Vutukuri *et al.* (1974), uni-
axial compression testing of rock cores involved placing
hard false-platens either end of the sample.   The false platens had a
h:d ratio of 1 and matched core sample diameter exactly.

The larger platens, between false-platens and testing machine platens,
are of mild steel and protect testing machine platen surfaces.

A sample of argillite (OB-W) is shown (h:d ratio of 1.5) failed from
axial cleavage during equipment trials.

APPENDIX 13

Uniaxial compressive strengths of Wellington greywacke-suite rocks :   tables

Stress-strain curves were derived from cores marked *.   Cores marked + were prepared for testing 18 months in advance of others, and, without exception their strengths are higher for any given lithology; accordingly, where numbers justify, their mean strengths are calculated separately.   Failure load marked # indicate premature failure not included in results.

Included are results from Bryant (1977); he tested samples which were 47.6 mm, 50.8 mm, 146.0 mm and 152.4 mm in diameter with a length:diameter ratio of 2,   loaded at approximately 14 MPa per minute.

Sample	Core No.	$\frac{h}{D}$ ratio	Core diameter D, inches	Bearing area inches^2	Failure load, lb	Strength lbf.in^{-2}	Strength MPa	Strength Mean	s.d.	Variance	Coefficient of variation, %
HQ-17 dry	1	2	0.985	0.762	25,400	33,333	230	221	25.6	581	11.6
	3*				24,700	32,415	224	n=9			
	5				23,500	30,840	213				
	7				20,900	27,428	189				
	9*				28,900	37,927	262				
	11				25,800	33,858	233				
	13				20,400	26,772	185				
	15*				22,700	29,790	205				
	16				27,300	35,827	247				
	1	1.5			28,300	37,139	256	256	-	-	-
wet	2	2			23,300	30,577	211	194	32.1	902	16.6
	4*				25,900	33,990	234	n=8			
	6*				23,500	30,840	213				
	8				18,000	23,622	163				
	10				19,500	25,591	176				
	12				15,300	20,079	138				
	14				24,000	31,496	217				
	17*				21,900	28,740	198				
SJ-3$_1$ dry	1	2	0.985	0.762	26,100	34,252	236	234	22.2	412	9.5
	3*				27,500	36,089	249	n=6			
	5				26,500	34,777	240				
	7				23,600	30,971	214				
	8*				22,300	29,265	202				
	10*				29,000	38,058	262				
	1	1.5			#22,700	29,790	205				
	2				31,800	41,732	288	288	-	-	-
wet	2	2			15,000	19,685	136	149	41.7	1452	28.0
	4				22,800	29,921	206	n=6			
	6*				19,400	25,459	176				
	9*				11,200	14,698	101 }				
	11				18,400	24,147	167 }	relatively coarse grained			
	12*				11,600	15,223	105 }				
KTW-14 dry	2*	2	0.985	0.762	32,600	42,782	295	260	23.5	472	9.0
	4				#19,400	25,459	176	n=7			
	6*				25,600	33,596	232				
	7				30,500	40,026	276				
	8				29,500	38,714	267				
	11				27,200	35,696	246				
	13*				25,900	33,990	234				
	16				29,900	39,239	271				
	1	1.5			31,200	40,945	282	282	-	-	-
wet	1	2			30,500	40,026	276	239	40.4	1401	16.9
	3*				28,000	36,745	253	n=7			
	5*				29,600	38,845	268				
	9				20,800	27,297	188				
	10*				23,200	30,446	210				
	12				21,400	28,084	194				
	14				31,300	41,076	283				
	15				# 9,300	12,205	84				

Sample	Core No.	h/D ratio	Core diameter D, inches	Bearing area inches²	Failure load, lb	Strength lbf.in⁻²	MPa	Mean	s.d.	Variance	Coefficient of variation, %
BQ-IXA dry	+ 1	2	0.985	0.762	34,900	45,800	+316	262	21.7	392.0	8.3
	+ 3				23,500	30,839	+213	n=6			
	+ 5				28,000	36,745	+253	+291	53.3	2371	18.3
	7				28,600	37,532	259	n=6			
	9				26,400	34,645	239				
	11*				28,900	37,926	262				
	+14				36,500	47,900	+330				
	+15				39,400	51,705	+357				
	17*				32,400	42,579	293				
	20				26,400	34,645	239				
	21*				30,900	40,550	280				
	+23				30,600	40,157	+277				
	1	1.5			27,100	35,564	245	242	12.2	124.6	5.04
	2				#18,600	24,409	168	n=6			
	3				28,000	36,745	253				
	4				28,600	37,532	259				
	5				26,300	34,514	238				
	6				25,300	33,202	229				
	7				25,400	33,333	230				
wet	2*	2			23,000	30,183	208	196	15.7	211.0	8.0
	+ 4				26,100	34,251	+236	n=7			
	6				24,600	32,283	223	+257	21.0	294.0	8.2
	8				21,400	28,084	194	n=3			
	10				20,000	26,246	181				
	+12				28,300	37,139	+256				
	13*				20,700	27,165	187				
	+16				30,700	40,288	+278				
	18				21,900	28,740	198				
	19*				19,800	25,984	179				
	+22				# 15,700	20,603	+142				
KS-2 dry	1	2	0.985	0.762	28,800	37,795	261	243	25.2	566	10.4
	3				28,100	36,877	254	n=9			
	6				#19,600	25,722	177				
	7*				22,900	30,053	207				
	9*				24,400	32,021	221				
	10*				28,900	37,927	262				
	12				29,600	38,845	268				
	14				30,000	39,370	272				
	17				26,400	34,646	239				
	18				23,400	30,709	212				
wet	2	2			19,500	25,591	176	182	33.7	1012	18.5
	4*				18,300	24,016	166	n=9			
	5				24,100	31,627	218				
	8				23,100	30,315	209				
	11				21,700	28,478	196				
	13*				17,000	22,310	154				
	15				25,100	32,940	227				
	16*				13,400	17,585	121				
	19				19,200	25,197	174				
DC-6 dry	1	1.5	0.985	0.762	39,100	51,312	354	354	–	–	–
	2				#21,400	28,084	194	n=1			
BQ-V dry	1*	2	0.985	0.762	31,500	41,338	285	263	19.7	258.7	7.5
	2*				28,400	37,270	257	n=3			
	3*				27,300	35,826	247				
	1	1.5			28,100	36,876	254	262	10.6	56.3	4.1
	2				29,700	38,976	269	n=2			
KTW-i dry	2	2	0.985	0.762	#26,400	34,645	239	324	42.3	1195	13.1
	4*				38,000	49,868	344	n=3			
	5*				30,400	39,894	275				
	6*				38,900	51,049	352				
wet	1*				30,400	39,894	275	278	4.2	9	1.5
	3*				# 20,800	27,296	788	n=2			
	7*				31,000	40,682	281				

Sample	Core No.	$\frac{h}{D}$ ratio	Core diameter D, inches	Bearing area inches²	Failure load, lb	Strength $lbf.in^{-2}$	MPa	Mean	s.d.	Variance	Coefficient of variation, %
SJ-T dry	1*	2	0.985	0.762	24,000	31,496	217	254 n=3	36.5	888.7	14.4
	2				28,200	37,007	255				
	5*				32,100	42,125	290				
	6				#21,000	27,558	190				
	8*				#21,600	28,346	195				
	1	1.5			39,400	51,705	357	321 n=2	51.6	1332	16.1
	2				31,400	41,207	284				
wet	3*				30,500	40,026	276	259 n=2	24.0	289	9.3
	4*				#17,700	23,228	160				
	7*				26,700	35,039	242				
OB-W dry	2	2	0.985	0.762	29,700	38,976	269	245 n=9	34.3	1048.0	14.0
	3*				26,400	34,646	239				
	5				26,000	34,121	235				
	6				21,900	28,740	198				
	7				#17,800	23,360	161				
	8*				23,100	30,315	209				
	13				32,600	42,782	295				
	16*				30,600	40,158	277				
	18				23,600	30,971	214				
	20				30,100	39,501	272				
	1	1.5			24,900	32,677	225	237 n=3	44.7	1330	18.9
	2				31,600	41,470	286				
	3				22,000	28,871	199				
wet	1	2			21,800	28,609	197	195 n=11	23.6	505	12.1
	4*				16,700	21,916	151				
	9				21,400	28,084	194				
	10				21,700	28,478	196				
	11				21,000	27,559	190				
	12*				19,300	25,328	175				
	14				23,300	30,577	211				
	15				25,400	33,333	230				
	17				18,600	24,409	168				
	19				24,200	31,759	219				
	21*				23,800	31,234	215				
HQ-22 dry	1*	2	0.985	0.762	17,500	22,966	158	147 n=4	30.6	702	20.8
	2				14,000	18,373	127				
	3*				20,400	26,772	185				
	6*				13,000	17,060	118				
	8				# 8,900	11,680	81				
	+ 1	1.5			23,000	30,184	+208	+204 n=2	5.7	16	2.8
	+ 2				22,100	29,003	+200				
	3				85.1 kN	25,128	173	153 n=4	20.9	327	13.7
	4				65.8 kN	19,429	134				
	5				66.9 kN	19,754	136				
	6				83.2 kN	24,567	169				
wet	4*	2			# 450	591	4				
	5*				# 100	131	0.9				
	7*				13,300	17,454	120	86 n=2	48.1	1156	55.9
	9				5,700	7,480	52				

Uniaxial compressive strengths and elastic properties (after Bryant, 1977)

Sample No.	Brief lithological description	Uniaxial compressive strength MPa	psi	Youngs modulus (Tangent mod. at 50% ultimate) GPa	psi x 10[6]	Poissons ratio,
1 1	Sandstone with some thin argillite beds	99.2	14,386	-	-	-
1 2	Sandstone with some thin argillite beds	128.7	18,664	-	-	-
1 3	Sandstone	49.3	7,153	-	-	-
1 4	Autoclastic breccia	99.2	14,386	-	-	-
1 5	Autoclastic breccia	98.5	14,285	64.4	9.34	0.36
1 6	Autoclastic breccia	83.5	12,109	68.7	9.97	0.24
1 7	Sandstone with very faint argillaceous bedding	102.9	14,930	-	-	-
1 8	Sandstone with some thin argillite beds	97.5	14,145	69.9	10.14	0.20
1 9	Sandstone with faint argillaceous bedding	20.8	3,022	84.0	12.18	0.13
1 10	Sandstone with faint argillaceous bedding	80.2	11,625	71.6	10.38	0.20
s 1	Sandstone with intersecting quartz veins	129.4	18,780	78.7	11.42	0.26
s 2	Siltstone with intersecting quartz veins	197.5	28,648	87.1	12.64	0.24
s 3	Sandstone and argillite interbedded	131.2	19,035	65.9	9.56	0.20
s 4	Sandstone quartz veins and argillite laminations	166.8	24,192	75.8	11.00	0.24
s 5	Argillite with some quartz veins	89.1	12,923	56.0	8.12	0.26
s 6	Argillite, massive	59.3	8,594	-	-	-
s 7	Argillite with interbedded sandstone	195.8	28,393	63.7	9.24	0.32
s 8	Sandstone with some quartz veins	148.8	21,581	72.2	10.47	0.25
s 9	Argillite with interbedded siltstone	122.5	17,762	56.3	8.16	0.20
s 10	Sandstone with some quartz veins	206.3	29,921	68.8	9.98	0.28
s 11	Sandstone with some quartz veins	197.1	28,584	60.9	8.83	0.22
s 12	Sandstone with some quartz veins	33.4	4,838	-	-	-
Mean values		121.1	17,593	69.6	10.1	0.24

APPENDIX 14

Stress-strain curves: methods and instrumentation

There is a wealth of data on the many dynamic and static strain measuring devices available but choice for this study was limited by finance and availability.

Study of basic principles and equipment characteristics and discussion by authors viz. Perry and Lissner (1962) Neubert (1967) Hawkes and Mellor (1970) Lama and Vutukuri (1978) led to the method adopted.

Strain measurement of rock cores and concrete cylinders was undertaken using TML series "P" polyester strain gauges, manufactured by Tokyo Sokki Kenkyujo Co. Ltd., Japan, the characteristics of which are given in Table A14.1. Type PL-20 were used for rock cores and the PL-60 for concrete.
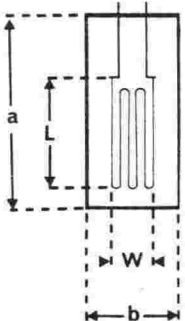
Strain gauge cement - Kyowa CC-15A (cyanoacrylate) - was used to attach the gauges which were positioned by template to preclude finger contact with the core surface.

Gauges were centred on the mid-point and parallel with the vertical axis of the sample, two diametrically opposed on rock cores and one on concrete cylinders.

To promote gauge adhesion, the attachment area surface dryness was ensured and concrete lightly dressed with medium grit emery paper to remove surface debris and laitance. Connector strips to facilitate soldered contacts between cables and gauges were cemented to the specimens at the same time as the gauges. Shielded cable was used for electrical connection, coaxial for rock samples, twin for concrete. Cables were all cut to the same length and the adequacy of shielding checked. Joints not soldered were made with high quality proprietary brand connectors.

Rock core gauges were connected in a full bridge configuration (Figure A14.1) with two "dummy" gauges mounted on a concrete specimen providing a reference and temperature compensation. Outputs were fed to a digital strain bridge (BLH Electronics, model 1200) connected to the X-axis of an X-Y plotter (Rikadenki - Kogyo model BW-133 serial number 59588). A load cell (safe working load 300 kN, gauge factor 2) used to detect rock core stress movement fed the Y-axis of the plotter via a strain bridge amplifier (San-ei, 6M51). Concrete specimens were connected in a half bridge configuration (Figure A14.1) using one "dummy" gauge. In these tests, the load cell was not used and Y-axis input was triggered manually from a low voltage source at load intervals of 10,000 lbs read from the compression test machine dial (Plate A14.1).

Table A14.1 : The series 'P' polyester strain gauge used for this study is a wire strain gauge utilising a transparent plastic backing impregnated with a polyester resin.   It may be used on metals, concrete, wood and synthetic resins.

Gauge Pattern	Type	Dimensions (mm)			Nominal Resistance (Ω)	Gauge factor (approx.)	Gauges per package
		Gauge length (L)	Gauge width (W)	Base (a x b)			
	PL-5	5	3	15 x 6	120 ±0.3	2.0	10
	PL-10	10	3	21 x 7	120 ±0.3	2.1	10
	PL-20	20	3	31 x 7	120 ±0.3	2.1	10
	PL-30	30	2	43 x 8	120 ±0.3	2.1	10
	PL-60	60	1	74 x 8	120 ±0.3	2.1	10
	PL-120	120	1	135 x 8	120 ±0.3	2.1	10

Gauge series	Material		Recommended adhesive	Operational temperature range ($^{\circ}$C)	Strain limit (%)		Fatigue life (x 10^5)	Gauge factor tolerance (%)	Maximum admissible current (mA)
	Sensing element	Carrier			Tension	Compression			
Series "P"	Cu - Ni wire	polyester	P-2 CN PS	-200~80	2	1.5	1*	±0.5	25

*Strain level 1500 x 10^{-6} vibratory frequency 40 Hz.
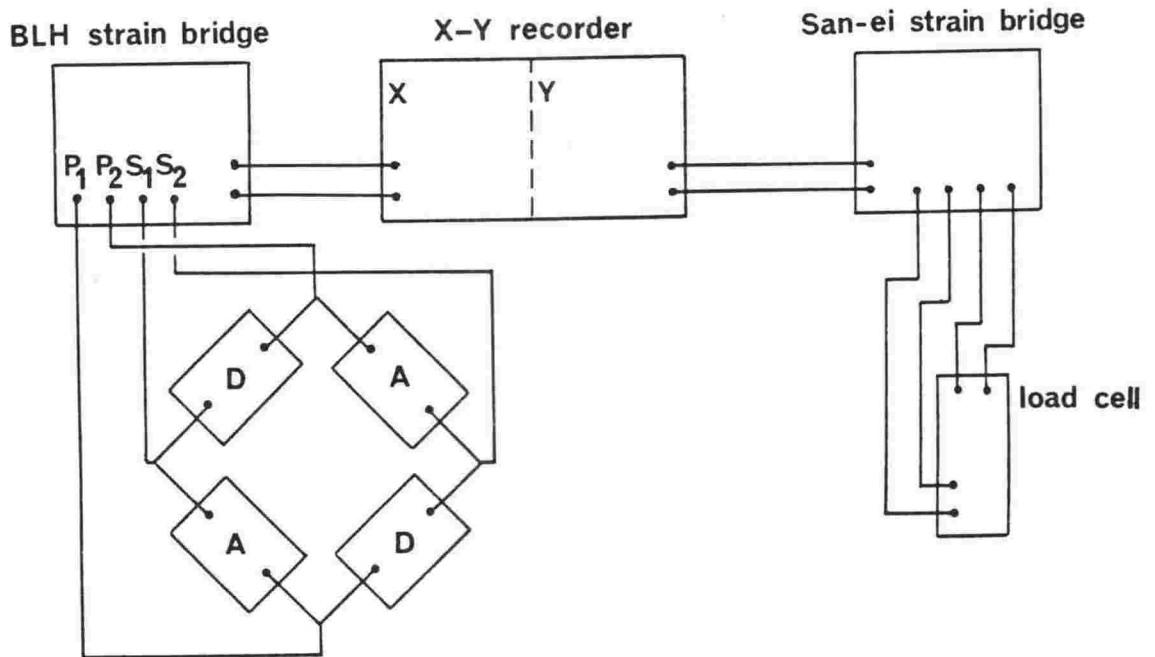
FULL-BRIDGE CIRCUITRY FOR ROCK CORE TESTING, ACTIVE GAUGES (A) ARE ON CORES, DUMMY GAUGES (D) ON A CONCRETE REFERENCE
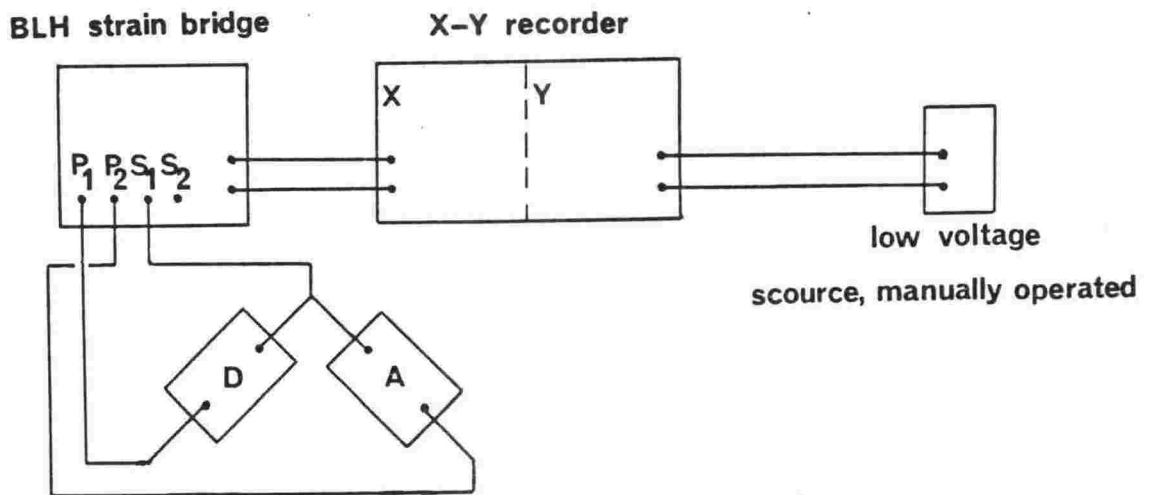
HALF-BRIDGE CIRCUITRY FOR CONCRETE CYLINDER TESTING

Figure A14.1 : Circuit arrangements for stress-strain recording of rock cores and concrete cylinders. Full-bridge layouts provide twice the strain signal of half-bridge layouts, important when calibrating strain axes.
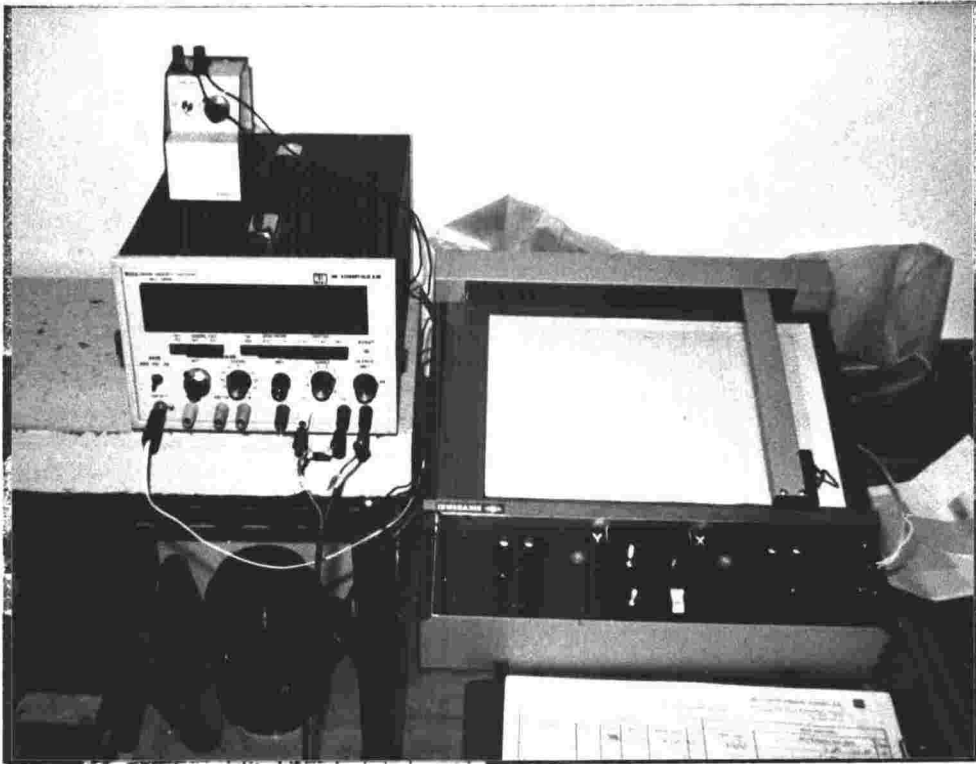
Plate A14.1 : (A) The Avery universal testing machine used for rock
                   core and concrete cylinder uniaxial compression
tests, and the arrangements of electronic apparatus.

               (B) Photograph showing the strain bridge, X-Y plotter
                   and low voltage source, used for 28 day concrete
stress-strain measurements using a half strain bridge circuit.

APPENDIX 15

Static elastic moduli determination and failure mode analysis of rock cores

1.   Static elastic modulus

The static elastic modulus, Young's modulus, compression modulus, modulus of elasticity or modulus of deformation is the ratio of stress to strain in a given material.   If a stress-strain curve is plotted for a perfectly elastic solid, the result will be a straight line and its slope which represents the elastic modulus (E) will be the same for all stress levels.   This is not the case with rocks where the stress-strain curve is not linear but a shape determined by constituent material (Figure A15.1).   Thus the slope of the curve, E, varies at different stress levels.

E can be represented at any point on the curve in two ways, firstly as a tangent at that point - this is tangental modulus E_t and secondly by a secant from the origin through the point - the secant modulus E_s.   The stress at that point is given by the Y intercept.

At any point on the near linear portion of the curve, tangental modulus will be more truly representative of E.

As the stress in rocks increases, elasticity becomes apparent and the curve nears linearity, generally in the vicinity of 50 percent of ultimate stress (C in Figure A15.1).   It is customary therefore to determine E at one or more of three discrete levels of stress - initial stress, 50 percent ultimate stress and ultimate stress;   the intial modulus E_i and the 50 percent modulus E_t both measured tangentally and the ultimate E_s as a secant modulus.   As the slope at the origin of the curve is difficult to ascertain, E_i tends to be the least accurate, particularly in curves where it would be of greatest use, i.e. types iii, iv, v and vi of Deere and Miller (1966) (Figure A15.2).

In this study all stress-strain curves were plotted on the first loading of specimens which continued to failure. E_i provides information on initial rock stress and the phenomenon of microcrack or pore closure, E_t was representative of the elastic portion of the stress-strain curve and reduced errors inherent in early portions of the strain history and E_s included the plastic or ductile portion of the curve from the yield point.   Moduli from this study are presented in Table A15.1.

The complete stress-strain curve for rock (Figure A15.1) illustrates the behaviour of rock in uniaxial compression.   The portion OC of the curve is a facsimile of those obtained from rocks of this study.   From O, the slope of the curve decreases to zero, with increasing stress - a situation observed at C.   Here, induced irreversable changes take place in the rock which passes to a brittle state and its ability to resist load decreases with increasing deformation.   The CD portion of the curve - the brittle field, is not observed from stress-strain curves presented in Figures A15.3 to A15.12 due to the characteristic of the machine used for tests in this study.

Energy stored in the machine during test is released when the sample reaches the stage of internal plastic deformation (Deere and Miller, 1966;   Jaeger 1972), i.e. when the material becomes ductile after yield point (Jaeger and Cook, 1976) and the sample sustains permanent deformation without loss of load bearing ability.   Rapid volume changes now occur marking transition to the brittle field and specimen failure, which can be violent and catastrophic.   Speed and violence of failure are related to test machine "stiffness"
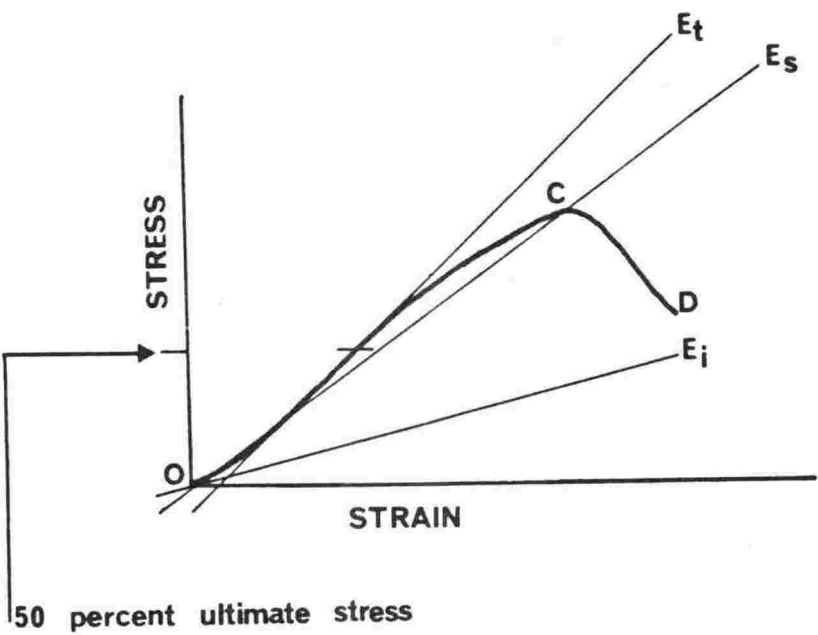
Figure A15.1 : A complete stress-strain curve for rock (from
Jaeger and Cook, 1969).
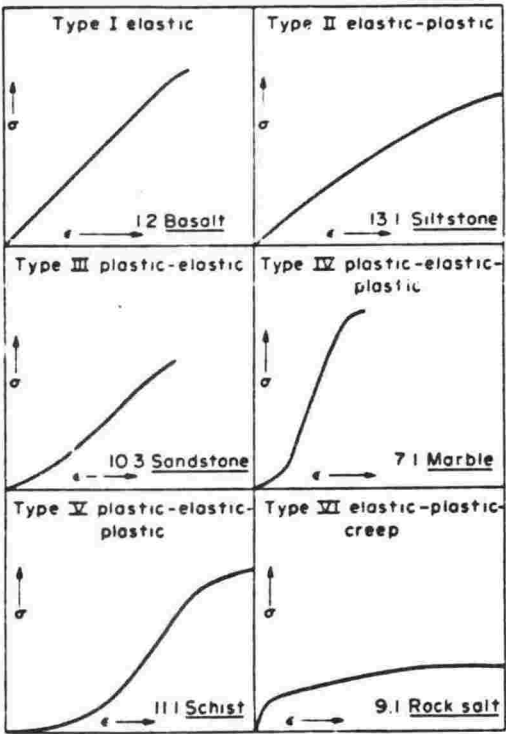
Figure A15.2 : Typical stress-strain curves for rock in uniaxial
compression. After Deere and Miller (1966).

Table A15.1 : Static elastic moduli of Wellington greywacke-suite rocks

CORES TESTED DRY

Sample		Initial tangent modulus				Tangent modulus at 50% ultimate stress				Secant modulus to ultimate stress			
		Stress MPa	Strain $\mu\xi$	E_i GPa	Mean E_i GPa	Stress MPa	Strain $\mu\xi$	E_t GPa	Mean E_t GPa	Stress MPa	Strain $\mu\xi$	E_s GPa	Mean E_s GPa
HQ-17	3	325	4991	65.1	69.5	230	3427	67.1	66.6	224	3335	67.2	67.2
	5	155	2304	67.3	n=3	219	3318	66.0	n=2				n=1
	9	175	2304	76.0									
SJ-3₁	8	391	5000	78.2	73.5	112	1495	74.9	73.7	202	2829	71.4	73.4
	3	320	5000	64.0	n=3	185	2604	71.1	n=3				n=2
	10	391	5000	78.2		197	2627	75.0		262	3479	75.3	
KTW-14	2	480	5600	85.7	77.8	300	3798	79.0	82.6	295	3651	80.8	80.6
	6	398	5000	79.6	n=3	303	3630	83.5	n=3	232	2861	81.1	n=3
	13	340	5000	68.0		295	3462	85.2		234	2933	79.8	
BQ-V	2	190	2825	67.3	67.1	315	5000	63.0	63.0	257	4000	64.3	64.3
	1	335	5000	67.0	n=3	315	5000	63.0	n=3				n=1
	3	335	5000	67.0		315	5000	63.0					
BQ-IXA	17	153	2500	61.4	74.7	153	2725	56.0	68.3	293	4550	64.4	64.4
	21	187	2500	74.8	n=3	218	3225	67.6	n=3				n=1
	11	220	2500	88.0		276	3400	81.2					
KS-2	10	251	5000	50.1	48.4	150	2625	57.1	56.3	262	4800	54.6	51.7
	9	226	5000	45.2	n=3	136	2475	55.0	n=3	221	4525	48.8	n=2
	7	250	5000	50.0		182	3200	56.9					
KTW-i	6	290	3600	80.6	77.7	220	3600	61.1	64.3	352	5612	62.7	63.3
	5	366	4600	79.6	n=3	304	4600	66.1	n=3				n=2
	4	366	4600	73.0		219	3335	65.7		344	5382	63.9	
SJ-T	5	235	2500	94.0	94.0	200	2750	72.7	72.7	251	3575	70.2	70.2
	1	235	2500	94.0	n=3	200	2750	72.7	n=3				n=1
	8	235	2500	94.0		200	2750	72.7					
OB-W	8	319	5000	63.8	63.9	165	3125	52.8	51.6	209	4100	51.0	48.1
	16	290	5000	58.0	n=3	130	2725	47.7	n=3	277	6325	43.8	n=3
	3	349	5000	69.8		185	3400	54.4		239	4825	49.5	
HQ-22	6	347	5000	69.4	68.3	160	2500	64.0	68.4	118	2325	50.8	60.9
	3	347	5000	69.4	n=3				n=2	309	5000	61.8	n=3
	1	330	5000	66.0		300	4125	72.7		158	2250	70.2	

CORES TESTED WET

Sample		Initial tangent modulus				Tangent modulus at 50% ultimate stress				Secant modulus to ultimate stress			
		Stress MPa	Strain $\mu\xi$	E_i GPa	Mean E_i GPa	Stress MPa	Strain $\mu\xi$	E_t GPa	Mean E_t GPa	Stress MPa	Strain $\mu\xi$	E_s GPa	Mean E_s GPa
HQ-17	6	390	5000	78.0	74.0	220	3364	65.4	65.1	213	3456	61.6	60.3
	4	330	5000	66.0	n=3	156	2465	63.3	n=3	234	4101	57.1	n=3
	17	390	5000	78.0		193	2903	66.5		198	3180	62.3	
SJ-3₁	6	186	2310	80.5	85.8	155	2241	69.2	67.5	176	3326	52.9	47.7
	12	343	5000	68.6	n=3	218	3502	62.3	n=3	105	2477	42.4	n=2
	9	250	2310	108.2		265	3733	71.0					
KTW-14	3	250	2750	90.9	88.8	170	2750	61.8	65.3	253	4300	58.8	58.8
	5	303	5000	60.6	n=3	170	2600	65.4	n=3				n=1
	10	230	2000	115.0		206	3000	68.7					
BQ-V		Not sufficient cores											
BQ-IXA	2	320	3927	81.5	81.5	115	1802	63.8	64.4	208	3049	68.2	66.5
	13	320	3927	81.5	n=3	115	1802	63.8	n=3	185	2857	64.8	n=2
	19	320	3927	81.5		195	2972	65.6					
KS-2	4	170	3220	52.8	46.1	80	1610	49.7	48.3	166	3335	49.8	51.7
	13	263	5000	52.6	n=3	160	2995	53.4	n=3	154	2880	53.5	n=2
	16	165	5000	33.0		126	3018	41.7					
KTW-i	7	330	5000	66.0	62.0	170	2742	62.0	59.5	281	4724	59.5	60.2
	1	310	5000	62.0	n=3	170	2857	59.5	n=3	275	4516	60.9	n=2
	3	290	5000	58.0		240	4217	56.9					
SJ-T	3	260	4389	59.1	59.1	190	2934	64.9	65.2	276	4528	61.0	61.0
	4	260	4389	59.1	n=2	155	2373	65.4	n=2				n=1
OB-W	21	160	2771	57.7	55.5	90	2309	39.0	37.1	215	6119	35.1	38.3
	4	255	5000	51.0	n=3	125	3438	36.4	n=3				n=2
	12	160	2771	57.7		110	3077	35.8		175	4231	41.4	
HQ-22	5	70	5000	14.0	14.0	44	3917	11.2	11.2	10	921	10.9	10.9
					n=1				n=1				n=1
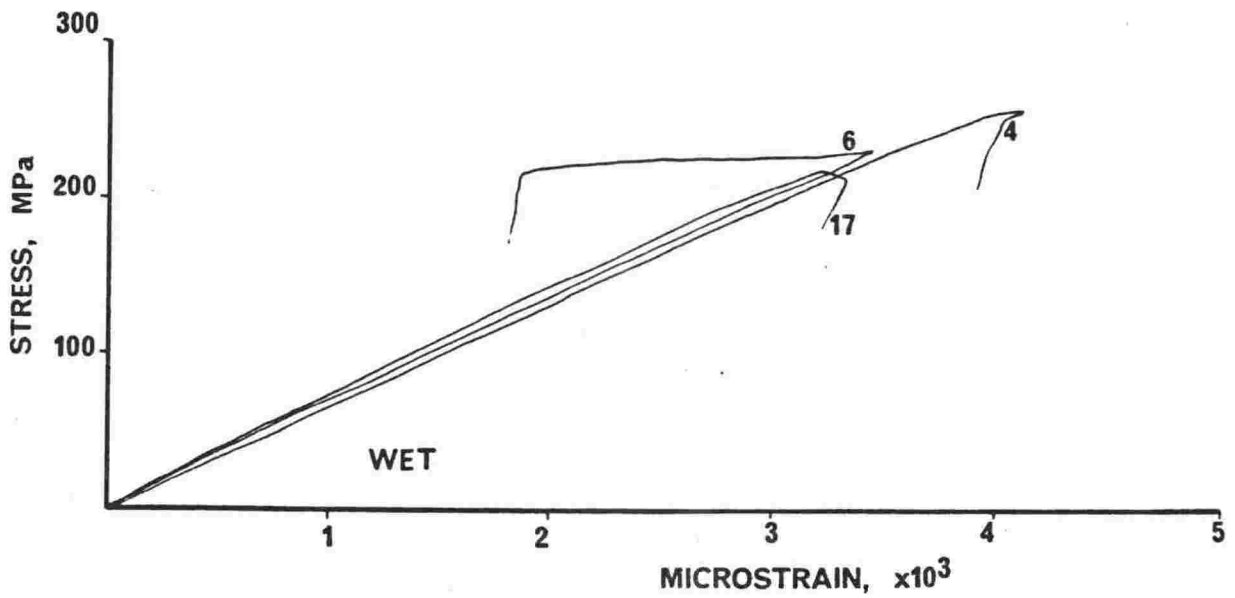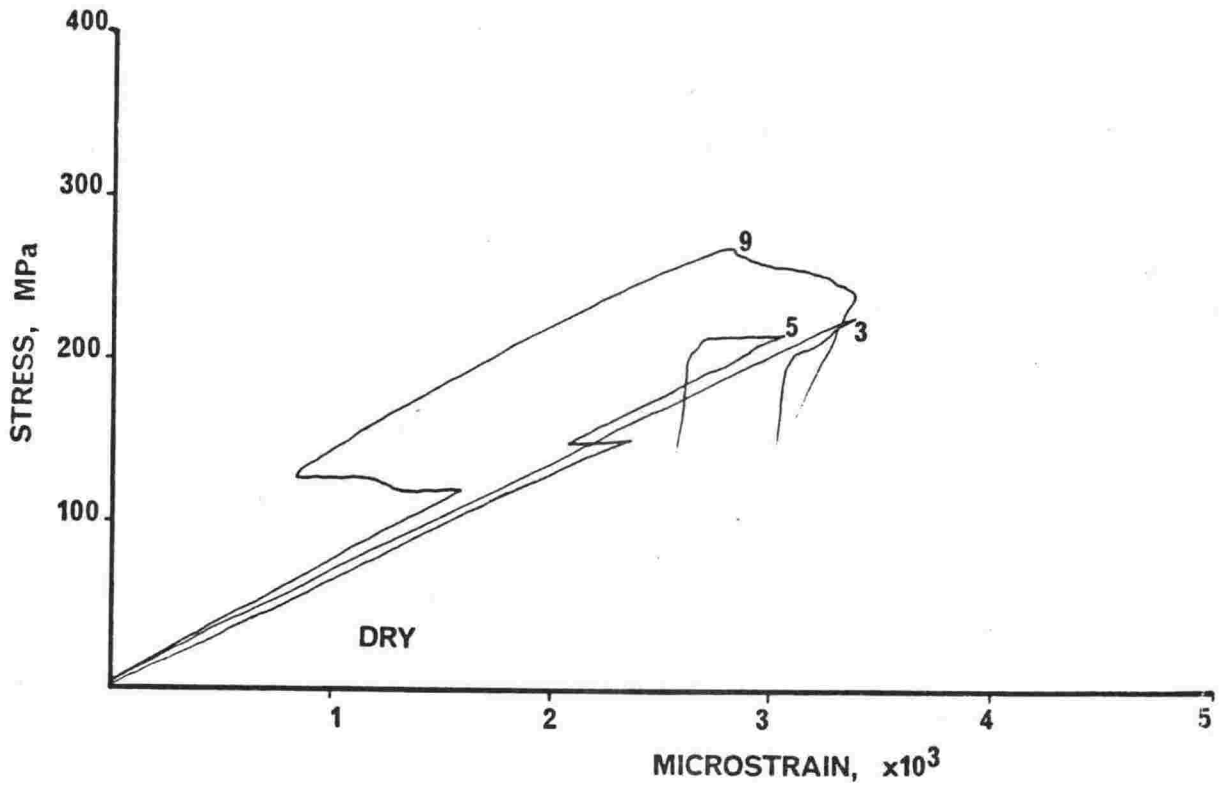
Figure A15.3 : Stress-strain curves of HQ-17 greywacke (1.3 phi, mean grain size). Curve numbers indicate core sample numbers.

Static elastic modulus figures are:

	dry	wet
E_i	69.5 GPa	74.0 GPa
E_t	66.6 GPa	65.1 GPa
E_s	67.2 GPa	60.3 GPa

N.B. 1000 microstrain = 1 mm.m^{-1}
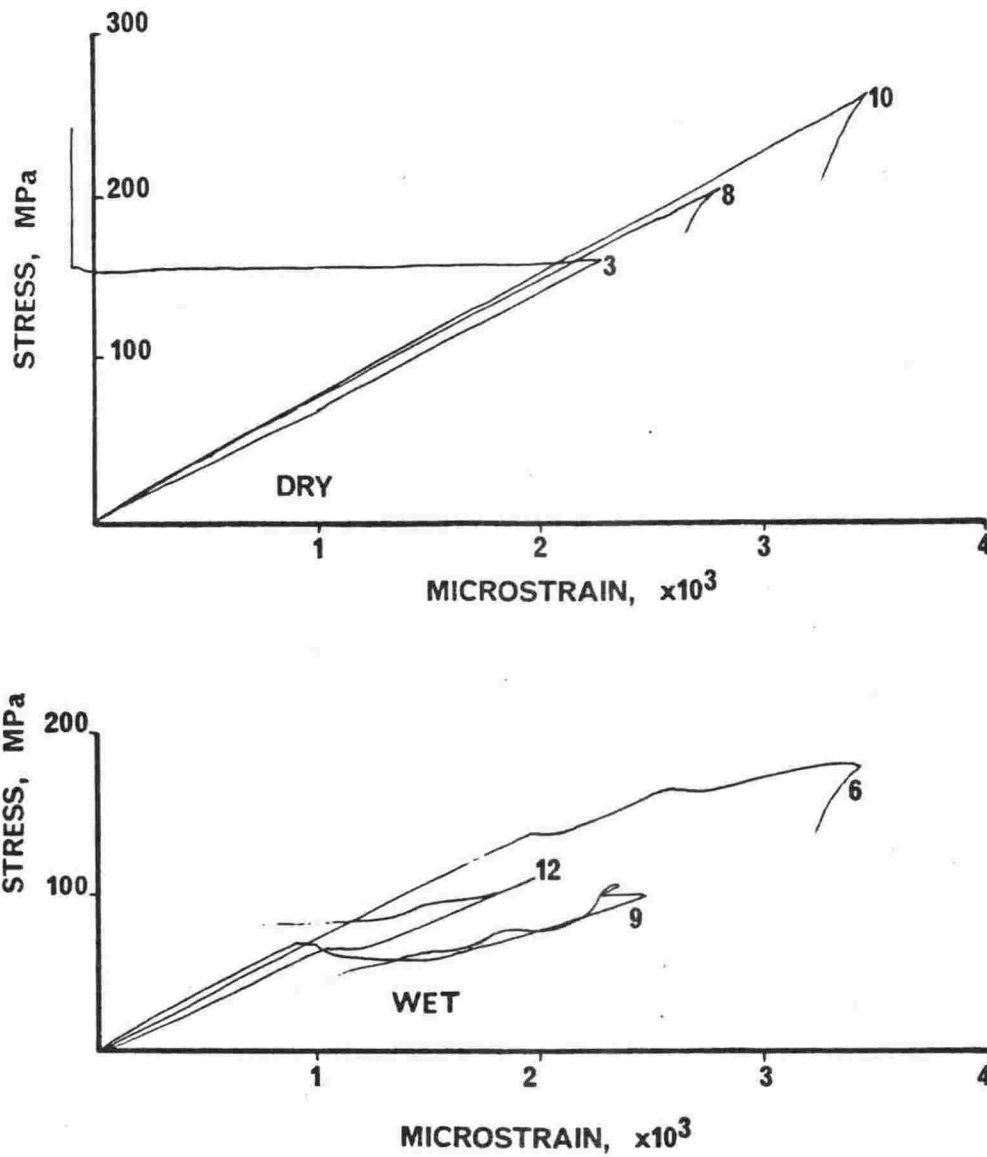
Figure A15.4 : Stress-strain curves of SJ-3$_1$ greywacke (1.3 phi,
mean grain size). Curve numbers indicate core
sample numbers.

Static elastic modulus figures are:

	dry	wet
E_i	73.5 GPa	85.8 GPa
E_t	73.7 GPa	67.5 GPa
E_s	73.4 GPa	47.7 GPa

N.B. 100 microstrain = 1 mm.m^{-1}
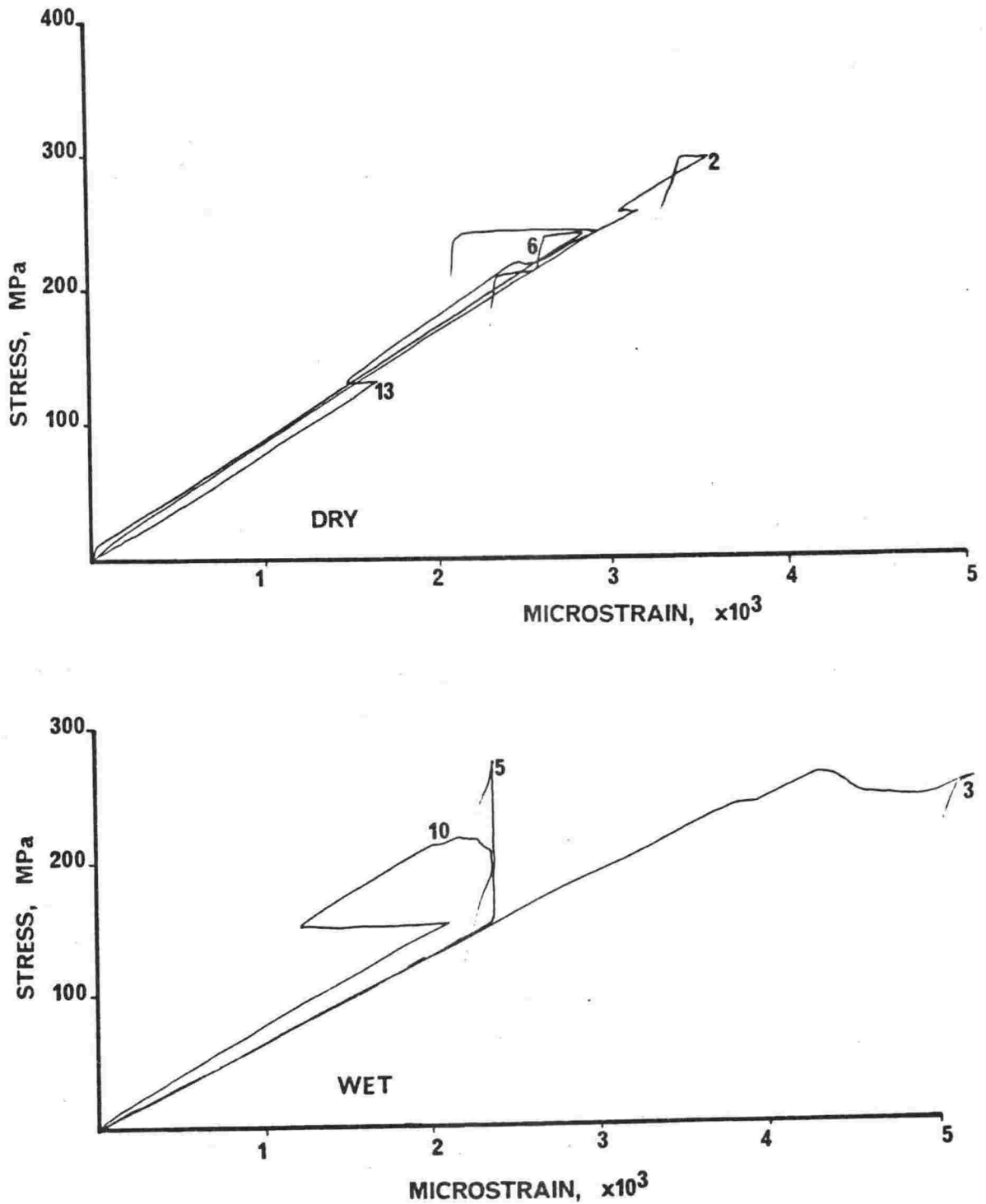
Figure A15.5 : Stress-strain curves of KTW-14 greywacke (2.6 phi, mean grain size). Curve numbers indicate core sample numbers.

Static elastic modulus figures are:

	dry		wet	
E_i	77.8	GPa	88.8	GPa
E_t	82.6	GPa	65.3	GPa
E_s	80.6	GPa	58.8	GPa

N.B. 1000 microstrain = 1 $mm.m^{-1}$
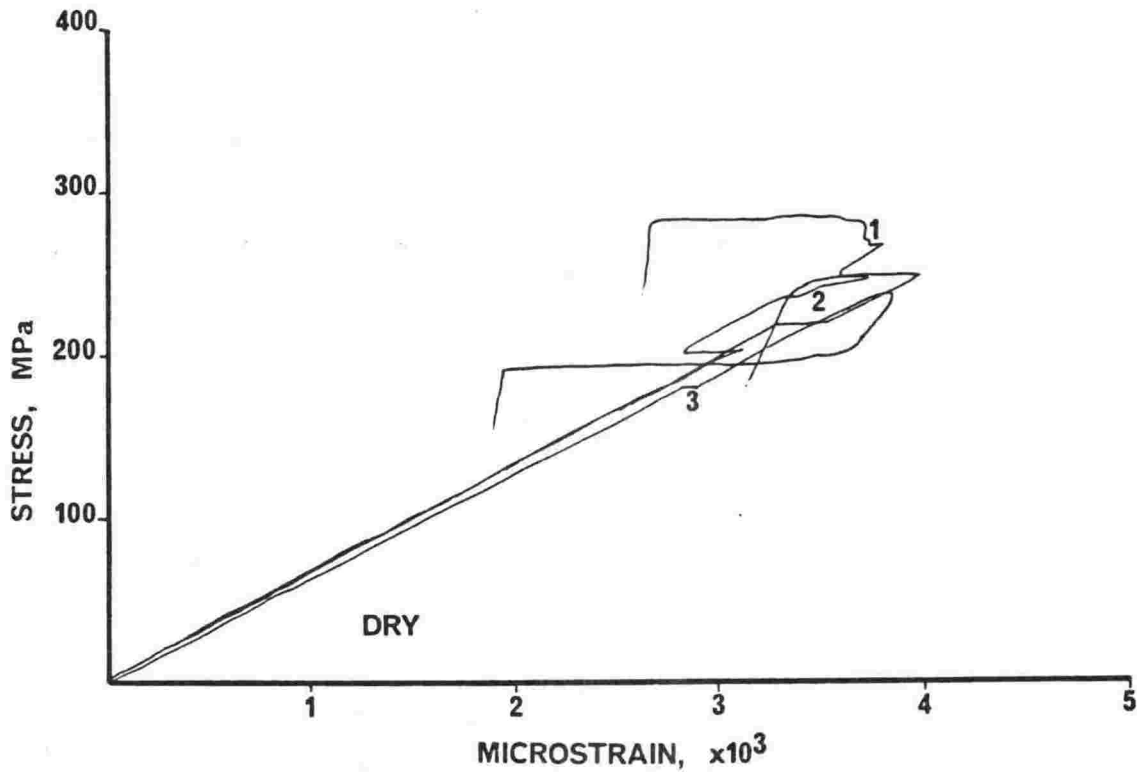
Figure A15.6 : Stress-strain curve of BQ-V greywacke (2.7 phi, mean grain size). Curve numbers indicate core sample numbers.

Static elastic modulus figures are:

	dry
E_i	67.1 GPa
E_t	63.0 GPa
E_s	64.3 GPa

N.B. 1000 microstrain = 1 $mm.m^{-1}$
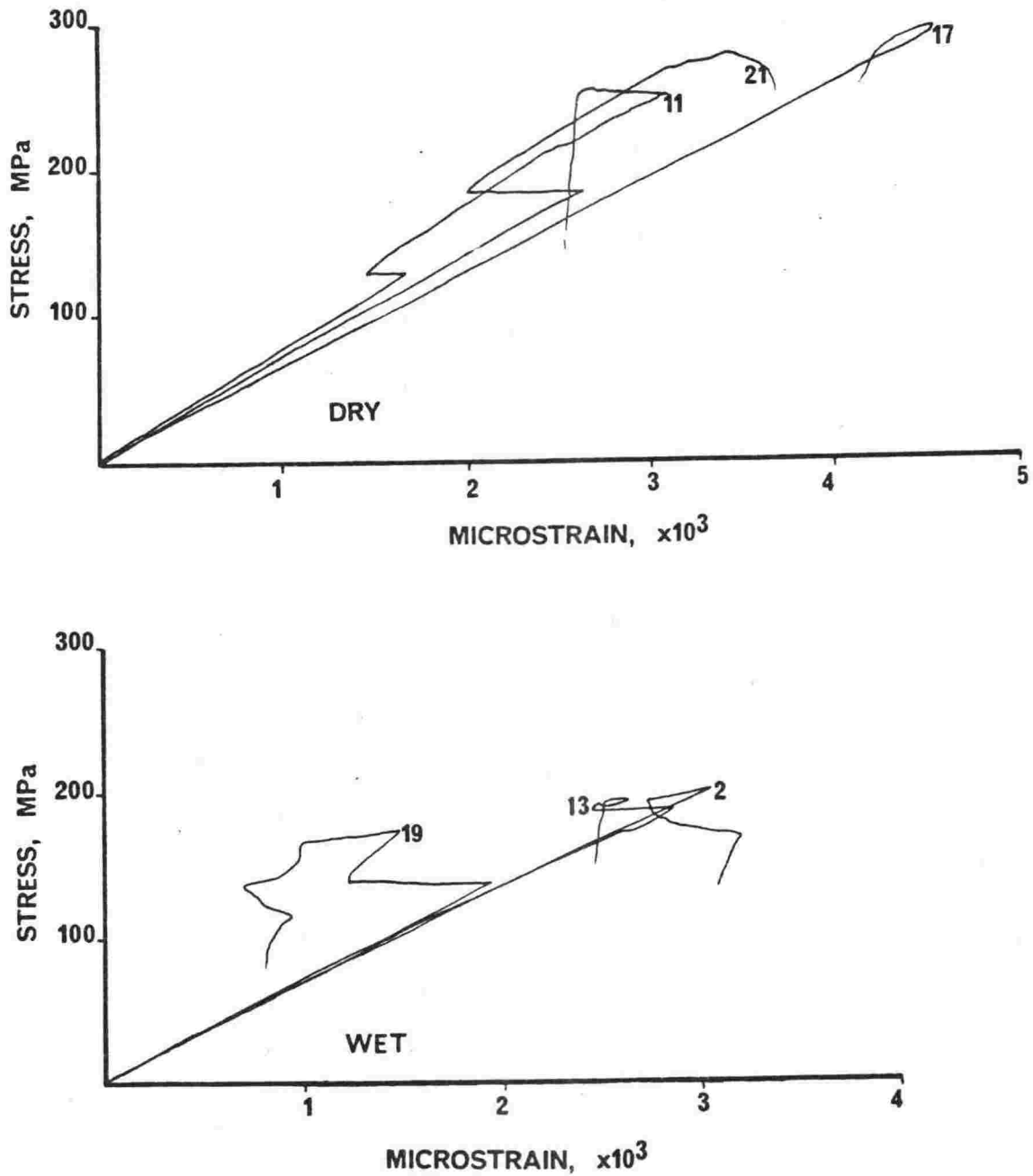
Figure   A15.7   :   Stress-strain curves of BQ-IXA greywacke (2.9 phi,
mean grain size).   Curve numbers indicate core
sample numbers.   Note, strain axes not identical scales.

Static elastic modulus figures are:

	dry		wet	
E_i	74.7	GPa	81.5	GPa
E_t	68.3	GPa	64.4	GPa
E_s	64.4	GPa	66.5	GPa

N.B.   1000 microstrain = 1 mm.m^{-1}
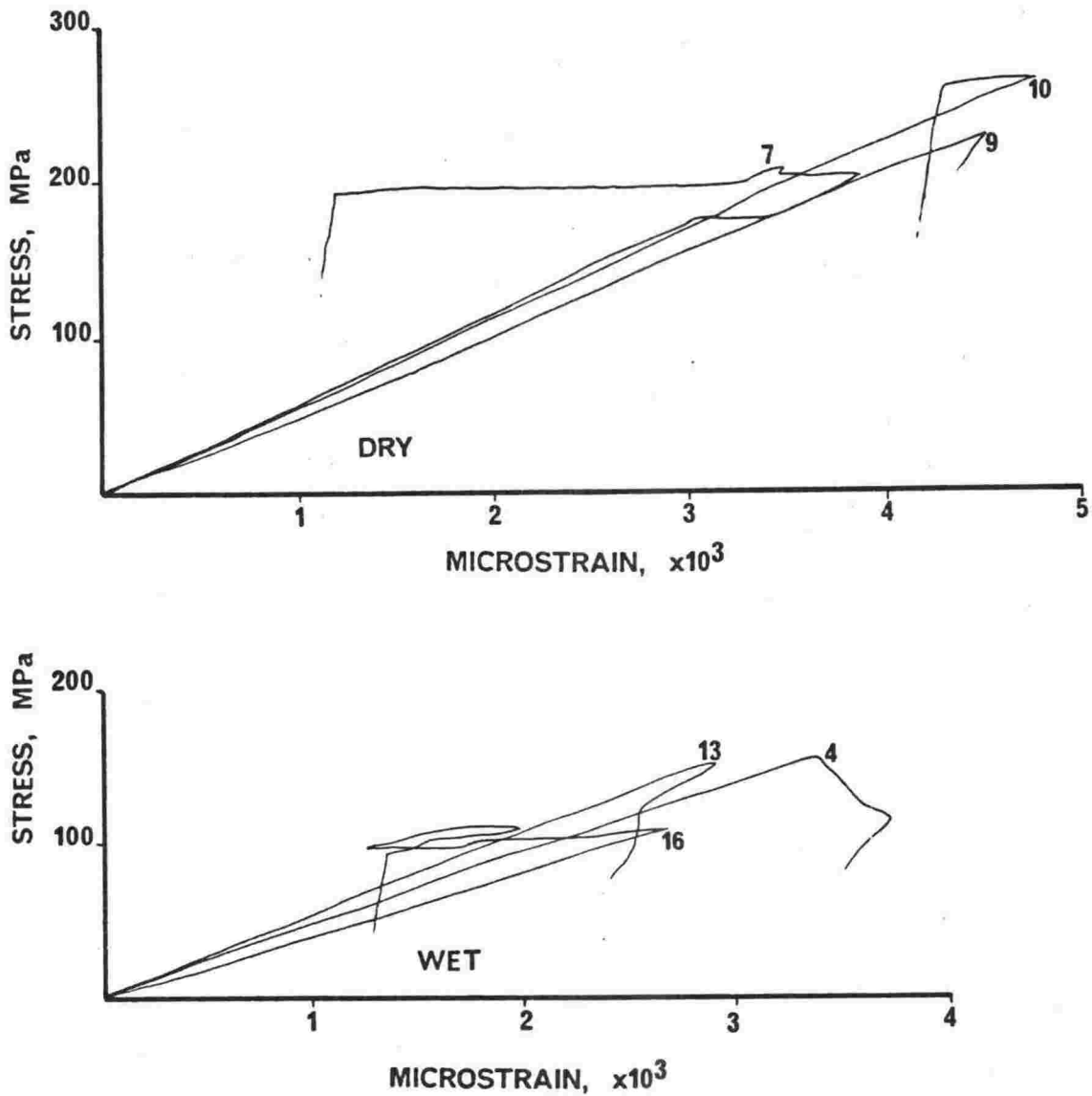
Figure A15.8 : Stress-strain curves of KS-2 greywacke (3.3 phi, mean grain size). Curve numbers indicate core sample numbers. Note, strain axes not identical scales.

Static elastic modulus figures are:

	dry		wet	
E_i	48.4	GPa	46.1	GPa
E_t	56.3	GPa	48.3	GPa
E_s	51.7	GPa	51.7	GPa

N.B.   1000 microstrain = 1 mm.m^{-1}
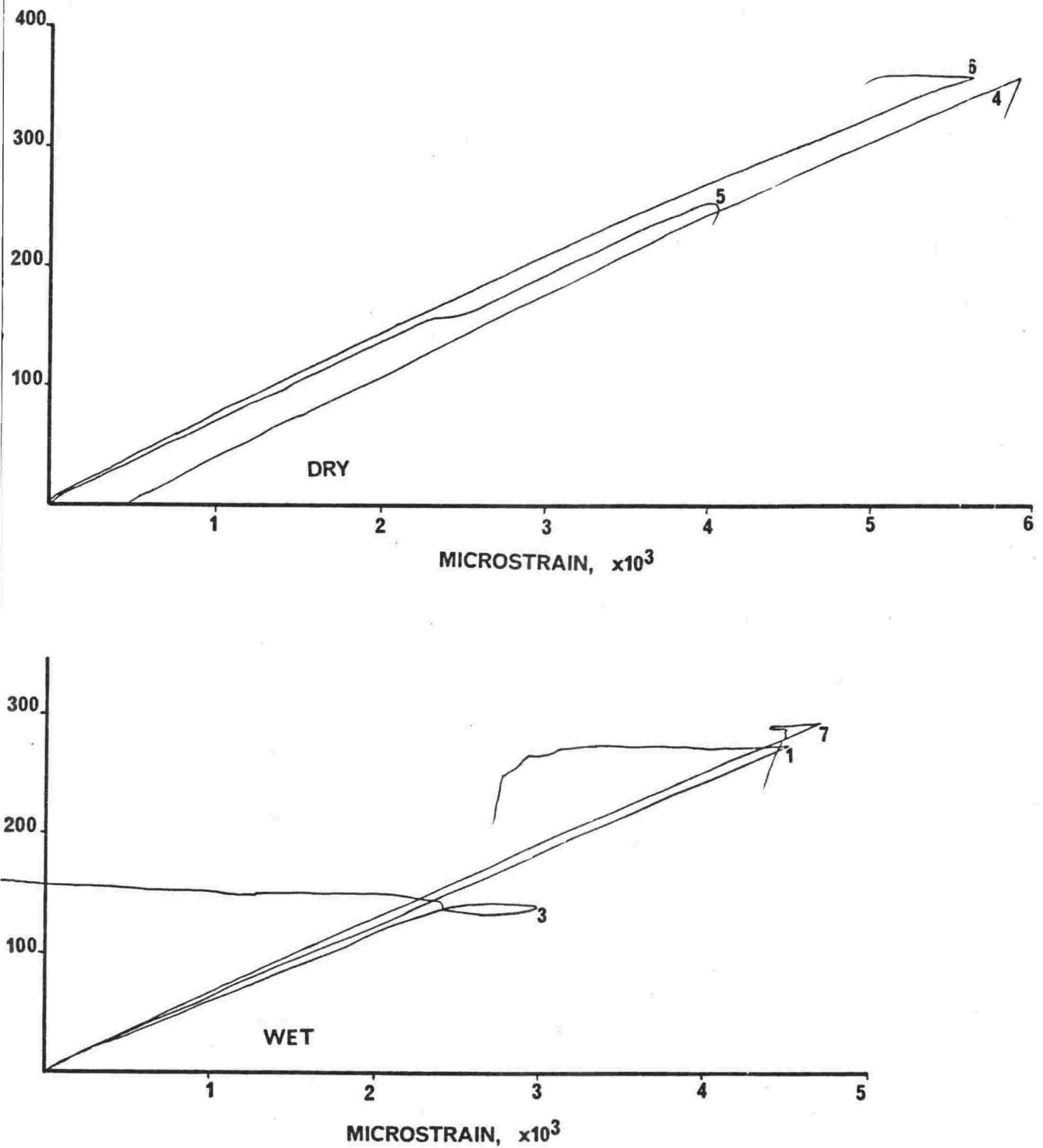
Figure A15.9 : Stress-strain curves of KTW-i greywacke (4.2 phi, mean grain size). Curve numbers indicate core sample numbers.

Static elastic modulus figures are:

	wet		wet	
E_i	77.7	GPa	62.0	GPa
E_t	64.3	GPa	59.5	GPa
E_s	63.3	GPa	60.2	GPa

N.B.   1000 microstrain = 1 $mm.m^{-1}$
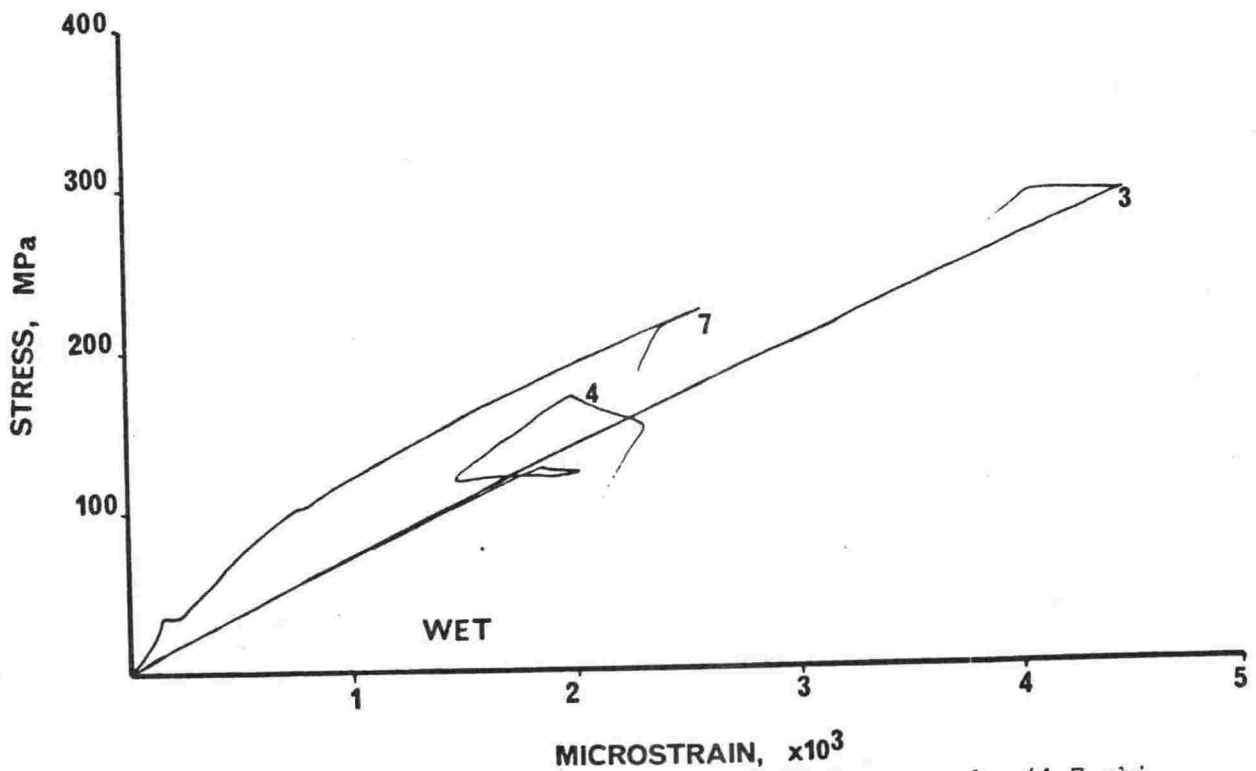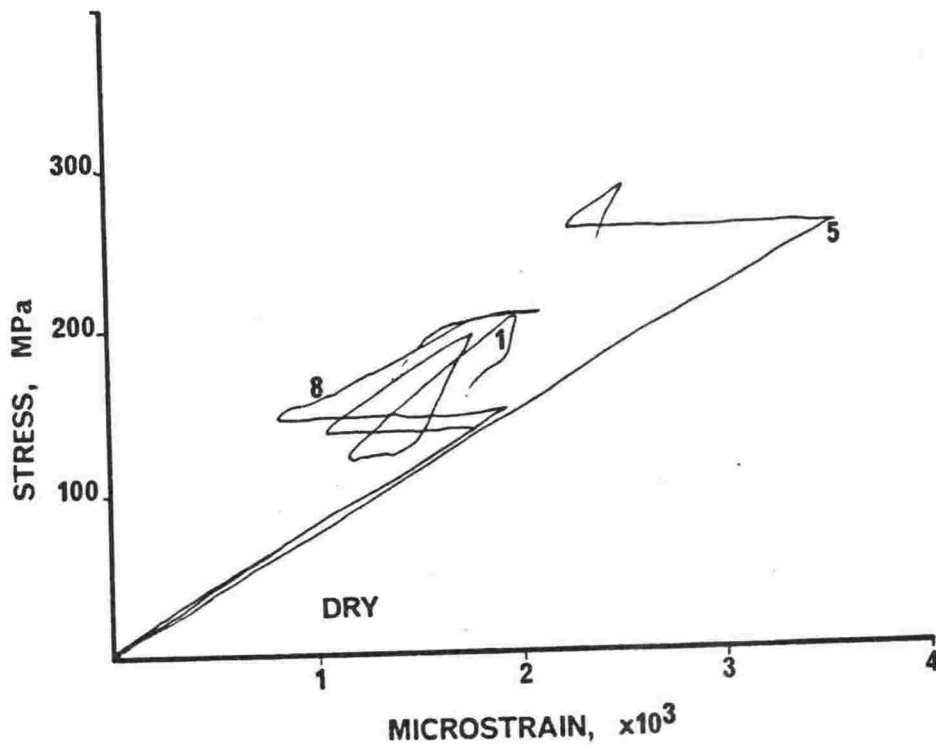
Figure A15.10 : Stress-strain curves of SJ-T greywacke (4.7 phi,
mean grain size). Curve numbers indicate core
sample numbers. Note, strain axes not identical scales.

Static elastic modulus figures are:

	dry	wet
E_i	94.0 GPa	59.1 GPa
E_t	72.7 GPa	65.2 GPa
E_s	70.2 GPa	61.0 GPa

N.B. 1000 microstrain = $1 \ mm.m^{-1}$
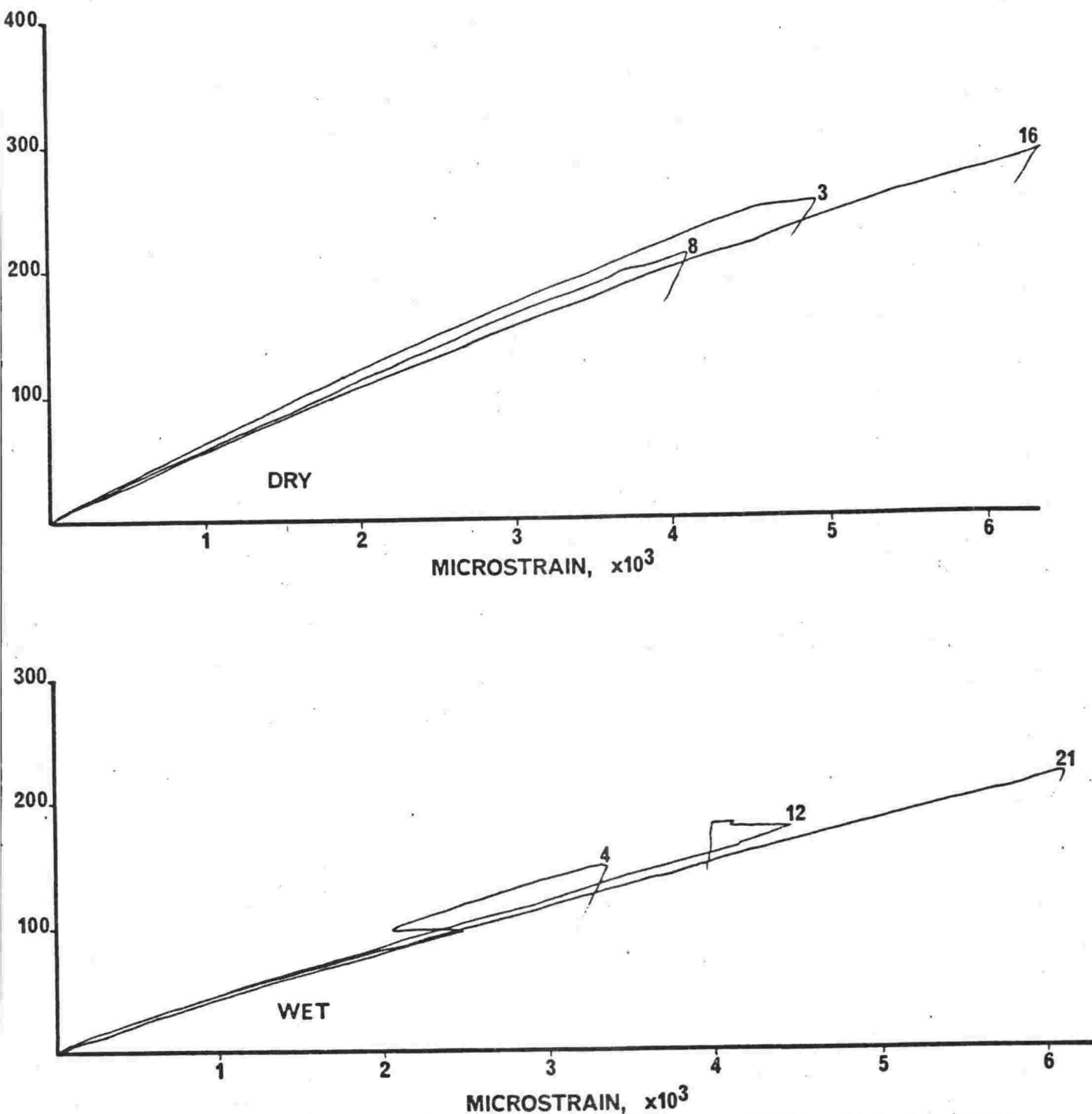
Figure A15.11 : Stress-strain curves of OB-W argillite (5.6 phi, mean
grain size).   Curve numbers indicate core sample
numbers.   Note, strain axes not identical scales.

Static elastic modulus figures are:

	dry	wet
E_i	63.9 GPa	55.5 GPa
E_t	51.6 GPa	37.1 GPa
E_s	48.1 GPa	38.3 GPa

N.B.   1000 microstrain = 1 mm.m^{-1}
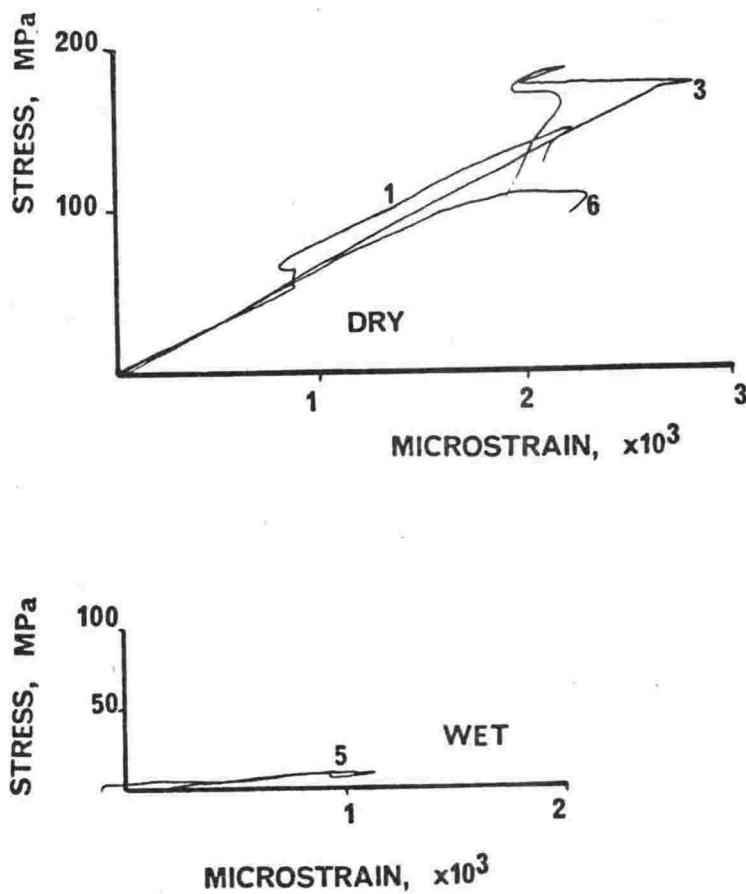
Figure A15.12 : Stress-strain curves of HQ-22 argillite (6.3 phi,
mean grain size). Curve numbers indicate core
sample numbers. Note, strain axes not identical scales.

Static elastic modulus figures are:

	dry		wet	
E_i	68.3	GPa	14.0	GPa
E_t	68.4	GPa	11.2	GPa
E_s	60.9	GPa	10.9	GPa

N.B. 1000 microstrain = 1 mm.m^{-i}

and test load respectively, the former inversely, the latter directly. Sudden failure, the usual result from all but the highest quality test equipment, masks the CD portion of the curve and may jeopardise the accuracy of ultimate stress determination.

Deere and Miller (1966) characterised six types of stress-strain curves (Figure A15.2), three of which apply to this study. In general, greywackes display type i elastic behaviour when dry but type ii elastic-plastic when wet. Some of the finer greywackes and all the argillites appear elastic - plastic wet or dry. In one case only was type iii plastic - elastic affinity noted, KS-2 greywacke, tested dry. The difference between wet and dry greywacke and argillites suggests moisture related promotion of plastic deformation at least in coarser examples.

An initial "plastic" closing of pores and/or fissures is generally thought to be the reason for the concave shape from the origin of the type iii curve - the elimination of this effect in KS-2 on saturation, indicates a pressure role by pore water in straightening this part of the stress-strain curve, though not enough to raise the mean initial tangent modulus (E_i) above that of the dry samples. All coarser grained greywackes have an increased E_i, probably due to an initial expulsion of water, requiring stress but not straining the sample. Strain fluctuations were apparent in both positive and negative senses, e.g. $SJ-3_1$, and KTW-i (dry) respectively, and it is suggested that these resulted from differences in failure mode.

2.   Core failure modes

Failure could be categorised in three groups, two main and one subordinate.

2.1   The first form of fracture mode (Plate A15.1A) is well reported in the literature under various names; extension failure (Griggs and Handin, 1960), axial cleavage fracture (Gramberg, 1965; Hawkes and Mellor, 1970), indirect tensile fracture or induced tensile fracture (Duncan, 1969), brittle fracture (Jaeger, 1972), typical "brittle" cataclasis type failure (Attewell and Farmer, 1976), longitudinal splitting (Jaeger and Cook, 1976), cataclastic failure (Bryant, 1977). This mode is the most common in rocks under uniaxial compression (Duncan, 1969) and is the type of failure experienced in rocks displaying the stress-strain curves of Figure A15.2, type i and ii (Griggs and Handin, 1960). During dry testing, failure would be so explosively violent as to completely eject all but small fragments of the sample from between the test platens; lower rates of loading, used in trials gave less violent results. Samples tested wet gave fewer, longer and therefore larger pieces, probably due to lower loads at failure.

The early formation of this type of fracture involves parting in tension across a surface, parallel to the direction of applied load. This occurs without relative displacement normal to the applied load. Extention fracturing in this way is characteristic of brittle materials (Handin, 1966). In the samples tested, this cracking which occurred at above 50 percent ultimate stress, although audible was invisible and rarely resulted in strain relief, appearing on the stress-strain curve as an X-axis displacement (Figure A15.7). This form of strain relief must be localised to interior zones and external ends of the specimen as the sample rarely lost its ability to bear load. The process occurred as frequently in wet tests as in dry and there appears to be no gradient change between displaced portions of the stress-strain curve. This is consistent with the analysis of stress distribution by Hawkes and Mellor (1970). Ultimate failure often resulted from cracking in this manner so that the sample, with increasing deformation, had decreasing ability to resist load - a brittle failure (KTW-i, wet). The effects described may have
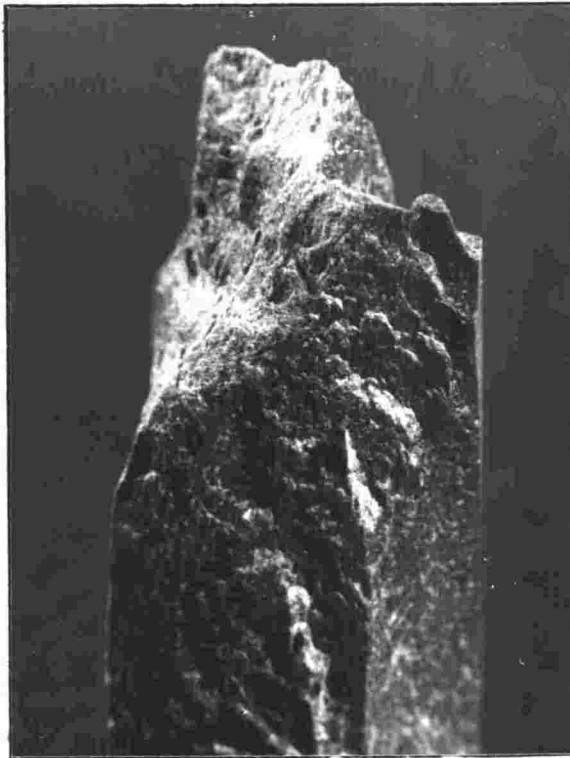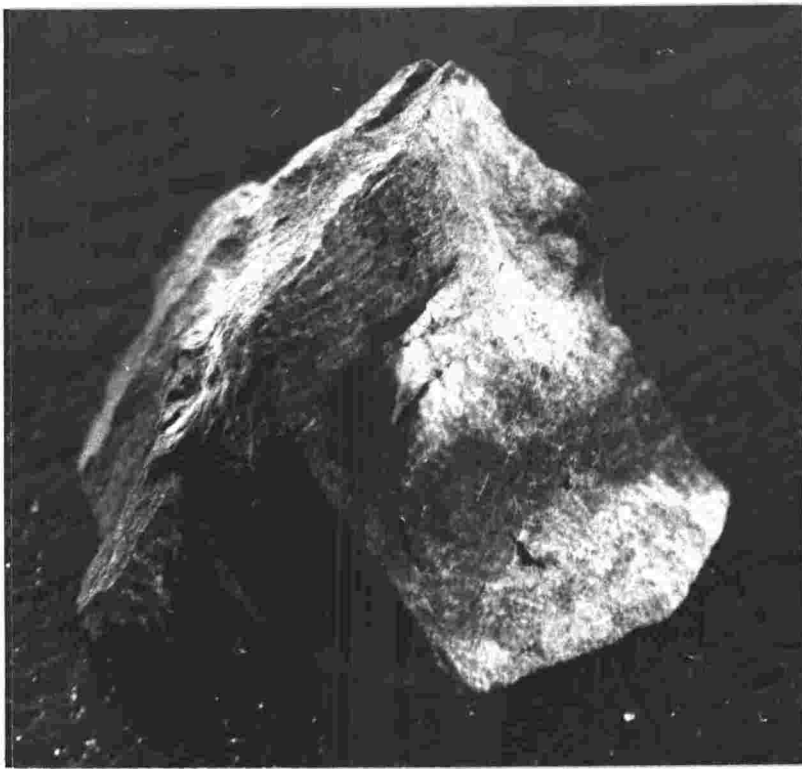
Plate A15.1 : (A) Axial cleavage failure mode in KTW-i with intense apical comminution and surface flaking.

(B) Bottom cone from a double cone failure of OB-W. Intense comminution and *en echelon* flaking are apparent.

been attributable to small sample size, end effects due to platen placement or end constraint, or uneven distribution of load on the end bearing surfaces, i.e. point loading. The effect merely indicates an unbalancing of one strain gauge in the testing system as it is momentarily relieved.

2.2   The second form of failure known variously as faulting (Handin, 1966), shear failure (Jaeger, 1972) or double cone failure (Vutukuri *et al.*, 1974) occurred more often in argillites.   It is more common in the testing of larger specimens or in concrete, developing from end constraint (Vutukuri *et al.*, 1972; Jaeger and Cook, 1976).   The distribution of stress in cylindrical specimens under uniaxial compression between metal surfaces is discussed by Hawkes and Mellor (1970) and Vutukuri *et al.* (1974).   The latter describe this type of failure as a "development of multiple cracks parallel to the direction of applied force at mid-height of the specimen near the surface and its extention to the ends and into the centre of the specimen".   On failure and collapse, conical end fragments remain along with large longitudinal slivers from around the periphery (Plate A15.1B, A15.2).   It is a predominance of this failure mode that imparts sudden strain increase to the stress-strain curves approaching failure stress; examples seemingly of greater magnitude, if not prevalence appears to be greater in samples tested wet and it is suggested that the effect is due to distortion of the strain gauge by sudden brittle failure, audible but invisible, occurring under the strain gauge attachment area "at the mid-height of the specimen near the surface" Vutukuri *et al.* (1974).

2.3   The third form of failure is shear fracture along a single oblique plane (Jaeger and Cook, 1976; Paterson, 1978).   Occurring rarely but more prevalent in wet tests, it resulted usually from an invisible flaw at a stress much lower than the true uniaxial strength of the rock.   In these cases results were not considered further.   Some failures may have been induced by machine geometry (Hawkes and Mellor, 1970) although efforts had been made to eliminate this cause.

Vutukuri *et al.* (1972) states all three of these failure modes may appear in a single specimen.   Bryant (1977), in a study of Kaimanawa greywackes, noted a range of failures involving all three failure modes.

Generally, dry samples in this study failed in a longitudinal splitting mode.   This is not unexpected since end constraint was reduced by using dummy platens of identical diameter to the cores tested (Plate A12.1).   Wet samples displayed a failure mode which encompassed both longitudinal splitting and cone formation.   Griggs and Handin (1960, plate 1) illustrate this well, though specimens in this study usually broke into fewer pieces, one end usually having a better formed end cone fragment.

3.   Surface features of failed rock cores

A study of broken surfaces proved interesting and is relevant to surface texture and dust generation considerations in bonding of rock aggregate in concrete (section 4.2.7).   Three main types of surface were produced by compression failure.

3.1   Cataclastic surfaces: Curved or planer faces on which intense comminution of surface grains was apparent.   These faces formed at angles of up to 40° from the longitudinal axis of the core.   Intense differential movement took place along the more planer surfaces in apical regions of wedge and cone shaped portions of fragments.   This surface, generally confined to the greywackes, sometimes displayed poorly developed slickensides in
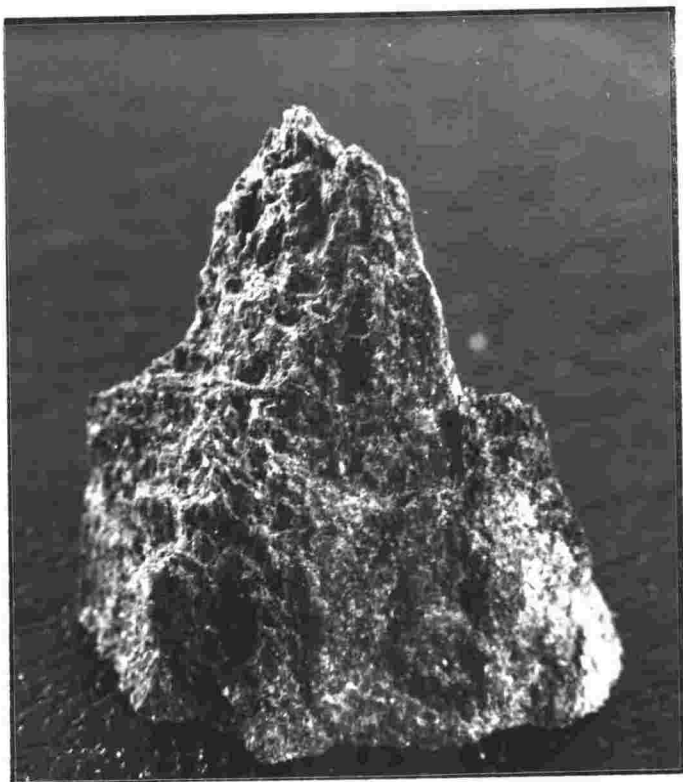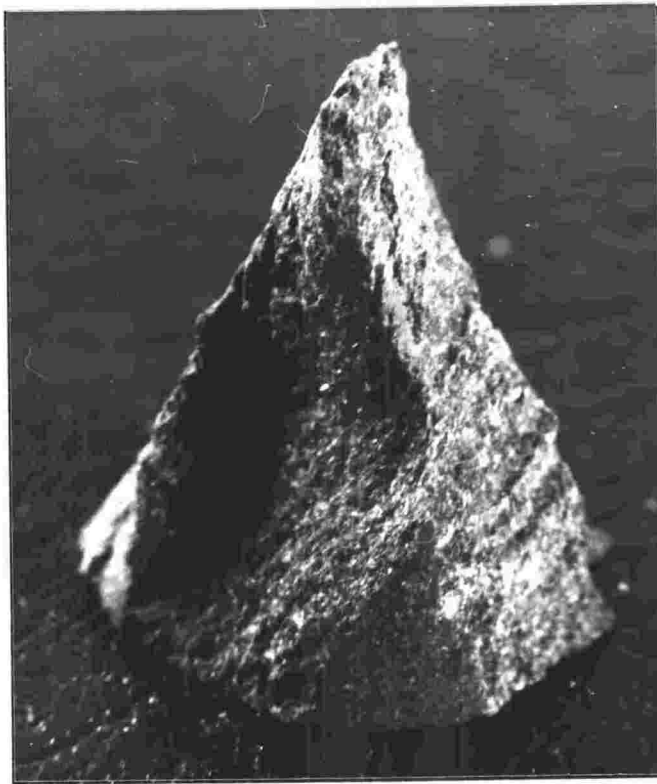
Plate A15.2 : Two views of HQ-17 (core 4) are shown, both are bottom cones from double cone failures showing surface flaking and *en echelon* flaking. Both fragments are 25 mm high.

intensely comminuted surface rock material. The fineness of comminution appeared directly related to the mean grain size of the parent rock and was a white powder in greywackes, grey in argillites. In all cases it was quite strongly bound to the rock surface (Plate A15.1A). Cataclastic surfaces are formed in association with all three failure modes but more strongly developed in longitudinal splitting and double cone failure modes. They developed regardless of rock moisture content.

3.2 Irregular planar surfaces: Surfaces were most commonly formed at angles between 0-15° to the longitudinal axis but smaller surfaces had orientations up to 90° (Plate A15.1A). These are the most commonly formed surfaces- a tensile splitting such that corresponding portions of the surface across the fracture do not come into frictional contact during or after core failure. These surfaces formed in all rock types in wet and dry test conditions; rather larger in wet. Surface colour is lighter (lower value) than that of the rock itself due to the presence of many very thin flakes of rock material which are partially detached from the surface. They remain as a non-comminuted flake, flat against the surface with perhaps one, two or three edges. Their surface extent is about two to three times the mean grain size of the rock in which they formed and they may have an irregular outline. Irregular planar surfaces, while not having any loose detritus was densely covered in a veneer of partly divorced thin (about 0.15 mm) flakes which would reduce bond strengths of aggregate in concrete (Alexander, 1963).

Irregular planar surfaces were most commonly formed in association with the logitudinal splitting failure mode.

3.3 Transition features: These formed in all rock types and were commonly associated with double cone failure modes. They represented a transition from the irregular planar surface to the cataclastic surface. They existed as a series of sharply *en echelon*, partly comminuted "ridges outlining a relatively broad zone of shear movement within the core (Plate A15.1B, A15.2). Their areal extent varied, but the fineness of the ridge structure was again a direct function of rock mean grain size - better developed in finer grained rocks. Core failure followed no obvious lithogical feature. Recemented shears (OB-W, see section 2.16.3) were traversed by failure planes. Because cores were cut perpendicular to bedding, no influence was apparent from the strength of grain orientation and hence fissility. Occasional fine veins (approximately 0.02 mm wide) in OB-W and HQ-22 were seen to "guide" some cracking but did not appear to reduce the load at failure compared with vein free cores. Larger veins (approximately 0.06 mm wide) promoted shear failure when orientated obliquely to applied load if they were of zeolite or calcite. Veins of quartz and prehnite showed no tendancy to become portions of fracture planes.

APPENDIX 16

Classification of intact rock by deformation characteristics, applied to Wellington greywacke-suite rocks

The significance of establishing uniaxial compressive strengths of rocks is explained elsewhere (section 3.5).   Results aid the choice of equipment required for winning and processing rock products and provides common ground between engineer and geologist.

Increasingly, engineering rock classification is finding favour as a means of quantitatively assessing *in situ* rock masses but systems derived to date fall well short of universal satisfaction and experience still outweighs calculated evaluation.

Lama and Vutukuri (1978) have summarised the development of intact rock classifications (i.e. the classification of rock "material removed from its environment and devoid of discontinuites") and show the importance of compressive strength and the stress-strain curve to these classifications.

The classification scale of Deere and Miller (1966) is now the most widely used (Figure A16.1) for describing and comparing intact rock characteristics.   Deformation characteristics of rock which are used for classification are related to compressive strength in a "modulus ratio" expressed either graphically or descriptively.
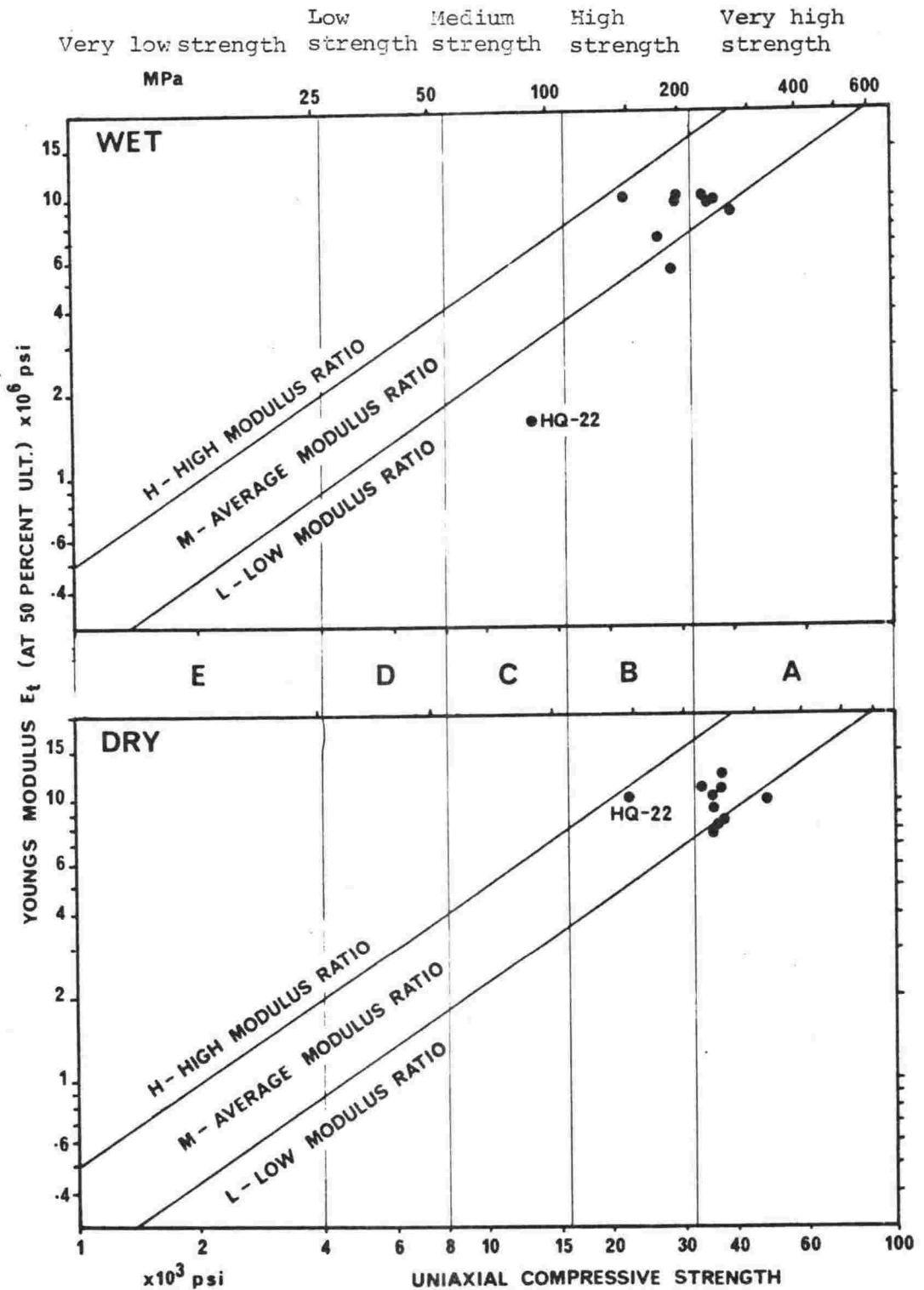
Figure A16.1 : Rock classification chart used by Deere and Miller (1966) originally for igneous rocks. Black dots show the classification of Wellington greywacke-suite rocks according to this scheme. Strength is subdivided into classes A, B, C, D and E for very high, medium, low and very low strengths respectively. Rocks are classified by both strength and modulus ratio e.g. wet samples would be classified AL, AM, BL, BM, CL; dry: AL, AM and BM.

APPENDIX 17

Angularity of rock particles: raw data

Included are photocopies of sectioned concrete cylinders from which particle angularity
was measured using a method of Lees (1964); Plate A17.1 to 12.   Figure A17.1 is the grid
used to select particles which were counted.   Raw data appears in Table A17.1.   Figures
A17.2, A17.3, A17.4 show relative frequency of particle angularity (A_{2D}) for each
aggregate.

The concrete cylinders were randomly selected from each of the groups of three tested in
uniaxial compression at three days.
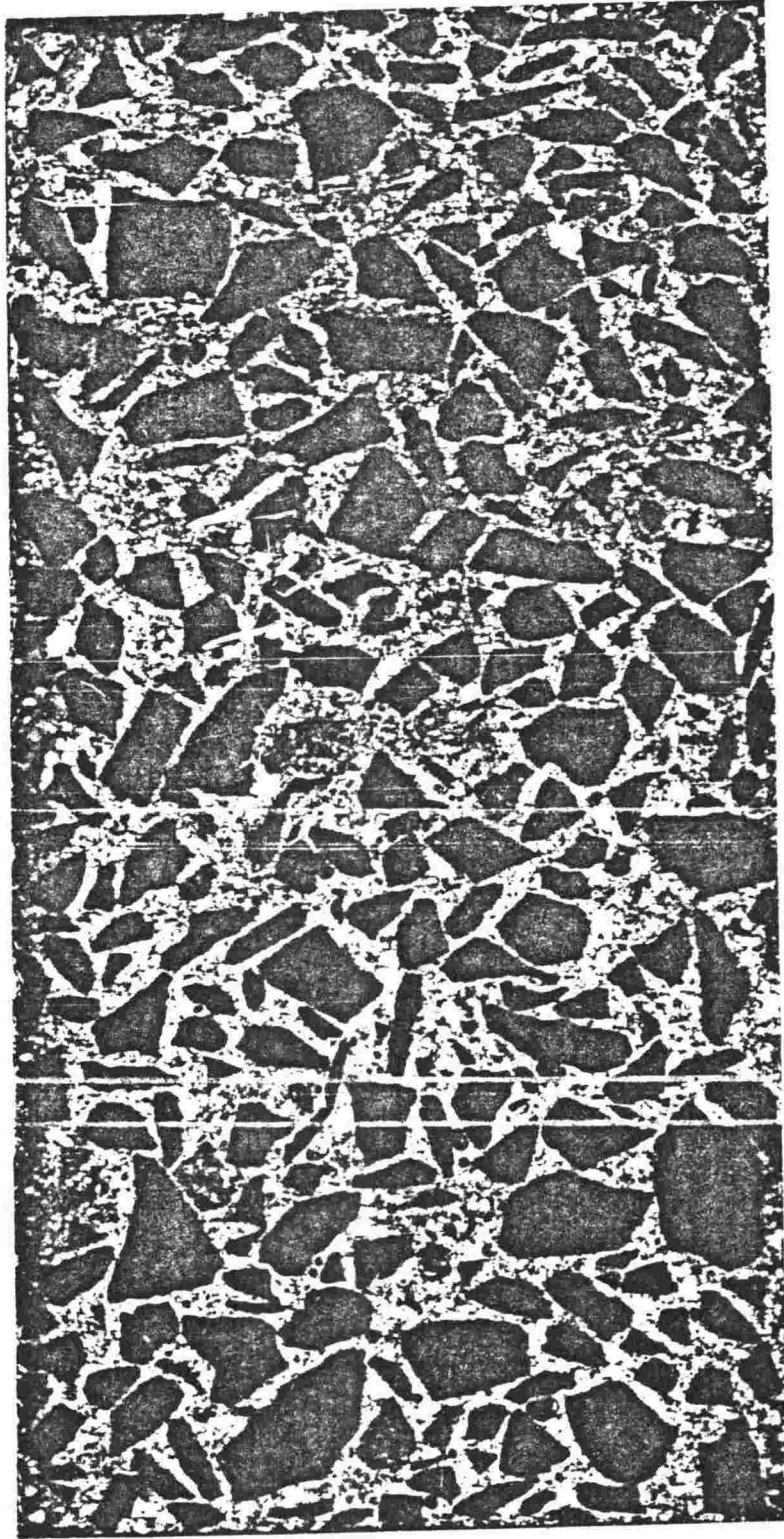
HQ-17 mix 1 (4)

Figure A17.1 to 12 : Photocopy images of sectioned concrete specimens from which angularity measurements were taken.
The top of the cylinder as cast, is to the top of the page. The number in brackets indicates the specimens place in the order angularity measurements were taken.
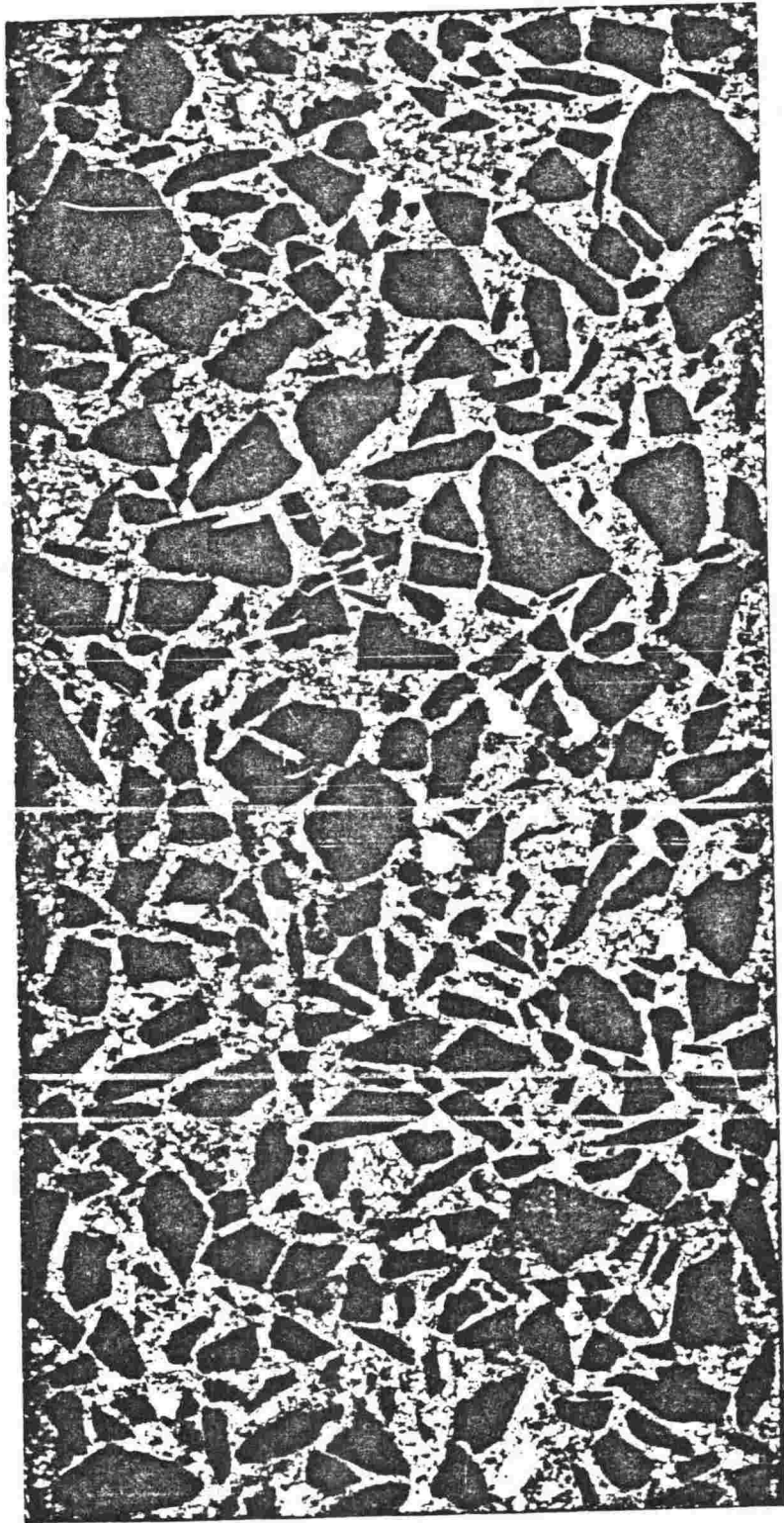
HQ-17   mix 2 (10)

KTW-14 mix 1 (2)
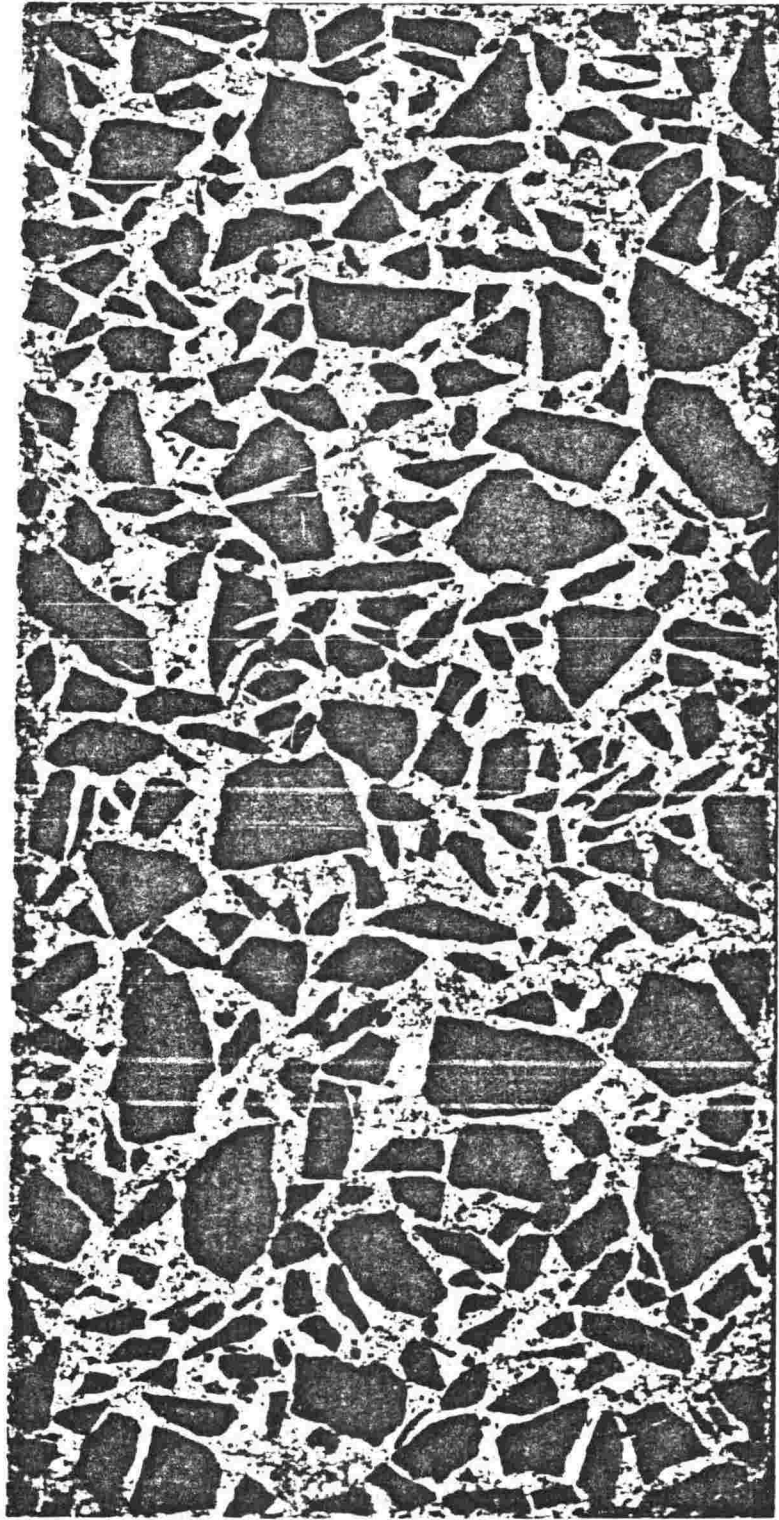
KTW-14   mix 2 (6)
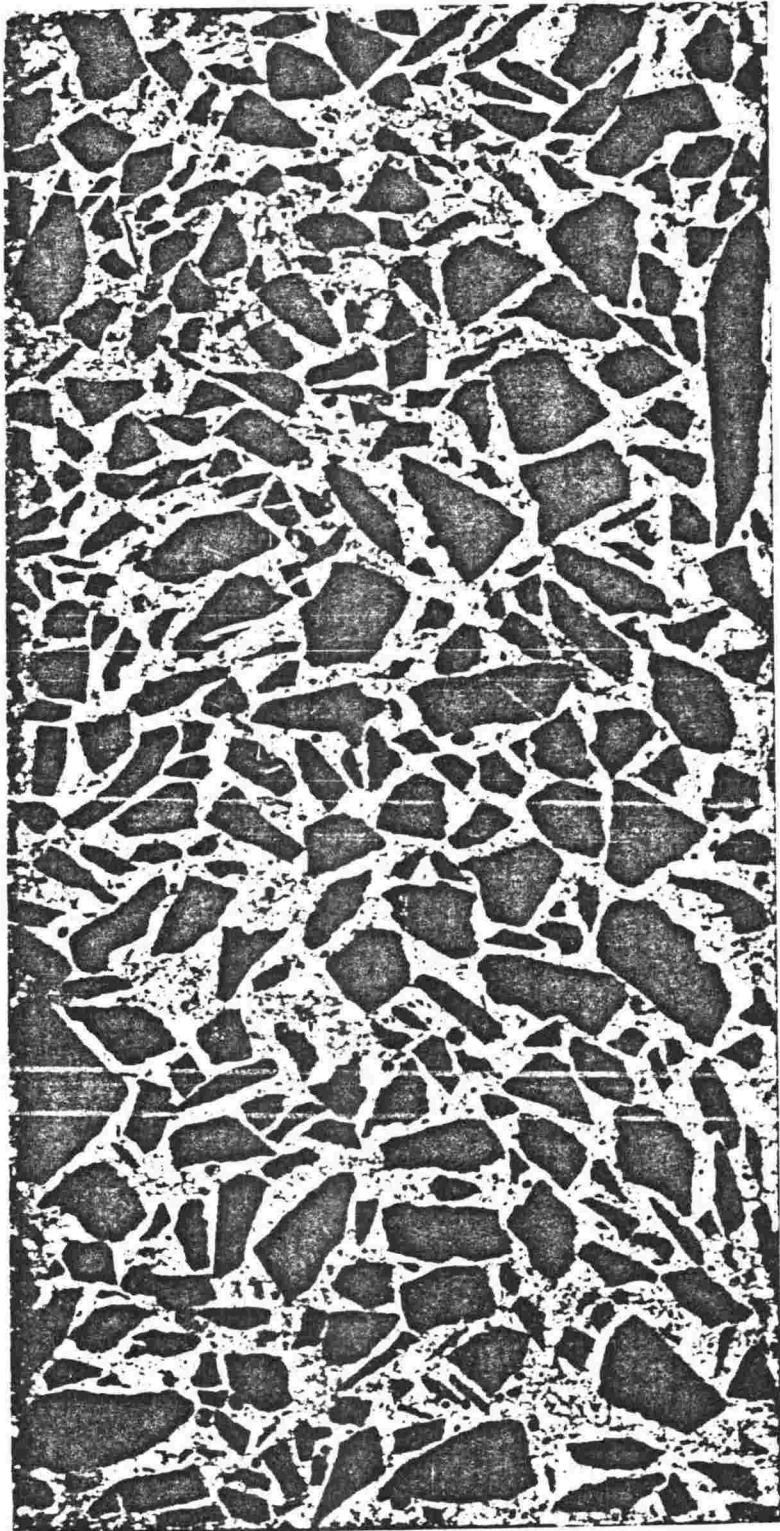
BQ-IXA   mix 1 (1)
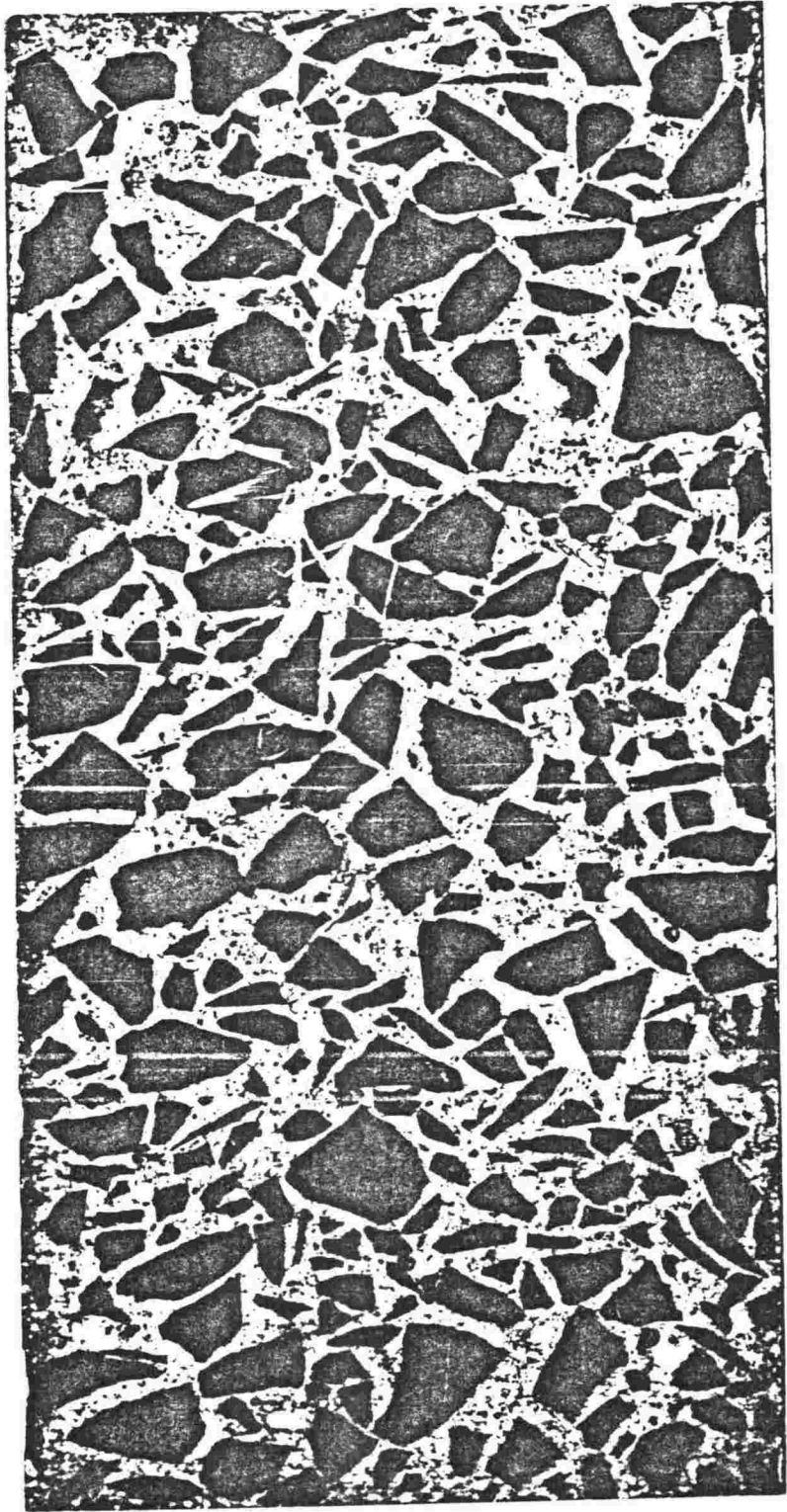
BQ-IXA mix 2 (9)
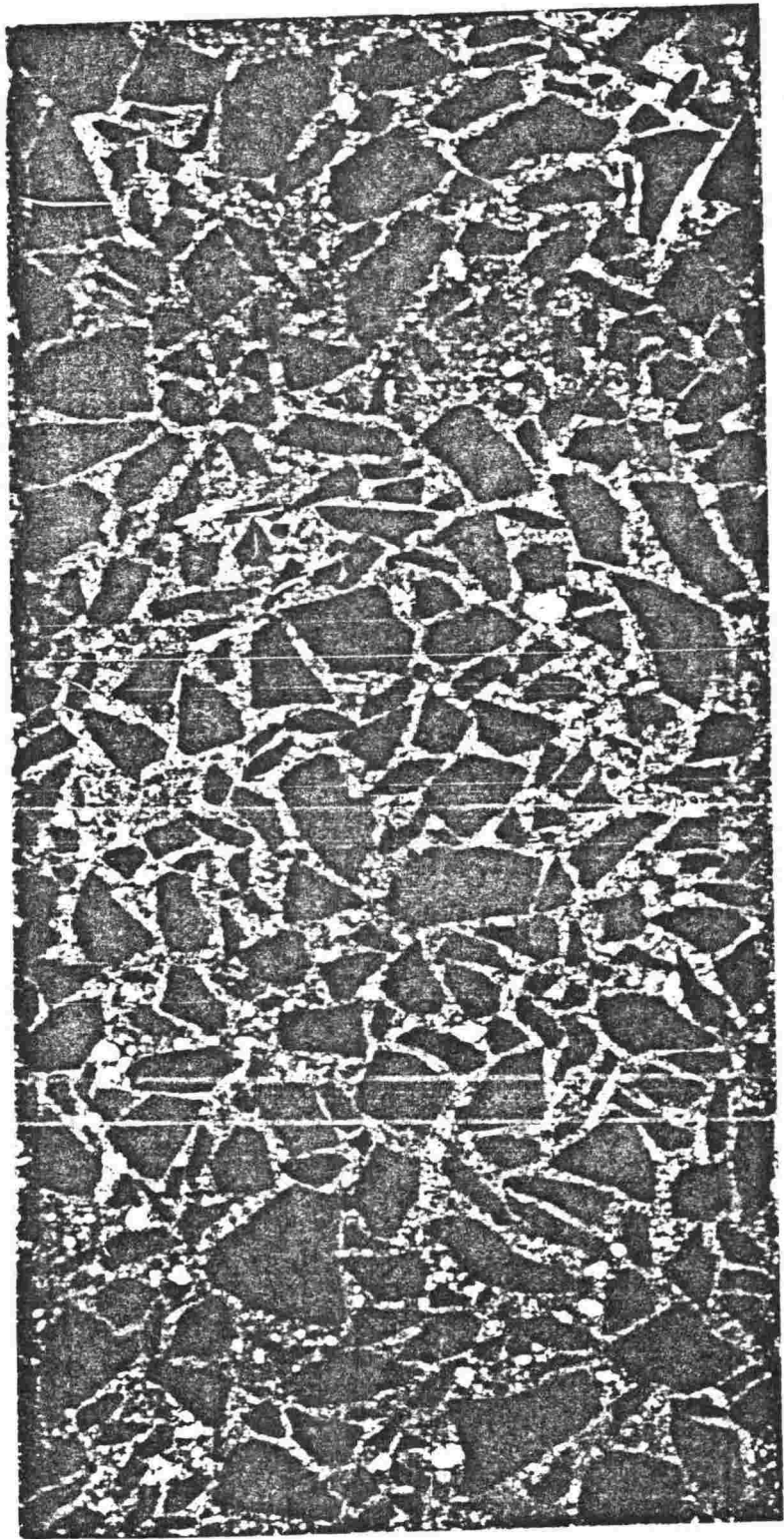
SJ-T mix 1 (7)

SJ-T   mix 2 (8)
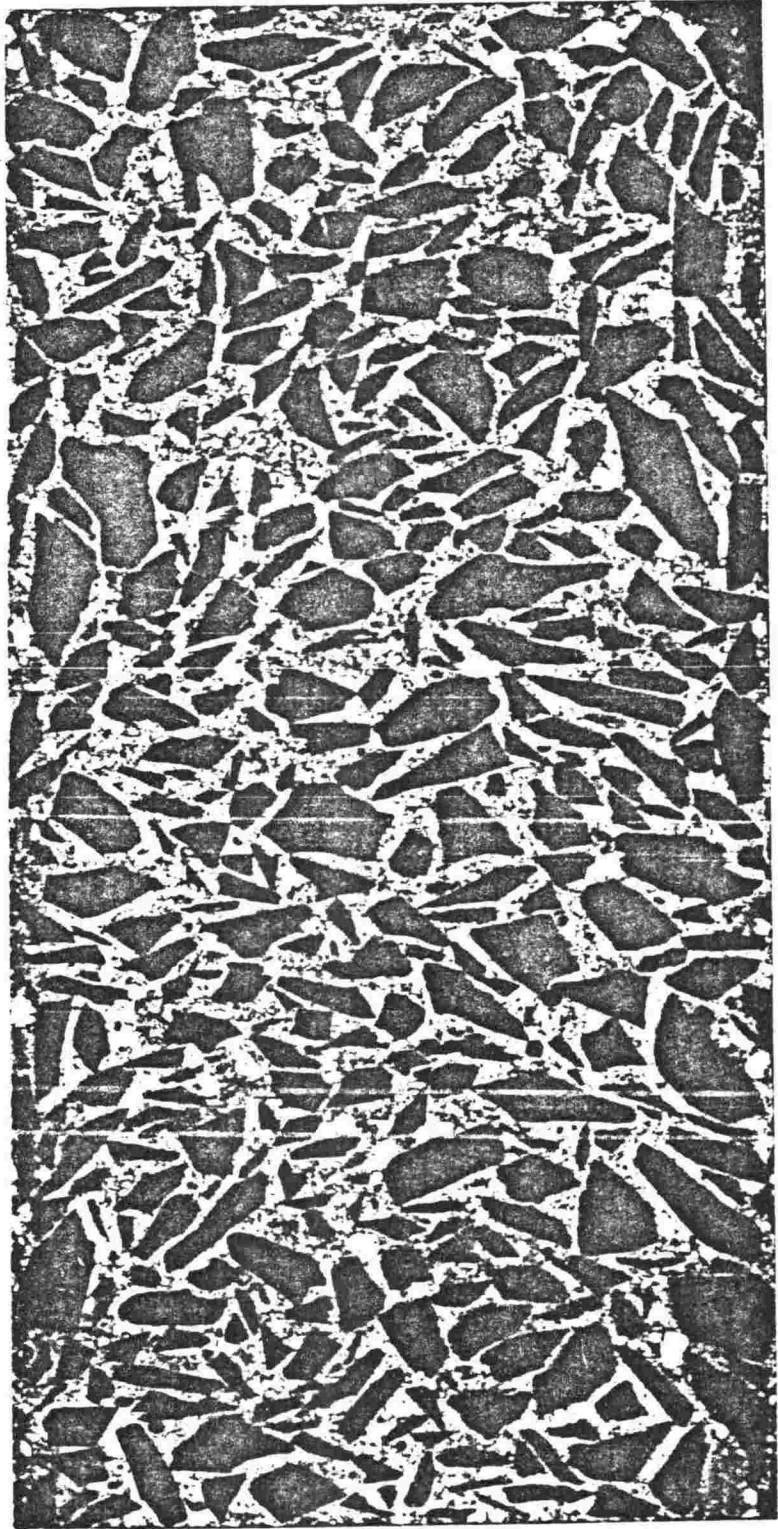
OB-W mix 1 (12)
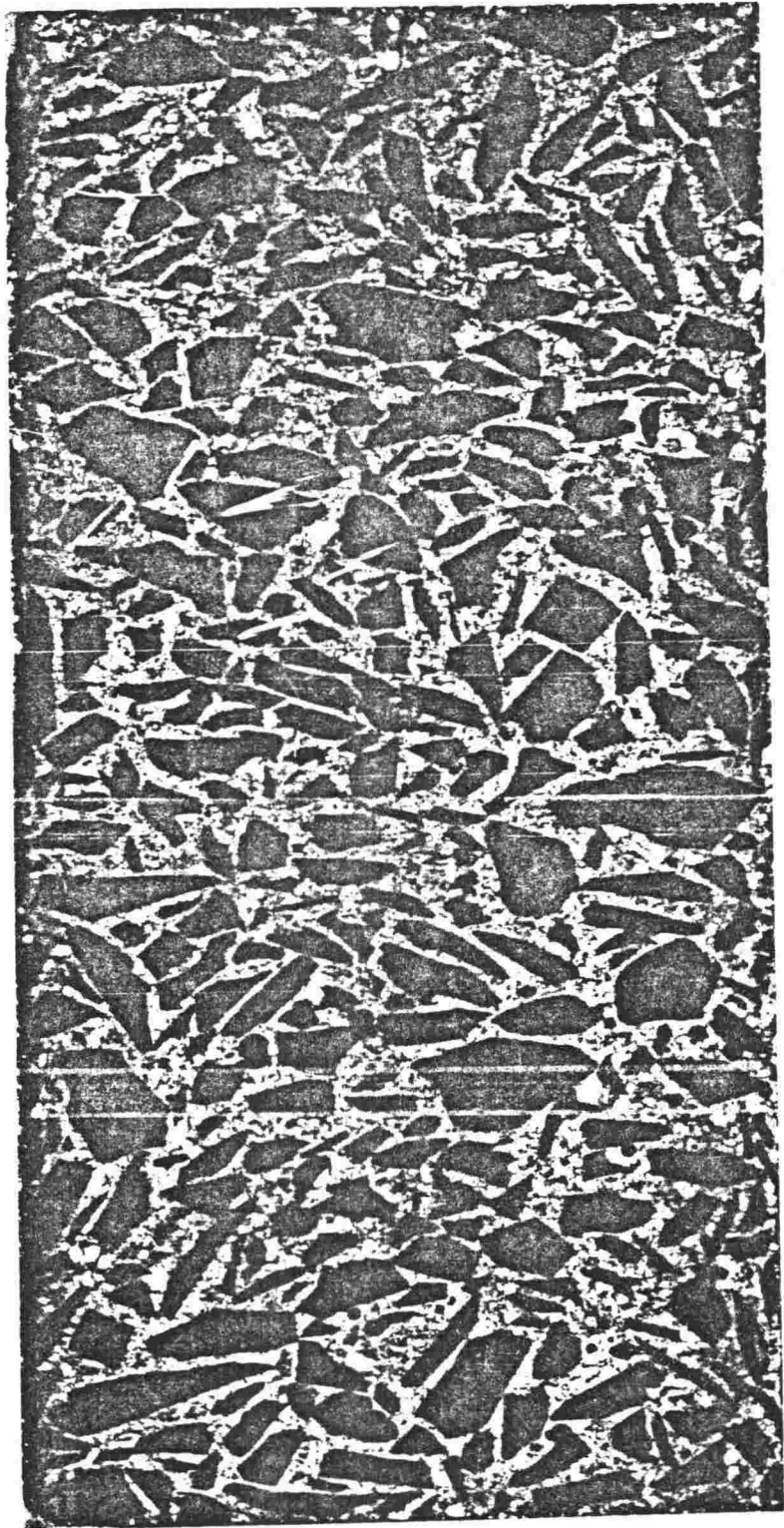
OB-W mix 2 (11)
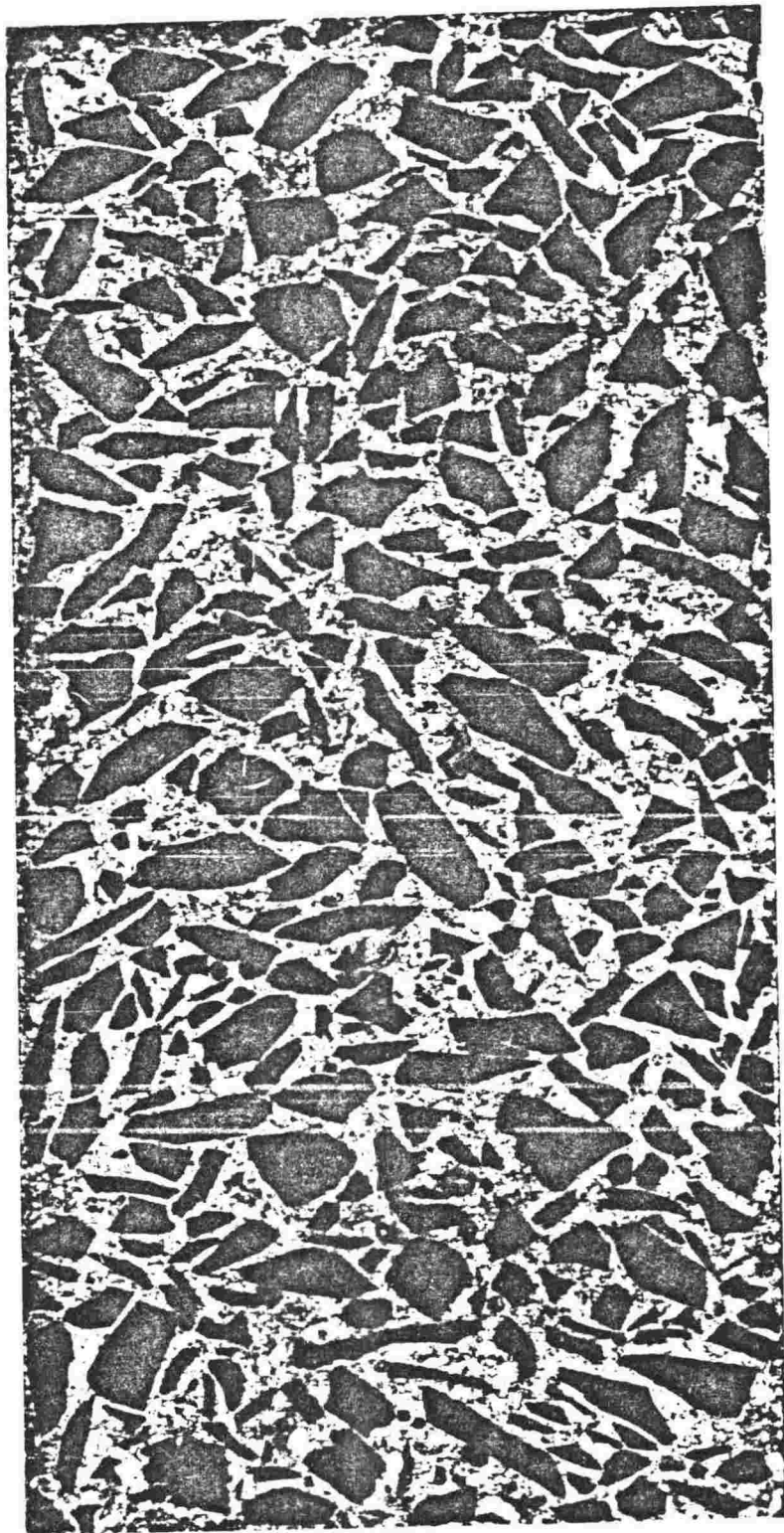
HQ-22 mix 1 (3)
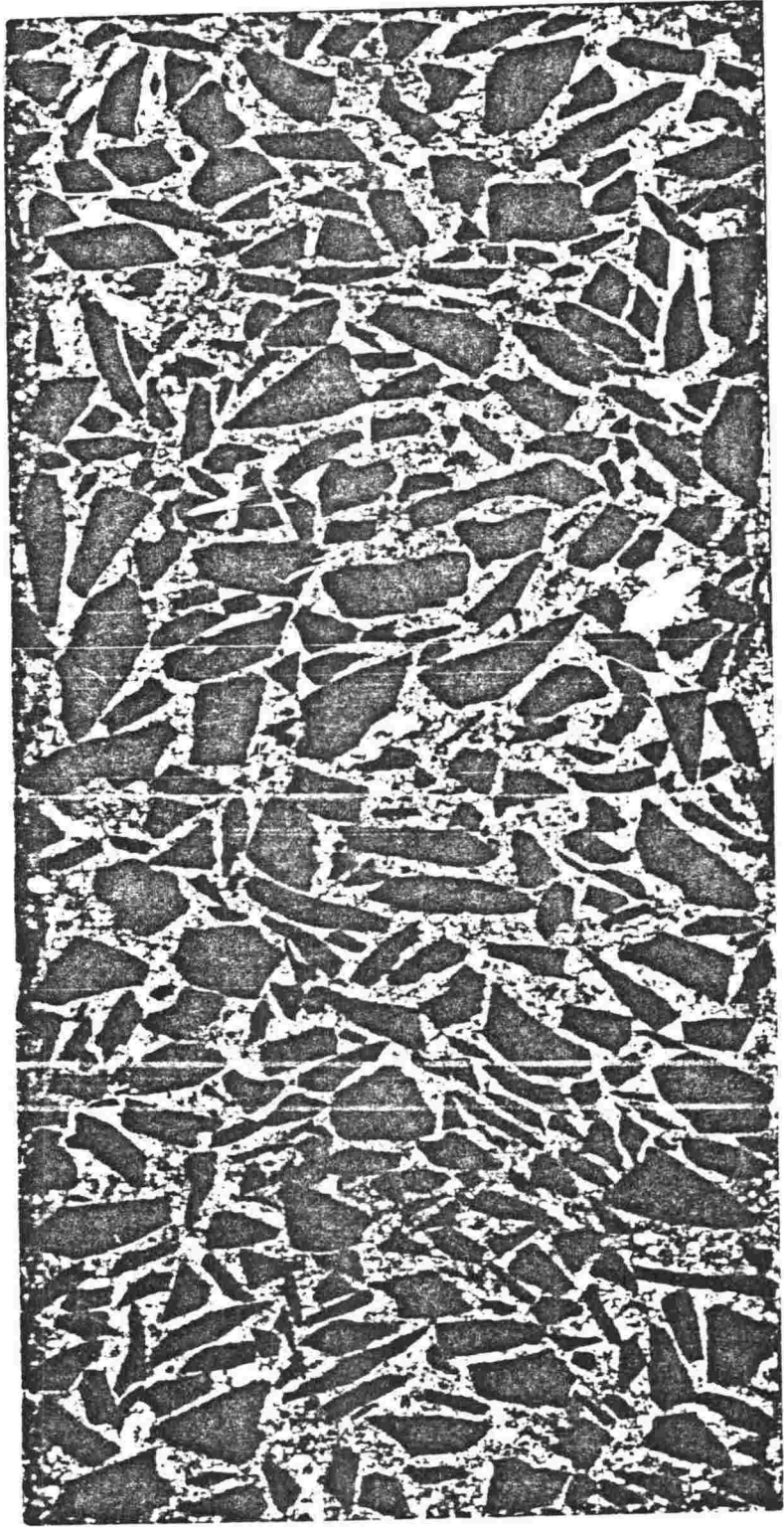
HQ-22 mix 2 (5)
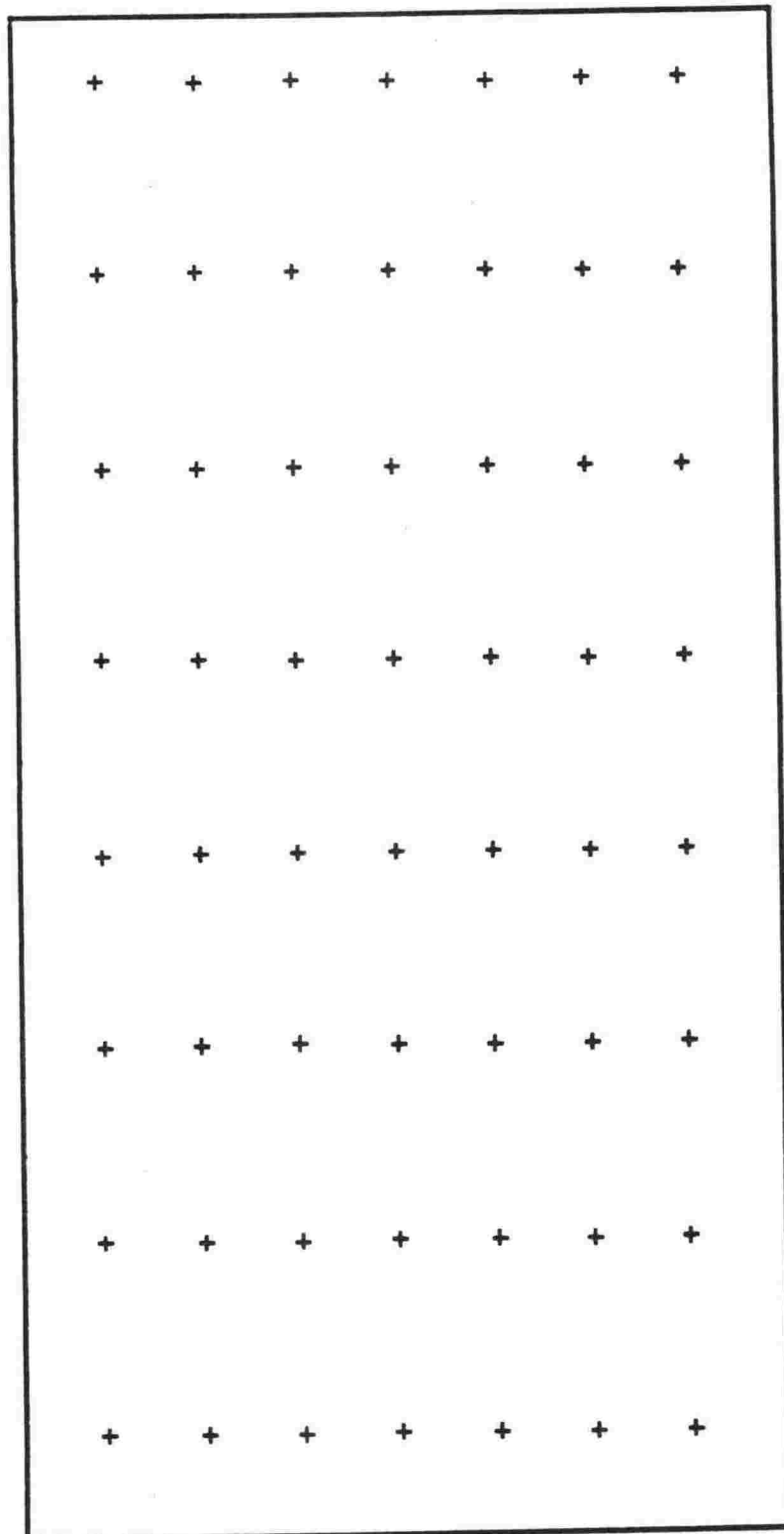
Figure A17.1 : Grid template used in particle selection for
angularity measurements. Crosses mark points from
which samples were taken. The border indicates the edge of the
photocopy image of the sectioned cylinder.

Table A17.1 : Angularity raw data for aggregate samples determined from sectioned concrete cylinders. At the base of each column in respective order are the total mean, standard deviation and coefficient of variation for angularity of the aggregate particles of the cylinder examined. The final value, n, is the number of aggregate particles.

HQ-17 1.3 phi		KTW-14 2.6 phi		BQ-IXA 2.9 phi		SJ-T 4.7 phi		OB-W 5.6 phi		HQ-22 6.3 phi	
Mix 1	Mix 2	Mix 1	Mix 2	Mix 1	Mix 2	Mix 1	Mix 2	Mix 1	Mix 2	Mix 1	Mix 2
450	885	665	960	615	680	630	1350	690	1058	825	920
485	445	485	895	470	590	755	955	1225	1200	1310	770
635	860	555	2740	745	1965	495	790	1805	675	765	1855
750	565	700	715	540	655	1743	480	810	760	588	1070
945	655	880	600	765	560	755	710	398	1845	455	1215
848	923	880	1275	1315	930	545	770	690	955	800	920
780	665	510	510	630	925	1040	600	1680	1100	1440	680
725	443	1070	415	590	1075	523	360	1175	1360	840	700
813	880	580	670	795	1295	1895	645	1185	1185	1450	875
440	620	838	775	810	915	415	1195	625	1610	1190	840
525	305	560	615	890	635	935	770	1660	900	870	570
390	645	1450	428	895	1140	1010	400	630	295	845	710
770	735	905	715	565	860	1030	790	2325	760	290	560
690	545	700	800	780	955	1250	890	1490	1205	535	1390
725	503	830	700	560	630	430	850	690	935	1235	970
1800	480	1095	1115	710	420	420	490	1275	975	565	765
450	880	625	1398	1005	615	960	605	1075	865	520	865
447	650	1735	805	452	940	1210	1130	600	740	755	1060
800	1300	520	685	940	900	745	680	350	1265	885	535
505	1260	515	1235	513	975	675	945	625	585	905	1050
490	770	585	945	445	840	780	420	740	498	855	790
1395	965	790	710	683	555	380	605	770	1245	995	1155
750	1015	670	760	400	465	980	625	530	570	820	940
650	1765	2320	870	775	950	980	570	980	1760	1095	885
765	495	1000	700	850	860	940	370	633	1130	985	710
1050	740	715	603	530	935	628	800	685	2495	1500	820
885	1750	740	695	1020	940	1320	340	1440	1030	1075	925
540	600	795	1325	1120	1125	960	960	1403	1320	500	1140
520	825	935	810	1230	875	415	755	2135	785	1730	1010
730	490	1100	710	820	385	480	685	990	1020	725	690
425	1310	645	675	705	1680	775	720	608	1110	680	725
635	790	595	545	570	1300	1345	1065	1115	1570	840	735
965	685	1890	685	1070	750	810	630	700	600	790	680
350	800	1070	880	1305	835	1165		1800	785	1235	1880
790	535	840	529	725	1160	810		785	785	865	775
1245	620	1090	805	715	695	495		1220	615	1880	670
1230	1060	460	440	885		730		740	820		1115
420	560		658					683	2160		1140
610	375							960	1030		1220
1430	825							995	1832		
793	1130							835	450		
								440			
								890			
								1980			
								970			
								855			
30640	32347	32338	31394	28432	32010	31453	23990	46883	43882	33624	36325
747	789	874	826	768	889	850	727	1019	1070	934	931
314	330	406	398	238	325	359	247	474	469	359	299
42.1	41.9	46.4	48.0	31.0	36.6	42.3	33.9	46.6	43.8	38.4	32.1
n=41	n=41	n=37	n=38	n=37	n=36	n=37	n=33	n=46	n=41	n=36	n=39
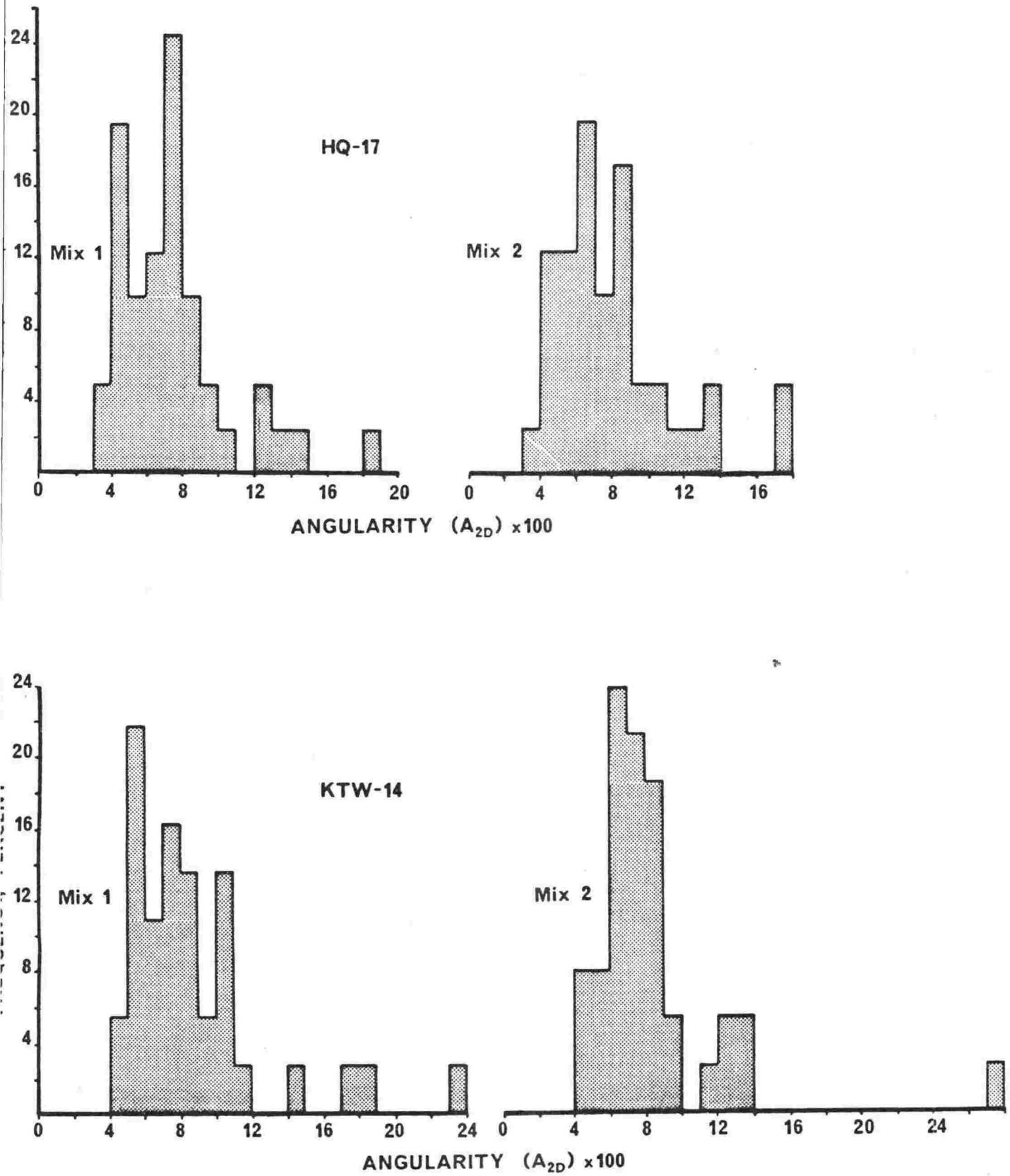
Figure A17.2 : Angularity frequency histograms of aggregate particles,
HQ-17 and KTW-14.
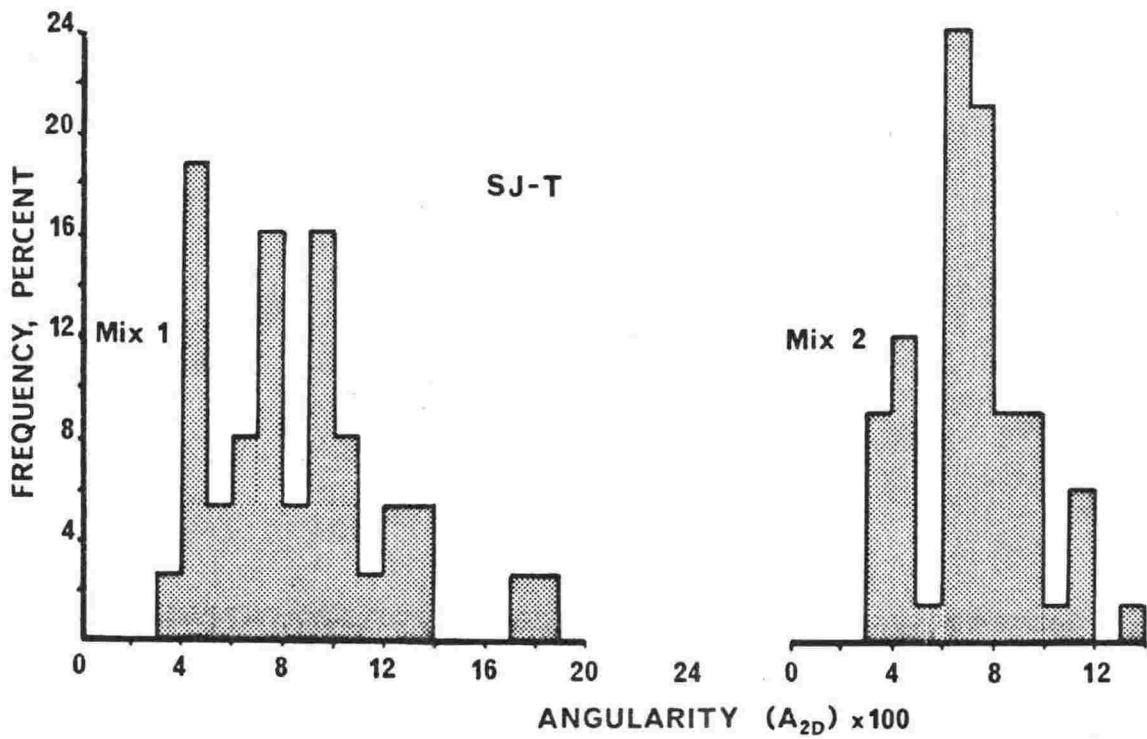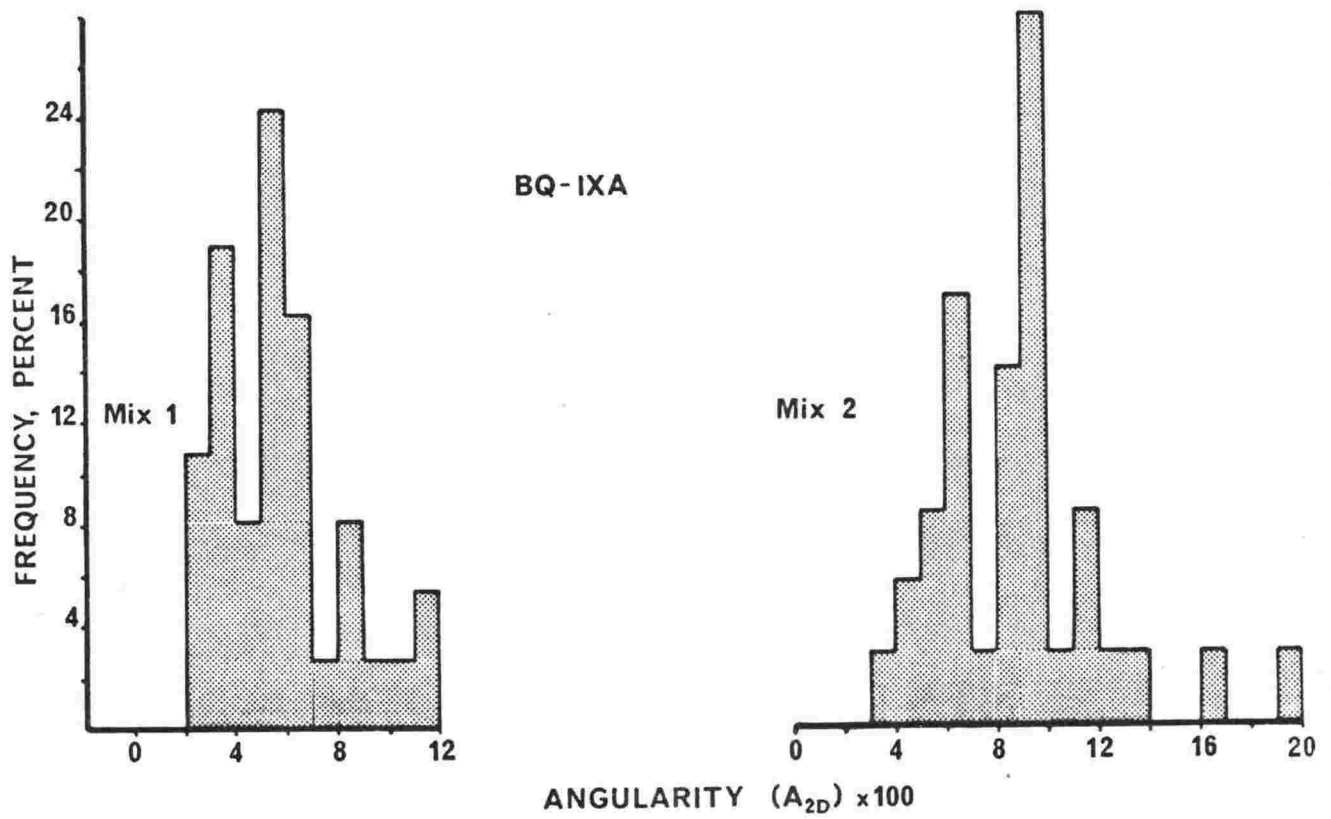
Figure A17.3 : Angularity freqency histogram of aggregate particles
BQ-IXA and SJ-T.
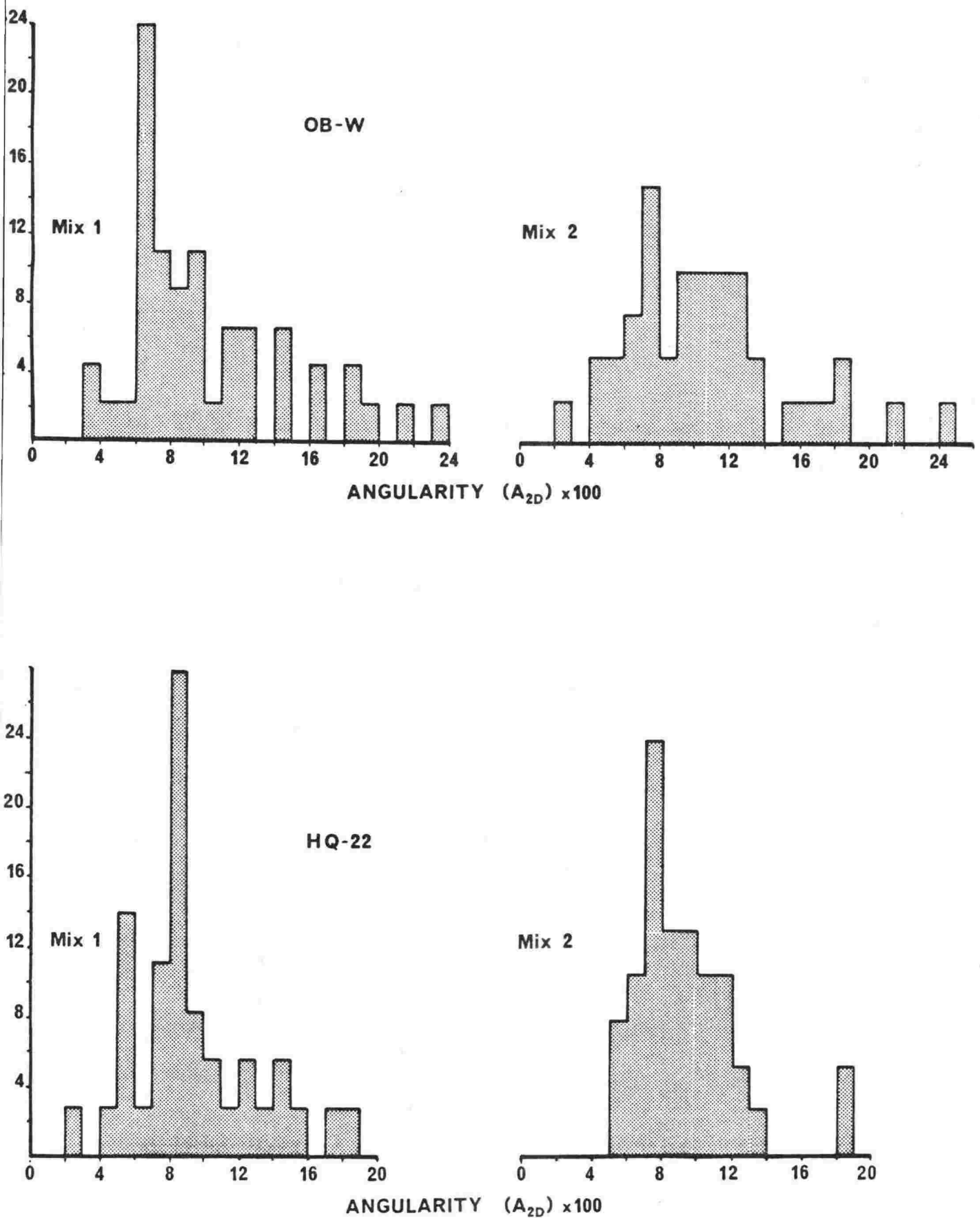
Figure A17.4 : Angularity frequency histogram of aggregate particles, OB-W and HQ-22.

APPENDIX 18

Comparison of the Los Angeles abrasion test with uniaxial compression test as a measure of rock strength

Recently a paper by Kazi and Al-Mansour (1980) presented data on igneous rock from Jeddah, Saudi Arabia, indicating that its use for engineering purposes could be assessed by its average unit mass and results of the Schmidt hammer test.   Indeed Los Angeles results may be predicted from Schmidt hammer test results, or uniaxial compressive strength.

Figure A18.1 is reproduced from Kazi and Al-Mansour (1980) and shows the relationship between Los Angeles abrasion test results and uniaxial compression strength.   Superimposed data from this study extends the graph from 170 MPa to 263 MPa.   The result for OB-W is attributable entirely to its high particle angularity (section 4.2.6, Figure 4.8).   It appears from this, that for rounded and strong aggregates, the Los Angeles test is ineffectual and that it is best utilised on rocks of strength ranging between 20 MPa and 100 MPa. Rocks stronger than this are delineated by particle shape rather than on resistance to abrasion and particle shape is better assessed by other means.
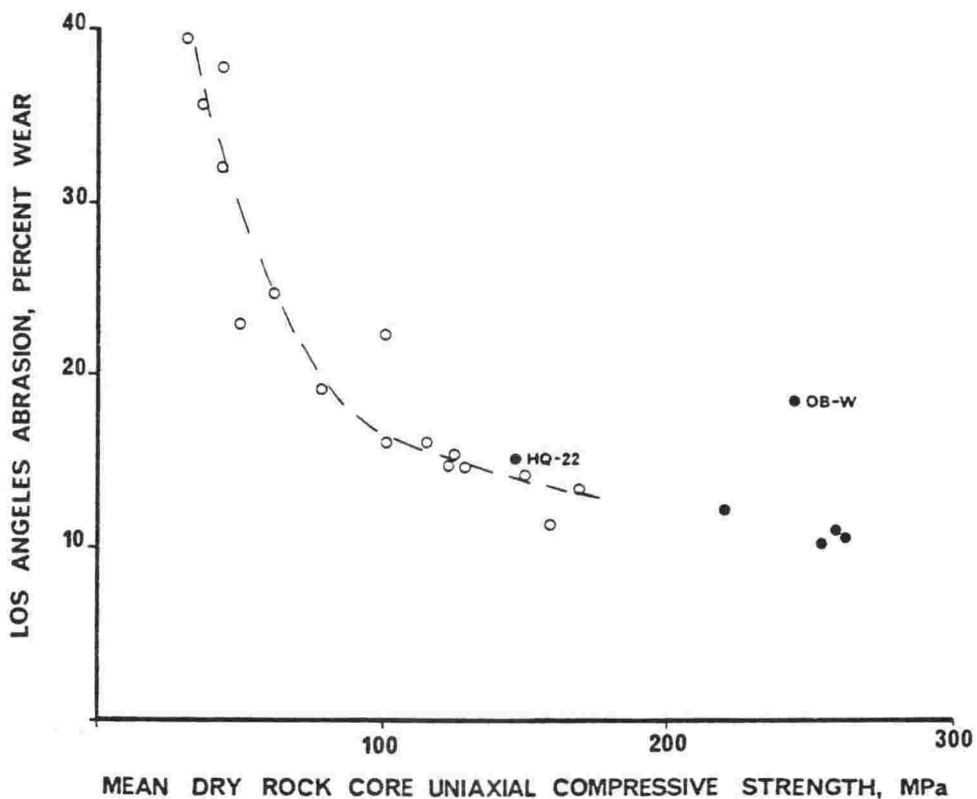
Figure A18.1 : The relationship of Los Angeles abrasion results and uniaxial compressive strength of rocks.   Data shown by open symbols are from Kazi and Al-Mansour (1980).   Solid symbols are from this study.

APPENDIX 19

Effect of moisture content on ultrasonic velocity of rock

A homogeneous, flaw free, right prism was prepared from a fine grained greywacke (KTW-i), grading at one end over approximately 50 mm into an argillite. The prism measured 209 x 50 x 50 mm, its long axis perpendicular to bedding. The sample was allowed to equilibrate at room temperature after cutting and was then immersed in tap water for 38 days. After a further 12 days drying at room temperature, the sample was placed in an oven at 105 ±5°C for one day, then left at room temperature a further eight days. During this time the effects of water was educed from daily tests with the PUNDIT apparatus, along the long axis of the prism.

Ultrasonic velocity in a solid depends on the density and elastic properties of the material. In porous materials the ultrasonic velocity may be enhanced by saturation with water, the water enabling a more complete acoustic path to be formed. This effect is shown by greywackes, so the state of saturation of the prism could be assessed by measuring the relative "completeness" of the acoustic path. Acoustic contact for trasducers was made using a paste of glycerin and talcum powder. Results are shown in Figure A19.1.

Within six days, the prism had reached saturation, and fluctuations in ultrasonic velocity over the next 32 days were within the 2 percent error of the apparatus. Release of water is a slower process than water uptake, considering the gradient of the line (Figure A19.1) showing acoustic change between day 38 and day 46, whilst the prism was drying at room temperature. After oven drying, a marked reduction in ultrasonic velocity was apparent. Moisture uptake from the atmosphere at room temperature appeared to take place at a rate, reflected in ultrasonic velocity change, similar to that of water immersion. A short-fall of 69 $m.s^{-1}$ was noticed after the experiment, compared with the initial ultrasonic velocity. This may be due to permanent moisture loss from the prism and/or cracking of the prism. Sparce microcracking had occurred in the argillaceous end of the prism before the end of the experiment.
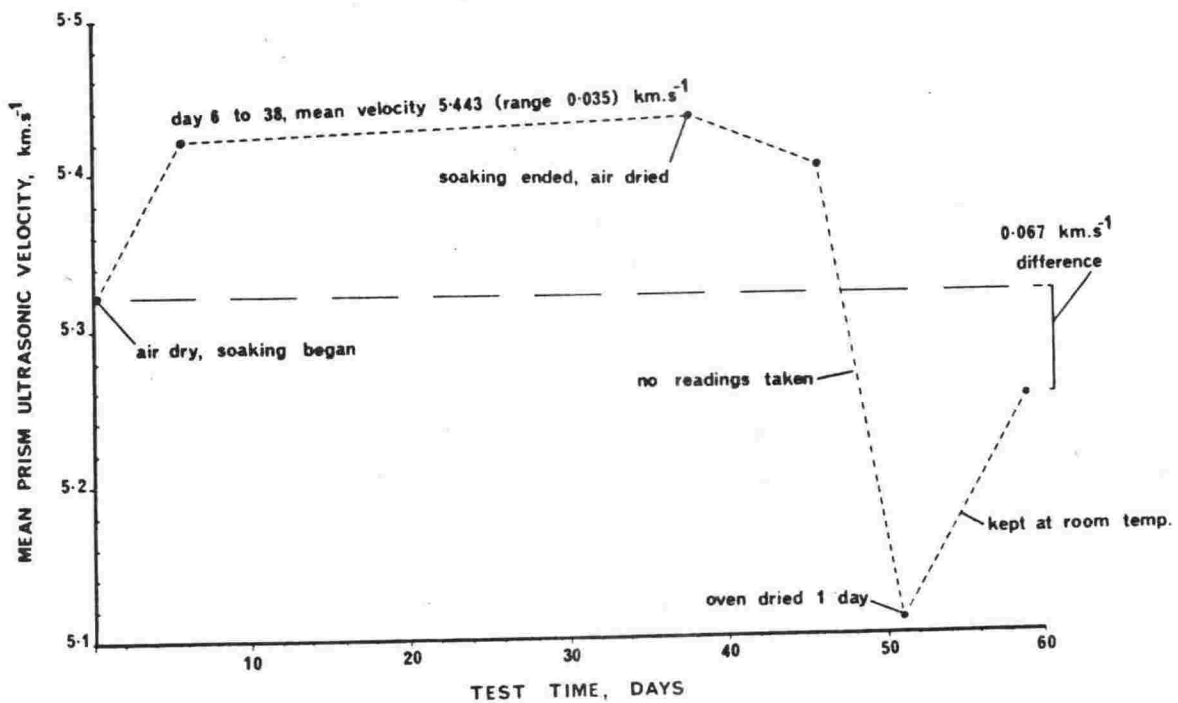
Figure A19.1 : The response of a prism of KTW-i greywacke (4.2 phi, 0.054 mm rock mean grain size) to various degrees of saturation measured by ultrasonic velocity variations. A permanent loss of moisture seems apparent after oven drying of rock.

APPENDIX 20

Measurement of unrestrained moisture movement in rock

The apparatus was made from a heavy retort stand with a heavy sliding collar fitted to its upright.   The collar had 3/16 inch WHIT. grub screws inserted in threaded holes at 90° so that it could be adjusted for height (Figure A20.1).   A lug welded to the collar enabled mounting of a dial gauge reading to 0.0001 inches.   A locating shoe with a conical recess, 5.5 mm diameter and 90° apical angle, centered in its lower face was fitted to the gauge spindle.   Apparatus using similar principles may be seen in Duncan (1969).

Samples were prepared from 25 mm diameter cores, cut perpendicular to bedding, one end ground plane and at right angles to the vertical axis; the other end, coarse ground ($\pm 20^\circ$), had a ball bearing (4.8 mm diameter) cemented (black, two part epoxy "Plastic Steel" was best) at its centre.

After drying for 24 hours at $50^\circ C$, samples were placed free standing in a vessel with a plane, flat base (inside and out) and of convenient size to completely accommodate the sample.   The vessel, filled with distilled water to the level of the ball bearing, was placed on the retort stand with the ball bearing centred under the dial gauge shoe.   Only the ball bearing was above the water level.

After ensuring the system was aligned correctly the dial guage was read and the time noted. Dial gauge readings were taken at intervals until no significant change was noted between readings or until the sample failed from internal air pressures.

Throughout all tests the apparatus was placed on a vibration free pad on a piece of firm carpet in a constant temperature room.   Vibration free conditions for each test period were further ensured by restricting access to the room.

40

thick walled
tubular collar,
smooth fit

dial gauge

175

12 D

water

vessel with plane,
smooth internal
bottom surface

15

baseplate 130 wide

160
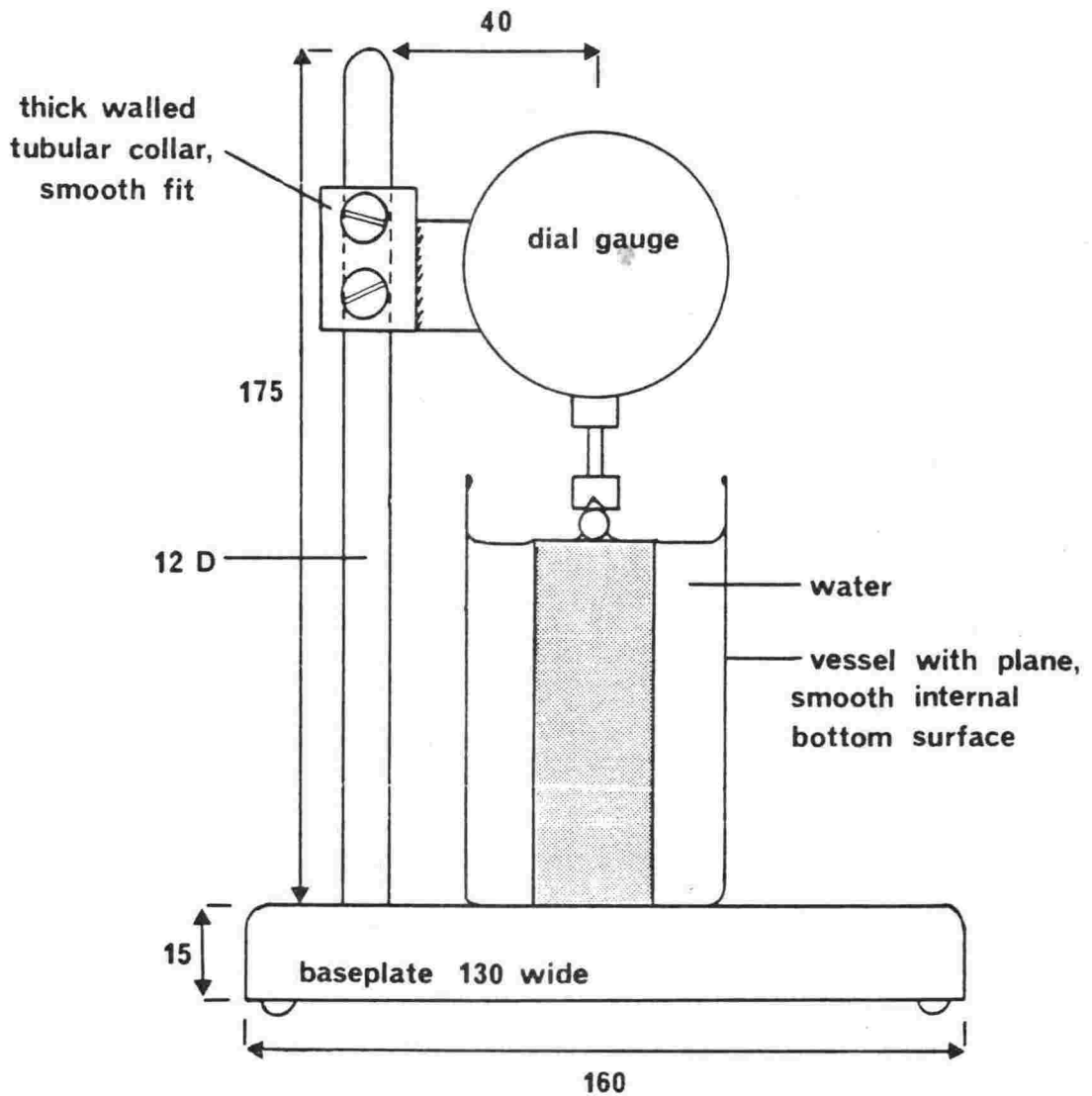
Figure A20.1 : Apparatus used for rock core unrestrained moisture
movement determinations. A rock core (shaded) with
ball bearing reference point afixed, is shown in position. Adjusting
feet keep baseplate level. All parts are mild steel except base-
plate and locating shoe which are cast iron and stainless respec-
tively. Dial gauge is adjusted to suit sample length.

Figure not to scale, dimensions in millimetres.

APPENDIX 21

Measurement of cyclic moisture movement in rock

Apparatus for this test series was identical with that shown by Duncan (1969, plate 18, p 97, and also Figure A21.1). It is also described in NZS 3112:1974, Method C1 "Determination of the drying shrinkage and wetting expansion of concrete". The method involves the use of a comparitor bar.

Samples with planar ends were cut from cores perpendicular to bedding. Ball bearings 4.8 mm diameter were cemented in the centre of each end. After intial drying to constant mass in a constant environment room (20 $\pm 1^{\circ}$C, 50 percent R.H.), samples were tested in a similar manner of Roper (1959), i.e. the comparitor bars and cores were measured and compared using a dial gauge mounted in the apparatus. Samples were then placed in distilled water at 20°C for four days $\pm$4 hours, measured, oven dried (50°C) for three days $\pm$4 hours then remeasured. The process was continued for several cycles.

The dial gauge provided reasings to 0.0001 inches and comparitor rods were made of invar and stainless steel for the rock prism (KTW-i) and rock cores tested respectively. All measurements were taken, and comparitor bars stored, in the constant environment room. Comparitor bars were used as a length standard against which correction could be made for changes in the dimension of apparatus.

Results were expressed as percentages, i.e. movement increments with respect to sample length before testing. The sample cross-section is irrelevant to the test and any convenient cross-section may be used.

bar, 30 wide, 12 thick, drilled to slide over uprights. Ends drilled and tapped for clamping bolts

160

dial gauge

350

adjust for sample height

12 D

baseplate 130 wide, 12 thick

200
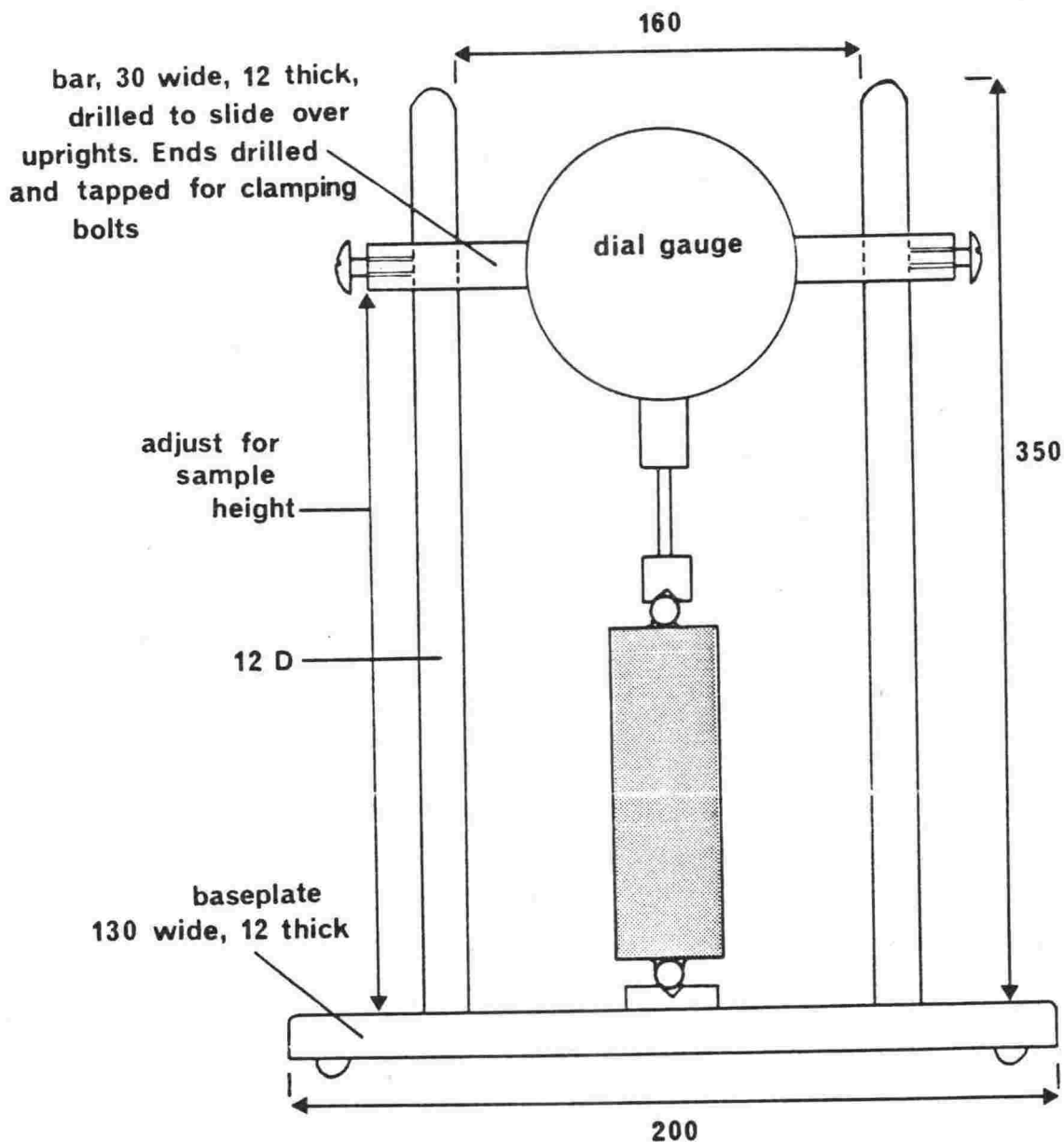
Figure A21.1 : Apparatus used for rock core cyclic moisture movement
determinations. A rock core (shaded) with ball
bearing reference points afixed, is shown in position for measure-
ment. Bottom locating shoe is vertically beneath dial gauge
locating shoe. Adjusting feet keep baseplate level. All parts
are mild steel except locating shoes which are stainless.

Figure not to scale, dimensions in millimetres.

APPENDIX 22

Measurement of rock permeability

1.   Sample preparation

Sample preparation was similar to that of Jaeger (1972).

Rock core, 25 mm diameter, was air dried for approximately one week, cut to a convenient length with one end finished as a plane surface perpendicular to the vertical axis and encapsulated with epoxy resin in a wax paper mould (drinking cup) in the following manner:

(i)   Epoxy was mixed in the following proportions

      100 parts Araldite GY252 resin
      100 parts Araldite CY208 resin
      30 parts Araldite HY956 hardener

CY208 resin was added to retard the exothermic reaction, allowing the soft walled mould to retain its shape during setting and to enable trapped air bubbles to surface.

Each rock sample was coated in a thin layer of the mixed epoxy to ensure air bubbles would not be trapped at the epoxy/rock interface, promoting a local increase in permeability at that point.

(ii)   Each sample was placed centrally in a waxed drinking cup (base 45 mm diameter, top 70 mm diameter, height 100 mm) and epoxy gently poured round the sample.   The cup was filled until the sample was just encapsulated.

(iii)   Encapsulation was timed to provide overnight setting.

(iv)   After 12 hours the paper cup was carefully peeled off and the quality of casting inspected.   Care was needed at this stage as the epoxy could still be deformed slightly under heavy finger pressure due to the retardant action of CY208 resin.   If successfully cast, samples were placed in an oven at $40^{\circ}C$ for 24 hours to cure.

(v)   Top and bottom surfaces of the epoxy were ground away until rock core ends were exposed.   Both surfaces were fine ground parallel.

(vi)   The upper face of the epoxy surround was drilled (3.7 mm) using a template to the pattern shown in Figure A22.1 and tapped (3/16 inch WHIT) to accept 3/16 inch WHIT gutter bolts.

2.   Apparatus

The apparatus used was of the falling head type illustrated by Curtis (1971), particularly applicable to materials of low permeability.   To simulate the natural movement of water, the most important media to move through rock, it was nesessary to ensure that there was no soluable or insoluable matter introduced which could "seal" the sample, so distilled water was used throughout the test.

62

51

chamfer

spigot, 7OD, 2·5 ID

TOP SURFACE OF
SAMPLE HOLDER

20

5·5 D holes

polythene tube

cadmium plated
gutter bolt $\frac{3}{16}$" WHIT.,
length to suit

5·5

'O' ring, 30 D,
2·5 section

epoxy casting
drilled and tapped
to $\frac{3}{16}$" WHIT. Top and
bottom surface fine
ground parallel
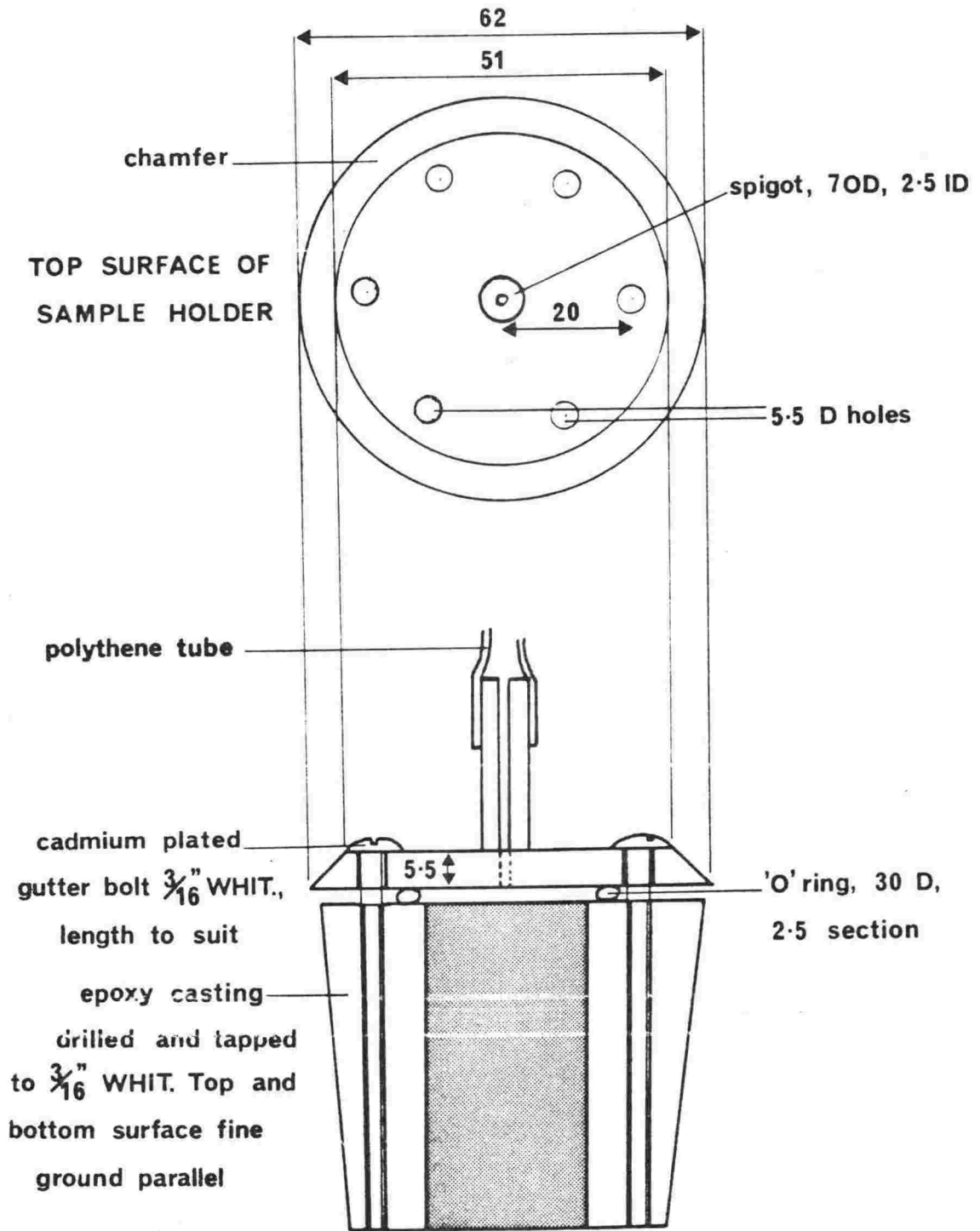
LONGITUDINAL SECTION ASSEMBLED SAMPLE AND HOLDER

Figure A22.1 : Permeability apparatus sample holder detail.
Figure not to scale, all dimensions in milli-
metres.   Sample holder made from brass.

The apparatus (Figure A22.2, Plate A22.1) consisted of a thick-walled precision calibration tube (2.27 mm internal diameter, measured with an optical micrometer) 600 mm long, fastened by a rubber bung in a 5 litre aspirator reservoir. A heavy walled polythene tube (2.5 mm internal diameter, 5.0 mm external diameter) was connected, at the outlet tap, and 16 m of this, taped to 5 mm polypropylene braided line at approximately 300 mm intervals, was connected to the brass sample holder (Figure A22.1).

3.   Permeameter operation

Samples were fixed to the sample holder using six gutter bolts and an "O" ring soaked in distilled water for at least one month. To ensure that no air bubbles were trapped in the system, the reservoir was filled and the feeder tube to the sample holder bled by opening the reservoir tap before the sample was finally fixed in place. Great care was taken to exclude all air from between sample and sample holder. The sample and sample holder as a unit were then lowered down a 1 m diameter concrete lined hole 15 m deep and made fast at the top of the hole by the 5 mm line. A maximum and minimum thermometer was lowered to the same depth as the sample.

Finally the calibration tube was extracted, the reservoir topped-up and the calibration tube replaced, allowing water displaced from the reservoir to rise in the tube.

4.   Minimising errors

Potential sources of error included:

(i)   Temperature change over the test duration.

(ii)   The tube between reservoir and sample holder changing dimension with time.

(iii)   Leakage.

(iv)   Elastic "relief" of the rubber bung holding the calibration tube in position.

(v)   The length of the calibration tube.

To check their probability, monitor their effects and minimise these where practicable, the following precautionary steps were taken:

(i)   Temperature change was monitored by a maximum and minimum thermometer reading to $0.1°C$. The hole down which testing took place was drilled in weathered rock beneath the building and air circulation was limited. Temperature change at the bottom of the hole was negligible over the duration of each test. Temperatures at the reservoir were higher but still stable over the duration of a test. The room in which the equipment was housed had no windows and was ventilated by an air condition/heating system. Access to the room by personnel was restricted.

The temperature gradient from reservoir to sample on test was continuous and water velocities in the tube so low as to ensure water in the tube was at equilibrium with the environment immediately surrounding it. In this way the viscosity of the water at the sample was maintained constant, for the temperature at that point. After change of sample, adequate time was allowed for the system to equilibrate with temperature before readings were taken.
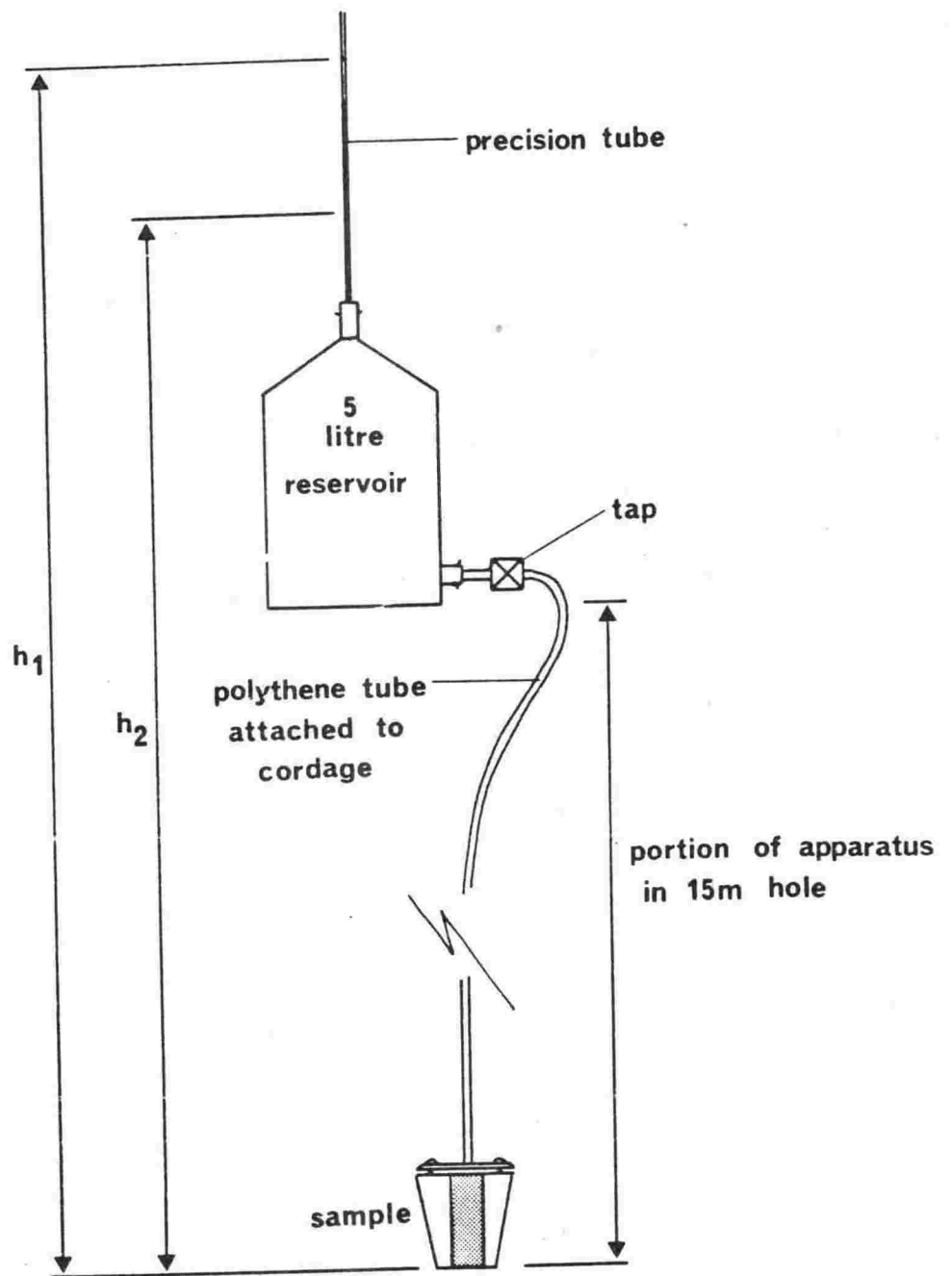
Figure A22.2 : Schematic diagram of the permeability apparatus.

Plate A22.1 : The falling head permeameter showing calibration
               tube protruding from the 5 litre reservoir vessel.
The sample was connected to this by polythene tube, seen entering the
15 x 1 m diameter hole via the small circular plate in the large
circular cover over the hole.

(ii)   It was assumed that the polythene tube from reservoir to sample holder would stretch both under the combined weight of sample assembly and its own weight and would also dilate, especially near the bottom of the hole - the two effects tending to negate any increase in the volume of water recorded as a loss of head in the calibration tube.

As a result of these assumptions:

(i)   A test was carried out over one week on an impermeable sample (a 7 mm thick Araldite disc, prepared in the same manner as the rock samples) prestretched the tube and allowed its behaviour to be observed.   There was no discernible reduction in head in the calibration tube.

This also confirmed the apparatus was free of leaks.

(ii)   Time was allowed after each sample change to offset the effects of tube stretch recovery, which occurred with the release of pressure.   This time was coincidental with temperature equilibrium time.

Because a rubber bung was used to hold the calibration tube in place some elastic recovery was observable after it was placed in the neck of the reservoir.   This recovery generally ceased after about 20 minutes.   It caused a significant drop in head level in the calibration tube.

Unfortunately the calibration tube was short, but was all that was available and the reduction of head in the fine bore tube over the period of one test required multiple fillings, each necessitating the removable of the bung and subsequent equilibration.   A calibration tube of small bore size was necessary as the sensitivity of a falling head permeameter is dependant on the ratio of the bore internal diameter to rock sample diameter, particularly important in rocks of low permeability.

After being placed on test at a noted date and time, a sample was critically observed over a period of generally one to two hours to check for possible leaks and ensure equilibrium of the system.   Subsequently, readings were taken of the head height above the reservoir (the difference in height between the neck of the reservoir and sample base was also known) and the time of each recording noted.

5.   Calculations

The following formula was used for the determination of permeability: in c.g.s. units).

$$k = 2.3 \, \frac{d^2 \mu L}{D^2 \rho g \Delta t} \cdot \log \frac{h_1}{h_2}$$

where: d is   internal diameter of the calibration tube (2.27 mm)
D is   the sample diameter (25.0 mm)
μ is   the viscosity of water
L is   the length of the specimen along the flow path
Δt the number   of seconds between observation of head heights h_1 and h_2 above the base of the sample
ρ is   the density of the water
g is   gravitational acceleration

To convert permeabilities expressed in square centimetres to Darcys, the following formula was used:

$$k_{cm^2} = 9.869 \times 10^{-9} \, k_{Darcys}$$

Values for μ and ρ were obtained from tables in Weast (1975).

6.   Comparison of apparatus performance

J. Hogan (Petroleum Corporation of New Zealand (Exploration) Ltd.,) kindly donated 25 mm core samples taken from core samples from the Kapuni-3 Well.   These were measured (parallel to bedding) by air permeability at the laboratories of KSEPL (KonoKlijke Shell Exploratie Petroleum Laboratoria;   Royal Shell Exploration Petroleum Laboratories) Hague, The Netherlands.   Measurements of the material by apparatus described provided correlations shown in Table A22.1 and Figure A22.3.

Repetitive tests confirmed that pore pressure took approximately the same time to equilibrate in new samples as in samples already thoroughly saturated by one cycle of permeability testing.   Variations in permeability generally occur extremely quickly stratigraphically and even within one sample.   Porosity influences permeability even if no constant relationship exists.   An average of a 10 fold increase in permeability results from a 3 percent increase in porosity (Archie, 1950).   Grain size, grading, grain shape and stratification also influence permeability.

Permeabilities also vary due to rock anistropy.   Vertical permeability, i.e. that permeability measured normal to bedding, is commonly considered lower than that parallel to bedding although there may be substantial directional variation within bedding planes.

In clayey (argillaceous) samples, water freed of air and salts has been found to give permeability values lower than, by as much as two orders of magnitude, those obtained using saline water.   This reflects an increase in structural water on clay particle surfaces when ion concentration is low.   Because finding compatable fluids can be impracticable, a non-polar fluid of low viscosity and high boiling point, e.g. kerosene, is often used. Determination of permeability using gas was not undertaken because values are higher than those given by any polar liquid and because water is the fluid usually encountered by aggregate.   Gas permeabilities however, may be of value in studying weathering greywacke-suite rocks.

Although Curtis (1971, figure 4) shows the bottom surface of permeability samples immersed in water, the apparatus made for this project had no such provision.   All samples were soaked for one month before testing and were wet at the exposed base of the sample after testing.

Table A22.1 : A comparison of distilled water permeabilities determined on Kapuni 3
rock cores also air permeability tested by the KSEPL, Hague, The
Netherlands. (see Hogan, 1979 for additional sample data).

Sample	Sample depth below rotary table	Method of permeability test	This study mD	KSEPL mD
KA-8	12,054 ft (3674.5 m)	air water	0.039	0.02
KA-2	11,950 ft (3642.6 m)	air water	0.845	0.23
KA-12	12,172 ft (3690.8 m)	air water	23.44	84.0
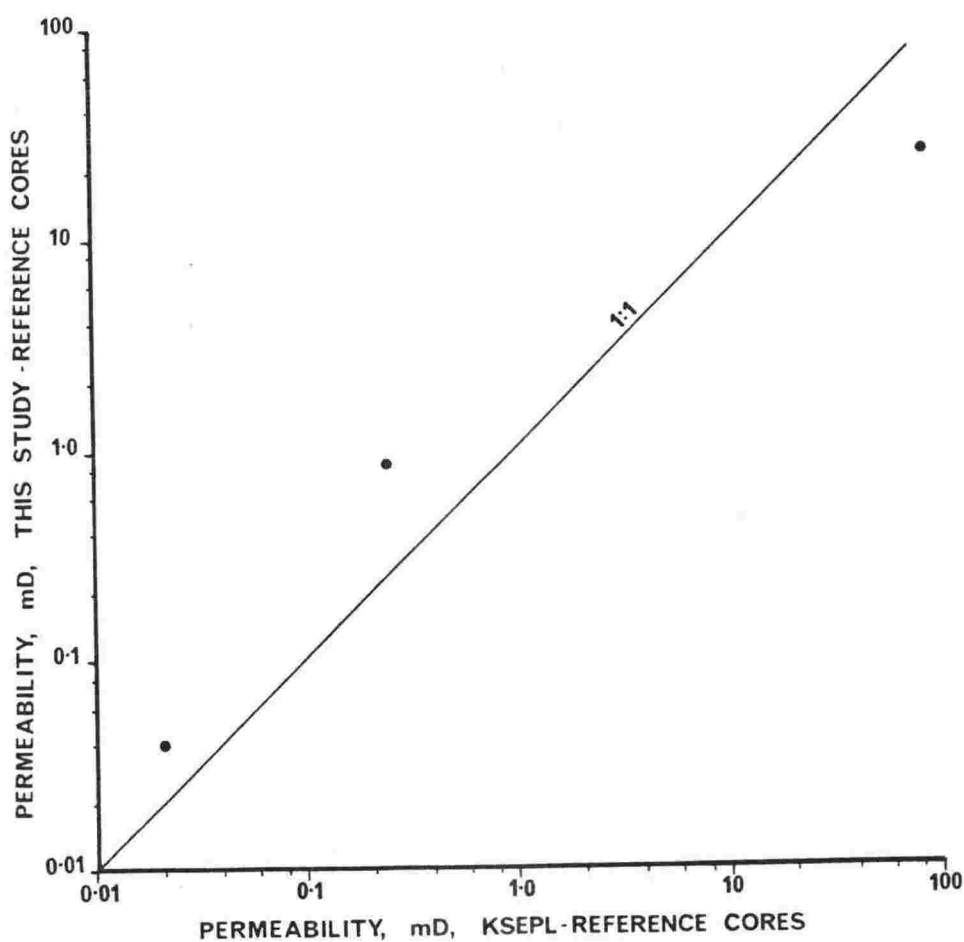
Figure A22.3 : A comparison of distilled water permeabilities
(this study) determined on rock cores from Kapuni 3
drill hole, with air permeabilities of the same material determined
by KSEPL, The Netherlands. see Hogan (1979) for additional sample
data.

APPENDIX 23

Aggregate degradation assessment of greywacke-suite rocks

1.   Introduction

Failure of basecourse aggregate used in the Auckland-Hamilton Motorway in 1964 prompted several investigations of the aggregate used (Cornwell, 1966; Reed, 1966; Buckland, 1967). The aggregation was quarried from greywacke-suite rocks, found extensively in New Zealand, and had passed the standard tests for strength and stability.

Sameshima (1977) after simulating in the laboratory the temperature/pressure environment of basecourse aggregate beneath a road surface, suggested that hydrothermal alteration increases the proportion of clay and the extent of hydration resulting in degradation of the aggregate and failure of the road.   He attributed this mainly to the increase in accessible montmorillonite and other swelling clays and devised a method for determining their abundance, in terms of "clay index" (Sameshima, 1977, p 56).

This Appendix examines the clay index, and its relationship to montmorillonite percentage, and reviews the clay index as an indicator of potential degradation of Wellington greywacke-suite rocks.

2.   The "clay index"

The clay index is found using methylene blue, which provides a means of estimating the amount of montmorillonite and other swelling clays by utilising the high cation-enchange capacity, surface area and state of dispersion of these clays (Jones, 1964).   He also gives figures that indicate an accuracy of about 0.33 volume percent if titration is taken to the nearest millilitre, or 0.1 volume percent by appraoching the end point a fraction of a millilitre at a time.

The "clay index" is defined as "the amount of dye, in ml., (4.5 gm/litre distilled water) 'consumed' by 1 gm of the sample", i.e. a basecourse or powdered rock sample finer than a BS 200 sieve (Sameshima, 1977; Sameshima and Black, 1979).   The Clay Index Grade is a classification of fines of an aggregate based on the "clay index", and a relationship between the clay index grade of aggregate fines and qualities of the basecourse is proposed (after Sameshima and Black, 1979):

Clay index	0 - 1	1.1 - 2	2.1 - 3	3.1 - 4	4.1 - 5n
clay index grade	1	2	3	4	5n
quality	sound	good	poor	unsound	unsound

3.   The methyline blue test as an indicator of montmorillonite:

It has been claimed that the methylene blue test can be used to estimate the percentage of montmorillonite (Sameshima, 1977).   However, the test has been widely used in a non specific way for "an estimation of cation exchange capacity of clays" (Baroid Drilling Mud Data Book, 1954; Fairbairn and Robertson, 1957); applicable particularly to drilling muds but also applied to aqueous dispersions of powdered clay, cores, drilled cuttings and foundry moulding sands.   However, minerals other than swelling clays can respond to the test especially if they have a large surface area.   Even albite shows some response, and

a standard illite sample yielded a value that is equivalent to a "montmorillonite percentage of 18 (Table A23.1). The Baroid Drilling Mud Data Book (1954) gives many other examples. Therefore the test results cannot be used to estimate, positively, abundance of montmorillonite or even of swelling clays with much reliability where other phyllosilicates are also abundant.

In assessing the reliability of methylene blue for estimating montmorillonite percentage, Sameshima has relied solely on X-ray diffractometry (XRD), and quotes values as low as 1 percent (Sameshima, 1977; Table A23.2). However, Carroll (1970), this study (Table 2.10) and Claridge, pers. comm. (1980) all suggest that standard XRD procedures are insensitive to montmorillonite abundances of less than 10 percent even for clay size material.

4. Response of Wellington greywacke-suite rocks to the methylene blue test:

The methylene blue test was carried out on 26 Wellington greywacke-suite rocks using the method according to Sameshima (1977), but with methylene blue being added in 0.1 ml, rather then 0.5 ml, increments. An additional three tests were carried out on quarry sludges, ultra-fine material settled out of quarry wash waters. Finally, four international standard minerals (albite, dickite, illite and montmorillonite) were tested along with VUW standard chlorite, 196/1/1(b). Results are shown in Tables A23.1, A23.3 and Figure A23.1. Repeated analyses indicate good precision of the method.

The data show that those greywacke-suite rocks with a mean grain size coarser than 5.5 phi (0.022 mm) have clay indices less than one (exceptions being KTW-G and DC-6 mentioned below). These are rocks that to not degrade (Rowe, 1979). However, rocks finer than 5.5 phi and which do degrade, have clay indices greater than one. These data suggest that the transition in clay index grade from "good" to "poor" would be better placed at the clay index value of 1 instead of 2 for Wellington greywacke-suite rocks.

An interpretation of the methylene blue test in terms of montmorillonite percentage indicates values ranging up to 3 percent in the fresh rock samples, but no montmorillonite was positively identified despite careful XRD study. However, montmorillonite was positively identified, by XRD, in quarry sludge, which certainly includes weathered material. Montmorillonite is present in soils in the Wellington area (New Zealand Soil Bureau Bulletin No. 26, Soils of New Zealand, 1968).

Occasional departures from the trend (KTW-G, DC-6) are in response to carbon and non-typical argillaceous rock fragment concentrations respectively, even though organic matter, such as lignites, polyacrylates and lignosulfonates, is removed by hydrogen peroxide. The relatively high metamorphic rank of rocks suggests that surface area effects of amorphous carbon (Bird, pers. comm.) are responsible.

Table A23.1 : A summary of some common minerals responding to the methylene blue test. Note the "Bentonite" sample contains 76 percent montmorillonite.

Mineral standard	Sample wt. (gm.)	Methylene blue solution titrated (ml)	Percent "montmorillonite" content	"Clay index"
Sodium feldspar (albite) No. 99, U.S. Dept. of Commerce, Bureau of Standards	2.0000	0.7	0.6	0.4
VUW standard chlorite, 196/1/1(b)	1.3358	0.4	0.5	0.3
*Dickite, No. 15A, San Juanito, Chihuahua, Mexico	2.0000	1.0	0.9	0.5
*Illite, No. 35, Fithian, Illinois	2.0000	20.5	17.5	10.3
*Montmorillonite, No. 20, Husband Mine (Bentonite), Polkville, Mississippi	1.0038	45.0	76.7	44.8

* Samples used in "American Petroleum Institute Clay Mineral Standards Project No. 49".

Table A23.2 : After Sameshima (1977) X-Ray modal analyses and methylene blue titration results for greywackes from the Whitehall Quarry, Waotu Quarry, Moutohora Quarry, Wellington area and Minors Road Quarry, Canterbury. Sample 8 is from Wellington.

	1.	2.	3.	4.	5.	6.	7.	8.	9.	10.	11.
Quartz	25	20	20	20	25	25	20	30	30	30	30
Plagioclase	40	20	30	30	25	30	30	30	35	35	35
Potash-feldspar	10	5	10	10	10	10	10	5	10	10	10
Hornblende	3	1	2	3	3	3	3	2	0	0	0
Prehnite	2	5	3	3	3	0	5	1	0	0	0
Calcite	1	0	1	0	1	0	0	1	0	0	0
Chlorite	10	10	20	15	15	10	10	15	10	10	10
Illite	5	2	3	3	3	5	2	10	5	10	7
Laumontite	1	10	1	2	2	10	15	0	0	0	2
Heulandite	0	10	2	1	2	0	0	0	0	0	0
Kaolin	0	10	3	5	3	3	5	5	5	5	3
Montmorillonite	1	10	1	5	2	1	3	1	3	1	2
Montmorillonite by titration %	0.8	11.1	0.8	3.2	1.4	0.6	2.4	1.1	3.1	1.1	1.9
Clay index	0.5	6.5	0.5	1.9	0.8	0.4	1.4	0.6	1.8	0.6	1.1

1. Whitehall Quarry, argillite. 2. Whitehall Quarry, stockpile aggregate fines. Heulandite include 5% stilbite. 3. Waotu Quarry, greywacke. 4. Ex Waotu Quarry aggregate fines from the State Highway No. 1, Ngutuwera-Pokaiwhenua Section. 5. Same as 4, separate sample. 6. Moutohora Quarry, greywacke. 7. Moutohora Quarry aggregate fines. 8. Titahi Bay, north of Wellington, greywacke. 9. West end Wainuiomata-Orongorongo tunnel greywacke, Reed (1957) sample No. 7328. Chemical composition in Appendix 4. 10. Ex Minors Road shingle Quarry aggregate fines from Cant. Univ. Test Track, 10^2EDA. 11. Same as 10, 10^5EDA.

Table A23.3 : Fresh greywacke-suite rock samples representing a textural range from
Wellington. X-ray diffractometry showed montmorillite to be present
only in sludge samples RSS-NS and RSS-F.

Rock sample	Sample weight (gm.)	Methylene blue solution titrated (ml.)	Percent "montmorillonite" content	Clay index	Mean grain size (phi)	
DC-6	2.0006	1.1	0.9	0.6	1.25	
HQ-17	2.0000	0.2	0.2	0.1	1.317	
SJ-3$_1$	1.9996	0.7	0.6	0.4	1.63	
KTW-13	1.9980	1.0	0.9	0.5	2.4	
HQ-21	2.0046	1.3	1.1	0.7	2.7	
BQ-V	1.9966	1.0	0.9	0.5	2.73	
BQ-IXA	1.9983	0.8	0.7	0.4	2.9	
repeated	2.0141	1.0	0.9	0.5	2.9	
OB-21	1.9989	1.1	0.9	0.6	2.93	Greywacke
HQ-19	2.0020	1.2	1.0	0.6	3.08	
KS-2	2.0050	1.7	1.5	0.9	3.27	
BQ-iii	2.0122	0.7	0.6	0.4	3.78	
KTW-G	2.0030	2.8	2.4	1.4	4.07	
RSS-iii	2.0072	1.0	0.9	0.5	4.08	
BQ-21	2.0119	1.3	1.1	0.7	4.13	
KTW-i	2.0069	0.8	0.7	0.4	4.23	
repeated	2.0156	0.9	0.8	0.5	4.23	
DC-8	1.9938	1.5	1.3	0.8	4.5	
BQ-i	2.0112	1.7	1.5	0.9	4.87	
RSS-ii	1.9996	1.5	1.3	0.8	5.18	
HQ-26	2.0226	1.7	1.4	0.8	5.4	
HQ-24	2.0000	2.5	2.1	1.3	5.58	
OB-W	2.0093	2.0	1.7	1.0	5.6	
HQ-20	2.0036	3.2	2.7	1.6	5.87	Argillite
HQ-18	2.0022	3.5	3.0	1.8	5.95	
BQ-vii	2.0047	2.3	2.0	1.2	6.11	
HQ-22	1.9985	3.0	2.6	1.5	6.28	
OB-13	1.9998	1.5	1.3	0.8	6.39	

Quarry sludge samples

RSS-NS	2.0000	11.0	9.4	5.5	-	
RSS-F	2.0000	19.0	16.3	9.5	-	
BQ-S	1.9753	5.4	4.7	2.7	-	
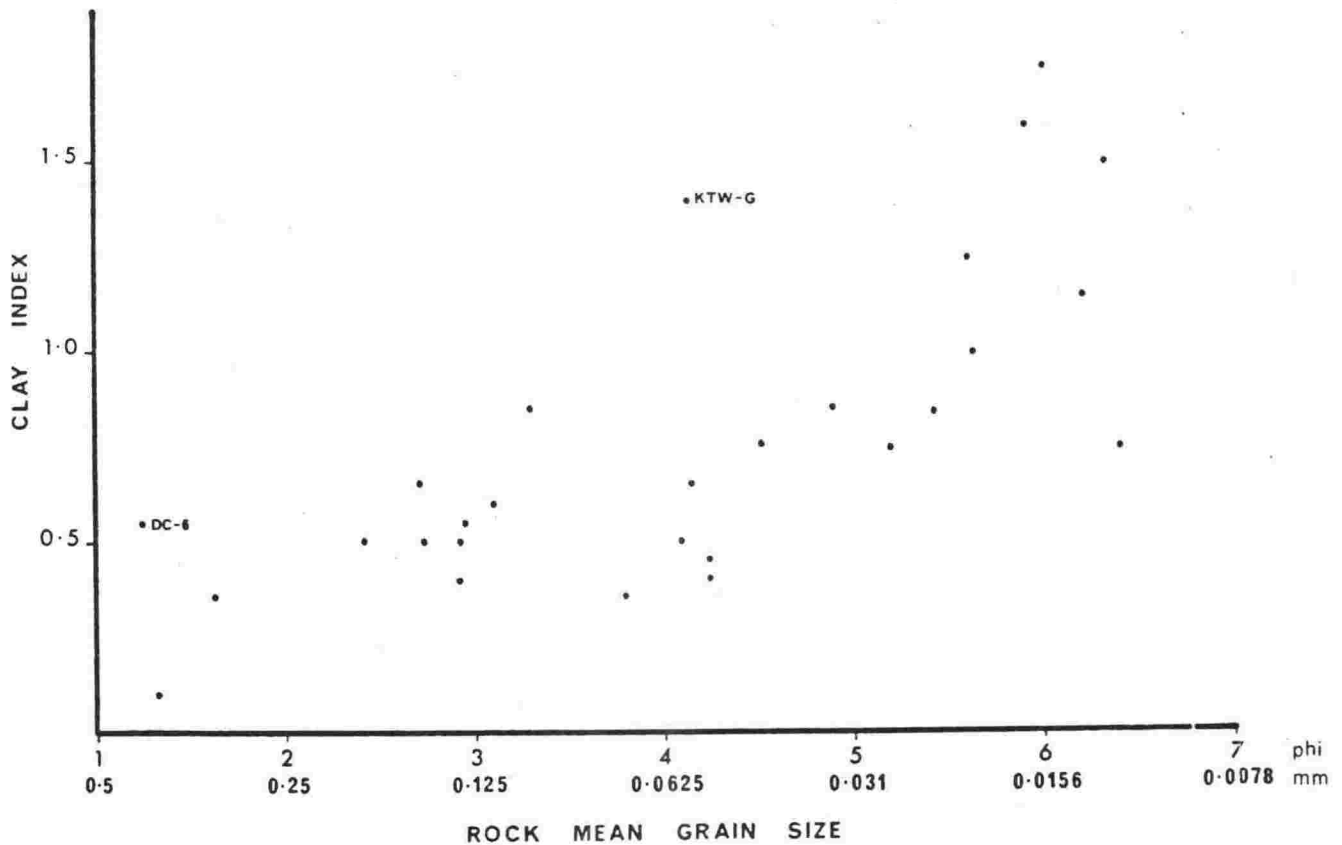
Figure A23.1 : Clay index increases directly with reduced mean grain
sizes of Wellington greywacke-suite rocks.   The rise
is steady from 1 to 5 phi (0.5 to 0.031 mm) and rises more steeply in
rocks finer than 5 phi.   KTW-G contains much organic matter and mica;
DC-6 contains many argillaceous clasts.

APPENDIX 24

Aggregate degradation: Washington degradation test and current research

1.   Introduction

The New Zealand National Roads Board Road Research Unit Newsletter 58 No. 6, 1978, described
preliminary results (Road Research Project BC/12-2) from an investigation assessing dura-
bility of basecourse and sub-base aggregate, with an accelerated attrition mill which
utilizes the basic principles of a large gem polisher. The mill operates at cascading
speed causing breakdown of the aggregate by attrition.

Tests on argillite and basalt indicated, among other things, that "the moist attrition mill
appeared to offer a method of assessing aggregate durability". The test method and
apparatus used is similar to those developed by Melville (1948), Ekse and Morris (1959) and
Minor (1959), as the traditional Los Angeles and Deval machine tests did not satisfactorily
identify poor aggregate. Improved resolution of potential degradation was achieved using
the Los Angeles machine, without the use of steel spheres, as an abrasive surcharge and by
determining Atterberg limits on the produced fines (Ekse and Morris, 1959). Further
refinement was added by including a "degradation factor", ranging from 0 - 100 (superior
materials having high values), based on the cleanness value of fines, produced by abrading
saturated aggregate in a 1 gallon polythene jar for one hour (Minor, 1959). Melville,
11 years before, also used a ball mill method of assessing aggregates. Each author con-
cluded that *conventional testing may not detect potential degradation in some aggregates.*

2.   The Washington degradation test

The degradation factor established by Minor (1959) has been refined, testing technique and
calculations have been simplified, and the method is now known as the Washington degradation
test (Marshall, 1967). Marshall has also shown good correlation between results of the
new and old methods.

To illustrate the discrepancies between different test methods, nine different commercially
produced basecourse aggregates from the Wellington region were tested by the Washington
method. The samples were supplied by Mr T. Grant-Taylor (NZ Geological Survey) after test
by conventional means to provide data for a publication (Grant-Taylor, 1976). They were
subjected to the Washington test carried out in strict adherence to the method of Marshall
(1967) except for one detail; the required 1.75" (44.45 mm) throw on the sieve shaker cam
could not be matched. The "ro-tap" machine used, had a throw of 1" (25.4 mm). Results
should therefore reflect maximum degradation factors for any particular sample, i.e. a "best"
result.

Table A24.1 lists the Washington test results along with results from Grant-Taylor (1976).

The methylene blue test was performed on aggregate fines (less than BS 100 sieve; finer
than 0.075 mm) and on fines generated by the Washington test.

Table A24.1 : Comparative data of nine greywacke-suite basecourse aggregates assessed using clay index, Washington test and X-ray diffractometry (this study) and by crushing resistance and Los Angeles tests (Grant-Taylor, 1976).

Basecourse sample locality

		Horokiwi	Carsons	River Shingle and Sand	Dry Creek	Owhiro Bay	Midway metal	Belmont	Waikanae	Kiwi Point
Grant-Taylor (1976)	Mean Los Angeles result, percent wear	22.8	18.0	19.0	19.0	18.9	19.5	20.1	–	17.5
	Mean crushing value*	3.0	3.8	4.0	2.8	2.2	6.1	–	1.7	5.4
	Degree of weathering	fresh	fresh or slightly discoloured	mainly fresh, slight local discoloration	fresh	fresh or very slightly discoloured	partly discoloured	slight discolouration	considerable discolouration	superficial weathering
	Subjective quality assessment (1 = best)	5	1	3	4	6	7	8	–	2
This study	Washington test degradation factor	84	81	74	74	67	58	41	16	15
	Average content of weathered particles, percent	0.3	9.5	1.4	0.6	5.1	17.3	21.0	65.0	58.5
Washington test fines	Material <5 µm	56	58	61	76	62	56	66	62	60
	Phyllosilicate content (1 = most)	8	7	–	4	1	2	6	3	5
	Phyllosilicates present	c i	c i v	–	c i v m	c i v m?	c i v	c i	c i v	c i v
Clay index	Natural basecourse fines	0.9	1.5	1.0	1.0	2.3	2.1	2.2	2.6	5.2
	Washington test fines	2.3	2.8	2.3	2.8	4.9	3.9	5.0	4.4	5.8

* percentage of fines passing 3/8" mesh sieve produced in standard cylinder under a load of 13.5 tonnes.

c = chlorite
i = illite
v = vermiculite
m = montmorillonite

3.   Observations

Subjective assessment is highly unreliable for recognising aggregates likely to degrade. Semi-quantitative assessment of clay mineral content and grain size analysis of fines from basecourse samples were undertaken (Table A24.1, Figure A24.1). Neither relate to the methylene blue test or the Washington test.   X-ray diffractometry of the fines from the Washington test indicates that approximately half of the less than 10 to 15 micron fraction (about 80 percent of the fines sample) is of phyllosilicate mineral composition. The grain size distributions of fines produced by the Washington test are similar (Figure A24.1).

The amount of weathered rock material in a basecourse also directly influences the methylene blue test for that basecourse, but the correlation is not as good as that from the Washington test (Figures A24.2, A24.3).

Recent work by Goonewardane (1977) on the Washington test has shown:

(i)   That comminution of aggregate particles does not occur.

(ii)   Fines are created by "leaching of hydrophilic minerals".

(iii) Autogenous grinding occurs, its influence depending on size, type and weathered nature of the sample.

All the basecourse aggregates tested were of similar type and particle size distributions were similar.

4.   Conclusions

(i)   Ball mill based tests are inconclusive unless augmented by other evidence.

(ii)   To date, no single test or subjective visual inspection of rock is sufficient to predict its engineering performance.

(iii) The inclusion of heavily weathered rock in road base layers involves high risk of degradation problems unless adequate stabilisation is utilised.
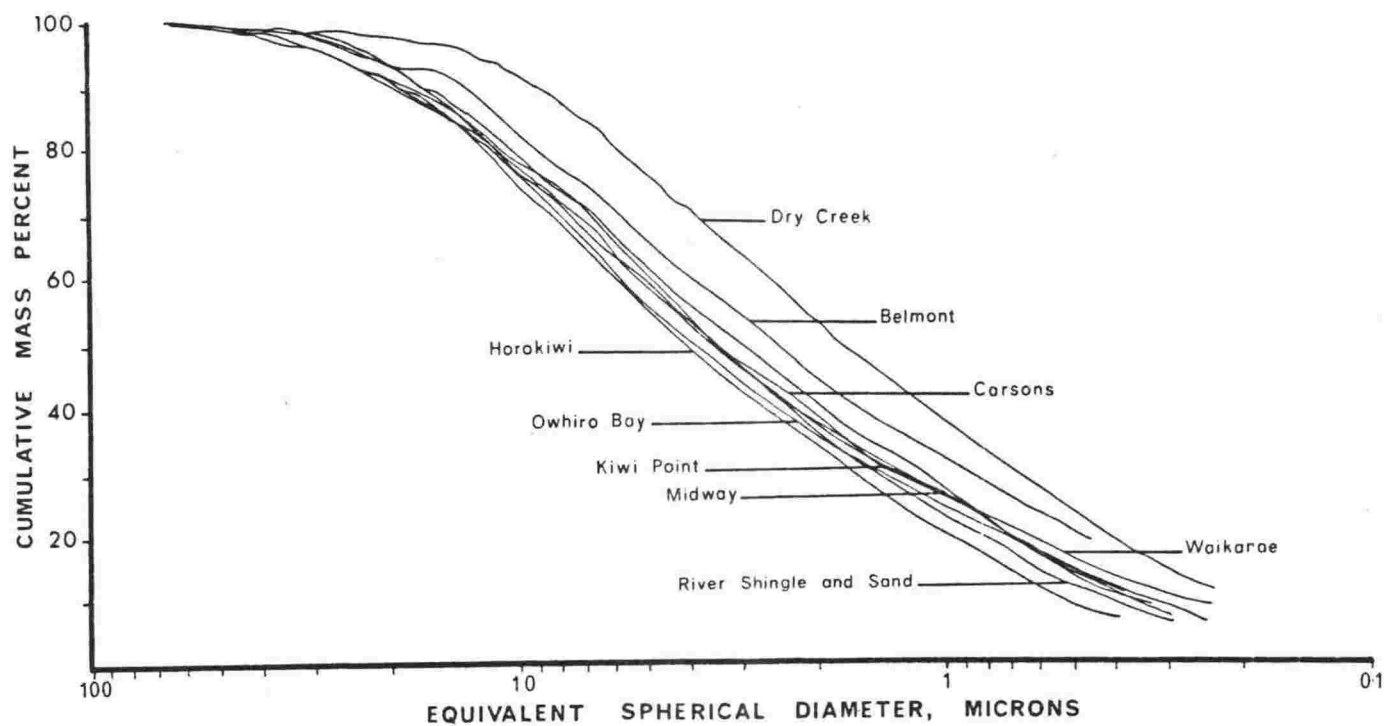
Figure A24.1 : Comparison of gradings of fine material generated by the Washington test, from nine basecourse aggregates.
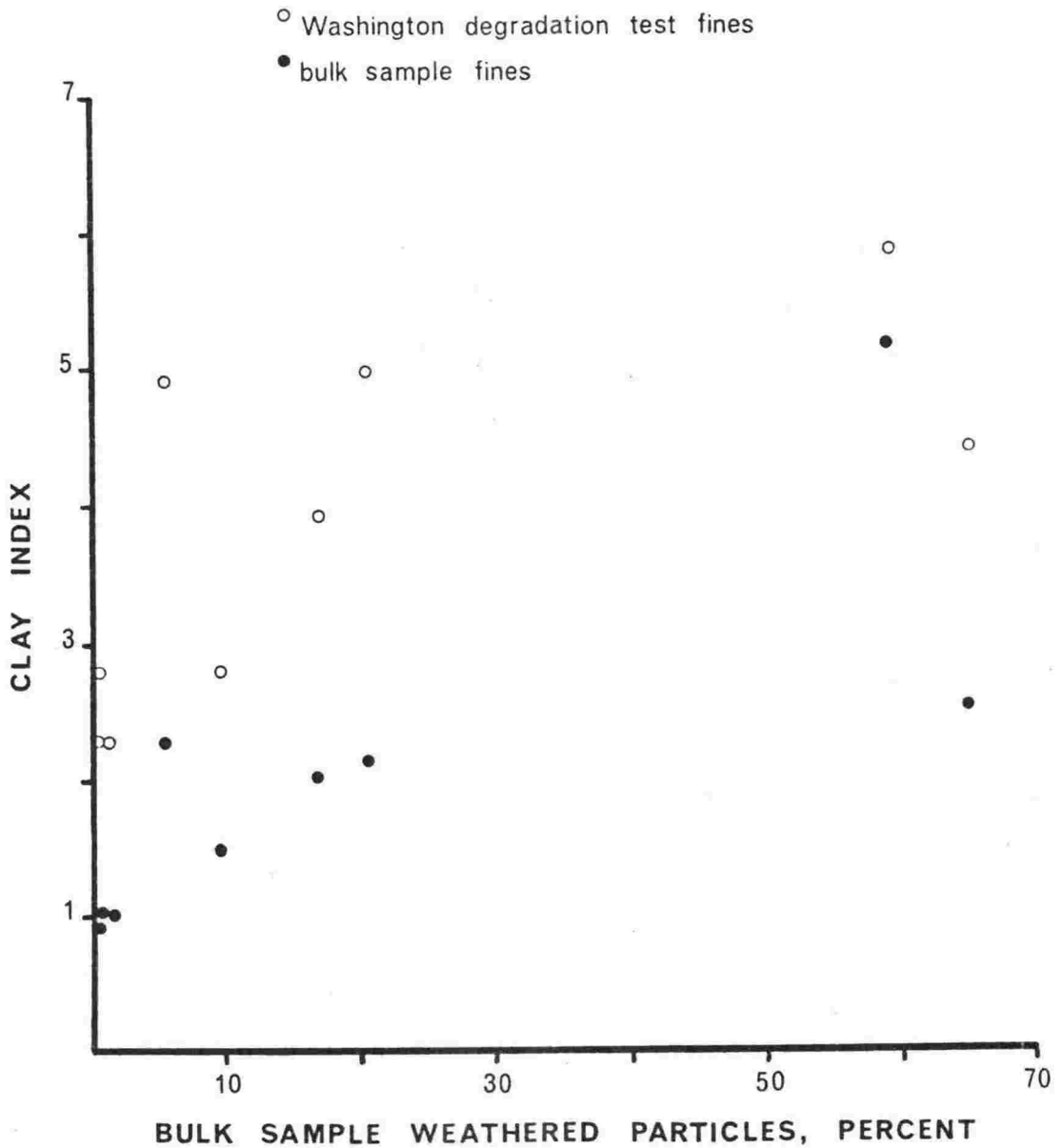
Figure A24.2 : Clay index is directly influenced by the percentage of
weathered particles in the aggregate tested.

Similar findings have been reported by Orchard (1976).   Generally,
fines generated by the Washington test give a clay index reading
double that of bulk sample fines, c.f. Figure A24.3.

○ Washington degradation test fines
● bulk sample fines
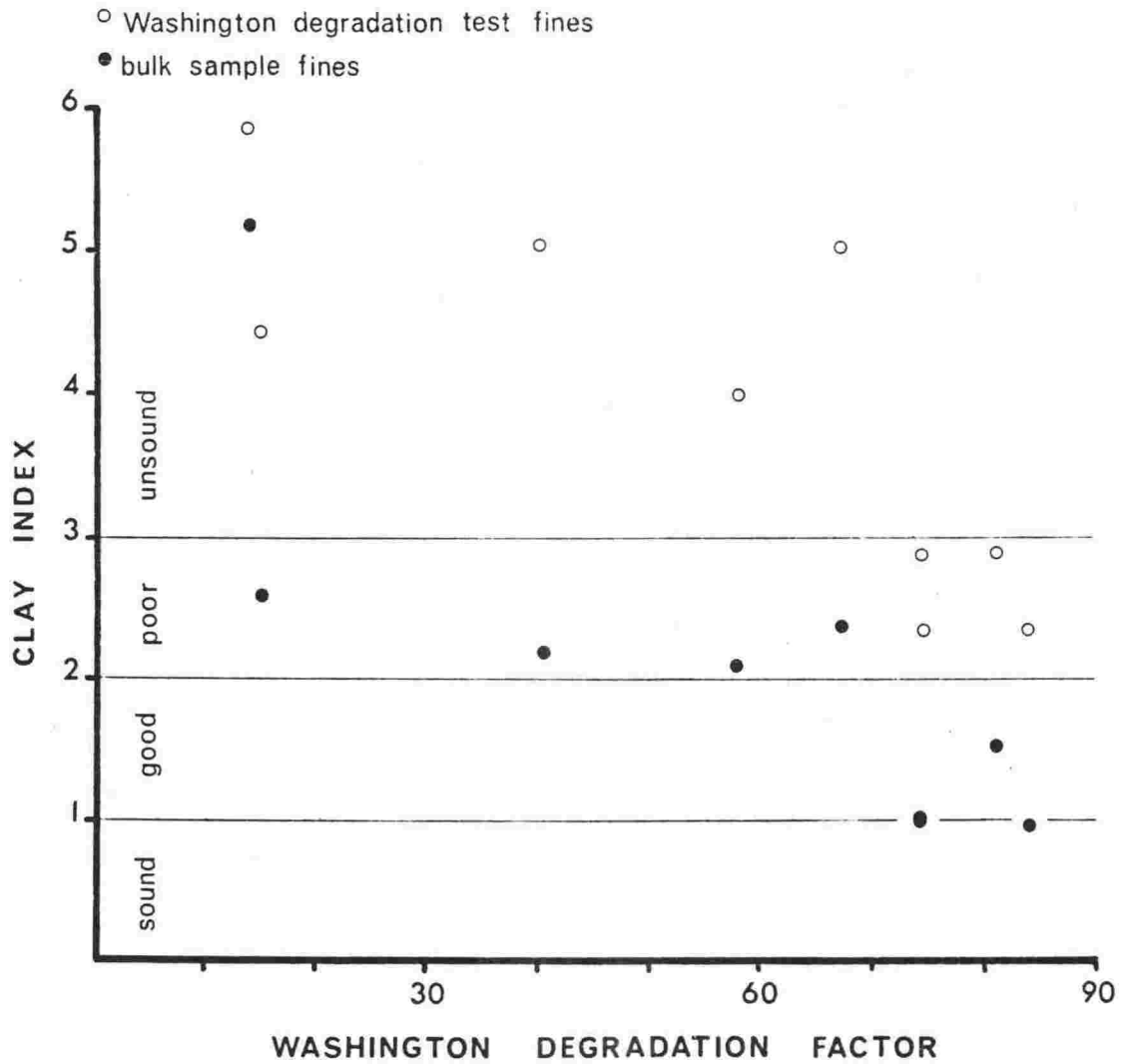
Figure A24.3 : Clay index and Washington test results are inversely
                related.   Note, only four samples comply with "sound"
and "good" categories of Sameshima (1977).   According to Orchard (1976)
the relationship may differ between rock types but this Figure (and
Figure A24.2)indicate the desirability of conducting both tests as, at
a high values of the Washington test, the clay index is relatively
insensitive.

APPENDIX 25

Storage of greywacke-suite aggregates

1.   Introduction

Elsewhere in this study (section 3.6; Appendices 23, 24), reference has been made to aggregate degradation.   The rate and process of this phenomenon has received little research attention.   It is the object of this Appendix to provide a better understanding of the natural agencies promoting degradation, the rate at which the process takes place, the sequence of the events which ultimately manifest themselves in degraded rocks and to provide an indication of how degradation losses in stockpiled aggregates may be minimised.

Generally, fresh argillite and fresh intensely zeolitised greywackes, are rock types most susceptible to degradation and can be expected to induce excess undersize materials in graded aggregate stockpiles.

2.   Outdoor observations on degradation

Lack of published material on quantification of degradation effects in the field, has prompted an attempt in this study to quantity degradation effects from a pebble garden and from two quarries.

The pebble garden studied consisted of nominal 38 mm Horokiwi aggregate placed over black plastic sheeting.   The aggregate was fresh and laid within a week of being processed. Exposure conditions approximated those of a stockpile surface, i.e., the surface was even and sloped at about 15 $^\circ$ (with a northerly aspect), was shaded about half the daylight hours and experienced occasional frost.   The entire surface received rain and was well drained. The surface was exposed over a period of four years and received only very light pedestrian traffic.

Assessment of degradation was made using a 0.25 m^2 frame divided into 100 mm squares by string lines to form a grid.   Aggregate particles were contained within squares and categorised according to a simple scheme (Table A25.1).   Over 2600 aggregate particles were assessed from about 8 percent of the garden's surface.

Particles which degraded had their requisite pieces adjacent, although detached (Plate A25.1).   Up to eight pieces, formerly one particle, could be seen juxtaposed in this way. Smaller (<10 mm) products of degradation were lost - removed to the base of the aggregate cover to lie on the plastic substrate.

Weathered particles did not degrade in the same manner as fresh rock.   Weathered material was reduced in size by removal of surface mineral grains, a quantity of mineral fines being obscured beneath the particles affected.

"Fresh zeolitised greywacke particles" were aggregate particles won from areas of the quarry where zeolite veining occurred on a millimetre interval scale, e.g., HQ-13 and HQ-14.

Results indicate that argillite and fresh zeolitised greywacke particles (the zeolite concerned being laumontite) required no mechanical stress to degrade.   Size reduction of graded aggregate is mostly influenced by zeolitised particles.   On average, a fresh

Table A25.1 : Results of observations on 2600 particles from a pebble garden. The aggregate had been crushed, washed and had a nominal 38 mm size.

Particle categories	As laid	After four years exposure
Whole fresh greywacke pieces	86.4	86.4
Whole fresh argillite pieces	5.3	4.2
Whole fresh zeolitised greywacke pieces	7.0	5.6
Whole weathered pieces	1.3	1.3
Degraded fresh zeolitised greywacke pieces	-	1.4
Degraded fresh argillite pieces	-	1.1
	100.0%	100.0%
Total whole fresh greywacke:whole fresh argillite ratio	18:1	22:1

Table A25.2 : Rock stability values of pebble garden aggregates and lithologies approximating them, show that laboratory prediction of degradation for the fresh zeolitised greywacke and fresh argillite categories is possible.

Representative particles of each aggregate category	Rock stability value	Average weight percent loss per day
Fresh greywacke	4.7	0.275
Fresh argillite	14.7	0.85
Fresh zeolitised greywacke	10.9	0.438
Weathered greywacke	6.5	0.263
Prepared rock specimens from Horokiwi Quarry approximating lithologies of the above aggregate particles		
HQ-17 fresh greywacke	6.1	0.267
HQ-22 fresh argillite	11.9	0.641
HQ-14 fresh zeolitised greywacke	8.1	0.289

A

B
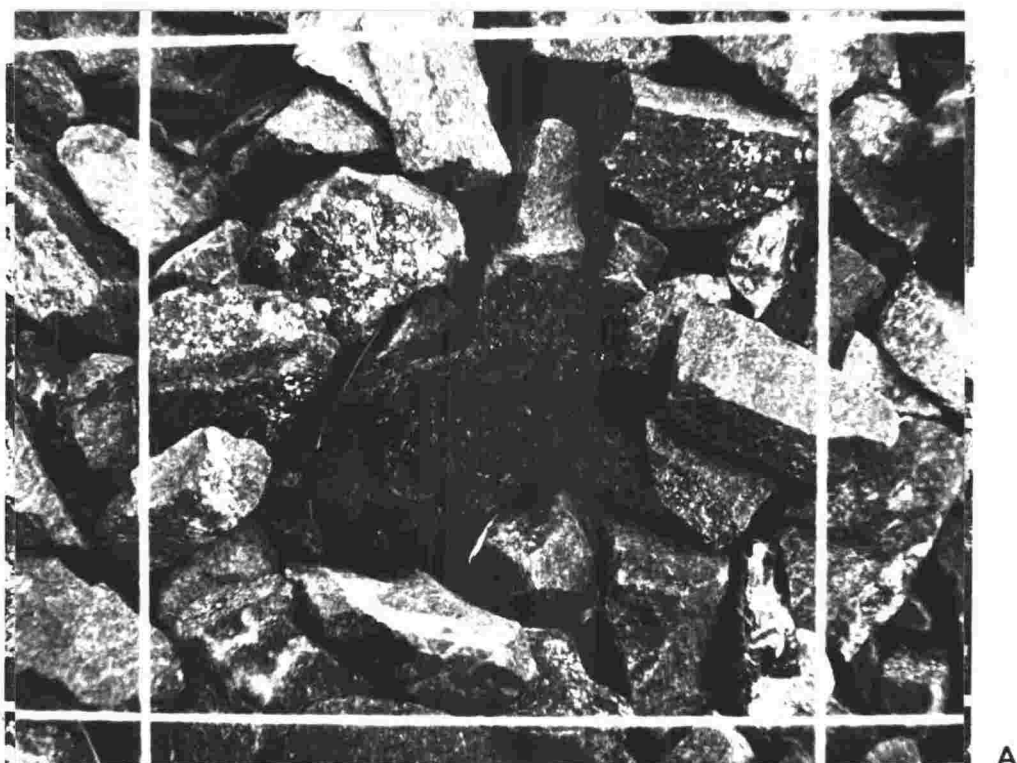
Plate A25.1 : (A) Degra-
dation of
argillite on exposure is
manifest simply as the
division of a particle into
smaller particles along planes
which may remain undetected
unless disturbed.

(B) Degra-
dation of fresh zeolitised
greywacke before (upper)
and after exposure. Degra-
dation products do not form
simply by parting; fines are
produced and therefore only
a crude reconstruction of
degraded pieces is possible.

The grid is 100 mm square.

zeolitised greywacke particle degraded into 3.4 pieces (range 2 - 8 pieces), the degree of size reduction being dependent on the degree of veining displayed. A 20 percent reduction of whole fresh zeolitised greywacke particles occurred in four years of exposure (Table A25.1). In terms of volume, the degradation of argillite appears more significant. Fresh argillite particles degraded into an average of 2.9 pieces (range 2 - 5 pieces), a 21 percent reduction in argillite particles in four years. Table A25.2 shows that Rock stability values (Rowe, 1979) of particles corresponds well with the observations of degradation. Degradation of argillite may be seen where quarrying has temporarily ceased. Blocks 0.01 m^3 to 0.25 m^3 in size at Owhiro Bay and Horokiwi quarries, were observed after eight years and four years of exposure respectively. The blocks become surrounded by debris in which microcracks propagated along planes, parallel and sub-parallel to bedding and sub-perpendicular to bedding. Original shape of blocks was often preserved but integrity so destroyed that attempts to move blocks resulted in their disintegration to slabby clasts of sub-equal size. Occasionally disaggregation of the surface portion only was apparent, giving a superficially cracked but otherwise intact interior bounded by curved surfaces, suggesting a volume change of the exterior (degrading) material, to provide tensile stresses exceeding the tensile strength of the rock at the curved interface. No fine material (sand or silt) is produced by this degradation process - pieces may be reassembled as a "jig-saw puzzle". Degradation pieces are usually a minimum size of 25 mm with relatively large surface area to volume ratios.

3.   Exposure of argillite to water

To observe the effects of water loss (section 3.5.1) a large (about 50 kg) sample of argillite (OB-W) from Owhiro Bay Quarry was cut parallel to bedding and three 25 mm diameter cores taken, perpendicular to bedding, from the centre portion of the block. Cores were approximately 75 mm long and were kept wet until the experiment began.

Cores were weighed in a saturated surface dry (SSD) condition before one was placed in each of three localities; a window ledge with a north-west aspect, a toilet cistern to ensure permanent fresh water wetness and after drying for 24 hours at room temperature in a thermostatically controlled oven (105 $\pm5^\circ$C). Cores remained in their respective locations for 14 months.

At the start of the experiemnt all cores were completely sound, with no microcracking apparent. Observations from each core with time were as follows:

Sample	Saturated surface dry (SSD) core weights on dates examined, gm.					Ultrasonic velocity on completion of experiment, $(m.s^{-1})$
	6.2.78 start	28.2.78	18.5.78	21.7.78	13.4.79 finish	
A Window ledge	100.00	-	100.30	100.26	NA	NA
B Permanently wet	104.20	-	-	-	104.30	5000
C Permanently dry	95.3	95.17	95.4	95.33	95.11	4704

NA - unavailable for test

The core from the window ledge was microcracked, at 25 mm intervals, within approximately eight weeks. After fourteen months the microcracks were only a few millimetres apart. One large, open diagonal crack 0.3 mm wide, developed after about 10 months of exposure. Edges of the crack developed yellow-brown weathering colouration within a further two months. The crack did not extend through the core, being limited to a depth of 10 mm. Its width was reduced when finger pressure was applied.

The permanently wet core showed no microcracking; no flaw whatever was found and its weight was constant throughout the test.

The oven dried core was microcracked at 10 mm spacings. Cracking was first noticed after 10 months. The core possibly lost weight, the technique of establishing SSD reference conditions for rock is subjective and weight variability may be the result of increasing amounts of water being held as microcracking increases.

Microcracks were, in all cases, approximately linear or gently curving, sub-parallel to bedding. They were invisible to the naked eye when the rock surface was dry. On wetting, water absorbed quickly into the microcracks, enlarging them and creating relatively dry crack margins. On drying, they retained water. They could be seen with the naked eye in both cases. They ranged to 0.004 mm in width.

The integrity of cores was established quantitatively by measuring their ultrasonic velocities parallel to their long axes. Cracks in the rock attenuate the signal pulse and lower the transmission time (New, 1976). Sound cores of OB-W had an average SSD ultrasonic velocity of 4945 $m.s^{-1}$ (range 4831 - 5072, n = 11). The velocity (5000 $m.s^{-1}$) for the core kept permanently wet is near the mean of velocities from sound cores and so this core may be considered unaffected by its experimental treatment. The core kept permanently dry gave a significantly lower ultrasonic velocity (4704 $m.s^{-1}$) from that of the lowest reading of sound cores, i.e., a difference in excess of the 2 percent accuracy of the PUNDIT apparatus used for the measurements. The core from the window ledge was unavailable for test.

The core experiments indicate that degradation may take place quickly (within two months) and requires wet and dry cycling to bring it about.

4.   The effects of wetting and drying on rock durability

To examine the role wetting and drying plays in degradation, two further experiments were completed to establish the volume change inherent in different rock types when wetted and to study the cyclic effects of wetting the drying, i.e., cycling these volume changes.

Eleven greywacke-suite rocks were tested for unrestrained moisture movement using an apparatus similar to that shown by Duncan (1969, vol. 1, plate 18), see also Appendix 20. Movement values are maxima as samples were 25 mm diameter rock cores cut perpendicular to bedding. Samples were measured over several days after initial drying (50°C for 24 hours). Three lithologies were retested, one of these (HQ-22) three times due to fractures forming during testing.

Results (Table A25.3, Figure A25.1) show unrestrained moisture movement in argillites to be an order of magnitude greater than that in greywackes.

Cyclic moisture movements were determined using a technique described by Roper (1959), see also Appendix 21. The cores used for unrestrained moisture movements were used for this experiment. In addition a prism of KTW-i greywacke (see Appendix 19 and Table A25.4)

Table A25.3 : Data from unrestrained moisture movement tests. Dial gauge used was calibrated in inches, therefore Δl is in inches. Mm_s is the unrestrained moisture movement, percent. L is sample length, M_z is rock mean grain size and RSV the Rock stability value.

HQ-17

L = 62.625 mm; 2.4656 inches
M_z = 1.317 phi; 0.4 mm
RSV= 6.1

Gauge reading	Δl ($\times 10^{-5}$)	Mm_s ($\frac{\Delta l}{L}\times 100$) percent	Hours
07.418	0	0	0
07.42	2	0.0008	23.5
07.425	7	0.0028	35.8
07.434	16	0.0065	48.0
07.446	28	0.0114	71.6
07.463	45	0.0183	95.5
repeat			
07.79	0	0	0
07.791	1	0.0004	1.8
07.7915	1	0.0006	4.4
07.794	4	0.0016	8.2
07.808	18	0.0073	22.7
07.819	29	0.0118	46.8
07.829	39	0.0158	59.5
07.839	49	0.0199	98.2

SJ-3₁

59.575 mm; 2.3455 inches
1.63 phi; 0.32 mm
6.6

Gauge reading	Δl ($\times 10^{-5}$)	Mm_s ($\frac{\Delta l}{L}\times 100$) percent	Hours
19.941	0	0	0
19.950	9	0.0038	11.0
20.00	59	0.0252	23.5
20.003	60	0.0256	52.6
20.004	60	0.0256	71.7
repeat			
20.30	0	0	0
20.306	6	0.0026	3.8
20.31	10	0.0043	9.67
20.312	12	0.0051	23.67
20.32	20	0.0085	48.69
20.321	21	0.0090	72.36
20.322	22	0.0094	95.14

KTW-14

76.4 mm; 3.0078 inches
2.6 phi; 0.165 mm
6.5

Gauge reading	Δl ($\times 10^{-5}$)	Mm_s ($\frac{\Delta l}{L}\times 100$) percent	Hours
14.81	0	0	0
14.823	13	0.0043	7.47
14.843	33	0.0110	22.55
14.853	43	0.0143	29.38
14.857	47	0.0156	31.71
14.861	51	0.0170	33.29
14.877	67	0.0223	47.46
14.881	71	0.0236	51.04
14.89	80	0.0266	71.96
14.898	88	0.0293	75.79
14.905	95	0.0316	95.41
14.905	95	0.0316	97.54

BQ-V

L = 68.0 mm; 2.6772 inches
M_z = 2.73 phi; 0.15 mm
RSV= 7.1

Gauge reading	Δl ($\times 10^{-5}$)	Mm_s ($\frac{\Delta l}{L}\times 100$) percent	Hours
01.591	0	0	0
01.591	0	0	0.95
01.592	1	0.0004	2.60
01.599	8	0.0029	4.77
01.60	9	0.0034	9.47
01.608	17	0.0064	14.10
01.617	26	0.0097	24.07
01.626	35	0.0131	29.52
01.630	39	0.0146	33.22
01.655	64	0.0239	48.30
01.665	74	0.0276	55.70
01.686	95	0.0355	71.68
01.701	110	0.0411	80.51
01.708	170	0.0437	96.01

BQ-IXA

78.4 mm; 3.0866 inches
2.9 phi; 0.134 mm
5.4

Gauge reading	Δl ($\times 10^{-5}$)	Mm_s ($\frac{\Delta l}{L}\times 100$) percent	Hours
22.35	0	0	0
22.355	5	0.0016	5.62
22.37	20	0.0065	11.62
22.385	35	0.0113	23.92
22.39	40	0.0129	31.84
22.407	57	0.0185	47.54
22.415	65	0.0211	57.37
22.422	72	0.0283	71.67
22.427	77	0.0249	100.17
22.43	80	0.0259	110.59

KS-2

70.7 mm; 2.7835 inches
3.27 phi; 0.104 mm
7.15

Gauge reading	Δl ($\times 10^{-5}$)	Mm_s ($\frac{\Delta l}{L}\times 100$) percent	Hours
11.695	0	0	0
11.733	38	0.0137	1.83
11.813	118	0.0424	5.50
11.878	183	0.0657	21.75
11.883	188	0.0675	48.17
11.884	189	0.0679	69.12
11.885	190	0.0683	71.67
11.885	190	0.0683	76.05
11.885	190	0.0683	77.58
11.885	190	0.0683	93.33

Table A25.3 : continued

	KTW-i				SJ-T				OB-W		

L = 75.0 mm; 2.9528 inches
M_z = 4.23 phi; 0.053 mm
3.9

64.5 mm; 2.5394 inches
4.72 phi; 0.038 mm
8.8

73.84 mm; 2.9071 inches
5.6 phi; 0.021 mm
11.3

Gauge reading	Δl $(\times 10^{-5})$	Mm_s $(\frac{\Delta l}{L} \times 100)$ percent	Hours	Gauge reading	Δl $(\times 10^{-5})$	Mm_s $(\frac{\Delta l}{L} \times 100)$ percent	Hours	Gauge reading	Δl $(\times 10^{-5})$	Mm_s $(\frac{\Delta l}{L} \times 100)$ percent	Hours
09.318	0	0	0	11.728	0	0	0	05.05	0	0	0
09.32	2	0.0007	1.72	11.732	4	0.0016	3.50	05.086	36	0.0124	2.6
09.329	11	0.0037	4.34	11.738	10	0.0039	5.47	05.11	60	0.0206	4.52
09.338	20	0.0068	7.27	11.740	12	0.0047	6.47	05.148	98	0.0337	7.63
09.367	49	0.0166	22.05	11.752	24	0.0095	13.59	05.213	163	0.0561	10.46
09.379	61	0.0207	30.62	11.77	42	0.0165	24.00	05.38	330	0.1135	21.79
09.409	91	0.0308	46.92	11.789	61	0.0240	34.13	05.41	360	0.1238	25.46
09.42	102	0.0345	54.72	11.808	80	0.0315	48.08	05.438	388	0.1335	29.16
09.44	122	0.0413	73.97	11.820	92	0.0362	59.08	05.444	394	0.1355	30.88
09.45	132	0.0447	93.97	11.836	108	0.0425	71.80	05.523	473	0.1627	45.96
				11.848	120	0.0473	85.42	05.535	485	0.1668	49.39
				11.869	141	0.0555	121.04	05.581	531	0.1827	70.38
				11.871	143	0.0563	146.42	05.59	540	0.1858	77.76
				11.872	144	0.0567	169.35	05.599	549	0.1889	93.79
								05.60	550	0.1892	96.96

HQ-22

L = 67.9 mm; 2.6732 inches
M_z = 6.28 phi; 0.013 mm
11.9

Gauge reading	Δl $(\times 10^{-5})$	Mm_s $(\frac{\Delta l}{L} \times 100)$ percent	Hours
07.791	0	0	0
07.997	206	0.0771	2.2
08.075	284	0.1062	6.75
08.123	332	0.1242	8.58
08.229	438	0.1639	13.18
08.367	576	0.2155	23.75
08.383	592	0.2215	28.42
08.411	620	0.2319	36.09
sample cracked?			
08.415	624	0.2334	48.12
08.415	624	0.2334	73.42
08.416	625	0.2338	95.59
repeat			
01.45	0	0	0
01.526	76	0.0284	0.70
01.705	255	0.0954	3.77
01.797	347	0.1298	6.15
01.863	413	0.1550	9.75
01.882	432	0.1616	13.62
sample cracked			
01.90	450	0.1683	24.22
01.918	468	0.1751	26.87
01.919	469	0.1755	47.87
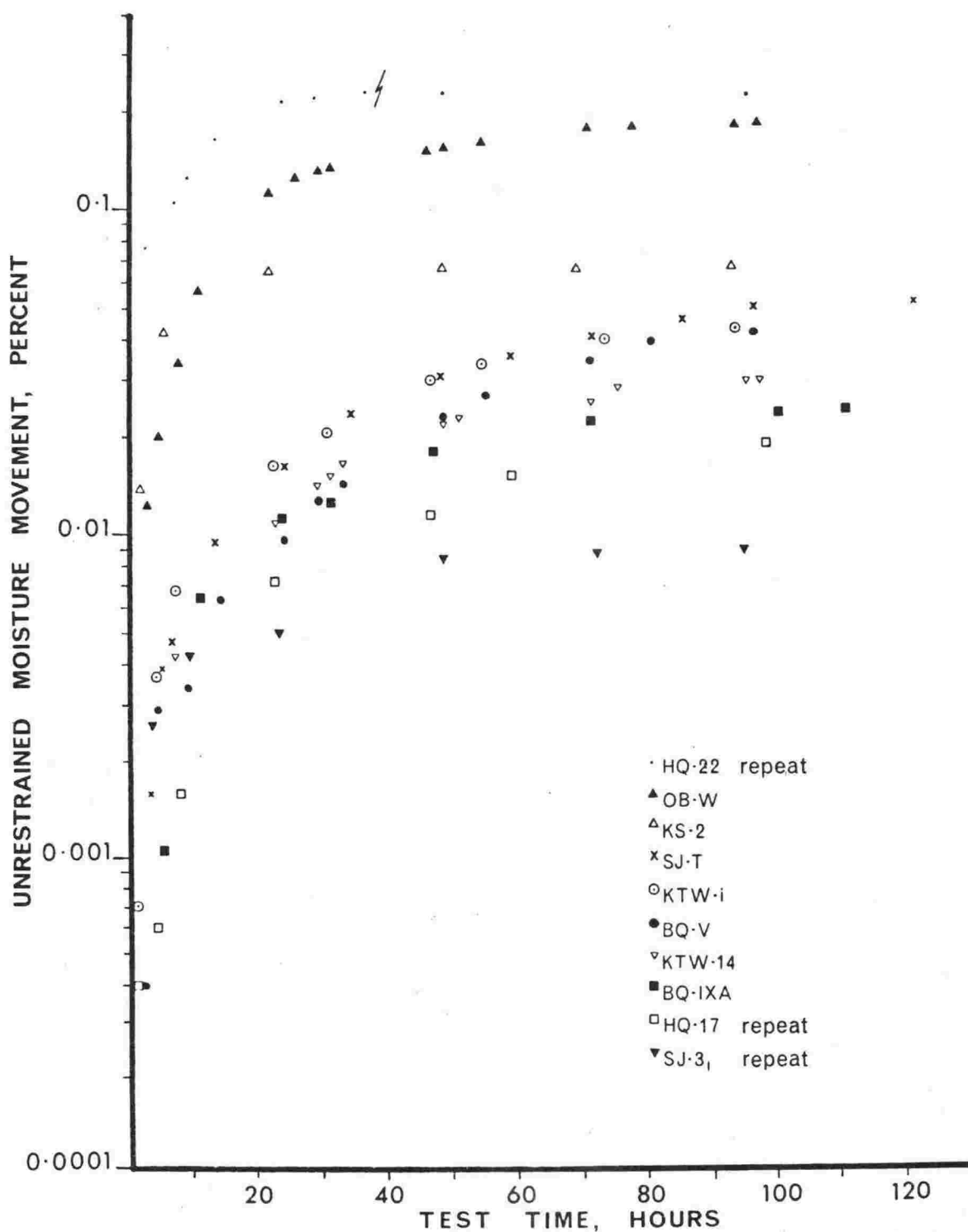
Figure A25.1 : Unrestrained moisture movement of greywacke-suite
              rocks takes place rapidly within the first 20 hours
of testing, gradually attaining equilibrium after approximately
90 hours (4 days). Note the log scale of the y-axis. Argillite
movements are an order of magnitude greater than greywackes.

Table A25.4 : Cyclic moisture movement values for prism KTW-i.   Compare with Figure
A25.2.

Length (L) = 20.9 cm

Cycle number	Comparitor measurement	Sample measurement	Δl x 0.001 cm	Mm_d $\frac{\Delta l}{L}$ x 100
1	0	05.677	0	0
1	0	05.428	-0.0249	-0.12
2	0	05.77	+0.0093	+0.05
2	+0.0001	05.43	-0.0247	-0.12
3	0	05.79	+0.0113	+0.05
3	0	05.45	-0.0227	-0.11
4	0	05.79	+0.0113	+0.05
4	0	05.45	-0.0227	-0.11
5	0	05.79	+0.0113	+0.05
5	0	05.47	-0.0207	-0.10
6	-0.0002	05.83	+0.0153	+0.07

was included.   Measurements were recorded with reference to an invar rod (for the prism)
and a stainless steel rod (for the cores).

Results (Table A25.5, Figure A25.2) show the argillite cores and the prism to have cumulative expansions.
Roper (1959) attributed this to crack formation and propagation.   Indeed, during the
experiment, argillite cores developed microcracks and a small argillaceous portion of the
prism further microcracked.   Comparison between KTW-i core and prism results show similar
percentages of expansion, indicating the greywacke to be cracking also (KTW-i core was
free of any argillite).

Roper (1959) concluded that volume changes were related to internal surface area.   Applied
to Figure A25.2, this suggests argillites to have larger internal surface areas than grey-
wackes, some of which indicated shrinkage tendancies.

5.   Permeability as an indicator of rock durability

Permeabilities of Wellington greywackes and argillites were studied to better understand
the role of internal surface area and rock degradation, and establish the effects water has
as it passes through a rock.

Factors influencing rock permeability include;   anisotropy, porosity, texture and
mineralogy.

Permeability measurements were made on 25 mm diameter cores of maximum integrity, with
axis orientation perpendicular to bedding and therefore the permeabilities measured are a
minimum.   This is the only orientation for which results could be confidently related
between samples, as permeability parallel to bedding varies due to fabric anisotropy.
Sample preparation is outlined in Appendix 22.   Calculations were based on a formula from

Curtis (1971) which determines k and may be related to pore geometry and internal surface characteristics of rocks. Absolute or specific permeability, k, is dimensioned as an area which may be considered as "average pore area" determining the rate of flow. It may be considered a characteristic of the rock provided the transmitted fluid does not alter the volume or internal surface of voids or solids.

Values of k, established for 10 different greywacke-suite rocks (Table A25.6), diminish with time (Figure A25.3) and appeared to stabilise after a minimum of 90 hours on test - an equilibrium time consistent with that of other tests (section 3.6; Appendix 19). However, all permeabilities were low, after 90 hours the mean value of k being 1.63×10^{-19} mD (standard deviation 0.87×10^{-19} mD) and values are masked by spurious change.

The reduction of k values with time is probably a response to pressure differences within the sample. As the rock becomes saturated, water is absorbed on internal surfaces. This water has a high viscosity, but is mobile and takes part in the flow (Neville, 1975), and surface tension within pores is increased. This process takes place regardless of the length of soaking period before testing (at least one month) and takes place even when a sample is retested.

Because of this k reduction (Figure A25.3), argillite permeability reduction rates tend to be faster and k, after 90 hours on test, is low.

It is probable that rates at which greywacke-suite rock come to equilibrium reflect their relative susceptability to degradation (see Mayer, 1963 and Farran and Thenot, in Mayer, 1963).

The equilibrated state of permeability after four days is mainly dependant on pore geometry, the chemical status of moisture within the rock, and the properties of organic and accessory minerals (Krynine and Judd, 1957). Initial permeabilities therefore may be better for comparative studies since these values are most likely to reflect mineralogy, textural and porosity differences.

The relationship of k with rock mean grain size is uncertain due to k changing with time; however a linear relationship does result after 75 hours of testing (r = -0.62, Figure A25.4). The initial, or three hour values of k show a relationship with rock mean grain size analogous to that shown by Rock stability value (RSV) and by Σ chlorite content (Rowe, 1979) but the trends for RSV and Σ chlorite are not linearly related to k at any test time.

Relationships of three hour permeability, chlorite content and RSV indicate that increasing phyllosilicate contents generally effect increases in k. The lower volumes of matrix (phyllosilicates) in coarser grained greywackes do not produce lower k values in these rocks since phyllosilicates are abundant in the sedimentary rock fragments the rocks contain and because zeolite, a permeable mineral, is often present also.

6.   Discussion: a sequence of degradation by natural agencies

From data presented, degradation appears strongly influenced by:

(i)   Water; both that influencing the rock from climatic conditions and that as an inherent component of the rock.

Table A25.5 : Data from cyclic moisture movement tests. Dial gauge used was calibrated in inches therefore $\Delta \ell$ is in inches. Mm_d is the cyclic moisture movement, percent and L is the sample length

Sample number length (L)		HQ-17 2.4115 inches			SJ-3$_1$ 2.3115 inches			KTW-14 2.348 inches		
Cycle number	Comparitor measurement	Sample measure-ment	Δl (x10^{-4})	Mm_d ($\frac{\Delta l}{L}$x100) percent	Sample measure-ment	Δl (x10^{-4})	Mm_d ($\frac{\Delta l}{L}$x100) percent	Sample measure-ment	Δl (x10^{-4})	Mm_d ($\frac{\Delta l}{L}$x100) percent
1	900	1067	0	0	2061	0	0	1691	0	0
1		1049	+18	+0.075	2036	+25	+0.108	1668	+23	+0.098
2		1061	+6	+0.025	2054	+7	+0.030	1685	+6	+0.026
2		1046	+21	+0.087	2039	+22	+0.095	1673	+18	+0.077
3		1064	+3	+0.012	2054	+7	+0.030	1685	+6	+0.026
3		1049	+18	+0.075	ball bearing register failed			1671	+20	+0.085
4		1062	+5	+0.021	2014	0	0	1683	+8	+0.034
4		1048	+19	+0.079	2012	+2	+0.008	1674	+17	+0.072
5		1063	+4	+0.017	2018	-4	-0.017	1682	+9	+0.038
5		1049	+18	+0.075	2010	+4	+0.017	1668	+23	+0.098
6		1061	+6	+0.025	2016	-2	-0.008	1680	+11	+0.047
6		1047	+20	+0.083	2010	+4	+0.017	1673	+18	+0.077
7		1063	+4	+0.017	2018	-4	-0.017	1685	+6	+0.026
7		1048	+19	+0.079	2012	+2	+0.008	1677	+14	+0.060
8		1063	+4	+0.017	2020	-6	-0.026	1689	+2	+0.009
8		1049	+18	+0.075	2014	0	-	1677	+14	+0.060
9		1058	+9	+0.037	2017	-3	-0.013	1683	+8	+0.034
9*		1032	+35	+0.145	2011	+3	-0.013	1660	+31	+0.132

* Water soak period prolonged three days i.e. was seven day soak.

Sample number length (L)		BQ-V 2.4027 inches			BQ-IXA 2.3865 inches			KS-2 2.3433 inches		
Cycle number	Comparitor measurement	Sample measure-ment	Δl (x10^{-4})	Mm_d ($\frac{\Delta l}{L}$x100) percent	Sample measure-ment	Δl (x10^{-4})	Mm_d ($\frac{\Delta l}{L}$x100) percent	Sample measure-ment	Δl (x10^{-4})	Mm_d ($\frac{\Delta l}{L}$x100) percent
1	900	1159	0	0	1312	0	0	751	0	0
1		1135	+24	+0.1	1284	+28	+0.117	ball bearing register failed		
2		1154	+5	+0.021	1307	+5	+0.021			
2		1144	+15	+0.062	1290	+22	+0.092			
3		1155	+4	+0.017	1309	+3	+0.013	737	0	0
3		1138	+21	+0.087	1289	+23	+0.096	721	+16	+0.068
4		1156	+3	+0.013	1307	+5	+0.021	734	+3	+0.013
4		1140	+19	+0.08	1293	+19	+0.08	719	+18	+0.077
5		1157	+2	+0.008	1308	+4	+0.017	733	+4	+0.017
5		1140	+19	+0.08	1286	+26	+0.109	717	+20	+0.085
6		1155	+4	+0.017	1302	+10	+0.042	731	+6	+0.026
6		1141	+18	+0.075	1285	+27	+0.113	716	+21	+0.09
7		1156	+3	+0.013	1302	+10	+0.042	732	+5	+0.021
7		1142	+17	+0.071	1285	+27	+0.113	716	+21	+0.09
8		1158	+1	+0.004	1304	+8	+0.034	732	+5	+0.021
8		1141	+18	+0.075	1291	+21	+0.088	717	+20	+0.085
9		1154	+5	+0.021	1302	+10	+0.042	730	+7	+0.03
9*		1130	+29	+0.121	ball bearing register failed			717	+20	+0.085

* Water soak period prolonged three days i.e. was seven day soak.

Table A25.5 : continued.

Sample number length (L)		KTW-i 2.4233 inches			SJ-T 2.398 inches			OB-W 2.3473 inches		
Cycle number	Comparitor measurement	Sample measure-ment	Δl (x10⁻⁴)	Mm_d ($\frac{\Delta l}{L}$x100) percent	Sample measure-ment	Δl (x10⁻⁴)	Mm_d ($\frac{\Delta l}{L}$x100) percent	Sample measure-ment	Δl (x10⁻⁴)	Mm_d ($\frac{\Delta l}{L}$x100) percent
1	900	951	0	0	1198	0	0	1701	0	0
1		933	+18	+0.074	1182	+16	+0.067	1664	+57	+0.243
2		946	+5	+0.021	1194	+4	+0.017	1699	+2	+0.009
2		924	+27	+0.111	1178	+20	+0.083	1642	+59	+0.251
3		945	+6	+0.025	1196	+2	+0.008	1699	+2	+0.009
3		929	+22	+0.091	1179	+19	+0.079	1642	+59	+0.251
4		943	+8	+0.033	1195	+3	+0.013	1692	+9	+0.038
4		929	+22	+0.091	1179	+19	+0.079	1644	+57	+0.243
5		942	+9	+0.037	1193	+5	+0.021	1696	+5	+0.021
5		921	+30	+0.124	1172	+26	+0.108	1642	+59	+0.251
6		938	+13	+0.054	1188	+10	+0.042	1695	+6	+0.026
6		925	+26	+0.107	1176	+22	+0.092	1643	+58	+0.247
								visible cracking		
7		941	+10	+0.041	1190	+8	+0.033	1697	+4	+0.017
7		925	+26	+0.107	1175	+23	+0.096	1643	+58	+0.247
8		940	+11	+0.045	1189	+9	+0.038	1697	+4	+0.017
8		924	+27	+0.111	1177	+21	+0.088	1642	+59	+0.251
9		935	+16	+0.066	1185	+13	+0.054	1696	+5	+0.021
9*		909	+42	+0.173	1155	+43	+0.179	1620	+81	+0.345

* Water soak period prolonged three days i.e. was seven day soak.

Sample number length (L)		HQ-22 (1) 3.123 inches			HQ-22 (2) 2.963 inches		
Cycle number	Comparitor measurement	Sample measure-ment	Δl (x10⁻⁴)	Mm_d ($\frac{\Delta l}{L}$x100) percent	Sample measure-ment	Δl (x10⁻⁴)	Mm_d ($\frac{\Delta l}{L}$x100) percent
1	900	182	0	0	1783	0	0
1		ball bearing register failed			ball bearing register failed		
2		115	0	0			
2		069	+46	+0.147			
3		113	+2	+0.006	1713	0	0
3		073	+42	+0.135	1673	+40	+0.135
4		112	+3	+0.009	1710	+3	+0.01
4		068	+47	+0.151	1672	+41	+0.138
5		112	+3	+0.009	1709	+4	+0.014
5		072	+43	+0.138	1669	+44	+0.149
6		110	+5	+0.016	1709	+4	+0.014
6		061	+54	+0.173	1668	+45	+0.152
		visible cracking					
7		108	+7	+0.022	1708	+5	+0.017
7		067	+48	+0.154	1664	+49	+0.165
					visible longitudinal crack		
8		110	+5	+0.016	1706	+7	+0.024
8		066	+49	+0.157	1663	+50	+0.169
9		105	+10	+0.032	1705	+8	+0.027
9*		062	+53	+0.17	1658	+55	+0.186

* Water soak period prolonged three days i.e. was seven day soak.

CYCLES OF WETTING AND DRYING
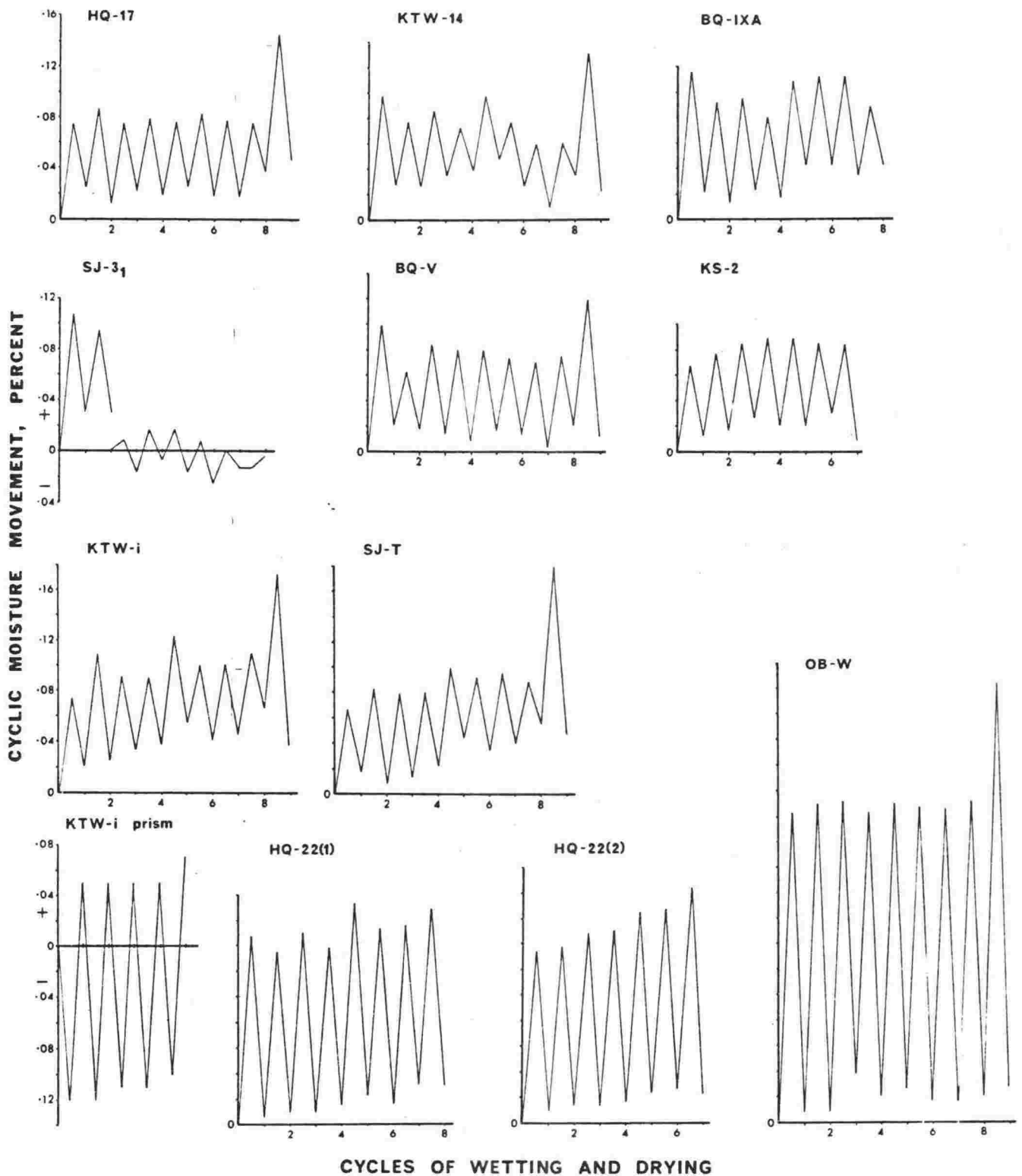
Figure A25.2 : From cyclic moisture movement measurements, greywackes
SJ-3$_1$ and BQ-V appear to shrink. Greywackes KTW-i and
SJ-T as well as all argillites tested, appear to expand.

Table A25.6 : Specific permeability, k, at nominal time intervals for all samples tested. The nearest recorded times, corresponding to the permeabilities calculated in millidarcies (x 10^{-19}), are shown in brackets.

Sample	Rock mean grain size, phi	Nominal time intervals, hours					
		3	20	48	75	100	130
HQ-17	1.317	19.6 (4)	11.6 (22)	88.34 (47)	3.02 (74)	0.71 (119)	1.25 (143)
SJ-3$_1$	1.32	18.37 (6)	11.24 (22)	3.34 (45)	1.09 (75)	-	-
KTW-14	2.6	14.6 (4.6)	10.7 (20)	2.47 (44)	3.19 (68)	0.8 (115)	1.34 (140)
BQ-V	2.73	7.34 (2)	5.11 (20)	3.22 (55)	2.88 (68)	2.65 (92)	2.62 (141)
BQ-IXA	2.9	3.79 (5)	4.09 (19)	3.74 (43)	3.06 (68)	2.95 (91)	-
KS-2	3.27	8.41 (3)	8.52 (22)	6.71 (42)	-	0.48 (103)	0.48 (138)
KTW-i	4.23	15.2 (4)	7.73 (23)	6.34 (47)	0.52 (79)	1.23 (96)	2.49 (131)
SJ-T	4.72	11.3 (4)	8.09 (22)	6.86 (51)	1.43 (70)	2.52 (117)	2.88 (143)
OB-W	5.6	23.61 (2)	-	4.1 (47)	1.24 (76)	1.45 (98)	1.76 (140)
HQ-22	6.28	9.28 (12.6)	7.29 (23)	6.42 (47)	0.57 (81)	0.91 (106)	1.14 (129)

Average k_{mD} after 90 hours = 1.63 x 10^{-19}

s.d. = 0.87
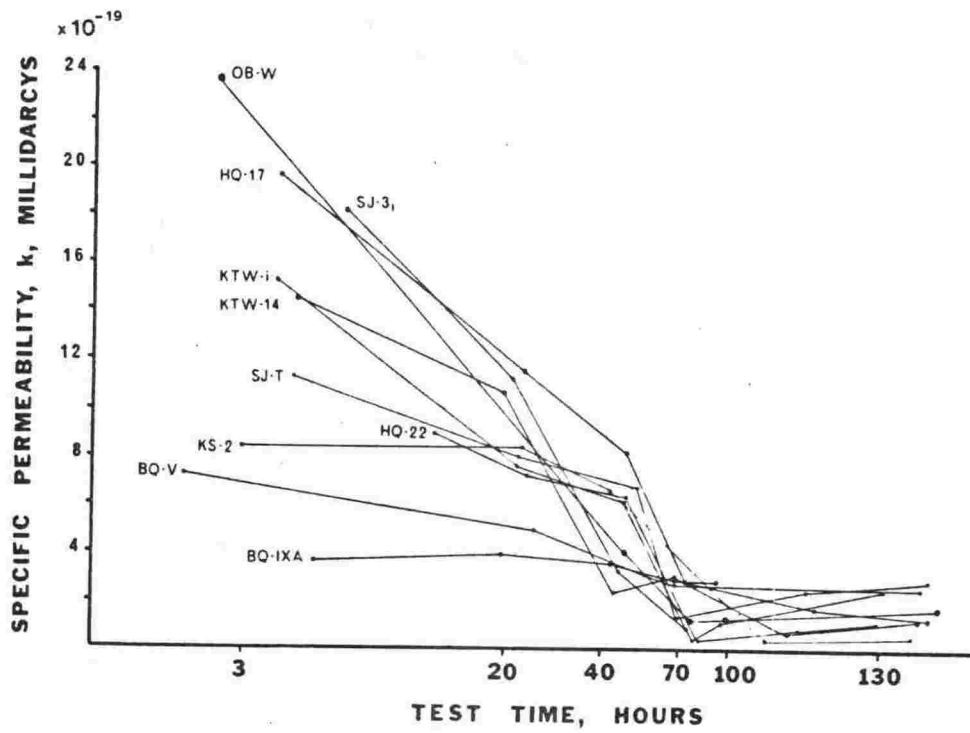
Figure A25.3 : Permeability is reduced with test time for all rocks
            tested.   Equilibrium is achieved after approxi-
mately 90 hours on test at a value less than 4×10^{-19} mD.
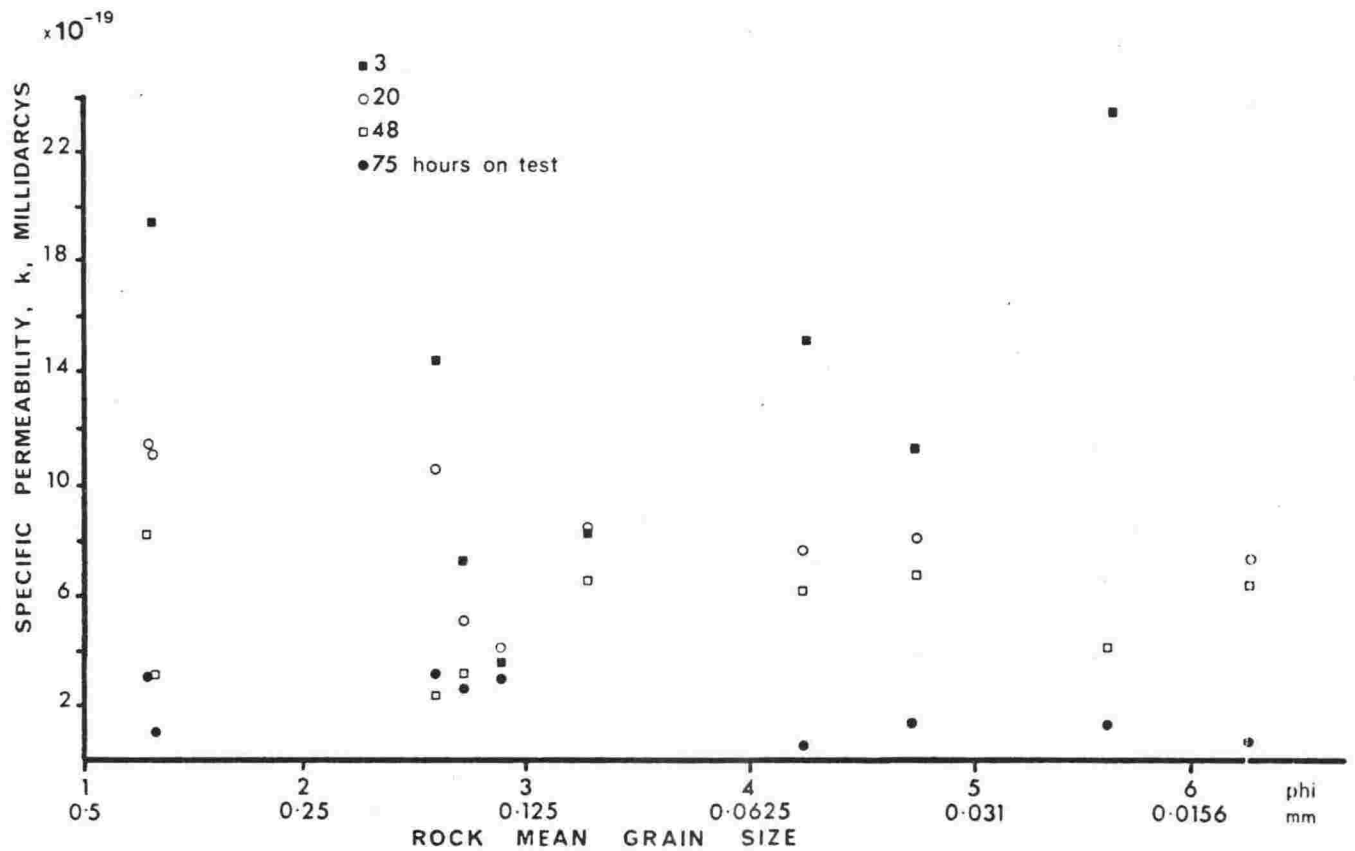
Figure A25.4 : Permeability shows an inverse relationship with finer
                rock mean grain sizes for times exceeding 20 hours on
test.   Initial permeabilities (three hours on test) show that grey-
wackes around 3 phi (0.125 mm) mean grain size have permeabilities
25 to 30 percent of those of the very coarse and very fine rocks in
the suite, with a gradation between minimum and maximum values.

(ii)   Mineralogy (which is related to rock mean grain size) and the presence of zeolite veining.

(iii)   Internal surface area of the rock.

The degradation process appears to commence at the moment of release from the quarry face and to be initiated by rock expansion. Perhaps this is best shown where ripping is used to loosen *in situ* material. The alternating greywacke and argillite, dipping nearly vertically, are confined - the greywacke less so than the argillite which because of its plasticity has developed recemented shears referred to by Clelland (1971) as "discontinuities effectively healed by later recrystallisation". Ripping of greywacke presents little difficultly but argillite presents a massive unyielding obstable; even when ripper depth is reduced the ripper will merely glide over the bed, often completely lifting the rear portion of very large machines. When the argillite finally yields, it breaks out as very large blocks. Ripper teeth have a life measured in minutes, rather than hours, in such conditions and a single ripper is generally used.

Rock expansion in response to pressure release, although not easily quantified, is a well documented phenomenon (Ollier, 1969; Winkler, 1973). Pressure release probably continues as dessication starts, i.e. dessication of both capillary and ordered water or quarry "sap" (Howie, 1910; Parks, 1911; Watson, 1911; Winkler, 1973). Accompanying pressure release and dessication, are thermal expansion effects (heating and cooling), as yet unresearched, and the effects of wetting and drying. From the ultrasonic velocity measurement of KTW-i prism (Appendix 19) and measurement of unrestrained moisture movement and permeability, equilibrium within an aqueous environment is achieved in approximately four days. The observation of Schaffer (1932) that a stress gradient is produced by rain, because rock is only soaked to a slight depth, may be significant for blocks of rock with relatively low surface area to volume ratios.

If some constraint is placed on rocks undergoing cyclic moisture movement they must experience an elastic deformation. In dessicated rocks, water penetrating into capillaries builds high vapour pressure in adjacent dry air spaces, due to the small meniscus radii (Mayer, 1963), which induces deformation - even complete disintegration. Indeed a measure of the ability of some shales to disintegrate in water is given by air-dried moisture content (Badger *et al.*, 1956), indicative of potential vapour pressures. Cyclic stress brings about the slabby degradation seen in cores cut perpendicular to bedding, the flaking effect along foliation planes and, in larger pieces of rock (reduced surface area to volume ratios), the concentric spalling observed (Plate A25.2, A25.3) - similar to that noted by Heidecker (1968). These observations are consistent with permeability effects or the ingress of water. Internal surface areas must be greater in rocks rich in phyllosilicates due to the presence of interlamellar spaces. Murray and Lyons (1960) have shown, for kaolinite, a relationship of surface area to base exchange capacity; total iron and titanium increasing with decreasing degrees of crystallinity. Chlorite is recognised as a mineral which decays early where weathering processes are active (Goldich, 1938; Loughnan, 1969), and has been shown by Marshall (1974) to be the first common mineral to be destroyed in the weathering of greywackes. Chlorite components occur in significant quantities in Wellington greywacke-suite rocks and have been shown to decrease in crystallinity with finer mean grain size of these rocks (section 2.14.3). The chlorites are rich in titanium and iron (Sameshima, 1977; Appendix 8) and the surface area and base exchange capacity is probably enhanced with reduced crystallinity.

Plate A25.2 : Degradation of argillite (OB-W shown) displays portions
                displaced from a central core along curvilinear planes;
(A), (B) and (C) show the phenomena, which is probably dependant on
surface area to volume ratios.   In (D) the control of degradation by
curved planes perpendicular to bedding and bedding plane fissility is
shown.

50 mm

C

8 mm

D

40 mm

A

B

38 mm
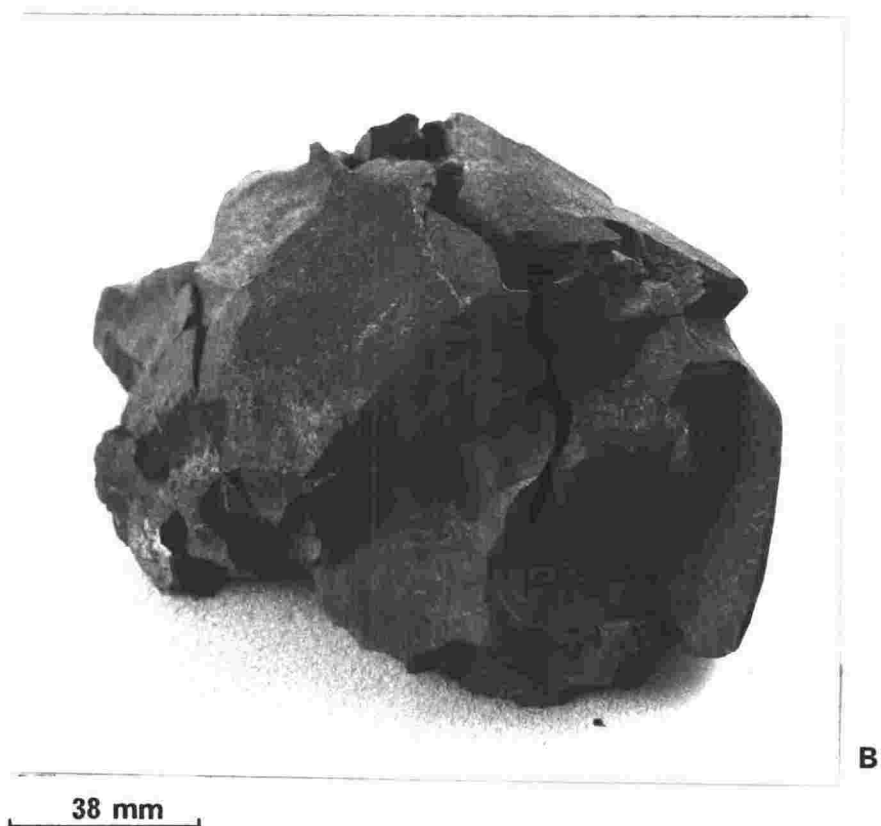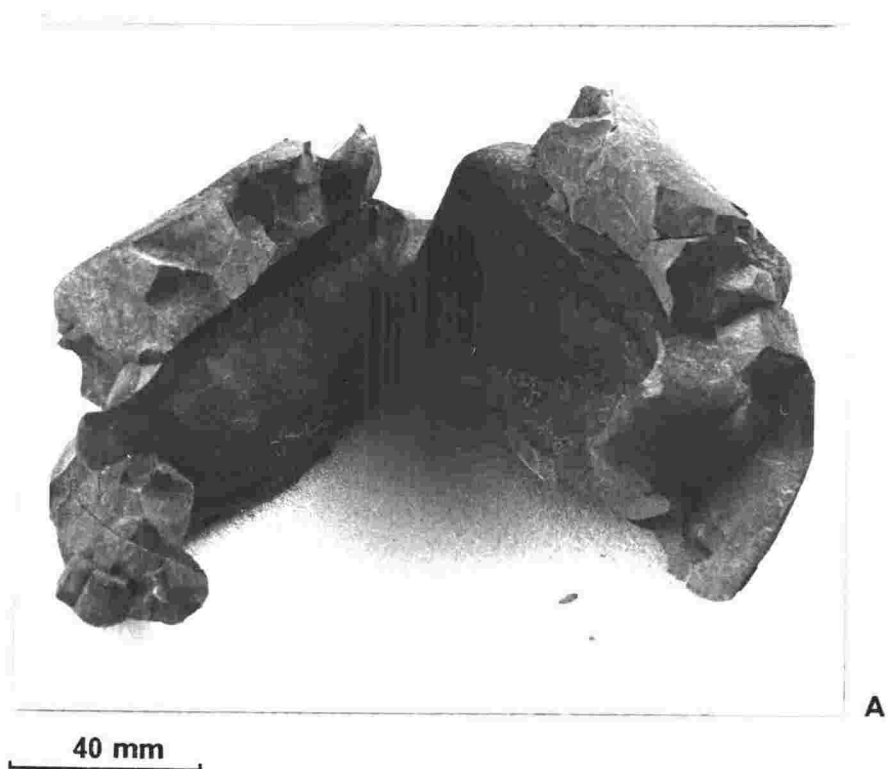
Plate A25.3 : Kawhia siltstone (KW-1) shows curved fracture surfaces
about a core after exposure to wetting and drying
cycles. Both (A) and (B) are of the same sample.

When microcracks develop due to cyclic wetting and drying, chemical weathering of a more obvious nature occurs at their edges and corners.

The dilation of crack openings and propagation of the crack with wetting of the rocks no doubt facilitates this development. The rock alters its colouration as yellow-brown, brown or red-brown oxides of iron are leached from chlorite and pyrite although this staining may be obvious only in thin section. The colouration is transmitted through the matrix material which both propagates and provides the iron oxides. The rock may now be considered to be incipiently weathered, to an extent that could certainly be detected by the Washington degradation test and probably by the clay index test (Appendix 23, 24).

Degradation, although decreasing physical size of rock particles, increases their surface area to volume ratios without reducing their strength. Only their physical integrity is destroyed. Indeed, on dessication most rocks gain strength, although pore pressure and weakened bond strength result in earlier compressive failure when rocks are tested wet (Michalopoulos and Triandafilidis, 1976; section 3.5.1; Appendix 13). Such a hardening/strengthening procedure is well known to stone masons, who speak of "seasoning" building stone prior to its use (Howie, 1910; Parks, 1911; Watson, 1911). Sir Christopher Wren insisted that the Portland stone chosen for the construction of St Pauls Cathedral, London, be seasoned for at least three years before use. (Schaffer 1932).

From the stage where physical strength is adversely affected by degradation, i.e. the stage at which iron oxides form, the rock and its associated engineering properties are most complicated and, as yet, little has been done to research geological aspects of these rocks, let alone marry geological properties to end use as engineering material.

Many engineering problems encountered, particularly with aggregates, have been attributable, at least in part, to excessive weathering; particles experiencing a loss of strength due to the formation of various chemical oxides. This variety of weathered (degraded) rock probably influenced failure of the Auckland-Hamilton motorway (Cornwell, 1966) and was certainly a factor in degradation mentioned by Dekker and Scott (1969).

Inconsistencies between petrographic prediction and performance tests (Clelland, 1971) have not helped in the establishment of limits for deleterious substances and physical property requirements for the end use of various aggregates for New Zealand (similar to ASTM C33-74a, table 3).

7.   Conclusions

(i)   The rate of degradation can be suprisingly rapid with cracks developing in argillites within two months of exposure.

(ii)   The measurement of internal rock surface area may lead to a better understanding of the degradation process.

(iii)   Chlorite content (and zeolite in veins) and degradation are directly related.

APPENDIX 26

Test results for sand (Walton Park) used in concrete mixes

The sand used in concrete mixes for this study was a natural rounded silica sand supplied by Walton Park Sand Co. Ltd., Green Island, Dunedin. The sand has impurities of iron oxide (less than 5 percent) imparting a yellow-orange-light brown stain to surface irregularities and cracks in the sand particles. The average diameter of the grains is 700 microns and all pass a 4.8 mm sieve. Two clean 200 litre (44 gallon) drums of the sand was homogenised by thorough mixing before being split to obtain representative samples for use in concrete.

The sand has been tested frequently by the New Zealand Concrete Research Association, over the last decade, and has been used as a standard repeatedly over this period. Results of tests conforming to NZS 1051:1953 and NZS 3111:1974, obtained in 1969 and 1978 respectively, are presented below (Table A26.1). Additional tests were carried out specifically for this study and are included with the 1978 test results.

Table A26.1 : Two sets of results of Walton Park sand tested ten years apart. Tests conformed to NZS 1051:1953 and NZS 3111:1974 for work done in 1969 and 1978 respectively. Sand represented by the sample tested in 1978 was used in concrete made for this study.

Test description	Test result 1969		Test result 1978	
Sand equivalent	75		75	
Sodium sulphate soundness test	Weight loss, 2.4 percent		-	
Bulk density and voids content	Dry rodded bulk density = 114.7 lb.ft^{-3} Dry rodded voids content = 29.2 percent Loose poured bulk density = 99.8 lb.ft^{-3} Loose poured voids content = 38.5 percent Flow time = 21.8 seconds		Loose poured bulk density = 1740 kg.m^{-3} Loose poured voids content = 37 percent Flow time = 21.5 seconds Oversize material = 1.2 percent	
Density and absorption	Density (SSD basis) = 2.61 gm.cm^{-3} Density (dry basis) = 2.60 gm.cm^{-3} Density (apparent) = 2.62 gm.cm^{-3} Absorption(dry basis) = 0.16 percent Absorption (SSD basis) = 0.16 percent		Density (SSD basis) = 2610 kg.m^{-3} Density (dry basis) = 2600 kg.m^{-3} Absorption (dry basis) = 0.42 percent Absorption (SSD basis) = 0.41 percent	
Organic impurities	-		No harmful impurities present	

Sieve analysis

Sieve size	Percent retained	Cumulative percent passing	Percent retained	Cumulative percent passing*
3/16"; 4.75 mm	0.3	99.7	0.7	99.3
#7; 2.36 mm	6.2	93.5	5.1	94.2
#14; 1.18 mm	20.3	63.2	16.1	78.1
#25; 600 um	33.9	39.3	38.9	39.2
#52; 300 um	14.8	24.5	30.1	9.1
#100; 150 um	15.2	9.3	7.4	1.7
#200; 75 um	8.2	1.0	1.6	0.1
PAN	1.0		0.3	-
Total:	99.9		100.2	
	Fineness modulus 2.61		Fineness modulus 2.78	

* Plotted in Figure A26.1
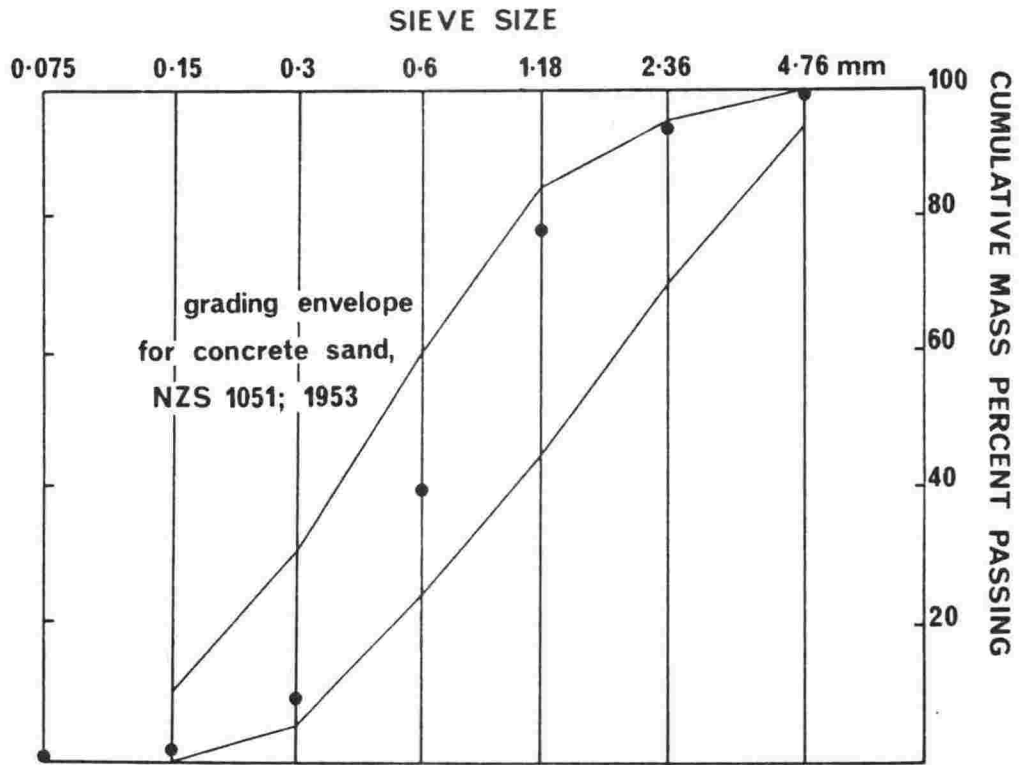
Figure A26.1 : Grading of Walton Park sand used for this study.

APPENDIX 27

Concrete mix designs

The concrete mix designs used in this study were based on work by McIntosh (1966), Shacklock (1974), Neville (1975) and Teychenne et $al.$ (1976), consistent with achieving two easily comparable mixes, of high strength, low water content, very low workability and high aggregate to cement ratio with coarse aggregate, particularly 19 mm aggregate, constituting 66 percent of the coarse aggregate blend.

Initial trials included water cement ratios of 0.4 and 0.5, but the contrast between such drastically different water to cement ratios, masked subtle workability affects imparted by aggregate and did not provide concrete of sufficient strength.

These mixes, designed specifically to attain high strength with high aggregate to cement ratios, would not normally be commercially viable because workability and cohesion are low due to lack of sand.

Mix 1 and 2 design calculations, for each aggregate, are given in Tables A27.1, A27.2.

Table A27.1 : Mix 1 concrete was designed on the basis of a $1m^3$ volume; values marked with an asterisk (*) indicate weights of components for a $1m^3$ volume of concrete.

Concrete sample		HQ-17	KTW-14	BQ-IXA	SJ-T	OB-W	HQ-22
Water:cement ratio		0.375	0.375	0.375	0.375	0.375	0.375
Density, cement	kg.m^{-3}	3140	3140	3140	3140	3140	3140
Density, sand	kg.m^{-3}	2600	2600	2600	2600	2600	2600
Density, 19 mm aggregate	kg.m^{-3}	2647	2660	2658	2691	2713	2671
Density, 9.5 mm aggregate	kg.m^{-3}	2632	2644	2651	2676	2699	2676
30 minute water absorption, sand	%	0.42	0.42	0.42	0.42	0.42	0.42
30 minute water absorption, 19 mm aggregate	%	0.22	0.15	0.17	0.21	0.26	0.33
30 minute water absorption, 9.5 mm aggregate	%	0.33	0.32	0.37	0.36	0.57	0.52
Dry mix proportions							
Cement content	*kg	350	350	350	350	350	350
Water demand; cement content x W:C ratio	kg	131.3	131.3	131.3	131.3	131.3	131.3
Total mix volumes;							
volume of water = $\frac{\text{water demand}}{1000}$	m^3	0.1313	0.1313	0.1313	0.1313	0.1313	0.1313
volume of cement = $\frac{\text{cement content}}{\rho \text{ cement x 1000}}$	m^3	0.1115	0.1115	0.1115	0.1115	0.1115	0.1115
air content (non-air entrained = 2 percent)	m^3	0.02	0.02	0.02	0.02	0.02	0.02
total volume of water, cement and air	m^3	0.2628	0.2628	0.2628	0.2628	0.2628	0.2628
∴ total volume of aggregate	m^3	0.7372	0.7372	0.7372	0.7372	0.7372	0.7372
Sand content;							
volume sand in total volume of aggregate	%	30	30	30	30	30	30
∴ volume of sand = volume of aggregate x 0.3	m^3	0.2212	0.2212	0.2212	0.2212	0.2212	0.2212
weight of sand = volume of sand x ρ sand x 1000	*kg	575.0	575.0	575.0	575.0	575.0	575.0
Coarse aggregate content;							
total volume of aggregate	m^3	0.7372	0.7372	0.7372	0.7372	0.7372	0.7372
volume of sand	m^3	0.2212	0.2212	0.2212	0.2212	0.2212	0.2212
∴ volume coarse aggregate	m^3	0.516	0.516	0.516	0.516	0.516	0.516

Table A27.1 : continued

Concrete sample		HQ-17	KTW-14	BQ-IXA	SJ-T	OB-W	HQ-22
19 mm aggregate content; volume 19 mm aggregate in coarse aggregate blend	%	66	66	66	66	66	66
volume 19 mm aggregate = total volume aggregate x 0.66 m^3		0.3416	0.3406	0.3406	0.3406	0.3406	0.3406
weight of 19 mm aggregate = volume 19 mm aggregate x ρ 19 mm aggregate x 1000	*kg	901.6	906.0	905.3	916.6	903.9	909.6
9.5 mm aggregate content; volume 9.5 mm aggregate in coarse aggregate blend	%	33	33	33	33	33	33
volume 9.5 mm aggregate = total volume aggregate x 0.33 m^3		0.1703	0.1703	0.1703	0.1703	0.1703	0.1703
weight of 9.5 mm aggregate = volume 9.5 mm aggregate x ρ 9.5 mm aggregate x 1000	*kg	448.2	450.2	451.5	455.7	459.6	455.7

Corrections for aggregate absorptions

		HQ-17	KTW-14	BQ-IXA	SJ-T	OB-W	HQ-22
Sand: weight of water required to bring sand to SSD condition = $\frac{\text{weight sand}}{100}$ x (30 min. water absorption - moisture content)	kg	2.42	2.42	2.42	2.42	2.42	2.42
19 mm aggregate: weight of water required to bring 19 mm aggregate to SSD condition = $\frac{\text{weight 19 mm aggregate}}{100}$ x (30 minute water absorption - moisture content)	kg	1.98	1.36	1.54	1.93	2.40	3.0
9.5 mm aggregate: weight of water required to bring 9.5 mm aggregate to SSD condition = $\frac{\text{weight 9.5 mm aggregate}}{100}$ x (30 min. water absorption - moisture content)	kg	1.48	1.44	1.67	1.64	2.62	2.37
Calculated water demand	kg	131.3	131.3	131.3	131.3	131.3	131.3
Corrected water demand	*kg	137.2	136.5	136.9	137.3	138.7	139.1

Batch weights for 0.03 m^3 concrete (i.e. twelve, 200 x 100 mm cylinder moulds)

		HQ-17	KTW-14	BQ-IXA	SJ-T	OB-W	HQ-22
water	kg	4.1	4.1	4.1	4.1	4.2	4.2
cement	kg	10.5	10.5	10.5	10.5	10.5	10.5
sand	kg	17.3	17.3	17.3	17.3	17.3	17.3
19 mm aggregate	kg	27.1	27.2	27.2	27.5	27.7	27.3
9.5 mm aggregate	g	13.5	13.5	13.6	13.7	13.8	13.7

Table A27.2 : Mix 2 concrete was designed on the basis of a 1 m^3 volume; values marked with an asterisk (*) indicate weights of components for a 1m^3 volume of concrete.

Concrete sample		HQ-17	KTW-14	BQ-IXA	SJ-T	OB-W	HQ-22
Water:concrete ratio		0.4	0.4	0.4	0.4	0.4	0.4
Density, cement	kg.m^{-3}	3140	3140	3140	3140	3140	3140
Density, sand	kg.m^{-3}	2600	2600	2600	2600	2600	2600
Density, 19 mm aggregate	kg.m^{-3}	2647	2660	2658	2691	2713	2671
Density, 9.5 mm aggregate	kg.m^{-3}	2632	2644	2651	2676	2699	2676
30 minute water absorption, sand	%	0.42	0.42	0.42	0.42	0.42	0.42
30 minute water absorption, 19mm aggregate	%	0.22	0.15	0.17	0.21	0.26	0.33
30 minute water absorption, 9.5mm aggregate	%	0.33	0.32	0.37	0.36	0.57	0.52
Dry mix proportions							
Cement content	*kg	350	350	350	350	350	350
Water demand; cement content x W:C ratio	kg	140	140	140	140	140	140
Total mix volumes;							
volume of water = $\frac{\text{water demand}}{1000}$	m^3	0.1400	0.1400	0.1400	0.1400	0.1400	0.1400
volume of cement = $\frac{\text{cement content}}{\rho \text{ cement x 1000}}$	m^3	0.1115	0.1115	0.1115	0.1115	0.1115	0.1115
air content (non-air entrained = 2 percent)	m^3	0.02	0.02	0.02	0.02	0.02	0.02
total volume of water, cement and air	m^3	0.2715	0.2715	0.2715	0.2715	0.2715	0.2715
∴ total volume of aggregate	m^3	0.7285	0.7285	0.7285	0.7285	0.7285	0.7285
Sand content;							
volume sand in total volume of aggregate	%	30	30	30	30	30	30
∴ volume of sand = volume of aggregate x 0.3	m^3	0.2186	0.2186	0.2186	0.2186	0.2186	0.2186
weight of sand = volume of sand x ρ sand x 1000	*kg	568.2	568.2	568.2	568.2	568.2	568.2
Coarse aggregate content ;							
total volume of aggregate	m^3	0.7285	0.7285	0.7285	0.7285	0.7285	0.7285
volume of sand	m^3	0.2186	0.2186	0.2186	0.2186	0.2186	0.2186
∴ volume coarse aggregate	m^3	0.5099	0.5099	0.5099	0.5099	0.5099	0.5099
19 mm aggregate content;							
volume 19 mm aggregate in coarse aggregate blend	%	66	66	66	66	66	66
volume 19 mm aggregate = total volume aggregate x 0.66	m^3	0.3365	0.3365	0.3365	0.3365	0.3365	0.3365
weight of 19 mm aggregate = volume 19 mm aggregate x ρ 19 mm aggregate x 1000	*kg	890.8	895.1	894.4	905.5	913.0	898.8
9.5 mm aggregate content;							
volume 9.5 mm aggregate in coarse aggregate blend	%	33	33	33	33	33	33
volume 9.5 mm aggregate = total volume aggregate x 0.33	m^3	0.1683	0.1683	0.1683	0.1683	0.1683	0.1683
weight of 9.5mm aggregate = volume 9.5 mm aggregate x ρ 9.5 mm aggregate x 1000	*kg	442.9	444.9	446.2	450.4	454.2	450.4
Corrections for aggregate absorptions							
Sand: weight of water required to bring sand to SSD condition = $\frac{\text{weight sand}}{100}$ x (30 min. water absorption - moisture content)	kg	2.39	2.39	2.39	2.39	2.39	2.39
19 mm aggregate: weight of water required to bring 19 mm aggregate to SSD condition = $\frac{\text{weight 19 mm aggregate}}{100}$ x (30 min. water absorption - moisture content	kg	1.96	1.34	1.52	1.90	2.37	2.97

Table A27.2 : continued

Concrete sample		HQ-17	KTW-14	BQ-IXA	SJ-T	OB-W	HQ-22
9.5 mm aggregate: weight of water required to bring 9.5 mm aggregate to SSD condition $= \dfrac{\text{weight 9.5 mm aggregate}}{100}$ x (30 min. water absorption - moisture content)	kg	1.46	1.42	1.65	1.62	2.59	2.34
Calculated water demand	kg	140.0	140.0	140 0	140.0	140.0	140.0
Corrected water demand	*kg	145.8	145.2	145.6	145.9	147.4	147.7

Batch weights for 0.03 m³ concrete (i.e. twelve, 200 x 100 mm cylinder moulds)

		HQ-17	KTW-14	BQ-IXA	SJ-T	OB-W	HQ-22
water	kg	4.4	4.4	4.4	4.4	4.4	4.4
cement	kg	10.5	10.5	10.5	10.5	10.5	10.5
sand	kg	17.1	17.1	17.1	17.1	17.1	17.1
19 mm aggregate	kg	26.7	26.9	26.8	27.2	27.4	27.0
9.5 mm aggregate	kg	13.3	13.4	13.4	13.5	13.6	13.5

APPENDIX 28

Concrete cylinders: Materials preparation, mixing, moulding, curing and test

1.   Preparation

Raw materials were prepared in the following manner:

(i)   Coarse aggregate preparation:
After crushing, the six test aggregates were graded (section 4.2.1), thoroughly hand washed, drained and slowly oven dried to constant mass at 105 ±3°C.   Washing was necessary to remove adhering surface coatings(section 4.2.7) enabling closer adherance to mix design and hence more accurate assessment of the aggregate as a rock type in concrete.   Oven drying obviates measurements of water content, an important mix parameter which must be determined for each size grading of aggregate but which is difficult to control, promotes aggregate storage problems and is both tedious and time consuming to obtain.   If aggregates are oven dried, the 30 minute absorption test supplies all the information necessary for design criteria.

(ii)   Sand:
The well rounded quartz sand from Walton Park, Dunedin, conforms fully to NZS 3111:1974 and has been used for several years by the NZ Concrete Research Association as a standard in many research and development programmes.   The Association test results are compared with those obtained in this study in Appendix 27.   This sand has the advantage of being monomineralic and light in colour - aiding studies of crushed and sawn concrete made from it.   (section 5.4.1 and Appendix 17).   For use in this study, two 200 litre (44 gallon) drums of sand was homogenised and a representative sample oven dried for each concrete mix.   No further pretreatment was necessary.

(iii)   Cement:
Cement used was a fresh shipment of bagged Wilsons Ordinary Portland cement, from one batch.   One 40 kg bag made two to three mixes and six bags were used in all.   No bag remained open longer than two days.   Storage was indoors.   Pending use, each bag was stored in two plastic bags with their open ends reversed and tightly tied closed.   In use, the open bag was kept in a waterproof metal container with a tightly fitting lid.

The cement was not tested, but assumed to be of good quality meeting NZS 3122:1974 "Portland cement (ordinary and rapid hardening)".

2.   Fresh concrete tests

Mix design is given in Appendix 27.   Two 0.03 m^3 mixes were made from each aggregate, utilising water to cement ratios of 0.375 (mix 1) and 0.4 (mix 2).   Each mix made sufficient concrete for 12 cylinders, 100 m diameter and 200 mm long, conforming to NZS 3112:1974, clause 201.

Tests were carried out to NZS 3112:1974 and results are given in Table 5.1.   A compaction factor test was also carried out to BS 1881:Part 2:1970, alternative number 1;   results also being listed in Table 5.1.

3.   Moulding and curing of concrete test cylinders

To optimise compaction of fresh concrete in the moulds, a vibrating table was used with visual monitoring of segregation and laitance.

Moulds were filled in three equal layers, marked for identification and placed in a curing chamber in an environment of 100 percent R.H. (atomised water spray) at 21 ±1°C.   Initially the cylinders were stacked horizontally with the seam uppermost but after removal from the moulds, placed vertically on galvanised expanded metal shelving.

4.   Testing of cylinders

The twelve cylinders from each batch were tested, in randomly selected groups of three, at 3, 7, 28 and 90 day ageing.   Cylinders were taken singly from the curing chamber and weighed immediately in air then in water.   Their long axis ultrasonic velocity was determined using the PUNDIT apparatus and they were measured lengthwise and across two diameters at mid-height, 22.5° either side of the mould seam.   They were then uniaxially compression tested.   Complete results are given in Appendix 29.   At 28 days, the static elastic modulus was determined using temperature compensated half bridge strain instrumentation, a single PL-60 strain gauge (60 mm gauge length) being attached parallel to the longitudinal axis of the cylinder centred on mid-height (Appendix 14).

APPENDIX 29

Concrete cylinders: tabulated test results.

Results presented in this Appendix are those obtained from tests outlined in Appendix 28.

Over the whole test programme the coefficient of variation did not exceed 6.8 percent and was generally considerably lower, averaging 2.8 percent for mix 1 and 2.5 percent for mix 2.

HQ-17   Mix 1   (0.375 w:c)

PUNDIT time	Age at test	Type of test	Wt. in air	Wt. in water	Density	Diam 1	Diam 2	Mean diam	Length	Load at failure	Strength	Mean strength	Range	Std dev	C of V	Ultra-sonic pulse velocity
µ sec	days		gms	gms	kg.m^{-3}	units in	units in	units in	units in	units lbf	MPa	MPa	MPa	MPa	%	m.s^{-1}
43.9			3880	2314	2478	3.932	3.928	3.930	7.878	52,800	30.0					4558
43.9	3	comp	3882	2310	2470	3.942	3.932	3.937	7.881	53,300	30.0	30.1	0.2	0.12	0.4	4560
43.6			3897	2324	2477	3.948	3.928	3.938	7.882	53,300	30.2					4592
42.2			3892	2321	2477	3.935	3.936	3.935	7.876	85,300	48.4					4741
42.5	7	comp	3891	2321	2478	3.949	3.920	3.934	7.880	87,200	49.5	49.3	1.7	1.00	2.0	4710
42.3			3885	2317	2478	3.934	3.928	3.931	7.878	88,200	50.1					4731
41.0			3876	2311	2477	3.929	3.928	3.928	7.884	131,000	74.5					4884
41.0	28	comp	3900	2329	2483	3.930	3.940	3.935	7.878	130,600	74.0	74.4	0.8	0.47	0.6	4881
40.7			3915	2340	2486	3.937	3.934	3.935	7.890	132,000	74.8					4924
40.3			3899	2326	2479	3.936	3.940	3.938	7.878	156,300	88.5					4965
40.4	90	comp	3889	2321	2480	3.927	3.935	3.931	7.876	151,500	86.1	88.0	3.3	1.95	2.2	4952
40.4			3886	2322	2485	3.928	3.931	3.930	7.876	157,300	89.4					4952

mean density kg.m^{-3} : 3 day: 2475   7 day: 2478   28 day: 2482   90 day 2481
reported in compliance with NZS 3111:1974 :   2480   2480   2480   2480
mean ultrasonic pulse velocity m.s^{-1} :   4570   4727   4896   4956

KTW-14   Mix 1   (0.375 w:c)

µ sec	days		gms	gms	kg.m^{-3}	in	in	in	in	lbf	MPa	MPa	MPa	MPa	%	m.s^{-1}
42.5			3899	2330	2485	3.940	3.928	3.934	7.886	55,400	31.4					4713
43.1	3	comp	3890	2321	2479	3.937	3.937	3.937	7.879	52,600	29.8	30.3	1.8	1.06	3.5	4643
42.6			3900	2329	2483	3.936	3.946	3.941	7.881	52,400	29.6					4699
41.5			3907	2337	2489	3.937	3.939	3.938	7.876	87,000	49.3					4821
42.1	7	comp	3895	2322	2476	3.942	3.935	3.938	7.876	89,200	50.5	49.8	1.2	0.71	1.4	4752
41.8			3890	2318	2475	3.936	3.941	3.938	7.876	87,400	49.5					4786
40.1			3879	2316	2482	3.929	3.930	3.929	7.875	131,400	74.7					4988
40.3	28	comp	3908	2336	2486	3.929	3.937	3.933	7.889	129,500	73.5	73.9	1.2	0.71	0.96	4972
40.2			3899	2329	2483	3.932	3.933	3.932	7.877	129,700	73.6					4977
40.4			3901	2330	2483	3.934	3.938	3.936	7.874	153,400	86.9					4951
40.3	90	comp	3906	2333	2483	3.938	3.942	3.940	7.874	144,800	81.9	85.5	5.7	3.4	3.9	4963
40.2			3902	2330	2482	3.913	3.944	3.929	7.876	154,000	87.6					4976

mean density kg.m^{-3} : 3 day: 2482   7 day: 2480   28 day: 2484   90 day: 2483
reported in compliance with NZS 3111:1974 :   2480   2480   2480   2480
mean ultrasonic pulse velocity m.s^{-1} :   4685   4786   4979   4963

BQ-IXA   Mix 1   (0.375 w:c)

PUNDIT time μ sec	Age at test days	Type of test	Wt. in air gms	Wt. in water gms	Density kg.m^{-3}	Diam 1 units in	Diam 2 units in	Mean diam units in	Length units in	Load at failure units lbf	Strength MPa	Mean strength MPa	Range MPa	Std dev MPa	C of V %	Ultra-sonic pulse velocity m.s^{-1}
43.7			3899	2326	2479	3.948	3.926	3.937	7.881	50,600	28.7					4581
43.5	3	comp	3932	2350	2486	3.933	3.942	3.937	7.937	56,600	32.1	29.8	3.4	2.01	6.7	4635
43.6			3902	2329	2481	3.937	3.937	3.937	7.889	50,700	28.7					4596
42.6			3896	2324	2478	3.938	3.940	3.939	7.883	87,300	49.4					4700
42.1	7	comp	3891	2324	2483	3.929	3.931	3.930	7.879	83,100	47.2	48.0	2.2	1.30	2.7	4754
42.2			3905	2330	2479	3.942	3.935	3.938	7.889	84,000	47.5					4748
40.4			3899	2331	2487	3.934	3.930	3.932	7.881	126,400	71.8					4955
40.5	28	comp	3909	2337	2487	3.934	3.935	3.934	7.876	130,000	73.7	74.0	4.7	2.77	3.8	4940
40.5			3891	2322	2480	3.932	3.933	3.932	7.881	134,800	76.5					4943
39.9			3904	2332	2484	3.935	3.943	3.939	7.876	154,600	87.5					5014
39.9	90	comp	3910	2338	2487	3.937	3.929	3.933	7.884	154,000	87.4	87.2	0.9	0.53	0.61	5019
40.0			3904	2333	2485	3.939	3.932	3.936	7.876	152,700	86.6					5001

mean density kg.m^{-3} : 3 day: 2482   7 day: 2480   28 day: 2491   90 day: 2485
reported in compliance with NZS 3111:1974 : 2480   2480   2490   2490
mean ultrasonic pulse velocity m.s^{-1} : 4604   4734   4946   5011

SJ-T   Mix 1   (0.375 w:c)

PUNDIT time μ sec	Age at test days	Type of test	Wt. in air gms	Wt. in water gms	Density kg.m^{-3}	Diam 1 units in	Diam 2 units in	Mean diam units in	Length units in	Load at failure units lbf	Strength MPa	Mean strength MPa	Range MPa	Std dev MPa	C of V %	Ultra-sonic pulse velocity m.s^{-1}
44.0			3932	2360	2501	3.938	3.932	3.935	7.882	49,600	28.1					4550
43.7	3	comp	3920	2350	2497	3.927	3.933	3.930	7.881	49,500	28.1	28.4	0.8	0.47	1.7	4581
44.2			3922	2354	2501	3.926	3.934	3.930	7.878	50,800	28.9					4527
42.4			3936	2359	2496	3.945	3.934	3.939	7.880	89,400	50.6					4721
42.6	7	comp	3941	2364	2499	3.944	3.943	3.943	7.884	85,500	48.3	49.9	2.4	1.42	2.8	4701
42.6			3915	2344	2492	3.940	3.937	3.938	7.884	89,600	50.7					4701
41.0			3929	2362	2507	3.936	3.940	3.938	7.874	129,000	73.0					4878
40.9	28	comp	3940	2365	2502	3.934	3.936	3.935	7.887	128,100	72.6	73.8	3.1	1.83	2.5	4898
41.1			3927	2354	2497	3.933	3.939	3.936	7.887	133,600	75.7					4874
40.3			3940	2369	2508	3.947	3.921	3.934	7.882	147,000	83.4					4968
40.5	90	comp	3931	2360	2502	3.932	3.936	3.934	7.882	152,500	86.5	83.4	6.3	3.7	4.5	4943
40.4			3946	2371	2505	3.936	3.941	3.939	7.879	141,700	80.2					4954

mean density kg.m^{-3} : 3 day: 2500   7 day: 2496   28 day: 2502   90 day: 2505
reported in compliance with NZS 3111:1974 : 2500   2500   2500   2510
mean ultrasonic pulse velocity m.s^{-1} : 4553   4708   4883   4955

OB-W   Mix 1   (0.375 w:c)

PUNDIT time μ sec	Age at test days	Type of test	Wt. in air gms	Wt. in water gms	Density kg.m^{-3}	Diam 1 units in	Diam 2 units in	Mean diam units in	Length units in	Load at failure units lbf	Strength MPa	Mean strength MPa	Range MPa	Std dev MPa	C of V %	Ultra-sonic pulse velocity m.s^{-1}
-			3939	2372	2514	-	-	3.940	7.887	53,600	30.3					-
45.9	3	comp	3964	2387	2514	3.943	3.940	3.941	7.886	56,300	31.8	31.4	1.8	1.06	3.4	4364
46.0			3941	2376	2518	-	-	3.940	7.887	56,800	32.1					4355
44.4			3965	2391	2519	3.936	3.943	3.939	7.894	85,500	48.4					4516
44.7	7	comp	3963	2392	2523	3.934	3.941	3.937	7.888	85,100	48.2	48.6	0.9	0.53	1.1	4482
44.5			3964	2390	2518	3.942	3.944	3.943	7.880	87,000	49.1					4498
43.2			3961	2390	2521	3.933	3.939	3.936	7.889	112,700	63.9					4638
43.1	28	comp	3954	2380	2512	3.943	3.939	3.941	7.876	113,100	63.9	62.7	3.5	2.07	3.3	4642
43.1			3966	2392	2520	3.939	3.944	3.941	7.877	106,900	60.4					4642
42.5			3953	2386	2523	3.929	3.926	3.928	7.875	111,800	63.6					4707
42.5	90	comp	3970	2398	2526	3.934	3.935	3.935	7.880	125,900	71.4	67.9	7.8	4.6	6.8	4710
42.7			3966	2393	2521	3.935	3.928	3.932	7.881	121,200	68.8					4688

mean density kg.m^{-3} : 3 day: 2515   7 day: 2520   28 day: 2518   90 day: 2523
reported in compliance with NZS 3111:1974 : 2520   2520   2520   2520
mean ultrasonic pulse velocity, m.s^{-1} : 4360   4499   4641   4702

HQ-22   Mix 1   (0.375 w:c)

PUNDIT time	Age at test	Type of test	Wt. in air	Wt. in water	Density	Diam 1	Diam 2	Mean diam	Length	Load at failure	Strength	Mean strength	Range	Std dev	C of V	Ultrasonic pulse velocity
μ sec	days		gms	gms	kg.m⁻³	units in	units in	units in	units in	units lbf	MPa	MPa	MPa	MPa	%	m.s⁻¹
45.1			3917	2344	2490	3.940	3.946	3.943	7.884	51,500	29.1					4440
45.2	3	comp	3903	2332	2484	3.938	3.941	3.939	7.879	52,000	29.4	29.9	2.0	1.18	4.0	4428
44.8			3910	2341	2492	3.934	3.931	3.932	7.885	54,800	31.1					4471
43.5			3920	2348	2494	3.932	3.944	3.938	7.879	84,400	47.8					4601
43.6	7	comp	3915	2346	2495	3.928	3.932	3.930	7.881	85,400	48.5	48.5	1.5	0.89	1.8	4591
43.7			3917	2345	2492	3.930	3.938	3.934	7.881	86,900	49.3					4581
42.0			3916	2349	2499	3.934	3.931	3.932	7.878	127,900	72.6					4764
41.8	28	comp	3926	2355	2499	3.943	3.928	3.935	7.876	126,100	71.5	71.3	2.9	1.7	2.4	4786
42.0			3918	2349	2497	3.932	3.931	3.931	7.874	122,700	69.7					4762
41.6			3915	2347	2497	3.907	3.914	3.911	7.852	142,700	81.9					4794
41.7	90	comp	3928	2356	2499	3.940	3.936	3.938	7.879	150,500	85.2	82.4	5.1	3.0	3.7	4799
41.9			3920	2349	2495	3.932	3.933	3.933	7.875	141,100	80.1					4774

mean density kg.m⁻³   :   3 day: 2489   7 day: 2494   28 day: 2498   90 day: 2497
reported in compliance with NZS 3111:1974 :   2490   2490   2500   2500
mean ultrasonic pulse velocity m.s⁻¹   :   4446   4591   4771   4789

HQ-17   Mix 2   (0.4 w:c)

PUNDIT time	Age at test	Type of test	Wt. in air	Wt. in water	Density	Diam 1	Diam 2	Mean diam	Length	Load at failure	Strength	Mean strength	Range	Std dev	C of V	Ultrasonic pulse velocity
44.6			3857	2289	2460	3.932	3.930	3.931	7.874	39,800	22.6					4484
44.5	3	comp	3869	2298	2463	3.934	3.933	3.933	7.880	38,400	21.8	22.1	0.8	0.47	2.1	4498
44.2			3872	2302	2466	3.928	3.939	3.933	7.883	38,700	22.0					4530
42.5			3870	2298	2462	3.937	3.934	3.935	7.895	74,900	42.5					4718
42.3	7	comp	3861	2296	2468	3.932	3.926	3.929	7.874	68,000	38.7	41.4	4.2	2.48	6.0	4728
42.6			3870	2298	2462	3.929	3.947	3.938	7.881	75,700	42.9					4699
41.1			3890	2314	2468	3.937	3.936	3.936	7.879	121,800	69.0					4869
41.1	28	comp	3879	2306	2466	3.933	3.939	3.936	7.875	115,800	65.6	66.9	3.4	2.0	3.0	4867
41.0			3890	2313	2467	3.938	3.941	3.939	7.877	117,000	66.2					4880
40.5			3888	2314	2470	3.933	3.940	3.937	7.877	141,500	80.2					4940
40.6	90	comp	3886	2312	2469	3.935	3.938	3.937	7.875	140,800	79.8	79.6	1.3	0.77	0.96	4927
40.5			3888	2316	2473	3.931	3.935	3.933	7.881	139,000	78.9					4943

mean density kg.m⁻³   :   3 day: 2463   7 day: 2464   28 day: 2467   90 day: 2471
reported in compliance with NZS 3111:1974 :   2460   2460   2470   2470
mean ultrasonic velocity m.s⁻¹   :   4504   4715   4872   4937

KTW-14   Mix 2   (0.4 w:c)

PUNDIT time	Age at test	Type of test	Wt. in air	Wt. in water	Density	Diam 1	Diam 2	Mean diam	Length	Load at failure	Strength	Mean strength	Range	Std dev	C of V	Ultrasonic pulse velocity
44.3			3869	2305	2474	3.924	3.931	3.927	7.879	43,700	24.9					4518
44.4	3	comp	3882	2312	2473	3.928	3.935	3.931	7.883	45,800	26.0	25.4	1.1	0.65	2.6	4551
44.3			3888	2316	2473	3.940	3.937	3.938	7.875	44,800	25.4					4515
42.3			3874	2307	2472	3.933	3.928	3.930	7.875	75,200	42.7					4729
42.0	7	comp	3900	2328	2481	3.938	3.938	3.938	7.877	73,000	41.3	42.1	1.4	0.83	2.0	4764
42.3			3865	2302	2473	3.926	3.925	3.925	7.875	74,400	42.4					4729
40.9			3890	2318	2475	3.937	3.935	3.936	7.878	119,000	67.4					4893
40.7	28	comp	3894	2324	2480	3.937	3.933	3.935	7.878	119,200	67.6	68.8	4.1	2.42	3.5	4917
40.6			3912	2336	2482	3.938	3.945	3.941	7.876	126,600	71.5					4927
40.3			3894	2324	2480	3.932	3.933	3.933	7.876	136,300	77.4					4964
40.2	90	comp	3882	2316	2479	3.931	3.931	3.931	7.871	142,600	81.0	80.0	4.1	2.42	3.02	4973
40.3			3897	2325	2479	3.935	3.938	3.937	7.875	143,900	81.5					4963

mean density kg.m⁻³   :   3 day: 2473   7 day: 2475   28 day: 2479   90 day: 2479
reported in compliance with NZS 3111:1974 :   2470   2480   2480   2480
mean ultrasonic velocity m.s⁻¹   :   4528   4741   4912   4967

BQ-IXA   Mix 2   (0.4 w:c)

PUNDIT time	Age at test	Type of test	Wt. in air	Wt. in water	Density	Diam 1	Diam 2	Mean diam	Length	Load at failure	Strength	Mean strength	Range	Std dev	C of V	Ultra-sonic pulse velocity
μ secs	days		gms	gms	kg.m^{-3}	units in	units in	units in	units in	units lbf	MPa	MPa	MPa	MPa	%	m.s^{-1}
44.4			3880	2307	2467	3.936	3.936	3.936	7.880	38,600	21.9					4508
44.8	3	comp	3868	2298	2464	3.932	3.932	3.932	7.879	38,400	21.8	21.7	0.5	0.30	1.4	4467
44.1			3881	2313	2475	3.935	3.932	3.934	7.873	37,700	21.4					4535
42.8			3880	2308	2468	3.936	3.934	3.935	7.877	68,000	38.6					4675
42.7	7	comp	3874	2304	2468	3.945	3.925	3.935	7.878	67,700	38.4	38.2	1.1	0.65	1.7	4686
43.0			3878	2306	2467	3.938	3.935	3.936	7.875	66,100	37.5					4652
41.2			3889	2318	2476	3.932	3.938	3.935	7.876	113,000	64.1					4856
41.4	28	comp	3880	2307	2467	3.938	3.931	3.934	7.876	119,500	67.8	65.9	3.7	2.18	3.3	4832
41.4			3870	2303	2470	3.931	3.931	3.931	7.879	116,000	65.9					4834
40.8			3882	2315	2477	3.934	3.930	3.932	7.877	134,500	76.4					4904
40.7	90	comp	3897	2324	2477	3.933	3.939	3.936	7.880	136,300	77.2	75.6	4.1	2.42	3.2	4918
40.8			3902	2326	2476	3.942	3.935	3.939	7.881	129,200	73.1					4906

mean density kg.m^{-3} : 3 day: 2469   7 day: 2468   28 day: 2471   90 day: 2477
reported in compliance with NZS 3111:1974 :   2470   2470   2470   2480
mean ultrasonic pulse velocity m.s^{-1} :   4503   4671   4841   4909

SJ-T   Mix 2   (0.4 w:c)

PUNDIT time	Age at test	Type of test	Wt. in air	Wt. in water	Density	Diam 1	Diam 2	Mean diam	Length	Load at failure	Strength	Mean strength	Range	Std dev	C of V	Ultra-sonic pulse velocity
44.3			3919	2347	2493	3.938	3.938	3.938	7.884	40,000	22.6					4520
44.5	3	comp	3901	2332	2486	3.931	3.928	3.930	7.881	40,400	23.0	22.8	0.4	0.24	1.0	4498
44.3			3912	2339	2487	3.942	3.940	3.941	7.876	40,500	22.9					4516
43.0			3930	2356	2497	3.942	3.944	3.943	7.878	66,000	37.3					4654
43.2	7	comp	3933	2358	2497	3.940	3.942	3.941	7.887	68,000	38.4	38.2	1.7	1.0	2.6	4637
43.0			3910	2336	2484	3.938	3.939	3.938	7.876	68,900	39.0					4652
41.8			3920	2344	2487	3.930	3.938	3.934	7.880	113,100	64.2					4788
41.9	28	comp	3913	2339	2486	3.936	3.939	3.937	7.882	114,800	65.0	64.0	2.3	1.36	2.1	4778
41.2			3916	2346	2494	3.933	3.932	3.932	7.877	110,400	62.7					4856
41.2			3925	2351	2494	3.930	3.944	3.937	7.886	128,600	72.8					4862
41.1	90	comp	3927	2354	2497	3.933	3.938	3.936	7.887	128,300	72.7	72.5	0.7	0.41	0.57	4874
41.2			3936	2362	2501	3.936	3.942	3.939	7.877	127,500	72.1					4856

mean density kg.m^{-3} : 3 day: 2489   7 day: 2493   28 day: 2489   90 day: 2497
reported in compliance with NZS 3111:1974 :   2490   2490   2490   2500
mean ultrasonic pulse velocity m.s^{-1} :   4511   4648   4807   4864

OB-W   Mix 2   (0.4 w:c)

PUNDIT time	Age at test	Type of test	Wt. in air	Wt. in water	Density	Diam 1	Diam 2	Mean diam	Length	Load at failure	Strength	Mean strength	Range	Std dev	C of V	Ultra-sonic pulse velocity
47.5			3936	2362	2501	3.923	3.948	3.935	7.882	42,500	24.1					4215
47.0	3	comp	3933	2365	2508	3.937	3.929	3.933	7.876	40,400	22.9	23.6	1.2	0.71	3.0	4256
47.0			3925	2358	2505	3.930	3.930	3.930	7.876	42,100	23.9					4256
44.7			3952	2379	2512	3.939	3.935	3.937	7.892	75,800	42.9					4485
45.2	7	comp	3950	2375	2508	3.937	3.940	3.938	7.880	73,700	41.7	42.4	1.2	0.71	1.7	4428
44.8			3951	2380	2515	3.930	3.937	3.933	7.900	75,000	42.6					4479
43.2			3956	2382	2513	3.936	3.938	3.937	7.875	108,200	61.3					4630
43.2	28	comp	3946	2374	2510	3.935	3.934	3.934	7.879	106,000	60.1	60.5	1.2	0.71	1.2	4633
43.3			3945	2377	2516	3.931	3.927	3.929	7.882	105,600	60.1					4624
42.7			3963	2389	2518	3.940	3.928	3.934	7.884	111,800	63,4					4690
42.6	90	comp	3957	2382	2512	3.929	3.941	3.935	7.880	116,200	65.9	65.4	3.6	2.1	3.3	4698
42.9			3942	2370	2508	3.932	3.934	3.933	7.877	118,000	67.0					4664

mean density kg.m^{-3} : 3 day: 2505   7 day: 2512   28 day: 2513   90 day: 2513
reported in compliance with NZS 3111:1974 :   2510   2510   2510   2510
mean ultrasonic pulse velocity m.s^{-1} :   4242   4464   4629   4684

HQ-22   Mix 2   (0.4 w:c)

PUNDIT time	Age at test	Type of test	Wt. in air	Wt. in water	Density	Diam 1	Diam 2	Mean diam	Length	Load at failure	Strength	Mean strength	Range	Std dev	C of V	Ultrasonic pulse velocity
μ sec	days		gms	gms	kg.$\bar{m}^3$	units in	units in	units in	units in	units lbf	MPa	MPa	MPa	MPa	%	m.s^{-1}
46.0			3899	2327	2480	3.931	3.937	3.934	7.881	42,400	24.1					4352
46.2	3	comp	3906	2334	2485	3.939	3.938	3.938	7.874	42,900	24.3	23.6	1.9	1.12	4.8	4329
46.2			3908	2334	2483	3.945	3.928	3.036	7.886	39,600	22.4					4336
44.4			3890	2319	2476	3.939	3.937	3.938	7.884	72,600	41.1					4510
44.5	7	comp	3910	2335	2483	3.942	3.937	3.939	7.889	74,500	42.2	41.1	2.3	1.36	3.3	4503
44.4			3910	2334	2481	3.949	3.939	3.944	7.881	70,700	39.9					4509
42.5			3919	2343	2487	3.942	3.943	3.942	7.881	121,100	68.4					4710
42.6	28	comp	3919	2343	2487	3.940	3.936	3.938	7.879	120,000	67.9	68.0	0.6	0.35	0.5	4698
42.5			3893	2325	2483	3.933	3.926	3.929	7.872	119,200	67.8					4705
42.2			3897	2329	2485	3.926	3.932	3.929	7.879	129,000	73.4					4742
42.1	90	comp	3918	2345	2491	3.939	3.931	3.935	7.883	125,300	71.0	72.8	2.9	1.7	2.4	4756
42.2			3894	2326	2483	3.933	3.936	3.935	7.875	130,300	73.9					4740

mean density kg.m^{-3} :   3 day: 2483   7 day: 2480   28 day: 2486   90 day: 2486
reported in compliance with NZS 3111:1974 :   2480   2480   2490   2490
mean ultrasonic pulse velocity m.s^{-1} :   4339   4507   4704   4746

APPENDIX 30

Measurement of rock specific heat

Specific heat tests by Mr G.R. Clark (New Zealand Concrete Research Association) and calcu-
lations by Mr A. Aldrige (Applied Maths Division, DSIR), were carried out in accordance with
ASTM C351-61 "Standard test method for mean specific heat of thermal insulation" but with
two minor changes in technique related to the physical properties of the sample.

As rock is a dense homogenious mass which can readily be brought to thermal equilibrium in
water, a sample holder was not necessary and pre-immersion temperature (C_i) was obtained as
a surface reading by thermometer, instead of by thermocouple at the geometric centre.   This
obviated mutilation of the sample and simplified calculation.

The method involves monitoring, in relation to time, temperature of a water bath into which
a heated sample is dropped.   The water temperature rises abruptly then decreases towards
ambient.   Specific heat is calculated from the formula:

$$C_s = \frac{(\text{mass of water} + K)\ (C_m - C_c)}{(\text{mass of sample})\ (C_i - C_m)}$$

where C_s = specific heat of sample, (cal/gm$^\circ$C)

C_i = temperature of sample at immersion, $^\circ$C.

C_c = ambient temperature of calorimeter, $^\circ$C

C_m = maximum theoretical temperature of calorimeter at immersion $^\circ$C

K = calorimeter constant (17.497 was used as the water equivalent of the
calorimeter and its accessories).

C_m is a theoretical temperature which would result from perfect thermal conductivity (between
sample and water): it was obtained from a plot of temperature against time by extrapolation
using least squares regression from maximum measured temperature.   Equipment calibration and
the use of Lagrangian interpolation gave a temperature plot accuracy of 0.01°C.   Results
are presented in Table A30.1.

Table A30.1 : Raw data and calculated specific heat values for Wellington greywacke-suite rocks. Two samples of two argillites were tested. Samples were off-cuts from 25 mm diameter cores.

Sample	Lithology	Rock mean grain size, phi	Sample Mass, gm.	Sample Temp., C_i, $^{\circ}C$	Duration of test seconds	Time sample added to water bath seconds	Tempera-ture recording intervals, seconds	Water mass, gm.	Calori-meter ambient, C_c, $^{\circ}C$	Mixture C_m, $^{\circ}C$	Specific heat, C_s, cal/gm.$^{\circ}C$
DC-6	greywacke		18.0517	103.7	520	240	20	301.22	13.033	13.978	0.1860
HQ-17	greywacke	1.317	23.2358	100.4	750	360	30	301.13	14.260	15.327	0.1720
SJ-3$_1$	greywacke	1.32	14.1193	102.6	390	240	15	303.75	14.220	15.046	0.2146
KTW-14	greywacke	2.6	14.7592	103.9	390	255	15	303.69	15.270	16.000	0.1805
BQ-V	greywacke	2.73	19.0108	101.7	520	240	20	302.5	12.913	13.889	0.1871
KS-2	greywacke	3.27	12.1689	101.9	390	180	15	300.76	15.426	15.987	0.1708
KTW-i	greywacke	4.23	17.2061	103.2	520	240	20	301.55	13.435	14.310	0.1825
SJ-T	greywacke	4.72	19.3121	105.3	520	260	20	304.98	14.781	15.814	0.1927
OB-W	argillite	5.6	12.7120	100.8	390	180	15	302.13	15.740	16.314	0.1708
OB-W(R)	argillite	5.6	11.8990	100.1	390	180	15	302.27	13.082	13.615	0.1656
HQ-22	argillite	6.28	6.4678	100.1	210	90	10	302.64	13.164	13.498	0.1909
HQ-22(R)	argillite	6.28	4.1534	101.3	120	60	5	302.82	13.164	13.382	0.1912

mean 0.1837

Based on determinations of 25 mm cores of concrete tested similarly, a standard deviation of 0.008 cal./gm.$^{\circ}C$ applied to the above samples, which at the 95 percent confidence interval, indicates values to be within 0.02 cal./gm.$^{\circ}C$ of the true value.

Specific heat in SI units (joules/kilogram.K) is obtained* from either the f.p.s. or c.g.s. values by multiplying by 4.1868×10^3.

* Rhodes, J.A. (1978) "Significance of tests and properties of concrete and concrete making materials". chapter 17 - Thermal properties; ASTM STP 169B: 242-61.

APPENDIX 31

Measurement of rock durability by ultrasonic cavitation test

This test was devised by the U.S. Bureau of Reclamation* to measure the resistance of rock to cavitation (de Puy 1965). A small disc of rock sample was attached by epoxy cement to the horn of a commercially available ultrasonic probe which was run in water for one minute at 20 kH$_z$ with a power output of 150 watts.

The possibility of flaking of the cement precluded evaluation by weight loss, so results were assessed by microscopic examination of the specimen surface in terms of a scale based on cavitation:

Durability rating	Amount of cavitation damage
0	Sample completely broken up before one minute
1	Sample broken up by end of one minute test
2	Severe deterioration
3	Severe general erosion
4	Severe pitting
5	Moderately severe pitting
6	Moderate pitting
7	Minor pitting or some intergranular erosion
8	Some minor intergranular erosion
9	Very slight pitting
10	No visual damage

More recently, Saltzman (1975) gave a full account of ultrasonic techniques in estimating rock quality for protective blankets (rip-rap). This author elaborated on some important imperfections in the original test.

Saltzmans' test was carried out on some representative greywacke-suite rocks with a Branson Sonifer ultrasonic cell disrupter, model B-30, producing up to 300 watts at 20 kH$_z$.

The horn tip measured 0.5 inch (12 mm). Samples were prepared from discs of varying thickness trimmed from rock cores prepared for use else here in this study. They measured 25 mm in diameter, were fine surface ground, oven dried to constant mass at 110°C, and cooled in a desiccator to room temperature.

Samples were placed in a heavy brass holder beneath the transducer horn, in a water bath measuring 220 mm in diameter at the top, tapering to 210 mm at its base and contained 60 mm of water (maintained at 50°C) which covered the sample.

The distance between sample and transducer could be adjusted without alteration to vertical axis alignment and was set to procure maximum transducer output (measured by wattmeter) Samples were tested for 10 minutes with the following results:

---

* U.S. Bureau of Reclamation (1965) Progress report: rip-rap testing research, comparison of an ultrasonic cavitation test with petrographic and physical tests to evaluate rock durability. Laboratory report ChE-23, Denver, Colorado.

Sample	Rock mean grain size, phi	Transducer wattage	Weight before testing, gm	Weight after testing, gm	Weight percent loss	Numerical durability rating
DC-6	1.25	125-130	18.0536	18.0335	0.1	5
HQ-17	1.317	125-130	23.2173	23.2094	0.03	9
SJ-3$_1$	1.32	125-130	14.1458	14.1039	0.3	6
KTW-14	2.6	150	14.7576	14.7412	0.1	7
BQ-V	2.73	150	19.0108	18.9773	0.2	6
BQ-IXA	2.9	150	4.9621	4.9364	0.5	7
KS-2	3.27	150	12.1779	12.1343	0.4	5
KTW-i	4.23	-	17.2081	17.1716	0.2	6
SJ-T	4.72	-	19.3369	19.2833	0.3	7
OB-W	5.6	125-130	11.8905	11.8572	0.3}	5
OB-W(R)	5.6	125-130	12.6866	12.6672	0.2} 0.25	7
HQ-22	6.28	125-130	4.1537	4.1272	0.6}	6
HQ-22(R)	6.28	125-130	6.4548	6.4305	0.4} 0.5	7

$\bar{x}$ 0.26

s.d. 0.16

Although some difficulty was experienced in maintaining power output, there is correlation between percentage weight loss and mean grain size - slightly positive

$$Y = 0.048x + 0.104, \quad r = 0.53$$

As samples had been prepared with preferred orientation perpendicular to the probe axis, the damage to argillites was probably rather less than may otherwise be expected, so only the greywacke results are considered representative. Some greywackes (SJ-3$_1$ and KS-2) showed relatively high loss.

Indications are that the test could provide valuable information on the suitability of various greywacke-suite rocks for rip-rap applications particularly rocks in the mean grain size range, 2.5 to 3.5 phi: (0.18 to 0.09 mm), a possibility reinforced by findings of this study.

APPENDIX 32

Quarry sludge properties

During quarrying operation, a significant portion of the rock is washed out as sludge.   This poses three related problems for the industry, i.e. product wastage, disposal and environmental.

The most attractive solution is commercial use, so sludge from two quarries was sampled to determine its properties.   Results are tabulated below:

Sample	pH on sampling	Moisture content on sampling %	Liquid limit	Plastic limit	Plasticity index	Drying shrinkage	Remarks
Belmont Quarry settling pond BQ-S	8	30	37	25	12	4.3 at plastic limit	sand size fraction up to 20 percent of sample
River Shingle and Sand Ltd., settling pond RSS-NS	7.6	54	-	-	-	-	
River Shingle and Sand Ltd., settling pond RSS-F	8.1	92	-	-	-	-	

Chemical data

	RSS-F	RSS-NS	BQ-S
SiO_2	60.47	57.82	59.58
Al_2O_3	16.31	16.99	16.46
TiO_2	0.53	0.62	0.67
*Fe_2O_3	5.76	6.82	5.78
FeO	-	-	-
MnO	0.12	0.16	0.10
MgO	2.09	2.06	2.02
CaO	2.73	2.37	3.28
Na_2O	1.68	1.88	2.07
K_2O	2.51	2.55	3.36
P_2O_5	0.13	0.16	0.18
LOI	7.71	8.06	5.84
Total	100.04	99.49	99.35

* All Fe represented as Fe_2O_3

Belmont Quarry also provided results of tests made by the New Zealand Geological Survey for the Wellington Regional Water Board.   These infra-red spectrophotometric modal analyses (weight percent) of sludge samples from the settling pond showed:

	Quartz	Feldspar	Illite	Kaolinitic clay mineral (halloysite)
Sample A	37 ±3	18 ±3	29 ±5	5
Sample B	31 ±3	16 ±3	35 ±5	5

In addition, up to 10 percent chlorite and rare calcite were detected. Mineralogy was confirmed by X-ray diffractometry.

To assess possible ceramic use, several firing tests were made, all thwarted by the very low green and dry strengths of the material, due to the pH and relatively high content of sand sized material. Most heavy ceramic clay bodies have:

(i)   Minimal sand-size material; less than 15 percent.

(ii)   Between 40 and 50 percent of particles finer than 0.005 mm.

(iii)   A mean grain size of about 0.015 mm (Figure A32.1).

Beneficiation of the sludge by sand removal may not be economic but the addition of $NaCO_3$ would ameliorate pH and improve knitting properties by deflocculation.

Suggested uses for the sludge materials, subject to research, may include fertilizer base, filter material, inert filler, or abrasive. With the addition of lime and/or cement it may be possible to use the material as a solid base material, low strength castable, or insulant. Higher strengths may be attainable from autoclaving.
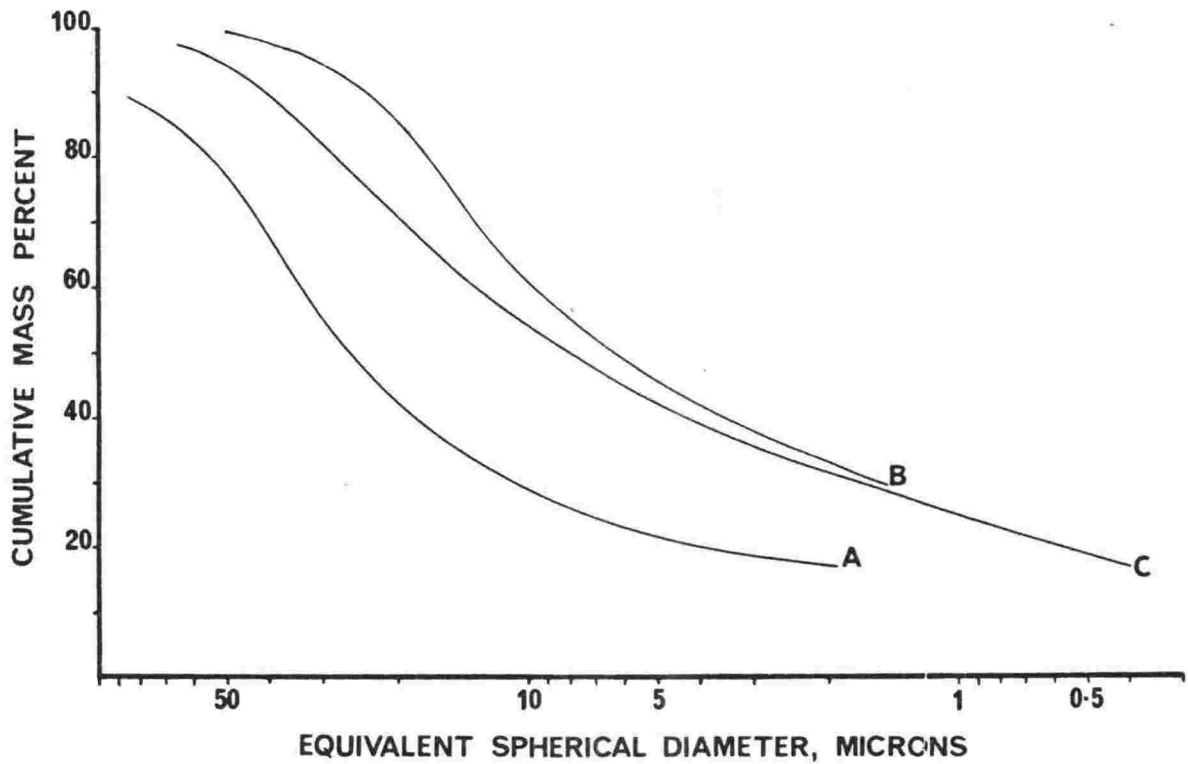
Figure A32.1 : Particle size gradings of two quarry sludges
(curves A and B) examined by the New Zealand
Geological Survey. Curve C is the particle size grading of a
typical earthware pipe clay.

APPENDIX 33

Sample number correlation with the petrology collection, Geology Department, Victoria University of Wellington.

VUW No.	This study	Short description	VUW No.	This study	Short description
13601	KW-1	Weathered siltstone from Kawhia Harbour. Subject of Plate A25.3			
13602	SJ-2	Greywacke	13656	KTW-1	Greywacke
13603	SJ-2A	Argillite, trace fossil bearing	13657	KTW-2	Greywacke
13604	SJ-3$_1$	Chipwacke	13658	KTW-4	Greywacke
13605	SJ-3$_2$	Greywacke	13659	KTW-13	Greywacke
13606	SJ-3$_3$	Greywacke	13660	KTW-14	Greywacke
13607	SJ-4	Greywacke	13661	KTW-15	Greywacke
13608	SJ-5	greywacke	13662	KTW-16	Greywacke
13609	SJ-6	Greywacke	13663	KTW-17	Greywacke
13610	SJ-T	Greywacke, trace fossil bearing	13664	KTW-i	Greywacke
			13665	KTW-ii	Greywacke
13611	KS-1	Greywacke	13666	KTW-iii	Argillite
13612	KS-2	Greywacke, contains floral debris, subject of Plate 2.4	13667	KTW-v	Argillite
			13668	KTW-viii	Greywacke
13613	KS-4	Greywacke	13669	KTW-G	Greywacke, contains floral debris
13614	KS-6	Greywacke			
13615	KS-7	Weathered greywacke			
13616	KS-8	Greywacke	13670	OB-1	Greywacke
13617	KS-10	Greywacke	13671	OB-11	Argillite
			13672	OB-12	Greywacke
13618	RSS-4	Greywacke	13673	OB-13	Argillite
13619	RSS-5	Greywacke	13674	OB-14	Greywacke
13620	RSS-6	Greywacke	13675	OB-21	Greywacke
13621	RSS-8	Greywacke	13676	OB-W	Argillite, subject of Plate A25.2A, B and C
13622	RSS-12	Greywacke			
13623	RSS-i	Greywacke			
13624	RSS-ii	Argillite	13677	HQ-13	Zeolitised greywacke
13625	RSS-ii(2)	Greywacke	13678	HQ-14	Zeolitised greywacke
13626	RSS-iii	Greywacke	13679	HQ-15	Argillite
13627	RSS-NS	Quarry sludge, naturally settled	13680	HQ-16	Greywacke
13628	RSS-F	Quarry sludge, flocculated	13681	HQ-17	Greywacke, zeolite bearing
			13682	HQ-18	Argillite
13629	WCC-2	Greywacke	13683	HQ-19	Greywacke
13630	WCC-5A	Argillite	13684	HQ-20	Argillite
13631	WCC-7	Greywacke	13685	HQ-21	Greywacke
13632	WCC-8A	Argillite	13686	HQ-22	Argillite
13633	WCC-13A	Greywacke	13687	HQ-23	Greywacke
13634	WCC-17	Greywacke	13688	HQ-24	Argillite
13635	WCC-18	Greywacke	13689	HQ-25	Greywacke
13636	WCC-22	Weathered greywacke	13690	HQ-26	Greywacke
31637	WCC-23A	Weathered laminated argillite, trace fossil bearing	13691	HQ-27	Greywacke
			13692	BQ-6	Greywacke
31638	DC-1	Greywacke	13693	BQ-8	Greywacke
13639	DC-2	Greywacke	13694	BQ-10	Greywacke
13640	DC-3	Greywacke	13695	BQ-11	Argillite
13641	DC-6	Chipwacke	13696	BQ-15	Argillite, trace fossil bearing
13642	DC-8	Greywacke			
13643	DC-10	Greywacke	13697	BQ-17A	Greywacke
13644	DC-LAM	Greywacke	13698	BQ-17B	Argillite
			13699	BQ-18	Greywacke
13645	NC-8	Greywacke	13700	BQ-20	Greywacke
13646	NC-15	Argillite	13701	BQ-21	Argillite
			13702	BQ-22	Greywacke
13647	IB-2	Weathered greywacke	13703	BQ-27	Greywacke
13648	IB-6	Greywacke	13704	BQ-i	Greywacke
13649	IB-7B	Greywacke	13705	BQ-ii	Argillite
13650	IB-8	Greywacke	13706	BQ-iii	Greywacke
13651	IB-11	Argillite	13707	BQ-iv	Greywacke
13652	IB-13A	intensely sheared and veined greywacke	13708	BQ-V	Greywacke
			13709	BQ-vii	Argillite
13653	IB-17	Weathered greywacke	13710	BQ-IXA	Greywacke
13654	IB-19	Weathered greywacke	13711	BQ-xviii	Greywacke
13655	IB-22	Weathered greywacke	13712	BQ-S	Quarry sludge, naturally settled

VUW No.	This study	Short description	VUW No.	This study	Short description
13713	DC-6				
13714	HQ-17				
13715	SJ-3$_1$				
13716	KTW-13				
13717	KTW-14		13777	BQ-IXA	Bond failure in concrete. Subject of Plates 5.1, 5.2
13718	RSS-12				
13719	HQ-21		13778	1/007	Walton Park concreting sand
13720	BQ-V				
13721	BQ-IXA		13779	8	Horokiwi Quarry basecourse
13722	OB-21		13780	5	Carsons Quarry basecourse
13723	HQ-19		13781	2	River Shingle and Sand basecourse
13724	KS-2		13782	9	Dry Creek Quarry basecourse
13725	KS-10		13783	4	Owhiro Bay Quarry basecourse
13726	BQ-iii		13784	3	Midway Metal basecourse
13727	KTW-G		13785	7	Belmont (formerly Kell's) Quarry basecourse
13728	RSS-iii				
13729	BQ-21	"Tema" ground specimens	13786	6	Waikanae Quarry basecourse
13730	KTW-i		13787	1	Kiwi Point Quarry basecourse
13731	DC-8				
13732	BQ-i		13788	DC-6	
13733	RSS-ii		13789	HQ-17	
13734	HQ-26		13790	SJ-3$_1$	
13735	HQ-24		13791	KTW-14	
13736	OB-W		13792	BQ-V	
13737	HQ-20		13793	BQ-IXA	Samples used for data presented in Appendices 30 and 31
13738	WCC-5A		13794	KS-2	
13739	HQ-18		13795	KTW-i	
13740	BQ-vii		13796	SJ-T	
13741	HQ-22		13797	OB-W	
13743	OB-13		13798	OB-W(R)	
13743	RSS-NS		13799	HQ-22	
13744	RSS-F		13800	HQ-22(R)	
13745	BQ-S				
			15852	KA-12	
13746	HQ-17		15853	KA-8	
13747	KTW-14		15854	KA-2	
13748	BQ-IXA	19 - 9.5 mm aggregate samples	15855	DC-6	
13749	SJ-T		15856	HQ-17	
13750	OB-W		15857	KTW-14	Samples used for permeability data presented in Appendix 25
13751	HQ-22		15858	BQ-IXA	
			15859	BQ-V	
13752	HQ-17		15860	KS-2	
13753	KTW-14		15861	KTW-i	
13754	BQ-IXA	9.5 - 4.8 mm aggregate samples	15862	SJ-T	
13755	SJ-T		15863	OB-W	
13756	OB-W		15864	HQ-22	
13757	HQ-22				
13758	HQ-17	Mix 1 concrete cylinders, cut in half parallel to the long axis. Aggregate particle angularity measurements were taken from these.	15865	HQ-17(4)	Subject of Plate A15.2
13759	KTW-14		15866	OB-W	Subject of Plate A15.1B
13760	BQ-IXA		15867	KTW-i	Subject of Plate A15.1A
13761	SJ-T		15868	KTW-i	Core fragment showing strain gauge and connector strip detail
13762	OB-W				
13763	HQ-22				
			15869	OB-W	Core failure showing *en echelon* ridges
13764	HQ-17	Mix 2 concrete cylinders, cut in half parallel to the long axis. Aggregate particle angularity measurements were taken from these.			
13765	KTW-14		15870	OB-W	Core failure showing failure plane independent of recemented shear
13766	BQ-IXA				
13767	SJ-T				
13768	OB-W		15871	OB-W(6)	Core failure dominated by vein
13769	HQ-22		15872	BQ-IXA	Axial cleavage failure
13770	Tinakori	Tinakori gun emplacement concrete	15873	KTW-i	Prism sample used in Appendices 19 and 25
13771	Karori Cem.	Karori Cemetry grave-surround concrete			
13772	I.R. Buildg.	Inland Revenue Building concrete, Courtney Place	15874	OB-W	Subject of Plate A25.2D
13773	Kelburn	18A St Michaels Crescent, foundation concrete	15875	IB-13B	Argillite, contains floral debris, subject of Plate 2.5
13774	Pearse	Old Pearse House concrete, Dixon St.	15876		Zeolite material from Horokiwi Quarry used for analysis in section 4.4
13775	Farrish	Cnr Farrish and Manners Sts. Structural concrete			
13776	Wilton	21 Wilton Rd, concrete from retaining wall	15877		Composite core fabricated for chlorite chemistry, Appendix 8
			15878		Typical cone failure in concrete made with OB-W. Tested at 90 days